

## Durham E-Theses

---

### *An investigation of the photoinitiated cationic cross-linking polymerization of some epoxy resins*

Matuszczak, Stephen

#### How to cite:

---

Matuszczak, Stephen (1987) *An investigation of the photoinitiated cationic cross-linking polymerization of some epoxy resins*, Durham theses, Durham University. Available at Durham E-Theses Online: <http://etheses.dur.ac.uk/6705/>

#### Use policy

---

The full-text may be used and/or reproduced, and given to third parties in any format or medium, without prior permission or charge, for personal research or study, educational, or not-for-profit purposes provided that:

- a full bibliographic reference is made to the original source
- a [link](#) is made to the metadata record in Durham E-Theses
- the full-text is not changed in any way

The full-text must not be sold in any format or medium without the formal permission of the copyright holders.

Please consult the [full Durham E-Theses policy](#) for further details.

AN INVESTIGATION OF THE PHOTOINITIATED  
CATIONIC CROSS-LINKING POLYMERIZATION  
OF SOME EPOXY RESINS

by

The copyright of this thesis rests with the author.  
No quotation from it should be published without  
his prior written consent and information derived  
from it should be acknowledged.

STEPHEN MATUSZCZAK, B.Sc. (York)

(Graduate Society)

A thesis submitted  
for the Degree of Doctor of Philosophy  
to the University of Durham

1987



13 JUN 1988

To My Parents and Sister  
for their encouragement and support  
throughout my education

MEMORANDUM

The work reported in this thesis was carried out in the Chemistry Department of the University of Durham between October 1982 and October 1985. This work has not been submitted for any other degree and is the original work of the author except where acknowledged by references.

Part of the work has been reported in *Polymer Communications* (27, 162, (1986)). Also aspects of the work have been presented at International Symposia concerning Polymer Surfaces and Interfaces (Durham, April 1985), New Trends in the Photochemistry of Polymers (Stockholm, August 1985) and The Radiation Curing of Polymers (Lancaster, September 1986).

ACKNOWLEDGEMENTS

First and foremost I would like to express my gratitude to my supervisor, Prof. W.J. Feast for his encouragement, guidance and help throughout the course of this work. My thanks also go to Camrex (Holdings) Ltd. (alas no more) for their financial support and to Dr. R. Kay, Dr. S. Furtardo, Mr.A. Prest and Mr. W. Woods for their encouragement and advice.

I am indebted to Dr. H. S. Munro for his helpful discussions of various aspects of the project especially those involving the use of ESCA and must also thank the members of the ESCA research group, particularly Dr. J.G. Eaves.

My thanks go to the colleagues with whom I have worked, especially Drs. Millichamp, Harper and Winters, along with Mr. D. Parker for the useful discussions and practical advice. My thanks also go to Mr. D. Barnes for the work carried out as part of his undergraduate project on the synthesis of the model epoxides. I would also like to express my thanks to the members of the technical staff, in particular, Messrs. Parkinson, McNeilly, Hart, Haswell and Coult along with Mrs. M. Cocks.

I must acknowledge the assistance given by Dr. R.S. Matthews in obtaining and interpreting the NMR spectra and the people concerned at Edinburgh and Newcastle Universities for running the samples. I must also offer my thanks to Drs. L.H. Williams and M.R. Crampton (unravelling the decay kinetics of the coloured species) and to the following members of Applied Physics. Dr. G.J. Russel (electron microscopy) and Dr. J.S. Thorp and Mr. C. Williams (ESR spectroscopy) for their assistance.

My sincere thanks also go to Mrs.E.M.Wood and Mrs.M.Wilson for their help in the production of this thesis and finally I must gratefully acknowledge the award of a grant by SERC.

by

STEPHEN MATUSZCZAK

Ph.D. Thesis - 1987

---

ABSTRACT

As well as dealing with general topics pertinent to the project, the first chapter gives the aims of the project and reviews the theories of network formation. Particular attention is paid to the occurrence of inhomogeneous cross-linking in non-linear chain-growth polymerizations. The second chapter reviews an important aspect of photoinitiated polymerizations, namely the photochemistry of the photoinitiator used, in this case diphenyliodonium hexafluorophosphate.

The preparation and characterization of the photoinitiator and the characterization of the commercial monomers are given in chapter three. The fourth chapter reports an investigation of the effect of various parameters on the degree of cross-linking as determined by a variety of techniques. The results can be interpreted in terms of inhomogeneous cross-linking and show that irradiation combined with thermal treatment produces the highest degree of cross-linking. Chapter five deals with a study of the photo-oxidative stability of two of the photocurable resin systems. Certain monomer systems were found to exhibit a transient colouration on cure and chapter six gives a possible explanation for this effect as well as the results of experiments designed to provide additional verification.

Finally, chapter seven reports the outcome of attempts to obtain low surface free energy films by the addition of small amounts of polyfluorinated monoepoxides to the conventional monomers in the hope that surface segregation of the fluorinated material would occur in the interval between application and cure of films.

CONTENTS

	<u>Page No.</u>
Memorandum	i
Acknowledgements	ii
ABSTRACT	iii
CHAPTER ONE - GENERAL BACKGROUND, AIMS OF THE PROJECT AND A REVIEW OF THE THEORIES OF NETWORK FORMATION	1
1.1 Surface Coatings	2
(A) Domestic Paints	3
(B) Industrial Coatings	4
(i) Chemically Resistant Coatings	4
(ii) Marine Coatings	6
1.2 Reasons for the Interest in the Photoinitiated Cure of Resins	8
1.3 Objectives of the Work Reported in this Thesis	9
1.4 Classification of Polymerization Reactions	10
(A) Step-Growth Polymerizations	11
(B) Chain-Growth Polymerizations	11
(C) Ring-Opening Polymerizations	13
1.5 Epoxy Resins	14
(A) Synthesis of Epoxy Resins	14
(B) Conventional Cure of Epoxy Resins	17
(i) Polyfunctional Amine and Amide Curing Agents	18
(ii) Acid Anhydride Curing Agents	19
(iii) Tertiary Amine Curing Agents	20
(iv) Polyfunctional Isocyanate Curing Agents	21
1.6 Cationic Ring-Opening Polymerizations of Epoxide Compounds	21
(A) Initiation	21
(B) Propagation	22
(C) Chain Transfer and Termination Processes	24
(D) Effect of Temperature on the Rate of Polymerization	26
1.7 Non-Linear Polymerizations	28
(A) The Flory-Stockmayer Theory of Non-Linear Polymerizations	29
(B) The Application of Cascade Theory to Non-Linear Polymerizations	33

	<u>Page No.</u>
(C) Intramolecular Reaction and Cyclization	36
(D) Application of Percolation Theory to Non-Linear Polymerizations	41
(E) Inhomogeneous Cross-Linking in Network Polymers	46
(i) Inhomogeneity in Conventionally Cross- Linked Epoxy Resins	46
(ii) Inhomogeneity in Chain Cross-Linking Polymerizations	48
(iii) Inhomogeneity in Photoinitiated Chain Cross-Linking Polymerizations	52
References - Chapter One	61
 CHAPTER TWO - A BRIEF SURVEY OF PHOTOINITIATORS AND THE PHOTOCHEMISTRY OF DIARYLIODONIUM SALTS	 65
2.1 General Aspects of Photochemistry	66
(A) Excited States and Photochemical Processes	66
(B) Quantum Yield	69
(C) Photosensitization	69
2.2 Photoinitiators for Free Radical and Cationic Polymerizations	70
(A) Free Radical Photoinitiators	70
(i) Carbonyl Photochemistry	71
(ii) Photoinitiators Producing Radicals by Fragmentation	72
(iii) Photoinitiators Producing Radicals by Abstraction	73
(iv) Disadvantages of Photoinitiated Free Radical Polymerizations	73
(B) Cationic Photoinitiators	75
(i) Aryldiazonium Salts	77
(ii) Diaryliodonium Salts	77
(iii) Sulphonium Salts	77
(iv) Triarylselenonium Salts	78
(v) Selection of a Photoinitiator for These Studies	79
2.3 Diaryliodonium Salts as Photoinitiators	79
(A) The Photochemistry of Diaryliodonium Salts	80
(i) Mechanism of Photolysis	80
(B) Mechanism of Initiation of Polymerization	82
(C) Photosensitization of Diaryliodonium Salts	84
(i) Direct Electron Transfer	85
(ii) Indirect Electron Transfer	86
(D) Applications of Diaryliodonium Salt Photoinitiators	88
References - Chapter Two	91

CHAPTER THREE - SYNTHESIS OF DIPHENYLIODONIUM HEXA- FLUOROPHOSPHATE AND THE ANALYSIS OF THE COMMERCIAL MONOMERS	93
3.1 Synthesis of the Diaryliodonium Salt Photoinitiators	94
(A) Synthetic Routes to Diaryliodonium Salts	94
(B) Preparation and Characterization of Diphenyliodonium Hexafluorophosphate	95
3.2 Analysis and Characterization of the Monomers	97
(A) Infra-Red Spectra of the Monomers	98
(B) Epoxide Content, Hydroxyl Content and the Molecular Weight of the Monomers	100
(C) $^1\text{H}$ -NMR and $^{13}\text{C}$ -NMR Spectra of the Monomers	101
(i) The DGEBA Resin	102
(ii) The DGEBF Resin	103
(iii) The Epoxy Novolac Resin	106
(iv) The Diglycidyl Ether of Butanediol	106
(D) Ultraviolet Spectra of the Monomers	108
References - Chapter Three	111
CHAPTER FOUR - THE EFFECT OF VARIOUS PARAMETERS ON THE PHOTOINITIATED CATIONIC CROSS-LINKING POLYMERIZATION OF EPOXY RESINS AND THE EVIDENCE FOR INHOMOGENEOUS NETWORK FORMATION	112
4.1 Introduction	113
4.2 Determining the Degree of Cure of Network Polymers	114
(A) Measuring the Extent of Reaction	114
(i) Infra-Red Spectroscopy	115
(ii) Differential Scanning Calorimetry	116
(B) The Glass Transition Temperature, $T_g$ , as a Measure of the Degree of Cross-Linking	117
(i) The Glass Transition	117
(ii) The Effect of Cross-Linking on $T_g$	120
(iii) The Effect of the Glass Transition on Cross-Linking Polymerizations	121
(C) Methods of Measuring $T_g$	122
(i) Differential Scanning Calorimetry	122
(ii) Thermo-mechanical Analysis	123
(D) Other Properties Related to the Degree of Cross-Linking	126
(i) Hardness	127
(ii) Gel Content	128

4.3	The Preparation and Irradiation of Films of the Monomers	129
	(A) Film Preparation	129
	(B) UV Sources used	130
	(i) The 100W Lamp	130
	(ii) The 1.8kW Lamp	130
4.4	An Overview of the Process of Network Formation <i>via</i> Photoinitiated Chain Cross-Linking Polymerization Emerging from this Study of the Cure of Epoxy Resins	132
4.5	An Initial Investigation of the Photoinitiated Cure of The DGEBA and Epoxy Novolac Systems using Infra-Red Spectroscopic Measurements of Conversion	135
4.6	Effect of Cure Exposure, Film Thickness and Light Intensity on the Cure of the DGEBA System	141
	(A) Infra-Red Spectroscopic Measurements of Epoxide Conversion	141
	(B) Measurement of the Gel Content	150
4.7	An Investigation of the Wavelengths of Light Responsible for Initiating Cure in the DGEBA System using Infra-Red Spectroscopic Measurements of Epoxide Conversion	153
	(A) Irradiation with the 100W Lamp	155
	(B) Irradiation with the 1.8kW Lamp	160
4.8	Effect of Photoinitiator Concentration on the Cure of the DGEBA and Epoxy Novolac Systems	164
	(A) Hardness Measurements	164
	(B) Infra-Red Spectroscopic Measurements of Epoxide Conversion	167
4.9	Effect of Temperature on the Cure of the DGEBA and Epoxy Novolac System as Determined by Hardness Measurements	170
4.10	Preliminary Investigation of the Effect of Adding a Pigment to the Photocurable Systems	174
4.11	The Use of TMA to Determine the Effect of Various Irradiation Conditions on the T <sub>g</sub> of the DGEBA System	175
	(A) Irradiation with the 1.8kW Source	176
	(i) An Initial Investigation of the T <sub>g</sub> of Films Irradiated on Steel	176
	(ii) Effect of Increasing Cure Exposure and Film Thickness on the T <sub>g</sub> of Films Irradiated on Steel	181

(iii)	Effect of Increasing Cure Exposure and Film Thickness on the Tg of Films Irradiated on Polyethylene	186
(iv)	Effect of Increasing Cure Exposure to Filtered Light	191
(B)	Irradiation with the 100W Source	196
(i)	Effect of Increasing Cure Exposure	196
(ii)	Effect of Increasing Cure Exposure to Filtered Light	200
4.12	The use of DSC to Investigate the Post-irradiation Thermal Cure of the DGEBA System	203
(A)	Irradiation with the 1.8kW Source	204
(i)	Effect of Increasing Cure Exposure	204
(ii)	Effect of Increasing Cure Exposure to Filtered Light	214
(B)	Irradiation with the 100W Source	222
(i)	Effect of Increasing Cure Exposure	222
(ii)	Effect of Increasing Cure Exposure to Filtered Light	227
4.13	Comparison of the Properties of Photocationically and Conventionally Cured Epoxy Resins Useful for Surface Coatings Applications	234
(A)	Chemical Resistance	235
(B)	Adhesion	239
(C)	Prohesion	240
	References - Chapter Four	242
CHAPTER FIVE - THE PHOTO-OXIDATION OF PHOTOCURABLE EPOXY RESIN SYSTEMS DURING CURE AND THEIR SUBSEQUENT PHOTO-OXIDATIVE STABILITY		244
5.1	Introduction	245
5.2	Electron Spectroscopy for Chemical Applications	246
5.3	A General Mechanism of the Photo-Oxidative Degradation of Polymers	248
5.4	Photo-Oxidation of Resins Photocured using Free Radical Photoinitiators	250
5.5	Photo-Oxidation Studies of Conventionally Cured Epoxy Resins and Model Compounds	251
5.6	Photo-Oxidation of the DGEBA System	259
(A)	Photo-Oxidation as a Result of the Curing Process	258
(i)	Effect of Increasing Cure Exposure to the 1.8kW Source	258

	<u>Page No.</u>
(ii) Elimination of the Photo-Oxidation Occurring During Cure	265
(iii) Effect of Increased Cure Exposure to Unfiltered and Filtered Light using the 100W Source	267
(B) Subsequent Photo-Oxidation of Cured Films on Prolonged Irradiation with Longer Wavelength UV Light ( $\lambda > 300\text{nm}$ )	269
(i) Effect of Increasing Cure Exposure	269
(ii) Effect of Increasing Cure Exposure to Filtered Light	280
5.7 Photo-Oxidation of the Diglycidyl Ether of Butanediol System	284
(A) Comments on the Cure of this System	285
(B) Photo-Oxidation as a Result of the Curing Process	291
(C) Subsequent Photo-Oxidation of Cured Films on Irradiation with Longer Wavelength UV Light ( $\lambda > 300\text{nm}$ )	298
References - Chapter Five	302
CHAPTER SIX - AN INVESTIGATION OF THE TRANSIENT COLOURATION OF THE DGEBA, DGEBF AND EPOXY NOVOLAC SYSTEMS WHEN PHOTOCATIONICALLY CURED	304
6.1 Introduction	305
6.2 UV/Visible Spectroscopic Analysis of Cured Films	306
(A) The Epoxy Novolac System	306
(B) The DGEBF System	307
(C) The DGEBA System	307
6.3 A Possible Explanation for the Transient Colouration	308
6.4 The Decay Kinetics of the Coloured Species	313
(A) The Epoxy Novolac System	313
(B) The DGEBF System	317
6.5 The Use of Model Epoxide Compounds and Polyethers to Investigate the Potential Reaction of the Initiating Species and the Resins to Generate Benzylic Cations	320
6.6 Preparation of the Model Epoxides	321
(A) Synthesis and Characterization of 4-(phenylmethyl)-phenoxymethyl oxirane (XXXVI)	322
(B) Synthesis and Characterization of 4-(1-phenylethyl)-phenoxymethyl oxirane (XXXVII)	325
(i) Synthesis and Characterization of the Precursor Phenol (XLI)	325

	<u>Page No.</u>
(ii) Reaction of (XLI) with ECH	329
6.7 Conventional Polymerization of the Model Epoxides	332
(A) Mechanistic and Stereochemical Aspects of Epoxide Polymerization using the $AlEt_3/H_2O$ System	333
(B) Preparation of the Catalyst Solution	336
(C) Polymerization of (XXXVI) and the Characterization of the Resulting Polyether (XXXVIII)	336
(D) Polymerization of (XXXVII) and the Characterization of the Resulting Polyether (XXXIX)	340
(E) Comments on the Bimodal Molecular Weight Distribution and the Tacticity of the Polyethers (XXXVIII) and (XXXIX)	343
6.8 Addition of the Model Epoxides and Polyethers to Sulphuric Acid	347
(A) Compound (XXXVI) and the Polyether (XXXVIII)	347
(B) Compound (XXXVII) and the Polyether (XXXIX)	350
6.9 Preparation of Poly(benzyl) and Poly(phenethyl)	353
(A) Poly(benzyl)	353
(B) Poly(phenethyl)	355
6.10 Irradiation of the Model Epoxides and Polyethers in the Presence of Photoinitiator	357
(A) Colouration of the Model Systems	357
(i) Compound (XXVI) and the Polyether (XXXVIII)	357
(ii) Compound (XXVII) and the Polyether (XXXIX)	359
(B) GLC Analysis	361
(i) Compound (XXXVI)	361
(ii) Compound (XXXVII)	362
(C) $^{13}C$ -NMR Spectroscopic Analysis	362
(i) Compound (XXXVI) and the Polyether (XXXVIII)	362
(ii) Compound (XXXVII) and the Polyether (XXXIX)	365
6.11 Conclusions	370
References - Chapter Six	371

CHAPTER SEVEN - ATTEMPTS TO OBTAIN FLUORINATED SURFACES VIA THE SURFACE SEGREGATION OF SMALL AMOUNTS OF POLYFLUORINATED MONOMER ADDED TO LACQUERS OF CONVENTIONAL EPOXY RESIN	372
7.1 Introduction	373
7.2 Surface Segregation of Low Surface Energy Species	374
7.3 Determination of the Surface Free Energy of Solid Polymers	375
7.4 Preparation of the Polyfluorinated Epoxides used in this Work	379
(A) Synthesis and Characterization of ((7,7,6,6,5,5,4,4,3,3,2,2-dodecafluoroheptyl) oxy)methyl oxirane (XLII)	381
(B) Synthesis and Characterization of ((3,3,3,2,2-pentafluoropropyl)oxy)methyl oxirane (XLIV)	384
(C) Synthesis and Characterization of 3,3,2,2-pentafluoropropyl oxirane (XLV)	387
7.5 Characterization and Surface Energy Measurements of Polymers Prepared by the Conventional Cationic Polymerization of Monomers (XLII) and (XLIII)	391
(A) Polymerization of (XLII) and the Character- ization of the Resulting Polyether (XLVII)	392
(B) Polymerization of (XLIII) and the Character- ization of the Resulting Polyether (XLVIII)	394
7.6 Addition of the Polyfluorinated Epoxides to Lacquers of Conventional Epoxy Resin	396
(A) Effect of Low Concentrations of (XLII) on the Surface Energy of Films	396
(B) Effect of Increasing the Concentration of (XLII) on the Surface Energy of Films	399
(C) Effect of Low Concentrations of (XLIII) Alone or with (XLII) on the Surface Energy of Films	404
(D) Effect of Low Concentrations of (XLIV) Alone or with (XLII) on the Surface Energy of Films	405
(E) Effect of Low Concentrations of (XLV) Alone or with (XLII) on the Surface Energy of Films	407
References - Chapter Seven	408

	<u>Page No.</u>
APPENDIX ONE - EXPOSURE OF THE UV CURABLE SYSTEMS TO SUNLIGHT	409
APPENDIX TWO - DETECTION OF $\text{PF}_6^-$ AT THE SURFACE OF FILMS IRRADIATED UNDER VARIOUS CONDITIONS	412
APPENDIX THREE - INSTRUMENTS AND APPARATUS	416
APPENDIX FOUR - INFRA-RED SPECTRA	421
APPENDIX FIVE - NUCLEAR MAGNETIC RESONANCE SPECTRA	427
APPENDIX SIX - MASS SPECTRA	445
APPENDIX SEVEN - DIFFERENTIAL SCANNING CALORIMETRY CURVES	449

CHAPTER ONE

GENERAL BACKGROUND,

AIMS OF THE PROJECT AND

A REVIEW OF THE THEORIES OF NETWORK FORMATION



## 1.1 Surface Coatings

The corrosion of a metal arises from chemical and electrochemical processes that occur on the surface of the metal where it is in contact with its environment. Other factors such as mechanical stress may help to initiate or increase the rate of corrosion. The cost of corrosion is quite substantial, generally accounting for approximately 1% of gross national product.<sup>1</sup> During the late nineteen seventies, for example, it was estimated that the protection or replacement of metal structures in America alone cost in the region of  $\$15 \times 10^9$  annually.<sup>2</sup> As well as being expensive corrosion is wasteful especially in view of the non-renewable source of metals.

The most common method used to prevent corrosion is to coat the surface of the metal with an impermeable membrane such as paint, which provides a barrier between the metal and its environment. Surface coatings may contain many components, the main ones being:

(a) the binder or medium, which is responsible for many of the protective properties of the film. The binder is usually a high molecular weight polymer or a polyfunctional resin that is polymerized after application to form a cross-linked, network polymer. Properties such as adhesion, toughness, abrasion resistance, flexibility and resistance to chemicals or solvents are determined by the binder

(b) pigments, which give the film opacity and colour, can also improve the durability, toughness, adhesion and chemical or solvent resistance of the coating. Some protection from ultraviolet radiation may also be achieved by the choice of an

appropriate pigment. A number of pigments, for example red lead, can inhibit corrosion of ferrous metals and are used extensively in primer coatings.

(c) extenders, which contribute to the opacity of the coating can reduce the need for the more expensive pigment, allowing the paint to be manufactured more economically. Extenders are chosen so that their use does not lead to a reduction in the effectiveness of the coating.

(d) solvents, which are used to aid the application of the paint to the substrate. Solvents may account for up to approximately 45% of the mass of a paint.

Other additives may be included to vary such properties as the viscosity, flow, wetting or the stability of dispersions. Special additives such as biocides may also be incorporated into the coating.

#### (A) Domestic Paints

Latex or alkyd resins are mostly used as the binders in domestic paints<sup>3</sup> which are employed more for decorative than protective purposes on substrates such as wood. Poly-(vinylacetate) or acrylics prepared by emulsion polymerization of the appropriate monomer are used as the binders in modern latex paints. The discrete particles of polymer, the pigment and other additives are dispersed in water. These paints have proved popular because of their ease of application and the lack of odour associated with the use of organic solvents. Alkyd resins are branched polyesters prepared from the reaction of polyols with polybasic acids. The addition of monobasic fatty acids to the polymerization reaction helps to produce polymer that can be readily dissolved in organic

solvents which have to be used with these paints. On application of the paint, the organic solvent or water slowly evaporates leaving the polymer or resin in the form of a continuous film with the pigment and other additives distributed throughout. In addition, unsaturated monobasic fatty acid units in the alkyd resin may react with oxygen to give some degree of cross-linking.

Exterior paints are based on similar formulations to those above but have to be more resistant to weathering.

#### (B) Industrial Coatings

In industry, coatings<sup>4</sup> are used on metal, wood, concrete and plastic substrates. The articles coated range from those produced in high volume manufacturing industries such as the car industry where the coating is carried out on a production line basis, to the coating of large structures such as ships. Protection of metal substrates from harsh environments may be essential so that durability, toughness, adhesion and resistance to chemicals or solvents become very important. Hence coatings based on cross-linked network polymers are widely employed. Chemically resistant coatings and marine coatings are examples of applications where the coating has to protect the substrate from harsh environments and where failure of the coating can incur a high economic penalty.

##### (i) Chemically Resistant Coatings

The protection of the ferrous metal used in the fabrication of, for example, pipelines and chemical tanks including those on cargo ships is very important as they may

carry aggressive chemicals or solvents. Chemically resistant coatings<sup>5</sup> are usually formulated for specific uses, as one type of coating cannot be expected to perform well against the wide variety of environments, chemicals or solvents that can be encountered. Coatings may also prevent the contents of the tank or pipeline from becoming contaminated with, for example, iron or rust.

The coating may be formulated so that it is impervious not only to air, oxygen, water or carbon dioxide but to electrons and ions. Restricting the mobility of electrons and ions may be the most important factor in preventing corrosion.<sup>6</sup> As far as possible the coating must be free of imperfections such as pinholes but if they do occur the adhesion of the coating to the substrate must be such that the damage is limited to the area of the imperfection. In general, adhesion and the preparation of the substrate surface are extremely important in industrial coatings. An alternative approach does not rely on the impermeable nature of the coating to prevent corrosion but on the use of pigments that inhibit corrosion in a primer coating. Generally inert coatings are used for structures which are subject to continual wetting or immersion where mechanical damage is unlikely to occur, as for example, in the interior of chemical tanks. Inhibitive coatings are used on structures which may be subject to weathering, high humidity or chemical fumes such as the exterior of chemical storage tanks.

The binders used in chemically resistant coatings are of four types:

- (a) Soluble polymers such as chlorinated rubbers or vinyl chloride-vinyl acetate copolymers. The polymer is dissolved in a suitable solvent in which other insoluble additives such as pigments are dispersed.
- (b) Cross-linked networks produced by the *in situ* reaction of two reagents. Epoxy resins cured with amine or amide compounds and the formation of polyurethane networks are examples of co-reacting systems. Solvents are generally used in such systems and although the cross-linking polymerization may proceed at ambient temperatures, heat may be required to give a high degree of cure.
- (c) Cross-linked networks produced by heating the resin with or without a curing agent. Examples of this type of coating include those based on phenol-formaldehyde resins either alone or in conjunction with epoxy resins, and epoxy powder coatings.
- (d) Inorganic binders such as zinc silicates. These coatings are formed by reacting an alkali metal silicate or hydrolysed ethylsilicate with metallic zinc to form a zinc silicate matrix surrounding particles of zinc.

Each of the above coatings system has its advantages and disadvantages but epoxy resins cured with polyfunctional amines or amides have the widest range of desirable properties and have been used very successfully in chemically resistant coatings.

(ii) Marine Coatings

Any unprotected metal such as steel, on ships or static structures, exposed to a marine environment will be rapidly subject to corrosion.<sup>7</sup> Surface coatings alone may

not provide total protection so that a combination of coating and electrical methods are used to prevent corrosion. The latter method involves placing an electrical charge on the object to be protected, preventing the electrochemical processes associated with corrosion from occurring. The coatings most widely used in marine environments tend to be of the co-reacting type, that is epoxy resins, coal-tar epoxies and polyurethanes. Again surface preparation of the substrate is very important so that the first coat adheres well to the substrate.

One of the undesirable consequences of immersion in a marine environment is the growth or attachment of marine organisms (animals and plants) to the structure. This is known as fouling and when it occurs on the hull of a ship it causes an increase in fuel consumption by increasing the frictional resistance to motion. On static structures, fouling may damage protective coatings and prevents proper inspection of the structure for fatigue or corrosion. Preventing the growth of these organisms is thus of considerable practical importance.

Fouling may be eliminated or reduced by the use of special paints that contain biocides of low water solubility capable of killing the organisms. Protecting the hull of a ship below the waterline usually involves a coating of impermeable or corrosion inhibitive primer followed by one or two coats of an anti-fouling paint which may continually release biocide in one of three ways.

The first approach involves formulating the coating so that the particles of biocide such as copper (I) oxide are in virtually continuous contact. As the biocide is leached

from the surface of the coating, water is able to penetrate into the bulk of the coating and leach out biocide, since the particles of biocide are in continuous contact. However the effectiveness of this type of anti-fouling paint does diminish with time. The second approach involves using a resin binder that is slightly soluble in sea water. As the binder slowly dissolves, a fresh surface containing biocide is continually exposed. Rosin, a natural resin obtained as a by-product from the timber industry, is commonly used as the binder in this type of anti-fouling paint. A third type of anti-fouling paint has been developed in which the binder is a polymer or copolymer containing an organo-tin moiety attached by an ester linkage to the polymer chain. On exposure to slightly alkaline water, the tin ester links are hydrolysed releasing the organo-tin biocide, leaving the polymer as a polyacrylate salt which slowly dissolves exposing fresh polymer. An added advantage of the latter two systems is the preferential removal of binder from high spots on the surface profile that protrude into the region of turbulent flow adjacent to the surface. The result is a decrease in the surface roughness of the coating. Thus viscous drag by fouling is prevented and as the surface of the coating becomes smoother with increased service, viscous drag is further reduced resulting in an additional saving of fuel.

## 1.2 Reasons for the Interest in the Photoinitiated Cure of Resins

In the late nineteen sixties there was growing concern about the environmental effects of the emission of organic solvents, particularly aromatic solvents, from industrial pro-

cesses such as surface coatings and printing inks. In America this concern led to legislation and severe restrictions on the amount and nature of solvents discharged into the atmosphere. Eliminating the use of solvents in surface coatings and printing inks is also economically desirable and reduces health and fire hazards.

The requirement for solvent free coatings gave impetus to the study and development of the photoinitiated cross-linking of resins, particularly to the development of new photoinitiators. Other potential advantages associated with the photocuring of resins are the energy efficiency of such systems since the heating stage required for some conventional coatings might not be necessary, the efficient cure of coatings on heat sensitive substrates, and the possibility of using one pack systems. The potential for eliminating the need for solvents in coatings is not now a prime reason for the use of photocurable systems.<sup>8,9</sup> Generally, where solvent free coatings have been required the use of high solids or water based coatings has predominated due to their similarity to the conventional solvent based systems. However there is continued interest in photocuring systems because of the quality of the coatings produced such as improved gloss and the rapidity of the curing process which contributes greatly to the cost effectiveness of such systems.

### 1.3 Objectives of the Work Reported in this Thesis

The work reported in this thesis is a result of a case project carried out in conjunction with Camrex (Holdings) Ltd.

The initial objectives were to investigate the factors affecting the photoinitiated cross-linking of commercially available epoxy resins and the properties of the cured resins relevant to the potential use of such systems as surface coatings. Although the work was carried out with a view to the use of the photocuring systems in the general area of industrial coatings, one of the applications of particular interest initially was their use as chemically resistant marine tank coatings.

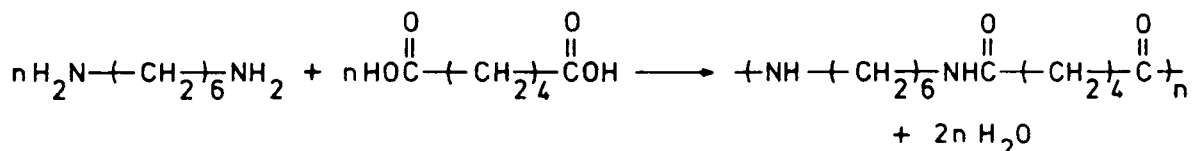
The project developed to include investigations into the effect of the photocuring process on the photostability of the cured systems and the transient colouration observed in certain resins when photocationically cured. Attempts were also made to prepare cured films with fluorinated surfaces. This involved the synthesis of fluorinated epoxides that were then added in small amounts to commercial resins in the hope that they would migrate to the surface prior to cure. The use of small amounts of material containing fluorine would not make such coatings expensive yet they would have the desirable surface properties of fluorinated polymers.

#### 1.4 Classification of Polymerization Reactions

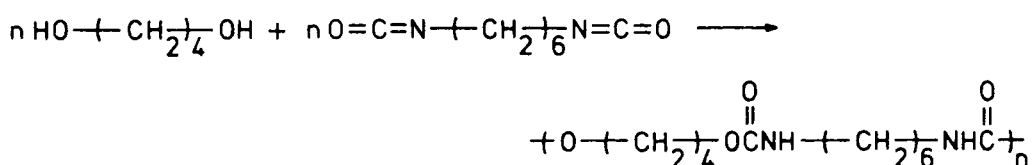
Polymerization reactions and the polymers formed were classified by Carothers as either condensation or addition depending on the mechanism of monomer reaction. Classification by this method is somewhat limited and has led polymerization reactions to be further classified on the basis of the mechanism by which the growth of polymer chains occurs.<sup>10,11</sup> The two possible mechanisms are step-growth and chain-growth.

(A) Step-Growth Polymerizations

The majority of condensation polymerizations proceed *via* a step-growth mechanism. A characteristic of condensation polymerizations is the elimination of a small molecule such as water from each reaction of a monomer molecule. An example of this type of polymerization is the formation of nylon 6,6 from hexanedioic acid and 1,6-diaminohexane:



An example of a step-growth polymerization that is also an addition polymerization is the formation of a polyurethane from a diol and a diisocyanate:



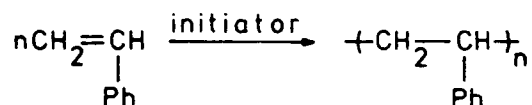
The cross-linking of epoxy resins using amine and acid anhydride curing agents proceeds *via* a step-growth addition mechanism.

The monomer molecules react in discrete steps with each other or with either end of a polymer chain. As a result, the rate of growth of polymer chains is slow and a wide distribution of chain lengths occurs. Polymer with a high number-average degree of polymerization,  $\overline{\text{DP}}_n$ , is only formed at high conversions of monomer functionality and can be difficult to obtain by such polymerizations.  $\overline{\text{DP}}_n$  is the average number of repeat units per polymer chain.

(B) Chain-Growth Polymerizations

Addition polymers are characterized by the repeat unit having the same molecular weight as the monomer and tend to be formed by a chain-growth mechanism although there are a

number of exceptions. The polymerization of alkenes such as styrene proceeds by a chain-growth mechanism to give an addition polymer:



A whole range of useful addition polymers may be prepared from monosubstituted alkenes.

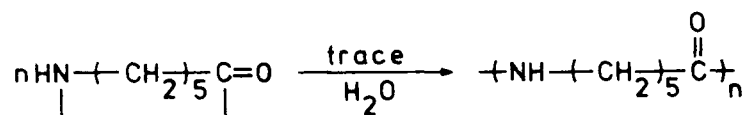
Three distinct reactions occur in chain-growth polymerizations unlike step-growth polymerizations where there is only one type of reaction. Initiation, propagation and termination are the three reactions. Initiation involves adding or generating *in situ* a species that reacts with a monomer molecule to produce an active centre. Propagation or growth of a polymer chain proceeds by the repeated reaction of a monomer with an active centre located at the end of the chain. The reactive species may be free radical, cationic, anionic or organometallic in nature. Since high average molecular weight polymer is rapidly formed, the polymerization mixture mainly consists of monomer and long chain polymer at any time. As the reaction proceeds, the amount of monomer present steadily decreases and the yield of polymer increases but the  $\overline{DP}_n$  of this material does not increase significantly. Under certain conditions, the termination processes that kill the growth of polymer chains can be eliminated giving rise to living polymerizations.

Problems in obtaining high molecular weight polymer can arise in chain-growth polymerizations due to the occurrence of transfer processes, in which, for example, the 'reactive species' is transferred from a growing polymer chain to a monomer molecule.

Growth of a new polymer chain then occurs from this monomer molecule.

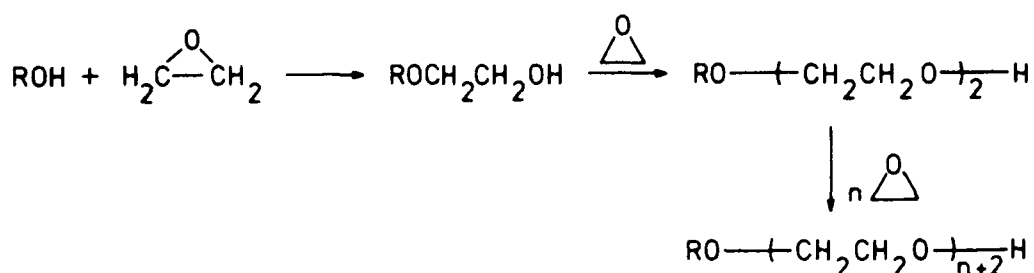
(C) Ring-Opening Polymerizations

Ring-opening polymerizations can be used to prepare polymers identical to those produced by condensation polymerization of non-cyclic monomers. Generally a compound is required to initiate the ring-opening polymerization. For example, caprolactam polymerizes in the presence of a small amount of water to yield nylon 6, which could be regarded as the condensation product of 6-aminohexanoic acid:



Polymer chain formation in this type of polymerization appears to be intermediate in character between step-growth and chain-growth.<sup>11</sup> Such polymerizations resemble step-growth polymerizations in that the  $\overline{DP}_n$  of the polymer formed generally increases as the reaction proceeds which is a consequence of the initiation and propagation steps being similar in rate and mechanism. However, like chain-growth polymerizations, monomer addition occurs exclusively to chain molecules and the yield of polymer increases as the reaction progresses.

The homopolymerization of epoxides such as oxirane may be initiated by, for example, alcohols or thiols and is catalysed by acid or base, *e.g.*



The growth of the polymer chains proceeds by a mechanism similar to that above. The cationic ring-opening homopolymerization of epoxides however proceeds by a chain-growth mechanism.

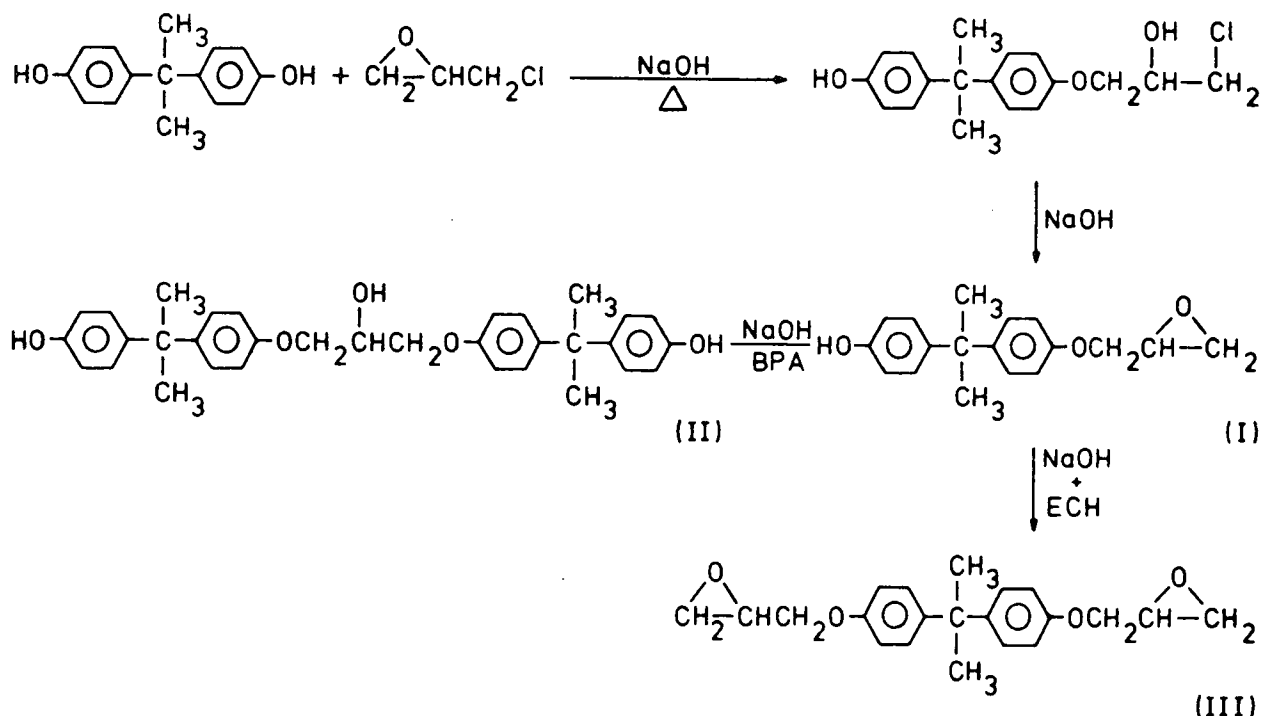
### 1.5 Epoxy Resins

When cured, commercial epoxy resins generally have good overall properties such as thermal stability, solvent and chemical resistance, mechanical strength, flexibility and adhesion.<sup>12,13,14</sup> The ability of epoxy resins to readily undergo photocationic cure combined with the potentially good properties of the cured resins were the reasons for their choice as the monomers to be used in this study.

#### (A) Synthesis of Epoxy Resins

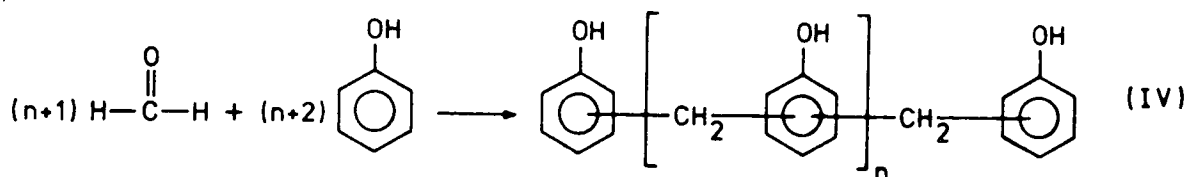
The first commercially developed and still the most widely used epoxy resins are those based on the reaction of epichlorohydrin, ECH, (chloromethyl oxirane) and bisphenol A, BPA, (4,4'-(1-methylethylidene)bisphenol). The main reasons for the development, which occurred in the early nineteen forties, and continued success of these resins are the cheapness and availability of bisphenol A and the properties of the resins when cured by a variety of cross-linking agents.

The reaction between BPA and ECH is shown overleaf.<sup>12</sup> The intermediate (I) can react with BPA to yield higher molecular weight diphenols (II) which will give rise to higher molecular weight resins containing secondary hydroxyl groups.

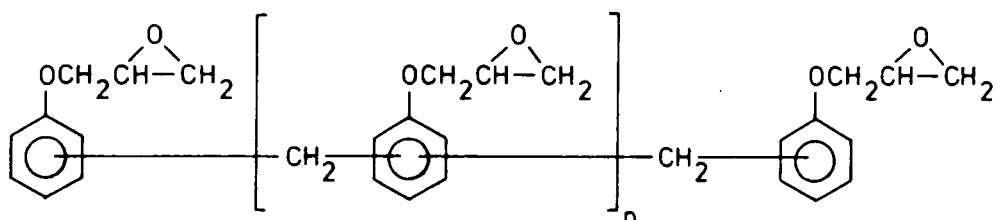


Alternatively (I) can react with ECH to produce the simple diglycidyl ether of bisphenol A, DGEBA, (2,2'-[[1-methylethylidene)bis(4,1-phenyleneoxymethylene)]bis oxirane), (III). Using a ratio of ECH to BPA of 10:1 greatly increases the yield of (III) but small amounts of the higher molecular weight material will still be produced.

Epoxy novolac resins provide greater cross-link density when cured because of the increased number of epoxide rings per resin molecule. Resins of this type are prepared from the reaction of polyhydroxy phenolic compounds, (IV), and ECH. Compounds such as (IV) are obtained from the acid catalysed condensation reaction of phenol and formaldehyde:



The methylene groups link the aromatic rings *via* the *ortho* or *para* positions. Reaction of compounds such as (IV) with epichlorohydrin, yields resins of the following general structure:



When  $n=0$ , (IV) is known as bisphenol F but  $n$  may be as high as three.

Epoxy resins based on bisphenol A are produced in the greatest amounts but other types of epoxy resins in addition to epoxy novolacs are commercially available for specialist use or as reactive diluents.<sup>12</sup> Table 1.1 shows some examples.

TABLE 1.1 Additional Examples of Commercially Available Epoxy Resins

Type	Example
aliphatic glycidyl ethers	
glycidyl esters	
glycidyl amines	
cycloaliphatic epoxies	

The first three types of resin are usually prepared by reacting the appropriate diol, dicarboxylic acid or amine with epichlorohydrin. Cycloaliphatic epoxies are prepared by

oxidation of the double bonds of the corresponding alkenes using peracids. The use of this latter type of resin in surface coatings used to prevent corrosion may become important, since they have a low ionic impurity content.

#### (B) Conventional Cure of Epoxy Resins

The conversion of an epoxy resin to an insoluble, three-dimensional network polymer is brought about by the use of a chemically active compound known as a curing agent. To obtain a cross-linked polymer, the resin and curing agent must have a combined functionality greater than or equal to five. For example the resin could be difunctional and the curing agent trifunctional or *vice versa*. The characteristics and properties of the cured resin will be dependant upon the structure of the cross-linked network. Hence the extent of reaction of functional groups, the density of cross-links, the structure of the resin between cross-links and the nature of the curing agent employed will affect the properties of the cured resin. The choice of resins and curing agents available gives a wide spectrum of possible properties, ranging from highly flexible, rubber-like films to hard or brittle films. This range of accessible properties has contributed greatly to the extensive use of epoxy resin systems in a variety of applications.

Generally curing agents will react with epoxy resins under ambient conditions which necessitates the use of two pack systems. The resin and curing agent are supplied separately and only mixed prior to application. Three classes of compound widely used as curing agents are polyfunctional amines and amides, acid anhydrides and tertiary amines.<sup>12,13</sup> Polyfunctional isocyanates are also used to cure epoxy resins but



act as latent initiators activated in the presence of moisture:

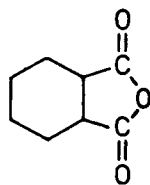


Aromatic primary and secondary amines are also used as curing agents. The chemistry of the cross-linking reaction is similar to that of aliphatic amines but as the amine groups are less basic, higher temperatures are required for efficient cure if accelerators are not used.

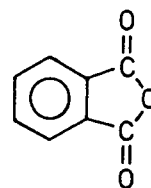
The polyfunctional amides used as curing agents are complex mixtures containing enough free amine hydrogens to react in a similar manner to amine curing agents.

(ii) Acid Anhydride Curing Agents

Two examples of this class of widely used curing agent are:

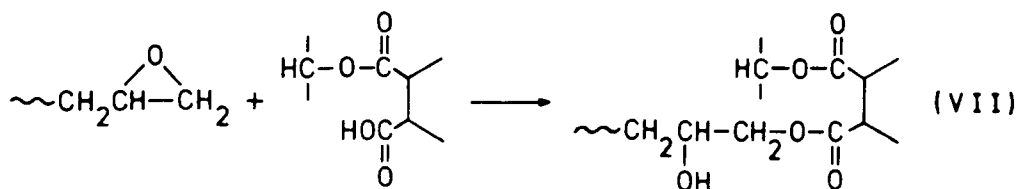
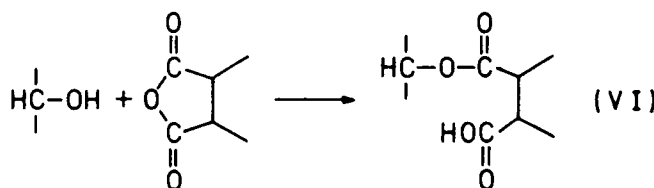


hexahydrophthalic anhydride



phthalic anhydride

Three processes may occur in the reaction of acid anhydrides with epoxy resins:





(iv) Polyfunctional Isocyanate Curing Agents

This class of curing agents do not react with the oxirane ring of epoxy resins but with hydroxyl groups on the resin molecule. Rapid reaction between the secondary hydroxyl groups of high molecular weight DGEBA resins and isocyanate groups occurs at or below room temperature to yield polymers with useful properties for surface coatings. Two disadvantages of using this type of system are the toxicity of the isocyanate curing agents and the constituents of the coating system must be as moisture free as possible.

1.6 Cationic Ring-Opening Polymerizations of Epoxide Compounds

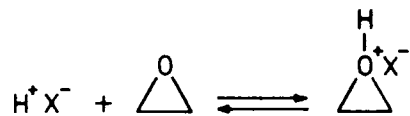
Cross-linking of epoxy resins by a step-growth mechanism can be rather slow at ambient temperatures. A chain-growth mechanism of cross-linking however offers the possibility of rapid network formation at ambient and low temperatures. Chain-growth polymerization of epoxides may proceed *via* a cationic or an anionic propagating species. Polymerization *via* a cationic species tends to be more rapid and more effective. As with all polymerizations of epoxide compounds the main thermodynamic driving force is the release of strain on opening the three-membered ring.<sup>15</sup>

(A) Initiation

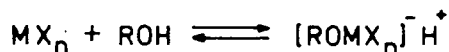
The initiation of cationic polymerization of cyclic ethers involves adding or generating *in situ* a species that reacts with a monomer molecule to form a cyclic oxonium ion which can react with another monomer molecule. Quite a large number of compounds are known to initiate the cationic polymerization of

cyclic ethers,<sup>16,17</sup> these include:

(a) Protonic acids with weakly nucleophilic anions such as  $\text{HFeCl}_4$ ,  $\text{HBF}_4$ ,  $\text{HSO}_3\text{F}$  and  $\text{HClO}_4$ . Initiators of this type act by protonating the oxygen atom of the ring:



(b) Friedel-Crafts catalysts such as  $\text{BF}_3$ ,  $\text{AlCl}_3$ ,  $\text{PF}_5$  and  $\text{SbCl}_5$ . Generally a co-initiator is used with such initiators but there is some confusion as to whether a co-initiator is essential for the initiation of polymerization. In many cases the mechanism of initiation is not clear. Water or alcohols are commonly used as co-initiators and the species responsible for initiation is considered to be a proton.



(c) Organometallic initiators such as triethyl aluminium may be used to initiate ring-opening polymerization of epoxides and are thought to do so by a cationic mechanism in certain cases. The mechanism of initiation and the use of triethyl aluminium is described in more detail in Chapter Six.

## (B) Propagation

Propagation is the reaction of monomer with the cationic species formed by the initiation step, giving rise to polymer chains. Reaction of the epoxide monomer with the cationic species at the chain end may proceed by an  $\text{S}_{\text{N}}1$  or  $\text{S}_{\text{N}}2$  type mechanism:



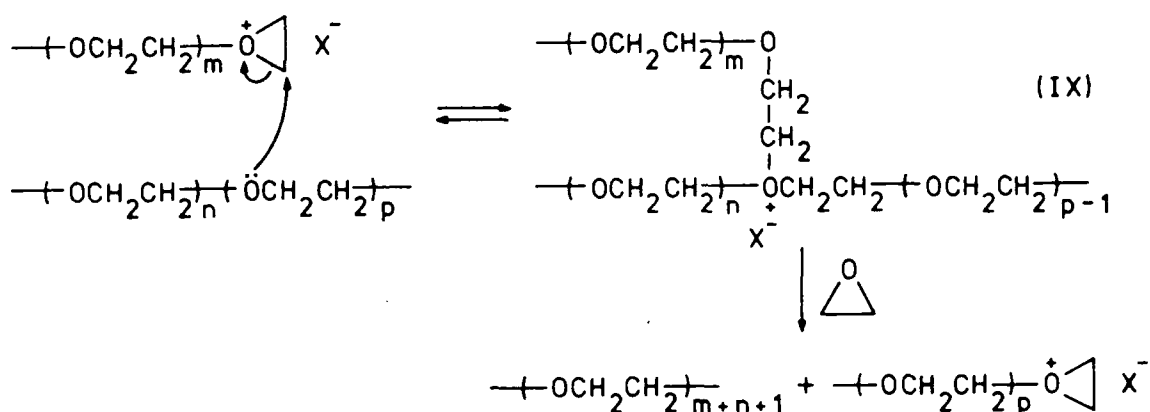
Since the propagating species is ionic, the dielectric constant of the reaction mixture and the nature of the anion should affect the rate of propagation. In the cationic polymerization of styrene increasing the dielectric constant of the solvent used increases the rate of propagation presumably due to a greater separation of the ion pairs.<sup>20</sup> However this effect does not occur with every alkene monomer. It has also been found that smaller, more tightly bound anions lead to a reduction in the rate of propagation and that free cations react faster than ion pairs. Solvent and anion effects on the rate of propagation for cyclic ethers are more complex probably because the monomers can participate in solvation of the charged species. Evidence has been obtained from the polymerization of tetrahydrofuran, THF, showing that the rate of propagation decreases slightly with increasing dielectric constant of the system.<sup>21</sup> Results from a study of the polymerization of the above monomer with anions such as  $\text{AsF}_6^-$ ,  $\text{PF}_6^-$ ,  $\text{CF}_3\text{SO}_3^-$ ,  $\text{SbF}_6^-$  and  $\text{FSO}_3^-$  present, indicate that the nature of the anion has little or no effect on the rate of propagation.<sup>22,23</sup> Also it has been found that the rate of propagation for a free cation and an ion pair are very similar.<sup>23,24</sup> These observations from the polymerization of THF may not necessarily apply to the polymerization of the less basic epoxide monomers.

### (C) Chain-Transfer and Termination Processes

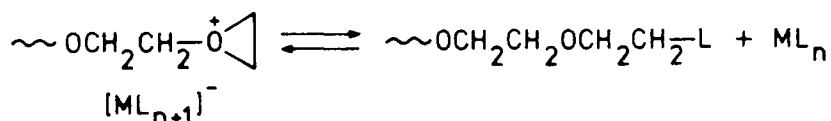
Generally there are many chain-transfer reactions possible in cationic polymerizations leading to the formation of low molecular weight polymers. Ring-opening cationic polymerizations of cyclic ethers suffer from this problem<sup>17</sup> even though



formation appears to be favoured,<sup>17,19</sup> but even with a methyl substituent present cyclic tetramer is formed in significant amounts.<sup>26</sup> Chain-transfer involving polymer chains can also occur intermolecularly,<sup>17</sup> as shown below.



Termination occurs if the oxonium ions (VIII) and (IX) are stable. Other causes of termination are reaction with a nucleophilic or basic impurity. Reaction with the anion may also lead to termination:<sup>17</sup>



#### (D) Effect of Temperature on the Rate of Polymerization

Understanding how both temperature and solvent affect the overall rate of cationic polymerizations is made difficult because of the numerous equilibria that may occur. In the cationic polymerization of a number of monomers, a decrease in temperature results in an increase in the rate of polymerization. This observation may be rationalised by considering the energetics of the initiation, propagation and termination reactions.<sup>20</sup> The overall rate of polymerization,  $k_o$ , is given by the expression,

$$k_o = k_i k_p / k_t$$

where  $k_i$ ,  $k_p$  and  $k_t$  are the rates of the initiation, propaga-

ation and termination steps respectively. The overall activation energy of polymerization is then given by the following expression:

$$E_o = E_i + E_p - E_t.$$

The activation energy of propagation is generally quite low, lower than  $E_i$  or  $E_t$  which tends to make  $E_o$  negative or slightly positive. When  $E_o$  has a negative value then decreasing the temperature results in an increase in the rate of polymerization. If  $E_o$  is positive then decreasing the temperature has the opposite effect.

The observation that the rate of polymerization increases with decreasing temperature can also be a consequence of an equilibrium between monomer or oligomer and polymer which gives rise to the ceiling temperature effect.<sup>27</sup> Thermodynamic considerations show that above a certain temperature, long chain polymer will not form. Reducing the temperature below this ceiling temperature however, results in a shift in the equilibrium and the formation of polymer occurs. This effect tends to be prevalent in the ring-opening polymerization of five, six and seven-membered rings but may account for the effect of temperature on the polymerization of oxirane where an equilibrium between polymer and cyclic dimer occurs.<sup>24</sup>

The temperature at which the reaction is carried out will affect the chain length of the polymer produced.<sup>20</sup> For example if the activation energy for chain-transfer is greater than that for propagation, which seems to be the case, an increase in temperature will result in a greater increase in the rate of chain transfer than of propagation. Polymer of lower average degree of polymerization will then result at higher temperatures.

In general, the commercial usefulness of cationic polymerizations is limited by the occurrence of chain-transfer processes. Even though the properties of a network polymer do not strictly depend on the attainment of high molecular weight material, the occurrence of chain transfer could have a deleterious effect on the course of chain cross-linking polymerizations.

### 1.7 Non-Linear Polymerizations

If a difunctional monomer is polymerized, then linear polymer chains are produced. Usually the polymer is soluble, regardless of the extent to which the monomer functional groups have reacted. Polymerization of certain monomers results in the formation of an insoluble, infusible product at a certain point in the reaction; the phenomenon is called gelation. This apparently sharp point is nearly always a characteristic of the use of a monomer or comonomer with a functionality greater than or equal to three as in the cure of epoxy resins. Gelation also occurs when polymer chains are cross-linked as in for example the vulcanization of rubber.

Carothers recognised that, for monomers with a functionality of three or more growth of polymer molecules can occur in three dimensions rather than one as for difunctional monomers.<sup>28</sup> This results in the formation of polymer molecules with complex structures. From his studies of step-growth condensation polymerizations Carothers derived an expression relating the extent of reaction,  $P$ , of functional groups, to the functionality of the monomer,  $f$ , and the  $\overline{DP}_n$  of the polymer produced:<sup>29</sup>

$$P = \frac{2}{f} - \frac{2}{\overline{DP}_n \cdot f} \quad (1)$$

For a difunctional monomer,  $f$  is two and the equation reduces to its simplest form namely:

$$P = 1 - \frac{1}{\overline{DP}_n} \quad (2)$$

In deriving equation (1) Carothers assumed that intramolecular reaction, that is reaction between functional groups on the same polymer molecule, did not occur. The gel point was assumed to be related to the formation of an infinitely large molecule which would occur as  $\overline{DP}_n$  approached an infinite value. This would give a value of  $P$  at the gel point equal to  $2/f$ . Carothers did note however that this value of  $P$  could be regarded as a maximum value for gelation to occur. The assumption that  $\overline{DP}_n$  is infinite at the gel point was later shown by Flory to be incorrect but the point at which  $P$  is equal to  $2/f$  is important as it represents the stage in the polymerization when a single molecule is formed. Any subsequent increases in  $P$  must then result from intramolecular reaction.

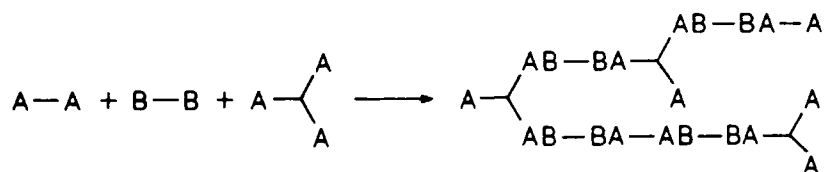
(A) The Flory-Stockmayer Theory of Non-Linear Polymerizations

Flory<sup>30</sup> agreed with the assertion made by Carothers that gelation was due to the unlimited growth of polymer molecules in three dimensions. Ultimately the size of one molecule approaches that of the container which is infinite on a molecular scale. It was noted that the main characteristic of such polymerizations was the occurrence of the gel point at a particular extent of reaction, independent of temperature, solvent or the presence of any catalyst. Gelation, it was also noted, occurred before all the monomer was bound into one molecule, indicating that smaller molecules of varying complexity

must be distributed throughout the gel. This material, known as the sol fraction, can be extracted by solvent.

Flory was the first to apply the statistical theory of probability to non-linear step-growth polymerizations<sup>11,30</sup> as he had done previously to linear step-growth polymerizations. To greatly simplify this approach, two assumptions were made. The first was that intramolecular reaction did not occur or was at least restricted to the gel phase giving rise to a network structure.<sup>31</sup> Secondly it was assumed that the reactivity of a functional group was independent of the number or configuration of other functional groups in the polymer molecule.

Considering the following type of polymerization,



where only A and B groups may react together, Flory derived equation 3:

$$\alpha = rP_A^2 \rho / [1 - rP_A^2 (1 - \rho)] = P_B^2 \rho / [r - P_B^2 (1 - \rho)] \quad (3)$$

The quantity  $\alpha$  is the probability that the functional group of a branch unit chosen at random leads to another branch unit. This is related to the extent of reaction,  $P$ , of A or B groups, the ratio of A groups on branch units to the total number of A groups,  $\rho$ , and the ratio of A to B groups,  $r$ . An expression was also derived relating  $\overline{DP}_n$  to the same three parameters. The value of  $\alpha$  necessary for the formation of an infinitely large molecule was deduced by the following reasoning. The probability that one of the  $(f-1)$  new chains emanating from an  $f$ -functional branch unit leads to another branch

unit is  $\alpha(f-1)$ . For the molecule to be infinite this probability must be equal to one. Therefore the critical branching probability  $\alpha_c$  is equal to  $1/(f-1)$  and when  $\alpha$  exceeds  $\alpha_c$  by a small amount, gelation occurs.

Flory carried out polymerizations of the above type measuring the extent of reaction up to the gel point, allowing  $\overline{DP}_n$  to be calculated. Also the viscosity of the polymerization mixture was measured which gave an indication of how the weight-average degree of polymerization,  $\overline{DP}_w$ , increased as the polymerization progressed. As had been noted previously for non-linear polymerizations, the viscosity increased slowly at first but as the gel point approached rose rapidly to become infinite. In contrast, the number-average degree of polymerization increased slightly as the conversion of monomer increased but was still relatively small at the gel point, reflecting the large number of species present. The expected value of  $P$  at the gel point was calculated from the critical value of  $\alpha$  using equation (3) and compared with the experimental value. It was found that the observed value of  $P$  was always greater than the calculated value, even allowing for the unequal reactivity of functional groups in the polymerization of certain monomers. This discrepancy between the two values of  $P$  could be accounted for by the occurrence of intramolecular reaction which would increase the critical extent of reaction since functional groups would react without producing any increase in the size of the polymer molecules.

Applying a more mathematical approach than Flory, but using identical assumptions, Stockmayer derived distribution functions for a number of types of non-linear step-growth

polymerizations.<sup>32</sup> The simplest of these is one where the monomer molecules possess the same number of functional groups with equal probability of reaction. Hence the branching coefficient  $\alpha$  is simply equivalent to the extent of reaction  $P$ . It is worth noting that in such a polymerization Flory would predict a value of  $\frac{1}{2}$  for  $P$  at the gel point whereas Carothers would predict a value of  $\frac{2}{3}$ , for a trifunctional monomer. Stockmayer derived an expression for the weight distribution of  $x$ -mers in a polymerization of this type showing that on a weight basis, monomer is present in the greatest amount up to the gel point. This is in contrast to linear step-growth polymerizations where the amount of monomer present rapidly diminishes as the reaction progresses. Expressions were also derived for  $\overline{DP}_n$  and  $\overline{DP}_w$ . The expression for the former was identical to that derived by Carothers, whilst that for the latter is shown below.

$$\overline{DP}_w = (1+\alpha)/[1-(f-1)\alpha]. \quad (4)$$

As expected, equation (4) shows that  $\overline{DP}_w$  becomes infinitely large as the gel point approaches.

Both Flory<sup>31</sup> and Stockmayer<sup>32</sup> derived expressions for the weight fraction of sol as a function of the extent of reaction in the polymerization of trifunctional monomers. The two expressions showed that the amount of sol would decrease as the extent of reaction increased, but in different ways. This difference between the two expressions was said by Stockmayer to be due to Flory's method inadvertently including intramolecular reaction which probably makes Flory's expression more relevant to real polymerizations.

Expressions have been derived that predict the occurrence of the gel point at a particular extent of reaction in the cross-linking of polymer chains and in the chain-growth copolymerization of difunctional vinyl and tetrafunctional divinyl monomers.<sup>33</sup> The latter system may be treated in a similar manner to the former system, if it is viewed as the cross-linking of primary polymer chains of weight average degree of polymerization,  $\overline{DP}_{w_0}$ . These primary chains are thought of as resulting from the severing of all the cross-links by, for example, chemical cleavage. The extent of reaction of vinyl groups  $P_c$  at the gel point is given by the expression

$$P_c = \frac{1}{\rho(\overline{DP}_{w_0} - 1)} \approx \frac{1}{\rho\overline{DP}_{w_0}} \quad (5)$$

The quantity  $\rho$  is the ratio of double bonds on the divinyl units to the total number of double bonds. Two of the assumptions made in deriving equation (5) are identical to those made for step-growth polymerizations whilst one further assumption is that at any time the fraction of material involved in the growth of chains is negligible in comparison to the amount of monomer and stable polymer. If the rates of all steps in the polymerization are independent of  $\rho$  then  $\overline{DP}_{w_0}$  is equivalent to the weight-average degree of polymerization of a polymer prepared from the pure monovinyl monomer under identical conditions.

(B) The Application of Cascade Theory to Non-Linear Polymerizations

The statistical theory of cascade processes was first applied to non-linear polymerizations by Gordon.<sup>34</sup> One of

the advantages of using cascade theory is that equations for various parameters, by which physical properties of the non-linear polymers are expressed, can be derived. However the derivation and manipulation of the equations used in this approach is quite complex. Again intramolecular reaction is assumed not to occur in the simplest approach and the resulting macromolecules are treated as tree-like structures.

Application of the theory to the simple step-growth polymerization of a trifunctional monomer gave similar expressions to those derived previously, the expression for the weight fraction of the sol being identical to that derived by Flory.<sup>34</sup> Good, who had originally developed the theory of cascade processes, also investigated simple polymerizations of  $f$ -functional monomers using cascade theory.<sup>35</sup> Expressions relating the weight fraction and the  $\overline{DP}_w$  of the sol fraction to the extent of reaction for tri- and tetrafunctional monomers were obtained. The theoretical treatment of polymerizations such as the copolymerization of hexanedioic acid and glycerol where the secondary hydroxyl groups of glycerol have different reactivities is made easier using cascade theory.<sup>34</sup> An identical expression to that obtained by Stockmayer for vinyl-divinyl copolymerizations<sup>34</sup> was obtained by the application of cascade theory to such polymerizations.

The applicability of cascade theory to real non-linear polymerizations was greatly enhanced when it was shown that a first shell substitution effect can be taken into account.<sup>36</sup> Such an effect occurs when the ease of making or breaking a link between two monomer molecules is dependent on the number of other links the two molecules have formed. The effect of

this non-random behaviour was investigated for irreversible and reversible bond formation. In both cases it was shown that the value of  $\alpha_c$  increased when the reactivity of functional groups was reduced and the value of  $\alpha_c$  decreased when the opposite occurred.

Cascade theory has been applied to the step-growth addition polymerization of epoxy resins with amine curing agents.<sup>37</sup> Expressions for molecular weight averages, the distribution of sol and gel fractions and the critical condition for gelation were derived as a function of the extent of reaction. It was assumed that no cyclization occurred and that a first shell substitution effect operated for the reaction of amine groups. The theoretically determined expressions were compared with experimental results for a DGEBA-hexamethylenediamine system.<sup>38</sup> Reasonable agreement was found indicating that the assumptions made and the application of cascade theory were valid.

The versatility of the application of cascade theory to non-linear polymerizations is exemplified by the range of systems to which it has been applied. These include the formation of elastic networks,<sup>39</sup> the cross-linking of polymer chains,<sup>40</sup> and chain-growth cross-linking polymerizations<sup>41,42</sup> as well as those systems mentioned above. Expressions for radii of gyration and other statistical parameters describing molecular dimensions have been derived for various systems.<sup>43</sup> Attempts to simplify the calculation of average properties of non-linear polymers by using a similar approach to cascade theory have been reported, the aim being to simplify the mathematics yet retain the versatility of cascade theory.<sup>44,45</sup>

(C) Intramolecular Reaction and Cyclization

Neglecting or limiting the occurrence of intramolecular reaction to the gel fraction as in the above approaches results in discrepancies between the calculated and observed values of the branching coefficient or extent of reaction at the gel point. Consideration of the space available for the growth of the infinite molecule after gelation leads to the conclusion that steric hindrance must result in intramolecular reaction in the gel fraction.<sup>46</sup> Unimolecular cyclization reactions are important, even prior to the gel point since their occurrence can affect the physical properties of the gel. For example it has been found that the glass transition temperature of a polyurethane gel decreases with increasing intramolecular reaction prior to the gel point.<sup>47</sup>

Stockmayer and Weil reported in 1945 that the extent of reaction at the gel point was directly proportional to the concentration of the polymerizing species in a step-growth polymerization. Extrapolation to zero dilution yielded values of  $P_c$  in agreement with theory. Intramolecular reaction arises from the segmental mobility of polymer molecules and is in competition with translational motion which leads to collision between polymer molecules and hence intermolecular reaction. Hence increasing the dilution results in a decrease in the frequency of collisions between molecules which will increase the probability of intramolecular reaction and raise the extent of reaction at the gel point.

The first theoretical approach to intramolecular reaction was made by Jacobson and Stockmayer for ring-chain equilibria in reversible linear polymerizations.<sup>48</sup> One of the main

postulates of this theory is that the probability of intramolecular reaction is determined by the frequency with which the chain ends coincide within a certain volume. Using Gaussian random flight statistics to determine the probability of the chain ends occurring within a certain volume gives rise to equation (6), for the reversible polymerization of a difunctional monomer such as dimethylsilanol.

$$\text{Concentration of } i\text{-mer rings } R_i = \left(\frac{3}{2\pi v}\right)^{3/2} \frac{(P')^i}{2i^{5/2} b^3} \quad (6)$$

where  $P'$  = the extent of reaction in the chain fraction

$v$  = the number of chain atoms per monomer unit

$b$  = the effective bond length for a chain molecule.

Ring formation is thus dependent on dilution and the structural features of the monomer such as the distance between functional groups and its flexibility. Comparison of a modified expression of the above form with experimental results<sup>49</sup> gave good agreement especially for the formation of larger rings.<sup>50</sup> This approach to intramolecular reaction provided the basis for the development of theories describing ring formation in linear, irreversible polymerizations. The further development of such theories for non-linear polymerizations has been reviewed recently.<sup>51</sup> Cyclization is however difficult to treat in non-linear polymerizations due to the number of functional groups available for intramolecular reaction, the long-range correlations involved and the effect of initial ring formation on subsequent cyclization.

Stepsto and coworkers studied non-linear step-growth polymerizations of the type  $RA_2 + RB_3$  such as the polymerization of a triol and diisocyanate.<sup>52</sup> These studies were mainly involved with the effect of cyclization on the gel point. In this

approach the difference in the observed and experimental values of the critical branching coefficient  $\alpha_c$  is related to a ring forming parameter  $\lambda$ .<sup>51</sup> An increase in the value of  $\lambda$  indicates a greater extent of intramolecular reaction. Equation (7) shows that this parameter can be related to the structure of the repeat unit, the chain flexibility and the dilution.

$$\lambda = \left( \frac{3}{2\pi\nu b^2} \right) \frac{\phi(1, 3/2)}{N C_{\text{ext}}} \quad (7)$$

$$\phi(1, 3/2) = \sum_{n=1}^{\infty} 1^n n^{-3/2}, \quad n \text{ being the number of units in a ring}$$

$N$  = Avagadro's constant

$C_{\text{ext}}$  = the concentration of functional groups that can react intermolecularly.

As predicted by the above expression, it is found that increasing the dilution or decreasing  $\nu$  by varying the monomer structure results in an increase in  $\lambda$  and hence  $\alpha_c$ . Also it is noted that the probability of intramolecular reaction increases with more flexible chains. Furthermore Stepto noted that the extent of intramolecular reaction should be solvent and temperature dependent since the parameter  $b$  is solvent and temperature dependent.<sup>47</sup> Recent results from a study of the formation of non-linear polyesters indicate that  $\lambda$  is temperature dependent.<sup>54</sup> In this study, increasing the temperature caused an increase in the stiffness of the polymer structure reducing  $\lambda$ .

To gain a better understanding of the effect of cyclization on non-linear polymerizations it is advantageous to obtain data on ring formation throughout the polymerization, not just at the gel point. This can be achieved by determining the number of ring structures per molecule  $N_r$ . Measuring the extent of reaction  $P$  and the number-average molecular weight  $\bar{M}_n$



Unreacted monomer will act as a solvent, diluting the chains formed initially. Hence the probability of reaction between the active centres (\*) at the ends of growing chains with pendant vinyl groups on other chains to produce cross-linking will be reduced. It is therefore expected that in the early stages of chain cross-linking polymerizations intramolecular reaction and ring formation will predominate. As the polymerization proceeds however, monomer will become incorporated into polymer chains and intermolecular reaction will become favoured.

In applying cascade theory to the homopolymerization of divinyl monomers, the formation of the cross-linked polymer is viewed as being equivalent to that resulting from the cross-linking of primary polymer chains. As in the Flory-Stockmayer<sup>33</sup> approach to vinyl-divinyl copolymerizations, these primary chains would be obtained if all the cross-links in the cross-linked polymer were severed. There will be three types of unit present in the primary chains; units that are involved in intermolecular reaction (cross-linking) or intramolecular reaction (cyclization) and units bearing pendant double bonds.

The results of the study indicate:-

- (a) The gel point conversion  $P_c$  increases with decreasing degree of polymerization of the primary chains.
- (b) Increasing the width of the distribution of primary chains increases  $P_c$ .
- (c) Intramolecular reaction results in an increase in  $P_c$ .
- (d) The fraction of units involved in intramolecular reaction at the gel point increases with increasing degree of polymerization of the primary chains.

- (e) Increasing the dilution gives an increase in the amount of intramolecular reaction.

A comparison of the results from this theoretical approach with experimental results from the free radical polymerization of diallylphthalate shows that the model used does predict the same trends as observed experimentally. However a significantly higher extent of reaction at the gel point was observed than that predicted. It is proposed that this discrepancy is due to the inability of the theory to take into account the high degree of intramolecular reaction that occurs initially, and its affect on subsequent cyclization reactions.

(D) Application of Percolation Theory to Non-Linear Polymerizations

From the previous section it is apparent that the Flory-Stockmayer approach to gelation, improved by the application of cascade theory, has some difficulty accommodating intramolecular reaction. Most of the applications of the previous theories have concerned step-growth polymerizations which are easier to treat than chain-growth polymerizations.

A relatively new approach to the phenomenon of gelation is the use of percolation theory.<sup>60</sup> In the simplest percolation model,  $f$ -functional ( $f \geq 3$ ) monomers are distributed on an infinitely large periodic lattice. Bonds are assumed to form randomly between nearest neighbours, and no restrictions are placed on the occurrence of intramolecular reactions. Gelation is taken as the point at which an infinitely large molecule is formed, *i.e.* one that spans the lattice. Step-growth polymerizations may be represented by this random bond percolation model. Figure 1.1 shows an example of percolation

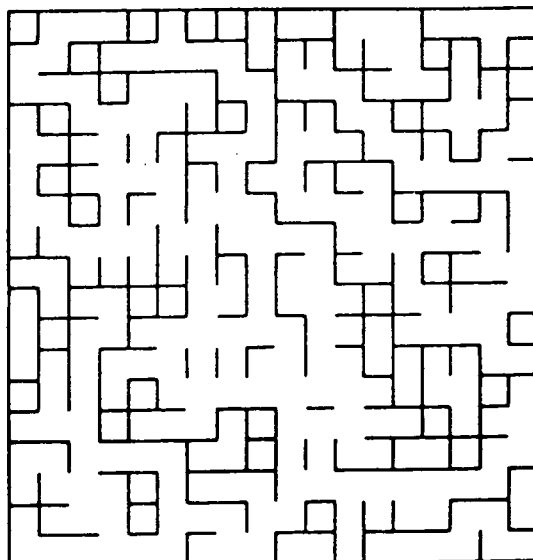


FIGURE 1.1 An Example of a Percolation Model Representing a Non-linear, Step-growth Polymerization

-----

at the gel point for a tetrafunctional monomer on a square lattice.<sup>61</sup> Bonds are represented by lines between the monomer units. As can be seen there are some nearly "infinite" molecules.

The advantages of applying percolation theory to non-linear polymerizations are that it takes into account intramolecular reaction, excluded volume effects and steric hindrance. The lack of molecular motion in simple percolation models is one criticism of their use,<sup>62</sup> another being the use of a fixed lattice but it has been shown that percolation on a lattice is similar to continuum percolation without a lattice.<sup>63</sup> Care must be taken in predicting critical extents of reaction from percolation models as the value obtained will depend on the nature of the lattice used. The development and application of percolation theory in its various forms to gelation in step-growth polymerizations has been reviewed in detail.<sup>61</sup>

Modification of the simple percolation model has allowed non-linear chain-growth polymerizations of the free radical type to be investigated using this technique. To obtain data from such models, a Monte Carlo computer simulation is generally carried out which is similar to a real experiment and allows "snapshots" of a lattice to be produced during the procedure. Simulations are usually carried out on lattices of increasing size and the results extrapolated to an infinite lattice.

Manneville and de Seze were the first to apply percolation theory to chain-growth polymerizations.<sup>64</sup> A model was developed by these two workers to investigate vinyl-divinyl copolymerizations which has provided the basis for subsequent studies. Equally reactive tetrafunctional and difunctional units were distributed randomly over the lattice. Activation of a given concentration of randomly selected units initiates the polymerization. Propagation was carried out by selecting an active centre and one of its first or second nearest neighbours at random. If the neighbouring unit chosen had an unreacted functionality then a bond formed between the two units, the active centre transferred to the neighbour and the process repeated. Termination can take place either by radical-radical combination or by trapping. The former takes place when two active centres are on neighbouring molecules whilst the latter occurs when an active centre is surrounded by fully reacted units. In spite of its simplicity, this model shows that the chain-growth process on a lattice leads to different structures than those predicted for step-growth polymerization using percolation models or the Flory-Stockmayer approach.

Percolation models of chain cross-linking polymerization have been developed further, becoming more complex. The

presence of solvent and, to a limited extent, mobility have been incorporated.<sup>65,66</sup> Using a model containing these features a qualitative investigation of the kinetics of a vinyl-divinyl polymerization have been carried out and the results compared with experimental observations.<sup>66</sup> Solvent molecules were randomly interspersed with tetrafunctional and difunctional monomer molecules on a lattice. Some degree of mobility is achieved by allowing solvent molecules to exchange positions with a nearest neighbour if that nearest neighbour is a solvent or unreacted monomer molecule.

The results show that the rate of reaction and the extent of reaction at the gel point,  $P_c$  are increased by:-

- (a) Increasing the concentration of initiator.
- (b) Decreasing the fraction of tetrafunctional monomer,  $f_t$ .

Increasing the amount of solvent present was found to decrease the rate of reaction but increased the extent of reaction at the gel point. Introducing mobility into the model raised the extent of reaction before trapping took place up to a maximum but then a decrease occurred. This effect is attributed to the lack of mobility of the large polymer molecules. However the inclusion of mobility did not change any of the above trends.

The Flory-Stockmayer approach to vinyl-divinyl copolymerization predicts that  $P_c \propto f_t^{-1}$  whereas results from the above percolation model indicate that  $P_c \propto f_t^{-0.5}$ . In another paper,<sup>67</sup> the same workers noted that in deriving the expression for the extent of reaction at the gel point in vinyl-divinyl copolymerizations, Stockmayer had used the weight average degree of polymerization of primary chains that would occur at the end

of the polymerization.<sup>33</sup> They pointed out that it would be more correct to set the value of  $\overline{DP}_w$  of the primary chains equal to that occurring at the gel point. If this amendment is made, Flory-Stockmayer theory then predicts that  $P_c \propto f_t^{-0.5}$ , in agreement with the percolation model.

Generally, the results from the above model agree qualitatively with experimental observations. The lack of quantitative agreement is hardly surprising in view of the simplicity of the model which as well as only having limited mobility does not take into account processes such as chain transfer or the spontaneous generation of radical species. Similarly termination by radical disproportionation or reaction with impurities is neglected but the prominence of trapping may help to offset this deficiency. In one case at least, however, a relationship predicted by the percolation model has been borne out experimentally. The model predicts that  $v_c \propto f_t^{-0.25}$  where  $v_c$  is the fraction of monomer units at the gel point that have reacted at least once. Results from a study of the copolymerization of acrylamide and N,N'-methylenebis-(acrylamide) give a very similar value for the exponent in the above relationship.<sup>68</sup> This shows that quantitative agreement between results from the percolation model and experimental measurements is possible and is further evidence of the validity of this approach to such polymerizations.

As will become apparent in the following sections, percolation models can be useful in illustrating another aspect of non-linear chain-growth polymerization.

(E) Inhomogeneous Cross-Linking in Network Polymers

(i) Inhomogeneity in Conventionally Cross-Linked Epoxy Resins

One of the first indications of inhomogeneous cure in thermosetting resins was reported in 1936 when de Boer calculated the expected tensile strength of a cured phenol-formaldehyde resin and compared the value obtained with experimental results.<sup>69</sup> The calculated value was found to be approximately 500 times greater than that observed experimentally. Quite a number of investigations have been carried out since, to determine whether the cross-linking in epoxy resin networks is inhomogeneous.

One of the methods most widely used to obtain experimental evidence of inhomogeneity is electron microscopy, EM.<sup>70,71,72</sup> Etched or unetched, free and fracture surfaces have been examined using this technique and the presence of nodular structures detected. If the nodular structures are not present initially then they may appear when the surface is etched chemically or by ions. The factors affecting the occurrence and physical appearance of the nodules which are assumed to be regions of high cross-link density include the curing agent used, the extent of cure and the cross-link density. For example epoxy resins cured by an acid anhydride and a catalytic curing agent were compared. The former system showed a nodular structure without etching whereas the latter system showed such structures only after etching.<sup>72</sup> Many of the studies using EM have involved replication of the surface under study and/or etching, both of which might give rise to spurious results. Nodular structures have been detected in the fracture surfaces of glassy polymers such as polymethyl

methacrylate treated in the same way as the cured epoxy resins.<sup>71</sup>

Further evidence of inhomogeneous cure in epoxy resins has been obtained from differential scanning calorimetry.<sup>73</sup> When cured epoxy resins were annealed close to, but below their glass transition temperature they subsequently showed an endothermic peak in the region of the glass transition. This observation is attributed to ordering of the cross-linked resin structure due to increased mobility at the annealing temperature. If however the resins were annealed well below their glass transition temperature, the glass transition then displayed two distinct steps. Phase separation of highly cross-linked and lightly cross-linked regions was given as the reason for this observation. The two regions act independently of one another, each giving rise to a glass transition. It must be noted that this effect was also observed in thermoplastics such as polystyrene.

Cured epoxy resins have been examined using small angle X-ray scattering.<sup>71</sup> The results from this study gave no indication of density fluctuations that would confirm the presence of nodules observed using EM. The application of cascade theory to the step-growth cross-linking of epoxy resins, as mentioned previously, gave no indication of inhomogeneous cross-linking.<sup>38</sup> The theoretical predictions agreed reasonably well with experimental results even though intramolecular reaction was neglected. Cyclization is thought to greatly influence the occurrence of inhomogeneity during cross-linking reactions. However the system studied was lightly cross-linked and it may be the case that inhomogeneity is more prevalent in systems that can be cross-linked to a higher degree.

Based on their results from study of the effects of such variables as the cross-link density of cured epoxy resins on the occurrence of nodular structures, Misra *et al* proposed a three stage curing mechanism.<sup>70</sup> The mechanism put forward is based on those proposed by previous workers and in particular accounts for the presence of two sizes of nodules and the formation of microgels prior to gelation. Highly cross-linked primary microgels are formed in the first stage which then agglomerate to form the larger, less coherent secondary microgels. Macroscopic gelation takes place when the secondary microgels coalesce, cross-linking of the material left in the interstices between the secondary microgels helping to link the secondary microgels together. Properties such as tensile strength are then determined by the degree of bonding between the secondary microgels.

The above studies presuppose that the resin and curing agent are thoroughly mixed. It has been shown, using UV fluorescent probe molecules, that poor mixing results in regions of inhomogeneity in the cured epoxy resins.<sup>74</sup>

(ii) Inhomogeneity in Chain Cross-Linking Polymerizations

Numerous investigations of free radical chain cross-linking polymerizations have been carried out.<sup>75</sup> The results of such studies strongly suggest that inhomogeneous cross-linking often occurs in polymerizations of this type.

Walling<sup>76</sup> found that the gel point conversions in methacrylate-ethylenedimethacrylate copolymerizations occurred at a much greater extent of reaction than predicted by the Stockmayer approach which neglects intramolecular reaction. Increasing the dilution or amount of tetrafunctional monomer

present increased this discrepancy. Other workers realized that the main cause of the discrepancy is the occurrence of intramolecular reaction.<sup>77</sup> Another effect was recognised that could contribute to the delay the onset of gelation in such polymerizations. This is shielding of the pendant vinyl groups by the polymer molecule to which they are attached leading to a reduction in their reactivity.<sup>78</sup>

Styrene-divinylbenzene copolymerizations in particular have attracted much interest due to the use of these cross-linked polymers as ion exchange resins and the stationary phase in gel permeation chromatography columns. To account for the effects of increasing the amount of divinylbenzene and the presence of an inert solvent on the cross-link density and the structure of the network formed, a mechanism of gelation involving the formation of microgels was proposed.<sup>79,80</sup> As in the cure of epoxy resins, gelation occurs when the microgels coalesce and bond together. Results from other studies have also produced evidence for the formation of microgels and allowed a better understanding of why they are formed.

A detailed investigation of the copolymerization of styrene and p-divinylbenzene showed that the number of pendant vinyl groups was virtually independent of the extent of reaction, only decreasing in the initial and final stages of the polymerization.<sup>81</sup> Also at the end of the polymerization there was still a substantial number of such groups present. The above effects became more pronounced as the amount of tetra-functional monomer used was increased. A comparison of the expected variation of the number of pendant vinyl groups as the reaction proceeds, assuming no intramolecular reaction, was made with that observed experimentally. At lower conversions,

fewer pendant vinyl groups are detected than expected whilst at higher conversions, more of these groups are present than theory would predict. Similar observations have been made in for example the polymerization of diallylphthalate.<sup>82</sup>

To explain these observations the following mechanism has been proposed.<sup>81,83</sup> In the initial stages of chain cross-linking polymerizations, intramolecular reaction predominates for the reasons discussed previously. Further intramolecular reaction is favoured in these cyclic and branched structures produced initially, which results in the formation of small densely cross-linked microgels with a reduced number of pendant vinyl groups. The occurrence of a greater number of pendant vinyl groups at higher conversions is attributed to the presence of such unreacted groups buried in the inaccessible core of the microgels and prevented from further participation in the polymerization. Pendant vinyl groups on the surface of microgels allow them to link together giving rise to macrogelation.

Other experimental results support the above mechanism of inhomogeneous cross-linking. The weight-average molecular weight of low conversion polyethylenedimethacrylate is found to be similar to that of primary chains of polymethylmethacrylate produced under the same conditions. Determination of the intrinsic viscosity of the non-linear polymer showed it to be significantly lower than that predicted for a branched polymer, suggesting the formation of compact polymer molecules.<sup>84</sup> A proportion of the repeat units in soluble styrene-ethylene-dimethacrylate copolymers are not detected in  $^1\text{H-NMR}$  spectra which is consistent with regions of restricted mobility such as would occur in the interior of microgels.<sup>85</sup>

A percolation model has been used to show the occurrence of inhomogeneity in chain cross-linking polymerizations of unsaturated monomers.<sup>86</sup> Using a model similar to those described previously, "snapshots" of the various stages of the polymerization of a tetrafunctional monomer proceeding by a step-growth and chain-growth mechanism were produced. Comparisons of the topology of the two systems were made at equivalent weight conversions. Extensive inhomogeneity was readily apparent in the chain-growth system which consisted of a small number of large polymer molecules. Pendant double bonds completely shielded by fully reacted polymer and unreacted monomer surrounded by polymer was present. Pendant double bonds were also seen on the boundaries of the polymer rich regions. In contrast the step-growth model produced a much more homogeneous system with a large number of small molecules distributed evenly over the lattice. The chain-growth mechanism was also carried out with 90% difunctional monomer present. Like the homopolymerization of tetrafunctional monomer by this mechanism there was a high degree of inhomogeneity. However there was much less cross-linking and the number of molecules formed was quite large so that if mobility were to be introduced, the inhomogeneity might be reduced.

Under conditions similar to those of the experimental study of the free radical copolymerization of styrene-p-divinylbenzene discussed previously,<sup>81</sup> the percolation model was used to predict the number of pendant double bonds present during the course of such a polymerization. Even though the percolation model is quite simple it predicted the same trends as seen experimentally especially at low conversions. Discrepancies did occur between the experimental and model studies, at high

conversions and on changing the amount of difunctional monomer used.

The occurrence of a high degree of cyclization during chain cross-linking polymerizations has been questioned. In one study, for example, it was found that in the early stages of a styrene-divinylbenzene copolymerization the difference in the number of pendant vinyl groups from that predicted by ring-free kinetic theory was negligible.<sup>87</sup> The delay in the gel point was then attributed to reaction of one double bond of the divinyl monomer reducing the reactivity of the second double bond.

Highly cross-linked copolymers that might be expected to exhibit inhomogeneity, give no indication of this in their mechanical properties. It is thought that lightly cross-linked copolymer forms in the voids between microgel particles and is bonded to the particles by pendant vinyl groups in the surface of microgels. Hence the inhomogeneity of the network is reduced. If however an inert solvent is present then a permanently inhomogeneous network containing voids may be formed. 83

(iii) Inhomogeneity in Photoinitiated Chain Cross-Linking Polymerizations

Only the method of generating the initiating species distinguishes photoinitiated free radical cross-linking polymerizations from those discussed in the previous section. The mechanism of inhomogeneous cross-linking as outlined in the previous section should therefore be applicable to photoinitiated free radical cross-linking polymerizations. It does not seem unreasonable to suggest that the photoinitiated cationic chain cross-linking polymerization of epoxides might proceed in a

similar way, resulting in the formation of microgels and inhomogeneous cross-linking. Such polymerizations would be expected to proceed *via* the formation of polyether chains with pendant epoxide groups which could undergo a high degree of intramolecular reaction in the early stages of the polymerization. Evidence for inhomogeneous cross-linking in both photoinitiated free radical and cationic cross-linking polymerizations has been reported.

In order to obtain an indication of the extent of reaction in cross-linked polymers, infra-red spectroscopy can be used to determine the amount of unreacted functionality present. Using this technique, the free radical photoinitiated cure of an unsaturated resin system was investigated.<sup>88</sup> The amount of unreacted functionality in a cured film was measured three times in three different places. Generally, quite a significant amount of scatter was observed in the three measurements which the authors attributed to inhomogeneous cross-linking. However the inhomogeneity must be occurring on a relatively large scale to be detected by infra-red spectroscopy. More positive evidence of inhomogeneous cross-linking has been obtained in such systems. The photoinitiated free radical cure of two resins, 1,6-hexanediol diacrylate, HDDA, and bis-(2-hydroxyethyl)bisphenol A dimethacrylate, HEBDM, were investigated.<sup>89</sup> Isothermal differential scanning calorimetry, DSC, was used to determine the degree of double bond conversion. Samples were irradiated ( $\lambda_{\max}=350\text{nm}$  bandwidth 45nm,  $0.2\text{mw cm}^{-2}$ ) in the sample holder of the calorimeter.

Five seconds irradiation at 20°C resulted in 60% and 35% conversion of HDDA and HEBDM respectively. Additional conversion occurred when the samples were heated to 80°C in

the dark, this post irradiation conversion was greater for the HEBDM resin. Irradiation for one hour at 20°C gave a greater conversion than for five seconds irradiation and then heating the samples to 80°C. However, there was still an additional conversion when the samples irradiated for the longer period were heated. The greatest degree of conversion (HDDA 89%; HEBDM 40%) was achieved by irradiating, for one hour, samples maintained at 80°C.

The above observations indicate that radicals are trapped at the end of the irradiation period which has been confirmed by electron spin resonance measurements. On heating, the trapped radicals become mobile leading to a significant increase in the degree of conversion. The results have been interpreted as being indicative of inhomogeneous cross-linking leading to regions of differing mobility. Radical species trapped in regions of low mobility after a short irradiation at 20°C may only continue to convert double bonds if the temperature and hence the mobility of the system is increased. If irradiation is continued for longer periods at 20°C, then further radicals are generated in regions of higher mobility resulting in a greater degree of conversion. Heating these samples again mobilises the trapped radicals leading to a further increase in the double bond conversion.

In divinyl polymerizations, conversion can be limited by the onset of vitrification which leads to the trapping of radicals. Increasing the temperature at which the polymerization is carried out increases the mobility and hence the extent of reaction at which trapping occurs. The observation that the additional conversion on heating samples of HDDA

irradiated at 20°C occurs over a wide range of initial conversions (14% to 79%) shows that this trapping occurs well before the limiting conversion is reached in the system examined.

The possibility of this inhomogeneity being due to phase separation is considered unlikely because of the small difference in monomer and polymer polarity and the absence of solvent. The inhomogeneous course of the cross-linking polymerization is attributed to local differences in the concentration of pendant vinyl groups due to intramolecular reaction. A percolation model, similar to those described previously, was used to predict the number of pendant double bonds as a function of the weight fraction of polymer produced for the chain-growth polymerization of a tetrafunctional monomer. As in a previous study, comparisons were made between a step-growth model and a chain-growth model of the polymerization of a tetrafunctional monomer on a two dimensional lattice. Figures 1.2 and 1.3 show the two systems for the same weight fraction of polymer produced. Thin lines represent single bonds and thick lines multiple connections.

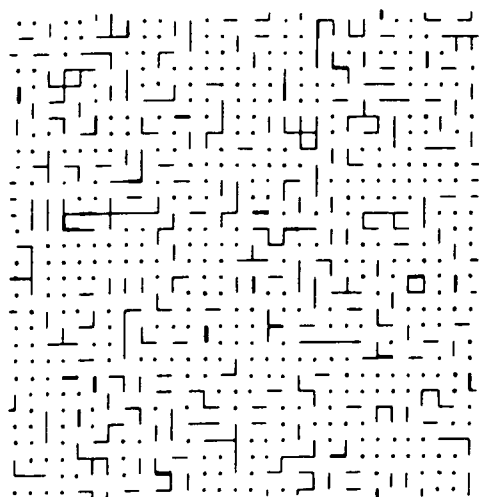


FIGURE 1.2 Step-growth  
Percolation Model

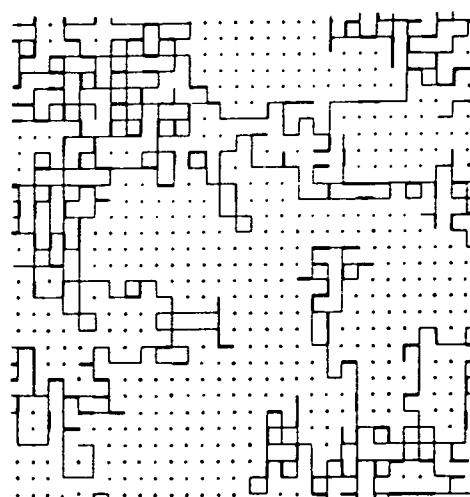


FIGURE 1.3 Chain-growth  
Percolation Model

The step-growth model shows the presence of numerous, relatively small molecules distributed homogeneously across the lattice whilst the chain-growth model shows a large inhomogeneously cross-linked polymer molecule with unreacted monomer trapped within it.

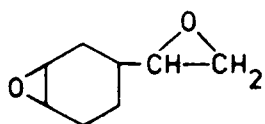
The number of pendant double bonds was determined in HDDA samples of increasing conversion,  $x$ , as measured by differential scanning calorimetry. Extractions of unreacted monomer and soluble polymer were carried out on the samples and the amount of monomer present measured from high pressure liquid chromatography traces. This allowed the fraction of polymer formed,  $P$ , to be evaluated. Quantitative retrieval of an inert compound added to the samples prior to irradiation showed that the extraction process was efficient. Using the expression below, the fraction of monomer units carrying pendant double bonds  $b$  was calculated:

$$b = \frac{2(P-x)}{P}$$

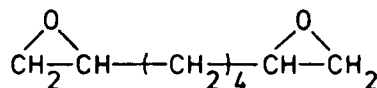
Results from calculations using a classical model of chemical kinetics and the percolation model were compared with those obtained experimentally. The number of pendant vinyl groups was found to be lower than predicted by the kinetic calculations at lower conversions but greater than predicted at higher conversions as had been found previously in studies of this type of polymerization. At lower conversions the percolation model predicted a lower number of pendant double bonds than the kinetic calculations, agreeing with the experimental results. However at higher conversions the percolation model underestimated quite significantly the number of pendant double bonds. This deviation could be due to the model under-

estimating the shielding of pendant vinyl groups or reduced efficiency of the photoinitiator in densely cross-linked regions. A similar deviation was observed in a study described previously which compared predictions from a percolation model with experimental results. Then, the discrepancy was attributed to inefficient extraction of monomer in the experimental study which is unlikely to be the explanation in this case.

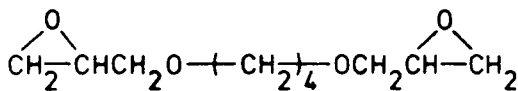
The application of a more subtle technique has shown the presence of inhomogeneous cross-linking in the photoinitiated cationic polymerization of the tetrafunctional epoxides shown below:<sup>90</sup>



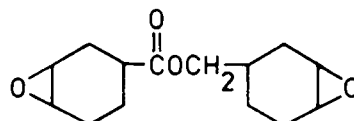
(X)



(XI)



(XII)



(XIII)

The photoinitiator used was bis(4-t-butylphenyl)iodonium hexafluoroarsenate.

The aim of the study was to investigate the properties of the cross-linked resins with a view of their use in optical systems. After exposure of the cross-linked resins to ultraviolet light, a long-lasting, bright blue emission was observed. Molecular mobility in polymers has been studied using luminescent probe molecules added to the system but in this investigation, intermediates from the photolysis of the

photoinitiator provided on intrinsic probe. The nature of this probe molecule is not known but it seems very likely that it is a free radical species.

Isothermal DSC measurements were used to determine the irradiation time required for maximum conversion. The samples were irradiated at 254nm in air. It is not stated whether subsequent heating produced any additional conversion of epoxide groups. All the cured resins exhibited fluorescence at 340nm. In addition resins (X), (XI) and (XIII) showed phosphorescence at approximately 480nm. The decay time of the phosphorescence was found to be 1.6 seconds and was independent of the resin structures. The intensity of both types of emission was found to be greatest when the samples were irradiated at 290nm.

To gain an insight into the polymerization of the diepoxides, emission spectra were recorded at increasing degrees of conversion. A rapid increase in the intensity of fluorescence was observed from the start of the polymerization. When phosphorescence did occur, it only appeared and increased in intensity after a certain irradiation time which was dependent on the structure of the resin. After twenty hours in the dark, the fluorescence intensity had decreased slightly and phosphorescence did not occur. Irradiation of the sample quickly regenerated the latter but prolonged irradiation resulted in the irreversible disappearance of both types of luminescence.

At ambient temperatures the decay time of the phosphorescence was found to be independent of the degree of conversion. The decay time,  $\tau$ , is given by the following expression,

$$\tau^{-1} = \tau_r^{-1} + \tau_{nr}^{-1}$$

where  $\tau_r$  is the radiative lifetime of the triplet state and  $\tau_{nr}$  the non-radiative lifetime. Inter- and intramolecular deactivation processes determine the latter. Chemical reaction or a high mobility of the species responsible for the luminescence will give rise to intermolecular quenching. If the cross-linking polymerization of the epoxides proceeded in a homogeneous manner then one would expect a gradual decrease in the mobility of the system as the cross-link density gradually increased. This should lead the phosphorescence decay time to increase gradually with conversion as the occurrence of intermolecular quenching would be reduced. The observation that the phosphorescence decay time remains constant with increasing conversion led the workers to propose that regions of high and low cross-link density and hence mobility occur in the network structure. In the regions of low mobility, which must be formed from the onset of phosphorescence, radiative decay predominates whereas non-radiative decay is dominant in the high mobility regions. The ratio of the phosphorescence and fluorescence intensities will give an indication of the volume fraction of low mobility regions. This ratio, which is found to depend on the resin structure, increases rapidly and then reaches a plateau value as the polymerization proceeds.

Phosphorescence is not observed at any extent of reaction in samples of resin (XII). It is considered that the structure of this resin is not rigid enough to limit mobility even in highly cross-linked domains, so that non-radiative decay predominates throughout the network. Cooling a cured sample of resin would be expected to favour radiative decay by reducing the internal mobility of the network structure.

Phosphorescence was indeed observed on cooling a cured sample of resin (XII).

Using ESR spectroscopy, trapped radical species were detected in freshly polymerized samples of each resin. The intensity of the signal increased with increasing conversion but the shape of the signal which is affected by the mobility of the species remained constant. The decay of the signal was found to be virtually independent of the structure of the resin and more interestingly the degree of conversion. These observations are consistent with the hypothesis that domains of high and low mobility are formed in such polymerizations. The increase of signal intensity with increasing conversion indicates that the volume fraction of low mobility domains increases as the polymerization progresses. The trapped radical species which are thought to be photolysis intermediates from the photoinitiator were detected in cured samples of resin (XII). Yet, assuming these radical species are responsible for the luminescence, the structure of this resin was considered too flexible to prevent non-radiative decay of the phosphorescence by intermolecular quenching.

Thus the above studies provide, from a variety of techniques, reasonably convincing evidence for the occurrence of inhomogeneous cross-linking in photoinitiated chain cross-linking polymerizations.

REFERENCES - CHAPTER ONE

1. P.W. Atkins, "Physical Chemistry", 1st Edition, Oxford University Press (1978).
2. E.A. Gilbransen, "McGraw-Hill Encyclopedia of Science and Technology", 5th Ed., Vol.3, McGraw-Hill Inc. (1982).
3. G.G. Schurr, "Kirk-Othmer Encyclopedia of Chemical Technology", Exec.Ed. M. Grayson, 3rd Ed., Vol.16, Wiley-Interscience (1981).
4. S. Hochberg, *ibid*, Vol.6 (1979).
5. C.M. Munger, *ibid*, Vol.6 (1979).
6. U.R. Evans, "An Introduction to Metallic Corrosion", 2nd Ed., Edwards Arnolds, (1973).
7. R.W. Drisko, "Kirk-Othmer Encyclopedia of Chemical Technology", Exec.Ed. M. Grayson, 3rd Ed., Wiley-Interscience (1979).
8. K. O'Hara, *Polymers, Paint and Colours Journal*, 141, 11 (1981).
9. L.H. Carblom, *Rad.Curing*, 10, 8 (1983).
10. R.W. Lenz, "Organic Chemistry of Synthetic High Polymers", Wiley-Interscience (1967).
11. P.J. Flory, "Principles of Polymer Chemistry", Cornell University Press (1953).
12. W.G. Potter, "Epoxy Resins", Plastics Institute (1970).
13. L.H. Lee and K. Neville, "Handbook of Epoxy Resins", McGraw-Hill (1967).
14. I. Skeist, "Epoxy Resins", Reinhart Book Corporation (1968).
15. K.C. Frisch and S.L. Reagan in "Ring-Opening Polymerizations", Eds. K.C. Frisch and S.L. Reagan, Marcel Dekker, London (1969).
16. A. Ledwith and D.C. Sherrington in "Reactivity and Structure in Polymer Chemistry", Eds. A.D. Jenkins and A. Ledwith, Wiley-Interscience, (1974).
17. S. Penczek, P. Kubisa and K. Matyjaszewski, *Adv.Polym.Sci.*, 37, 1 (1980).
18. R.E. Parker and N.S. Isaacs, *Chem.Revs.*, 59, 737 (1959).
19. A. Sato, T. Hirano, M. Suga and T. Tsuruta, *Polym.J.*, 9, 209 (1977).
20. J.M.G. Cowie, "Polymers: Chemistry and Physics of Modern Materials", Intertext Books (1973).

21. K. Matyjaszewski, P. Kubisa and S. Penczek, *J.Polym.Sci., Polym.Chem.Ed.*, 13, 763 (1975).
22. K. Matyjaszewski, S. Slomkowski and S. Penczek, *J.Polym.Sci., Polym.Chem.Ed.*, 17, 69 (1979).
23. K. Matyjaszewski, S. Slomkowski and S. Penczek, *J.Polym.Sci., Polym.Chem.Ed.*, 17, 2413 (1979).
24. D.J. Worsfold and A.M. Eastham, *J.Am.Chem.Soc.*, 79, 900 (1957).
25. Y. Kowakami, A. Ogawa and Y. Yamashita, *J.Polym.Sci., Polym.Chem.Ed.*, 17, 3785 (1979).
26. S.G. Entelis and G.V. Karovina, *Makromol.Chem.*, 175, 1253 (1974).
27. K.J. Ivin in "Reactivity, Mechanism and Structure in Polymer Chemistry", Eds. A.D. Jenkins and A. Ledwith, Wiley-Interscience (1974).
28. W.H. Carothers, *Chem.Revs.*, 8, 353 (1931).
29. W.H. Carothers, *Trans.Farad.Soc.*, 32, 39 (1936).
30. P.J. Flory, *J.Am.Chem.Soc.*, 63, 3083 (1941).
31. P.J. Flory, *Chem.Revs.*, 39, 137 (1946).
32. W.H. Stockmayer, *J.Chem.Phys.*, 11, 45 (1943).
33. W.H. Stockmayer, *J.Chem.Phys.*, 12, 125 (1944).
34. M. Gordon, *Proc.Roy.Soc. (London)*, A268, 240 (1962).
35. I.J. Good, *Proc.Roy.Soc. (London)*, A272, 54 (1963).
36. M. Gordon and G.R. Scantlebury, *Farad.Soc.Trans.*, 60, 604 (1964).
37. K. Dusek, M. Ilavsky and S. Lunak, *J.Polym.Sci., Polym.Symp.*, 53, 29 (1975).
38. S. Lunak and K. Dusek, *J.Polym.Sci., Polym.Symp.*, 53, 45, (1975).
39. G.R. Dobson and M. Gordon, *J.Chem.Phys.*, 43, 705 (1965).
40. V. Vojta and K. Dusek, *Brit.Polym.J.*, 12, 1 (1980).
41. K. Dusek and M. Ilavsky, *J.Polym.Sci., Polym.Symp.*, 53, 57 (1975).
42. K. Dusek and N. Ilavsky, *J.Polym.Sci., Polym.Symp.*, 53, 75 (1975).
43. G.R. Dobson and M. Gordon, *J.Chem.Phys.*, 41, 2389 (1964).

44. C.W. Mocasko and D.R. Miller, *Macromols.*, 9, 199 (1976).
45. C.W. Mocasko and D.R. Miller, *Macromols.*, 9, 206 (1976).
46. M. Gordon, T.C. Ward and R.S. Whitney in "Polymer Networks: Structure and Mechanical Properties", Eds. A.J. Chomppff and S. Newman, Plenum Press, New York (1971).
47. R.F.T. Stepto, *Polymer*, 20, 1324 (1979).
48. M. Jacobson and W.H. Stockmayer, *J.Chem.Phys.*, 18, 1600 (1950).
49. J.F. Brown and G.M.J. Slusaczuk, *J.Am.Chem.Soc.*, 87, 931 (1965).
50. P.J. Flory and J.A. Semlyen, *J.Am.Chem.Soc.*, 88, 3209 (1966).
51. R.F.T. Stepto, *Developments in Polymerization*, 3, 81 (1982).
52. R.F.T. Stepto, *Farad.Trans.*, 69, 57 (1974).
53. W. Hopkins, R.M. Peters and R.F.T. Stepto, *Polymer*, 15, 315 (1974).
54. Z. Ahmad, R.F.T. Stepto and R.M. Still, *Brit.Polym.J.*, 17, 205 (1985).
55. J.L. Stanford and R.F.T. Stepto, *Brit.Polym.J.*, 9, 124 (1977).
56. M. Gordon and G.R. Scantlebury, *Proc.Roy.Soc. (London)*, A292, 380 (1966).
57. M. Gordon and G.R. Scantlebury, *J.Chem.Soc.*, B, 1 (1967).
58. S.B. Ross-Murphey, *J.Polym.Sci., Polym.Symp.*, 53, 11 (1975).
59. K. Dusek, *Makromol.Chem., Suppl.*, 2, 35 (1979).
60. D. Stauffer, *J.Chem.Soc., Farad II*, 72, 1354 (1976).
61. D. Stauffer, A. Coniglio and M. Adam, *Adv.Polym.Sci.*, 44, 103 (1982).
62. M. Galina and M. Gordon, *Europhysics Conference Abstracts*, 51, 50 (1981).
63. D. Stauffer, *Physica*, 106A, 177 (1981).
64. P. Manneville and L. de Seze in "Numerical Methods in the Study of Critical Phenomena", Eds. J.Della Dora, J.Demongeot and D. Lacoll, Springer-Verlag (1981).
65. M.J. Herrmann, D. Stauffer and D.P. Landau, *J.Phys.A.: Math.Gen.*, 16, 1221 (1983).
66. R. Bansil, M.J. Herrman and D. Stauffer, *Macromols.*, 17, 998 (1984).

67. R. Bansil, M.J. Herrmann and D. Stauffer, *J.Polym.Sci., Polym.Symp.*, 73, 175 (1985).
68. R. Nossal, *Macromols*, 18, 49 (1985).
69. J.H. de Boer, *Trans.Farad.Soc.*, 32, 10 (1936).
70. S.C. Misra, J.A. Manson and L.H. Sperling, *ACS Symp.Ser.*, 114, 157 (1979).
71. K. Dusek and J. Malinsky, *Polymer*, 19, 393 (1980).
72. T. Takahama and P.H. Geil, *Makromol.Chem., Rapid Commun.*, 3, 389 (1982).
73. U.T. Kreibich and R. Schmid, *J.Polym.Sci., Polym.Symp.*, 53, 177 (1975).
74. M. Ghaemy, N.C. Billingham and P.D. Calvert, *J.Polym.Sci., Polym.Lett.*, 20, 439 (1982).
75. K. Dusek, *Developments in Polymerization*, 3, 143 (1982).
76. C. Walling, *J.Am.Chem.Soc.*, 67, 441 (1945).
77. M.Gordon and R.J. Roe, *J.Polymer Sci.*, 21, 75 (1956).
78. L. Minnema and A.J. Staverman, *J.Polym.Sci.*, 29, 281 (1958).
79. B.T. Storey, *J.Polym.Sci.*, A3, 265 (1965).
80. J.R. Millar, D.G. Smith and T.R.E. Kressman, *J.Chem.Soc.*, 304 (1965).
81. J. Malinsky and J. Klaban, *J.Macromol.Sci-Chem.*, A5, 1071 (1971).
82. K. Ito, Y. Murase and Y. Yamashita, *J.Polym.Sci., Polym.Chem.Ed.*, 13, 87 (1975).
83. K. Dusek, M. Galina and J. Mikes, *Polym.Bull. (Berlin)*, 3, 19 (1980).
84. H. Galina, K. Dusek, Z. Tuzor, M. Bohdanecky and J. Stokr, *Eur.Polym.J.*, 16, 1043 (1980).
85. J. Spevacek and K. Dusek, *J.Polym.Sci., Polym.Phys.Ed.*, 18, 2027 (1980).
86. H.M.J. Boots and R.B. Pandey, *Polym.Bull.(Berlin)*, 11, 415, (1984).
87. R. Okasha, G. Mild and P. Remppe, *Eur.Polym.J.*, 15, 975 (1979).
88. A. Rais-Ali and M.O.W. Richardson, *Brit.Polym.J.*, 12, 57 (1980).
89. J.G. Kloosterboer, G.M.M. van de Hei and H.M.J. Boots, *Polym.Comm.*, 25, 354 (1981).
90. E.W. Meijer, D.M. de Leeuw, F.J.A.M. Greidanus and R.J.M. Zwiers, *Polym.Comm.*, 26, 45 (1985).

CHAPTER TWO

A BRIEF SURVEY OF PHOTOINITIATORS  
AND THE PHOTOCHEMISTRY  
OF DIARYLIODONIUM SALTS

## 2.1 General Aspects of Photochemistry

Photochemistry<sup>1</sup> is the study of the chemical or physical processes that occur when molecules absorb a quantum of radiation from the visible or ultraviolet regions of the electromagnetic spectrum. Essentially, radiation of wavelength 200 to 700 nm is utilized.

### (A) Excited States and Photochemical Processes

Electrons occupy a set of molecular orbitals of increasing energy. On absorption of a photon of sufficient energy, an electron is promoted to a molecular orbital of higher energy. Photochemical reactions occur from this excited state as opposed to thermal reactions which occur from the electronically unexcited ground state. In a number of molecules, the electrons associated with a particular group of atoms, known as a chromophore, are excited.

Electrons possess a spin quantum number which may take the value  $+\frac{1}{2}$  or  $-\frac{1}{2}$  depending on the direction of the spin. The expression  $2S+1$ , where  $S$  is the sum of the spin quantum numbers of electrons, gives the multiplicity of an electronic configuration. Most organic molecules have an even number of electrons distributed in pairs, with their spins opposed, in molecular orbitals. The multiplicity of this electronic configuration is then one and the term singlet state is used to describe it. The excitation of electrons is governed by a number of selection rules, one of which forbids transitions that occur with a change of spin. Therefore the excited states of most organic molecules reached by direct electronic excitation are singlets.

The energy of the photon absorbed is often greater than the energy required to promote an electron. This results in the electron attaining an upper vibrational level of the excited state. Before any other processes occur, the excess vibrational energy is lost by internal conversion, IC. The main processes by which the excess electronic energy is lost can occur concurrently and are summarized in Figure 2.1.

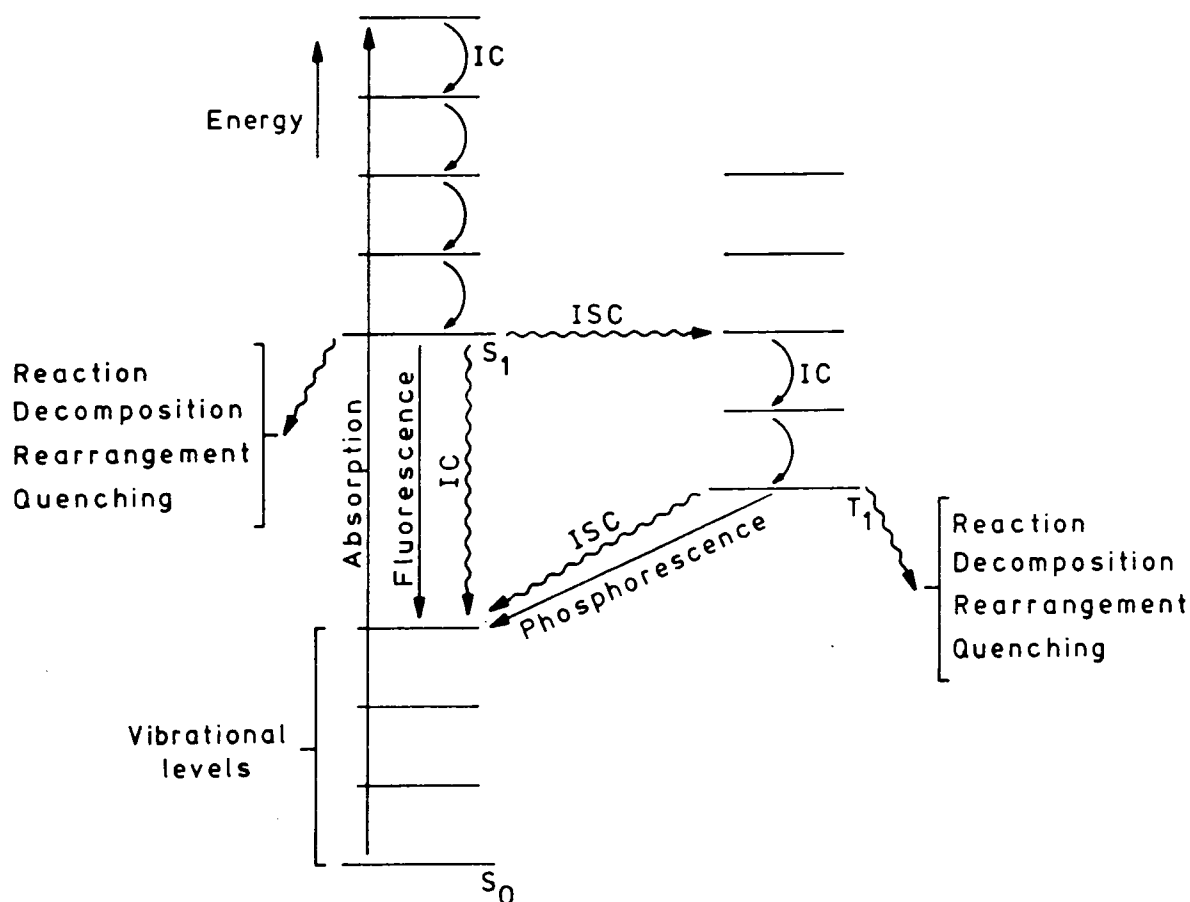
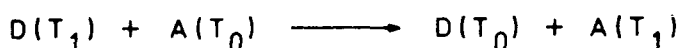


FIGURE 2.1 Excited Electronic States and Their Possible Fates

Emission of a photon results in the electron returning to one of the various vibrational levels of the ground state and gives rise to fluorescence. Ideally, the absorption and fluorescence emission spectra will be mirror images with the fluorescence spectrum at longer wavelengths. Internal conversion can produce the same transition, without emission of

a photon, through collisions with the surrounding medium.

Quenching of the excited state occurs through interaction with an acceptor molecule, A, most importantly by an energy transfer mechanism. The excited state donor molecule, D, returns to the ground state whilst the acceptor molecule is raised to an excited state as shown below:



This process can only occur if the excited state of the acceptor molecule is of lower energy than that of the donor molecule.

If the excited state of a molecule is of sufficient energy then a weak bond, close to the site of excitation, may be cleaved. This produces radical or molecular species, dissipating the excess energy. Alternatively, the energy rich molecule may undergo intermolecular chemical reaction or an intramolecular rearrangement, giving rise to products or isomers in the ground state. Intermolecular processes involving the singlet excited state tend to be disfavoured because of the short lifetime of this state.

A change in multiplicity of the excited state can be weakly allowed and is known as intersystem crossing, ISC. Likewise the transition from a triplet excited state to a singlet ground state is possible. If the latter transition is accompanied by the emission of a photon then the process is known as phosphorescence. Unlike fluorescence, which ceases as soon as the light source is removed, phosphorescence may continue for a lengthy period after irradiation. This

is a reflection of the inefficiency of transitions between states of different multiplicity. The excess energy of the triplet excited state may be lost by other processes which are similar to those of the singlet excited state. The longer lifetime of the triplet state gives intermolecular processes a better chance of occurring.

#### B. Quantum Yield

The quantum yield  $\phi$ , is a measure of the efficiency of a process and is defined as follows:

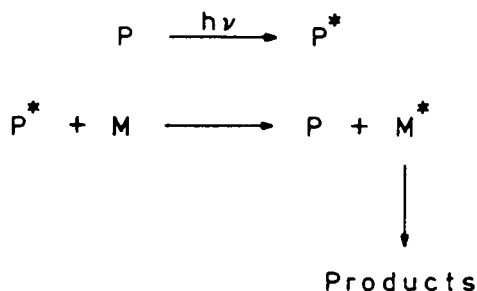
$$\phi = \frac{\text{number of molecules undergoing a process}}{\text{number of quanta absorbed}}$$

For photochemical reactions the quantum yield for product formation gives an insight into the mechanism of reaction. If  $\phi$  is equal to one then a molecule reacts for each quantum of radiation absorbed. A value of  $\phi$  less than one may indicate, for example, that deactivation of the excited state or radical recombination is occurring. By contrast when  $\phi$  is greater than one, a chain process is probably occurring.

#### C. Photosensitization

An alternative to the direct irradiation of a molecule to produce an excited state is the process of photosensitization. This technique can be used when the wavelengths emitted by the light source do not match those absorbed by a molecule which is required to undergo a photochemical process. A compound is chosen that must fit two requirements. Firstly the photosensitizer must absorb wavelengths emitted by the light source and thus be raised to an electronically excited state.

Secondly the photosensitizer must be capable of interacting with the molecule of interest to produce the same effect as direct irradiation. Generally energy transfer is the most important process by which photosensitization occurs. The molecule, M, is raised to an excited state whilst the photosensitizer, P, is returned to its ground state.



## 2.2 Photoinitiators for Free Radical and Cationic Polymerizations

The term photoinitiated polymerization is used to describe the initiation of chain-growth polymerization by a species produced from the photochemical reaction of a specific photoinitiator. This is in contrast to photopolymerizations, where each propagation step requires the absorption of a photon.<sup>2</sup>

The two main types of chain-growth polymerization for which photoinitiators have been extensively developed are those that proceed by free radical and cationic mechanisms. The availability of free radical and cationic photoinitiators allows the cross-linking polymerization of both vinyl and epoxy resins to be carried out.

### A. Free Radical Photoinitiators

A brief summary of the photochemistry and the types of free radical photoinitiators is presented here. More detailed reviews of this area have been published.<sup>3,4,5,6</sup>

The main requirements for a photoinitiator, especially ones for commercial use are:-

- (a) efficient absorption of wavelengths from available ultraviolet lamps;
- (b) efficient photochemical production of species, effective at initiating polymerization;
- (c) thermal stability.

Free radical photoinitiators such as peroxides have been known for many years but they do not meet the first and third requirements. Some aromatic carbonyl compounds fulfil all of the above requirements. This has led to their development and predominant use as free radical photoinitiators in the curing of unsaturated polyesters, acrylates, isocyanate acrylates and epoxy acrylates.

(i) Carbonyl Photochemistry

The molecular orbitals associated with the carbonyl group are shown below in order of increasing energy:<sup>7</sup>



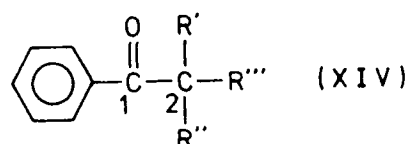
There are electron pairs in the  $\sigma$  and  $\pi$  orbitals and in two non-bonding orbitals on the oxygen atom. Two transitions may be readily observed,  $n \rightarrow \pi^*$  and  $\pi \rightarrow \pi^*$ . The former transition is usually of lower energy than the latter but this order may be reversed depending on the substituents present in the molecule or on the solvent used. The two possible excited states have different reactivities. For example the  $n, \pi^*$  excited state results in a decrease of electron density on the oxygen atoms making hydrogen abstraction reactions more favourable.

Also the  $n, \pi^*$  state may undergo intersystem crossing to yield a relatively long-lived triplet state more easily than the  $\pi, \pi^*$  excited state.

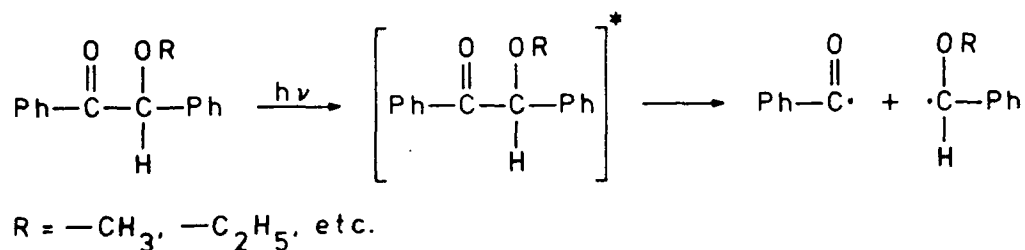
Free radical photoinitiators produce the radical initiating species by either fragmentation of intermolecular hydrogen abstraction.

(ii) Photoinitiators Producing Radicals by Fragmentation

The majority of aromatic carbonyl compounds used as photoinitiators that act in this way have the general structure, (XIV), and can be regarded as  $\alpha$ -substituted acetophenones:



The excited state molecule undergoes homolytic cleavage of the bond between carbons 1 and 2 in structure (XIV) to give two radical species, as shown below for benzoin alkyl ethers. This type of process is known as a Norrish Type I cleavage.



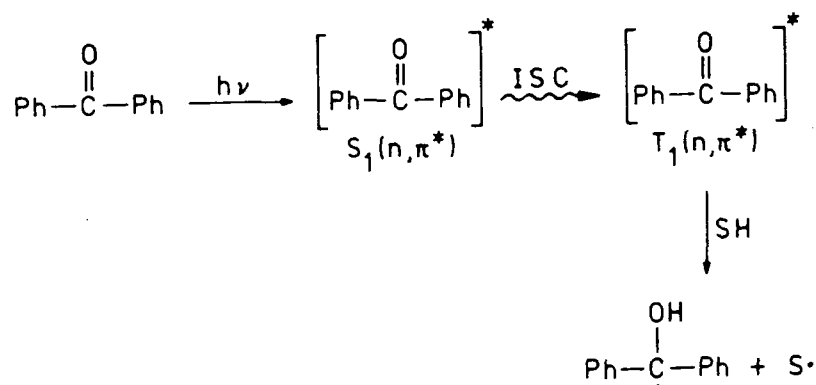
In the case of benzoin alkyl ethers, both radical species or the benzyl radical alone may initiate polymerization, depending on the monomer used, its concentration and the photoinitiator concentration.

Other compounds with the general structure (XIV) used as photoinitiators include benzoin, benzyl ketals, dialkoxyaceto-

phenones and di- or trichloroacetophenones.

(iii) Photoinitiators Producing Radicals by Hydrogen Abstraction

An example of this type of photoinitiator is benzophenone. The  $\pi, \pi^*$  triplet excited state of this molecule abstracts a hydrogen atom from a donor molecule:



Alcohols, ethers and amines with hydrogen atoms  $\alpha$  to the heteroatom as well as thiols are used as hydrogen donors. Of the two radical species produced, experimental evidence indicates that those resulting from the hydrogen donor, are primarily responsible for initiating polymerization.

Other examples of photoinitiators that act by hydrogen abstraction include Michlers ketone, thioxanthenes, and anthroquinones.

(iv) Disadvantages of Photoinitiated Free Radical Polymerizations

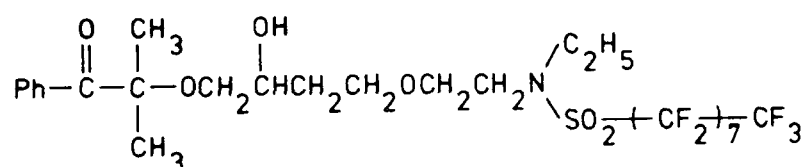
Although widely employed in areas such as photoresist technology, wood coatings, adhesives and printing inks there are a number of drawbacks associated with the use of photoinitiated free radical cross-linking polymerizations. Termination of polymerization by radical-radical combination

can create problems especially at high initiator concentrations or at low viscosities, the desirable high rates of polymerization only occurring above a threshold viscosity.

Oxygen inhibition of polymerization, is however, the major problem associated with the use of such systems. Free radical polymerizations in general may be inhibited by the reaction of oxygen with the propagating species to form relatively unreactive peroxy radicals. The problem is further exacerbated when photoinitiators are used since oxygen can efficiently quench the triplet excited states of carbonyl compounds, preventing radical formation. In systems irradiated in air, tacky surfaces can result due to the greater oxygen concentration at the film-air interface.

Several solutions to this problem have been developed. These include irradiation of samples under nitrogen, the use of high intensity, UV lamps, or the addition of a wax which segregates to the surface preventing further diffusion of oxygen into the sample. If photoinitiators based on benzophenone are used then the addition of tertiary amines can reduce the effects of oxygen. Also using a mixture of photoinitiators acting by fragmentation and hydrogen abstraction can prove helpful.

One of the more recent solutions to this problem is the use of photoinitiators such as (XV) which contain a long perfluoroalkyl chain.<sup>8</sup> Surface segregation of the low surface free energy



(XV)

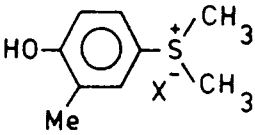
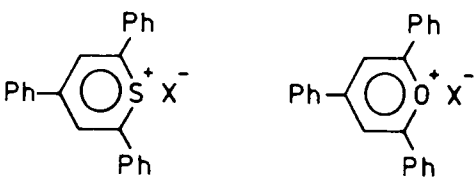
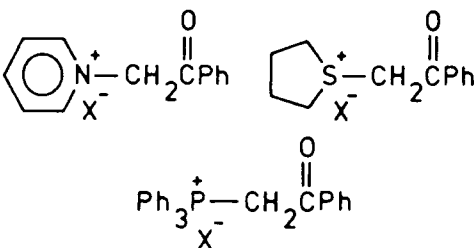
fluorinated compound results in an increased concentration of initiator in the surface layer. A sufficient concentration of radicals is then produced in the surface to react with oxygen and to initiate polymerization. The surface segregation of fluorine containing monomers is discussed in more detail in a later chapter.

#### B. Cationic Photoinitiators

Of the compounds able to act as photoinitiators for the cationic polymerization of epoxides, onium salts are generally the most effective.<sup>9</sup> Aryldiazonium tetrafluoroborates were the first class of onium salts discovered to be efficient cationic photoinitiators.<sup>10</sup> Since 1975, numerous patents and papers have appeared concerning the use of a whole range of onium salts able to act as photoinitiators for the polymerization of cyclic ethers such as epoxides and other cationically polymerizable monomers. Table 2.1 gives an indication of the range of onium salts that can act as photoinitiators.

An important feature of these onium salts is the use of non-nucleophilic anions which reduces termination by reaction of the anion with the propagating cationic species. Photoinitiated cationic polymerizations do not suffer the disadvantages of photoinitiated free radical polymerizations outlined previously. In particular the lack of oxygen inhibition combined with fewer termination processes gives such systems the potential for continued polymerization after irradiation in air. High initiator concentrations can also be tolerated in such systems.

TABLE 2.1 Examples of Onium Salt Photoinitiators

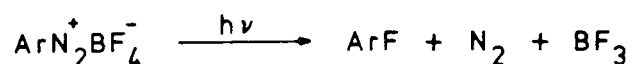
Class of onium salt	Example
aryldiazonium	$\text{PhN}_2^+ \text{X}^-$
diaryliodonium <sup>11</sup>	$\text{Ph}_2\text{I}^+ \text{X}^-$
arylonium salts of sulphur <sup>12</sup> selenium <sup>13</sup> and phosphorus <sup>14</sup>	$\text{Ph}_3\text{S}^+ \text{X}^-$ $\text{Ph}_3\text{Se}^+ \text{X}^-$ $\text{Ph}_4\text{P}^+ \text{X}^-$
dialkyl-4-hydroxyphenyl- sulphonium salts <sup>15</sup>	
sulphoxonium salts <sup>16</sup>	$\begin{array}{c} \text{O} \\    \\ (\text{ArO})_2\text{S}^+ \text{Ar} \\ \text{X}^- \end{array}$
thiopyrillium <sup>17</sup> and pyrillium salts <sup>18</sup>	
phenacylonium salts of nitrogen, <sup>19</sup> sulphur <sup>20</sup> and phosphorus <sup>21</sup>	
$\text{X}^-$ includes $\text{SbF}_6^-$ , $\text{AsF}_6^-$ , $\text{PF}_6^-$ and $\text{BF}_4^-$	

-----

In addition to the three requirements of a photoinitiator stated previously, other factors such as the nature and fate of the products of photolysis, the ease of synthesis and the cost should be taken into account when selecting a photoinitiator. The last two points may become important in the commercial use of photoinitiators.

(i) Aryldiazonium Salts

On photolysis, aryldiazonium salts produce a Lewis acid which initiates polymerization,<sup>22</sup> for example:



Although aryldiazonium salts are relatively cheap and easy to produce they are thermally unstable, which prevents the long-term storage of one pack systems, and one product of photolysis is nitrogen which can cause bubbles and pinholes in thicker films.

(ii) Diaryliodonium Salts

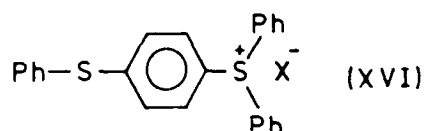
The diaryliodonium salts of chlorine, bromine and iodine are very photosensitive and can act as cationic photo-initiators. Diaryliodonium salts have received the most attention because unlike the others, they are thermally stable and fairly easy to synthesise.<sup>23</sup> The photolysis<sup>24</sup> and the effectiveness of diaryliodonium salts as photoinitiators for epoxide polymerization<sup>25</sup> has been studied by Crivello *et al.* It is thought that photolysis results in the formation of a Brönsted acid which is responsible for initiating cationic polymerization. Although these salts only absorb strongly below 300nm, photosensitization can be used to produce photolysis using longer wavelength UV or visible light.

(iii) Sulphonium Salts

The properties of triarylsulphonium salts are comparable to those of diaryliodonium salts. The synthesis, characterization and use of such compounds as photoinitiators has been reported.<sup>26</sup> The mechanism of photolysis and the

species initiating polymerization is thought to be the same as diaryliodonium salts. However one of the products of photolysis is diphenylsulphide which has a strong odour.<sup>27</sup> This can be disadvantageous in some surface coating applications. Photosensitization of triarylsulphonium salts is more difficult than with diaryliodonium salts but it can be achieved using aromatic hydrocarbons.<sup>28</sup>

A solution to the last two problems is the use of 'complex' triarylsulphonium salts<sup>27,29</sup> such as diphenyl-4-thiophenoxyphenylsulphonium salts (XVI).



A less volatile residue is produced on photolysis and in addition these salts possess absorption bands in the 300nm region. Dialkylphenacyl<sup>20</sup> and 4-hydroxyphenylsulphonium<sup>15</sup> salts also possess additional absorption bands in the 300nm region. On irradiation, a reversible process occurs resulting in the formation of a sulphur ylid and a Brönsted acid. The reversibility of the photolysis process makes these salts less effective photoinitiators than triarylsulphonium salts.

Thiopyrillium salts have been investigated as potential photoinitiators but they are substantially less efficient than triarylsulphonium salts.<sup>17</sup>

#### (iv) Triarylselenonium Salts

The photolysis of these onium salts has been studied and they have been shown to initiate the polymerization of epichlorohydrin on irradiation.<sup>13</sup> However they are slightly

less efficient photoinitiators than triarylsulphonium salts.

(v) Selection of a Photoinitiator for These Studies

Very little has been reported about the use of the remaining onium salts in Table 2.1 other than their ability to act as photoinitiators for epoxide polymerization. The choice of photoinitiator for the investigation of the photoinitiated cationic curing of epoxy resins lay between diaryliodonium and triarylsulphonium salts since they fulfil most of the criteria required of a photoinitiator. It was noted however that one of the more effective synthetic routes to the latter class of onium salts involves the use of diaryliodonium salts.<sup>26</sup> Taking this into account, diaryliodonium salt photoinitiators were chosen for the study. However, since the commencement of this project some concern has arisen over the commercial use of diaryliodonium salt photoinitiators because of their toxicity.

2.3 Diaryliodonium Salts as Photoinitiators

Although diaryliodonium salts appear somewhat unusual at first sight in that the central iodine atom has an oxidation state of +3 and a coordination number of two, they were first synthesised as early as 1894.<sup>30</sup> Since that time numerous synthetic routes to such compounds have been devised and their chemistry investigated.<sup>31</sup> Usually diaryliodonium salts are isolated with a halide counter ion. Salts with such anions, although photosensitive, are not effective as photoinitiators because of the nucleophilicity of the anions.

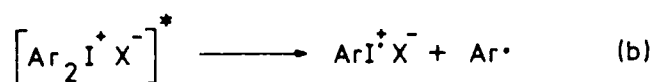
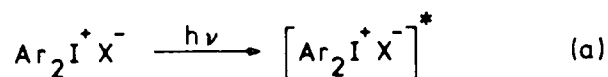
(A) The Photochemistry of Diaryliodonium Salts

Diaryliodonium salts usually show strong absorption bands in the 200-210nm and 230-260nm regions.<sup>24</sup> The anion has virtually no effect on the position or intensity of the bands. Substituents on the aromatic rings can affect the intensity and position of these bands especially the longer wavelength one. Methoxy or other electron donating substituents in the para position result in a shift to longer wavelengths.<sup>32</sup>

The rate of photolysis is unaffected by the anion but is slightly affected by the structure of the cation.<sup>24</sup> Increasing the temperature and the presence of oxygen have no effect on the rate of photolysis, which is directly proportional to the light intensity.

(i) Mechanism of Photolysis

Identification of the photolysis products of bis(4-tert-butylphenyl)iodonium tetrafluoroborate in acetonitrile, acetone and acetone/water led Crivello and Lam to propose a mechanism,<sup>24</sup> similar to one proposed by other workers,<sup>33</sup> that accounted for the major products:



The excited state photoinitiator produced in step (a) is thought to be singlet in nature, since photolysis is unaffected by the presence of triplet quenchers.<sup>9a</sup> Homolytic

cleavage of a carbon-iodine bond, in the excited state molecule rapidly occurs, step (b). This results in the formation of an arylodinium radical-cation and an aryl radical. Strong evidence for the formation of an arylodinium radical-cation has recently been obtained from laser-flash photolysis studies of diaryliodonium salts.<sup>34</sup> Identification of biphenyl compounds as photolysis products was taken to indicate that aryl radicals were the other primary photoproducts. The observation that diaryliodonium salts can act as photoinitiators of free radical polymerizations further supports the formation of radical species on photolysis.<sup>35</sup> The radical-cation abstracts a hydrogen atom from the monomer or solvent (SH) to yield the species  $\text{ArIH}^+ \text{X}^-$  from which an iodoaryl compound and a Brönsted acid may be formed as shown in steps (c) and (d).

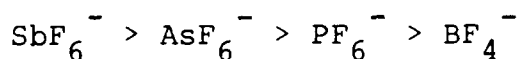
The photolysis products of diphenyliodonium hexafluorophosphate, irradiated in methanol have been reported.<sup>36</sup> The major product was benzene (70%) with fluorobenzene (16%) and biphenyl (10%) as the other products. The formation of biphenyl was not attributed to the recombination of aryl radicals as by Crivello and Lam but to attack of an aryl radical on the diphenyliodonium cation. A photoinduced ionic process was proposed to account for the formation of fluorobenzene. The absence of iodobenzene was attributed to this compound's ability to readily undergo photodecomposition.

Crivello and Lam determined the quantum yield for the formation of 4-tert-butyliodobenzene from the photolysis of bis(4-tert-butylphenyl)iodonium hexafluoroarsenate.<sup>24</sup> Values of  $\sim 0.20$  and  $\sim 0.19$  were obtained at wavelengths of 313nm and 366nm respectively. The former value was found to be independent

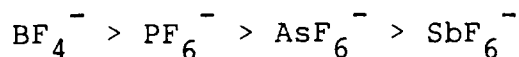


polymerization of monomer in the dark indicating that long-lived cationic species are formed.<sup>37</sup> Also the formation of polymer is completely suppressed when proton traps that do not interfere with Lewis acids are added.<sup>35</sup>

Although the anion has a negligible effect on the rate of photolysis of diaryliodonium salts of the same cation structure, the overall rate of polymerization of epoxides is markedly dependent on the anion.<sup>25</sup> The rate of polymerization decreases in the following order as determined by isothermal DSC measurements.



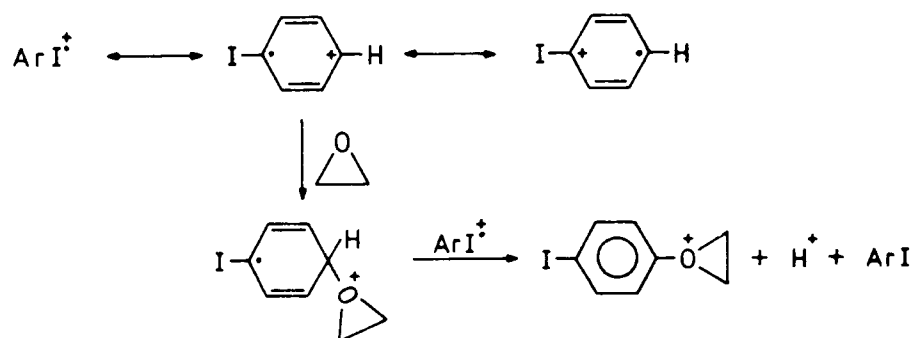
No conclusive explanation for this trend has yet been found but it has been suggested that the nucleophilicity of the anions and their stability towards fluoride ion loss must be relevant. The nucleophilicity of the anions decreases in the order:



Increased nucleophilicity of the anion will result in a decrease in the ion pair separation of the propagating species and hence a decrease in the rate of propagation. This effect should be most pronounced in the polymerization of less basic monomers. The tendency of the anions to eliminate a fluoride ion follows the same order as their nucleophilicity. On going from  $\text{BF}_4^-$  to  $\text{SbF}_6^-$  the frequency of the termination of polymerization by reaction of the cationic species with the anion should therefore decrease giving rise to the observed trend. The nucleophilicity of the monomer will be important in determining the occurrence of this termination process. Polymerization of a more nucleophilic monomer should be less subject

to such termination reactions. However if fluoride ion abstraction is significant with the anions  $\text{BF}_4^-$  and  $\text{PF}_6^-$  then  $\text{BF}_3$  and  $\text{PF}_5$  will be produced which are known to be effective initiators of the polymerization of epoxides.

In addition to initiation by a Brönsted acid, Ledwith has proposed that the radical-cation produced on the photolysis of iodonium and sulphonium salt photoinitiators may directly initiate polymerization by the mechanism shown below:<sup>18</sup>



This mechanism has received support from laser-flash photolysis studies of Pappas *et al* who found that the phenyliodonium radical-cation produced by irradiation of iodobenzene reacted with cyclohexene oxide and tetrahydrofuran.<sup>34</sup> This radical-cation was found to react with other nucleophiles such as methanol, water and acetone.

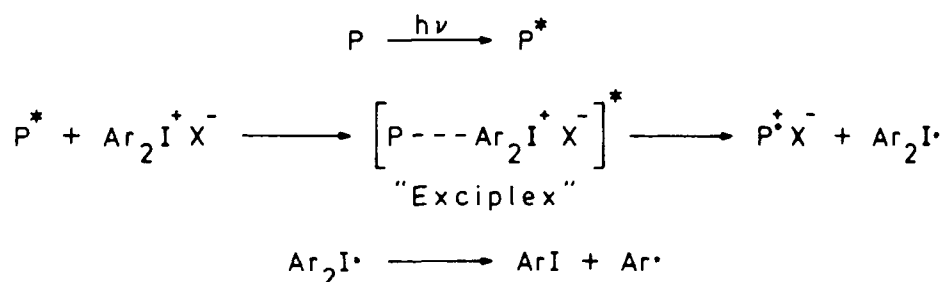
### (C) Photosensitization of Diaryliodonium Salts

A wide range of dyes,<sup>38</sup> aromatic hydrocarbons,<sup>37</sup> and aromatic ketones<sup>37</sup> will act as photosensitizers for the photolysis of diaryliodonium salts. Examples of such compounds are acridine orange, acetophenone and anthracene. Triplet-triplet energy transfer from photosensitizers such as acetophenone is favourable and does occur as is evidenced by the quenching of the phosphorescence of acetophenone by diphenyliodonium hexafluoroarsenate. However the quantum yield of phenyliodide

is very low,  $<0.05$  (this value is significantly lower than that quoted by Crivello and Lam under similar conditions). This eliminates energy transfer as the mechanism of photosensitization and also indicates that the triplet excited state of diaryliodonium salts is inactive as regards bond cleavage. However, two other mechanisms of photosensitization have been found to occur.

(i) Direct Electron Transfer

In this process, electron transfer occurs from the excited state photosensitizer to the ground state photoinitiator.<sup>37</sup>



The process may proceed *via* the formation of an "exciplex".<sup>39</sup> These excited state complexes are usually stabilized by charge transfer and their formation can be deduced from the occurrence of longer wavelength fluorescence than that from the free excited species. The "exciplex" may undergo charge separation leading to the formation of a radical cation species from the photosensitizer and a radical species from the diaryliodonium salt. The radical-cation derived from the photosensitizer is the species responsible for initiating cationic polymerization.

Sensitization using dyes and aromatic hydrocarbons is thought to take place by this mechanism. The products from the photosensitized photolysis of diaryliodonium salts have been analysed and found to correspond to those expected from the above mechanism.<sup>35</sup> Ledwith has reported that the N-ethyl-

2-ethylphenothiazine radical-cation can be observed in the photosensitized photolysis of diaryliodonium salts.<sup>18</sup> Similarly the perylene radical-cation has been observed in the photosensitization of sulphonium salts.<sup>35</sup>

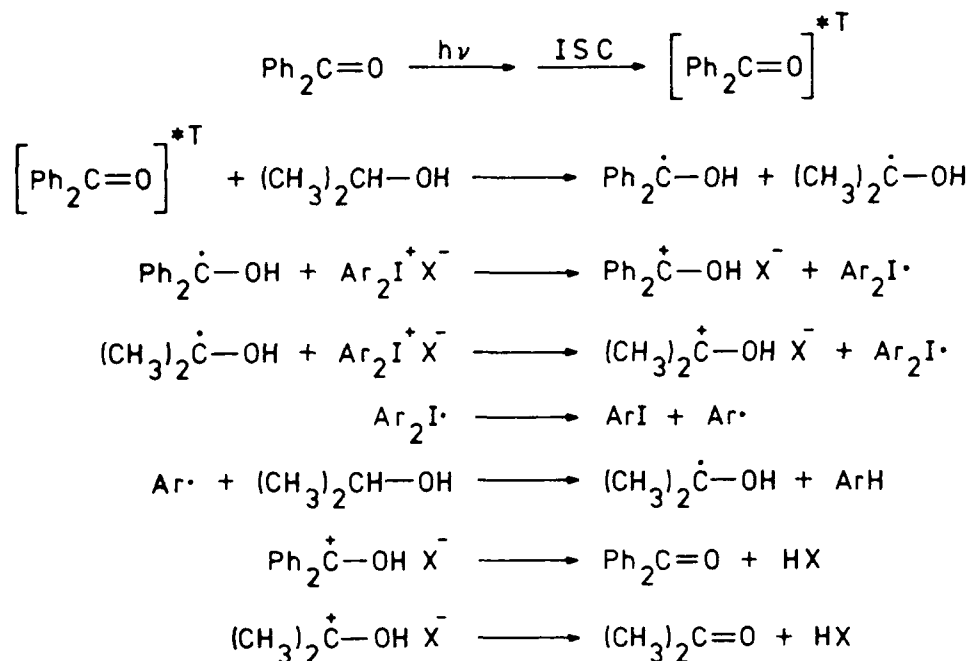
The thermodynamic favourability of both energy and electron transfer processes for a range of photosensitizers have been determined.<sup>37</sup> This has shown that in a number of cases where sensitization occurred, the former process is unfavourable whilst the latter process is favourable.

(ii) Indirect Electron Transfer

The quantum yield of phenyliodide from the benzophenone photosensitized photolysis of diphenyliodonium hexafluoroarsenate irradiated at 366nm in acetonitrile has been found to be very low. Electron transfer from benzophenone is unfavourable which agrees with the above observation.<sup>37</sup> However, the benzophenone/diphenyliodonium salt combination was found to initiate the cross-linking of a commercial epoxy resin, 3,4-epoxycyclohexyl-methyl-3',4'-epoxycyclohexane carboxylate, when irradiated with 366nm light. A possible explanation for this observation was proposed, involving hydrogen atom abstraction by the excited state benzophenone. The benzophenone photosensitized photolysis of the iodonium salt in acetonitrile was repeated with hydrogen donor molecules present. With tetrahydrofuran and propan-2-ol present, quantum yields for the formation of iodobenzene were found to be 3.3 and 2.4 respectively. The latter value increased to 4.9 when the measurement was repeated under vacuum. Addition of tetrahydrofuran to the sensitized photoinitiated cross-linking of the epoxy resin resulted in a significant decrease

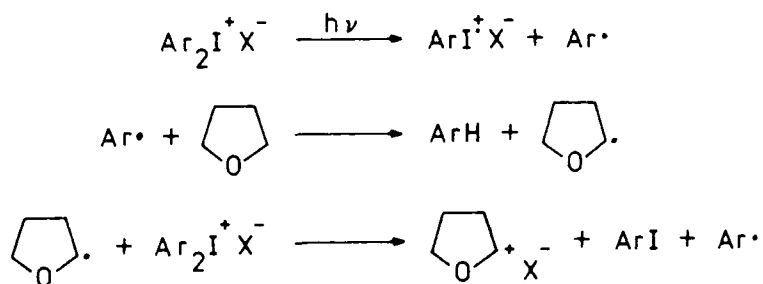
in the irradiation time required to produce gelation.

The results from the quantum yield studies indicate that a chain process involving free radicals is occurring. The mechanism proposed to account for the above effect involves the reduction of the diphenyliodonium salt by free radicals and is shown below with propan-2-ol as the hydrogen donor.



Free radical photoinitiators that undergo a Norrish Type I cleavage such as 2,2-dimethoxy-2-phenylacetophenone can also be used as photosensitisers.<sup>40</sup> In this case it is proposed that the radical species from the cleavage of the free radical photoinitiator are oxidized by the diphenyliodonium salt to yield cationic species that initiate polymerization.

Apparently the quantum yield of phenyliodide is significantly greater than one when diaryliodonium salts are photolysed in tetrahydrofuran at 366nm.<sup>35</sup> Again this is indicative of a chain-process and the following mechanism is proposed:

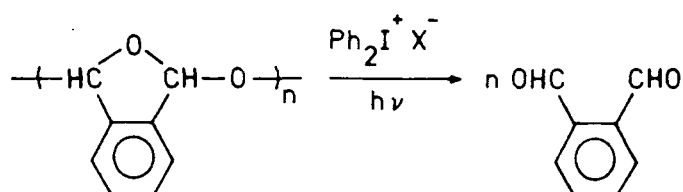


Ledwith however has reported that very little polymer formation occurs when diaryliodonium salts are used in the photoinitiated polymerization of tetrahydrofuran and irradiated at longer wavelengths.<sup>40</sup> In this experiment, the samples were irradiated through pyrex which absorbs light below approximately 300nm. This would indicate that high quantum yields for the photolysis of photoinitiators are no guarantee that rapid or effective initiation of polymerization will occur. Ledwith has noted this effect in a study of the photolysis of triarylsulphonium salts.<sup>18</sup> Unlike other triarylsulphonium salts, diphenyl-4-thiophenoxyphenylsulphonium salts were found to undergo a chain photodegradation process. Even though the quantum yield of photolysis was 1.5 and 3 in tetrahydrofuran and cyclohexene oxide respectively irradiated at 304nm, the quantum yield for polymer formation in the former monomer is only 0.06.

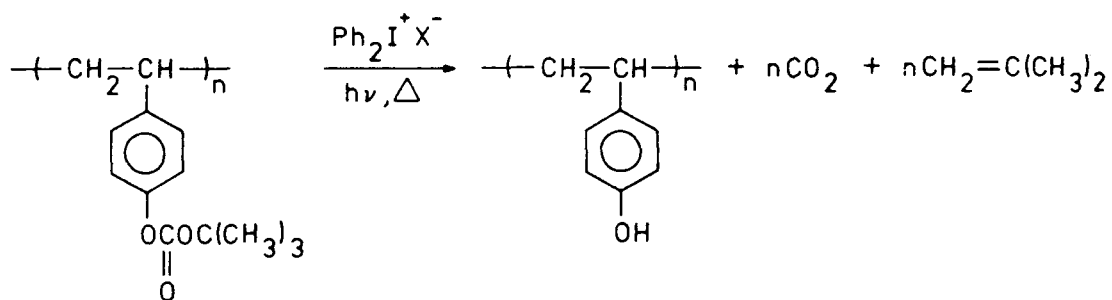
#### (D) Applications of Diaryliodonium Salt Photoinitiators

The ability of diaryliodonium salts to efficiently photoinitiate the cationic cure of epoxy resins in air has led to the possible commercial use of such systems as printing inks and adhesives as well as surface coatings. Since diaryliodonium salts only become active on irradiation another possible use is in photoresist systems<sup>6</sup> where light is used to induce a chemical change leading to a difference in solubility between

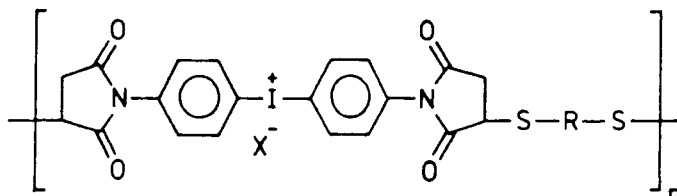
the unexposed and exposed regions of the photoresist. In negative photoresist systems, a decrease in solubility occurs in the irradiated areas whereas the opposite effect occurs in positive photoresist systems. Since cross-linked resins are insoluble, negative photoresist systems involving the photo-initiated cross-linking of epoxy resins have been reported.<sup>41</sup> Positive photoresist systems have been developed that make use of the strong Brönsted acid produced on the photolysis of diaryliodonium salts. For example the Brönsted acid can be used to catalyse the depolymerization of polymers such as poly(phthalaldehyde):<sup>41</sup>



The photogenerated acid has been shown to catalyse the thermalysis of t-butyloxycarbonyl group in poly(p-t-butoxycarbonyloxystyrene) to give poly(p-hydroxystyrene) which is preferentially soluble in polar solvents:<sup>41</sup>



A positive photoresist system in which diaryliodonium salt moieties have been incorporated into the backbone of a polymer chain has been reported:<sup>42</sup>



On irradiation, photolysis of the iodonium salt moiety leads to cleavage of the polymer chain and an increase in solubility.

Diaryliodonium salt photoinitiators can be used in the surface modification of bulk polymers.<sup>43</sup> A polymer such as polystyrene is doped with small amounts of an iodonium salt photoinitiator which on irradiation initiates polymerization of a monomer such as a vinyl ether adsorbed on the surface. The monomer is not grafted onto the bulk polymer but forms a homopolymer. Irradiation may be carried out with monomer present or prior to the introduction of monomer.

Thermal initiation of cationic polymerization can be achieved using diaryliodonium salt photoinitiators. The combination of free radical thermal initiators such as benzpinacol and iodonium salts has been shown to be effective at initiating polymerization.<sup>40,44</sup> The latter compounds oxidize the free radicals produced by the former compounds to give cationic species capable of initiating polymerization. The thermal decomposition of diaryliodonium salts, catalysed by copper (II) compounds yields a species capable of initiating cationic polymerization.<sup>45</sup> A trace amount of a reducing agent is usually necessary for the decomposition to occur. In addition, it has been found that diaryliodonium salts accelerate the cure of epoxy resins when anhydride curing agents are used.<sup>46</sup>

REFERENCES - CHAPTER TWO

1. C.H.J. Wells, "Introduction to Molecular Photochemistry", Chapman and Hall, London (1972).
2. F.C. De Schryver, N. Boens and G. Smets, J. Polym. Sci., Polym. Chem., 11, 1687 (1972).
3. S.P. Pappas and V.D. McGinnis in "UV Curing: Science and Technology", Ed. S.P. Pappas, Vol. 1, Technology Marketing Corporation (1978).
4. S.P. Pappas in "UV Curing: Science and Technology", Ed. S.P. Pappas, Vol. 2, Technology Marketing Corporation (1978).
5. G.E. Green, B.P. Stark and S.A. Zahir, J. Macro. Sci.-Revs. Macro. Chem., C21, 187 (1981-1982).
6. C.G. Roffey, "Photopolymerizations of Surface Coatings", Wiley-Interscience (1982).
7. A. Ledwith, J. Oil Col. Chem. Assoc., 59, 157 (1976).
8. A. Hult and B. Ranby, ACS Polym. Preprints, 25, 329 (1984).
9. (a) J.V. Crivello in Ref. 3.  
(b) W.R. Watt in Ref. 4.
10. J.J. Licari, W. Crepeau and P.C. Crepeau, U.S. Pat. 3205 257 (1965); C.A. 63:17368a.
11. J.V. Crivello and J.H.W. Lam, J. Polym. Sci., Polym. Symp., 56, 383 (1976).
12. J.V. Crivello and J.H.W. Lam, ACS Symp. Ser., 114, 1 (1978).
13. J.V. Crivello and J.H.W. Lam, J. Polym. Sci., Polym. Chem. Ed., 17, 1047 (1978).
14. J.V. Crivello, Ger. Offen. 2518 652, (1975); C.A. 84:60556e.
15. J.V. Crivello and J.H.W. Lam, J. Polym. Sci., Polym. Chem. Ed., 18, 1021 (1980).
16. G.E. Green and E. Irving, Eur. Pat. Appl. 22 081, (1981); C.A. 94:192949b.
17. A.D. Ketley and J.H. Tsao, J. Rad. Curing, 6, 22 (1979).
18. A. Ledwith, Reprints, Div. of Polym. Chem., ACS, 23, 323 (1982).
19. J.V. Crivello, Ger. Offen. 2 518 656, (1975); C.A. 84:75119.
20. J.V. Crivello and J.H.W. Lam, J. Polym. Sci., Polym. Chem. Ed., 17, 2877 (1979).
21. J.V. Crivello, U.S. Pat. 4 069 056, (1978), C.A. 88:138079s.
22. S.I. Schlesinger, Photog. Sci. and Eng., 18, 387 (1974).

23. J.V. Crivello and W.H. Lam, *J.Polym.Chem., Polym.Lett.*, 16, 563, (1978).
24. J.V. Crivello and W.H. Lam, *Macromols.*, 10, 1307 (1977).
25. J.V. Crivello, J.H.M. Lam and C.N. Volante, *J.Rad.Curing*, 4, 2 (1977).
26. J.V. Crivello and J.H.W. Lam, *J.Polym.Sci., Polym.Chem.Ed.*, 17, 977 (1977).
27. J.V. Crivello and J.H.W. Lam, *J.Polym.Sci., Polym.Chem.Ed.*, 18, 2677 (1980).
28. J.V. Crivello and J.H.W. Lam, *J.Polym.Sci., Polym.Chem.Ed.*, 17, 1059 (1979).
29. J.V. Crivello and J.H.W. Lam, *J.Polym.Sci., Polym.Chem.Ed.*, 18, 2697 (1980).
30. C. Hartmann and V. Meyer, *Chem.Ber.*, 27, 426 (1894).
31. G.A. Olah, "Halonium Ions", Wiley-Interscience (1975).
32. F.M. Beringer and I. Lillien, *J.Am.Chem.Soc.*, 82, 5136 (1960).
33. J.W. Knapczyk, J. Luminkowski and W.E. McEwan, *Tet.Lett.*, 35, 3739 (1972).
34. S.P. Pappas, B.C. Pappas, L.R. Gatechair, J.H.Jilek and W. Schnabel, *Polym.Photochem.*, 5, 1 (1984).
35. J.V. Crivello, *Adv.Polym.Chem.*, 62, 1 (1984).
36. R.S. Davidson and J.W. Goodin, *Eur.Polym.J.*, 18, 589 (1982).
37. S.P. Pappas and L.R. Gatechair, *Proceedings of the Water Borne and Higher Solids Coatings Symposium*, 8, 85 (1981).
38. J.V. Crivello and W.H. Lam, *J.Polym.Sci., Polym.Chem.Ed.*, 16, 2441 (1978).
39. D. Phillips, *J. Oil Col.Chem.Assoc.*, 59, 202 (1976).
40. F.A.A. Abdul-Rasoul, A. Ledwith and Y. Yogci, *Polymer*, 19, 1219 (1978).
41. M. Ito and C.G. Wilson, *ACS Symp.Ser.*, 242, 11 (1984).
42. J.V. Crivello and J.H.W. Lam, *J.Polym.Sci., Polym.Chem.Ed.*, 17, 3845 (1979).
43. A. Hult, S.A. MacDonald and C.G. Wilson, *Macromols.*, 18, 1804 (1985).
44. A. Ledwith, *Polymer*, 19, 1217 (1978).
45. J.V. Crivello, T.P. Lockhart and J.L. Lee, *J.Polym.Sci., Polym.Chem.Ed.*, 21, 97 (1983).
46. D.S. Johnson, U.S. Pat. 4 398 013 (1983); C.A. 99:123655u.

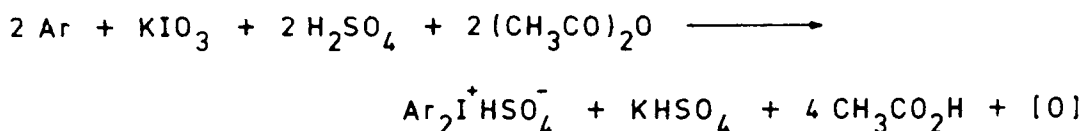
CHAPTER THREE

SYNTHESIS OF DIPHENYLIODONIUM  
HEXAFLUOROPHOSPHATE AND THE ANALYSIS  
OF THE COMMERCIAL MONOMERS

### 3.1 Synthesis of the Diaryliodonium Salt Photoinitiators

#### (A) Synthetic Routes to Diaryliodonium Salts

Crivello and Lam used three methods for synthesising symmetrical diaryliodonium salts having electron donating or withdrawing substituents and unsymmetrical diaryliodonium salts.<sup>1</sup> Method A is that used to prepare dialkyl substituted diaryliodonium salts or the simple diphenyliodonium salt:<sup>2</sup>



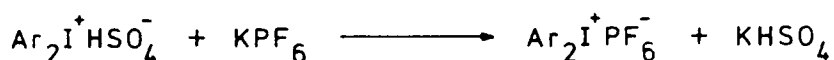
#### Method A

The synthesis of diaryliodonium salts bearing electron donating substituents can be carried out using Method B:<sup>3</sup>



#### Method B

Crivello and Lam<sup>1</sup> found that the bisulphate anion could be replaced quite easily by complex anions such as  $\text{AsF}_5^-$ ,  $\text{PF}_6^-$  and  $\text{SbF}_6^-$  by simple metathesis with the alkali metal salt of the complex anion, for example:



Richards<sup>4</sup> attempted the synthesis of bis(4-ethylphenyl)iodonium hexafluorophosphate using Methods A and B, both proved unsuccessful. The synthesis of diphenyliodonium hexafluorophosphate was successful using Method A but not Method B. Using Method A, bis(4-methylphenyl)iodonium and bis(3,4-dimethylphenyl)iodonium hexafluorophosphate were synthesised. However the anion exchange step and the purification of these two salts proved difficult. Since diphenyliodonium hexafluorophosphate is easily prepared and purified it was decided that this iodonium salt should be prepared and used as the photoinitiator.

(B) Preparation and Characterization of Diphenyliodonium Hexafluorophosphate

Potassium iodate (12.5g, 0.06 moles), acetic anhydride (14 cm<sup>3</sup>, 0.15 moles) and benzene (12 cm<sup>3</sup>, 0.04 moles) were placed in a 100 cm<sup>3</sup> round-bottom, three-neck flask equipped with a condenser, dropping funnel and a thermometer. The mixture was stirred using a magnetic follower (in subsequent preparations a mechanical stirrer was used) and cooled to -5°C. A mixture of concentrated sulphuric acid (10 cm<sup>3</sup>) and acetic anhydride (14 cm<sup>3</sup>) was prepared using an ice bath to maintain a low temperature. The addition of the concentrated sulphuric acid/acetic anhydride mixture to the contents of the flask was carried out slowly so that the temperature did not rise above 5°C. When all the sulphuric acid/acetic anhydride mixture had been added, the contents of the flask and the ice-bath were allowed to reach room temperature. To allow completion of the reaction, the contents of the flask were left stirring for sixty hours. At the end of this time the reaction mixture was cooled to 0°C and 25 cm<sup>3</sup> of distilled water added slowly so that the temperature did not rise above 5°C. Diethyl ether (15 cm<sup>3</sup>) was then added and the mixture filtered to remove potassium bisulphate. The filtrate was extracted twice with diethyl ether (15 cm<sup>3</sup>) and then once with 30/40 petroleum ether (15 cm<sup>3</sup>).

Potassium hexafluorophosphate (12.6g, 0.07 moles) was added to the aqueous layer, which gave a white precipitate. The mixture was diluted with water by a factor of four and left on a flask shaker for 2 hours. The solid was then filtered off and washed thoroughly with distilled water. After drying for

twenty hours at 56°C under vacuum in a drying pistol the yield was 40%. The product was then recrystallised from butanone and dried as before. In subsequent preparations, it was found that the product could be adequately dried under vacuum over P<sub>2</sub>O<sub>5</sub> and that it could be purified by reprecipitation from butanone using petroleum ether as a non-solvent.

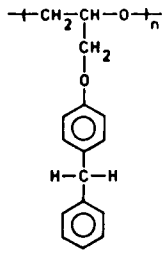
The melting point of the purified product was 134-136°C (lit. value<sup>5</sup>: 138-141°C). Elemental analysis gave the following:

	%C	%H	%I	%P	%F
Calculated	33.8	2.4	29.8	7.3	26.8
Found	34.0	2.5	30.6	7.0	27.8

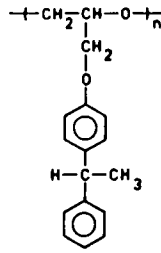
No potassium impurity was detected.

The infra-red spectrum (Appendix Four, No.1) was identical to that obtained by Richards<sup>4</sup> and did not indicate the presence of moisture or butanone. The spectrum contains peaks at 3080 cm<sup>-1</sup> and 3060 cm<sup>-1</sup> due to the aromatic C-H stretch, 1570 cm<sup>-1</sup> due to the aromatic breathing mode, 1465 cm<sup>-1</sup> and 1445 cm<sup>-1</sup> due to the substituted aromatic C-H bend and an intense peak at 830 cm<sup>-1</sup> due to P-F stretch. The <sup>1</sup>H-NMR spectrum recorded on a Brüker Spectrospin HX 90E showed resonances at 8.26 and 7.55 ppm due to the aromatic protons. No further resonances were detected other than those from the solvent, acetone. The <sup>19</sup>F-NMR spectrum showed a doublet at 71.03 ppm upfield of CFCl<sub>3</sub>. The doublet is due to coupling between the fluorine atoms and the central phosphorus atom with J<sub>P-F</sub> equal to 703 Hz.

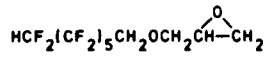
The ultraviolet spectrum of the photoinitiator was recorded using methanol, ethanol and acetonitrile as the solvents.



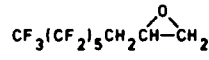
(XXXVIII)



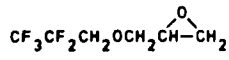
(XXXIX)



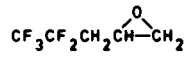
(XLII)



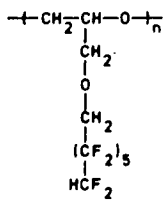
(XLIII)



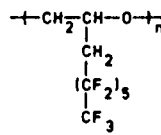
(XLIV)



(XLV)

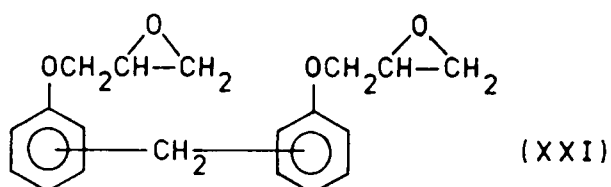


(XLVII)



(XLVIII)

Richards<sup>4</sup> found that films of the resins CY 179 and CY 177 containing photoinitiator, only cured at the surface even after prolonged irradiation. This is contrary to reports in the literature<sup>6,7</sup> which indicate that resins of this type cure faster than those of the glycidyl ether type. The DGEBA, (XVIII), epoxy novolac, (XIX), and aliphatic diglycidyl ether (XX) resins were found to undergo satisfactory cure to give tack-free films. These three resins along with a "purified" sample of the diglycidyl ether of bisphenol F, DGEBF, (XXI)



also obtained from Ciba-Geigy were used in the work reported in this thesis.

#### (A) Infra-Red Spectra of the Monomers

The infra-red spectra of the four resins are shown in Appendix Four (Spectra Nos. 2-5). Table 3.2 shows the assignments of a number of bands in the spectra.

All the resins show an absorption at  $\approx 3500 \text{ cm}^{-1}$  in their spectrum, attributable to hydroxyl functionality although in the case of the DGEBF resin this was very small. In all cases the presence of hydroxyl functionality could be due to the presence of small amounts of chlorohydrin groups, (XXII) or  $\alpha$ -glycol groups (XXIII)

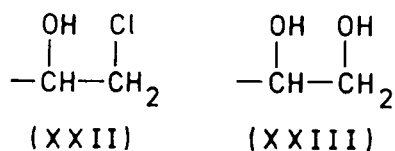
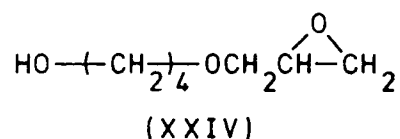


TABLE 3.2 Assignment of Bands in the IR Spectra of the Monomers

Frequency/cm <sup>-1</sup>	(XVIII)	(XIX)	(XXI)	(XX)
3500 - 3400	O-H stretch	O-H stretch	O-H stretch	O-H stretch
3060 - 3010	Oxirane C-H stretch + aromatic C-H stretch	Oxirane C-H stretch + aromatic C-H stretch	Oxirane C-H stretch + aromatic C-H stretch	Oxirane C-H stretch
2990 - 2840	Aliphatic C-H stretch	Aliphatic C-H stretch	Aliphatic C-H stretch	Aliphatic C-H stretch
1610 - 1605	Aromatic ring breathing	Aromatic ring breathing	Aromatic ring breathing	
1520 - 1330	Aliphatic C-H bend + aromatic ring breathing	Aliphatic C-H bend + aromatic ring breathing	Aliphatic C-H bend + aromatic ring breathing	Aliphatic C-H bend
1250 - 1240	Aromatic ether asymmetric stretch	Aromatic ether asymmetric stretch	Aromatic ether asymmetric stretch	
1100				Aliphatic ether asymmetric stretch
1035 - 1020	Aromatic ether symmetric stretch	Aromatic ether symmetric stretch	Aromatic ether symmetric stretch	
915 - 900	Oxirane ring stretch	Oxirane ring stretch	Oxirane ring stretch	Oxirane ring stretch
855 - 830	Oxirane ring stretch	Oxirane ring stretch	Oxirane ring stretch	Oxirane ring stretch

The DGEBF, epoxy novolac and DGEBF resins may also contain glycerol ether links as shown in the structure of the DGEBA resin (XVIII), which introduces secondary alcohol functionality. The incomplete reaction of butanediol with epichlorohydrin will result in the resin (XX) containing some monoglycidyl ether (XXIV) which may account for most of the hydroxyl functionality present in this resin.



(B) Epoxide Content, Hydroxyl Content and the Molecular Weight of the Monomers

Richards<sup>4</sup> determined the epoxide group content, the hydroxyl content and the number-average molecular weight of the three monomers (XVIII), (XIX) and (XX). The epoxide group content of each resin was determined by a chemical method and the results are shown in Table 3.3.

A chemical method and spectroscopic method were used to determine the hydroxyl content of the resins. The latter method involved reacting any hydroxyl groups with hexafluoroacetone and then determining the amount of adduct formed using <sup>19</sup>F-NMR. The results from both techniques are shown in Table 3.3. The number-average molecular weight of each resin shown in Table 3.3 was determined using a vapour pressure molecular weight apparatus.

The value of  $\bar{M}_n$  for the DGEBA resin indicates that the value of n in the structural formula (XVIII) is ~0.03 since it is expected that the secondary hydroxyl group of the glycerol

TABLE 3.3. Molecular Weight and Chemical Analysis of the Monomers

Monomer	$\bar{M}_n$	Epoxide functionality	Hydroxyl functionality (chem. analysis)	Hydroxyl functionality (spect. analysis)
(XVIII)	347	1.95	0.25	0.03
(XIX)	628	3.36	0.37	0.17
(XX)	184	1.64	0.14	0.10

ether links will account for the majority of the hydroxyl functionality present, this would tend to agree with the hydroxyl content as determined by the spectroscopic method.

The value of  $n$  in the structural formula (XIX) of the epoxy novolac resin is 1.95 from the number-average molecular weight determination. The molecular weight for the pure aliphatic diglycidyl ether resin would be expected to be 202. The measured value seems a little low which could be due to some low molecular weight impurity. Taking a value of 0.12 for the hydroxyl content and assuming that the majority of this arises from the monoglycidyl ether (XXIV) then the value of  $\bar{M}_n$  for the mixture is *c.a.* 196.

(C)  $^1\text{H-NMR}$  and  $^{13}\text{C-NMR}$  Spectra of the Monomers

Richards<sup>4</sup> recorded the  $^1\text{H-NMR}$  and  $^{13}\text{C-NMR}$  spectra of the three monomers (XVIII), (XIX) and (XX) on spectrometers operating at frequencies of 22.6 MHz for  $^{13}\text{C}$ -nuclei and 60 MHz for  $^1\text{H}$ -nuclei. Since those spectra were recorded, access to instruments operating at much higher frequencies has become available. The assignment of resonances and interpretation of  $^1\text{H-NMR}$  spectra in particular can be made easier when they are recorded on instruments operating at higher

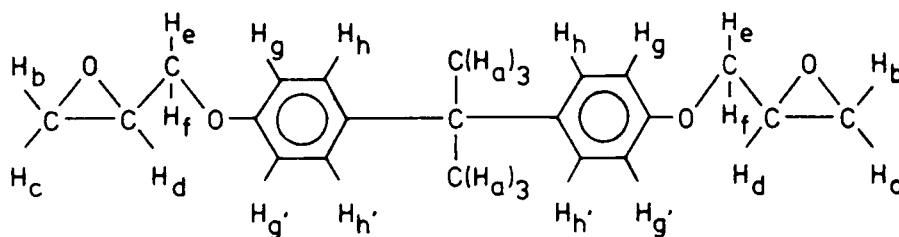


frequencies since the frequency separation of proton resonances is increased. More information was obtained from the spectra of the resins, particularly the  $^1\text{H-NMR}$  spectrum of the aliphatic glycidyl ether of butanediol, run on an instrument operating at 300 MHz for  $^1\text{H-nuclei}$  and 75 MHz for  $^{13}\text{C-nuclei}$ .

(i) The DGEBA Resin

The  $^1\text{H-NMR}$  spectrum of the DGEBA resin (Appendix Five, Spectrum No.1) shows numerous small peaks, presumably due to impurities, the most intense ones having shifts of 1.66 and 2.28 p.p.m. The  $^1\text{H-NMR}$  data given in Table 3.4 is consistent with this resin being a diglycidyl ether of bisphenol A.

TABLE 3.4  $^1\text{H-NMR}$  Data for (XVIII)

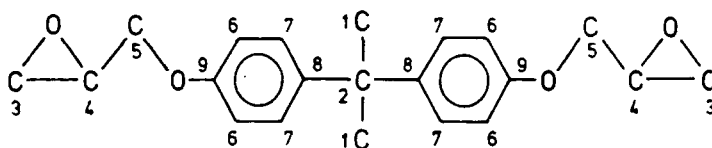


Proton	Shift/ppm	Splitting	Integration
$\text{H}_a$	1.59	Singlet	6
$\text{H}_b$	$\delta_A = 2.62$	$\text{AB}_q$ $J_{b-c}^2 \sim 4.5 \text{ Hz}, J_{c-d}^3 \sim 4.3 \text{ Hz}$	2
$\text{H}_c$	$\delta_B = 2.75$	$J_{b-d}^3 \sim 2.3 \text{ Hz}$	2
$\text{H}_d$	3.22	Multiplet	2
$\text{H}_e$ or $\text{H}_f$	$\delta_A = 3.81$	$\text{AB}_q$ $J_{e-f}^2 = 11.0 \text{ Hz}$	2
$\text{H}_e$ or $\text{H}_f$	$\delta_B = 4.11$	$J_{e/f-d}^3 = 5.8 \text{ Hz}, J_{f/e-d}^3 = 2.6 \text{ Hz}$	2
$\text{H}_g$ or $\text{H}_{g'}$	$\delta_A = 6.78$	Pseudo $\text{AB}_q$	4
$\text{H}_h$ and $\text{H}_{h'}$	$\delta_B = 7.10$	$J_{g-h} = J_{g'-h'} = 8.4 \text{ Hz}$	4

The "Handbook of Epoxy Resins"<sup>8</sup> was particularly useful in assigning the proton resonances in this spectrum.

The assignment of the resonances in the  $^{13}\text{C}$ -spectrum of (XVIII) (Appendix 5, Spectrum No.2) is shown in Table 3.5. The assignment of the oxirane carbons was helped by the work of Moniz and Poranski<sup>9</sup> whilst the assignment of the aromatic carbons agreed with those for bisphenol A given in "Carbon-13 Nuclear Magnetic Resonance Spectroscopy".<sup>10</sup>

TABLE 3.5 Assignment of  $^{13}\text{C}$  Resonances in the Spectrum of (XVIII)

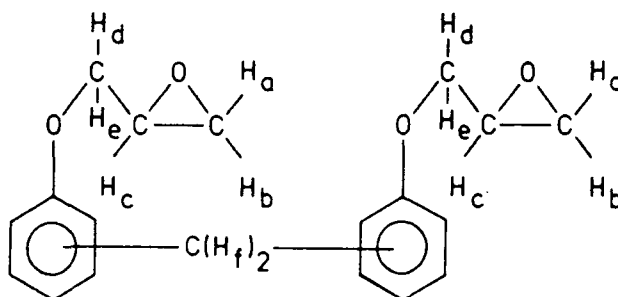


Nucleus	Shift/PPM	Nucleus	Shift/PPM
C <sub>1</sub>	30.94	C <sub>6</sub>	114.00
C <sub>2</sub>	41.57	C <sub>7</sub>	127.64
C <sub>3</sub>	44.35	C <sub>8</sub>	143.45
C <sub>4</sub>	50.01	C <sub>9</sub>	156.32
C <sub>5</sub>	68.74		

(ii) The DGEBF Resin

The complexity of the spectrum (Appendix 5, Spectrum No.3) indicated that there were a number of isomers of this compound present. From the  $^{13}\text{C}$  spectrum it becomes apparent that there are three isomers present, with the methylene groups linking the two aromatic rings para-para (P-P), para-ortho (O-P) and ortho-ortho (O-O) to the glycidyl ether groups. Table 3.6 shows the assignment of the resonances in the  $^1\text{H}$ -NMR spectrum.

TABLE 3.6 Assignment of the  $^1\text{H}$  resonances in the Spectrum of (XXI)



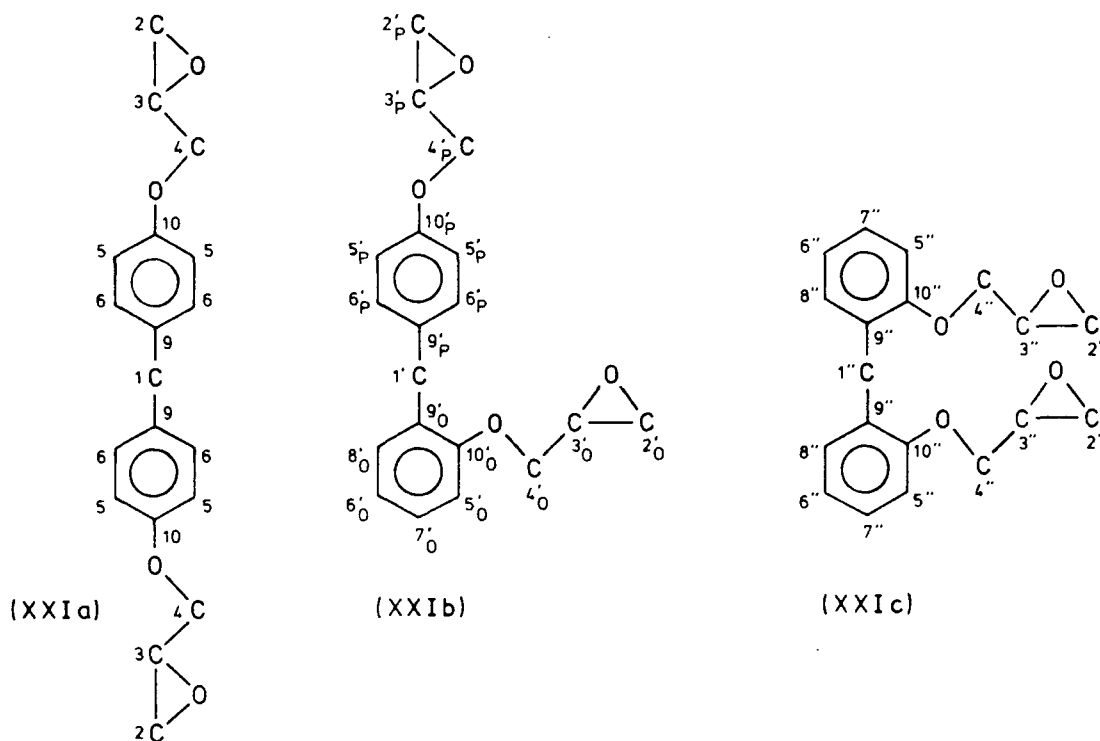
Proton	Shift/PPM	Splitting	Integration
$\text{H}_a$	$\delta_A \sim 2.60$	Overlapping $\text{AB}_q\text{s}$	2
$\text{H}_b$	$\delta_B \sim 2.74$		2
$\text{H}_c$	3.20	Multiplet	2
$\text{H}_d$ or $\text{H}_e$	$\delta_A \sim 3.80$	Overlapping $\text{AB}_q\text{s}$	4
+ $\text{H}_f(\text{P-P})$			$(2\text{H}_f + 2\text{H}_{d/e})$
$\text{H}_d$ or $\text{H}_e$	$\delta_B \sim 4.87$		2
$\text{H}_f(\text{O-P})$	4.01	Singlet	
$\text{H}_f(\text{O-O})$	4.05	Singlet	
Aromatic	6.80	Multiplet	4
protons	7.07	Multiplet	4

-----

The initial assignment of three resonances in the  $^{13}\text{C}$ -NMR spectrum to the methylene carbons linking the aromatic groups in the three isomers allowed the amount of each isomer to be determined. The percentage of each isomer (XXIa), (XXIb) and (XXIc) shown in Table 3.7 is 31%, 51% and 18% respectively. This observation combined with simple calculations based on additivity increments<sup>11</sup> allowed the

assignment of the remainder of the resonances in the  $^{13}\text{C}$  spectrum (Appendix 5, Spectrum No.4) to be made, as shown in Table 3.7.

TABLE 3.7 Assignment of Resonances in the  $^{13}\text{C}$  Spectrum of DGEBF



Nucleus	Shift/PPM	Nucleus	Shift/PPM
1''	30.04	7'	127.15
1'	35.20	7' <sub>O</sub>	127.38
1	40.10	6	129.75
2+2' <sub>O</sub> + 2' <sub>P</sub> + 3''	[ 44.32 44.39	6' <sub>P</sub>	[ 129.87 130.39
3+3' <sub>O</sub> + 3' <sub>P</sub> + 3''	50.06	8' <sub>O</sub> +8'''+9' <sub>O</sub> +9''	[ 130.48 130.67
4+4' <sub>O</sub> + 4' <sub>P</sub> + 4''	68.97	9' <sub>P</sub>	133.74
5''	111.89	9	134.21
5' <sub>O</sub>	111.99	10' <sub>O</sub>	156.30
5' <sub>P</sub>	114.63	10''	156.56
5	114.79	10' <sub>P</sub>	156.87
6''	121.00	10	157.00
6' <sub>O</sub>	121.14		

The assignment of the aromatic carbons agrees with those made for the three isomers of dianisylmethane reported in the literature.<sup>10</sup>

(iii) The Epoxy Novolac Resin

Since there are at least seventeen different ways of joining the four aromatic rings present in this resin through the methylene groups with the links being ortho or para to glycidyl ether groups it is not surprising that the <sup>1</sup>H-NMR spectrum is very complex (Appendix 5, Spectrum No.5). The resonances of the methylene protons of the oxirane ring occur at ~2.7 ppm and ~2.8 ppm, with that of the methine proton at ~3.3 ppm. The methoxy protons and those of the methylene linkages between the aromatic rings give resonances between 3.8 ppm and 4.2 ppm. The aromatic protons resonate at ~6.7 ppm and ~7.2 ppm.

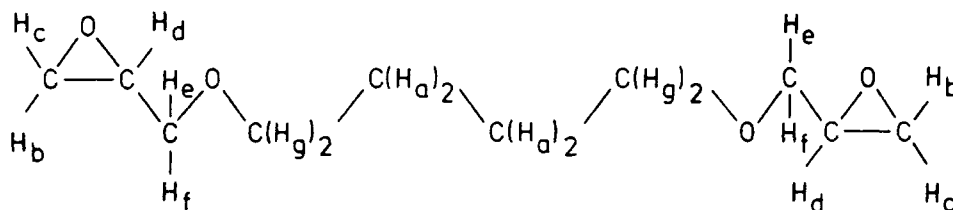
The <sup>13</sup>C-NMR spectrum (Appendix 5, Spectrum No.6) is again complicated due to the possible number of isomers present. The peaks at 29.52, 34.64 and 39.48 ppm are due to the carbons of the methylene groups linking the aromatic rings and indicate that 30.1% link para-para, 52% link ortho-para and 18% link ortho-ortho to the glycidyl ether groups. Generally the spectrum shows resonances with similar shifts to those in the spectrum of DGEBF, indicating that carbon atoms in similar environments are present.

(iv) The Diglycidyl Ether of Butanediol

The <sup>1</sup>H spectrum of this diglycidyl ether of butanediol (Appendix 5, Spectrum No.7) shows the presence of aromatic

protons due to some impurity at 7.5 ppm which occurred in all the samples of this resin and also peaks at  $\sim 3.6$  ppm from the aliphatic protons of some impurity. Table 3.8 gives the assignments of the major resonances

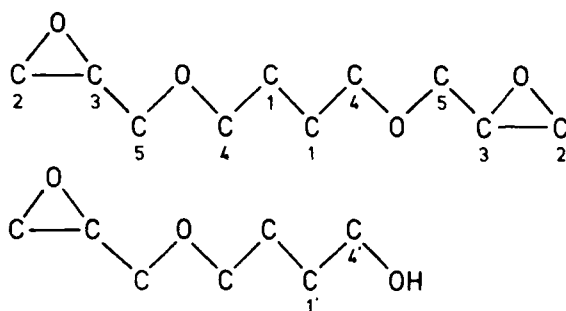
TABLE 3.8 Assignment of the  $^1\text{H}$  Resonances in the Spectrum of (XX)



Proton	Shift/ppm	Splitting	Integration
H <sub>a</sub>	1.64	Multiplet	4
H <sub>b</sub>	$\delta_A = 2.58$	$AB_q$ $J_{b-c}^2 = 5.1 \text{ Hz}$	2
H <sub>c</sub>	$\delta_B = 2.76$	$J_{c-d}^3 = 4.3 \text{ Hz}, J_{b-d}^3 = 2.7 \text{ Hz}$	2
H <sub>d</sub>	3.11	Multiplet	2
H <sub>e</sub> or H <sub>f</sub>	$\delta_A = 3.34$	$AB_q$ $J_{e-f}^2 = 11.5 \text{ Hz}$ $J_{e/f-d}^3 = 5.9 \text{ Hz}$	2
H <sub>e</sub> or H <sub>f</sub>	$\delta_B = 3.71$	$J_{f/e-d}^3 = 2.9 \text{ Hz}$	2
H <sub>g</sub>	3.49	Multiplet	4.4

The  $^{13}\text{C}$  spectrum (Appendix 5, Spectrum No.8) shows many small peaks due to impurity. Two of these peaks at 29.6 and 62.1 ppm could possibly be due to the presence of the mono-glycidyl ether (XXIV). Table 3.9 shows the peak assignments.

TABLE 3.9 Assignment of the  $^{13}\text{C}$  Resonances in the Spectrum of (XX)



Carbon	Shift/PPM	Carbon	Shift/PPM
1	26.36	4'	42.14
1'	29.62	4	71.14
2	44.02	5	71.46
3	50.77		

-----

(D) Ultraviolet Spectra of the Monomers

It is of interest to know the UV absorption characteristics of the resins for comparison with those of the photoinitiator. Table 3.10 gives the wavelengths of maximum absorption by each resin and the values of the extinction coefficient. The latter values will be very approximate since the resins do not have well defined molecular weights and will contain species that absorb at similar wavelengths but to different extents.

The aliphatic diglycidyl ether, (XX), shows a small absorption at  $\sim 220$  nm which appears to be a shoulder on an absorption below 200 nm. Absorption of light by this resin would not be expected to compete with absorption by the photoinitiator above 230 nm. However there is a small but significant absorption present at 275 nm which is indicative

TABLE 3.10 Data from the UV Absorption Spectra of the Monomers

Resin	Solvent	$\lambda_{\max}/\text{nm}$	$\epsilon_{\max}/\text{cm}^{-1}\text{mol}^{-1}\text{dm}^3$
(XX)	ethanol	220(s)	44
(XVIII)	ethanol	227(s)	$2.01 \times 10^4$
		276	$3.3 \times 10^3$
		283(s)	
(XXI)	ethanol	224(s)	$1.74 \times 10^4$
		272(s)	
		277	$3.4 \times 10^3$
(XXI)	chloroform	275(s)	
		278	$3.4 \times 10^3$
(XIX)	chloroform	278	$7.1 \times 10^3$

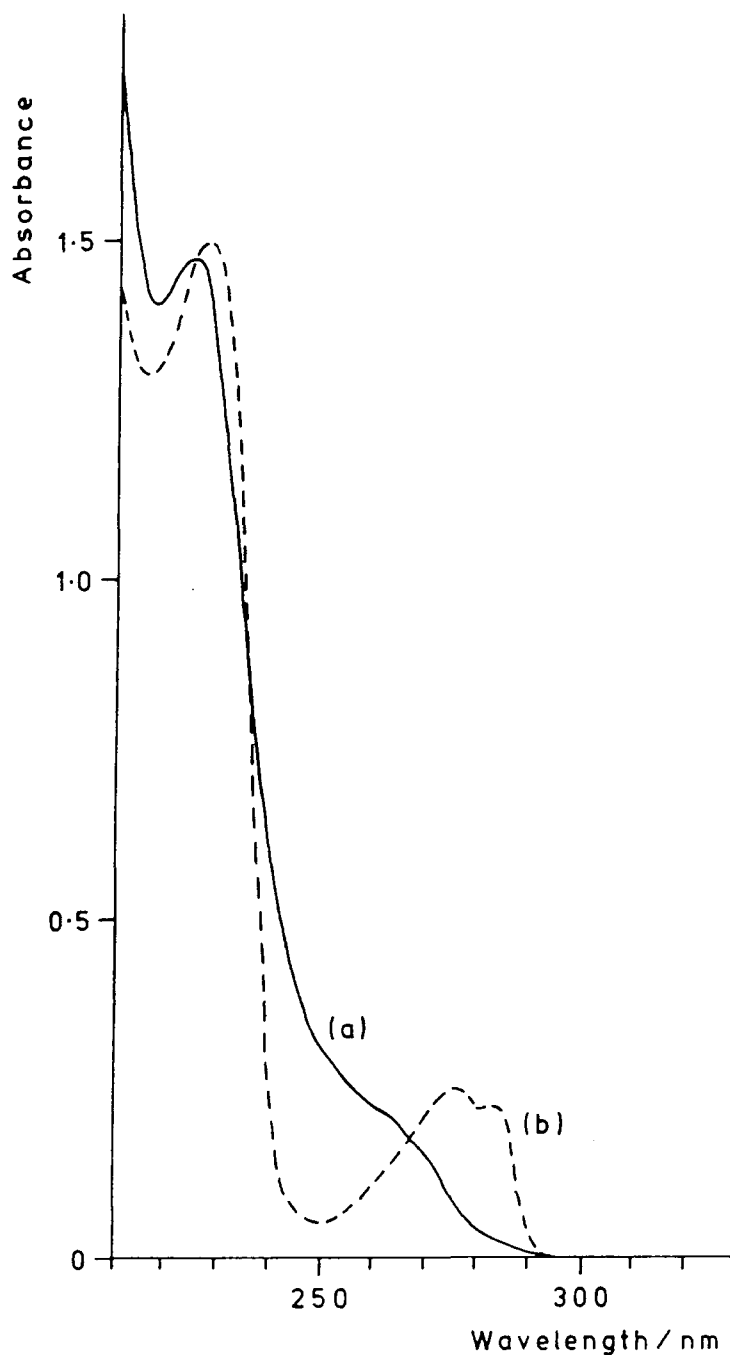
(s) = shoulder

of an aryl chromophore. The presence of an aromatic impurity has already been inferred from the  $^1\text{H-NMR}$  spectrum of this resin.

The remainder of the resins all contain aryl ether chromophores and are expected to absorb strongly below 300 nm.

The DGEBA and DGEBF resins show an intense absorption band in the 220-230 nm region as will the epoxy novolac resin. Absorption in this region by the resins will interfere strongly with that of the photoinitiator. The resins also absorb in the 270-280 nm region which will again compete with absorption of light by the photoinitiator. From Figure 3.1 which shows the absorption spectra of diphenyliodonium hexafluorophosphate and the DGEBA resin it is apparent that the photoinitiator absorbs more strongly than this resin

FIGURE 3.1 UV Absorption Spectra of diphenyliodonium hexafluorophosphate ( $\sim 8.8 \times 10^{-5} \text{ mol dm}^{-3}$ ), (a), and (XVIII) ( $\sim 7.6 \times 10^{-5} \text{ mol dm}^{-3}$ ), (b)



in the 250nm region. This also applies to the other resins of this type. However, in the photocurable composition of the resin and photoinitiator, the resin is present in far greater amounts than the photoinitiator and would be expected to absorb much more of the incident light at shorter wavelengths possibly hindering the photolysis of photoinitiator.

REFERENCES - CHAPTER THREE

1. J.V. Crivello and J.H.W. Lam, J.Polym.Sci., Polym.Symp., 56, 383 (1976).
2. F.M. Beringer, M. Drexler, E.M. Gindler and C.C. Lumpkin, J.Am.Chem.Soc., 75, 2705 (1953).
3. I. Masson and E. Race, J.Chem.Soc., 2, 1718 (1937).
4. D.S. Richards, M.Sc. Thesis, Durham (1982).
5. J.V. Crivello and W.H. Lam, Macromols., 10, 1307 (1977).
6. J.V. Crivello in "UV Curing Science and Technology", Ed. S.P. Pappas, Vol.1, Technology Marketing Corporation (1978).
7. J.V. Crivello, J.H.W. Lam and C.N. Volante, J.Rad. Curing, 4, 2 (1977).
8. H.L. Lee and K. Neville, "Handbook of Epoxy Resin", McGraw-Hill (1967).
9. W.B. Moniz and C.F. Poranski, ACS Symp.Ser., 114 (1978).
10. G.C. Levy, R.L. Lichter and G.L. Nelson, "Carbon-13 Nuclear Magnetic Resonance Spectroscopy", 2nd Ed., Wiley-Interscience (1980).
11. R.M. Silverstein, G.C. Bassler and T.C. Morrill, "Spectroscopic Identification of Organic Compounds", 4th Ed., J.Wiley and Sons (1981).

CHAPTER FOUR

THE EFFECT OF VARIOUS PARAMETERS  
ON THE PHOTOINITIATED CATIONIC  
CROSS-LINKING POLYMERIZATION OF  
EPOXY RESINS AND THE EVIDENCE FOR  
INHOMOGENEOUS NETWORK FORMATION

#### 4.1 Introduction

One of the main factors affecting the properties and characteristics of a cured resin is the degree of cure or cross-linking. For example, better chemical resistance properties of a cured resin are obtained when the maximum degree of cross-linking is achieved.<sup>1</sup> The rate and final degree of cure in the photoinitiated cross-linking of resins might be expected to be related to the film thickness, the irradiation time, the light intensity and wavelength, the temperature and the concentration of the photoinitiator. The effect of temperature on the curing process is an important factor in possible marine tank coating applications. If such systems showed promising chemical or solvent resistance and cured rapidly at temperatures as low as 0°C then they would have an advantage over conventionally cured epoxy resins. The photoinitiator will be one of the more expensive components in photocurable surface coatings, so it is desirable to ascertain the lowest acceptable concentration of photoinitiator. One of the potential disadvantages of photoinitiated cure is the deleterious effect of pigments on the penetration of light into the interior of the coating,<sup>2</sup> preventing or reducing the initiation of polymerization. Although unpigmented photocurable coatings could be used as varnishes for example, the scope for such systems in surface coating applications would be greatly enhanced if they could be pigmented.

The nature of cationic polymerizations means that photocationically cured systems have the potential to undergo further cross-linking after irradiation.<sup>3</sup> As the cross-linking continues, the properties of the material could change significantly which may have a bearing on any potential applications.

Knowledge of the extent to which this continued polymerization occurs and the time scale over which it takes place are therefore important.

This chapter reports the results of investigations into the affect of the factors outlined above on the photoinitiated cationic cure of, principally, the DGEBA resin. In addition the chemical resistance, adhesion and ability of photocationically and conventionally cured epoxy resins to prevent corrosion are compared.

#### 4.2 Determining the Degree of Cure of Network Polymers

There are two approaches to obtaining a measure of the degree of cure of network polymers, namely, determining the extent of reaction of functional groups or alternatively measuring some physical property related to the degree of cross-linking.<sup>1</sup>

##### (A) Measuring the Extent of Reaction

This approach is widely used as an indication of the degree of cross-linking in network polymers including cured epoxy resins. However it must be noted that the consumption of epoxide functional groups does not necessarily imply that the degree of cross-linking has increased.

Although cross-linked epoxy resins are insoluble, which makes the investigation of such systems difficult, chemical analysis can be used to determine the amount of unreacted epoxide functionality present by swelling the powdered material in a suitable solvent.<sup>4</sup> Until quite recently, infra-red spectroscopy was the only spectroscopic technique available to measure the amount of unreacted functionality present in cross-linked resins.

Recently it has been demonstrated that the relatively new technique of solid state NMR can be used for such measurements;<sup>5</sup> however this technique is not routinely available.

In this study infra-red spectroscopy was used to determine the extent of reaction of epoxide functionality whilst DSC was used to investigate the potential for post-irradiation thermal cure. The use of these two techniques is described below in more detail.

(i) Infra-Red Spectroscopy

Infra-red spectroscopy is a readily available analytical technique that can provide a rapid, quantitative measure of the disappearance or appearance of functionality during the curing process. Dannenberg and Harp<sup>4</sup> measured the percentage of unreacted epoxide groups in an amine cured resin by both chemical analysis and IR spectroscopy. The two techniques were found to give comparable results. Quantitative IR measurements, for example, have been used in a detailed study of the cure kinetics of epoxy resins using anhydride curing agents and found to be satisfactory.<sup>6</sup>

To measure the absorbance of a particular functional group a baseline is defined as, for example, in Figure 4.1. The relatively arbitrary nature of the baseline is one of the factors contributing to the lack of accuracy which can occur with quantitative IR measurements.

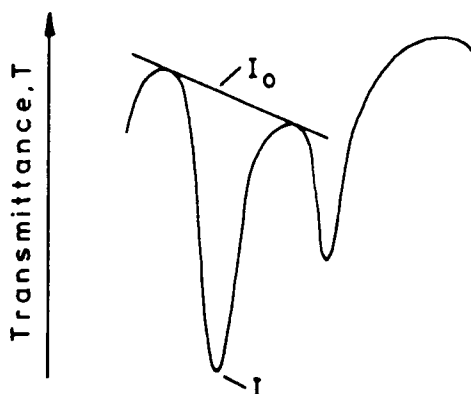


FIGURE 4.1 Example of Baseline Construction

The absorbance,  $A$ , at a particular wavelength can be calculated using the following expression:

$$A = \log_{10} \left( \frac{T_{I_0}}{T_I} \right)$$

As the expression indicates, absorbance is not directly proportional to transmittance and small changes in the 0 to 20% transmittance region result in large changes in the absorbance value. Therefore in the interests of accuracy the use of absorption bands in this transmittance range should be avoided for quantitative measurements.

Variations in sample thickness can be allowed for when comparing different samples by expressing the absorbance of the peak of interest as a ratio of the absorbance of a reference peak. The reference peak may be due to some other functional group of the material or to some inert compound present in known amounts. The simplest method of quantifying the amount of unreacted functionality in a cured resin is to express the normalized absorbance due to the functional group as a percentage of the normalized absorbance due to the functional groups in the uncured system. This assumes that the absorption characteristics of the material are similar in the solid and liquid states.

(ii) Differential Scanning Calorimetry

The information that can be obtained from DSC makes it a powerful tool for the thermal analysis of polymerization reactions and polymers. In the scanning mode the calorimeter records the differential power supplied to the sample and reference holder required to maintain them at identical temperatures, as the temperature is raised. Chemical reactions and first order transitions such as melting points give rise to peaks on the DSC trace. The area under such a peak is proportional to

the enthalpy change of the process. An absolute value for the enthalpy change of the process can be obtained by prior calibration. Isothermal measurements can also be carried out, in which the rate of heat taken in or given out by the sample is recorded as a function of time at a particular temperature. Again the area under the isothermal peak is a measure of the enthalpy change of the process.

Both the isothermal and scanning modes have been used to investigate the thermal cure of epoxy resins by conventional curing agents.<sup>7,8</sup> Assuming that the enthalpy change at a particular point in the process is proportional to the extent of reaction allows the percentage conversion of functional groups to be determined by comparison with the total enthalpy change for the reaction, assuming that this corresponds to complete conversion of functional groups.

Isothermal DSC has proved useful for determining the extent of reaction in both photoinitiated free radical and cationic chain cross-linking polymerizations.<sup>9,10,11</sup> In the studies reported, the calorimeter has been modified to allow the irradiation of samples while in the sample holder. A continuous measure of monomer conversion is then provided by the heat evolved from the sample as it is irradiated.

(B) The Glass Transition Temperature,  $T_g$ , as a Measure of the Degree of Cross-Linking

(i) The Glass Transition

Generally as a hard, glassy, amorphous polymer is slowly heated it will eventually soften and show rubber-like behaviour. This change in behaviour occurs over quite a narrow temperature range. A glass transition can also take place if a soft, rubbery, amorphous polymer is cooled. In this case the

change is to glass-like behaviour. Although the glass transition occurs over a temperature range, a single temperature known as the glass transition temperature,  $T_g$ , is defined. The  $T_g$  has an important bearing on the potential applications of amorphous polymers. A lower temperature limit is set on the uses of elastomers and rubbers whilst an upper limit is set on the use of rigid linear and cross-linked polymers.

On a molecular scale, the change from glass-like to rubber-like behaviour is associated with the onset of segmental motion of the polymer chains.<sup>12</sup> At temperatures below  $T_g$ , there is some vibrational motion of the chain segments about a fixed position or possibly some rotational motion of side groups. As the temperature is raised, the amplitude and cooperative nature of the vibrational movements increases until secondary intramolecular forces are overcome. Loops and segments of polymer chain may then undergo rotational and translational cooperative motion giving rise to the rubber-like behaviour. The translational motion of whole polymer chains in linear polymers is prevented by entanglements, but as the temperature is further raised this restriction is surmounted and the polymer acts like a viscous liquid. In a truly crystalline polymer only a melting transition is observed whereas in a semi-crystalline polymer a glass transition may be observed due to the above type of molecular motion in the amorphous regions.

The relatively simple picture of changes in molecular motion being responsible for the difference in behaviour of an amorphous polymer above and below its  $T_g$ , belies the complex nature of the glass transition and the difficulty in obtaining a theoretical model that satisfactorily accounts for all the features of this phenomenon.<sup>12,13,14</sup>

A first order thermodynamic transition such as a melting point is characterized by a discontinuity in the first derivatives of free energy such as enthalpy or entropy. A discontinuity in the heat capacity or coefficient of expansion which are second derivatives of free energy is a characteristic of second order transitions. Early workers were prompted to refer to the glass transition as a second order transition because of the similarity in the behaviour of the heat capacity of polymers on passing through the glass transition. However significant differences in the behaviour of the second derivatives of free energy do exist for the two types of transition. Furthermore the glass transition cannot be regarded as a true thermodynamic transition since the value of  $T_g$  obtained is dependent on the thermal history of the sample and the heating rate used in carrying out the measurement. An increase in the value of  $T_g$  is observed with increasing heating rate which is not solely a consequence of the rate of heat transfer to the sample but also results from the slowness of relaxation processes at temperatures close to or below  $T_g$ .<sup>15</sup>

One of the more successful theoretical approaches to describing the glass transition is the free volume theory.<sup>14,16</sup> The glass transition temperature is related to the free volume of the polymer, that is the difference between the actual volume and the volume occupied by the polymer chains. The effect of such factors as the chain structure, molecular weight, presence of small molecules and cross-linking on the  $T_g$  of a polymer can be explained in terms of a change in the free volume of the system or, alternatively a change in the segmental mobility of the polymer chains. Increasing the free volume or the segmental mobility results in a decrease of  $T_g$ .

(ii) The Effect of Cross-Linking on Tg

An important but complex example of the effect of cross-linking on the Tg of a polymer is the vulcanization of rubber. Well over a hundred years ago, it was found that a series of products ranging from soft, rubbery materials to a hard substance called ebonite resulted, when the amount of sulphur reacted with natural rubber was increased. The reaction of sulphur with natural rubber leads to cross-linking and an increase in Tg which explains the above observation.<sup>13</sup>

When polymer chains are cross-linked both the free volume and segmental mobility are decreased leading to an increase in Tg. The structure of highly cross-linked polymers may be so rigid that a glass transition cannot be observed, degradation of the polymer occurring before Tg is reached.

Fox and Loshaek<sup>17</sup> copolymerized styrene with various amounts of divinylbenzene by a free radical mechanism to yield polymers with various degrees of cross-linking. The Tgs of this series of network polymers were found to obey a semi-empirical expression of the form:

$$T_g = T_{g_\infty} + (\text{constant} \times \Gamma)$$

The constant  $T_{g_\infty}$  is the Tg of an infinite molecular weight linear polymer composed of the same repeat units as the cross-linked polymer, in this case polystyrene. The quantity  $\Gamma$  is the cross-link density of the polymer which may be defined as the number of cross-links per unit volume. Styrene-divinylbenzene copolymers with well defined average molecular weight between cross-links,  $\bar{M}_c$ , have been prepared by anionic living polymerizations and their Tg measured.<sup>18</sup> It was found that the Tg of the polymers was linearly related to the inverse of

$\bar{M}_c$ . This is in accord with the relationship found by Fox and Loshaek since  $\bar{M}_c$  is inversely proportional to  $\Gamma$ .

It has been shown qualitatively that  $T_g$  increases with the degree of cross-linking in conventionally cured epoxy resins by measuring the  $T_g$  of samples as a function of the cure temperature and time.<sup>19</sup> More quantitative measurements using DSC have shown that  $T_g$  increases with increasing percentage conversion of functional groups for amine cured epoxy resins.<sup>8,20</sup> The increase of  $T_g$  in such systems with conversion will not only be a consequence of an increase in cross-linking but also of a reduction in the plasticizing effect of monomer and oligomers as they become bound into the network. The variation of  $T_g$  with  $\bar{M}_c$  for amine cured epoxy resins has been investigated.<sup>21</sup> A series of DGEBA resins of increasing average molecular weight were fully cured and their  $T_g$ s determined. The results showed that  $T_g$  is inversely proportional to  $\bar{M}_c$  again indicating the increase of  $T_g$  with cross-link density.

(iii) The Effect of the Glass Transition on Cross-Linking Polymerizations

As a polymerization reaction proceeds, the  $T_g$  of the system increases significantly. If  $T_g$  becomes equal to the temperature at which the polymerization is carried out then the mobility of the system is greatly reduced and the polymerization becomes diffusion controlled. Polymerization may cease completely if the  $T_g$  becomes significantly greater than the temperature of the polymerizing system. This effect known as vitrification occurs in both linear and non-linear bulk polymerizations. If an epoxy resin is cured at a temperature below the  $T_g$  of the fully cured system then on subsequent heating additional conversion occurs.<sup>7</sup> As indicated in Chapter One

this effect also occurs in chain cross-linking homo- and copolymerizations of vinyl monomers.<sup>11</sup>

Gillham *et al*<sup>22,23</sup> have studied in detail, using torsional braid analysis, the conventional cure of epoxy resin systems. Three distinct types of behaviour were observed depending on the temperature of cure,  $T_c$ , relative to the glass transition temperature of the ungelled system,  $T_{gg}$ , and the fully cured system  $T_{g\infty}$ . When  $T_c$  is lower than  $T_{gg}$  vitrification and the cessation of reaction occurs prior to gelation. If  $T_c$  is raised so that it is between  $T_{gg}$  and  $T_g$ , gelation and then vitrification of the cross-linked system is observed. Only gelation is observed when  $T_c$  is greater than  $T_{g\infty}$ .

### (C) Methods of Measuring $T_g$

Since numerous physical properties of a polymer show a change on passing through a glass transition, it is not surprising that a variety of techniques ranging from dilatometry to broad line  $^1\text{H-NMR}$  may be used to determine  $T_g$ . Comprehensive lists<sup>15,24</sup> of the techniques available have been recorded in the literature. In this study, thermo-mechanical analysis (penetrometry), TMA, and DSC were used to measure the  $T_g$  of a photo-cured epoxy resin system.

#### (i) Differential Scanning Calorimetry

The second derivative of free energy, heat capacity, shows a discontinuity or step increase on passing through a glass transition. Since the signal from the calorimeter is proportional to the specific heat capacity of the sample, a step in the baseline is observed when such a transition occurs, as shown in Figure 4.2.

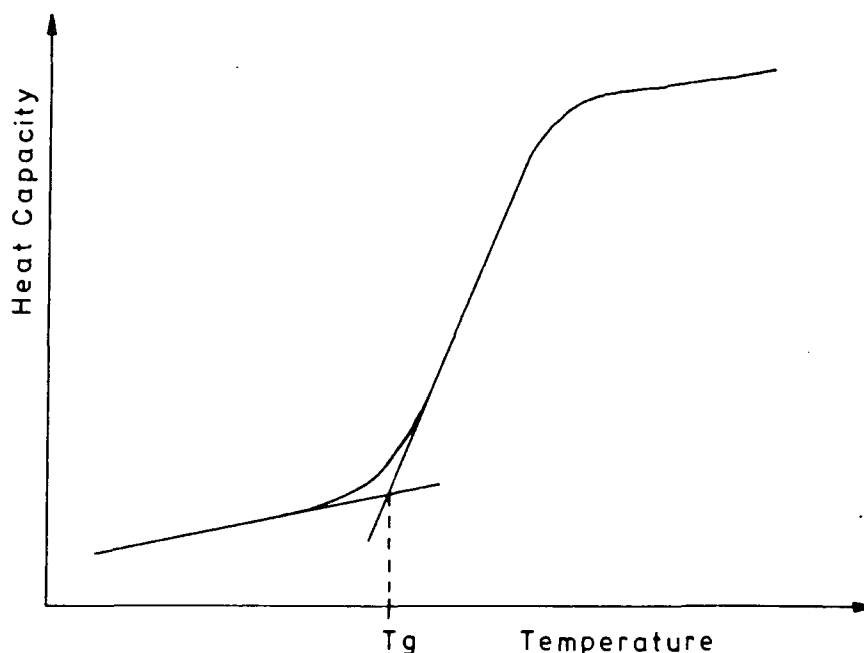


FIGURE 4.2 Change in Heat Capacity for a Glass Transition

In this study the glass transition temperature was taken from the intersection of the extrapolation of the baseline with the extrapolation of the inflexion as shown in Figure 4.2, rather than determining the temperature of the mid-point of the shift in the baseline which is often quoted as  $T_g$ . The adopted procedure gives a temperature corresponding to the onset of the transition.

(ii) Thermo-mechanical Analysis

The basis of the technique of penetrometry is that the increased segmental mobility at the glass transition allows a probe to penetrate the polymer sample. This method of  $T_g$  determination is both rapid and relatively simple. The dimensional changes associated with the glass transition measured by TMA are greater than the heat capacity changes measured by DSC, glass transitions are thus much easier to detect using the former technique.<sup>25</sup> The values of  $T_g$  obtained by penetrometry tend to be lower than those obtained using DSC which has been attributed to the stress activation of relaxation processes by the penetrometer method.<sup>8</sup>

A Stanton Redcroft TMA 691 was used in this work with which both penetrometric and dilatometric measurements of  $T_g$  may be carried out. For penetrometric measurements a quartz probe with a  $1 \text{ mm}^2$  tip is used which rests on the polymer sample. The load on the probe can be varied (0-200g) to give a reasonable degree of penetration at the glass transition. A temperature control unit allows the sample to be heated at a controlled rate. Any movement of the probe as the sample is heated is translated into an electrical signal proportional to the magnitude of the movement and displayed on a chart recorder along with the sample temperature. Figure 4.3 shows an example of a trace obtained for polymethylmethacrylate, PMMA, and indicated the temperature corresponding to the onset of penetration was defined at the  $T_g$  of the sample.

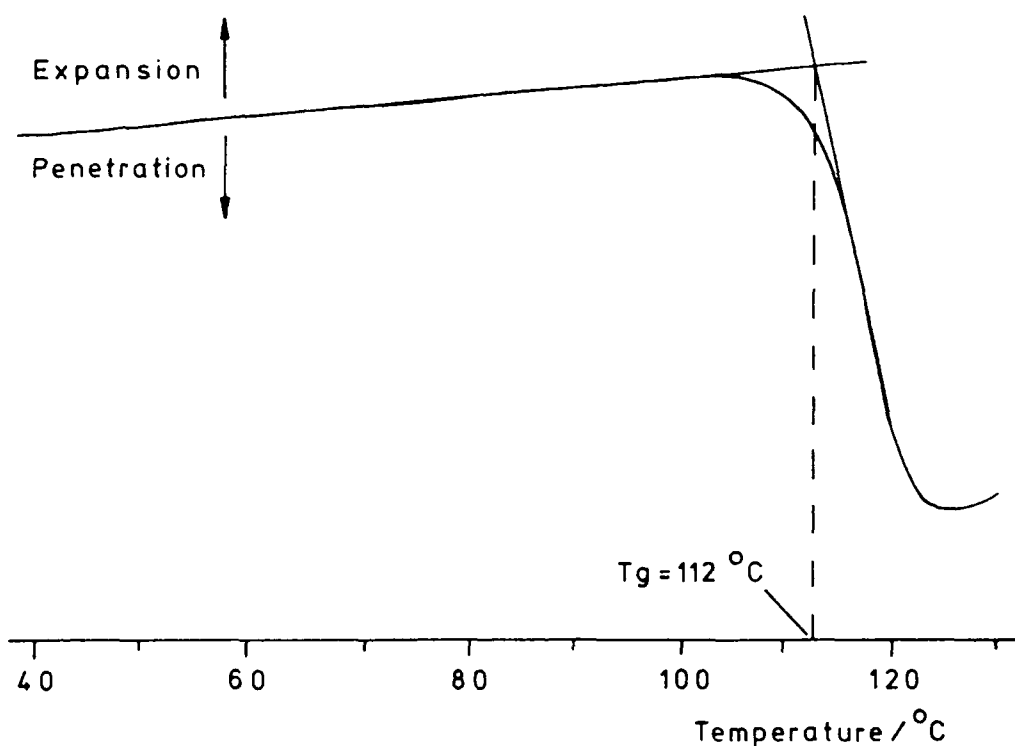


FIGURE 4.3 Example of a TMA Trace of PMMA

The thermocouple measuring the sample temperature was calibrated against a thermometer certified by the National Physical Laboratory using an oil bath as a heat source. Agreement between the thermocouple and the thermometer to within  $1^{\circ}\text{C}$  was found at  $50^{\circ}\text{C}$ ,  $100^{\circ}\text{C}$  and  $150^{\circ}\text{C}$ . Using samples taken from a piece of injection moulded PMMA the effect of heating rate, load and thermal history on the measured value of  $T_g$  as well as the reproducibility of this technique were investigated. Unless otherwise stated, each measurement was carried out on a fresh sample at a heating rate of  $5^{\circ}\text{C min}^{-1}$ , using a 20g load.

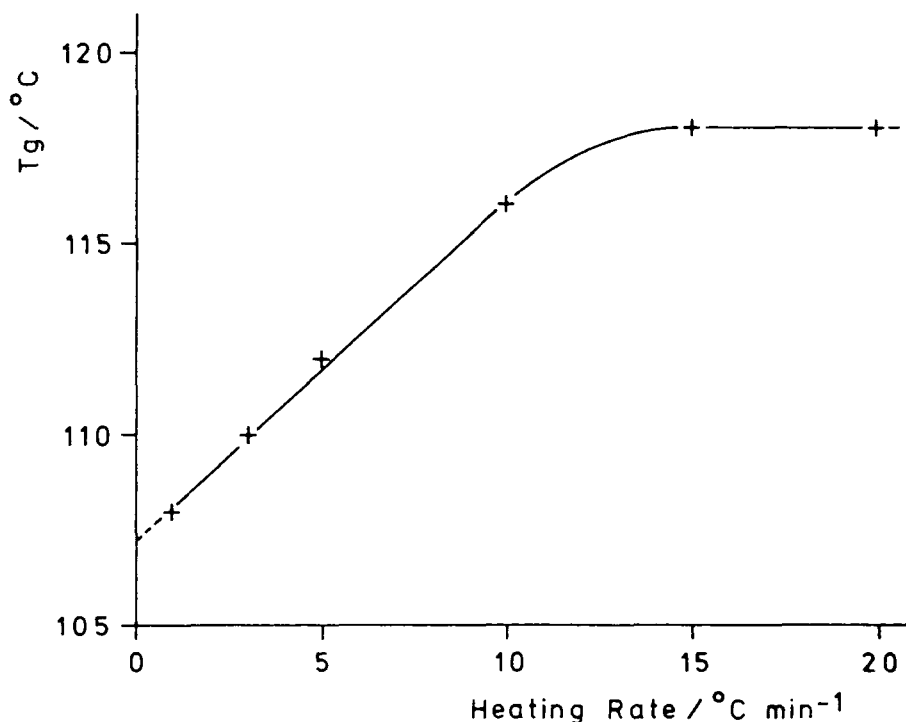


FIGURE 4.4 Effect of Heating Rate on the  $T_g$  of PMMA as measured by TMA

Figure 4.4 shows the dependence of  $T_g$  on heating rate for the PMMA samples. As expected the  $T_g$  increases with increasing heating rate until at high heating rates a constant value of  $T_g$  is obtained. Extrapolation to the physically meaningless point of zero heating rate yields a  $T_g$  of  $107^{\circ}\text{C}$ .

In view of the numerous variables affecting the measurement of Tgs and the unknown characteristics of the samples used, this value and the ones obtained at lower heating rates agree very well with the value of  $105^{\circ}\text{C}$  quoted in the literature.<sup>15</sup> The magnitude of the load used on the probe was found not to have a significant affect on the Tg value obtained. The average of ten measurements was found to be  $112^{\circ}\text{C}$  with a standard deviation of  $\pm 1^{\circ}\text{C}$  showing the method is quite reproducible. When the Tg measurement of a sample was repeated a slight increase in Tg was observed but no further increase occurred on subsequent measurements.

The Tgs of commercial samples of other polymers were measured. These samples of polystyrene, polycarbonate of bisphenol A and polyethersulfone gave Tg values of  $88^{\circ}\text{C}$ ,  $151^{\circ}\text{C}$  and  $226^{\circ}\text{C}$  respectively which are in only reasonable agreement with the literature values of  $100^{\circ}\text{C}$ ,  $145^{\circ}\text{C}$  and  $214^{\circ}\text{C}$  respectively,<sup>15</sup> and probably illustrate the variation of Tg with the thermal history of the sample and the measuring technique used. The TMA trace of the polycarbonate sample tended to show two steps, indicating the occurrence of two glass transitions, the second one being some  $15^{\circ}\text{C}$  to  $20^{\circ}\text{C}$  higher than that quoted above. This effect may be due to the fact that the probe rested on the curved surface of a granule of polymer rather than a flat surface as with the other polymer samples.

#### (D) Other Properties Related to the Degree of Cross-Linking

A number of subjective tests are used, particularly in the field of surface coatings, to follow the cure of resins. An example of such a test is the tack-free test, in which the time taken for the coating to become non-tacky to the touch is determined. In an attempt to remove some of the subjectivity of

this test, Watt has developed an instrument to determine the tack-free time of photocurable resin systems.<sup>3</sup> Tests of this type offer no quantitative information about the degree of cross-linking and in photocured systems probably do not reflect the extent of cure in the bulk of the sample.

The interaction of a network polymer with a suitable solvent leads to swelling of the polymer which can be used to quantify the degree of cross-linking. The magnitude of the swelling is inversely proportional to the cross-link density providing a qualitative measure of the degree of cross-linking, in for example, cured epoxy resins.<sup>4</sup> More quantitative data from swelling measurements such as the average molecular weight between cross-links has been obtained for amine cured epoxy resins.<sup>26</sup>

Analysis of the pulsed  $^1\text{H}$ -NMR decay curves and the measurement of the dielectric constant are other techniques which have been used to follow the cross-linking of the photocured monomers.<sup>27</sup> In this work, hardness measurements and gel content were used as guides to the degree of cure in the cross-linked resins.

(i) Hardness

The hardness of a resin is related to the degree of cross-linking as well as the structure of the network polymer between cross-links and can be used to follow the cross-linking of a given resin system. A quite subjective but simple qualitative procedure for determining the hardness of a cured resin is to establish the type of pencil lead (2B, HB, *etc.*) required to mark the surface. Richards<sup>28</sup> used this technique to follow the post-irradiation hardening of photocured epoxy resins.

More quantitative measurements of hardness have been used to investigate the free radical photoinitiated cure of dimethacrylate resins at various depths into the sample as a function of irradiation time.<sup>29</sup>

In this study the hardness of the photocured resins was determined semiquantitatively using a micro-indentation tester. This instrument accurately measures the depth to which a diamond-tipped probe under a known load penetrates the sample. When carrying out the measurements, films of the sample were prepared on rigid substrates. With the sample held firmly in place, the probe is lowered so that it is in contact with the surface of the film. A small primary weight is placed on the probe to ensure good contact. After a given time has elapsed the heavier secondary weight is applied to the probe. The depth of penetration of the probe is then read from a micrometer gauge after a given time.

(ii) Gel Content

As indicated in Chapter One, not all the monomer becomes bound into the polymer network and in addition soluble polymer may be formed. The amount of insoluble gel can be determined by extracting the soluble material using a suitable solvent. This technique is quite widely used in the study of network polymers as a measure of the degree of cross-linking.<sup>24</sup>

A known amount of the cross-linked polymer is extracted for a given time at a given temperature either by placing it directly in the solvent or using a Soxhlet apparatus. Either the gel or sol fraction can be recovered dried and weighed. Expressing the amount of insoluble material as a percentage of the original weight of the sample gives the gel content.

### 4.3 The Preparation and Irradiation of Films of the Monomers

#### (A) Film Preparation

The DGEBA resin, (XVIII), was prone to slow crystallization. To obtain this resin in a liquid form, it was dissolved in toluene, filtered and then the toluene removed under reduced pressure. Gently warming the resin prepared in this way, if it showed any subsequent signs of crystallizing, ensured it was all in the liquid form. The DGEBF, (XXI), resin also tended to crystallize but was obtained in a liquid form by gentle warming. Simple lacquers containing resin, photoinitiator and acetone were prepared from the DGEBA, DGEBF and aliphatic diglycidyl ether, (XX), resins. The photoinitiator was dissolved in acetone to aid its dispersion in the resin. The epoxy novolac resin (XIX) is a solid with a melting point close to room temperature and the preparation of a mobile lacquer required the addition of 12-14% w/w toluene. All the lacquers prepared were mixed thoroughly by hand prior to use.

Films of the lacquers of the DGEBA and epoxy novolac resins were generally prepared using a draw-down block. This is a metal cube with a hole drilled between two opposite faces and a channel cut from the hole to one of the edges, the width of this channel being equal to the diameter of the hole. The face of the cube with the channel cut into it is placed on the substrate, the hole filled with lacquer and the block drawn down the substrate in the opposite direction to the channel, leaving a film of lacquer. The depth of the channel determines the thickness of the film produced.

A different technique of film preparation was used for lacquers of mobile resins such as the aliphatic diglycidyl ether or if large areas of film were required. In those instances,

adhesive tape was used to provide barriers within which the lacquer was spread. The thickness of adhesive tape ("sellotape") is  $\sim 50\mu\text{m}$  so the film thickness could be increased from  $50\mu\text{m}$  in  $50\mu\text{m}$  steps. Unless otherwise stated, draw-down blocks were used to prepare films of the lacquers.

(B) UV Sources used

(i) The 100W Lamp

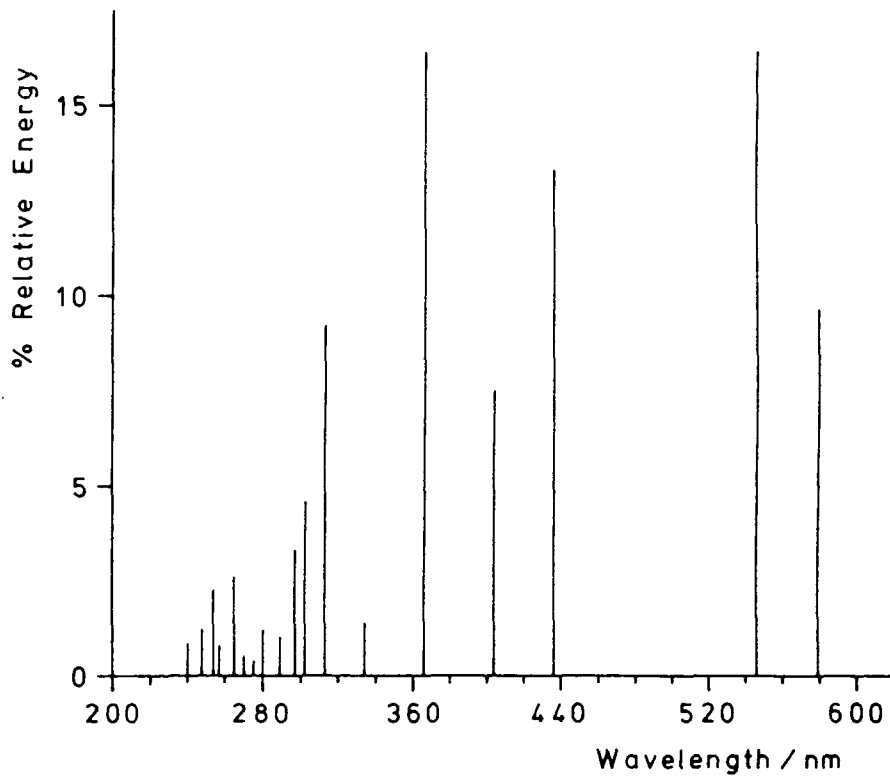
This UV source was taken from a Hanovia 1 litre photo-chemical reactor. The lamp was mounted horizontally with its quartz envelope and thimble in place. Water was passed between the envelope and thimble to cool the lamp and to prevent heating of the sample being irradiated. Ozone formation could be suppressed by flushing the envelope with nitrogen. The sample to be irradiated was placed on a laboratory jack at the desired distance from the lamp. An aluminium shield that covered the lamp and the sample could be used to prevent the escape of stray radiation.

The power consumption of this medium pressure mercury arc lamp is 100W, giving a radiative flux of  $\sim 25\text{W}$  including emission in the visible and infra-red regions. Figure 4.5(a) shows the spectral distribution of the radiation emitted by the lamp in the UV and visible regions.

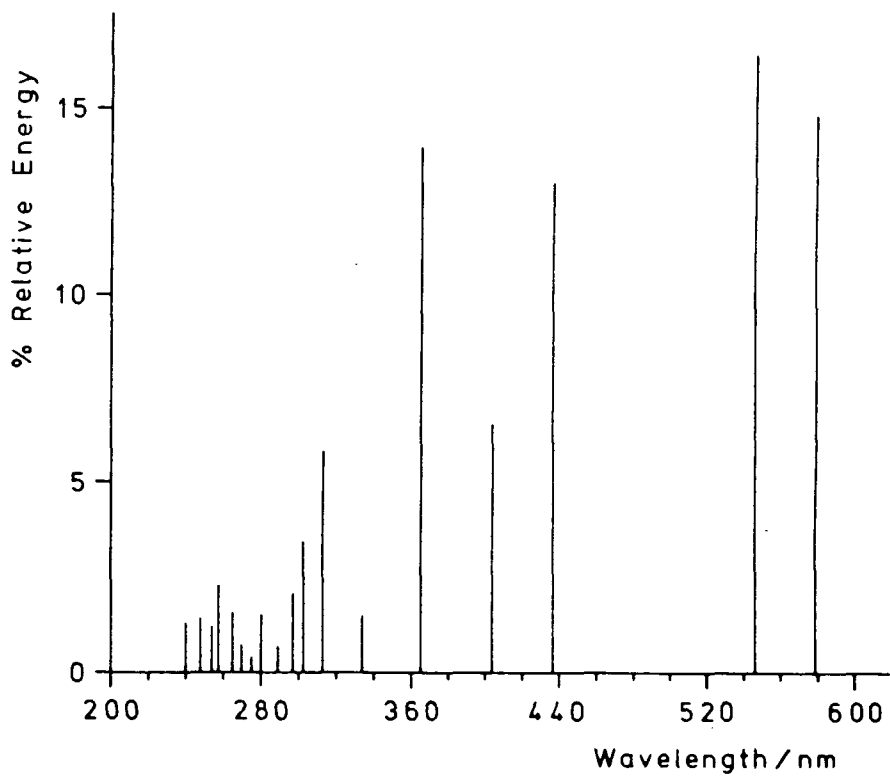
(ii) The 1.8kW Lamp

A mini-cure UV curing apparatus (Primarc Ltd.) was also used for irradiating films of the resins. The mini-cure unit contains a variable speed conveyor belt that carries the samples under two medium pressure mercury arc lamps with elliptical reflectors. An extraction system helps to cool the lamps

FIGURE 4.5 Spectral Distribution of the Medium Pressure Mercury Arc Lamps



(a) The 100W Lamp



(b) The 1.8kW Lamp

and removes ozone but in spite of the cooling system, samples can still become quite warm as the number of passes under the lamp increases. The lamp housing is enclosed in a virtually light tight cowling above the conveyor. To allow the passage of filters under the lamps, the lamp housing and the cowling were raised by  $\sim 0.5$ cm making the height of lamps above the conveyor  $\sim 8.5$ cm. This modification may have reduced the efficiency of irradiation since the samples may no longer pass through the focal point of the elliptical reflectors.

The power consumption of each lamp is 1.8kW of which 846W are emitted as ultraviolet, visible and infra-red radiation. Figure 4.5(b) shows the spectral distribution of the radiation emitted in the UV and visible regions. Comparing this distribution with that of the 100W lamp shows the latter source emits a greater proportion of its radiation at 313nm and 302.5nm whilst the 1.8kW source emits a greater proportion of its radiation in the infra-red and 240 to 265nm regions.

Unless otherwise stated, the mini-cure apparatus was used with only one of the 1.8kW lamps functioning. Also the conveyor speed used throughout this work was  $\sim 7.6$  m min<sup>-1</sup> giving an exposure time of  $\sim 5$  seconds for each passage under the lamp.

#### 4.4 An Overview of the Process of Network Formation via Photo-initiated Chain Cross-Linking Polymerization Emerging from this Study of the Cure of Epoxy Resins

As stated previously, the degree of cure in photocured resins might be expected to be a function of a number of interdependent parameters. The analysis of such multivariable problems tends to be complex. In addition the nature of three dimensional polymer networks makes them difficult to study and

the solutions to questions arising from the results in this investigation may be related to the photochemistry and/or the polymerization of the system. A number of techniques were used to study the effect of the various parameters on the photo-initiated cure of epoxy resins in an attempt to accumulate sufficient data to gain an insight into this process. At the simplest level the results of the experiments show the effect of a particular parameter, for example the irradiation time, on the cure of a particular resin. More detailed analysis of the results and correlations between different techniques strongly suggest that inhomogeneous cross-linking is occurring. At this point the broad picture of network formation by chain cross-linking polymerizations emerging from this study is presented, prior to the detailed analysis of the results of each experiment. It must be pointed out that the results of individual experiments that have been interpreted as being indicative of inhomogeneous cross-linking, with varying degrees of certainty, could have other explanations but taken as a whole the mass of results make quite a convincing case for inhomogeneous network formation.

It is assumed that one starts with a film of lacquer with photoinitiator distributed evenly throughout. On irradiation, cationic species capable of initiating polymerization are generated and ring-opening, chain cross-linking polymerization commences. In spite of the possibility of initiating species not being formed uniformly throughout the thickness of the film due to the attenuation of light, it appears that in the very early stages of the process when the concentration of initiating and hence propagating species is low, a homogeneous lightly cross-linked network is formed. As the degree of cross-linking

increases, either by the further generation of initiating species or the continued polymerization of the lightly cross-linked system, inhomogeneity of the network begins to develop as a relatively low threshold of cross-linking is exceeded. This gives rise to domains of high and low cross-link density, and to the trapping of reactive species and unreacted functionality in the highly cross-linked regions. It may be that the areas of high cross-link density are embedded in a continuous phase of less cross-linked material. The rate of formation of initiating species and hence polymerization may have a bearing on the formation of two phase network, an apparently more homogeneous network resulting from faster initiation. One can speculate as to how a lower rate of initiation could give rise to a different network topology than a faster rate of initiation. For a lower rate of initiation the concentration of propagating centres and hence primary polymer chains in the early stages of the polymerization will be lower, giving rise to the potential for a greater degree of intramolecular cross-linking. This could then result in the formation of a greater proportion of more densely cross-linked regions than for a faster rate of initiation since under the latter conditions the concentration of growing polymer chains will be greater and hence intermolecular cross-linking between the polymer chains will be more favoured.

As cross-linking continues, the potential for reaction in the areas of high mobility is exhausted and although reaction can continue *via* species present in low mobility regions the rate of reaction is so slow as to be almost imperceptible over short time periods. This continued reaction however does manifest itself by an increase in  $T_g$  and a reduction in the two phase nature of the network over prolonged time periods. The form-

ation of an inhomogeneous network, the relative mobility of the two types of region formed and the trapping of species does not appear to be affected by the introduction of highly mobile, flexible, reactive diluents probably due to the increased flexibility being offset by an increased degree of cross-linking as a result of improved mobility of reactive species and functional groups.

The trapping and immobility of species capable of producing further cross-linking gives rise to the potential for post-irradiation thermal cross-linking, the application of heat increasing the mobility of the system. Thus heating the films after irradiation results, for example, in an increase in  $T_g$  and when inhomogeneity is initially present an apparently more homogeneous network is formed. To increase the degree of cross-linking after irradiation, the system could therefore be left for a long time or heated. From a commercial point of view the latter would appear to be the most desirable option but as will become apparent this course of action may not be the most effective.

The detailed interpretations of the results that justify the above view of network formation in these systems are presented in the following sections.

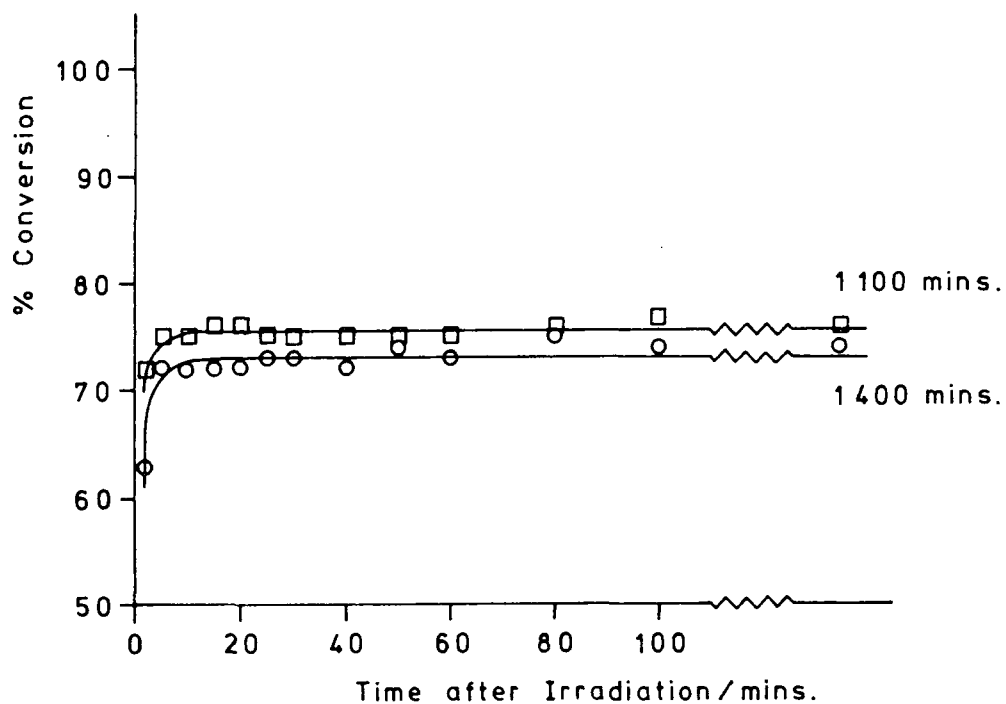
#### 4.5 An Initial Investigation of the Photoinitiated Cure of the DGEBA and Epoxy Novolac Systems using Infra-Red Spectroscopic Measurements of Conversion

The photoinitiated cure of the DGEBA and epoxy novolac resins were investigated using infra-red spectroscopy. The percentage conversion of epoxide functionality was monitored at intervals after irradiation to follow any post-irradiation cure.

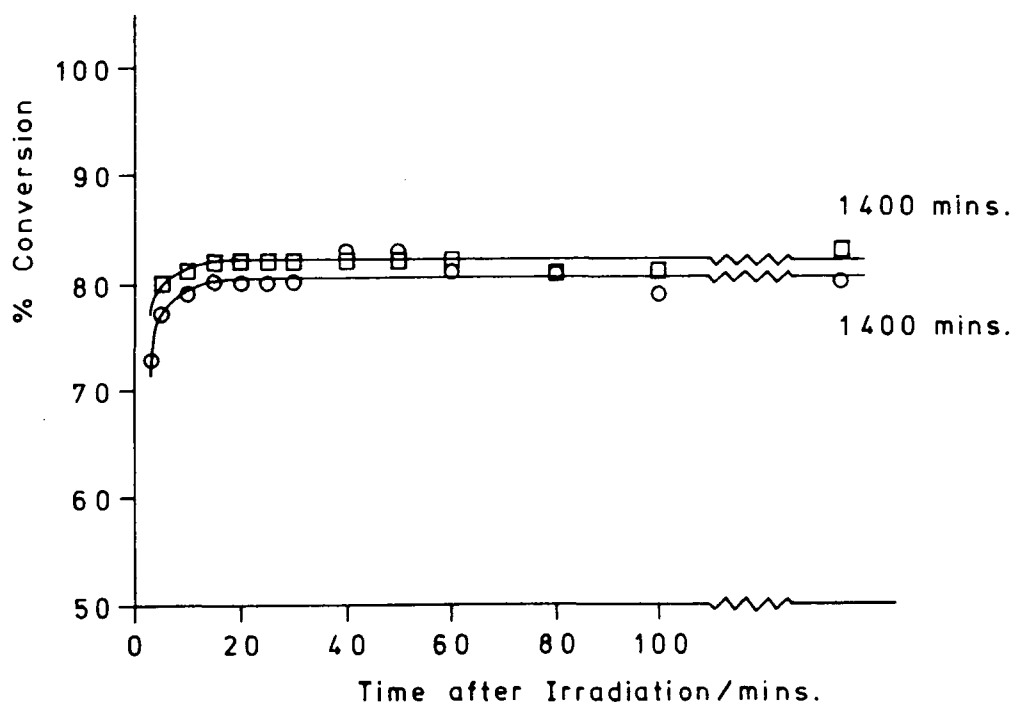
In the investigations of the cure of epoxy resins using IR spectroscopy mentioned previously<sup>4,5</sup> films of the resin were either cured between KBr or NaCl plates or samples of the cured material taken and incorporated into KBr discs to obtain the spectra. With the former technique free standing films cannot be obtained on which other measurements can be carried out whilst the latter technique is time consuming and can give variable results. The approach adopted in this study was to irradiate films of the resin lacquer on thin polyethylene sheet and to record the infra-red spectrum of the film whilst still on the polyethylene substrate, with identical polyethylene sheet in the reference beam of the spectrometer, since polyethylene does not absorb in the regions of interest. Free standing films were not used because of the possibility of leaving uncured resin on the substrate.

Films of 100 $\mu$ m nominal thickness were prepared from a lacquer of the DGEBA resin containing 96.9% resin, 2.1% photoinitiator and 1.0% w/w acetone. Films of the epoxy novolac system containing 82.9% resin, 14.1% toluene, 2.0% photoinitiator and 1.0% w/w acetone were similarly prepared. The films were irradiated at a distance of 18cm from the 100W source, with the aluminium shield in place, for 5 and 10 minutes. From the infra-red spectra of the irradiated films, the absorbance at 915  $\text{cm}^{-1}$  due to the oxirane ring stretch was expressed as a ratio of the absorbance at 1605  $\text{cm}^{-1}$  due to an aromatic breathing mode. This latter absorption band should not be significantly affected by the curing process. The ratio in the cured films was expressed as a percentage of the same ratio measured in the uncured lacquer to give an estimate of the degree of conversion of epoxide groups. The percentage conversion thus

FIGURE 4.6 Epoxide Conversion as a Function of Cure Exposure  
(□, 10; ○, 5 min. Irradiation) and the Time  
after Irradiation



(a) The DGEBA System



(b) The Epoxy Novolac System

measured will be an average of the conversion through the film thickness.

Figures 4.6(a) and (b) show the percentage conversion of epoxide groups for the two resin systems plotted as a function of the time after irradiation. From Figure 4.6(a), 5 minutes' irradiation of a film of the DGEBA lacquer results in ~60% conversion of the epoxide groups, which is increased to 73% by continued reaction during the next 10 minutes. No apparent further increase in conversion occurred after this period. Irradiation for ten minutes gives a conversion of 70% which increases over a 10 minute period after irradiation to an apparently constant value of 76%.

Similar trends are seen in Figure 4.6(b) for the epoxy novolac system, that is a longer irradiation time results in a greater conversion immediately after irradiation and a smaller post-irradiation conversion than the shorter irradiation time. Although the conversion of functionality in this system is greater than in the DGEBA system, the post-irradiation conversion takes place over a similar time scale.

The films appeared to be well cured throughout, in spite of the absorption of shorter wavelength light by the resins as indicated in Chapter Three. Simple calculations involving the extinction coefficient of the DGEBA resin and the photoinitiator at various wavelengths emitted by a medium pressure mercury lamp offer a possible explanation for this apparently reasonable through cure of the films. Using the Beer-Lambert Law, the depth at which a given proportion of monochromatic incident radiation is absorbed by a film of lacquer can be calculated. The absorption of light by lacquer is assumed to be related to the sum of the absorption by individual components, in this case

the DGEBA resin and the photoinitiator, the absorption of light by acetone being considered negligible for the purposes of the calculation. Similar calculations have been carried out to illustrate the effect of increasing the concentration of photoinitiator present in a film on the depth of penetration of light into the film.<sup>30</sup>

Table 4.1 offers a guide to the depth in micrometers at which 50%, 90% and 99% of the incident radiation at a given wavelength,  $\lambda$ , is absorbed for a film containing 97% DGEBA resin, 2% photoinitiator and 1% acetone.

TABLE 4.1 Depth of Penetration of Light into a Film of a Lacquer of the DGEBA System containing 2% w/w Photoinitiator

$\lambda/\text{nm}$	Depth at which 50% of light is absorbed $/\mu\text{m}$	Depth at which 90% of light is absorbed $/\mu\text{m}$	Depth at which 99% of light is absorbed $/\mu\text{m}$
313	370	1200	2500
303	190	630	1300
297	40	130	260
265	1	2	4
254	1	4	8
249	1	5	10

The data in Table 4.1 indicates that light of 265, 254 and 248nm wavelength will be totally absorbed within a few micrometers of the surface of the film. Longer wavelength light, 315 and 303nm in particular, is able to penetrate much further into a film without a serious loss of intensity. It would therefore appear that the longer wavelength light is primarily responsible for the through cure of thicker films. The fraction of the total light absorbed,  $I_A$ , which is absorbed by the photoinitiator,  $I_{AP}$ , or the resin,  $I_{AR}$ , can be calculated using

the following expression<sup>31</sup>

$$I_{AP} = 1 - I_{AR} = \frac{\epsilon_P C_P}{\epsilon_P C_P + \epsilon_R C_R} I_A$$

where  $\epsilon_P$  and  $\epsilon_R$  are the molar absorptivity of the photoinitiator and resin respectively whilst  $C_P$  and  $C_R$  are the concentration of the photoinitiator and resin respectively. The results expressed as a percentage of the total light absorption are shown in Table 4.2.

TABLE 4.2 Percentage of Total Light Absorption due to the Photoinitiator (2%w/w) and DGEBA Resin

$\lambda/\text{nm}$	$\frac{I_{AP}}{I_A} \times 100$	$\frac{I_{AR}}{I_A} \times 100$
313	13	87
303	13	87
297	6	94
265	2	98
254	9	91
248	12	88

It would appear that the absorption of light at a given depth for each wavelength is mostly due to the resin which is not surprising since it is present in a greater concentration. Even though the proportion of light absorbed by the photoinitiator is low at longer wavelengths, the intensity of light of these wavelengths at a given depth is much greater than for the shorter wavelengths. Furthermore, in spite of the photoinitiator being a weak absorber of longer wavelength light, the number of photons absorbed and hence the number of molecules undergoing photolysis will depend on the intensity of the incident light. It might be that the intensity of the light reaching the films,

emitted by the lamp at 303nm or 313nm, is sufficient to produce a significant amount of photolysis of the photoinitiator and hence initiate polymerization deeper in the film.

Another explanation for this effect, involving the photosensitization of photoinitiator photolysis by some mechanism similar to those discussed in Chapter Two, with the resin or acetone acting as the photosensitizer, might also be possible.

#### 4.6 Effect of Cure Exposure, Film Thickness and Light Intensity on the Cure of the DGEBA System

Films of 50, 100, 150, 200 and 250 $\mu$ m nominal thickness were prepared from lacquers containing 97.0% resin, 2.0% photoinitiator and 1.0% acetone or 96.9% resin, 2.1% photoinitiator and 1.0% acetone. The films were irradiated 9, 18 and 36cm from the 100W lamp. The aluminium shield could not be used effectively with the films 36cm from the source and not at all with them 9cm distant. A thermopile detector was used to measure the photon flux at each distance from the source. This detector measures the total intensity of radiation from emissions in the ultraviolet, visible and infra-red regions of the electromagnetic spectrum.

##### (A) Infra-Red Spectroscopic Measurements of Epoxide Conversion

Irradiation times of 10 seconds, 1, 2, 2.5, 3, 8, 20 and 45 minutes were originally chosen. However a film of 100 $\mu$ m nominal thickness irradiated 18cm from the source was found to require a minimum of 2.5 minutes irradiation to produce a sufficient initial degree of cure to allow infra-red spectra of the film to be recorded. Films of 150, 200 and 250 $\mu$ m

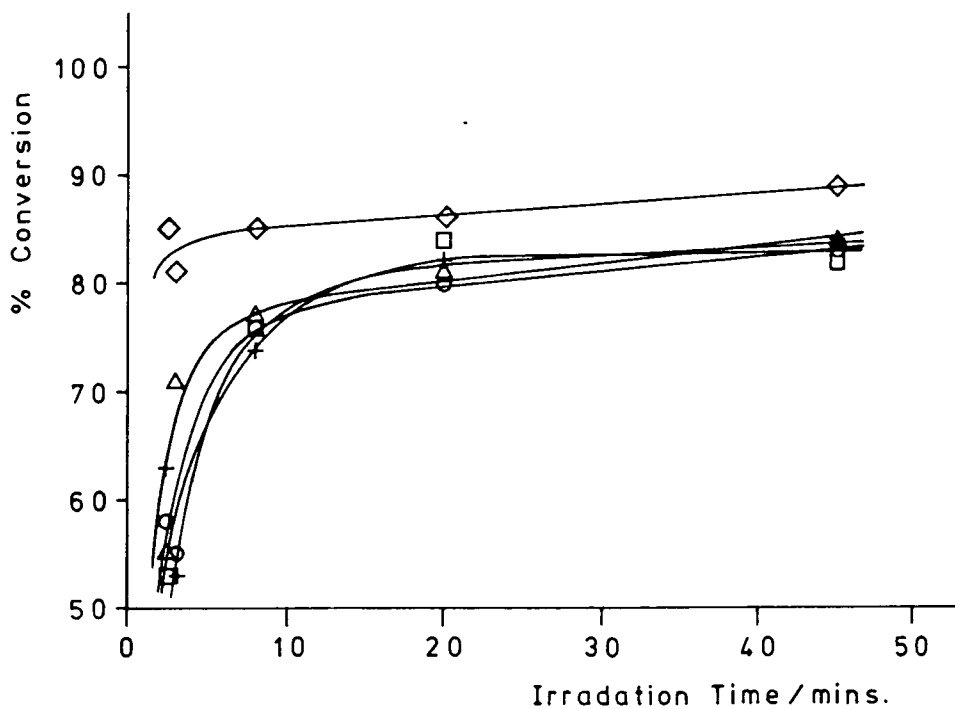
nominal thickness given 2.5 and 3 minutes irradiation 18cm from the source only showed surface cure; as did all the films receiving smaller radiation doses. The IR spectra of such films could not be recorded because of the presence of mobile material.

IR spectra of the films which appeared to be cured throughout were recorded at intervals over a period of 1 to 50 hours after irradiation. There was no apparent increase in the extent of reaction during this period; however, there was some scatter in the measurements and consequently an average value of the measurements for each film was taken. In addition, irradiation of films of 100 $\mu$ m nominal thickness 18cm from the source for various times and subsequent infra-red analyses, were carried out three times. Similar trends and degrees of conversion were obtained in each experiment. In comparing the conversion in films of different thickness it is assumed that the Beer-Lambert Law is obeyed.

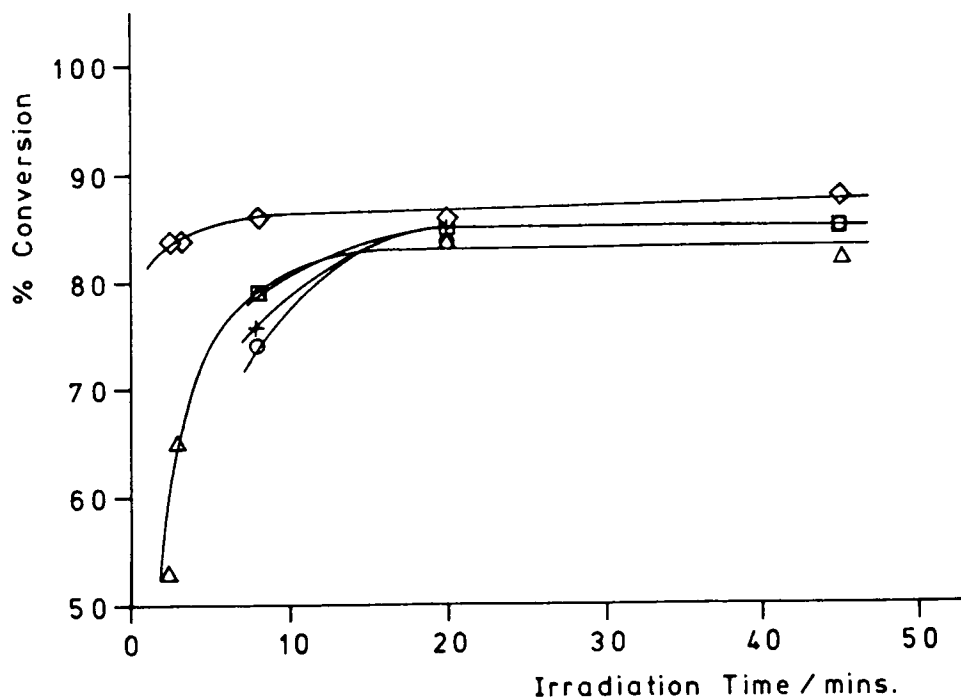
Figure 4.7(a) shows the final percentage conversion plotted against irradiation time for films of differing thickness irradiated 9cm from the source. Figures 4.7(b) and (c) show similar plots for films irradiated at distances of 18 and 36cm from the source. These plots indicate that longer irradiation times result in a greater conversion of functional groups, especially for thicker films and lower light intensities.

Since Crivello and Lam<sup>32</sup> have shown that the extent of photolysis of iodonium photoinitiators increases with increasing irradiation time, it seems reasonable to suggest that the increase of conversion with irradiation time observed in the films of the DGEBA lacquer is related to an increase in the number of initiating species produced. Therefore because fewer

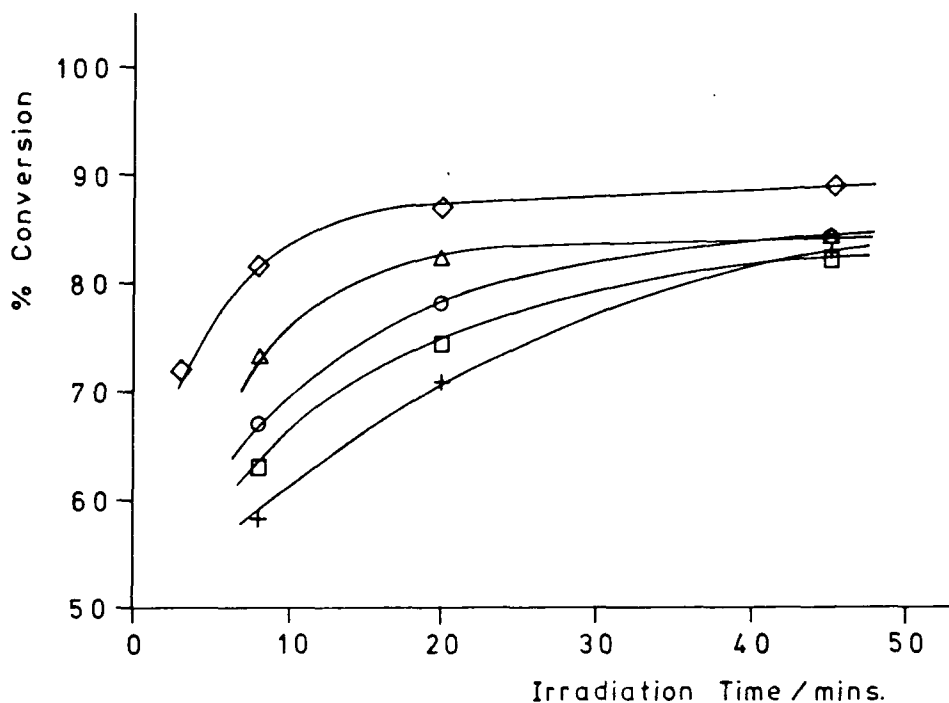
FIGURE 4.7 Epoxide Conversion as a Function of Cure Exposure for Different Film Thicknesses ( $\diamond$ , 50;  $\triangle$ , 100;  $\circ$ , 150;  $\square$ , 200;  $+$ , 250 $\mu\text{m}$ ) and Light Intensities



(a) Films Irradiated 9cm from the source



(b) Films Irradiated 18cm from the Source



(c) Films Irradiated 36cm from the Source

initiating species result in a lower conversion of functional groups, some process must be occurring that limits the kinetic chain length, that is the average number of monomer molecules reacted per initiating species.

Kloosterboer *et al*<sup>33</sup> found in their study of the photo-initiated free radical polymerization of polyfunctional vinyl resins that an increase in the conversion of double bonds occurred with increasing cure exposure. As described in Chapter One they hypothesised that the trapping of radical species due to inhomogeneous cross-linking resulted in a limited kinetic chain length. The trapping of cationic species in the DGEBA network system would account for the effect of increased irradiation time on the conversion and it has been shown that inhomogeneous network formation resulting in domains in which species can be trapped can occur in the photoinitiated chain

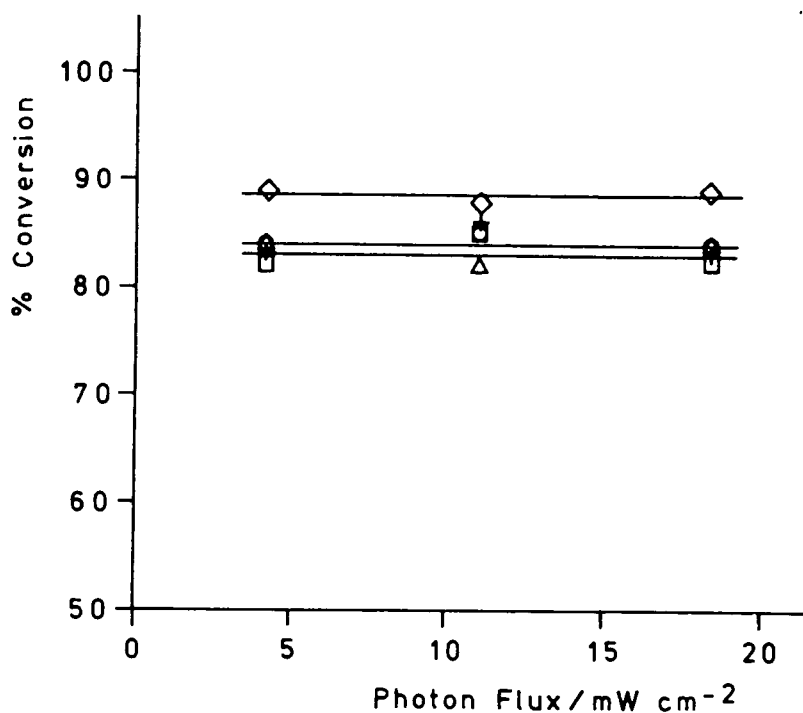
cross-linking polymerization of epoxy resins.<sup>34</sup> Other processes limiting the kinetic chain length such as termination of the propagating species might possibly account for the observed effect of increasing irradiation time in the photoinitiated cationic polymerization of epoxide compounds since Crivello and Lam<sup>10</sup> have reported a similar effect in the polymerization of monoepoxide compounds using cationic photoinitiators. It must be noted however that the conversion measurements in this latter study made no allowance for continued polymerization after irradiation.

Figure 4.8(a) shows the percentage conversion in films of different thickness irradiated for 45 minutes plotted against the light intensity. It appears that a four-fold decrease in light intensity has no effect on the conversion of epoxide groups even in the thicker films, for this irradiation time. Figures 4.8(b), (c) and (d) show similar plots for irradiation times of 20, 8 and 3 minutes respectively. These plots again show that longer irradiation times, thinner films and a higher light intensity result in a greater degree of conversion.

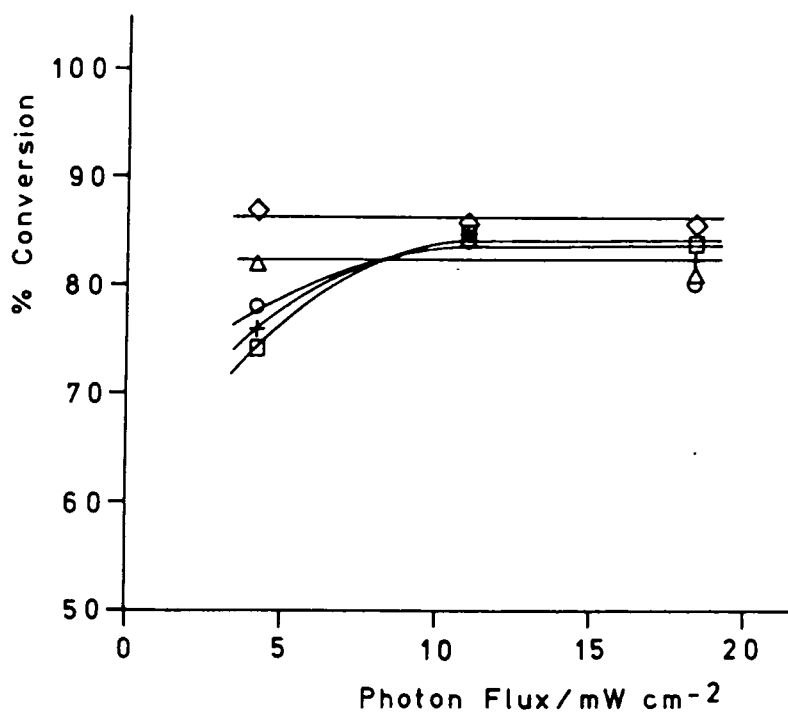
The effect of light intensity on the extent of reaction can again be explained in terms of the number of initiating species produced and a limited kinetic chain length. Over a 45 minute irradiation period, enough initiating species could be produced at all intensities to give similar degrees of conversion. As the irradiation time is reduced fewer protons are generated, leading to a reduction in the final conversion because of the limited kinetic chain length; this effect becoming more pronounced as the film thickness is increased.

Dutch workers<sup>11</sup> have reported a lowering of the maximum extent of reaction achieved in free radical photoinitiated

FIGURE 4.8 Epoxide Conversion as a Function of Light Intensity for different Film Thicknesses ( $\diamond$ , 50;  $\triangle$ , 100;  $\circ$ , 150;  $\square$ , 200; +, 250 $\mu\text{m}$ ) and Cure Exposures

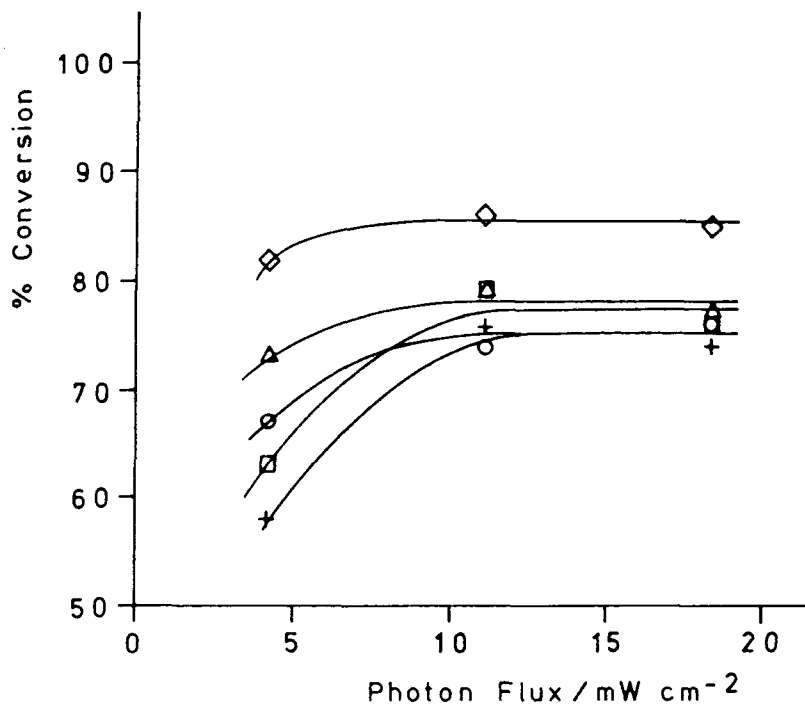


(a) Films Irradiated for 45 Minutes

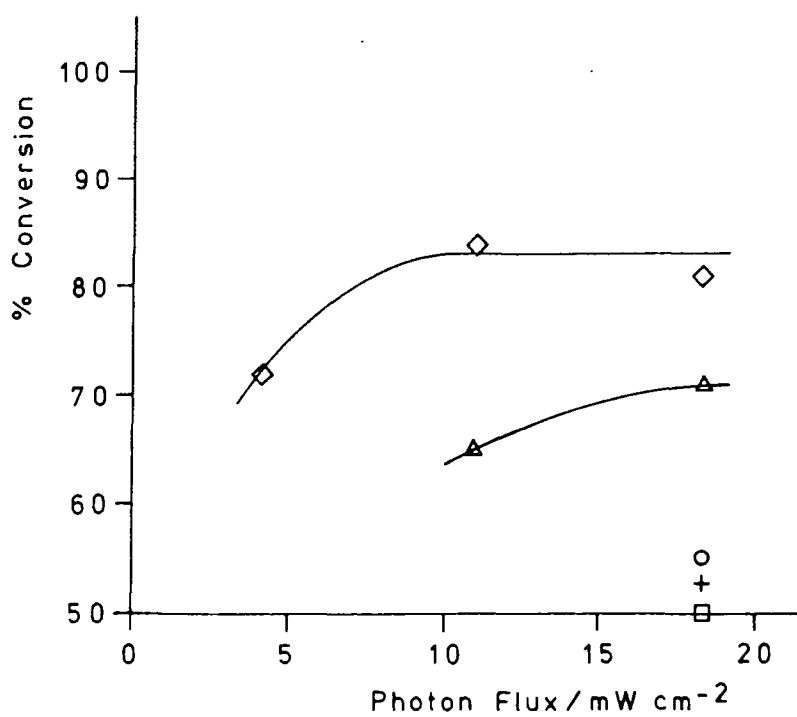


(b) Films Irradiated for 20 Minutes

FIGURE 4.8 (contd.....)



(c) Films Irradiated for 8 Minutes

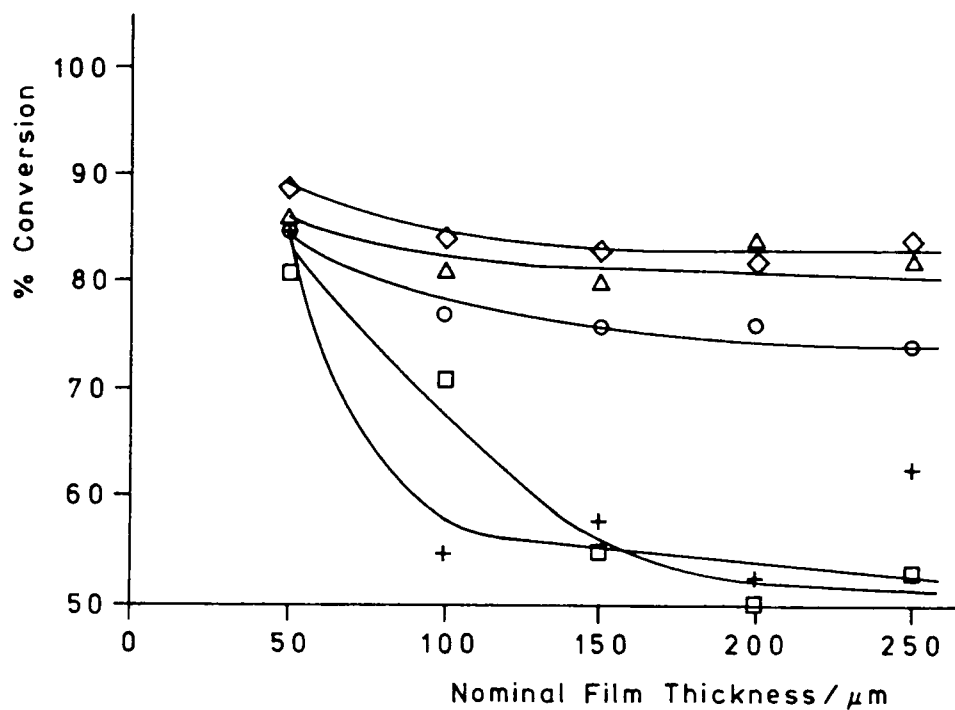


(d) Films Irradiated for 3 Minutes

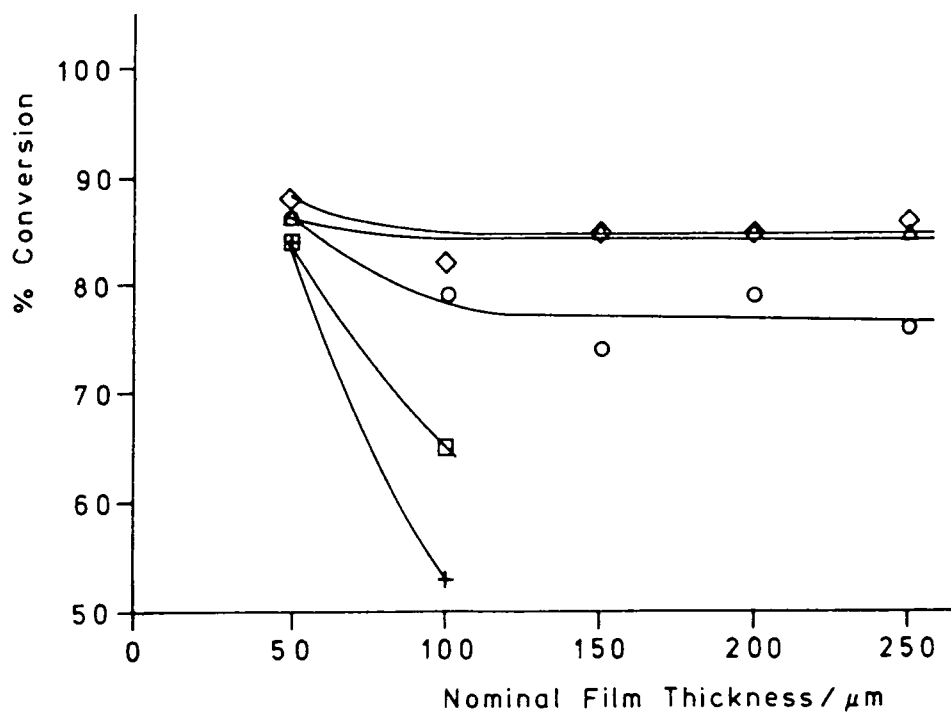
polymerizations as the light intensity is reduced. These workers followed the rate of shrinkage with irradiation time and compared it to the rate of double bond conversion under similar conditions. This showed that the maximum rate of shrinkage and its decay lagged behind the maximum rate of double bond conversion and its decay. The occurrence of this time lag between conversion and volume relaxation was used to account for the effect of light intensity on the final conversion. At higher light intensities the rate of initiation is faster because of the increased photolysis of the photoinitiator. Consequently a higher degree of conversion is reached before volume relaxation reduces the mobility of functional groups and hence their probability of reacting. Lower light intensities result in a lower rate of initiation and consequently allows volume relaxation to have a significant effect on the probability of reaction at low degrees of conversion. In this study no significant change in the percentage conversion was observed for the longest irradiation time when the light intensity was decreased as shown in Figure 4.8(a). However such an effect as that observed by the Dutch workers might become apparent if the light intensity were further decreased since cyclic ether compounds can show some shrinkage on polymerization although to a much lesser degree than vinyl compounds.<sup>35</sup>

Figures 4.9(a), (b) and (c) show more clearly the effect of film thickness on the percentage conversion. Each line on a plot represents a different irradiation time and each plot a different light intensity. The same conclusions can be drawn as from the previous figures. It would appear that attenuation of the wavelengths responsible for cure, thought to be mainly 303nm and 313nm is significant as is evidenced by the decrease in conversion in thicker films. This effect can be offset

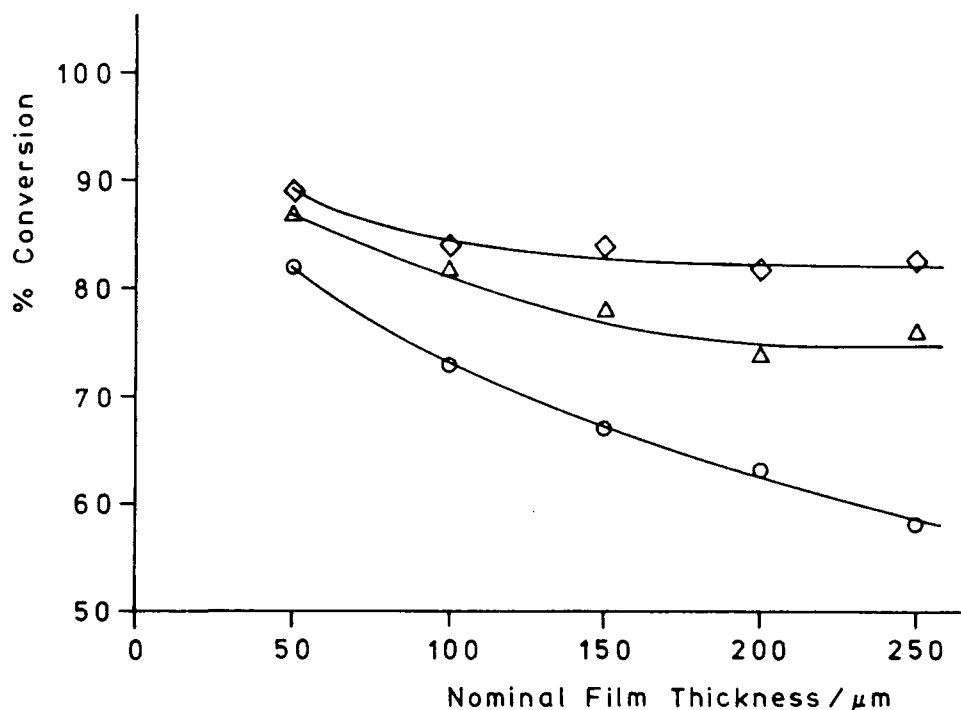
FIGURE 4.9 Epoxide Conversion as a Function of Film Thickness for Different Cure Exposures ( $\diamond$ , 45;  $\triangle$ , 20;  $\circ$ , 8;  $\square$ , 3; +, 2.5 mins. irradiation) and Light Intensities



(a) Films Irradiated 9cm from the Source



(b) Films Irradiated 18cm from the Source



(c) Films Irradiated 36cm from the Source

somewhat by using longer irradiation times or higher intensities of light both of which will increase the number of photons available for the photolysis of photoinitiator.

The thickness of films prepared in a similar manner to those above was measured using a micrometer. Films of 50, 100 and 250 $\mu\text{m}$  nominal thickness were found to be approximately 25, 50 and 125 $\mu\text{m}$  thick respectively, indicating that the actual film thickness is approximately half the nominal value. This difference in actual and nominal film thickness is highly unlikely to be due totally to shrinkage.

#### (B) Measurement of the Gel Content

The gel content of the films was determined using the following procedure. An accurately weighed sample of the film to be extracted was placed in a round bottom flask equipped with

a condenser. Analar grade toluene ( $70 \text{ cm}^3$ ) was added and refluxed for five hours. After cooling, the solution was filtered through a sintered glass funnel (No.3) to remove the gel. The solution was transferred to a preweighed flask and the solvent removed using a rotary evaporator. The sol was then dried to constant weight on a vacuum line. Recovery of the sol rather than the gel was carried out because it was thought it would be easier to dry than the gel. The weight of film used in these extractions was quite small being between 0.01 and 0.1g.

Although some films were initially not sufficiently cured to obtain infra-red spectra, they did appear to harden over a period of 20 to 30 hours after irradiation. Attempts to obtain infra-red spectra at this point proved unsuccessful as the surface of the films wrinkled when they were placed in the infra-red beam. However such films could later be removed from the substrate and the gel content determined.

Table 4.3 shows the percentage gel found in each film. The error in these measurements is likely to be high owing to the small sample size; however, when the totality of the data is considered some general trends become discernible and some tentative conclusions can be made. Generally the results show that high amounts of gel are formed for the longer irradiation times at each distance from the source and each film thickness indicating that most of the monomer has been incorporated into the network structure. Shorter irradiation times result in a decrease in the gel content which is more pronounced for thicker films and lower light intensities. It is noted that for films of  $50 \mu\text{m}$  nominal thickness, irradiated at 18 and 36cm from the source, the amount of gel increased with a decrease in irradiation

TABLE 4.3 Percentage Gel Content as a Function of Cure Exposure  
Film Thickness and Light Intensity

Nominal film thickness/ $\mu\text{m}$	Irradiation time/mins	Distance from the UV source/cm		
		9	18	36
50	45	90	80	50
	20	97	82	64
	8	90	94	73
	3	96	99	41
	2½	95	82	n.c.
100	45	93	-	89
	20	86	94	84
	8	90	90	82
	3	71	80	84
	2½	83	65	n.c.
150	45	93	94	94
	20	86	98	95
	8	94	82	81
	3	93	72	61
	2½	70	n.c.	n.c.
200	45	-	94	92
	20	99	97	-
	8	98	96	68
	3	89	79	n.c.
	2½	-	n.c.	n.c.
250	45	98	98	92
	20	97	100	85
	8	92	96	61
	3	85	44	n.c.
	2½	62	n.c.	n.c.

n.c. - not cured sufficiently to remove the film from the substrate.

time. This effect is likely to be spurious. There is some evidence that for longer irradiation times, the increased conversion results from intramolecular cross-linking. For example, films irradiated 9cm from the source for 20 minutes show a small but significant increase in epoxide conversion over films irradiated for 8 minutes, yet the gel content of these films is approximately the same.

An infra-red spectrum of the sol extracted from one of the films showed the presence of a high proportion of unreacted epoxide functional groups. Infra-red spectra of the gel from two of the films (both of 250 $\mu$ m nominal thickness given 8 and 3 minutes' irradiation, 36 and 18cm from the source respectively) showed the presence of a significant amount of epoxide functionality. It would appear that a reasonable proportion of the epoxide functionality remaining in thinner films irradiated for longer periods at higher intensities is attached to the network since such films showed a high gel content yet contained a significant amount of unreacted functionality as seen in the previous infra-red measurements. There are at least two possible explanations for this unreacted functionality. Vitrification of the system may have occurred limiting the probability of functional groups reacting or alternatively an inhomogeneous cross-linking may be taking place giving rise to highly cross-linked domains in which functional groups are trapped.

#### 4.7 An Investigation of the Wavelengths of Light Responsible for Initiating Cure in the DGEBA System using Infra-Red Spectroscopic Measurements of Epoxide Conversion

As will become apparent in the next chapter, it may be necessary to prevent the irradiation of resins containing an

aryl ether moiety with certain wavelengths during the curing process. It is therefore important to determine whether these wavelengths interact with the diphenyliodonium salt to initiate polymerization. Also knowledge of the wavelengths responsible for the photolysis of the photoinitiator could allow a more effective choice of lamp to be made, thus improving the efficiency of the curing process.

To remove shorter wavelength UV light a 'pyrex' filter was used and as is shown by the UV absorption spectrum in Figure 4.10, the filter starts to absorb at about 370nm and totally absorbs all wavelengths below 275nm. This filter was made from a 'pyrex' petri dish so that the space beneath could be flushed with nitrogen. A UV cut-off filter purchased from

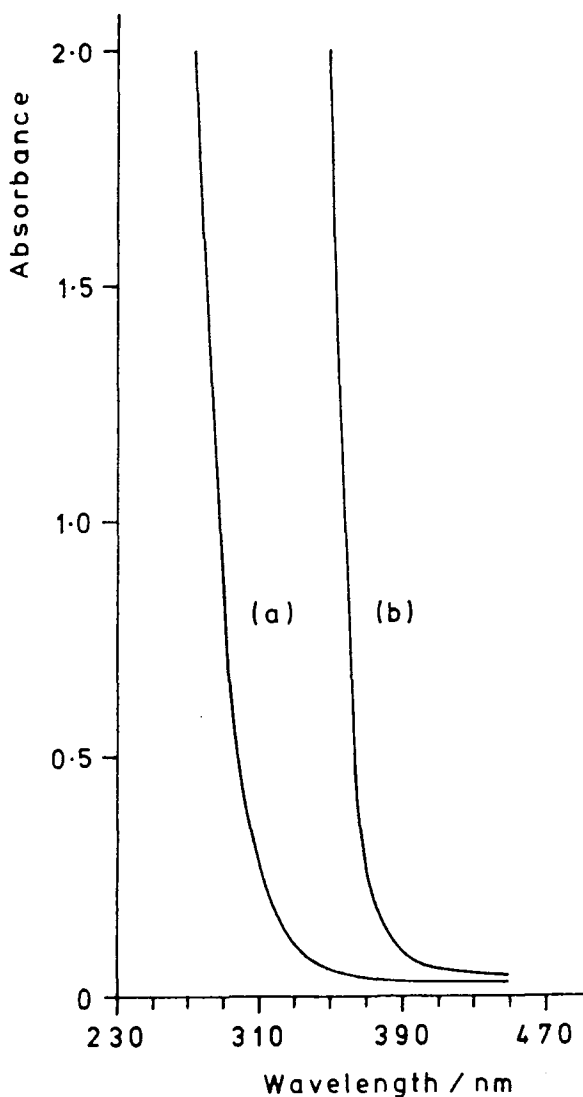
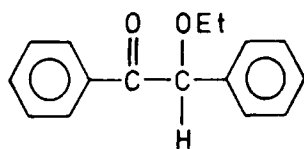


FIGURE 4.10 UV Spectra of the 'Pyrex' Filter, (a) and the UV Cut-Off Filter, (b)

Applied Photophysics was also used in this work, the UV absorption spectrum in Figure 4.10 indicating that the filter starts absorbing at *ca.* 400nm and totally absorbs all wavelengths below 350nm.

Films of the resin containing a 1:1 molar ratio of benzoin ethyl ether, BEE, to photoinitiator were prepared:



BEE

The BEE was added in the hope that it would (by an indirect electron transfer mechanism as described in Chapter Two) act as a photosensitizer allowing the photolysis of photoinitiator to take place on irradiation with longer wavelength light.

(A) Irradiation with the 100W Lamp

The two lacquers used in the initial set of experiments contained 97.0% resin, 2.0% photoinitiator and 1.0% w/w acetone or 95.9% resin, 2.1% photoinitiator, 1.0% BEE and 1.0% w/w acetone films of 100 $\mu$ m nominal thickness being prepared from the lacquers. The intensity of the light 9cm from the 100W lamp was measured using the thermopile and found to be 18.1 mW cm<sup>-2</sup>. Two films, one of each lacquer, were irradiated at this distance from the lamp for 3 minutes as controls. With the UV cut-off filter in place, the intensity of the light was measured and the distance of the detector varied so that it registered a similar photon flux (18.3mW cm<sup>-2</sup>) to that without the filter present. Films were then irradiated at this distance from the source with the filter in place for increasing lengths of time. The procedure was repeated with the 'pyrex' filter in place using an intensity of 18.5mW cm<sup>-2</sup>. The films thus receive a

similar number of photons with and without the filters in place and although the wavelength distribution is different, the photo-initiator has approximately the same chance of interacting with a photon.

The results of the IR spectroscopic measurements of conversion are given in Table 4.4. The error in each figure refers to the standard deviation from the mean of several measurements made at the given time after irradiation.

TABLE 4.4 Percentage Epoxide Conversion in Films Irradiated with Filtered Light using the 100W Source as a Function of Cure Exposure

Irrad. time/ mins.	U.V. Cut-off filter				'Pyrex' filter			
	0% BEE		1% BEE		0% BEE		1% BEE	
	I+1hr	I+46hr	I+1hr	I+46hr	I+1hr	I+46hr	I+1hr	I+46hr
3	n.c.	n.c.	n.c.	n.c.	72±3	70±3	69±4	65±4
8	n.c.	44±6	n.c.	47±8	82±2	79±2	74±4	74±5
20	51±9	51±6	49±1	48±7	85±2	83±2	79±3	79±3
45	59±3	63±5	68±4	68±4	85±2	87±3	81±3	82±4

I + 1 hr = 1 hour after irradiation, n.c. = not cured sufficiently.

-----

The percentage conversions in the control film containing no BEE were found to be 78%±2% and 80%±3%, 1 and 46 hours after irradiation, respectively. The conversion in this film appears to be somewhat greater than in films cured previously under similar conditions. The extent of reaction in the control film containing 1.0% BEE was found to be 72%±2% and 74%±2%, 1 and 46 hours after irradiation respectively.

A film containing no BEE given 3 minutes' irradiation with light of wavelengths greater than 350nm is apparently not cured initially and remains so whereas a film given 8 minutes' exposure under these conditions although still mobile 1 hour after irradiation

iation, hardens within *ca.* 45 hours. Films irradiated for 20 and 45 minutes were fairly rigid within 1 hour of irradiation. The extent of reaction in the films given 8, 20 and 45 minutes' irradiation increased as the irradiation time increased. However the film given 45 minutes' irradiation still showed a significantly lower degree of conversion than for a film irradiated with unfiltered light for 3 minutes. As with the other films, it is difficult to say with certainty whether the conversion increases with the time after irradiation because of the scatter in the measurements. Light of 366nm is most probably responsible for the cure of these films, the reduced conversion reflecting the inefficiency of light absorption by the photoinitiator at this longer wavelength. Films containing BEE ( $\epsilon_{366} \sim 44 \text{ dm}^3 \text{ mol}^{-1} \text{ cm}^{-1}$ ) irradiated under similar conditions showed the same trends as that observed in the BEE free films, with similar or only slightly higher epoxide conversion, indicating that photosensitization by the BEE is not occurring.

Films containing no BEE irradiated through the 'pyrex' filter show the trend of increasing conversion with increasing irradiation time. The film given 3 minutes' exposure was soft and tacky immediately after irradiation but soon hardened. The conversion in this film was found to be significantly lower than that of the control but again the general trend of an increase in conversion with increasing cure exposure is apparent. Comparison of the conversion in the films given 8, 20 and 45 minutes' irradiation with those for similar films cured previously using the full output of the source as reported in Section 4.6(A) shows a greater degree of reaction in the former films which is again indicative of some irreproducibility in either the preparation and irradiation of

films or the conversion measurements. However the results indicate that the films given longer cure exposures are at least as well cured as films given equivalent exposures to the full output of the lamp. The poor cure of the film given 3 minutes' irradiation may be attributable to the lack of rapid cure in surface regions of the film due to the absorption of shorter wavelength UV light by the photoinitiator. Films containing BEE ( $\epsilon_{303} \sim 184 \text{ dm}^3 \text{ mol}^{-1} \text{ cm}^{-1}$ ,  $\epsilon_{313} \sim 170 \text{ dm}^3 \text{ mol}^{-1} \text{ cm}^{-1}$ ) irradiated through the 'pyrex' filter show the same trends as that observed in the films irradiated under similar conditions without photosensitizer present. If anything, the conversion is slightly lower in the films containing BEE compared with the films without this potential photosensitizer present.

The above set of experiments, except those involving BEE, were repeated some time later. For these measurements a lacquer containing 97.0% resin, 2.0% photoinitiator and 1.0% w/w acetone was used. Films were prepared in a similar manner to those in the previous experiments and irradiated with light intensities of  $16.2 \text{ mW cm}^{-2}$ ,  $16.3 \text{ mW cm}^{-2}$  and  $16.3 \text{ mW cm}^{-2}$  with no filter, the UV cut-off filter and the 'pyrex' filter in place, respectively.

Table 4.5 shows the conversion of epoxide function in each film as measured by infra-red spectroscopy. Although the same trends are observed as in the films irradiated in the previous set of experiments, the extent of reaction in some cases is higher and in others lower than those recorded in Table 4.4. During the course of the project further films of similar composition to those above were irradiated with and without the 'pyrex' filter present using similar light intensities and irradiation times. The conversion in these films were found to be in the region of 90%, independent of the irradiation time

TABLE 4.5 Further Percentage Epoxide Conversion Measurements in Films Irradiated with Unfiltered and Filtered Light using the 100W Source

Irrad. time/ mins.	No filter			UV Cut-off filter			'Pyrex' filter		
	I+1hr	I+24hr	I+48hr	I+1hr	I+24hr	I+48hr	I+1hr	I+24hr	I+48hr
3	72±2	74±4	75±2	n.c.	n.c.	n.c.	57±5	57±6	57±8
8	75±4	79±3	80±4	n.c.	n.c.	33±7	76±2	77±2	79±3
20	77±4	81±2	79±3	40±7	48±6	40±7	80±2	82±2	82±2
45	82±3	82±4	85±2	67±3	69±4	69±3	81±2	83±2	83±3

n.c. = not cured sufficiently.

-----

or the use of the filter, contrary to what had been observed previously.

In spite of attempts to standardise the lacquer and film preparation, the irradiation procedure and the IR spectroscopic measurements it would appear that some minor change in the above procedures gives rise to a significant variation in the results obtained.

The above discrepancies between experiments carried out under similar conditions provide an illustration of the considerable difficulties involved in designing totally reproducible experimental procedures in the field of network polymers. Neither the small variations in the composition of the lacquers used nor the small variations in the incident intensity are fully consistent with the irreproducibility observed. The same batch of resin was used throughout the work but several batches of photoinitiator were used during the course of the above experiments, and it might be that variations in the purity of the photoinitiator could have contributed to these discrepancies. Another factor which was not controlled and as will be seen later can affect the cure of films is the temperature at which the irradiations were carried out. This may have varied between

10 and 22°C. Quantitative IR spectroscopy has a number of inherent difficulties associated with its use. Possible differences in the light scattering or morphology of the samples used, slight differences in the position of the sample in the beam and in the operational characteristics of the instrument may also have contributed to the above discrepancies.

The results however strongly indicate that irradiation with wavelengths between 275nm and 350nm can give a degree of cure similar to irradiation with the total spectral output of the lamp. This tends to confirm the earlier assertion that the wavelengths of 297, 303 and 313nm emitted by the lamp have an important role in the photolysis of the photoinitiator and hence the cure of films of the DGEBA system, and probably the epoxy novolac system too, with wavelengths greater than 350nm and less than 275nm making a smaller contribution to the photolysis of the photoinitiator, especially throughout the film thickness in the case of wavelengths less than ~275nm. Further observations on the cure of the DGEBA system on irradiation with longer wavelength light are reported in Appendix One.

(B) Irradiation with the 1.8kW Lamp

The following experiments were carried out to determine the extent of reaction in films of the DGEBA system as a function of the radiation dose received and to investigate the effect on the extent of reaction of irradiating films through the 'pyrex' filter. Using the 100 W lamp, the irradiations could be carried out in such a way that the number of photons reaching the sample were similar with and without the filter present. This was not possible when the mini-cure apparatus was used to irradiate films. In fact the intensity of longer wavelength light reaching the

films will be reduced since the filter also absorbs slightly in this region.

Films of 100 $\mu$ m nominal thickness were used in all the following experiments. Table 4.6 gives the percentage conversion measured by IR spectroscopy in films containing 97.0% resin, 2.0% photoinitiator and 1.0% w/w acetone given an increasing number of passes under the 1.8kW lamp with and without the 'pyrex' filter present.

TABLE 4.6 Percentage Epoxide Conversion in Films Irradiated with the 1.8kW Source, with and without the Filter in Place

Conditions	Time after irradiation / hrs	Number of passes					
		1	2	3	5	10	20
No filter	24	61 $\pm$ 3	74 $\pm$ 3	73 $\pm$ 3	74 $\pm$ 3	76 $\pm$ 4	79 $\pm$ 3
'Pyrex' filter	48	54 $\pm$ 6	61 $\pm$ 5	65 $\pm$ 6	72 $\pm$ 7	76 $\pm$ 3	79 $\pm$ 3

-----

It was noted that the film given 1 pass under the lamp with the 'pyrex' filter in place was still mobile immediately after irradiation although it did harden with time.

These results indicate that in general the extent of reaction increases with increasing exposure to the source and that the use of the filter reduces the degree of conversion especially in films given shorter cure exposures. However during the course of the work further films were irradiated under similar conditions and the extent of reaction measured. The results are recorded in Table 4.7, the composition of the lacquers used being given in Table 4.8.

TABLE 4.7 Further Measurements of Percentage Epoxide Conversion in Films Irradiated using the 1.8kW Source with and without the 'Pyrex' Filter in Place

Run No.	Conditions	Time after irradiation /hrs	Number of passes					
			1	2	3	5	10	20
1	No filter	48	84±2	82±2	83±2	82±4	85±1	86±2
2	No filter	48	78±2	75±1	76±4	77±3	79±5	85±2
3	No filter	24	90±1	87±1	89±2	88±1	-	92±1
4	No filter	24	74±3	77±3	79±2	78±2	80±3	82±2
5	'Pyrex' filter	48	82±2	81±2	80±3	82±2	78±3	81±2

TABLE 4.8 Composition (w/w) of the Lacquers used to Prepare the Films

Run	% Resin	% Photoinitiator	% Acetone
1 and 5	77.0	2.0	1.0
2 and 4	96.9	2.0	1.1
3	96.8	2.1	1.1

Unlike the previous experiment, each set of films was irradiated at a different time. Again it was noted that the film given 1 pass under the lamp with the 'pyrex' filter in place was still mobile after irradiation although it did appear to harden with time.

As with films cured using the 100W lamp the discrepancies in the conversion measurements between the different sets of films (Table 4.7) cured under similar conditions do not appear to be related to the minor variations in lacquer composition. Explanations similar to those proposed to account for the irreproducibility seen in the conversion measurements for films irradiated using the 100W lamp apply to the above measurements,

including the effect of the temperature at which irradiations are carried out. Even though the films are heated as they pass under the high intensity lamp, the magnitude of this heating effect will depend upon the initial temperature of the samples. The mini-cure has a conveyor system to take the samples under the lamp and although the same speed setting was used throughout the work, a small variation in the actual speed of the belt may have contributed to the irreproducibility. An attempt to determine the reproducibility of the infra-red spectroscopic measurements of conversion was made. Five films of similar thickness and composition to those used previously were each given 5 passes under the lamp. The average extent of reaction of epoxide functionality in the five films, measured 48 hours after irradiation, was found to be 80% with a standard deviation of  $\pm 2\%$  showing that under these conditions the technique provides a fairly reproducible measure of conversion.

In spite of the discrepancies, taking the data as a whole, a number of tentative conclusions may be drawn. In the majority of the runs, the conversion appears to increase with increasing cure exposure as for films irradiated with the 100W lamp. In the case of films irradiated without the filter present, the heating of the films may have contributed to this observation. Giving more credence to the measurements carried out at the same time, reported in Table 4.6, and taking into account the observation that 1 pass with the filter in place does not result in a rigid film immediately after irradiation, it may be concluded that the use of the filter has a deleterious effect on the cure of films given shorter cure exposures although the conversion measurements in Table 4.7 for films cured with the filter in place indicate that there is very little effect on the conversion, if any. The wide variations in the conversion measurements on

films irradiated with the 1.8kW lamp make it difficult to compare the extent of conversion achieved in these films with those irradiated using the 100W source.

Further films were irradiated under the 'pyrex' filter using the 1.8kW source but with the space beneath the filter flushed with nitrogen, as part of the work reported in the following chapter. The extents of reaction in these films were measured as a function of the cure exposure but unfortunately the wide variation in the results between different runs made it difficult to ascertain whether the nitrogen atmosphere had any effect on the cure of the films.

#### 4.8 Effect of Photoinitiator Concentration on the Cure of the DGEBA and Epoxy Novolac Systems

##### (A) Hardness Measurements

Lacquers of the DGEBA and the epoxy novolac resins were prepared containing various concentrations of photoinitiator as shown in the Tables below.

TABLE 4.9 Composition (w/w) of the DGEBA Lacquers

% Resin	% Photoinitiator	% Acetone
96.1	2.8	1.1
96.7	2.2	1.1
97.8	1.1	1.1
98.3	0.7	1.1

TABLE 4.10 Composition (w/w) of the Epoxy Novolac Lacquers

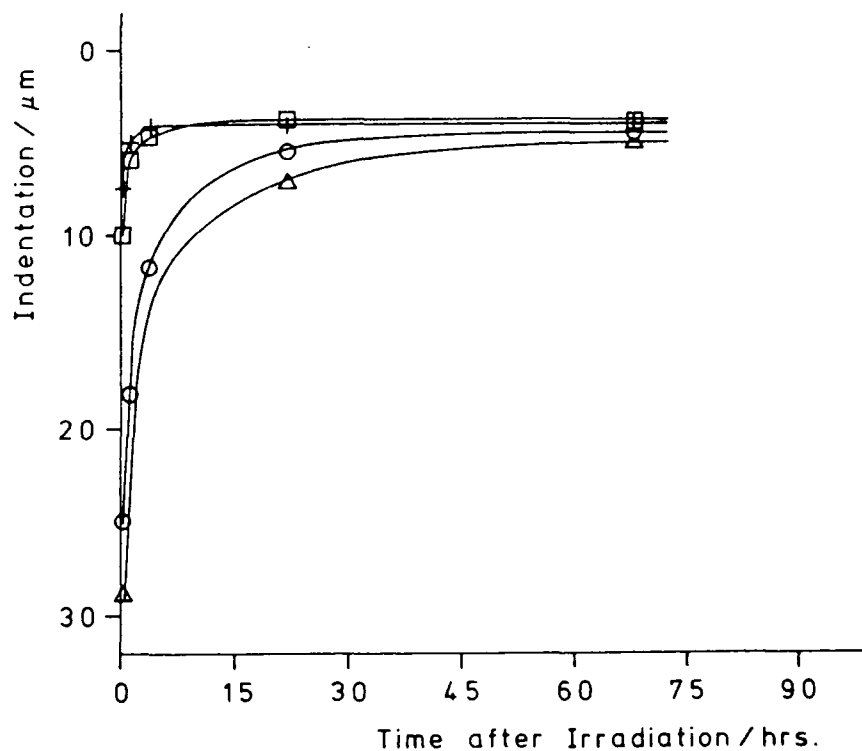
% Resin	% Toluene	% Photoinitiator	% Acetone
83.4	12.4	3.1	1.1
84.3	12.6	2.2	0.9
85.2	12.7	1.0	1.0
85.5	12.8	0.7	1.1

The lacquers were applied to glass plates to give films of 125 $\mu$ m nominal thickness. The films were irradiated for 8 minutes, 18cm from the 100W lamp as in previous experiments. When carrying out the hardness measurements the indenter with a primary weight of 0.25g was applied to the film for 30 seconds after which the secondary weight of 10g was added and the depth of penetration measured 30 seconds later. The measurements were carried out at intervals after irradiation, each measurement being repeated three times and an average taken.

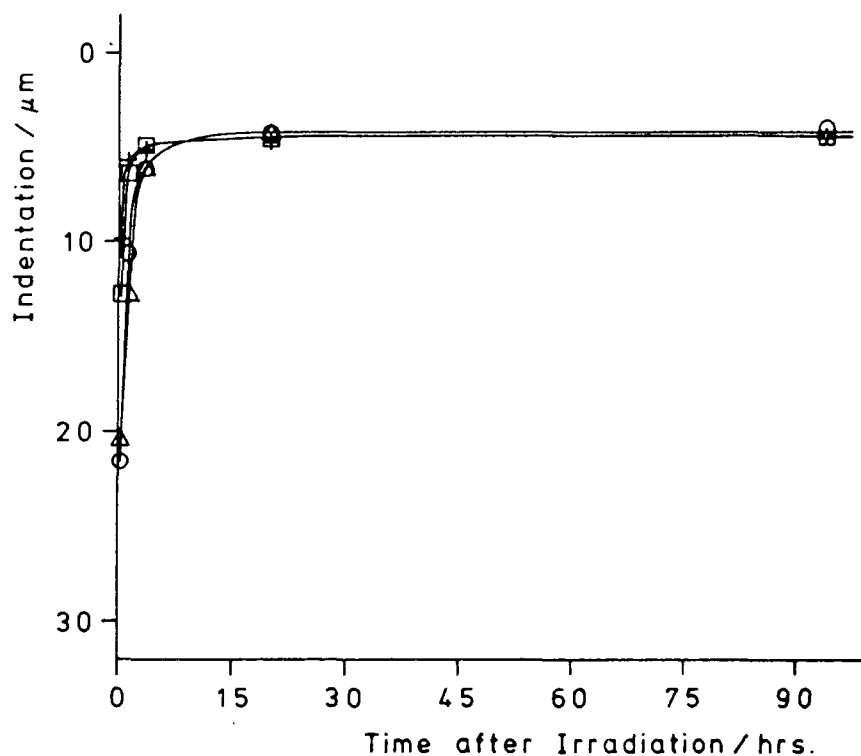
Figure 4.11(a) is a plot of the penetration depth against the time after irradiation for a film of each lacquer of the DGEBA system whilst Figure 4.11(b) is a similar plot for the epoxy novolac system. In general the two plots show that decreasing the concentration of photoinitiator results in softer films immediately after cure and a slower rate of post-irradiation hardening. The effect of lower photoinitiator concentrations is more pronounced for the DGEBA system with the final hardness values of this system also showing some dependence on the photoinitiator concentration.

From the results it would appear that increasing the amount of photoinitiator above 3% would not have any further beneficial effect. Similar results have been reported for the cure of 3,4-epoxycyclohexylmethyl-3',4'-epoxycyclohexane carboxylate with increasing concentrations of a diaryliodonium hexafluoroarsenate photoinitiator, the irradiation time required to produce a film that could no longer be deformed by thumb pressure being taken as a measure of the rate of cure.<sup>10</sup> The fact that photoinitiator concentrations above 3% w/w were found not to increase the rate of cure was attributed to limitations imposed by the light intensity.

FIGURE 4.11 Hardness as a Function of Photoinitiator Concentration and Time after Irradiation



(a) The DGEBA System (+, 2.8; □, 2.2; ○, 1.1; Δ, 0.7% w/w photoinitiator)



(b) The Epoxy Novolac System (+, 3.1; □, 2.2; ○, 1.0; Δ, 0.7% w/w photoinitiator)

On completion of the experiment the actual thickness of the films were measured. This was carried out by embedding a sample of each film in an epoxy resin and then using a microscope equipped with a graticule to measure the film thickness. Films of the DGEBA lacquer were on average  $85 \pm 6 \mu\text{m}$  thick whilst those of the epoxy novolac system were  $75 \pm 6 \mu\text{m}$  thick. Again this is significantly less than the nominal thickness of the film of wet lacquer.

(B) Infra-Red Spectroscopic Measurements of Epoxide Conversion

The previous experiment was repeated using lacquers of the following composition:

TABLE 4.11 Composition (w/w) of the DGEBA Lacquers

% Resin	% Photoinitiator	% Acetone
95.9	3.0	1.1
96.9	2.0	1.1
97.9	1.0	1.1
98.4	0.5	1.1

TABLE 4.12 Composition (w/w) of the Epoxy Novolac Lacquers

% Resin	% Toluene	% Photoinitiator	% Acetone
83.4	12.5	3.1	1.0
84.3	12.6	2.1	1.0
85.1	12.7	1.0	1.2
85.7	12.8	0.5	1.0

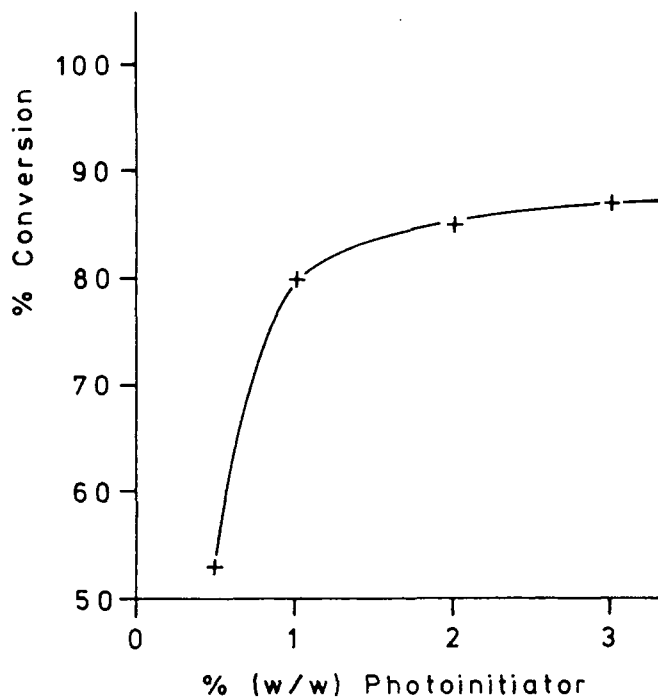
Similar films to those used in the previous experiment were prepared and irradiated using the same conditions. One very important difference however is that the films were pre-

pared on polyethylene rather than glass panels. As will be seen later, the substrate can have a significant effect on the cure of films. IR spectroscopy was used to determine the extent of reaction in each film at intervals over a period of 13 minutes to 75 hours after irradiation.

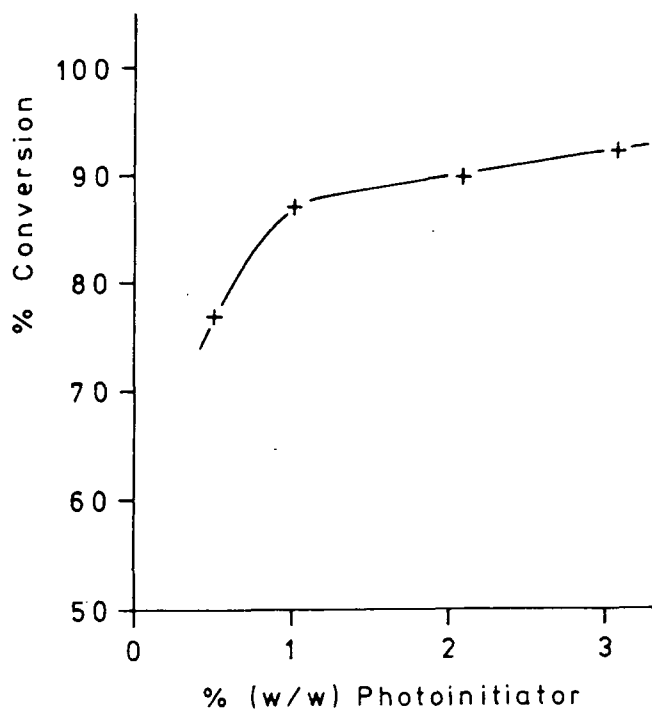
In spite of the scatter in the conversion measurements, there was some indication of post irradiation cure especially in the films containing 0.5 and 1.0% photoinitiator. The average final conversion values are plotted as a function of the photoinitiator concentration for the two systems in Figures 4.12(a) and (b). These two figures indicate that the final conversion is dependent on the photoinitiator concentration, the effect being more pronounced in the DGEBA system. The increase of conversion with increasing photoinitiator concentration can again be interpreted as evidence of inhomogeneous cross-linking leading to the trapping of reactive species. The use of different substrates prevents detailed comparison between the hardness and conversion measurements but both techniques indicate that the DGEBA system is more sensitive to the concentration of photoinitiator.

It is noted that the film of DGEBA containing 2% photoinitiator shows a significantly greater conversion than that measured in a similarly irradiated film in Section 4.6(a). This again illustrates the problems of reproducibility but the general trend is still clear.

FIGURE 4.12 Effect of Photoinitiator Concentration on the Conversion of Epoxide Functionality



(a) The DGEBA System



(b) The Epoxy Novolac System

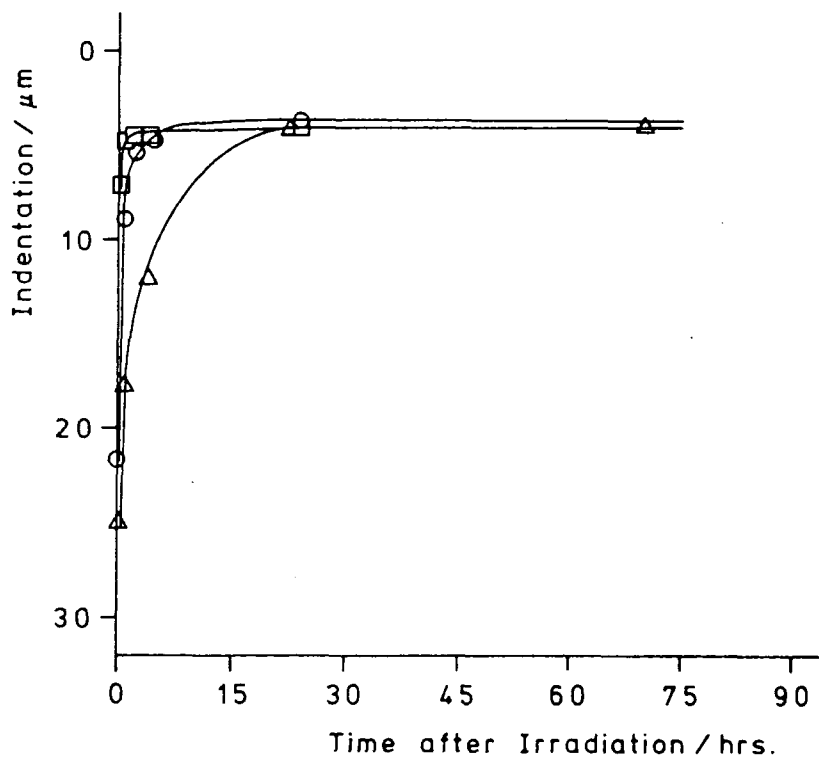
#### 4.9 Effect of Temperature on the Cure of the DGEBA and Epoxy Novolac System as Determined by Hardness Measurements

The 100W lamp was set up in a Fisons Climatic Cabinet so that the temperature at which irradiations were carried out could be controlled to within  $1^{\circ}\text{C}$ . Some control over the relative humidity, RH, was also possible. Films were irradiated at temperatures of  $5^{\circ}\text{C}$  (65% RH),  $10^{\circ}\text{C}$  (65% RH),  $21^{\circ}\text{C}$  (67% RH) and  $31^{\circ}\text{C}$  (62% RH).

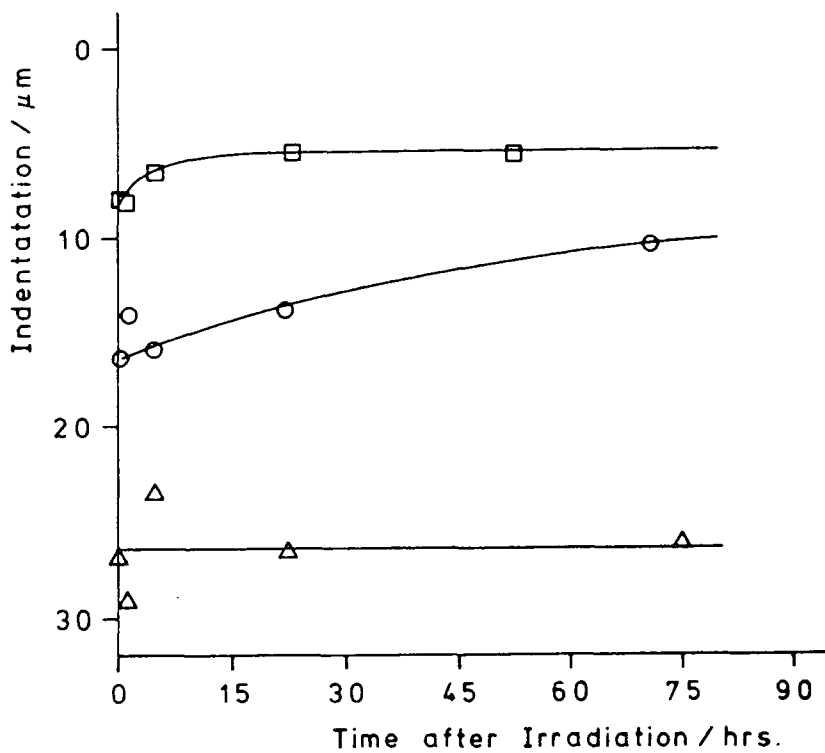
The lacquers of the DGEBA and epoxy novolac resins used contained 96.9% resin, 2.1% photoinitiator and 1.0% w/w acetone and 84.3% resin, 12.6% toluene, 2.0% photoinitiator and 1.0% w/w acetone respectively. Six films of each lacquer were prepared for irradiation at each temperature, the nominal film thickness being  $125\mu\text{m}$ . The films were placed in the climatic cabinet to equilibrate and then irradiated for 8 minutes, 18cm from the source. The microindentation tester was used as previously to measure the hardness of the films at intervals after irradiation. Six separate films were prepared and irradiated for each lacquer and temperature so that one could be removed and its hardness quickly measured, whilst for the next measurement another film was removed and so on. This procedure was adopted so that any warming or cooling of a film whilst a measurement was being taken would not affect subsequent measurements.

The plot of indentation *versus* the time after irradiation in Figure 4.13(a) for films irradiated at 31, 21 and  $10^{\circ}\text{C}$ , shows that the lower the temperature, the softer the film immediately after cure and that the post-irradiation hardening becomes faster as the temperature of irradiation and storage increases although the same hardness values are eventually reached. A similar plot for the epoxy novolac system in Figure 4.14(a) shows the

FIGURE 4.13 Hardness of Films of the DGEBA System as a Function of Temperature and Time after Irradiation

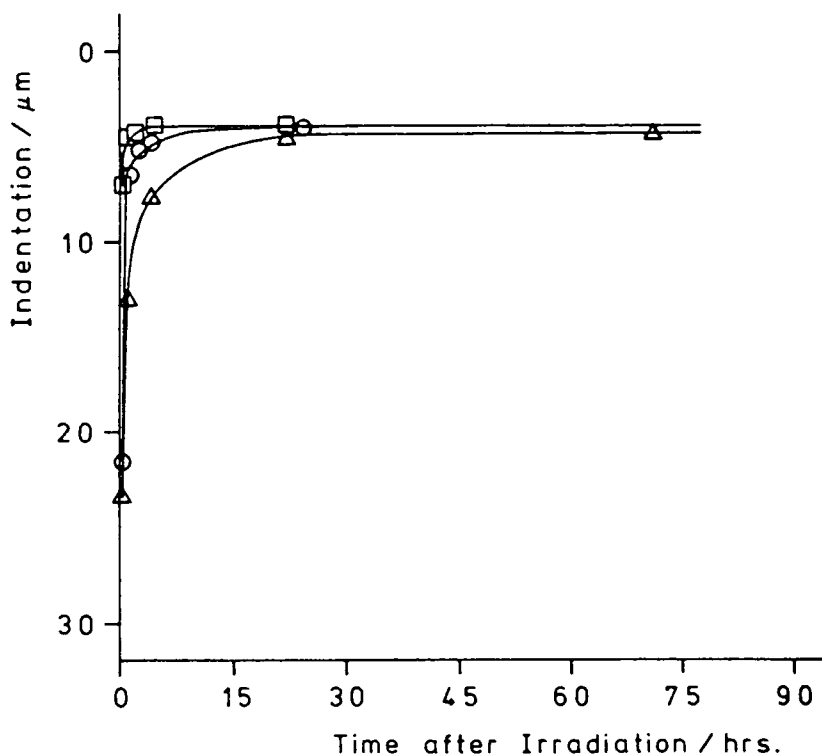


(a) 8 Minutes Irradiation at 10 ( $\Delta$ ), 21 ( $\circ$ ) and 31°C ( $\square$ )

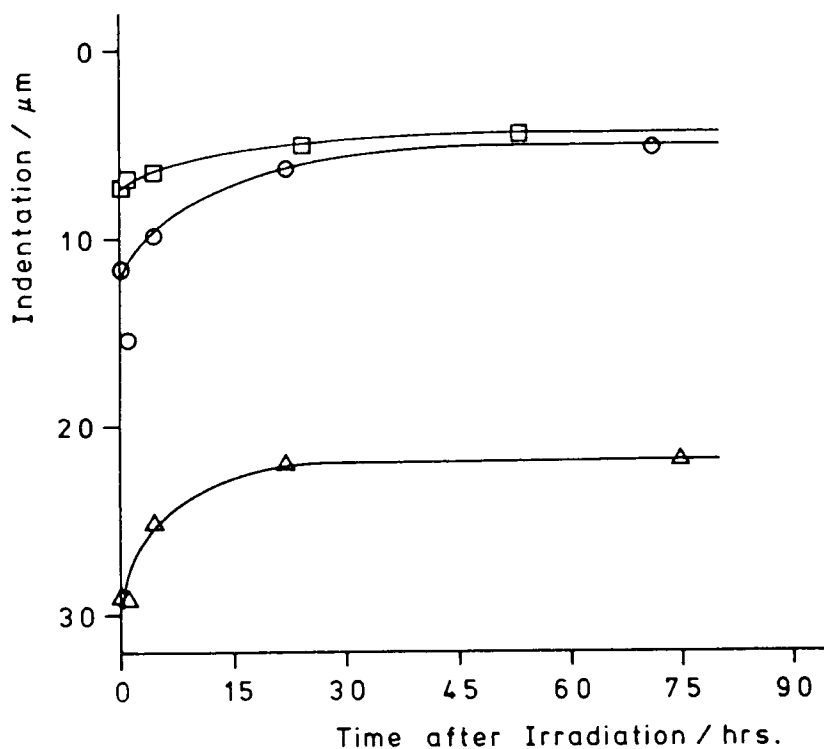


(b) Effect of Increasing Cure Exposure ( $\Delta$ , 8;  $\circ$ , 20;  $\square$ , 45 mins. irradiation) at 5°C.

FIGURE 4.14 Hardness of Films of the Epoxy Novolac System as a Function of Temperature and Time after Irradiation



(a) 8 Minutes Irradiation at 10 ( $\Delta$ ), 21 ( $\circ$ ) and 31°C ( $\square$ )



(b) Effect of Increasing Cure Exposure ( $\Delta$ , 8;  $\circ$ , 20;  $\square$ , 45 mins. irradiation) at 5°C

same trends although the effect of the lower temperature is not as great. As shown in Figure 4.13(b) for the DGEBA system, 8 minutes' irradiation at 5°C results in a much softer film with no post-irradiation hardening. Increasing the irradiation time to 20 and then 45 minutes produces an increase in the initial hardness of the films and there is some degree of post-irradiation hardening. The film irradiated for 45 minutes is still significantly softer 52 hours after irradiation than the films given much shorter cure exposures at higher temperatures. A similar trend is seen in Figure 4.14(b) for the epoxy novolac system irradiated at 5°C. However this system appears to be less affected by this lower temperature; 8 minutes' irradiation results in some degree of post-irradiation hardening, the difference in hardness resulting from 20 and 45 minutes' irradiation is much less than that for the DGEBA system and the films irradiated for 45 minutes approach the hardness of those irradiated at higher temperatures.

The results indicate that the overriding effect of a reduction in the temperature at which irradiations are carried out is a decrease in the rate of polymerization as a result of a reduction in the mobility. The formation of an inhomogeneously cross-linked network could explain why an increase in the irradiation time at the lowest temperature results in an increased degree of cross-linking and hence hardness. The effect of temperature on the photoinitiated cationic cure of epoxy resins has been reported in the literature. Using isothermal DSC to measure the extent of reaction, Crivello and co-workers found that increasing the temperature at which 3,4-epoxycyclohexylmethyl-3',4'-epoxycyclohexane carboxylate containing diaryliodonium hexafluoroarsenate photoinitiator was irradiated resulted in a decrease in the time to reach the maximum cure rate.<sup>10</sup> In

another study Watt<sup>36</sup> found that the time after irradiation at which films of a DGEBA/aryldiazonium salt system became tack-free, decreased with increasing temperature. Films cured at high temperatures (110-120°C), however, were found to be soft and rubbery and when irradiation was carried out above 120°C, no cure was observed. This was attributed to the increased occurrence of chain transfer reactions at elevated temperatures.

The humidity in the climatic cabinet was kept constant and at a reasonable level because it is reported by Watt<sup>36</sup> that high humidity inhibits photoinitiated cationic polymerizations. This is yet another possible variable that could affect the cure of such systems. However the same author notes that films prepared from epoxy resins containing photoinitiator dispersed in water can be cured satisfactorily and that this observation presents something of a paradox.

#### 4.10 Preliminary Investigation of the Effect of Adding a Pigment to the Photocurable Systems

The pigment chosen for this experiment was the rutile form of titanium dioxide. Lacquers of both the DGEBA and epoxy novolac resins were prepared containing *ca.* 5, 10 and 20% w/w of this white pigment, with concentrations of photoinitiator and acetone similar to those used previously.

Irradiation of 125µm nominal thickness films of each lacquer for 8 minutes, 18cm from the 100W source resulted in surface cure only. Increasing the irradiation time to 20 and then 45 minutes did not lead to through cure. The surfaces of these films exhibited wrivelling or wrinkling, an effect noted in other pigmented UV curable systems and which is thought to be due to the rapid cure of the surface introducing stress which is allev-

iated by adopting a convoluted surface profile.<sup>37</sup> Films of 50 $\mu$ m nominal thickness containing 10 and 20% TiO<sub>2</sub> did not cure satisfactorily even after 45 minutes' irradiation whereas the films of both systems containing 5% of the pigment were cured after the longer irradiation period.

Since the rutile form of TiO<sub>2</sub> starts to absorb at  $\sim$ 410nm, reaching a maximum and constant absorption value (ca. 5% transmittance) at  $\sim$ 370nm,<sup>37</sup> the effect of TiO<sub>2</sub> on the cure of two systems is hardly surprising and illustrates the difficulty of pigmenting UV curable systems. The number of variables that can affect the cure of a pigmented film include the photoinitiator and pigment concentration, the absorption and scattering of radiation by the pigment, the film thickness and the spectral distribution of the source make the formulation of pigmented systems complex.<sup>2</sup>

Possible solutions to the pigmentation of the systems examined in this work would be to either choose pigment that does not absorb in the region of 275-313nm or probably more realistically use a photosensitizer that absorbs in a different region of the electromagnetic spectrum to the pigment.

#### 4.11 The Use of TMA to Determine the Effect of various Irradiation Conditions on the Tg of the DGEBA System

Infra-red spectroscopic measurements of the extent of epoxide conversion in films of the photocured epoxy resins have proved quite useful for showing trends such as the increase of conversion with increasing cure exposure. Qualitative measurements of the hardness of the photocured resins, a property related to the degree of cross-linking, proved to be a reasonably sensitive technique for monitoring post-irradiation cure. As

indicated previously the glass transition temperature,  $T_g$ , of a network polymer is another physical property related to the degree of cross-linking. The  $T_g$ s of films of the DGEBA system irradiated under various conditions were measured using penetrometry in an attempt to provide a guide to the relative degree of cross-linking which could be related to the conditions of irradiation and to determine whether the same trends are observed as with IR spectroscopy measurements of epoxide conversion. However the use of  $T_g$ , measured by penetrometry, as a guide to the degree of cross-linking turned out to be much more complicated than originally envisaged.

The  $T_g$  measurements were carried out on samples of films removed from the substrate using the cork-borer. A load of 50g applied to the probe of the TMA instrument and a heating rate of  $5^\circ\text{C min}^{-1}$  were the conditions employed in all the measurements carried out.

(A) Irradiation with the 1.8kW Source

(i) An Initial Investigation of the  $T_g$  of Films Irradiated on Steel

Films of  $200\mu\text{m}$  nominal thickness containing 97.0% resin, 2.0% photoinitiator and 1.0% w/w acetone were prepared on mild steel panels. The films were irradiated using the mini-cure apparatus with both the 1.8kW lamps functioning. It was found that even with the second lamp operational, films required at least 4 passes under the lamps before gelation occurred, whereas a similar film on polyethylene irradiated using only 1 lamp gave a rigid film after 1 pass. The UV reflectance of the substrate can have a significant effect on the cure of films but it would seem unlikely that polyethylene could have a greater reflectance than metal. When using polyethylene as the substrate, it was

attached to a glass panel but it is improbable that reflection from the glass could give rise to the above effect since films on polyethylene attached to metal panels were polymerized after 1 pass. Another possible explanation could be that the films on polyethylene are more easily warmed by the heat from the lamps whereas films in intimate contact with the metal are not heated as efficiently. It is also reported that the substrate can inhibit or prevent the cure of films if it is reactive towards the acid initiator or propagating species.<sup>3</sup> Since it was noted that the steel under a cured film was slightly discoloured, reaction of the acidic initiating species with the steel substrate is a distinct possibility.

The  $T_g$  of samples of a film given 4 passes under the lamp were measured over a period of time starting from 96 hours after irradiation. Figure 4.15 shows an example of a TMA trace obtained.

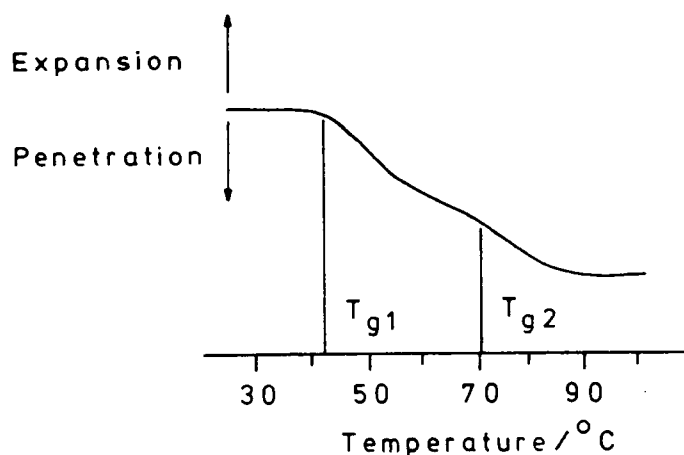


FIGURE 4.15 Example of the TMA Trace for a Film of the DGEBA System Cured on Steel

The above trace was reproducible with fresh samples of film but repetition of the measurement on the same sample gave only one transition as did subsequent runs. The temperature of the onset of the two transitions are shown in the Table below, along with the  $T_g$  values recorded on subsequent measurements.

TABLE 4.13 Effect of Repeating the Tg Measurements on a Sample of Film Cured on Steel

Run	1	2	3	4	5	6
Tg/°C	Tg <sub>1</sub> =43, Tg <sub>2</sub> =70	63	72	75	68	77

The two transitions could be indicative of two relaxation processes occurring independently of one another. This may be interpreted as being a consequence of the network containing domains of high and low mobility, the formation of these regions resulting from an inhomogeneous mechanism of cross-linking as detailed in Chapter One. As the temperature of the sample is raised, the less cross-linked more mobile regions could undergo relaxation at a lower temperature than the less mobile regions giving rise to a penetrometry trace of the above form. The attenuation of light penetrating the film resulting in a reduction in the number of initiating species produced deeper in the film and hence a lower degree of cross-linking could contribute to the above observation. It is unlikely that it is the sole cause however since one might expect this effect to give a gradual decrease in the degree of cross-linking on going deeper into the film and not such a pronounced difference in the degree of cross-linking as is indicated by the TMA traces.

Repeating the measurement on the same sample which was heated to 102°C in the first measurement results in only one observable transition, the onset of which occurs at a temperature mid-way between those of the two transitions observed for the pristine sample. This would indicate that as the temperature of the network is raised, the mobility increases and trapped reactive species become active leading to further cross-linking, especially in regions of low cross-link density. The result is a decrease in the two phase nature of the system and only one

observable glass transition on subsequent measurements. The temperature of the onset of this single transition indicates that the cross-link density has not increased to equal that of the domains of high cross-link density in the unheated network. However, subsequent heating of the sample during further measurements does result in  $T_g$  becoming similar to the value of  $T_g$  attributed to regions of high cross-link density in the unheated network. The observed increase of  $T_g$  in heated samples may not be solely due to increases in the degree of cross-linking. Thermo-gravimetry, the measurement of weight change with temperature, showed that a sample of the above film started to lose weight in the region of  $100^\circ\text{C}$  when heated at  $10^\circ\text{C min}^{-1}$  under a nitrogen atmosphere and that the film had lost 3.5% of its weight at  $200^\circ\text{C}$ . The loss of low molecular weight species which may include unreacted monomer, moisture, photoinitiator residues or photodegradation products would also contribute to an increase of  $T_g$ .

The thermal treatment of the system was further investigated by heating samples of a film under a variety of regimes. Samples heated to 80, 102 and  $134^\circ\text{C}$  for 1 hour gave  $T_g$ s of *ca.* 80, 85 and  $93^\circ\text{C}$  respectively after repeated measurements. The sample heated to  $134^\circ\text{C}$  did not show a significant increase after the first measurement whereas the others did. An increase in the degree of cross-linking in the sample heated to the higher temperature perhaps combined with a greater loss of low molecular weight species could account for its higher  $T_g$ .

Two glass transitions were also observed in the trace from a sample of a  $200\mu\text{m}$  nominal thickness film of the epoxy novolac system of similar composition to that used previously and irradiated on steel in a similar way to the above films. The

first transition occurred at 35°C whilst the second occurred at 75°C; repeating the measurement on the same sample resulted in one transition at 51°C. Heating a sample of the film to 128°C for 1 hour gave a single Tg in the region of 90-100°C after a number of measurements.

The effect of adding a reactive diluent to the DGEBA system was investigated. Lacquers in which up to 20% w/w of the DGEBA resin was replaced by the diglycidyl ether of butanediol were prepared and films of 200µm nominal thickness irradiated as above. It was found that even in the film containing 20% w/w of the reactive diluent, the temperature of the onset of the two transitions, 46 and 72°C respectively, were very close to those observed in a film containing no reactive diluent. After being heated to 134°C for 1 hour and a number of measurements, the Tg of a sample of the film containing 20% of the diluent was found to be 90°C which, again, is quite close to the value obtained for a film containing no reactive diluent. In view of the flexible structure of the diluent, one might expect the Tg of the system containing the diluent to be lowered. Addition of the diluent however reduced the viscosity of the system and it may be that this increase in mobility leads to an increase of monomer conversion and hence cross-link density, offsetting the increased flexibility of the system; an effect that has been observed in other photocurable systems.<sup>38</sup> Inhomogeneous cross-linking however still persists even with the addition of diluent. Other possible explanations for the above observation could involve the formation of polymer rich in one of the monomers, with other areas of the network rich in the other monomer for reasons of differences in compatibility or reactivity. If the two areas of network acted independently then under the conditions adopted for measuring Tg, relaxation

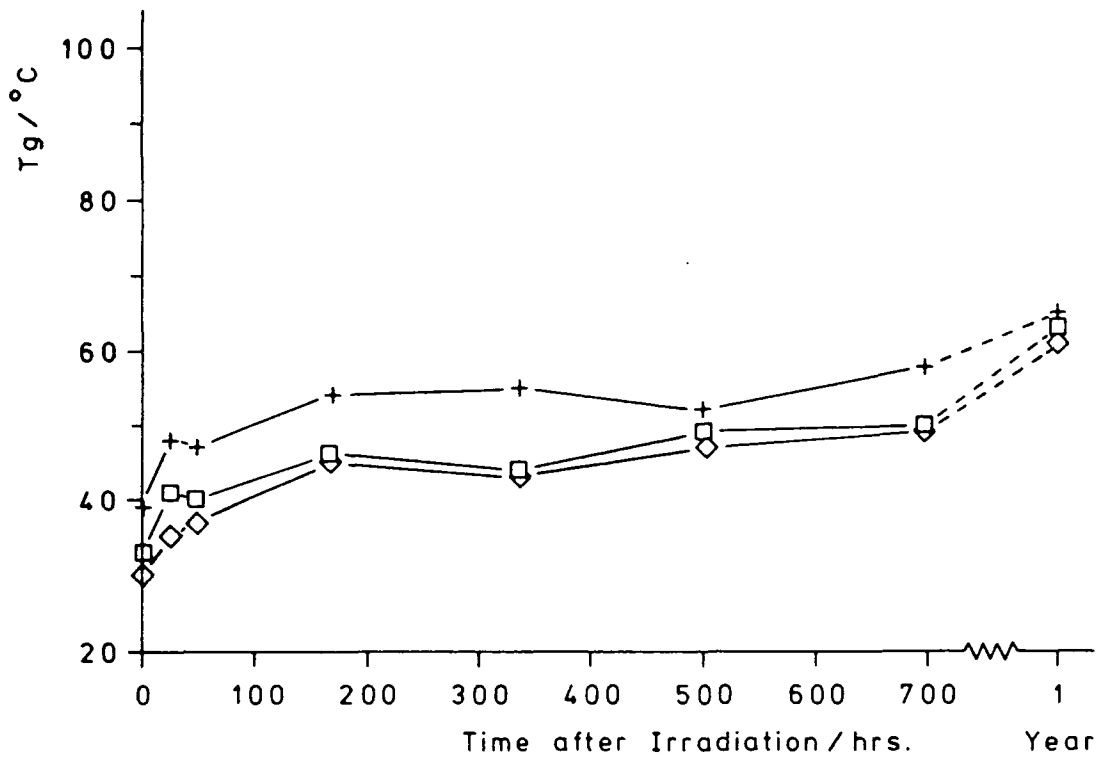
processes in the areas rich in diluent probably would not be detected since the examination of a film of homopolymer of the diluent indicated that the  $T_g$  is below room temperature.

(ii) Effect of Increasing Cure Exposure and Film Thickness on the  $T_g$  of Films Irradiated on Steel

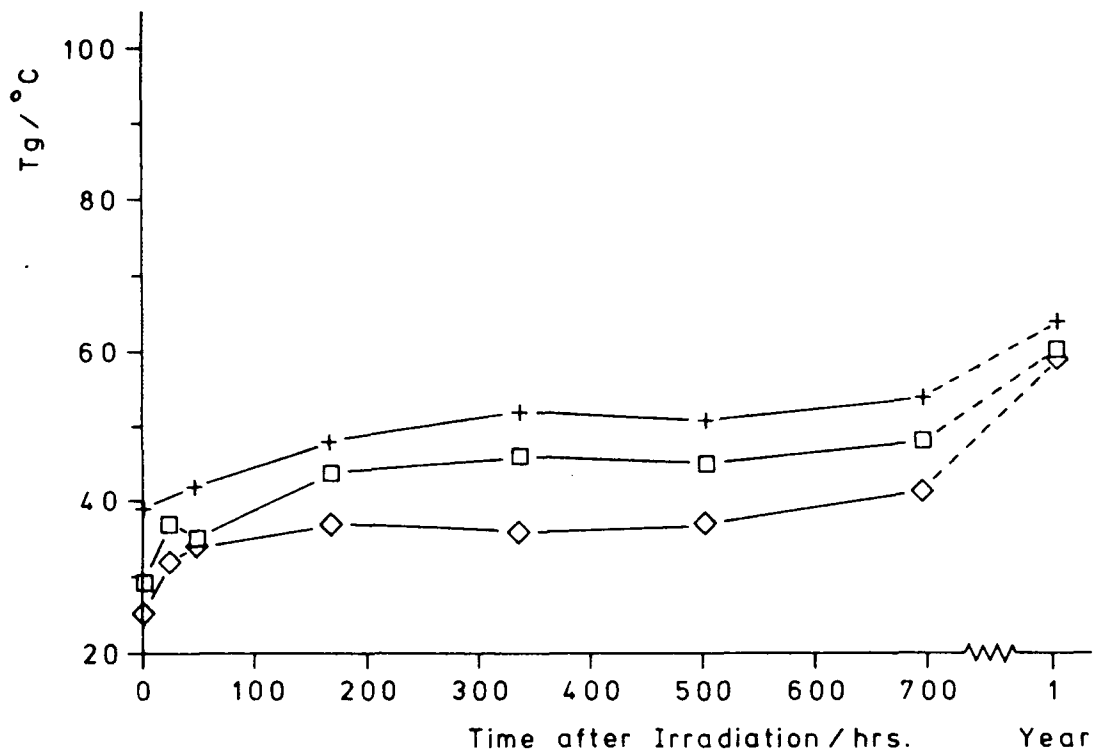
Films of 100 and 200 $\mu$ m nominal thickness prepared on steel from a lacquer containing 96.9% resin, 2.1% photoinitiator and 1.0% w/w acetone were irradiated using the mini-cure apparatus with only one of the 1.8kW lamps functioning. The films were given 5, 10 and 20 passes under the lamp, 5 passes being the lowest exposure required to produce a rigid film and then stored in the dark. The first  $T_g$  measurement on each film was carried out 10 minutes after irradiation.

Figures 4.15(a) and (b) show the temperature of the onset of initial penetration plotted against the time after irradiation for the 100 $\mu$ m and 200 $\mu$ m films respectively. In both sets of films this initial  $T_g$  increases with increasing cure exposure, although the difference between films given 5 and 10 passes is not as pronounced in the thinner films. The increase of the initial  $T_g$  with cure exposure could be a combination of an increase in photoinitiator photolysis or the temperature of films leading to a greater degree of conversion and hence cross-linking. Generally there is a marked increase in the initial  $T_g$  of a film over the first 168 hours after irradiation, the bulk of this increase occurring within 24 hours and probably within 1 hour of irradiation, followed by a slight drift upwards in the  $T_g$  value over the next 500 hours or so. In all cases the initial  $T_g$  measured 1 year after irradiation shows a significant increase over the value obtained 696 hours after irradiation, indicating that the system continues to react albeit very slowly. This continued reaction leads the difference in the

FIGURE 4.16 Initial Tg as a Function of Cure Exposure and Time after Irradiation for Films Irradiated on Steel using the 1.8kW Source ( $\diamond$ , 5;  $\square$ , 10; +, 20 passes)



(a) Films of 100µm Nominal Thickness



(b) Films of 200µm Nominal Thickness

initial Tg due to increasing cure exposure to diminish as time progresses. The thicker films tend to show a lower initial Tg than the thinner films given an equivalent cure exposure although this difference again diminishes with time. However the thicker film given 20 passes does show a higher initial Tg than the thinner film given 10 passes for example.

All the films of 200 $\mu$ m nominal and those of 100 $\mu$ m nominal thickness given 5 or 10 passes under the lamp showed a higher temperature transition, the values being shown in Table 4.14.

TABLE 4.14 Second Tg ( $^{\circ}$ C) as a function of Cure Exposure, Sample Thickness and Time after Irradiation for Films Cured on Steel using the 1.8kW Source

Time after irradiation /hrs.	100 $\mu$ m			200 $\mu$ m		
	5 passes	10 passes	20 passes	5 passes	10 passes	20 passes
0.17	70	73	-	-	-	-
24	69	69	71	63	62	-
48	69	61	-	63	64	71
168	68	69	-	68	70	70
336	74	71	-	72	72	74
504	72	71	-	69	69	75
696	71	72	-	71	72	75
1 year	-	-	-	80	-	-

The temperature of the onset of this second transition in films of 100 $\mu$ m thickness given 5 and 10 passes under the lamp does not change significantly in the 696 hour period after irradiation but after approximately 1 year, only one transition is observed. Although the 200 $\mu$ m films do not exhibit a second transition 10 minutes after irradiation, one becomes discernible when the TMA trace is recorded 24 or 48 hours after irradiation. The temperature at which this second transition occurs in these films does

appear to increase with time but less so in the film given 20 passes. After 1 year however only the film given 5 passes showed a clearly discernible second transition.

The above observations, in particular the occurrence of two transitions again lend support to the hypothesis of inhomogeneous cross-linking and the trapping of reactive species. The increase in the lower  $T_g$  with irradiation time is consistent with the interpretation of the results of IR spectroscopic measurements of conversion as a function of the cure exposure. The apparent decrease in the mobility of these less cross-linked regions could be due to an increased proportion of more highly cross-linked domains exerting a 'stiffening' effect on the low cross-link density regions as well as a possible increase in the cross-link density of these regions.

The onset of penetration at a lower temperature in the thicker films is probably a consequence of a reduction in the generation of initiating species in the lower reaches of the films due to attenuation of the light penetrating the films. The fewer propagating centres result in a lower degree of conversion and hence cross-linking prior to trapping. No second transition was observed in these films immediately after irradiation, possibly because at this stage the system is still fairly homogeneous as substantial regions of the network have not really become highly cross-linked due to the reduced number of initiating species but as the polymerization progresses these areas are formed and two transitions become apparent. The maximum number of initiating species will be produced in the thinner film given the longest cure exposure which may explain why this film tends to show one transition, the greater number of initiating species resulting in a more homogeneous distribution of cross-linking. The  $T_g$  of this film is still quite low however indicating that

material of lower cross-link density is present.

It would appear that the films do continue to react in the dark after irradiation. Although quite rapid initially the rate of this reaction becomes very slow but it does still occur. In all but the thickest film given the least cure exposure this continued reaction leads to a loss of the two phase nature of the system and only one observable transition 1 year after irradiation. Although it is proposed that reactive species become trapped in highly cross-linked regions they must still have a small degree of mobility to give rise to the above observation.

The potential for thermal reaction was investigated after a year's storage, the results in Table 4.15 showing the effect of repeating the measurement after the sample has been heated to 150°C in the first measurement.

TABLE 4.15 Effect of Repeating the T<sub>g</sub> Measurement on Films Cured on Steel using the 1.8kW Source and Stored for One Year

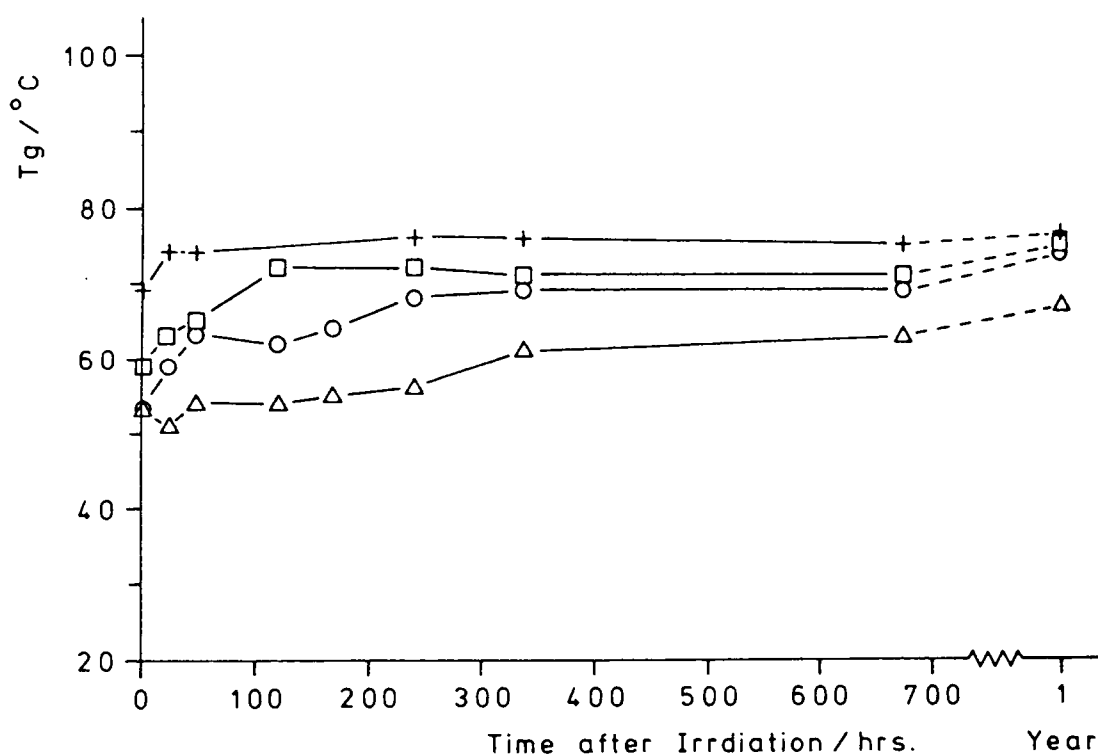
Film thickness/ $\mu\text{m}$	100				200			
Number of passes	5		20		5		20	
Run	1	2	1	2	1	2	1	2
T <sub>g</sub> /°C	59	74	65	90	59,80	70	64	83

Heating the film of 200 $\mu\text{m}$  nominal thickness given 5 passes results in only one observable transition at a temperature between those of the two transitions observed in the initial run. Heating the other films results in an increase in the temperature of the onset of the single transition, the magnitude of the increases being greater in the thinner film given a longer cure exposure. This increase in T<sub>g</sub> may be due to a combination of the loss of low molecular weight species and an increase in the degree of cross-linking.

(iii) Effect of Increasing Cure Exposure and Film Thickness on the Tg of Films Irradiated on Polyethylene

Films of 100 and 200 $\mu$ m nominal thickness were prepared on polyethylene from lacquers containing 97.0% resin, 2.0% photoinitiator and 1.0% w/w acetone, irradiated using the mini-cure apparatus and then stored in the dark. The experiment with films of 100 $\mu$ m nominal thickness was repeated three times, similar lacquer compositions being used. All three runs showed similar trends. In the majority of measurements, only one transition was observed but occasionally a second transition did become discernible which may be indicative of some inhomogeneity in the cure over the area of a film.

FIGURE 4.17 Tg as a function of Cure Exposure and Time after Irradiation for Films of 100 $\mu$ m Nominal Thickness Irradiated on Polyethylene using the 1.8kW Source ( $\Delta$ , 1; O, 3;  $\square$ , 10; +, 20 passes)



The results from one of the experiments using 100 $\mu$ m films are shown in Figure 4.17, the first Tg measurement being carried out 10 minutes after irradiation. Although films were given 1,2,3,5,10 and 20 passes under the lamp, the results for only four of these films are plotted to avoid congestion of the Figure. As with the films cured on steel, the Tg of a film tends to increase with increasing cure exposure implying that the degree of conversion increases, a trend indicated by IR spectroscopic measurements of conversion on similarly irradiated films. The Tg of the films given 3, 10 and 20 passes show a marked increase over the first 168 hours or so after irradiation, with a slight increase after this period so that after 1 year the films have very similar Tg values. The film given 1 pass appears to show a more gentle increase throughout the period after irradiation and after 1 year the Tg of this film is still lower than that of the other films.

Infra-red spectroscopic measurements were carried out on similar films stored in the dark for 1 year, to determine whether any increase in conversion has occurred over this time period. The results in Table 4.16 indicate that there is some increase in the extent of reaction over this period in all the films except that given 20 passes.

TABLE 4.16 Epoxide Conversion after 1 year's Storage for Films of 100 $\mu$ m Nominal Thickness Cured on Polyethylene using the 1.8kW Source

Number of passes	% Conversion	
	I + 48 hours	I + 1 year
1	78 $\pm$ 2	82 $\pm$ 2
3	76 $\pm$ 1	80 $\pm$ 1
10	79 $\pm$ 5	86 $\pm$ 1
20	85 $\pm$ 2	85 $\pm$ 2

The fact that the above films only show one transition does not necessarily rule out the occurrence of inhomogeneous cross-linking, which the interpretation of the increase of  $T_g$  with cure exposure implies is taking place. Possibly, the difference in the mobility of the high and low cross-link density regions is not sufficient to give rise to two detectable transitions.

Interestingly, unlike the above films cured on polyethylene, films of similar composition and thickness irradiated on steel tend to show two transitions with the initial penetration of the probe occurring at a lower temperature for all cure exposures suggesting that the degree of cross-linking is lower. Even if the induction period associated with the gelation of the films on steel were to be related to the reaction of the initiating species with the substrate, the rate of photolysis of the photoinitiator or a reduction in the heating of films, one might expect the films given 10 or 20 passes to show at least a similar degree of cross-linking to a film on polyethylene given 1 pass under the lamp. Contrary to expectation it may be that the degree of cross-linking is lower in the films on steel given longer cure exposures. The lower rate of initiation and hence polymerization might result in the formation of a network structure that facilitates the trapping of reactive species possibly at an earlier stage in the cross-linking process thus reducing the kinetic chain length. Alternatively, the results may indicate that the slower rate of polymerization of films on steel affects the topology of the network produced so that even though the overall degree of cross-linking is greater for the films on steel given longer cure exposures than for a film on polyethylene given a short cure exposure, the network contains a greater proportion of less cross-linked material. After 1 year's storage

the films on steel given 10 and 20 passes do show a similar  $T_g$  to that of the film cured on polyethylene given 1 pass due to continued polymerization but the values are still significantly lower than for films on polyethylene given greater cure exposures.

FIGURE 4.18  $T_g$  as a Function of Cure Exposure ( $\Delta$ ,1;  $O$ ,3;  $\square$ ,10;  $+$ ,20 passes) and Time after Irradiation for Films of 200 $\mu$ m Nominal Thickness Irradiated on Polyethylene using the 1.8kW Source

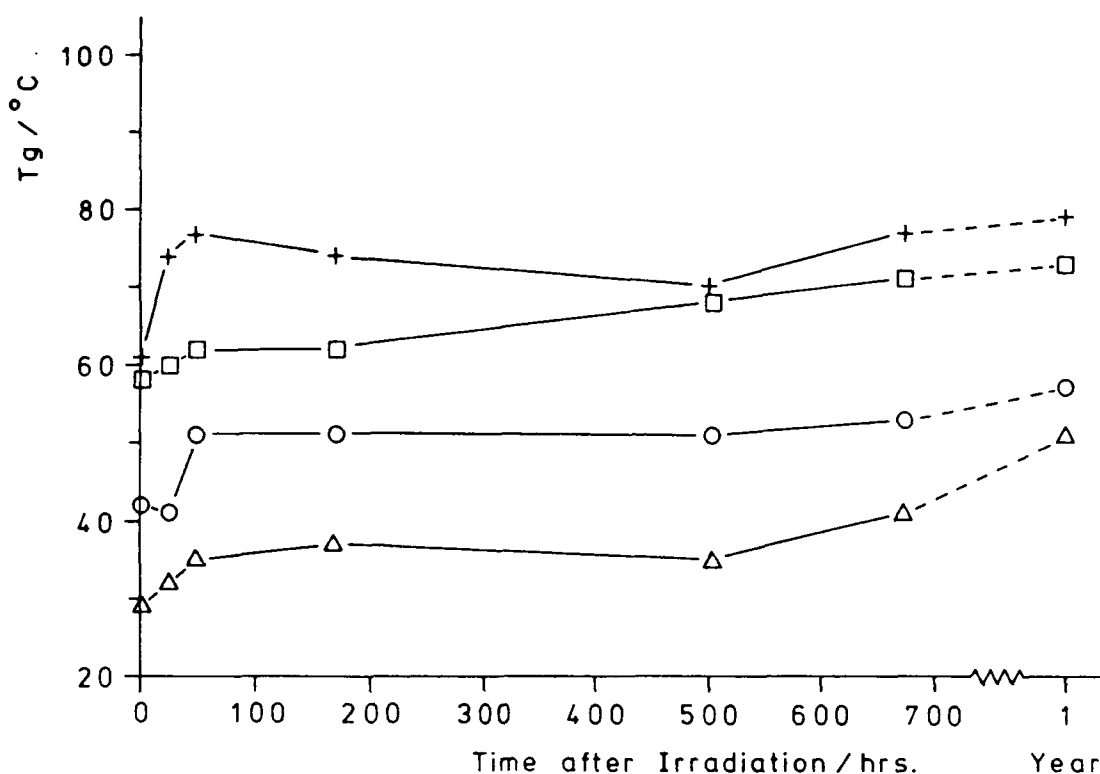


Figure 4.18 shows that the  $T_g$  of 200 $\mu$ m films increases with increasing cure exposure and as with the films of 100 $\mu$ m, an increase in the  $T_g$  of the films occurs within 168 hours of irradiation with only a slight increase occurring after this period. Even after 1 year there is still a significant difference in the  $T_g$ s of the films. Comparison of Figures 4.17 and 4.18 shows that the difference in  $T_g$ s between the 200 $\mu$ m films is more pronounced than for the 100 $\mu$ m films and that the films given

1 and 3 passes show a significantly lower  $T_g$  than the similarly cured films of  $100\mu\text{m}$  thickness. The difference between the 200 and  $100\mu\text{m}$  films given 10 and 20 passes is much less, showing the effect of film thickness on the extent of cure can be offset somewhat by increasing the radiation dose.

The penetrometry traces for the film of  $200\mu\text{m}$  thickness given 1 pass did not show a very smooth penetration of the probe into the sample possibly indicating that there were two unresolved transitions and indeed in three of the traces two transitions were discernible. However the temperature of the onset of penetration is of the same order as that of a film of the same thickness given 5 passes on steel, yet in the latter film two transitions were clearly discernible. Also the temperature of penetration is significantly lower than a film of  $100\mu\text{m}$  on steel which again showed two transitions. If the form of the penetrometry trace were to be simply related to the degree of cross-linking, the film of  $200\mu\text{m}$  on polyethylene given 1 pass would be expected to show two distinct transitions. Since two transitions are not clearly discernible this may be further evidence that a lower rate of polymerization resulting from the cure of films on steel affects the topology and  $T_g$  of the network formed. Similar conclusions can be arrived at when comparing the  $T_g$  of the film of  $200\mu\text{m}$  thickness on polyethylene given 3 passes with the  $T_g$  of films irradiated on steel.

The thermal treatment of films cured on polyethylene after a year's storage was investigated, the results being shown in Table 4.17.

Repeating the measurement after heating the film to  $150^\circ\text{C}$  in the first measurement results in an increase in the  $T_g$  of the sample, the magnitude of this increase being greater in the thinner film given the greater cure exposure.

TABLE 4.17 Effect of Repeating the Tg Measurement on Films Cured on Polyethylene using the 1.8kW Source and Stored for 1 Year

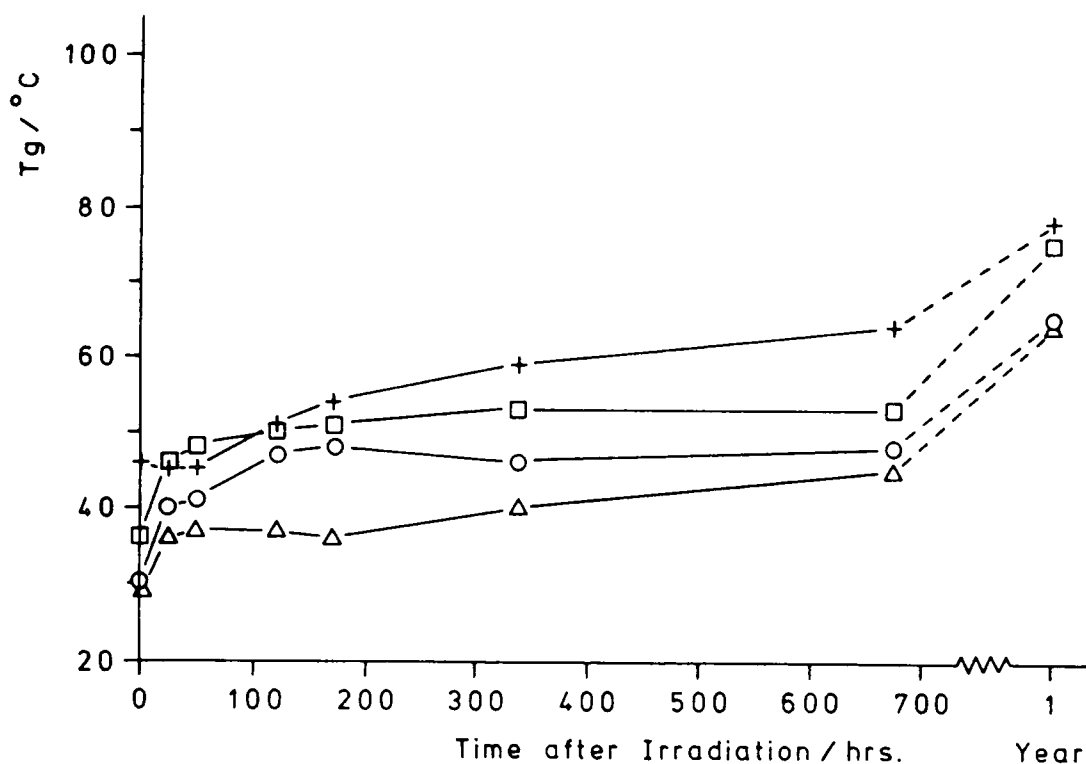
Film thickness/ $\mu\text{m}$	100						200					
	1		5		20		1		5		20	
Run	1	2	1	2	1	2	1	2	1	2	1	2
Tg/ $^{\circ}\text{C}$	67	83	74	88	76	99	53,96	61	64	73	78	95

(iv) Effect of Increasing Cure Exposure to Filtered Light

Films of 100 $\mu\text{m}$  nominal thickness were prepared on polyethylene from a lacquer containing 97.0% resin, 2.0% photo-initiator and 1.0% w/w acetone, irradiated using the mini-cure apparatus with the 'pyrex' filter in place and then stored in the dark. A sample of the films given 3, 10 or 20 passes under the lamp could be removed immediately to obtain a Tg measurement 10 minutes after irradiation whereas the tackiness of the film given 1 pass prevented the removal of a sample for at least 2½ hours after irradiation.

The majority of the traces recorded at intervals after irradiation showed two transitions and it is the temperature of the onset of initial penetration that is plotted in Figure 4.19. As seen for the other films investigated this initial Tg tends to increase with increasing cure exposure. After a marked increase of this Tg over a period of 168 hours, the rate of increase shows considerably and any further increase only becomes apparent on going from 672 hours to 1 year after irradiation. After 1 year's storage, the difference in Tg between the films given 1 and 3 passes diminishes as does that between the films given 10 and 20 passes but the difference between films given 3 and 10 passes still remains.

FIGURE 4.19 Initial Tg as a Function of Cure Exposure ( $\Delta$ , 1;  $\circ$ , 3;  $\square$ , 10;  $+$ , 20 passes) and Time after Irradiation for Films Irradiated with Filtered Light using the 1.8kW Source



The temperatures at which the second transition occurs are recorded in Table 4.18 as a function of the cure exposure and time after irradiation.

The films given 1 and 3 passes do not show a second Tg 3 hours and 10 minutes after irradiation respectively which may indicate that as with the films of 200 $\mu$ m on steel, the reduced number of initiating species formed results in a more homogeneous lightly cross-linked network for a short period after irradiation. Only three of the measurements on the film given 20 passes showed a second transition but the penetration of the probe into the sample for the remaining measurements was not smooth perhaps indicating that two overlapping transitions may be present but

TABLE 4.18 Second Tg ( $^{\circ}$ C) Function of the Cure Exposure and Time after Irradiation for Films Irradiated with Filtered Light using the 1.8kW Source

Time after irradiation/ hrs.	1 Pass	3 Passes	10 Passes	20 Passes
0.17	- *	-	66	-
24	63	65	72	76
48	65	63	65	80
120	-	69	70	81
168	65	68	69	-
336	-	-	67	-
672	66	66	71	-
1 year	89	94	-	-

\* 3 hours after irradiation

not resolved. The temperature at which this second transition occurs only shows a marked increase on going from 672 hours to 1 year after irradiation for the films given 1 or 3 passes. The continued reaction in the film given 10 passes results in an apparently more homogeneous network as only one transition is observed after 1 year's storage. The occurrence of two transitions may again be interpreted as being indicative of an inhomogeneously cross-linked network.

Infra-red spectroscopic measurements were carried out on films left in the dark for one year to determine whether continued conversion of epoxide groups occurred. Table 4.19 shows the results which indicate that there is virtually no change in conversion after 1 year's storage whereas TMA implies that an increase in conversion does occur.

In the 692 hour period after irradiation, the initial penetration of the probe occurs, for all cure exposures, at a

TABLE 4.19 Epoxide Conversion after 1 Year's Storage for Films Irradiated with Filtered Light using the 1.8kW Source

Number of passes	% Conversion	
	I + 48 hrs	I + 1 year
1	82 ± 2	79 ± 2
3	80 ± 3	80 ± 2
10	78 ± 3	80 ± 2

-----

lower temperature in the above films than in the films irradiated with the full output of the lamp and also the above films tend to show two transitions. It might be expected that a film irradiated with filtered light shows a lower degree of cross-linking than a film given an equivalent cure exposure using the full output of the source. In the case of films given lower cure exposures this may be due to a reduction in the light intensity reaching the films since the filter absorbs longer wavelength UV light as well as totally absorbing shorter wavelength light whilst for longer cure exposures the reduction in cross-linking could also possibly be due to a combination of network relaxation and the low rate of polymerization limiting the extent of reaction as is thought to occur in the photoinitiated free radical cure of unsaturated resins. However one would expect the extent of photoinitiator photolysis to be greater in films given 10 and 20 passes with the filter in place than in a film given 1 pass using the full output of the lamp and hence the degree of cross-linking to be greater as the IR spectroscopic measurements of conversion in Section 4.7(B) suggest is the case unlike the TMA results. Indeed the conversion measurements would tend to suggest that the extent of reaction in films given

the longer cure exposures with and without the filter in place are quite similar. Contrary to expectation and the conversion measurements, the films given longer cure exposure may be less well cured than the film given a short exposure to the source, without the filter present. Again this could be a result of the lower rate of initiation and hence polymerization giving rise to a mechanism of network formation amenable to the trapping of reactive species possibly at an earlier stage in the process, thus reducing the kinetic chain length. Alternatively the above observation may indicate that the slower rate of polymerization resulting from the use of the filter affects the topology of the network produced, giving rise to a greater proportion of higher mobility regions even though the overall degree of cross-linking may be similar to, or greater than, that of a network produced by a more rapid rate of polymerization. After 1 year's storage, the films given 10 and 20 passes with the filter in place show only one transition which occurs at a similar temperature to the films given equivalent cure exposures using the full output of the lamp indicating that continued polymerization results in a similar topology and rigidity of the network in films given longer cure exposures with and without the filter in place. The films given 1 and 3 passes with the filter in place still show two transitions after 1 year's storage and the initial penetration of the probe occurs at a lower temperature than films given equivalent cure exposures using the full output of the source perhaps reflecting a reduction in the formation of initiating species in the former films.

The potential for an increase in the  $T_g$  due to heating, even after one year's storage, was again demonstrated by repeating the  $T_g$  measurements on such films. Table 4.20 shows the results.

TABLE 4.20 Effect of Repeating the Tg Measurement on Films Irradiated with Filtered Light using the 1.8kW Source and Stored for 1 Year

Number of passes	1		5		20	
Run	1	2	1	2	1	2
T <sub>g</sub> /°C	64,89	69	68,96	83	78	93

-----

Initially the films given 1 and 5 passes show two transitions but on repeating the measurement only one transition is apparent. The temperature of the onset of the single transition for the film given 5 passes is significantly higher than that for the first transition seen in the first run whilst that for the film given 1 pass is only slightly greater. The film given 20 passes showed one transition initially, the temperature of the onset of this transition showing a marked increase on subsequent measurement.

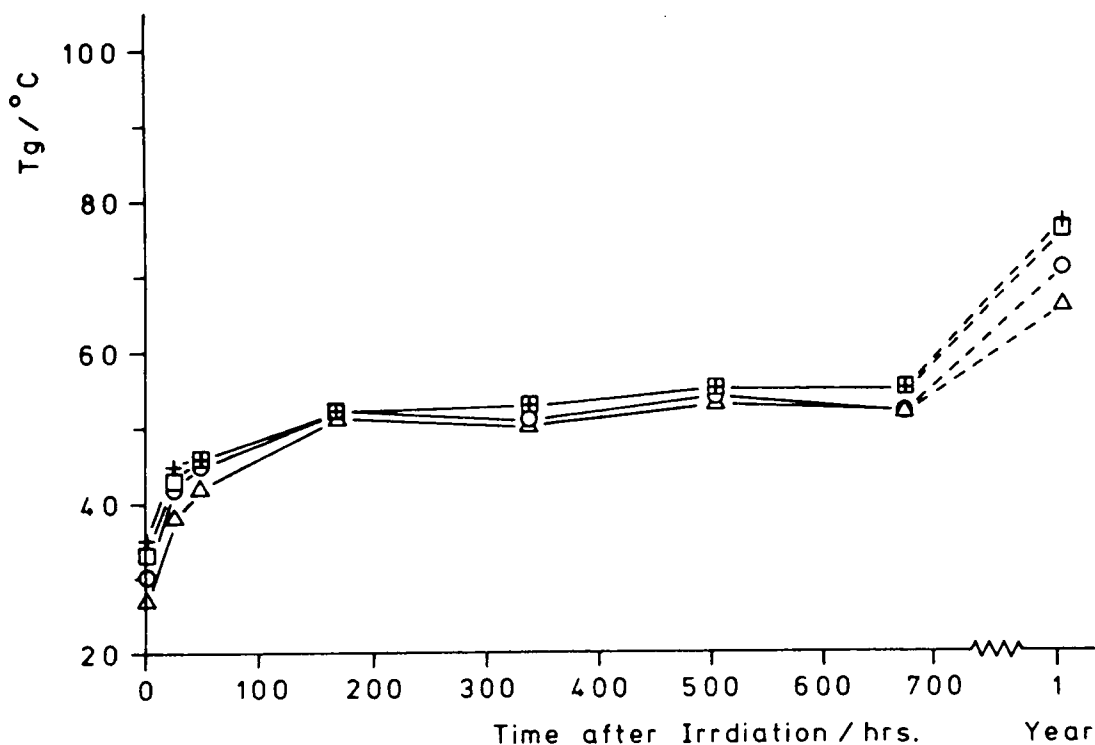
(B) Irradiation with the 100W Source

(i) Effect of Increasing Cure Exposure

Films of 100µm nominal thickness comprising 97.0% resin, 2.0% photoinitiator and 1.0% w/w acetone were prepared on polyethylene and irradiated with the 100W lamp, the intensity of light reaching the films being 16.7 mW cm<sup>-2</sup>. Initial T<sub>g</sub> measurements were carried out 10 minutes after irradiation, the films being stored in the dark prior to this measurement and between subsequent measurements.

The films tended to show two transitions, Figure 4.20 shows a plot of the temperature of the onset of initial penetration against the time after irradiation and indicates a slight increase of this T<sub>g</sub> with irradiation time implying that

FIGURE 4.20 Initial Tg as a Function of Cure Exposure and Time after Irradiation for Films Irradiated using the 100W Source ( $\Delta$ , 3;  $\circ$ , 8;  $\square$ , 20; +, 45 mins. irradiation)



the cross-linking and hence the extent of epoxide conversion increases, a trend also indicated by IR spectroscopic measurements of epoxide conversion. This initial Tg of the films increases markedly within 168 hours of irradiation, the bulk of the increase occurring within 24 hours of irradiation. A much slower increase in this Tg then occurs after this period leading to a marked increase only becoming apparent after a prolonged storage time.

The temperature of the onset of the second transition recorded in Table 4.21 show that it increases with cure exposure and time after irradiation as shown with other films.

Only one transition was apparent in the film irradiated for 3 minutes when TMA was carried out 10 minutes after irradiation which again suggests that lower extents of photo-

TABLE 4.21 Second T<sub>g</sub> (°C) as a Function of Cure Exposure and Time after Irradiation for Films Irradiated with the 100W Source

Time after irradiation/hrs.	3 mins. irradiation	8 mins. irradiation	20 mins. irradiation	45 mins. irradiation
10 minutes	-	65	71	74
24	65	68	70	74
48	69	69	72	74
168	71	71	75	76
336	74	74	77	76
504	74	74	78	77
672	72	74	77	78
1 year	99	106	-	-

initiator photolysis and hence polymerization appears to result in an initially homogeneous network in which inhomogeneous cross-linking subsequently develops. After 1 year's storage the films given the two shorter irradiation times still show a discernible second transition whereas the films given longer irradiation times do not, implying that in the latter films continued polymerization results in a decrease in the two phase nature of the network.

Infra-red spectroscopic measurements were carried out on similar films that had been stored in the dark for 1 year.

The results in Table 4.22 indicate that there may be some increase in conversion over the period of a year but it is not apparent in all the films.

From the IR data reported in Sections 4.6(A) and (B) it was difficult to compare the cure of films irradiated with the 1.8kW and 100W sources. Comparison of the TMA data on the films irradiated using the two sources indicates that, in the 672 hour period after irradiation, the degree of cross-linking

TABLE 4.22 Epoxide Conversion after 1 Year's Storage for Films Irradiated using the 100W Source

Irradiation time/mins.	1 + 24 hours	1 + 1 year
3	75 ± 3	76 ± 5
8	80 ± 4	83 ± 2
20	79 ± 3	84 ± 4
45	85 ± 2	84 ± 5

-----

is lower in the films irradiated with the 100W source for all cure exposures since the initial penetration occurs at a lower temperature and two transitions are readily apparent. However one might expect that a greater number of initiating species would be generated by 45 minutes' irradiation with the low intensity source than by 1 pass under the high intensity lamp and hence the degree of cross-linking to be greater in a film given the former cure exposure as the IR spectroscopic measurements in Sections 4.6(A) and (B) do suggest. However the TMA results indicate that this is not the case and may be further evidence for a reduction in the rate of initiation and hence polymerization producing a network structure containing a greater proportion of lower cross-link density regions than is produced by a faster rate of polymerization even though the overall degree of cross-linking is greater. However as mentioned in connection with similar comparisons in previous sections the degree of cure might be lower in the films given longer exposures to the low intensity source than in a film given a short exposure to the high intensity source contrary to expectation and the conversion measurements. After one year's storage the temperature of the onset of penetration becomes similar in the two sets of films

indicating that continued polymerization gives rise to networks of similar rigidity in the films irradiated with the two sources. However, the films given shorter cure exposures with the low intensity source still show two transitions, a possible explanation being that the lower number of initiating species and hence trapped reactive species in these films are unable to reduce the two phase nature of the network.

The effect of thermal treatment on the Tgs of the films was investigated after 1 year's storage. The results in Table 4.23 show that repeating the measurement on a sample heated to 150°C in the first measurement results in only one transition and/or an increase in the temperature at which initial penetration occurs.

TABLE 4.23 Effect of Repeating the Tg Measurement on Films Irradiated using the 100W Source and stored for 1 year

Irradiation time/hrs.	3		8		45	
	1	2	1	2	1	2
Tg/°C	66,99	79	71,106	87	77	91

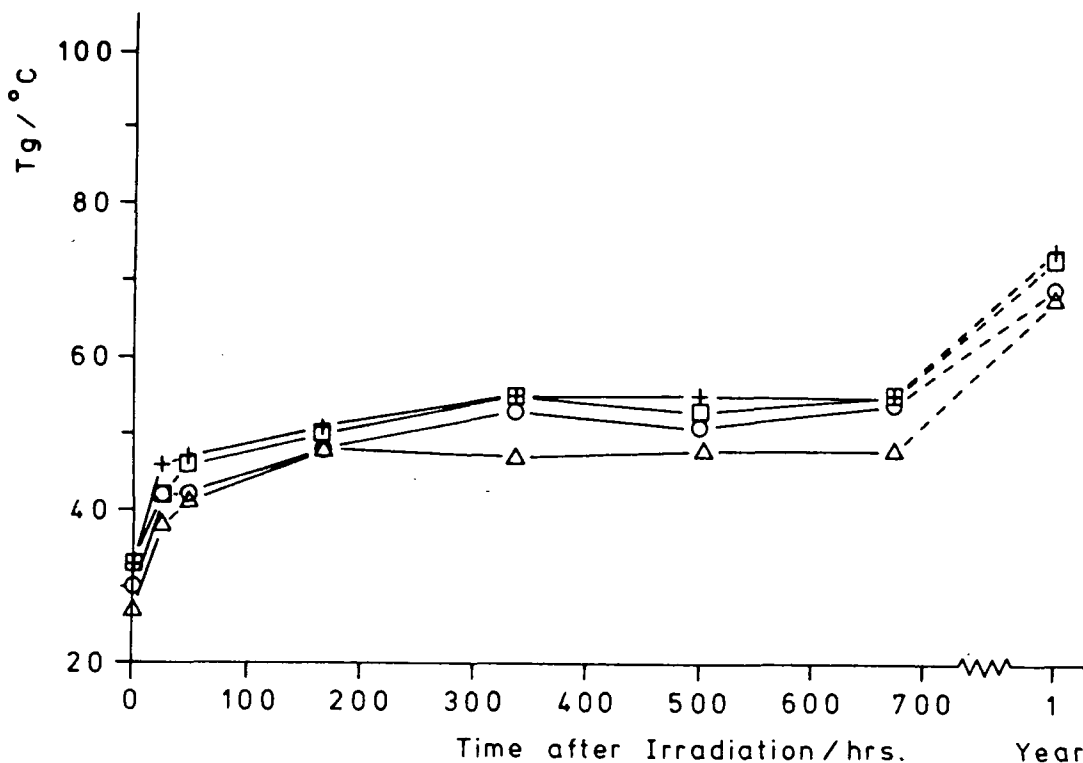
(ii) Effect of Increasing Cure Exposure to Filtered Light

Films of similar composition and thickness to those used in the previous experiment were prepared and irradiated at such a distance from the source with the 'pyrex' filter in place so that they received a photon flux similar to that received by films in the previous experiment. The samples were treated in the same way as in the previous experiment, the Tg measurements being carried out at the same times after irradiation.

As with the films irradiated with the full output of the source, these films also tended to show two transitions,

Figure 4.21 showing the temperature of the onset of the first transition plotted against the time after irradiation.

FIGURE 4.21 Initial Tg as a Function of Cure Exposure ( $\Delta$ , 3;  $\circ$ , 8;  $\square$ , 20; +, 45 mins. irradiation) and Time after Irradiation for Films Irradiated with Filtered Light using the 100W Source



The same trends as those observed in the similar plot, Figure 4.20, for films irradiated with the full output of the lamp occur in the above plot. Comparing the TMA data in Figures 4.20/4.21 shows that over the 672 hour period after cure, the initial Tg of the film given 3 minutes' irradiation with filtered light is lower than that of the film given a similar cure exposure using the full output of the lamp, although after 1 year's storage these two films do show similar initial Tgs. Films given longer cure exposures with and without the filter in place show similar initial Tgs at all times. The results indicate that irradiation with wavelengths greater than 275nm results in no

significant decrease in the degree of cross-linking compared with irradiation using a similar intensity of light with both long and short wavelength UV light present, except for the shortest irradiation time. This conclusion was also inferred from the infra-red spectroscopic measurements of the degree of conversion of such films in Section 4.6(B).

Table 4.24 gives the temperature of the onset of the second transition as a function of the cure exposure and time after irradiation. The results show the same trends as those for films irradiated with the full output of the lamp. The similarity of the values for films given equivalent cure exposures with and without the filter in place tends to suggest that any effect of using the filter is limited to the lower cross-link density regions.

TABLE 4.24 Second Tg as a Function of Cure Exposure and Time after Irradiation for Films Irradiated with Filtered Light using the 100W Source

Time after irradiation /hrs.	3 mins. irradiation	8 mins. irradiation	20 mins. irradiation	45 mins. irradiation
0.17	-	65	72	74
24	67	68	69	74
48	64	67	71	75
168	69	71	74	75
336	69	75	77	78
504	74	75	76	79
672	73	75	77	77
1 year	98	99	-	-

-----

The infra-red spectroscopic measurements shown in Table 4.25 indicate that there is no detectable increase in the

conversion of epoxide groups over a year's storage unlike the TMA results.

TABLE 4.25 Epoxide Conversion after 1 Year's Storage for Films Irradiated with Filtered Light using the 100W Source

Irradiation time/mins.	% Conversion	
	I + 24 hrs.	I + 1 year
3	57 ± 5	56 ± 6
8	79 ± 3	78 ± 3
20	82 ± 2	-
45	83 ± 3	82 ± 2

The effect of the thermal treatment of films after one year's storage was investigated as in previous experiments. The results in Table 4.26 show that repeating the Tg measurement on a film heated to 150°C in the first measurement again gives rise to one transition and/or an increase in the Tg value.

TABLE 4.26 Effect of Repeating the Measurement of Tg on Films Irradiated with Filtered Light using the 100W Source and Stored for 1 Year

Irradiation time/mins.	3		8		45	
	1	2	1	2	1	2
Tg/°C	68,98	77	69,99	80	74	89

#### 4.12 The use of DSC to Investigate the Post-irradiation Thermal Cure of the DGEBA System

Thermo-mechanical analysis of unheated and heated films of the photocured DGEBA resin indicated that a thermal reaction might be occurring, resulting in one observable transition and/or

an increase in the temperature of the onset of penetration. As mentioned previously a number of studies of both free radical and cationic polymerizations have involved the use of mainly isothermal DSC, but in this study the scanning mode was used to determine whether a thermal reaction does indeed occur on heating these films.

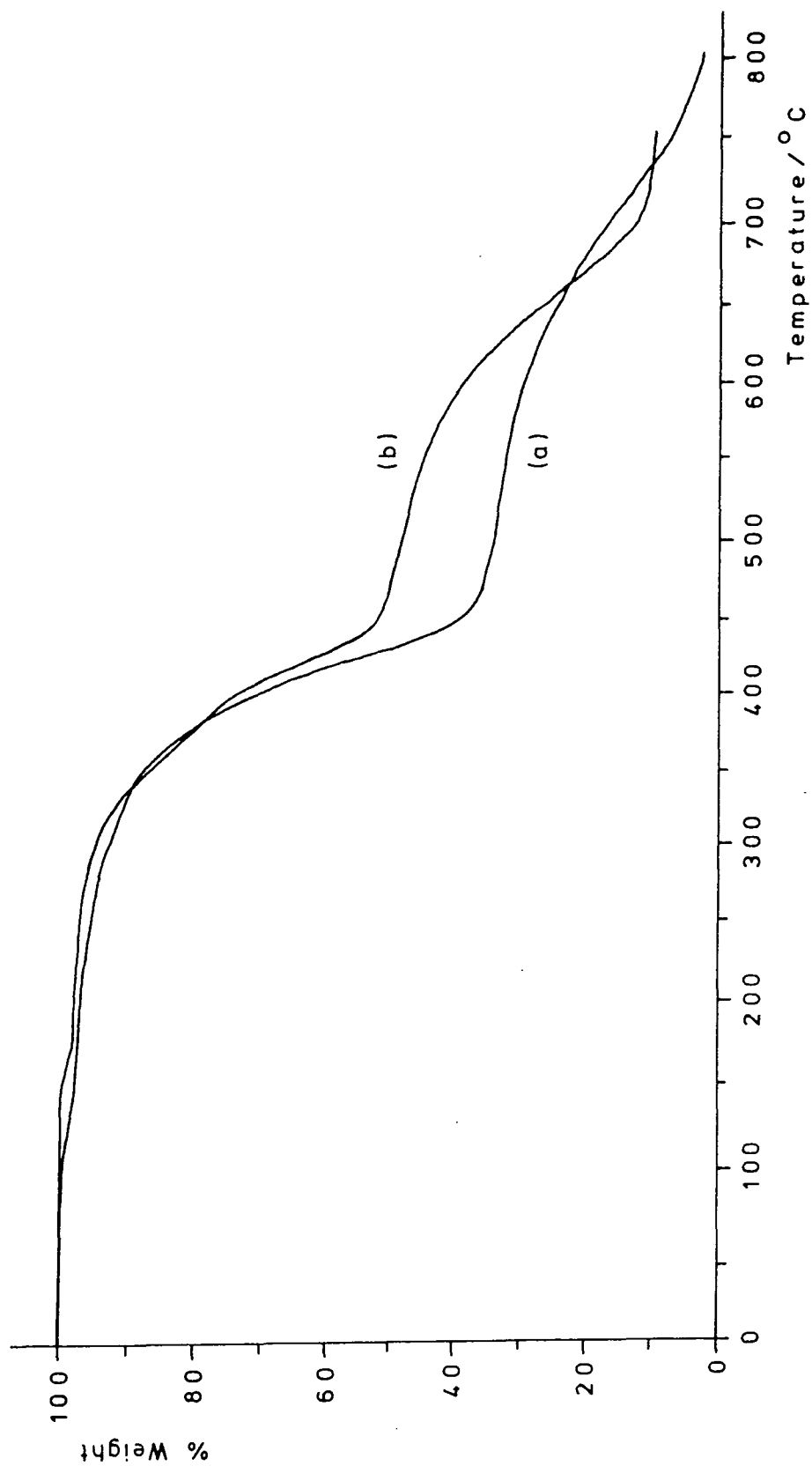
The films of 100 $\mu$ m nominal thickness prepared on polyethylene and irradiated under various conditions for the following experiments, contained 97.0% resin, 2.0% photoinitiator and 1.0% w/w acetone or were close to this composition. The procedure adopted for the DSC analyses was to punch several discs from a cured film using a cork-borer and encapsulate a known weight of these discs in an aluminium sample pan. All the samples were heated at a rate of 10 $^{\circ}$ C min $^{-1}$ , under a nitrogen atmosphere. A sample of uncured lacquer heated to 150 $^{\circ}$ C under the above conditions showed no evidence of a thermal reaction.

(A) Irradiation with the 1.8kW Source

(i) Effect of Increasing Cure Exposure

Films were given an increasing number of passes under the high intensity source and samples taken for the DSC analysis 1, 168 and 504 hours after irradiation. Other samples were taken from similarly cured films that had been stored in the dark for 1 year. In all cases the samples were heated to 220 $^{\circ}$ C during the analysis. The thermogravimetric traces, reproduced in Figure 4.22, of similar films given 2 and 20 passes under the lamp, show that there is some weight loss when the films are heated to this temperature, amounting to 3% for the film given 2 passes and 2% for the film given 20 passes, but no major thermal degradation. Visual examination of the samples after they were heated to this temperature also gave no indication of degradation. Interestingly

FIGURE 4.22 TGA Traces of Films Given 2 and 20 Passes Under the 1.8kW Source



the overall appearance of the two thermogravimetric traces in Figure 4.22 suggests that the details of thermal decomposition are dependent on the cure exposure.

The DSC curves obtained for films given 1, 3, 10 and 20 passes under the lamp are shown in Appendix Seven to illustrate the trends outlined below. The major feature of the DSC curves recorded 1 hour after irradiation is the presence of a number of overlapping exothermic peaks between 30 and 100°C with a further quite small, very broad exothermic peak at a higher temperature. As the number of passes under the lamp increases, the higher temperature peaks of the overlapping peaks become more prominent and, qualitatively, the area under the peaks diminishes. It had been hoped to quantify this residual heat of polymerization but no consistent method of constructing a baseline could be found to allow the area under the peaks to be determined. Gross changes in the area under the peaks, however, can be detected qualitatively. On re-running each sample no exothermic events were detected only an endothermic step in the baseline, attributed to a glass transition, which was not observed in the first run. This effect occurred for all the films examined and at all times after irradiation.

After 168 hours' storage in the dark, the film given 1 pass showed a quite sharp exothermic peak with possibly a small second peak overlapping on the high temperature side. Immediately prior to this exothermic peak there is the onset of either an endothermic peak or a shift in the baseline which could be indicative of the onset of either stress release or a glass transition. This effect does not appear in any of the other traces. As the number of passes received by the film increases, the area under the main exothermic peak appears to diminish whilst the higher temperature overlapping peak becomes progress-

ively more prominent. The traces again showed a small, very broad exothermic higher temperature peak. Comparison of the areas under the main exothermic peaks in these traces with those in the traces recorded 1 hour after irradiation indicates that continued polymerization has occurred. Similar comments can be made about the curves recorded 504 hours after irradiation with the magnitude of the diminution of the area under the exotherms being less than that on going from 1 to 168 hours after irradiation. The DSC curves of samples stored for 1 year showed at least two small, broad, overlapping peaks, with perhaps a slightly smaller area under the exotherms than in the curves recorded after 504 hours. This, however, indicates that there is still the potential for a thermal reaction 1 year after irradiation. It was also noted that the difference in area under the main exothermic peaks, due to different cure exposures tended to diminish as time progressed.

The temperatures of the onset,  $T_o$ , and the peak maximum,  $T_m$ , of the lower temperature overlapping exotherm were defined as in Figure 4.23.

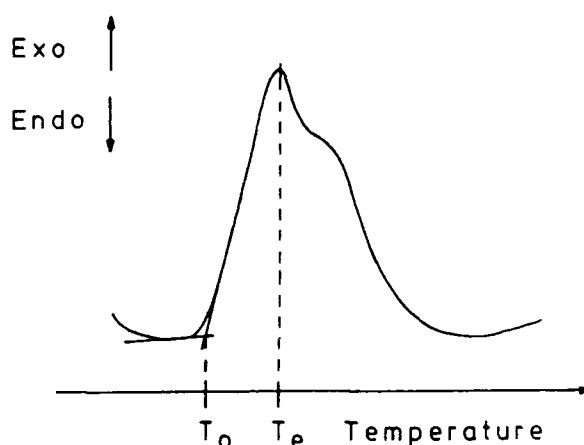


FIGURE 4.23 Definition of  $T_o$  and  $T_e$ .

The values of  $T_o$  and  $T_e$  along with the glass transition temperature,  $T_{g_d}$ , measured from the re-run samples are given in Table 4.27 for films given 1, 3, 10 and 20 passes. In

addition, after re-running the samples to measure  $T_{g_d}$ , the glass transition temperature,  $T_{g_p}$ , was measured using penetrometry. These values are also shown in Table 4.27.

TABLE 4.27 Values of  $T_o$ ,  $T_e$ ,  $T_{g_d}$  and  $T_{g_p}$  as a Function of Cure Exposure and Time after Irradiation for Films Irradiated using the 1.8kW Source

Number of passes	Time after irradiation/ hrs.	$T_o/^{\circ}C$	$T_e/^{\circ}C$	$T_{g_d}/^{\circ}C$	$T_{g_p}/^{\circ}C$
1	1	~37	48	68	86
3		~39	56	89	89
10		43	63	97	83,112
20		45	69	107	87,119
1	168	59	64	80	90
3		61	69	92	-
10		62	75	100	89,118
20		61	86	107	85,118
1	504	64	68	80	89
3		65	72	91	96
10		65	75	102	93,123
20		65	86	104	96,122
1	1 year	71	-	94	-
3		79	-	94	-
10		70	-	120	-
20		70	-	120	-

-----

The DSC curves recorded 1 hour after irradiation show a slight increase in  $T_o$  with increasing exposure to the source whilst at the same time the area under the peaks decreases. Assuming that  $T_o$  is representative of the temperature at which the network is sufficiently mobile for trapped reactive species to become active, then these observations indicate that the

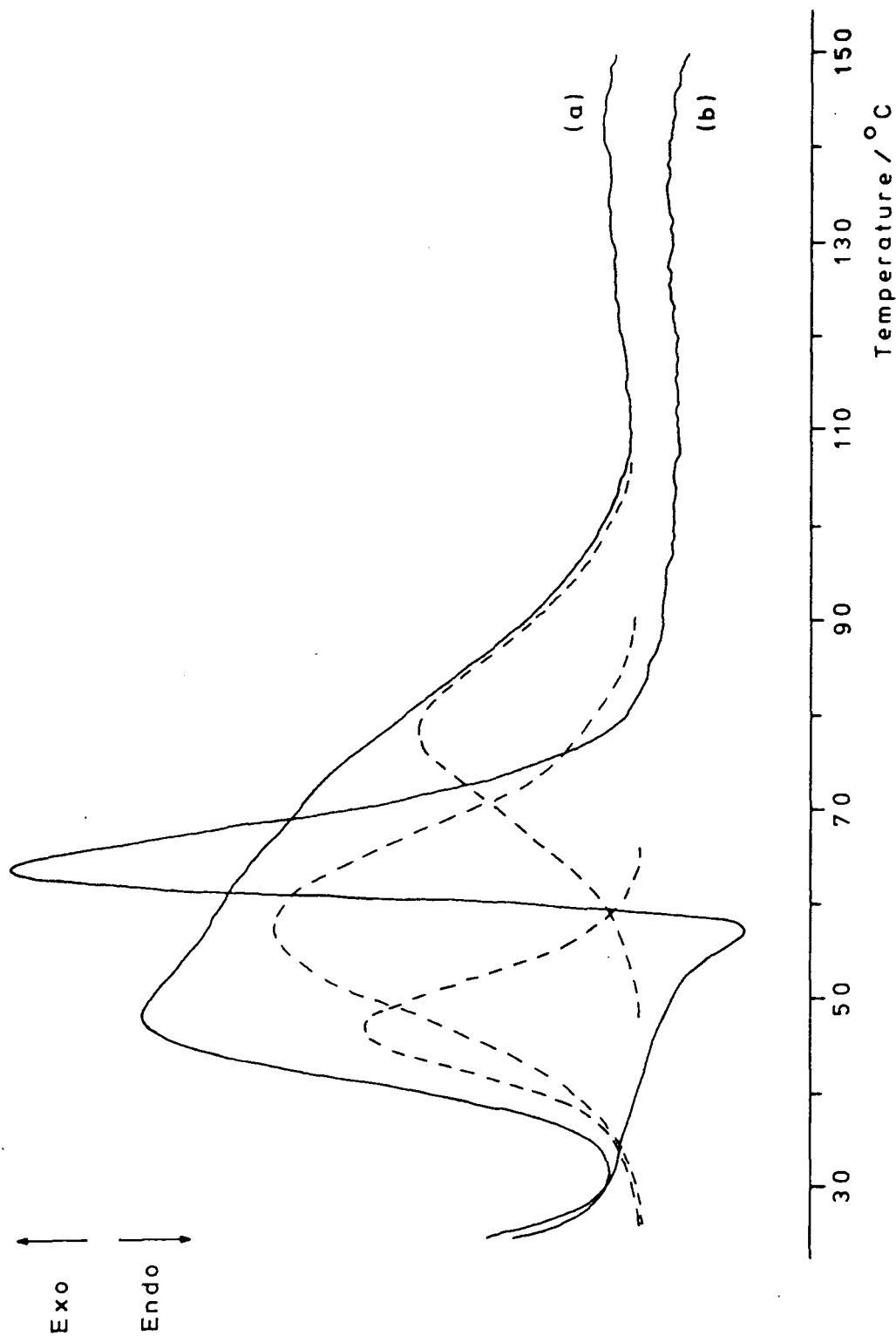
rigidity of the system increases and the amount of unreacted functionality present in the films decreases with increasing cure exposure. This is consistent with increased cure exposure generating further initiating species and a warming of the films both of which could result in an increased conversion and hence cross-linking. The IR spectroscopic measurements of epoxide conversion and the results of TMA on similarly cured films led to this conclusion. The parameter  $T_0$  however is substantially lower than the temperature of the onset of penetration plotted in Figure 4.17 for similar films, 10 minutes after irradiation. As defined by the extrapolation procedure, the temperature of the onset of penetration does not correspond with the temperature at which the network first shows indications of mobility, indeed the first signs of penetration occur at a significantly lower temperature than the value of  $T_g$  quoted. This combined with a greater sensitivity of the trapped reactive species towards network mobility could explain the above observation. The parameter  $T_e$  shows a more marked increase with cure exposure, reflecting an increase in the difference between  $T_0$  and  $T_e$ .

After storage for 168 hours, the difference in  $T_0$  between the films has virtually disappeared and the value of  $T_0$  has apparently increased markedly. This combined with the diminution of the area under the exotherms suggests that an increase in monomer conversion and hence cross-linking has occurred at ambient temperatures. The same conclusions can be drawn from the data obtained 504 hours after irradiation although the increase in  $T_0$  is not as great as that observed on going from 1 to 168 hours' after irradiation. Similarly,  $T_0$  has increased slightly and the area under the main exotherms diminished

slightly in the curves recorded 1 year after irradiation compared with the curves obtained after 504 hours' storage. The parameter  $T_e$  also increases markedly on going from 1 to 168 hours after irradiation but less so on then going to 504 hours but the increase of this parameter with increasing cure exposure, although reduced, is still significant. It is interesting to note that the temperature of the onset of penetration plotted in Figure 4.17 for similarly irradiated films shows an increase over a period of 168 hours after irradiation and DSC indicates that there is a more marked increase in conversion and rigidity of the system over this time period.

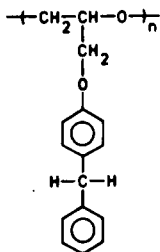
Closer inspection of the traces recorded 1 hour after irradiation shows an interesting feature. The lower temperature exothermic peak of the overlapping exotherms appears to diminish and virtually disappear with increasing cure exposure to leave at least two overlapping peaks in the trace of the film given 20 passes under the lamp. Thus the increase of  $T_0$  and the decrease of the area under the exotherms is partly due to this first exotherm diminishing which also explains why  $T_e$  shows a more marked increase with increasing cure exposure. From this it seems reasonable to propose that there are at least three overlapping exothermic peaks in the film given one pass under the lamp. A more detailed examination of the traces recorded 1 and 168 hours after irradiation for films given 1 and 3 passes, indicates that the two overlapping exotherms observed in the curves recorded after the longer storage period could correspond to the two higher temperature exotherms of the overlapping exotherms observed in the curves recorded 1 hour after irradiation. Figure 4.24 is an attempt to illustrate this point. The curve recorded 1 hour after irradiation for the film given 1 pass (a), has been resolved into three Gaussian peaks and the trace from a

FIGURE 4.24 DSC Curves of a Film Given 1 Pass Under the  
1.8kW Lamp Recorded 1 Hour (a) and 168 Hours (b)  
after Cure

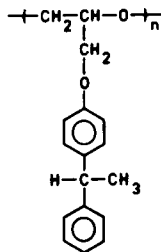


sample of the same film recorded 168 hours after irradiation, (b), superimposed on this. It must be stressed that the deconvolution of the trace is very arbitrary and can only be taken as an approximate guide to the "component peaks" present under the envelope. As time progresses it would appear that the lowest and highest temperature exotherms virtually disappear leaving the middle exotherm which partly accounts for the increase in  $T_0$  on going from 1 to 168 hours after irradiation.

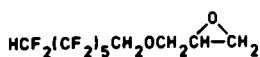
In spite of the fact that  $Tg_d$  is measured after the films have been heated to  $220^{\circ}\text{C}$  and the thermal reaction completed, the results in Table 4.27 indicate that at a given time after irradiation  $Tg_d$  tends to increase with increasing cure exposure. Also it would appear, especially for films given shorter cure exposures, that  $Tg_d$  increases with storage time and as time progresses the difference in  $Tg_d$  between films given 1 and 3 passes diminishes. These observations might be rationalized as follows. The film given the least exposure to the source has the greatest potential for post-irradiation thermal polymerization. If this film is heated, further polymerization occurs but the rate of chain transfer or termination processes is also markedly increased. Therefore although the degree of cross-linking has increased it is not as high as it would have been in the absence of such processes. A film given a longer cure exposure has a greater degree of cross-linking prior to thermal treatment and so shows a higher  $Tg_d$  value even though the occurrence of chain transfer or termination will have reduced the effectiveness of the thermal polymerization to produce a more rigid network. If the film given a lower cure exposure is left at ambient temperature then continued polymerization occurs but the rate of chain transfer is low. Therefore after storage the film has a higher degree of cross-linking and hence gives a higher  $Tg_d$  value after heating.



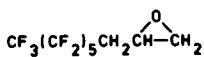
(XXXVIII)



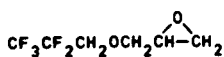
(XXXIX)



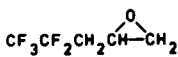
(XLII)



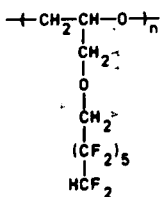
(XLIII)



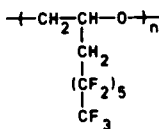
(XLIV)



(XLV)

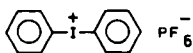


(XLVII)



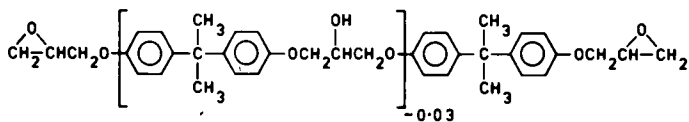
(XLVIII)

# KEY

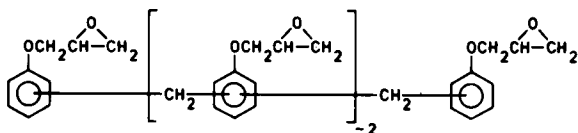


PHOTOINITIATOR

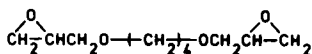
DIPHENYLIODINIUM HEXAFLUOROPHOSPHATE



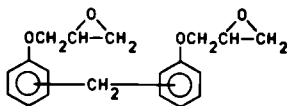
DGEBA (XVIII)



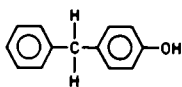
EPOXY NOVOLAC (XIX)



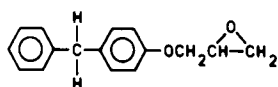
DIGLYCIDYL ETHER OF BUTANEDIOL (XX)



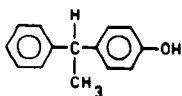
DGEBF (XXI)



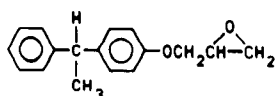
(XL)



(XXXVI)



(XLI)



(XXXVII)

(CONTO ....)

The fact that the films given 1 and 3 passes initially show a significant difference in their  $Tg_d$  values but after long storage time there is little difference in the values indicates that although fewer initiating species and hence propagating centres may be generated in the film given the lower cure exposure they eventually produce a degree of cross-linking similar to that of the film given the longer cure exposure.

Penetrometry was used to measure the  $Tg$  of samples of each film after they had been heated to  $220^{\circ}\text{C}$  and then  $142^{\circ}\text{C}$ . The results are complicated by the occurrence of two transitions in the traces of films given 10 and 20 passes under the lamp but it does appear as in similar trends to those observed in the  $Tg_d$  values are occurring. Generally the  $Tg_p$  values tend to be slightly higher than the  $Tg_d$  values. This result is difficult to rationalize in view of the stress activation of relaxation processes but it may be that in re-running the samples to measure  $Tg_d$  further low molecular weight material is lost resulting in a higher value of  $Tg_p$ . The penetrometry measurements were repeated on the sample of the films analysed after 1 hour's storage, the samples having been heated to  $\sim 150^{\circ}\text{C}$  in the first measurement. No change in either the values of  $Tg_p$  or the occurrence of the two transitions occurred. The apparent presence of regions of higher and lower mobility in the films given 10 and 20 passes is difficult to explain as is why this apparent difference in mobility is 'locked' into the system and why two glass transitions are not detected in the DSC curves.

Crivello has published DSC curves of a 3,4-epoxycyclohexylmethyl 3',4'-epoxycyclohexane carboxylate/triphenylsulfonium hexafluoroarsenate system recorded immediately and 24 hours after irradiation.<sup>39</sup> The two curves indicate a similarity in the behaviour of the above system with that studied in

this work. The trace recorded immediately after irradiation shows two overlapping exothermic peaks whilst in the trace recorded after 24 hours' storage the lower temperature exotherm has diminished. It is interesting to speculate that this behaviour which occurs for the DGEBA system may be a result of inhomogeneous cross-linking as discussed previously. If the network were composed of regions of different mobility then as heat is applied the reactive species present in the regions of higher mobility will become more active leading to the conversion of functional groups and the lower temperature exotherm but as the temperature is further raised, the species trapped in lower mobility regions will become active leading to a second apparently overlapping exotherm. The curves recorded one hour after irradiation would therefore indicate that the proportion of species present in higher mobility regions decreases with increasing cure exposure. After 168 hours' storage the lower temperature exotherm is absent which suggests that the cationic species present in the high mobility regions have reacted at ambient temperatures. This qualitative analysis of the DSC data is reasonably self-consistent and not inconsistent with the other interpretations of the results from techniques used to analyse the system. However some of the aspects of the DSC data such as the occurrence of a third higher temperature overlapping peak would either require a much deeper understanding of the processes that can occur in these systems or progressively more fanciful interpretations of the data.

(ii) Effect of Increasing Cure Exposure to Filtered Light

Samples of films given increasing cure exposures under the high intensity source with the 'pyrex' filter in place were removed at intervals after irradiation for DSC analysis as in the previous experiment. Other samples were taken from simil-

arly irradiated films that had been stored in the dark for 1 year. The DSC curves obtained for films given 1, 3, 10 and 20 passes are reproduced in Appendix 7 to illustrate the trends outlined below.

The DSC curve of the film given 1 pass recorded 3 hours after irradiation shows what appears to be a fairly broad single exothermic peak in the region of 30-100°C whilst the curve for the film given 3 passes, recorded 1 hour after irradiation, shows at least two overlapping exothermic peaks with the lower temperature peak more prominent. As the number of passes is increased to 10 and then 20, what is possibly a third higher temperature overlapping exothermic peak becomes apparent and the prominence of the lower temperature peak of these overlapping exotherms diminishes. All the traces show a very broad, quite small, high temperature exothermic peak. The area under the main exotherms appears to increase markedly on going from 1 to 3 passes mainly because of the growth of the second overlapping exotherm and on going from 3 to 10 passes because of the growth of a third overlapping exotherm, whereas on going from 10 to 20 passes there is a slight decrease in the area under the exotherms.

After 168 hours' storage the DSC curve of the film given 1 pass again shows a single fairly broad exotherm in the region of 30-100°C whilst the other films show a reasonably sharp exothermic peak with a small overlapping peak on the high temperature side which increases in prominence with increasing cure exposure. Both the curves for the films given 1 and 3 passes show the onset of an endothermic peak or shift in the baseline immediately before the main exothermic event, an effect observed in the DSC curve of a film given 1 pass using the full output of the lamp recorded after 168 hours' storage. Again a

small, broad high temperature exothermic peak is present in the curves. The area under the main exotherms in each curve appears to have decreased since the last analysis. In the film given 3 passes this decrease is mainly due to the diminution of the low temperature overlapping exotherm whilst in the films given 10 and 20 passes the third higher temperature overlapping exotherm diminishes as well. Similar curves are obtained after 504 hours' storage with a slight decrease in the area under the exotherms occurring since the analysis carried out after 168 hours' storage. After storage for 1 year the DSC curves of similar films show a broad exothermic event with, in the curves of the films given 1 and 3 passes, the onset of an endothermic event immediately before the onset of the exotherm. This shows there is still the potential for reaction one year after irradiation. It was noted that as time progressed the difference in the areas under the main exotherms, due to the different cure exposures, diminished.

The parameters  $T_o$  and  $T_e$  were defined as in the previous section and the values obtained are shown in Table 4.28 along with those of  $Tg_d$  and  $Tg_p$ .

In the curves recorded 1 hour after irradiation,  $T_o$  tends to increase slightly with cure exposure indicating that the rigidity of the network increases. The area under the main exothermic peaks however shows more complex behaviour. Contrary to what one might expect, the area under the main exothermic peak in the curve of the film given 1 pass is less than the area under the exotherms in the film given 3 passes. This effect may arise because the residual heat of polymerization will be related to the number of reactive species trapped as well as the amount of unreacted functionality present. In the film given 1 pass the number of initiating and hence propagating

TABLE 4.28 Values of  $T_o$ ,  $T_e$ ,  $Tg_d$  and  $Tg_p$  as a Function of Cure Exposure and Time after Irradiation for Films Irradiated with Filtered Light using the 1.8kW Source

Number of passes	Time after irradiation /hrs.	$T_o/^{\circ}C$	$T_e/^{\circ}C$	$Tg_d/^{\circ}C$	$Tg_p/^{\circ}C$
1	3	~31	55	~29	-
3	1	~30	44	62	-
10	1	~37	49	85	-
20	1	~39	54	92	-
1	168	50	66	55	62
3		56	62	76	80
10		61	68	90	86
20		60	68	93	82
1	504	60	66	64	67
3		63	66	80	86
10		64	70	94	93
20		64	71	97	93
1	1 year	73	-	79	-
3		76	-	87	-
10		76	-	97	-
20		-	-	-	-

-----

centres produced and trapped may be very low leading to an apparently lower residual heat of polymerization even though there is possibly a greater number of unreacted functional groups present in the system whereas 3 passes results in a greater number of trapped reactive species which are able to convert a greater proportion of the unreacted functional groups giving rise to a larger exotherm. The increase in area under the exotherms on going from 3 to 10 passes may not be due to a greater potential for thermal polymerization but to the occurrence of some other process since this increase is mainly due to the appearance of

a third overlapping exotherm and in spite of the increase in area,  $T_0$  increases. On going from 10 to 20 passes the area under the exotherms appears to decrease slightly and  $T_0$  increases which is at least in part due to the diminution of the lower temperature peak of the overlapping exotherms. This is consistent with an increase in the conversion of functional groups and an increase of the rigidity of the system with increasing exposure. The values of  $T_0$  in the films are close to the temperature of the onset of penetration measured 10 minutes after irradiation, reported in Section 4.11(A) (iv). The behaviour of  $T_e$  is more complicated since it decreases on going from 1 to 3 passes under the lamp and then increases with further cure exposure reflecting the complex relationship between the overall rate of polymerization and the form of the resulting DSC curve.

After a further 167 hours' storage  $T_0$  has increased significantly, but still shows an increase with increasing cure exposure. This increase of  $T_0$  combined with the decrease in the area under the exotherms over the same period indicates that the rigidity of the network and the extent of reaction have increased at ambient temperatures. The value of  $T_0$  from the curves recorded 504 hours after irradiation shows an increase, especially in the films given shorter cure exposures, over the value obtained after 168 hours' storage but the magnitude is significantly less than that observed on going from 1 to 168 hours' storage. Also the value of  $T_0$  now increases only slightly with increasing cure exposure. The area under the exotherms appears to diminish slightly on going from 168 to 504 hours' storage which, combined with the increase of  $T_0$ , is indicative of further reaction and cross-linking. Similarly the DSC curves recorded after 1 year's storage indicate that the extent of reaction and rigidity of the network has increased over

the lengthy period since the analysis carried out 504 hours after irradiation. The parameter  $T_e$ , although increased in each film, still shows a decrease on going from 1 to 3 passes and then an increase with further cure exposure in the traces recorded 168 hours after irradiation. After a further 336 hours' storage  $T_e$  has again increased, although only slightly, in all the films except that given 1 pass. It is interesting to note that the temperature of the onset of penetration into films cured in a similar manner showed a marked increase within 168 hours of irradiation and that the DSC data also indicates a marked increase in conversion and cross-linking over this same period.

The values of  $T_{g_d}$  obtained from the re-run samples given in Table 4.28 show quite clearly an increase with increasing cure exposure and storage time. The values of  $T_{g_p}$  obtained from samples that have been heated to 220°C and then 137°C show the same trends as the  $T_{g_d}$  values. Unlike the TMA traces of films irradiated without the filter present, only one transition was apparent in all the above samples. Comparison of the two measures of  $T_g$  indicate that  $T_{g_d}$  is only higher than  $T_{g_p}$  in the films given longer cure exposures.

The DSC curves of these films may again be loosely interpreted as being indicative of inhomogeneous cross-linking, leading to the formation of a two phase network. One hour after irradiation the DSC curve of the film given 3 passes shows two overlapping exotherms which may be attributed to species trapped in regions of high and low mobility becoming active, leading to the conversion of residual functional groups. As the cure exposure increases, the lower temperature exotherm diminishes in prominence indicating that a greater proportion of species are trapped in regions of low mobility. After 168

hours' storage the lower temperature exothermic peak of the overlapping exothermic peaks has disappeared, which contributes to the increase in  $T_0$ , leaving at least one higher temperature exotherm which could correspond to reactive species trapped in low mobility regions becoming active, the reactive species in high mobility regions having reacted at ambient temperatures. The DSC curve of the film given 1 pass recorded 3 hours after irradiation shows the presence of a single quite broad exothermic peak perhaps suggesting that the two phase nature of the system has not developed because of the slower rate of polymerization as a result of a reduction in the formation of initiating species. Continued reaction during 168 hours' storage results in a marked increase in  $T_0$  indicating that the reactive species are more firmly held in the network. It is interesting to note that the penetrometry trace of a similarly cured film showed only one transition 3 hours after irradiation whereas 24 hours later two transitions become apparent. The picture of an inhomogeneous network outlined above from the DSC data is consistent with that outlined for the films irradiated using the full output of the lamp with the same limitations applying.

The DSC analyses carried out one hour after irradiation indicate that for each cure exposure the films irradiated with filtered light have a lower degree of cure than films irradiated with the full output of the lamp since the area under the main exothermic peaks is greater (excepting the film given 1 pass) whilst the values of  $T_0$  and  $T_{g_d}$  are lower. As time progresses the values of  $T_0$  become equivalent in the two sets of films whilst the difference between the areas and the main exothermic peaks and the values of  $T_0$  tend to diminish. The results from the TMA of similarly irradiated films also suggested that for each cure exposure, irradiation with filtered light results in

a lower degree of cure which may not be unreasonable. However the DSC analysis indicates that the additional conversion on heating is greater for films given 10 or 20 passes with the filter in place than for a film given 1 pass using the full output of lamp even though the values of  $T_{g_d}$  are significantly greater in the former films and the values of  $T_o$  similar. With the progression of time the difference in the area under the main exothermic peaks and the values of  $T_{g_d}$  tend to diminish. As reported in Section 4.11(A) (iv), TMA also indicated that the degree of cure in films given longer exposures to filtered light was lower than that in a film given a short exposure to unfiltered light. As mentioned previously in connection with the TMA results, one might expect the former films to show a similar or higher degree of cure than a film irradiated under the latter regime as is indicated by IR spectroscopic measurements of the epoxide conversion in such films. Contrary to expectation and the conversion measurements it might be that films given 10 or 20 passes with the filter in place are less well cured, formation of the network by a lower rate of polymerization due to the use of the filter possibly facilitating the trapping of propagating species at an earlier stage in the cross-linking process thus shortening the kinetic chain length. If this were to be the case then it is difficult to explain why the value of  $T_{g_d}$  is higher in the two films cured using filtered light since it is proposed that the magnitude of  $T_{g_d}$  is dependent on the degree of cross-linking prior to heating. An alternative proposition is that even though the overall degree of conversion and cross-linking is greater in the films given longer cure exposures using filtered light than the film given a shorter cure exposure without the filter in place, the lower rate of initiation and hence polymerization as a result of using the

filter gives rise to a network structure containing a greater proportion of lower mobility regions as is indicated by the TMA results. The larger exotherm on heating the two films given longer cure exposures to filtered light might then result from a combination of a greater number of trapped propagating species and a greater probability of residual functionality in high mobility regions reacting even on heating. The higher  $T_{gd}$  values would then be explained by the greater overall degree of cross-linking

(B) Irradiation with the 100W Source

(i) Effect of Increasing Cure Exposure

Samples of films irradiated for 3, 8, 20 and 45 minutes with a light intensity of  $17.1 \text{ mW cm}^{-2}$  were removed at intervals after cure for DSC analysis. Other samples were taken from similarly irradiated films that had been stored in the dark for 1 year. The DSC curves obtained are shown in Appendix 7 to illustrate the trends outlined below.

The DSC curve recorded 1 hour after irradiation of a film for 3 minutes shows at least two overlapping exothermic peaks in the region of 30 to  $100^{\circ}\text{C}$ . As the cure exposure increases a third higher temperature overlapping peak becomes apparent and the lower temperature peak becomes less prominent. In addition all the curves exhibit a minor, very broad, higher temperature exothermic peak. The area under the main peaks appears to increase on going from 3 to 8 minutes' irradiation, mainly due to the appearance of the third overlapping exotherm, whilst the area decreases on going to 20 and then 45 minutes' irradiation. The curves recorded 168 hours after irradiation show a quite sharp exothermic peak in the region of  $30\text{-}100^{\circ}\text{C}$  with a second, smaller, overlapping peak on the higher temperature

side. The very broad, higher temperature, exothermic peak is still present. Immediately before the main exothermic event, in the traces for the films given 3 and 8 minutes' irradiation, there is the onset of either an endothermic peak or shift in the baseline indicative of either stress release or a glass transition. The area under the main exothermic peaks appears to have decreased somewhat in the trace of the film given 3 minutes' irradiation over the 167 hour period since the previous run mainly because of the lower temperature peak of overlapping exotherms diminishing whilst the decrease of the area under the main exothermic peaks, over the same period, in the curves for films given longer cure exposures is due to a diminution of both the higher and lower temperature peaks of the three overlapping exotherms. Similar curves were obtained 504 hours after irradiation with a slight decrease in the area under the main exothermic peaks occurring over the period of storage since the last analysis. The DSC curves of films stored for 1 year show at least two overlapping exotherms with the lower temperature one being quite distinguishable. As with the previous DSC analyses, all the above samples showed an endothermic shift in the baseline when re-run, attributed to a glass transition.

The parameters  $T_o$ ,  $T_e$  and  $Tg_d$  measured from the curves as in previous DSC analyses. The values of these parameters along with the temperature of the onset of penetration,  $Tg_p$ , for samples of each film measured after the DSC analysis are recorded in Table 4.29.

The values of  $T_o$  from the curves recorded 1 hour after irradiation show a slight increase with increasing irradiation time. This increase of  $T_o$  indicates that the network becomes more rigid with increasing cure exposure but is at least

TABLE 4.29 Values of  $T_o$ ,  $T_e$ ,  $Tg_d$  and  $Tg_p$  as a Function of Cure Exposure and Time after Irradiation for Films Irradiated with the 100W Source

Irradiation time/mins.	Time after irradiation/hrs	$T_o/^\circ\text{C}$	$T_e/^\circ\text{C}$	$Tg_d/^\circ\text{C}$	$Tg_p/^\circ\text{C}$
3	1	~35	47	64	76
8		~36	48	88	87
20		39	52	92	-
45		42	55	95	90,113
3	168	55	63	78	82
8		59	65	92	92
20		59	66	98	93
45		60	67	97	93
3	504	60	66	79	86
8		63	68	91	93
20		63	69	98	97
45		63	70	99	98
3	1 year	68	-	88	80
8		70	80	93	91
20		71	83	97	92
45		70	82	95	96

partly due to the diminution of the lower temperature peak of the overlapping exothermic peaks. The increase in area under the main exothermic peaks on going from 3 to 8 minutes' irradiation may not be a consequence of an increase in the potential for polymerization since it is mostly due to the appearance of a third overlapping exotherm and  $T_o$  increases which is taken as being indicative of an increase in the rigidity of the network and hence the conversion of epoxide functionality. The values of  $T_o$  are quite close to the temperature of the onset of pene-

tration measured in similarly irradiated films, plotted in Figure 4.20. The values of  $T_e$  also show an increase with increasing cure exposure.

After a further 167 hours' storage the values of  $T_o$  in each film have increased and the difference in  $T_o$  between films given longer cure exposures has become negligible. This increase of  $T_o$  combined with a decrease in the area under the main exothermic peaks indicates, as seen with other films, that the extent of conversion and the rigidity of the system have increased. An additional 336 hours' storage results in a slight increase of  $T_o$  and  $T_e$  with a decrease in the area under the main exothermic peaks. The DSC curves of similarly irradiated films stored in the dark for one year, show a further slight increase of  $T_o$  and  $T_e$  over the values obtained 504 hours after irradiation whilst the area under the exothermic peaks has again diminished slightly.

The values of  $Tg_d$  in Table 4.29 show the trend of increasing with increasing cure exposure and storage time although the difference resulting from increased cure exposure diminishes with increased storage time and the magnitude of the increase on going from 336 to 504 hours' storage is significantly less than that on going from 1 to 168 hours' storage. The values of  $Tg_p$  show similar trends to those exhibited by the  $Tg_d$  values. The TMA trace of the film given 45 minutes' irradiation, recorded after 1 hour's storage and the DSC analysis, showed two transitions but subsequent traces recorded after further storage and DSC analyses showed one transition. It would appear that as seen for other films, the value of  $Tg_p$  is lower than  $Tg_d$  in films given shorter cure exposures.

The presence of overlapping exothermic peaks in the DSC curves recorded 1 hour after irradiation and the diminution

of the lower temperature overlapping peak with increasing cure exposure and after storage of the films may again be interpreted as being indicative of inhomogeneous cross-linking.

Comparison of the DSC data from the analysis of films irradiated with the 1.8kW and 100W sources suggests, in spite of the values of  $T_{gd}$  and  $T_o$  being in the same range, that the films irradiated with the latter source are less well cured since the area under the main exothermic peaks is greater although the difference does tend to diminish with time. TMA of similarly irradiated films also suggested that the degree of cross-linking in the films irradiated with the low intensity lamp was lower. As already mentioned in connection with the TMA results in Section 4.11(B)(i) one might expect the film irradiated with the 100W source for 45 minutes to show a degree of cure similar to or greater than that of a film given 1 pass under the high intensity lamp as the IR spectroscopic measurements of the epoxide conversion in similarly irradiated films indicate. The DSC analyses, like the results from TMA, suggest that this is not the case even though the value of  $T_{gd}$  is initially significantly lower for the film given 1 pass under the 1.8kW source. As time progresses the values of  $T_{gd}$  tend to become equivalent for the two films and the difference in the area under the main exothermic peaks diminishes. The possibility exists that, in spite of what might be expected and the conversion measurements, the film given 45 minutes' irradiation with the 100W source is less well cured than the film given the shorter cure exposure to the high intensity lamp. The lower rate of initiation and hence polymerization (resulting from the use of the low intensity source under the above conditions) might, as proposed previously, facilitate the trapping of propagating species possibly at an earlier stage in the cross-linking process thus shortening the

kinetic chain length. Again an alternative proposition is that the overall degree of conversion and hence cross-linking might be greater in the film given the longest exposure to the low intensity lamp but the lower rate of polymerization results in a network composed of a greater proportion of lower mobility regions. The larger exotherm on heating the film irradiated for 45 minutes using the 100W source might then result from a greater probability of residual functionality in high mobility regions reacting perhaps combined with the presence of a greater number of trapped reactive species. The increased overall degree of cross-linking might also account for the higher  $T_{g_d}$  value.

(ii) Effect of Increasing Cure Exposure to Filtered Light

Films were irradiated for 3, 8, 20 and 45 minutes with the 'pyrex' filter in place, so that they received a similar light intensity,  $17.1 \text{ mW cm}^{-2}$ , to the films irradiated in the previous experiment without the filter present. Samples were taken at intervals after cure for DSC analysis whilst other samples were taken from similarly irradiated films stored in the dark for 1 year. The DSC curves obtained are shown in Appendix 7 to illustrate the trends outlined below.

One hour after irradiation, the DSC curve of the film irradiated for 3 minutes shows a quite broad exothermic peak in the region of 30 to  $100^{\circ}\text{C}$  with perhaps a smaller peak overlapping on the high temperature side. The curve of the film irradiated for 8 minutes shows two overlapping exothermic peaks in the region of 30- $100^{\circ}\text{C}$ . As the irradiation time is increased to 20 and 45 minutes the lower temperature exotherm peak becomes less prominent and a third higher temperature overlapping peak appears. The area under the main exothermic peaks

appears to increase on going from 3 to 8 minutes' irradiation due to the growth of the second overlapping peak. There is little difference in the area under the main exothermic on going from 8 to 20 minutes' irradiation as the decrease in the lower temperature exotherm is offset by the growth of the third overlapping peak. The area under the main exothermic peaks in the curve of the film given 45 minutes' irradiation is slightly less than that for the film irradiated for 20 minutes.

In the curves obtained after 168 hours' storage, a fairly sharp exothermic peak is observed in the 30 to 100°C region with a second exotherm overlapping on the high temperature side which becomes more prominent as the cure exposure received by the film increases. Immediately prior to the main exothermic event in the curve for the film given 3 minutes' cure exposure there is the onset of either an endothermic peak or shift in the baseline due to a release of strain or a glass transition. The small, broad, higher temperature exotherm is still apparent in these curves. Overall the area under the exothermic peaks has decreased since the last analysis. In the case of the film given 8 minutes' irradiation this decrease in area is due to the diminution of the lower temperature overlapping exothermic peak whilst for films given 20 and 45 minutes' irradiation it is due to both the diminution of the lower and higher temperature overlapping peaks. Similar curves are obtained 504 hours after irradiation with a slight decrease in the area under the main exothermic peaks compared with the traces recorded after 168 hours' storage. The DSC curves of samples stored for 1 year after being cured show the presence of at least two overlapping exotherms with the lower temperature one being quite distinguishable. All the curves show the onset of either an endothermic peak or shift in the baseline prior to the exothermic

event and again the area under the exothermic peaks appears to be less than that in the curves obtained after 504 hours' storage. As time progresses it appears that the difference in area under the main exothermic peaks, due to different cure exposures, tends to diminish. All of the above samples showed an exothermic shift in the baseline when re-run which was again attributed to a glass transition.

The parameters  $T_o$ ,  $T_e$  and  $Tg_d$  were defined as in previous analyses and are shown in Table 4.30 along with the values of  $Tg_p$ .

TABLE 4.30 Values of  $T_o$ ,  $T_e$ ,  $Tg_d$  and  $Tg_p$  as a Function of Cure Exposure and Time after Irradiation for Films Irradiated with Filtered Light using the 100W Lamp

Irradiation time/mins.	Time after irradiation/hrs.	$T_o/^{\circ}C$	$T_e/^{\circ}C$	$Tg_d/^{\circ}C$	$Tg_p/^{\circ}C$
3	1	~36	49	41	51
8		~36	48	72	82
20		43	55	93	85
45		45	59	94	83,110
3	168	55	63	65	75
8		59	64	87	89
20		60	67	98	92
45		61	68	99	91
3	504	60	60	71	86
8		63	67	86	90
20		64	70	97	95
45		64	70	100	95
3	1 year	71	78	86	95
8		72	79	93	95
20		72	82	94	96
45		71	81	95	98

The values of  $T_o$  from the DSC curves recorded 1 hour after irradiation tend to increase with increasing cure exposure, the diminution of the lower temperature overlapping exotherm contributing at least in part for this increase, especially on increasing the irradiation time from 8 to 20 and then 45 minutes. The area under the main exothermic peaks shows more complex behaviour.

Like the film given the least exposure to the 1.8kW source with the 'pyrex' filter in place the film irradiated for 3 minutes shows a broad single exothermic peak again illustrating the complex relationship between the number of initiating and hence propagating species produced on irradiation and the magnitude and form of the post-irradiation exotherm. Increasing the irradiation time to 8 minutes results in an increase in the area under the exothermic peaks probably because a greater number of initiating species are produced and hence a greater number of propagating centres are trapped leading to a greater proportion of the residual functionality to be converted on heating. There is virtually no difference in the area under the exothermic peaks in the curves of films given 8 and 20 minutes' irradiation, the decrease of the lower temperature overlapping exotherm being offset by the growth of a third overlapping exotherm yet  $T_o$  increases indicating that the conversion of functional groups and the rigidity of the network have increased. On going from 20 to 45 minutes' irradiation there is a decrease in the area under the exotherms and slight increase in  $T_o$ . The parameter  $T_e$  behaves in a more complex manner, decreasing slightly on going from 3 to 8 minutes' irradiation but increasing with further cure exposure.

The data from the curves recorded 168 hours' after irradiation indicates that further polymerization has occurred

since  $T_o$  has increased and the area under the main exothermic peaks has diminished. The difference in  $T_o$  between films given 8, 20 and 45 minutes' irradiation has become negligible but the value of  $T_o$  for the film given 3 minutes' irradiation is somewhat lower. The values of  $T_e$  have also increased and now show a slight increase with increasing cure exposure even on going from 3 to 8 minutes' irradiation. A further 336 hours' storage results in a smaller increase in the  $T_o$  values and decrease in the area under the main exothermic peaks. The DSC analysis of films stored for a year shows that  $T_o$  has again increased and the area under the exotherms has diminished compared with the samples run after 504 hours' storage. It is interesting to note that the temperature of the onset of penetration of similarly irradiated films plotted in Figure 4.21 show a marked increase within 168 hours of irradiation and a much slower increase with further storage time and that the DSC data indicates a similar trend for the conversion of epoxide functionality and rigidity of the network.

The  $Tg_d$  values shown in Table 4.30 again show the trend of increasing with increasing cure exposure although the difference is very small for 20 and 45 minutes' irradiation and, especially with films given the two shorter irradiation times, an increase with increasing time after irradiation so that 1 year after irradiation the  $Tg_d$  values are much closer in each of the films. The  $Tg_p$  values show similar trends to the  $Tg_d$  values. As seen in other experiments the  $Tg_p$  value for the film given lower cure exposures are significantly higher than the  $Tg_d$  values whereas for films given longer cure exposures, the value of  $Tg_p$  is similar or lower. Like the film given 45 minutes' irradiation in the previous analyses, the film given 45 minutes' irradiation in this set of films shows two transit-

ions in the penetrometry trace recorded 1 hour after irradiation, but only one glass transition on subsequent analyses.

The form of the DSC curves may again be interpreted as being indicative of inhomogeneous cross-linking leading to the formation of high and low mobility regions. The curve for the film given 3 minutes' irradiation obtained after 1 hour's storage essentially shows one main exothermic peak which may be a result of the two phase nature of the network not having developed at this stage due to a reduction in the rate of polymerization. The penetrometry trace of a similarly irradiated film recorded 10 minutes after cure showed only one transition whereas 24 hours later two transitions were apparent. A film irradiated for 3 minutes without the filter present also only showed one transition in the TMA trace recorded 10 minutes after irradiation and two transitions in the trace obtained 24 hours later. However the DSC curves of a similarly irradiated film recorded one hour after cure exhibited two overlapping exothermic peaks, as described previously, which is interpreted as indicating regions of different mobility. It is probable that a greater number of initiating species are produced in the film irradiated without the filter present so that the rate of polymerization is such that in the 50 minute interval between the TMA and DSC analyses the two phase nature of the system develops.

Comparison of the DSC data for the films irradiated for 45 minutes with and without the filter in place indicates that they possess similar degrees of cure since the values of  $T_0$  and  $Tg_d$  are similar as are the areas under the main exothermic peaks. Likewise the DSC analysis of films irradiated for 20 minutes with and without the filter in place indicates that

they have similar degrees of cure. The above conclusions were also reached from the IR spectroscopic measurements of conversion and the TMA of similarly irradiated films. Using the DSC data it is more difficult to comment on the relative degree of cure of films given shorter cure exposures with and without the filter present. Contrary to expectation, one hour after cure, the area under the main exothermic peaks is greater for the film given 8 minutes' irradiation without the filter present than for the film irradiated with the filter present even though the values of  $T_0$  are similar, but this difference is mainly due to the presence of a third higher temperature overlapping exothermic peak which may not be related to the thermal cure of the films. However the value of  $Tg_d$  is lower for the latter film indicating that the degree of cross-linking is lower at this point in time after irradiation. Subsequent analyses of the two films show that  $Tg_d$  becomes similar indicating that the degree of cross-linking becomes similar. The area under the exothermic peak in the DSC curve of the film given 3 minutes' irradiation with the filter in place, recorded 1 hour after cure, is less than the area under the main exothermic peaks for the film irradiated for 3 minutes using the full wavelength output of the lamp even though the values of  $T_0$  are similar. In spite of this, it is reasonable to suggest that the former film has a lower degree of cure, the disparity in the magnitudes of the post-irradiation exotherms being attributable to a reduction in the number of initiating species formed. This is further supported by the value of  $Tg_d$  being significantly lower for the film irradiated with the filter in place. As time progresses, however, the value of  $Tg_d$  for the film irradiated with the filter in place approaches that of the film irradiated without the filter present which is interpreted as indicating that although

fewer initiating species are generated and the magnitude of the post irradiation exotherm is lower, a network of similar cross-link density is eventually achieved. Infra-red spectroscopic measurements of the epoxide conversion and TMA also indicated that a film given 3 minutes' irradiation with the filter present had a greater degree of cure than a film irradiated for 3 minutes without the filter present. In addition, the TMA results like the DSC results indicated that the degree of cure of the two films becomes similar.

#### 4.13 Comparison of the Properties of Photocationally and Conventionally Cured Epoxy Resins Useful for Surface Coatings Applications

The chemical resistance, adhesion and ability of the photocured DGEBA and epoxy novolac systems to prevent corrosion of the substrate,prohesion,were compared with three conventional coatings systems. The commercial systems used were 'camkote EP' an epoxy novolac/polyfunctional amine system; 'camkote A', a DGEBA/polyfunctional amide system and 'camkote N', a polyurethane system. The commercial systems consisted of just the resin,curing agent and solvent.

The substrate used was mild steel and to aid the adhesion of the coatings, the surface of the steel had been roughened and then degreased. The curing agent and base resin of the commercial systems were mixed in the appropriate proportions and using adhesive tape as a barrier, films of 200µm nominal thickness prepared on the panels. The films were then placed in an oven at 60°C for three days. Films of the two UV curable systems were prepared in a similar way and irradiated for 45 minutes, 9cm from the 100W source. The lacquer of the DGEBA

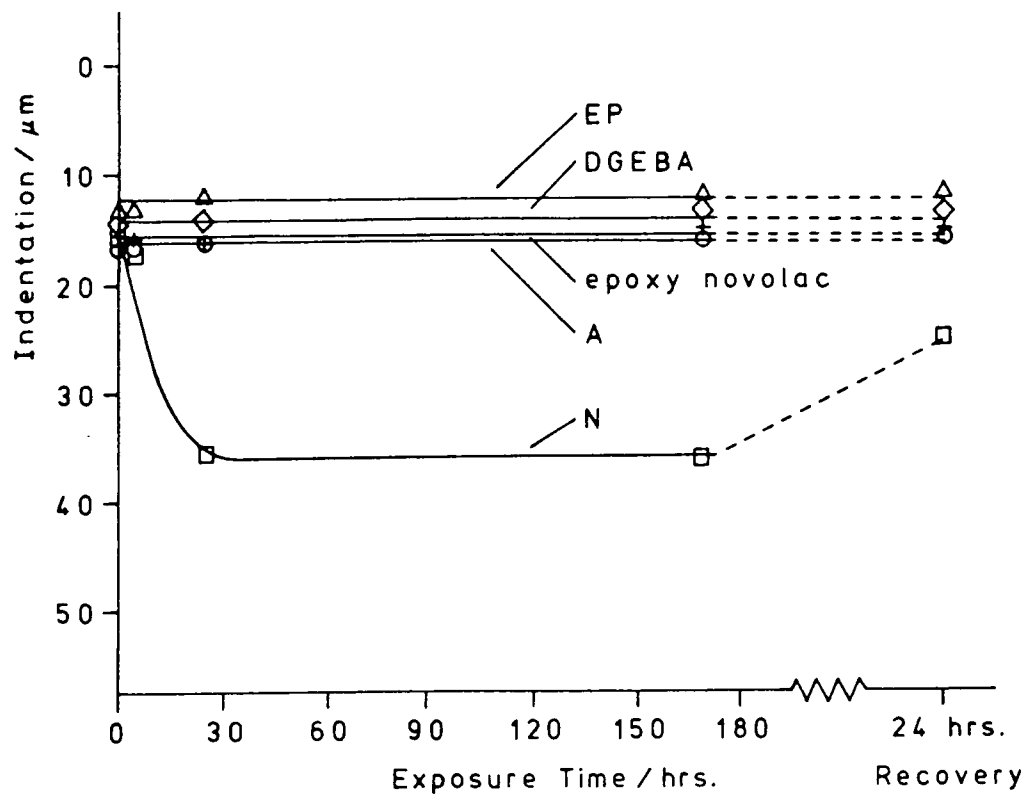
resin contained 96.9% resin, 2.0% photoinitiator and 1.1% acetone whilst that of the epoxy novolac contained 84.4% resin, 12.6% toluene, 2.0% photoinitiator and 1.0% w/w acetone. The films were then left for at least 24 hours after irradiation before use in the tests.

(A) Chemical Resistance

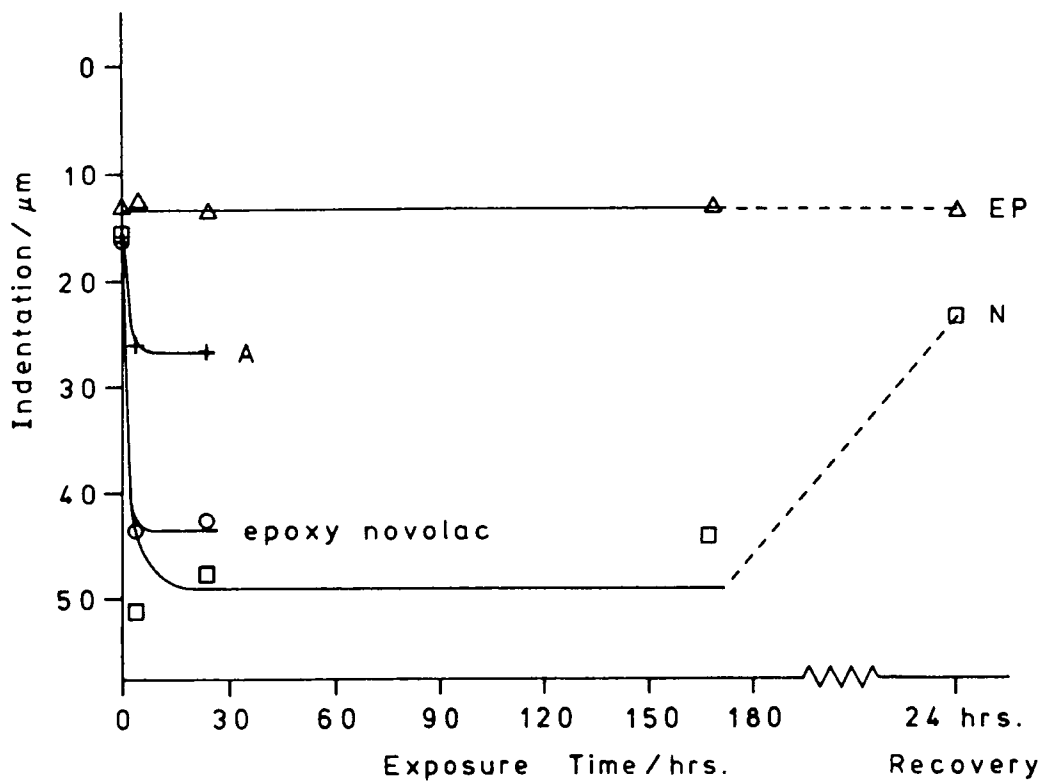
Two films of each system were used in the chemical resistance tests. The initial hardness of each film was measured with the micro-indentation tester using a primary weight of 1g and a secondary weight of 100g, each applied for 30 seconds. The cells used to contain the chemicals were then placed on the panels using grease to hold them in place and prevent any leakage of the contents. The ten chemicals chosen were white spirit (hydrocarbon fractions), xylene, oxitol (2-ethoxyethanol), acetone, methanol, triethylamine, water, 5% acetic acid solution, 30% sulphuric acid and 50% sodium hydroxide. After 4 hours' exposure the cells were emptied and the area of film beneath the cell exposed to the chemical checked for softening. This was repeated after 24 and 168 hours' exposure. After 168 hours' exposure the film was left for 24 hours and then the hardness measured again to determine whether any recovery occurred if the film had been softened by the chemical.

White spirit, 5% acetic acid, 30% sulphuric acid and 50% sodium hydroxide had no effect on the hardness of any of the systems. Water caused a slight softening of the films of the epoxy novolac and 'camkote A' but the films recovered over the 24 hour period after exposure. Triethylamine produced a slight hardening of the 'camkote' film but slightly softened 'camkote N', and had no effect on the remaining systems. Figures 4.25 (a), (b), (c) and (d) show the indentation depth plotted against

FIGURE 4.25 Hardness of the Photocured and Conventionally Cured Epoxy Resins as a Function of Exposure Time to Various Chemicals

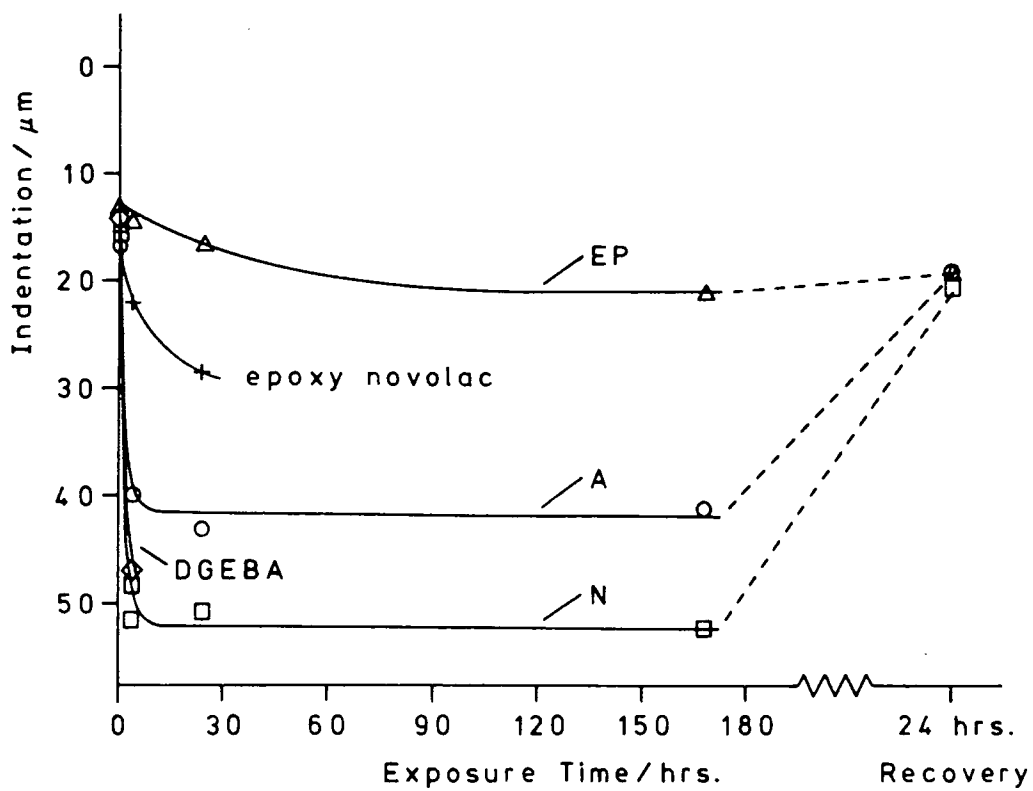


(a) Xylene

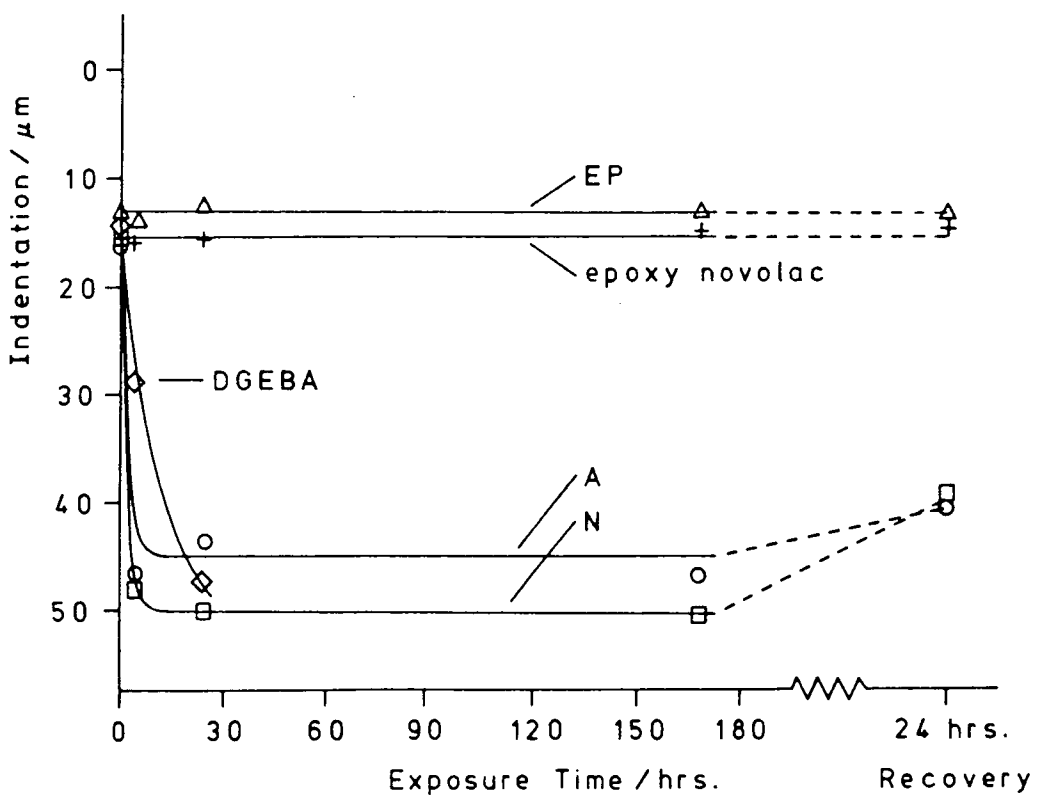


(b) Acetone

FIGURE 4.25 (contd...)



(c) Methanol



(d) Oxitol

the time of exposure to xylene, acetone, methanol and oxitol respectively. As can be seen from Figure 4.25(a), xylene produced marked softening of the polyurethane system, 'camkote N', but did not affect the other systems. Figure 4.25(b) shows that acetone softened the 'camkote N' system but the film remained intact whereas the photocured systems and 'camkote A' were softened and detached from the substrate, after only 4 hours' exposure in the case of the photocured DGEBA system; 'camkote EP' was unaffected. Exposure to methanol, Figure 4.25(c) led to softening of all the films but the two photocured systems were detached from the substrate. The 'camkote EP' system was least affected. Exposure to oxitol, Figure 4.25(d) resulted in softening of the 'camkote N' and 'A' systems as well as the photocured DGEBA system with the latter being detached from the substrate; the 'camkote EP' and photocured epoxy novolac systems were unaffected. In all cases where softening occurred and the film remained intact, some recovery was seen 24 hours after exposure. When softening of the photocured systems occurred, they were detached from the substrate which may be a reflection of the poor adhesion of these systems.

Visual observations were also recorded and are given in Table 4.31.

The discolouration of steel seen in some cases, such as with exposure to acetone, is probably due to moisture being carried through the film and attacking to the steel. In time this could lead to underfilm corrosion.

Generally the UV cured systems held up well against the acids, alkalis and less aggressive solvents. Against more aggressive solvents that led to softening, such as acetone,

TABLE 4.31 Visual Observations made after 168 Hours' Exposure of the Conventionally Cured and Photocured systems of Various Chemicals

Chemical	System	Comments
Acetone	'Camkote N'	Slight discolouration of the steel
	'Camkote EP'	Discolouration of the steel
Methanol	'Camkote A'	Slight discolouration of the steel
Water	DGEBA	Discolouration of the steel
	Epoxy Novolac	Slight discolouration of the steel
	'Camkote EP'	Discolouration of the steel
5% Acetic acid	DGEBA	Discolouration of the steel
	Epoxy Novolac	Discolouration of the steel
	'Camkote N'	Discolouration of the steel
	'Camkote EP'	Small blisters and underfilm corrosion
30% sulphuric acid	'Camkote EP'	Severe blistering and underfilm corrosion

-----

the UV cured systems fared worse than the conventional systems with the epoxy novolac system showing more potential than the DGEBA system.

(B) Adhesion

The adhesive properties of a coating have an important bearing on its protective properties. The adhesion of the UV cured systems to steel might be expected to be lower than that of the conventionally cured epoxy resins since they contain fewer hydroxyl groups and no amine moieties which are reputedly responsible for good adhesion.<sup>40</sup>

The adhesion of the five systems to steel was determined

by measuring the force required to detach the films from the substrate. Metal stubs were attached to each film using a rapid cure, epoxy adhesive. The stubs were then pulled off using an Elcometer pull-off gauge which consists of a 'hook' that slots around the stub and can then be raised pulling the stub and hopefully the film, from the substrate. The force required to achieve this is measured by the gauge. It is quite a subjective test since the rate of application of the force required to remove the stub and film can affect the result.

The force required to remove a film of each system from the substrate is recorded in Table 4.32.

TABLE 4.32 Force required to detach films of the conventionally cured and photocured systems from Steel

System	Elcometer reading/kg cm <sup>-2</sup>
DGEBA	16
Epoxy Novolac	18
'Camkote N'	>16
'Camkote EP'	17
'Camkote A'	>17

-----

The results from this relatively simple test indicate that the UV cured systems adhere just as well as the commercial systems to steel. Of the two UV cured systems the epoxy novolac system has the better adhesion.

(C) Prohesion

A film of each system as prepared previously was scored with a cross to expose the substrate. The films were then placed in a prohesion cabinet for five days. In the cabinet, the films are alternately sprayed with an aqueous salt solution

and then dried, which mimics, for example, a marine environment. The salt solution contained ammonium sulphate and sodium chloride.

The three commercial systems showed the least amount of underfilm corrosion, rusting of the steel being limited to the exposed areas. The two UV cured systems, however, showed a greater degree of underfilm corrosion, with the epoxy novolac system faring slightly better.

REFERENCES - Chapter Four

1. W.G. Potter, 'Epoxide Resins', Plastics Institute, London (1970).
2. Wicks and S.P. Pappas in "UV Curing: Science and Technology", Vol.1, Ed. S.P. Pappas, Technology Marketing Corporation (1978).
3. W.R. Watt in "Epoxy Resin Chemistry", Ed. R.S. Bauer, American Chemical Society, Washington (1978).
4. H. Dannenberg and W.R. Harp, Anal.Chem., 28, 86 (1956).
5. A.N. Garroway, W.B. Moniz and H.A. Resing in "Carbon-13 N.M.R. in Polymer Science", Ed. M. Pasika, American Chemical Society, Washington (1979).
6. G.C. Stevens, J.Appl.Polym.Sci., 26, 4259 (1981).
7. R.A. Fava, Polymer, 9, 137 (1968).
8. J.M. Barton, J. Macromol.Sci.-Chem., A8(1), 25 (1974).
9. J.E. Moore in Reference 2.
10. J.V. Crivello, J.H.W. Lam, and C.N. Volante, J.Rad.Curing, 4, 2 (1977).
11. J.G.Kloosterboer, G.M.M. van de Hei, R.G. Gossink and G.C.M. Dortant, Polym.Comm., 25, 322 (1984).
12. I.M. Ward, "Mechanical Properties of Solid Polymers", 2nd Ed., Wiley-Interscience (1978).
13. J.A. Byrosos in "Polymer Science - Vol.II", Ed. A.D. Jenkins, North-Holland Publishing Company (1972).
14. R.N. Haward in "Molecular Behaviour and the Development of Polymeric Materials", Eds. A. Ledwith and A.M. North, Chapman and Hall, London (1975).
15. W.A. Lee and R.A. Rutherford in "Polymer Handbook", 2nd Ed., Eds. J. Brandrup and E.H. Immergut, John Wiley (1974).
16. T.G. Fox and P.J. Flory, J.Appl.Phys., 21, 581 (1950).
17. T.G. Fox and J. Loshaek, J.Polym.Sci., 15, 371 (1955).
18. F. Rietsch, D. Daveloose and D. Froelich, Polymer, 17, 859 (1976).
19. N.D. Danielely and E.R. Long, J.Polym.Sci., Polym.Chem., 19, 2443 (1981).
20. A.P. Gray, Thermal Analysis Application Study, No. 2, Perkin-Elmer Corporation (1972).
21. L. Banks and B. Ellis, Polymer, 23, 1466 (1982).
22. J.K. Gillham and J.A. Benci, J.Polym.Sci., Polym.Symp., 46, 279 (1974).

23. J.B. Enns and J.K. Gillham, *J.Appl.Polym.Sci.*, 28, 2567 (1983).
24. J.F. Rabek "Experimental Methods in Polymer Chemistry", Wiley-Interscience (1980).
25. T. Daniels "Thermal Analysis", Kogan Page, London (1973).
26. T.K. Kwei, *J.Polym.Sci.*, A1, 2977 (1963).
27. J.L. Barrett, *J.Rad.Curing*, 6, 20 (1979).
28. D.S. Richards, M.Sc. Thesis, Durham (1982).
29. W.D. Cook, *J.Macromol.Sci.-Chem.*, A17, 99 (1982).
30. S.P. Pappas in Reference 2.
31. R.C. Michaelson and L.F. Loucks, *J.Chem.Ed.*, 52, 652 (1975).
32. J.V. Crivello and J.H.W. Lam, *Macromol.*, 10, 1307, (1977).
33. J.G. Kloosterboer, G.M.M. van de Hei and H.M.J. Boots, *Polym.Comm.*, 25, 354 (1984).
34. E.W. Meijer, D.M. de Leeuw, F.J.A.M. Greidanus and R.J.M. Zwiers, *Polym.Comm.*, 20, 45 (1985).
35. W.J. Bailey, H. Iwama, R. Tsushima, *J.Polym.Sci., Polym.Symp.*, 56, 117 (1976).
36. W.R. Watt in "U.V. Curing: Science and Technology", Vol.2, Ed. S.P. Pappas, Technology Marketing Corporation (1984).
37. B.E. Hulme, *J.Oil Col.Chem.Assoc.*, 59, 245 (1976).
38. A. Priola, F. Renzi and S. Cesca, 55, 63 (1983).
39. J.V. Crivello in Reference 2.
40. H. Lee and K. Neville, "Handbook of Epoxy Resins", McGraw-Hill Inc. (1967).

CHAPTER FIVE

THE PHOTO-OXIDATION OF PHOTOCURABLE  
EPOXY RESIN SYSTEMS DURING CURE AND  
THEIR SUBSEQUENT PHOTO-OXIDATIVE STABILITY

## 5.1 Introduction

When exposed to longer wavelength UV light present in sunlight ( $\lambda > 290\text{nm}$ ) all commercial polymers will sooner or later exhibit signs of photo-oxidative degradation, that is the generation of oxygen containing species such as hydroxyl and carbonyl groups, *via* the photochemical formation of species capable of reacting with oxygen. This generally results in a deterioration of the optical and mechanical properties of the polymer. Whether a polymer interacts with light of a particular wavelength will not only be determined by the structure of the polymer but also the conditions of its preparation and the presence of any additives. Much research effort has been expended over a number of years to investigate the processes that give rise to photo-oxidation, allowing techniques to be developed that reduce or eliminate the occurrence of this problem. However, research in this area of polymer science is still very active in an attempt to develop more photostable polymer systems.

Potential applications of the photocured epoxy resins studied in this work, may require prolonged exposure to sunlight; this chapter reports the results of an investigation into their photostability. Since the formation of a cross-linked network in these systems involves irradiation with UV light, the occurrence of photo-oxidation during the curing process may influence the subsequent photostability of the cured system. Electron spectroscopy for chemical applications, ESCA, and transmission infra-red spectroscopy were used to examine the surfaces and the bulk of films for evidence of photo-oxidation during the curing process and on subsequent

prolonged exposure to longer wavelength UV light.

## 5.2 Electron Spectroscopy for Chemical Applications

ESCA is a very useful tool for the analysis of polymer surfaces, a wealth of data on structure and bonding can be obtained ranging from elemental composition to structural isomerism. Detailed reviews of instrumentation<sup>1</sup> and applications of ESCA in general, and to polymer surfaces in particular, have been published.<sup>1,2</sup>

The ESCA spectrometer measures the kinetic energy of electrons emitted by the interaction of molecules with photons of the required energy; knowing the energy of the incident radiation and measuring the kinetic energy of the electrons emitted allows the energy required to remove an electron from a given orbital to be determined; this is known as the binding energy. In most ESCA studies, electrons ejected from core orbitals rather than valence orbitals are investigated. The reasons for this are the greater probability of photoionization of an electron from a core orbital and core orbitals give rise to photoelectrons of a binding energy characteristic of a particular element. To study the photoionization of core electrons, photons in the low wavelength X-ray region of the electromagnetic spectrum are required. The ESCA spectrometer thus essentially consists of a source for generating a beam of soft, monochromatic X-rays, an instrument for differentiating between electrons of different kinetic energy, an instrument for detecting and 'counting' the electrons, and a means of displaying the data.

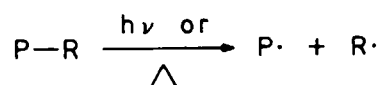
The interior of the spectrometer is kept under quite a high vacuum ( $10^{-8}$  torr) so as to limit the scattering of the emitted electrons by collision with gas molecules and to limit surface contamination of the sample. The surface sensitivity of ESCA arises from the short mean-free path of electrons in solids, the electrons detected resulting from photoionization occurring within a few nanometers of the surface of the sample.

The data from the spectrometer is presented in the form of a plot of the number of electrons 'counted' against their kinetic or binding energy. The peaks due to photoionized electrons in core level ESCA spectra are characteristic of the elements present in the surface so for example, peaks arising from the photoionization of electrons in the  $1s$  core orbitals of carbon, fluorine and oxygen may easily be distinguished. The elemental composition of the surface can be determined quantitatively using the area under the peaks due to different elements and a calibration factor obtained from the spectra of well characterized model compounds. Core electrons might not be expected to reflect the bonding environment of an atom but this is not the case. Small but significant shifts in the binding energy of electrons do occur depending on the environment of the atom. For example, characteristic shifts in binding energy due to carbons associated with hydrocarbon functionality (carbon atoms exclusively bound to hydrogen or other carbons),  $\underline{C}$ -H, carbon atoms singly bound to oxygen,  $\underline{C}$ -O, carbonyl functionality,  $\underline{C}=\underline{O}$ , and carboxylate functionality,  $\underline{O}-\underline{C}=\underline{O}$ , can be distinguished in the  $C_{1s}$  spectra which is useful for the study of photo-oxidation. Although the shifts are small, producing overlapping peaks, data handling systems can be used to resolve the spectra allowing the relative areas under the component peaks to be determined and hence the percentage of carbon atoms in each environment.

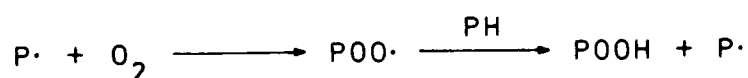
#### 5.4 A General Mechanism of the Photo-Oxidative Degradation of Polymers

The mechanism of the photo-oxidation of polyalkenes is thought to be quite similar to that of their thermal oxidation.<sup>3,4</sup> In the former type of oxidative degradation light is absorbed by a chromophore resulting in the homolytic cleavage of a weak bond to generate the initial radical species whereas in the latter type, thermal energy results in bond cleavage. This difference in initiation leads to differences in the rates of subsequent processes but photo-oxidative degradation can be represented by the same general free radical chain mechanism as for thermo-oxidative degradation which is shown below. P<sup>•</sup> represents a radical species on the polymer chain.

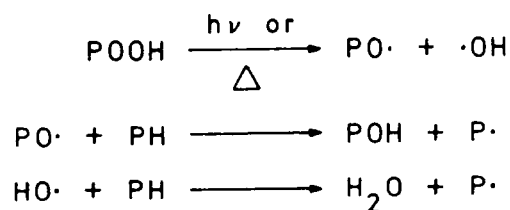
##### Initiation



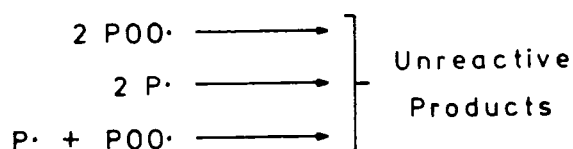
##### Propagation



##### Branching



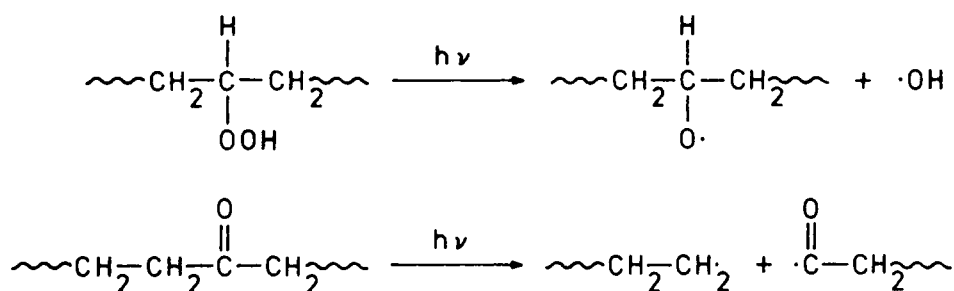
##### Termination



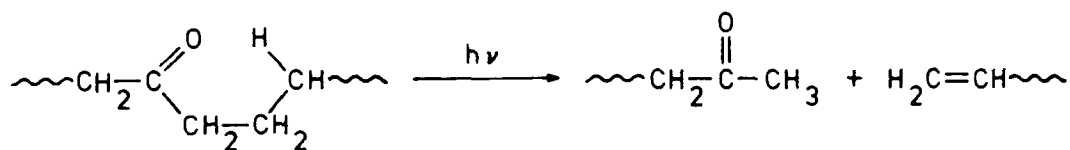
Although the above general type of mechanism is proposed to account for photo-oxidation in polymers, auto-catalytic behaviour may not be apparent. The absence of such behaviour has been attributed to an increased rate of initiation and a limited kinetic chain length for the branching processes.<sup>3</sup>

The occurrence of photo-oxidation is expected to be a function of the wavelength of irradiation. Polystyrene for example, undergoes photodegradation when irradiated with UV light of 254nm since the aromatic moiety absorbs light of this wavelength.<sup>5</sup> Photo-oxidation would not be expected to occur when polystyrene is irradiated with the longer wavelength UV light present in sunlight, yet it does.<sup>5</sup> Similarly other polymers such as polyethylene possess no inherent chromophore capable of absorbing longer wavelength UV light but again photo-oxidation does occur on exposure to sunlight especially in commercial samples. The absorption of longer wavelength UV light by polyalkenes is attributed to the presence of a combination of impurity chromophores arising from oxidation of the polymer during manufacture or processing, catalyst residues, and a complex photophysical interaction between the polymer and oxygen to generate hydroperoxides.<sup>6</sup>

Two types of chromophore thought to result from the oxidation of polyalkenes during manufacture are carbonyl and hydroperoxide groups. Photolysis of carbonyl and hydroperoxide groups proceeds as follows to generate radical species:



In addition to the Norrish Type I process shown above, carbonyl groups may undergo a Norrish Type II process giving rise to alkene and ketone functionality:



Generation of radical species from carbonyl groups is one of the processes resulting in chain scission, a feature common to photo- and photo-oxidative degradation, although cross-linking due to the recombination of radical species in the termination steps can more than equal the occurrence of chain scission.

The general scheme outlined above shows how photo-oxidation gives rise to hydroxyl groups. The formation of carbonyl species as a result of photo-oxidative degradation is shown in a following section in reference to the photo-oxidation of epoxy resins.

#### 5.4 Photo-Oxidation of Resins Photocured using Free Radical Photoinitiators

At least two studies have indicated that the presence of residual free radical photoinitiators can markedly affect the photostability of resins cured by this technique. Allen *et al*<sup>7</sup> investigated the photo-oxidative stability of UV and electron beam cured acrylate resins. Photo-oxidation occurred much more readily in the UV cured systems than the electron beam cured systems, which was attributed to the photolysis of residual photoinitiator in the former systems. The latter method of cure does not involve the use of photoinitiators, collision of energetic electrons with monomer molecules produces radical species capable of initiating polymerization. Furthermore the photo-oxidative stability of the UV cured systems depended

on the nature of the photoinitiator used. Hult *et al*<sup>8</sup> also showed that the presence of residual free radical photoinitiator in UV cured systems can affect the subsequent photostability. In this study solutions or films of polystyrene containing photoinitiator were irradiated. The initial rate and extent of degradation of the polystyrene were found to increase with increasing photoinitiator concentration and were dependent on the nature of the photoinitiator.

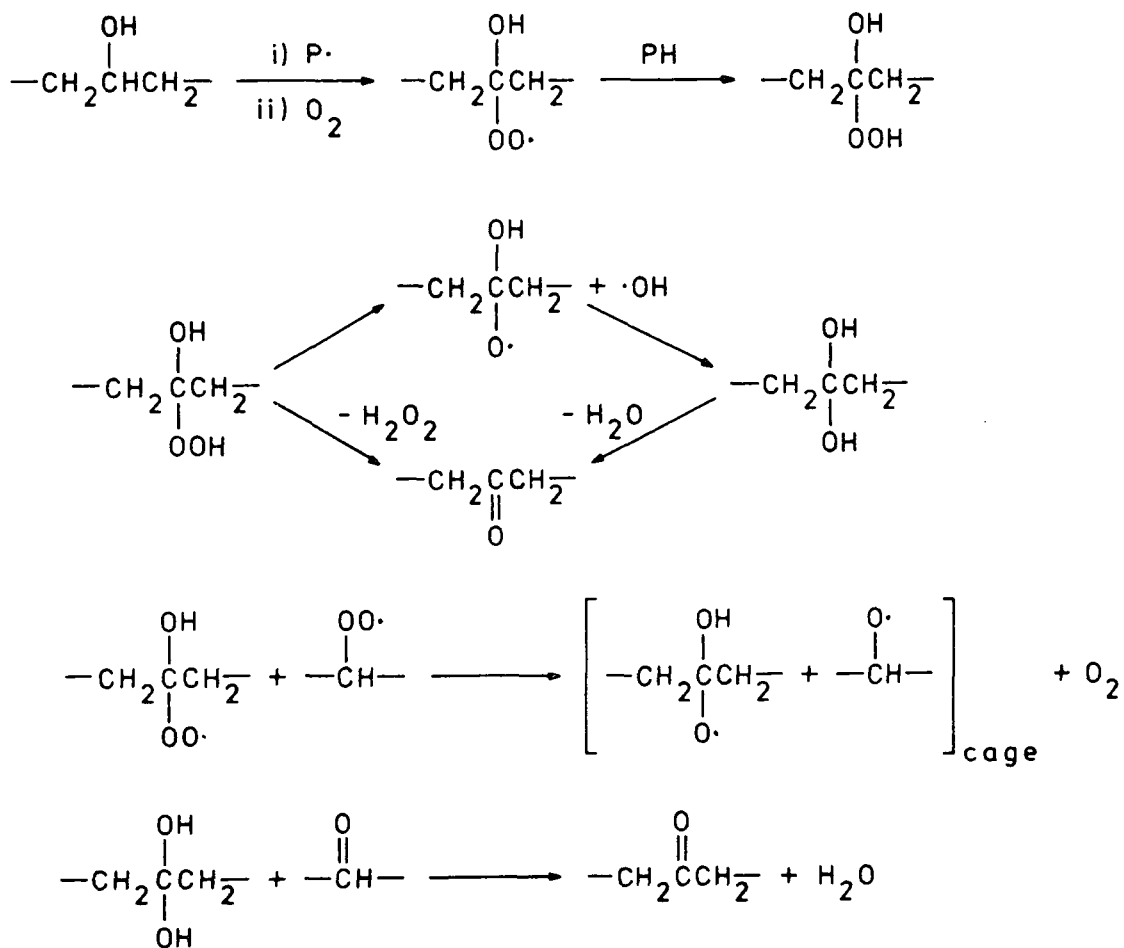
Photo-oxidation occurring during the UV cure of unsaturated resins was also investigated by Hult *et al*.<sup>8</sup> Comparison of the C<sub>1s</sub> and O<sub>1s</sub> ESCA spectra of the top and bottom surfaces of a UV cured film of an acrylated urethane system indicated that photo-oxidation does occur during cure but is limited to a thin surface layer. Subsequent irradiation of a film during ageing experiments resulted in an increase in the extent of photo-oxidation at the surface to a constant value leading the workers to propose that photo-oxidation of the surface proceeds rapidly as long as residual photoinitiator is present.

#### 5.5 Photo-Oxidative Studies of Conventionally Cured Epoxy Resins and Model Compounds

Many of the applications of conventionally cured DGEBA and epoxy novolac resins involve prolonged exposure to sunlight which unfortunately results in a deterioration of the desirable mechanical or optical properties of the cured resins due to photo degradation.<sup>9,10,11</sup> A number of studies have been carried out in an attempt to ascertain the chromophore responsible for light absorption and the mechanism of photo-oxidation.

Bellenger *et al*<sup>12</sup> investigated the photo-oxidative stabil-

ity of DGEBA resin cured with various aliphatic amine curing agents. Films of the cured resin were irradiated using a source emitting light between 300-450nm. Infra-red spectroscopy showed the growth of carbonyl ( $1725-1735\text{ cm}^{-1}$ ) and amide ( $1650-1660\text{ cm}^{-1}$ ) functionality with increasing irradiation time. The growth of the carbonyl functionality appeared to increase with increasing hydroxyl content of the system which led the workers to propose the following scheme for carbonyl formation from secondary hydroxyl groups resulting from the curing process or initially present in the structure of the uncured DGEBA resin:

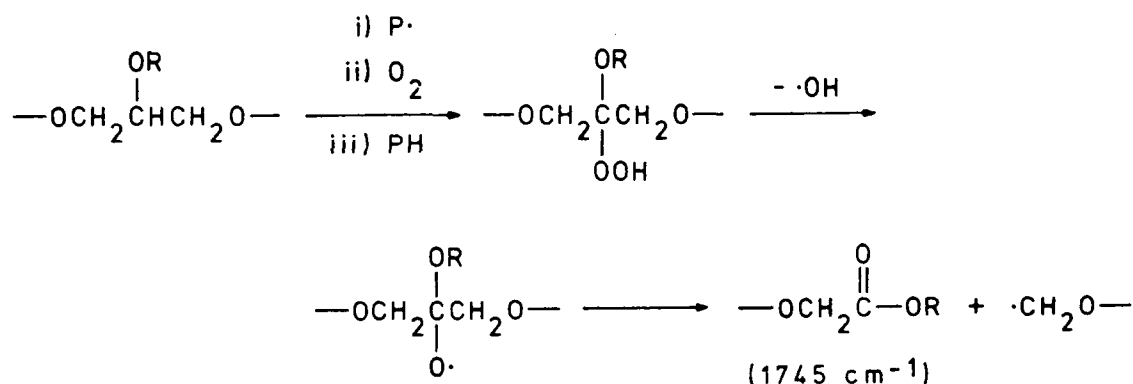


On irradiation, the  $T_g$  of the cured resin system decreased indicating the occurrence of chain scission which was attributed to Norrish Type I and II processes involving the carbonyl groups. Bellenger and Verdu<sup>13</sup> went on to study the photo-oxidative stability of DGEBA and DGEBF resins cured with aromatic curing agents and irradiated under conditions similar to those in the

previous study.<sup>12</sup> Again carbonyl and amide formation were observed, the rate of formation of these species showing auto-inhibition which was attributed to unreacted amine curing agent acting as a radical scavenger. Hydroperoxide formation was also followed and observed to increase rapidly on irradiation then decrease to a steady state concentration. Light absorption by the cured resin was found to be related to the structure of the epoxy resin rather than the curing agent. Absorption of light by the epoxy resin was attributed to the phenoxy moiety or to the presence of impurities perhaps as a result of thermal oxidation of the resin during manufacture. In the previous study,<sup>12</sup> carbonyl species formed during the curing process were found to act as photosensitizers increasing the rate of carbonyl formation.

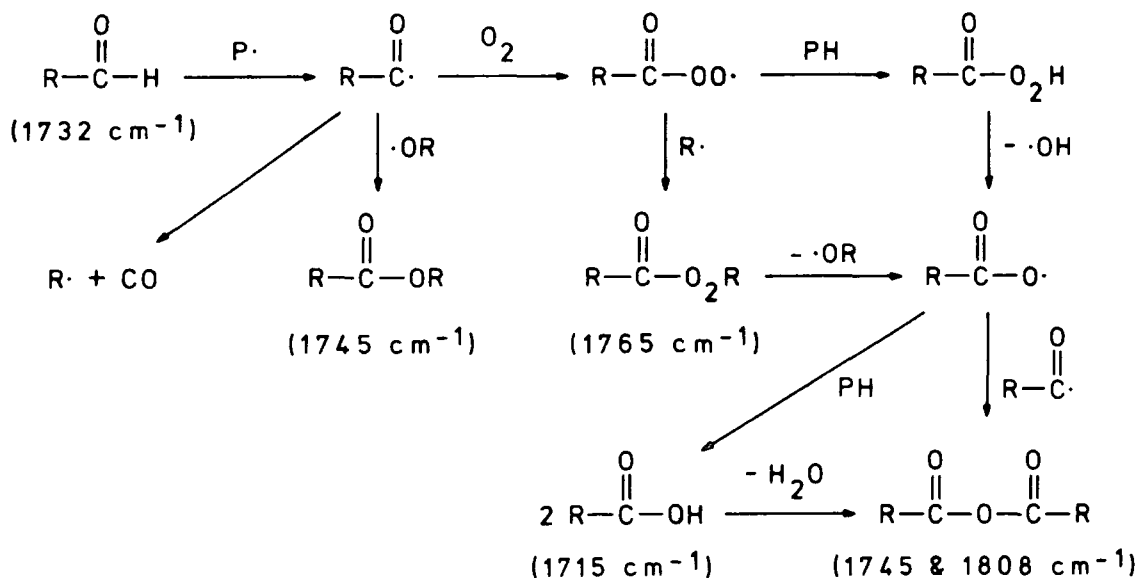
Allen *et al*<sup>10</sup> reached the same conclusions from their investigation of the spectroscopic properties and photosensitivity of commercial epoxy resins. Absorptions at  $1760\text{ cm}^{-1}$  were observed in the IR spectra of the commercial resins which it was suggested might be due to perester functionality,  $\text{R}(\text{C}=\text{O})\text{OOR}$ . This shows that some oxidation of the resins has occurred but perester impurities are not expected to contribute to the photosensitivity of epoxy resins to longer wavelength UV light since they should only absorb light well below 300nm. However the UV derivative spectra of cured resins did show the presence of impurity chromophores absorbing above 300nm which it was suggested might be due to quinone groups formed during the manufacture or cure of the resins. It was also suggested that the phenoxy moiety of the epoxy resin may absorb light at the higher energy end of the solar emission spectrum to initiate photo-oxidation.

Linn *et al*<sup>14</sup> compared the thermo- and photo-oxidative degradation of a DGEBA resin cured using trimethylboroxine which results in homopolymerization of the resin. Fourier transform infra-red spectroscopy was used to detect any changes in the structure of the resin on degradation. Thermo-oxidative degradation resulted in an increase in, or the appearance of, absorptions due to carbonyl functionality at 1808, 1784, 1765, 1745, 1732, 1715 and 1665  $\text{cm}^{-1}$  as well as an absorbance at 885  $\text{cm}^{-1}$  due to hydroperoxide groups and an increase in the hydroxyl group absorption. The following scheme was proposed to account for the formation of the carbonyl functionality.



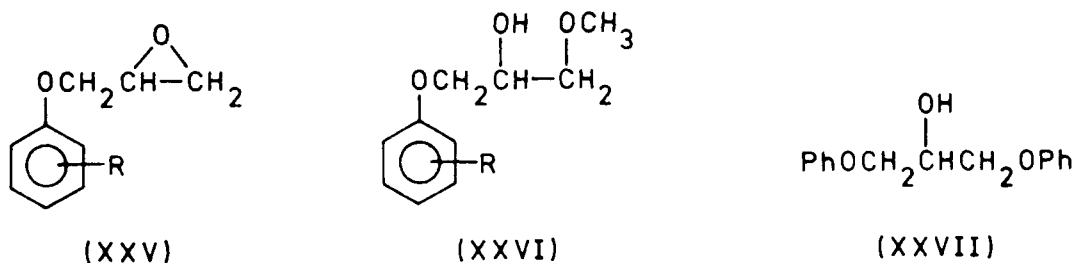
The cured resin structure contains hydrogen atoms on three carbons  $\alpha$  to ether groups. The above scheme shows hydrogen abstraction from a secondary carbon atom but abstraction from the two primary carbon atoms can occur although not as readily as from the secondary carbon atom. This will result in the formation of aldehyde groups which it is proposed may give rise to other carbonyl species by the route shown overleaf.

The remaining absorption at 1685  $\text{cm}^{-1}$  was attributed to the formation of semi-quinone moieties. Photo-oxidation on irradiation with light from a xenon-mercury source resulted in similar absorptions in the infra-red spectrum of the cured resin. The workers thus proposed that the carbonyl function-



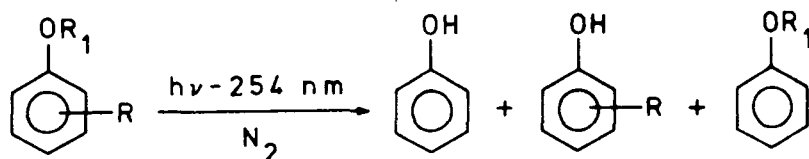
ality resulted from the same processes as in thermal oxidation. The infra-red spectrum of the uncured resin showed an absorption at  $1732 \text{ cm}^{-1}$  attributed to aldehyde groups formed by rearrangement of the epoxide group during the preparation of the resin and an absorption at  $1765 \text{ cm}^{-1}$  attributed to perester functionality resulting from oxidation of the aldehyde groups.

Tempe *et al*<sup>15</sup> have investigated the photochemistry of a number of aryl ether compounds, such as (XXV) (XXVI) and (XXVII), related to the structure of epoxy resins:

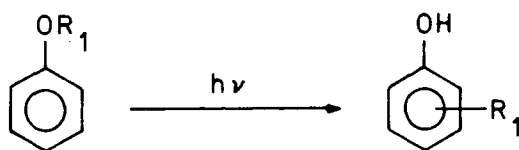


e.g. R = H, p-CH<sub>3</sub> and p-OCH<sub>3</sub>

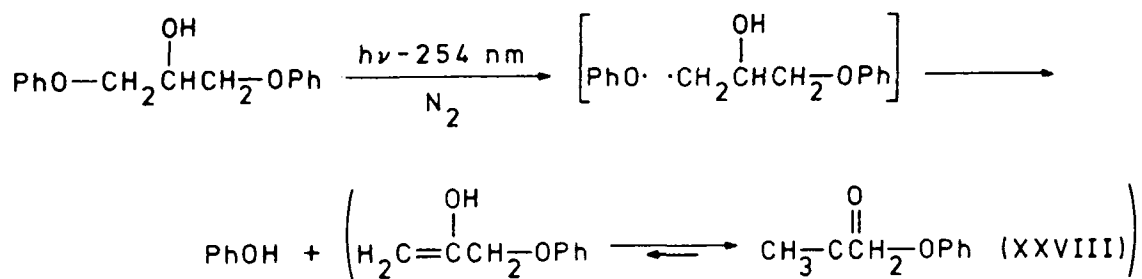
The UV absorption spectra and the fluorescence emission spectra of the model compounds and DGEBA were very similar indicating that the photochemistry of the model compounds and DGEBA are similar. Irradiation of compounds (XXV) and (XXVI) in solution under a nitrogen atmosphere with 254nm light gave phenol and substituted phenols as the major products detected.



No products from the expected Photo-Fries rearrangement, shown below, were detected.



The formation of the phenols was proposed to occur *via* formation of phenoxy and alkyl radicals due to the homolytic cleavage of the phenoxy-alkyl bond. Similarly the loss of the substituent on the phenyl ring may proceed *via* the homolytic cleavage of the bond attaching the substituent to the ring. Absorption of light of this wavelength was attributed to the phenoxy chromophore indicating that excitation of this moiety results in homolytic bond cleavage. More interestingly photolysis of (XXVII) under a nitrogen atmosphere using 254nm light yielded phenol and phenoxyacetone (XXVIII) as the major products. A possible mechanism accounting for the formation of phenoxyacetone *via* the enol tautomer was proposed:



Repeating the irradiation of (XXVII) with air present just resulted in faster rates of phenol formation. However, irradiation of (XXVII) with longer wavelength light in the presence of air yielded phenyl formate (XXIX) as a major volatile product along with minor amounts of phenol, phenoxyacetone and phenoxyacetic acid (XXX). The following mechanism, involving a charge transfer complex between (XXVII) and oxygen, was proposed to account for the formation of (XXIX) and (XXX):



The above studies have indicated the presence of a number of sites in the DGEBA and diglycidyl ether of butanediol resins which could undergo oxidation and these sites will also be present in the structure of the photocured resins prepared in this work, the photo-oxidative stability of which are described in the following sections.

### 5.6 Photo-Oxidation of the DGEBA System

The lacquers of the DGEBA resin used in the following experiments contained 97.0% resin, 2.0% photoinitiator and 1.0% w/w acetone or were close to this composition. Unless otherwise stated films of 100 $\mu$ m nominal thickness were prepared on polyethylene for the ESCA measurements and films of 50 $\mu$ m nominal thickness for the infra-red spectroscopic measurements.

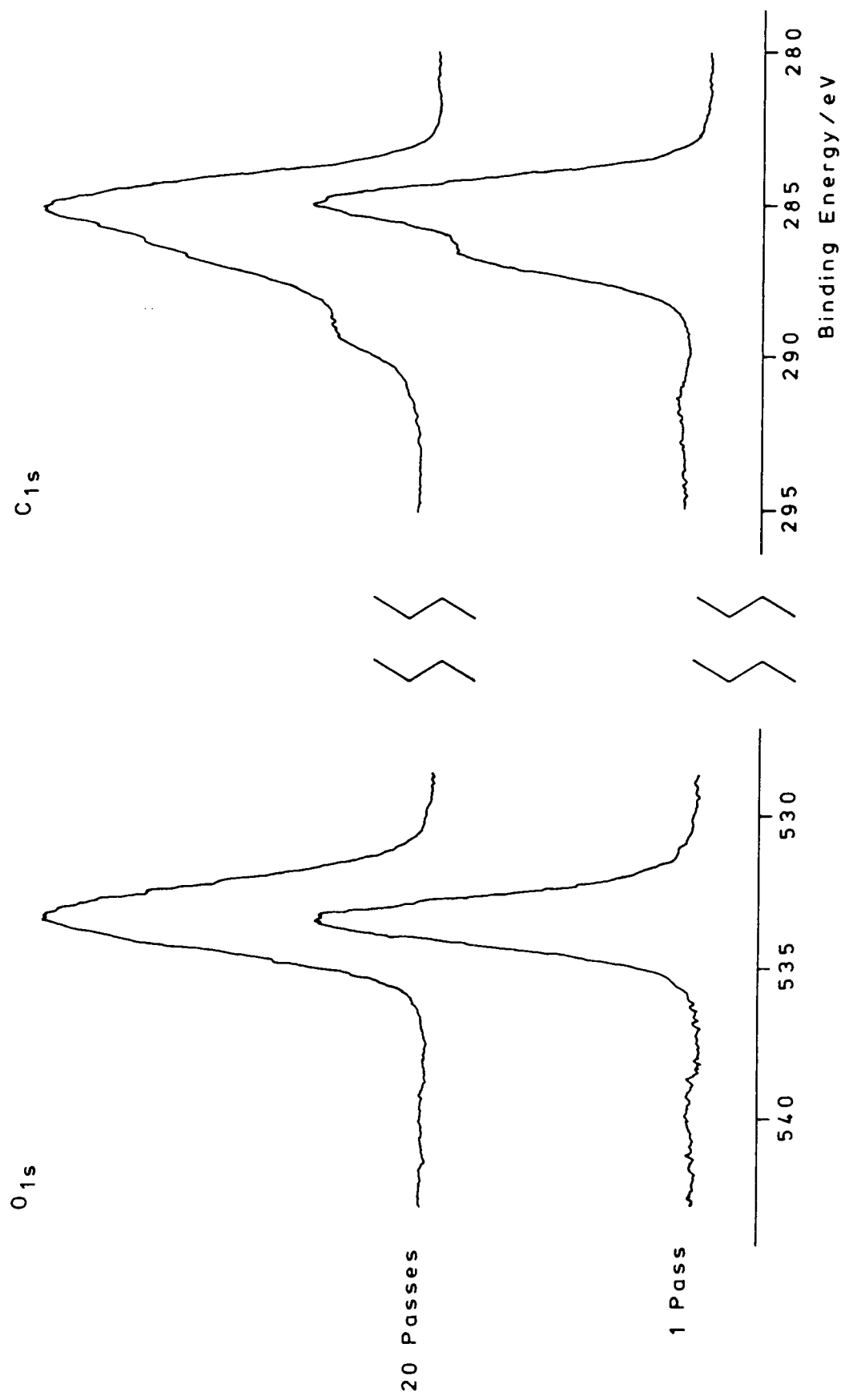
For the prolonged irradiation of samples with UV light of wavelengths similar to those present in sunlight, a UV fluorescent lamp (Phillips, 40W) was used. The emission of light by this source commences at  $\sim$ 300nm and peaks at 360-365nm. Samples were placed at a distance of 2mm from the source and received a photon flux of  $1.2\text{mW cm}^{-2}$ , as measured by the thermopile detector, at a temperature of 27 $^{\circ}$ C.

#### (A) Photo-Oxidation as a Result of the Curing Process

##### (i) Effect of Increasing Cure Exposure to the 1.8kW Source

ESCA spectra of films given on increasing number of passes under the 1.8kW source were recorded  $\sim$ 24 hours after irradiation. The configuration of the X-ray source, sample and detector in the spectrometer gave a sampling depth of  $\sim$ 40 $\text{\AA}$ . The  $\text{C}_{1s}$  and  $\text{O}_{1s}$  core level spectra in Figure 5.1 illustrate the

FIGURE 5.1  $C_{1s}$  and  $O_{1s}$  Core Levels for Films of the DGEBA System Given 1 and 20 Passes Under the 1.8kW Source



trends observed. The  $C_{1s}$  spectra show the growth of carbon environments with higher binding energies in the surface of films given longer cure exposures whilst the peak in the  $O_{1s}$  spectra broadens with increasing cure exposure indicating an increase in the number of oxygen environments. The  $C_{1s}$  spectrum of the film given 1 pass contains an envelope of peaks with a small satellite peak at higher binding energy. The latter peak arises from the process known as shake-up, where the transition of a valence electron from an occupied to an unoccupied molecular orbital accompanies photoionization, a feature commonly observable in the ESCA spectra of polymers containing unsaturated units. A small satellite peak at higher binding energy due to shake-up is also visible in the  $O_{1s}$  spectra. Deconvolution of the  $C_{1s}$  envelope for the film given 1 pass shows the presence of two component peaks. The peak at lower binding energy is attributed to  $\underline{C}$ -H functionality which occurs at 285.0 eV. The other component peak occurs at  $286.7 \pm 0.1$  eV relative to the  $\underline{C}$ -H peak and corresponds to  $\underline{C}$ -O functionality.<sup>16</sup> The shake-up peak,  $\pi \rightarrow \pi^*$ , occurs at a binding energy of  $291.6 \pm 0.1$  eV which is close to that found for polystyrene.<sup>17</sup> Figure 5.2 is the deconvoluted spectrum of the film given 20 passes. This shows the presence of additional component peaks at  $286.8 \pm 0.1$  eV and  $289.4 \pm 0.1$  eV which correspond to carbonyl,  $\underline{C}=\underline{O}$ , and carboxyl or carboxylate functionality,  $\underline{O}-\underline{C}=\underline{O}$ , respectively.<sup>16</sup>

A second set of films were prepared, irradiated and analysed in a similar way to those described above, the good agreement between the two sets of data give confidence in the analytical method. The average composition of the surface of the films given 1 pass was found to be 64.8%  $\underline{C}$ -H and 35.2%  $\underline{C}$ -O

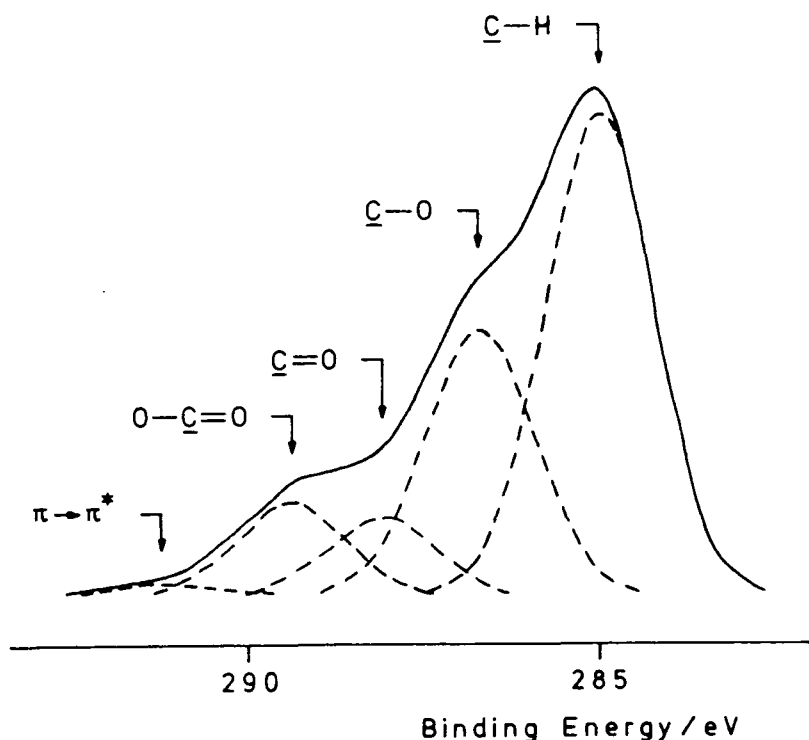


FIGURE 5.2 C<sub>1s</sub> Core Level Spectrum of a Film Given 20 Passes  
Showing the Component Peaks

with a ratio of carbon to oxygen atoms of  $\sim 1:0.21$ . The expected composition of the surface from the structure of the DGEBA resin (XVIII) and the composition of the lacquer would be 62.4%  $\underline{\text{C}}\text{-H}$  and 37.2%  $\underline{\text{C}}\text{-O}$  with a ratio of carbon to oxygen atoms of  $\sim 1:0.19$ . The surface composition of the cross-linked network as determined by ESCA is therefore reasonably close to that expected from the resin structure.

The effect of increased cure exposure on the  $\text{O}_{1s}/\text{C}_{1s}$  intensity ratio is shown in Figure 5.3, each point representing the average for two films. There appears to be an induction period before the relative amount of oxygen at the surface starts to increase linearly with increasing cure exposure. After 20 passes, the carbon to oxygen atom ratio has doubled to  $\sim 1:0.4$ . Figure 5.4 clearly shows decreases in the  $\text{C-H}$  and  $\underline{\text{C}}\text{-O}$  component intensities and the formation and increase in the intensities of  $\underline{\text{C}}\text{=O}$  and  $\text{O-}\underline{\text{C}}\text{=O}$  components with increasing cure exposure.

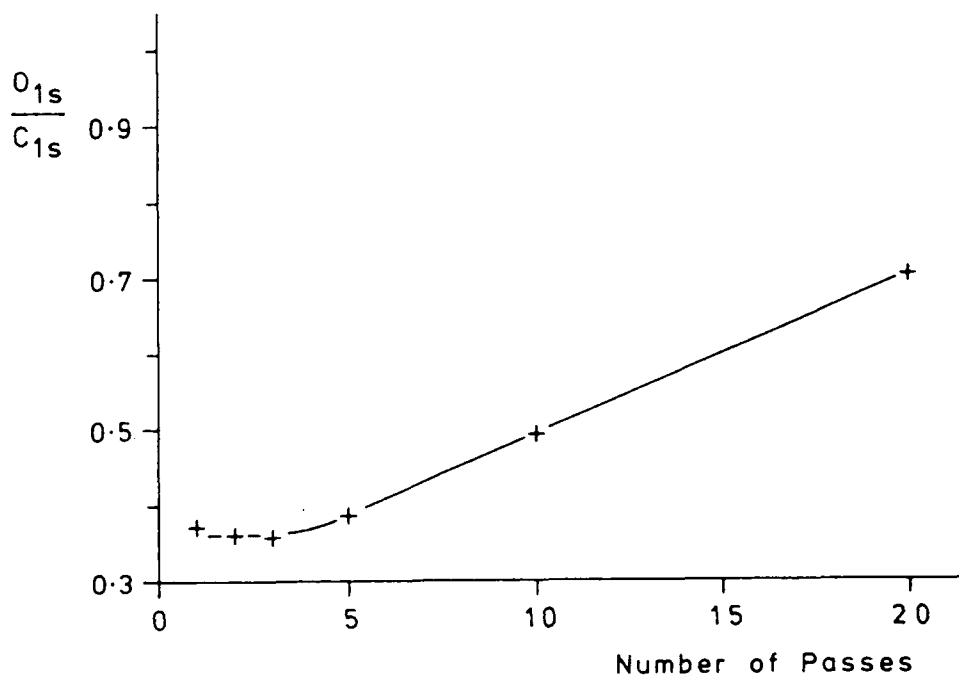


FIGURE 5.3  $O_{1s}/C_{1s}$  Intensity Ratio as a Function of Cure Exposure

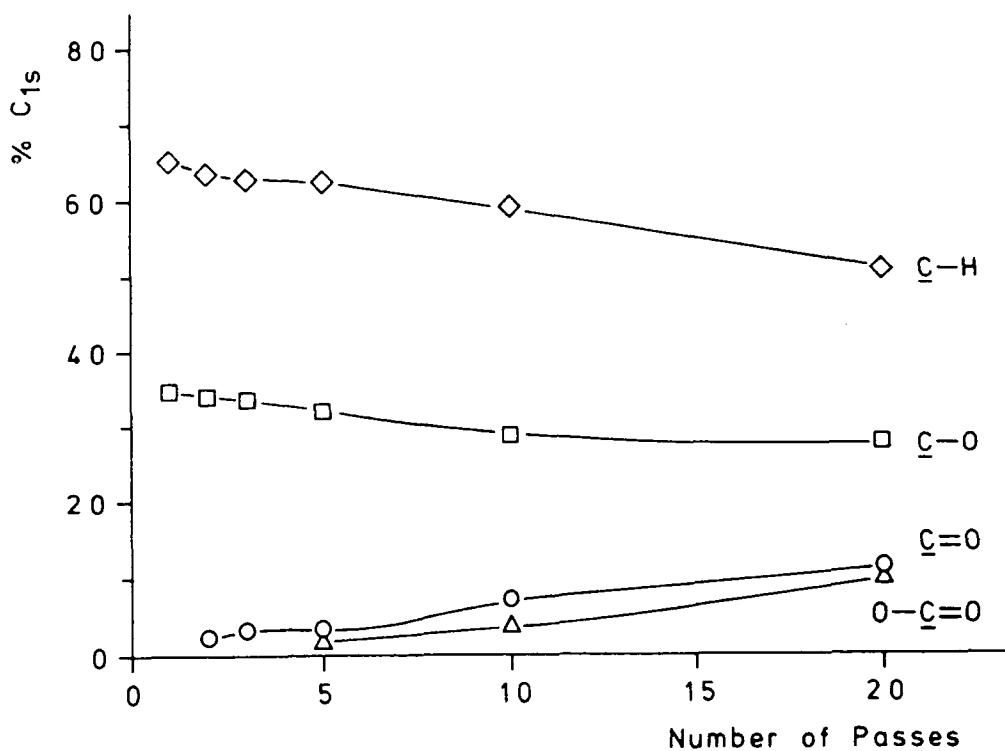


FIGURE 5.4  $C_{1s}$  Component Intensities as a Function of Cure Exposure

It is interesting to note that the induction period associated with the formation of O-C=O functionality is similar to that associated with the increase in the  $O_{1s}/C_{1s}$  ratio.

The decrease in the C-H component intensity as the C=O and O-C=O components are formed and increase implies that photo-oxidative degradation of the bisphenol A moiety of the resin structure is taking place since this accounts for the C-H component. One might expect that the isopropylidene bridging unit would be particularly susceptible to photo-oxidation but there is also evidence for photo-oxidative degradation of the phenyl rings.

TABLE 5.1  $\pi \rightarrow \pi^*$  Component Intensity as a Function of Cure Exposure

No. of passes	1	2	3	5	10	20
% $C_{1s}$	2.1	1.8	1.8	1.8	1.8	1.0

Table 5.1 shows the intensity of the  $\pi \rightarrow \pi^*$  shake-up transition diminishes with increasing cure exposure and hence may be indicative of a loss of aromaticity due to the degradation of the phenyl rings. Photo-oxidative degradation of the bisphenol A moiety, including the aromatic rings, has been observed in bisphenol A poly(sulphone) for example.<sup>18</sup> The decrease in the intensity of the C-O component with increasing cure exposure implies that the loss of ether or hydroxyl functionality due to the degradation of the polyether network is not compensated for by the generation of new hydroxyl, hydroperoxide or ester groups.

It must be noted that ESCA can only give the relative amount of each component present at the surface. Changes in the relative intensities of the component peaks could therefore

be due to the growth of one type of functionality at the expense of another or to the loss of a particular component as a result of the formation of volatile species, both processes contributing to the changes in surface composition. Indeed, the high vacuum conditions employed in the ESCA spectrometer probably result in an increased loss of photo-oxidation products from the surface.

Infra-red spectra of lacquers of the DGEBA resin show the presence of two weak absorptions that can be attributed to carbonyl groups. One is at  $\sim 1710 \text{ cm}^{-1}$  and does not appear in the infra-red spectrum of the resin alone so is presumably due to the trace of acetone in the lacquer. The other absorption occurs at  $\sim 1750 \text{ cm}^{-1}$  and does appear in the infra-red spectrum of the resin alone and may be due to non-conjugated ester carbonyl groups or perhaps to perester functionality. Infra-red spectra of  $100\mu\text{m}$  films given 1 to 20 passes showed the presence of these two absorption bands with no further bands appearing in the carbonyl region. The two absorbances were expressed as a ratio of the absorbance at  $1605 \text{ cm}^{-1}$ . The two normalized absorbances showed no change with increasing cure exposure and were no greater than the same ratios in the uncured lacquer. This would strongly suggest that the photo-oxidation occurring during the curing process is limited to a thin surface layer. In addition the  $\text{O}_{1s}$  and  $\text{C}_{1s}$  ESCA spectra of the underneath of a film given 20 passes under the lamp gave no indication of photo-oxidation products whereas the top surface has suffered extensive photo-oxidation, further supporting the conclusion that photo-oxidation during cure does not occur throughout the bulk.

Since the films are irradiated with short as well as long wavelength UV light it seems probable that the chromophore responsible for the initiation of photo-oxidation is the aryl ether moiety of the resin. The above results would tend to support this conclusion since it was shown in the previous chapter, Section 4.5, that the DGEBA resin absorbs much of the shorter ( $\lambda < 297\text{nm}$ ) wavelength UV light emitted by the source within a few micrometers of the surface of a film of a lacquer of similar composition to those used in these experiments. Therefore if the aryl ether chromophore were to be responsible for the initiation of photo-oxidation then one might expect it to be limited to the surface as appears to be the case.

(ii) Elimination of the Photo-Oxidation Occurring During Cure

As photo-oxidative degradation requires oxygen as well as light of the appropriate wavelength, the initial approach to eliminating its occurrence was to irradiate the system with longer wavelength UV light in the absence of oxygen. Films were prepared from a degassed lacquer under a nitrogen atmosphere and irradiated using the 1.8kW source through the 'pyrex' filter, the space beneath the filter being flushed with nitrogen. ESCA was carried out on the films approximately 24 hours after cure. The  $C_{1s}$  component analysis in Figure 5.5 shows that the  $\underline{C-H}$  and  $\underline{C-O}$  component intensities remain constant and no  $\underline{C=O}$  or  $O-\underline{C=O}$  functionality is formed as the cure exposure is increased. Likewise the  $O_{1s}/C_{1s}$  intensity ratio remains constant with increasing cure exposure as is also shown in Figure 5.5. Thus the occurrence of surface photo-oxidation has been eliminated.

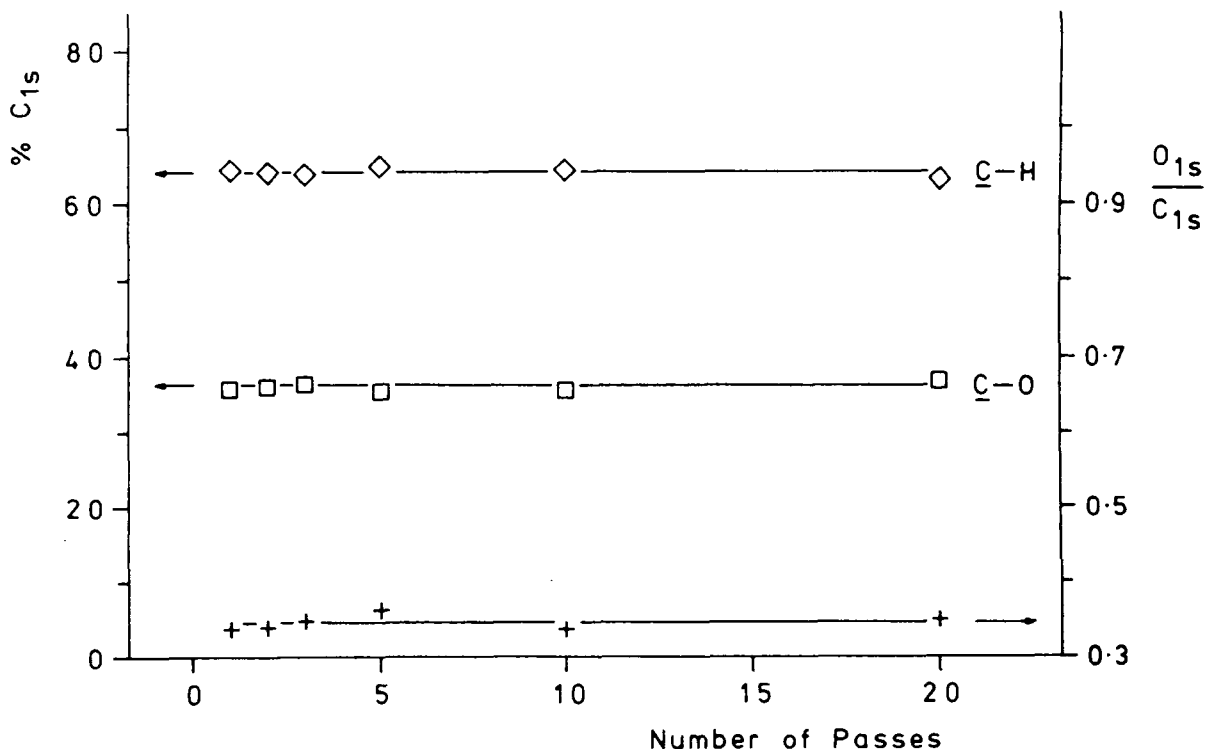


FIGURE 5.5 Effect of increasing Cure Exposure to Filtered Light under a Nitrogen Atmosphere on the  $O_{1s}/C_{1s}$  Intensity Ratio and  $C_{1s}$  Component Intensities

The photo-oxidation of films prepared from a non-degassed lacquer and irradiated through the 'pyrex' filter in air was also investigated. Interestingly the results, Figure 5.6, again show the absence of photo-oxidation.

Since the filter removes all wavelengths below 275nm, as shown in Figure 4.10, photo-oxidation during cure may be eliminated or substantially reduced by removing wavelengths strongly absorbed by the DGEBA resin, tending to confirm that the aryl ether chromophore of the DGEBA resin is responsible for the absorption of shorter wavelength light leading to the initiation of photo-oxidation. As the resin still cures on irradiation with the longer wavelength light, albeit not as effectively as when irradiated with the total output of the lamp under these conditions, direct or sensitized photolysis of the photo-initiator must be occurring which will give rise to radical species.

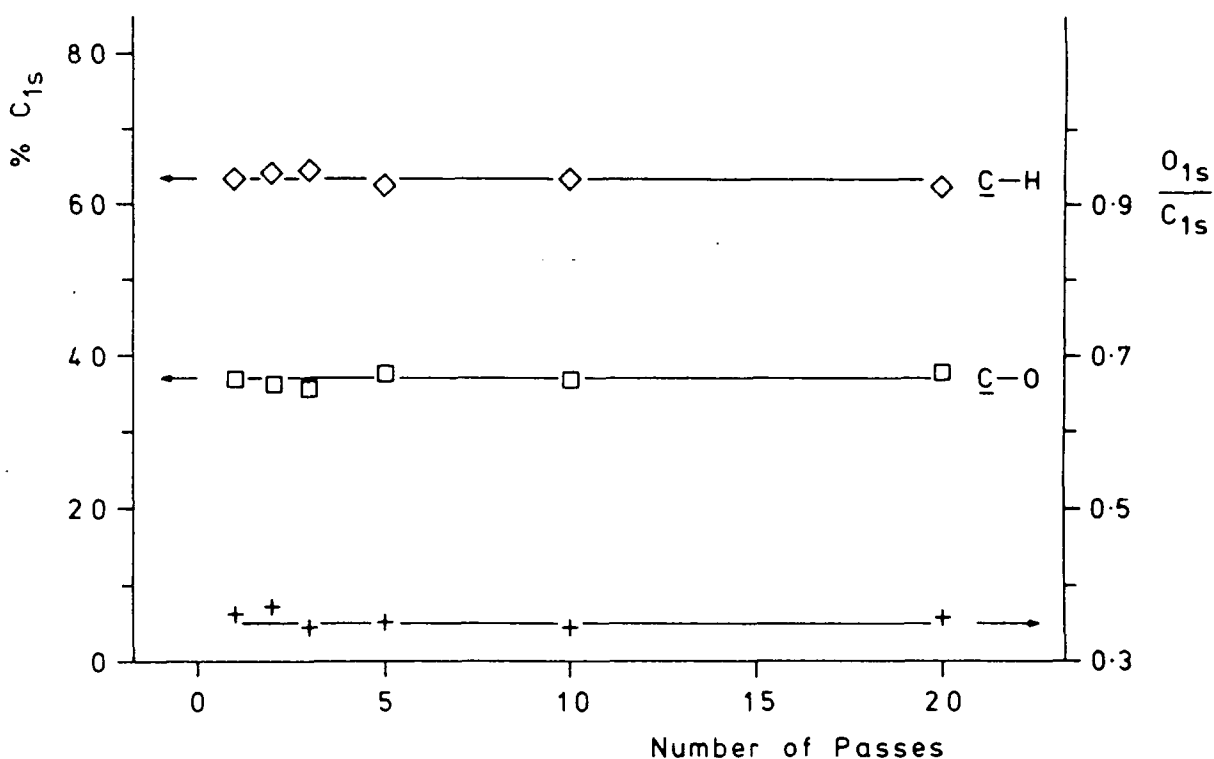


FIGURE 5.6 Effect of increasing Cure Exposure to Filtered Light in Air on the  $O_{1s}/C_{1s}$  Intensity Ratio and  $C_{1s}$  Component Intensities

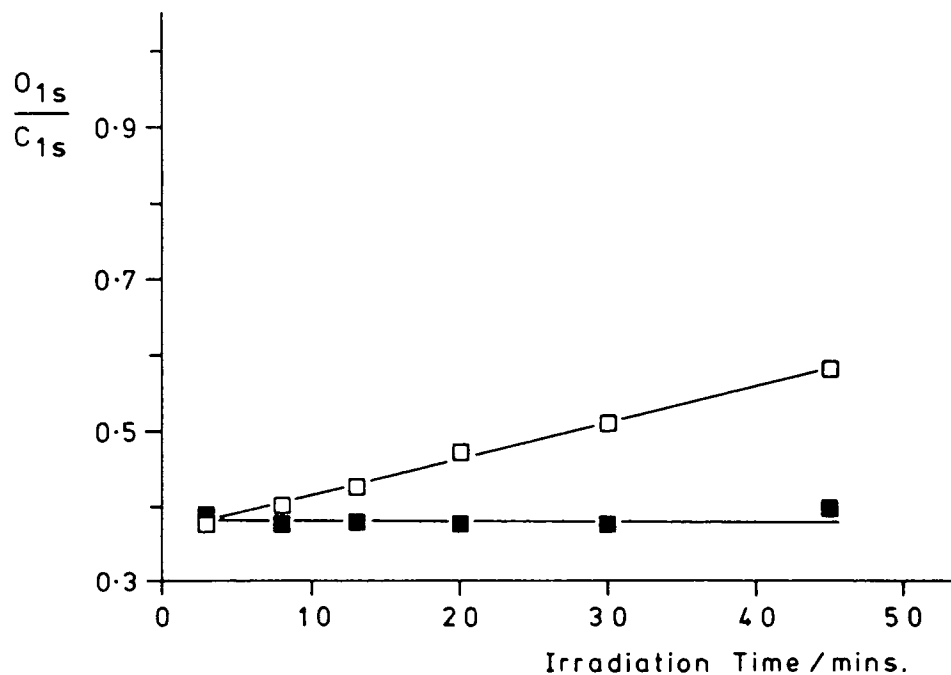
These radical species (even with oxygen present) must, therefore, have little or no bearing on the photo-oxidation of this resin.

(iii) Effect of Increased Cure Exposure to Unfiltered and Filtered Light using the 100W Source

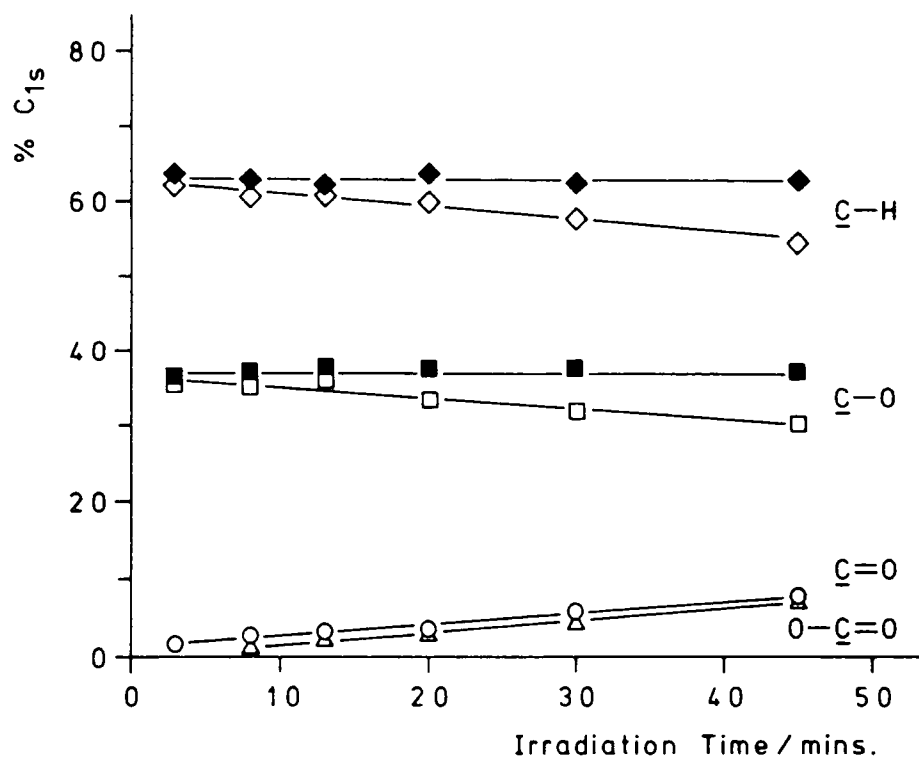
Although the filter absorbs all radiation below 275nm the possibility remains that its effectiveness in preventing surface photo-oxidation is related to a reduction in the number of photons reaching the films and not to the removal of shorter wavelength light. This experiment was carried out to eliminate the above possibility since irradiations using the 100W source can be carried out so that films irradiated with unfiltered and filtered light receive a similar light intensity.

Films were irradiated with and without the 'pyrex' filter in place as in previous experiments so that they received

FIGURE 5.7 Effect on the Surface Photo-oxidation of Increased Cure Exposure to Unfiltered (Open Symbols) and Filtered (Filled Symbols) Light using the 100W Source



(a)  $O_{1s}/C_{1s}$  Intensity Ratio



(b)  $C_{1s}$  Component Intensities

a photon flux of 17.4 and 17.6 mW cm<sup>-2</sup> respectively. Figures 5.7(a) and (b) indicate that photo-oxidation of the films irradiated without the 'pyrex' filter in place does occur and increases with increasing exposure. IR spectroscopy indicated that the normalized carbonyl absorbances at 1750 and 1710 cm<sup>-1</sup> were no greater than in the uncured lacquer and did not increase with increasing cure exposure. The results from the analysis of films irradiated with the 'pyrex' filter in place are also shown in Figures 5.7(a) and 5.7(b) and indicate that photo-oxidation is not occurring, supporting the conclusions reached in the previous section.

(B) Subsequent Photo-Oxidation of Cured Films on Prolonged Irradiation with Longer Wavelength UV Light ( $\lambda > 300\text{nm}$ )

(i) Effect of Increasing Cure Exposure

The following work was carried out to determine whether the surface photo-oxidation of films of the DGEBA resin during cure affects the subsequent photo-oxidative stability on prolonged exposure to longer wavelength UV light as is present in sunlight. A preliminary experiment was carried out, using films exhibiting the greatest degree of surface photo-oxidation to determine an optimum exposure time that would result in a degree of photo-oxidation detectable by IR spectroscopy yet not so long that films given different cure exposures would show the same degree of photo-oxidation detectable by both ESCA and IR spectroscopy.

Films of 100 $\mu\text{m}$  nominal thickness given 20 passes under the 1.8kW source were left in the dark for 24 hours and then irradiated using the fluorescent lamp. IR spectra of a free standing film were recorded at intervals and samples of another film taken for surface analysis. The table overleaf shows the ESCA results.

TABLE 5.2 Effect of Prolonged Irradiation ( $\lambda > 300\text{nm}$ ) on the Surface Composition of a Film given 20 Passes

Irradiation time/hrs.	% C <sub>1s</sub>					O <sub>1s</sub> /C <sub>1s</sub>
	C-H	C-O	C=O	O-C=O	$\pi \rightarrow \pi^*$	
0	51.0	27.8	11.4	9.8	1.2	0.704
96	45.7	26.9	10.3	16.1	1.0	0.889
142	47.1	24.1	10.7	17.0	1.1	0.879
504	46.6	25.1	9.3	17.8	1.1	0.771

Irradiation for 96 hours results in a marked decrease in the C-H component intensity, a slight decrease in the C-O and C=O component intensities with the  $\pi \rightarrow \pi^*$  component intensity remaining constant whilst the O-C=O component intensity and the O<sub>1s</sub>/C<sub>1s</sub> ratio increase significantly. Further irradiation results in only slight changes in the C<sub>1s</sub> component intensities but does lead to a decrease in the O<sub>1s</sub>/C<sub>1s</sub> ratio, possibly due to the evolution of CO<sub>2</sub>. Although quite heavily oxidized initially the surface of the film does undergo further oxidation.

The IR spectra recorded as a function of the irradiation time showed the growth of at least three overlapping peaks in the carbonyl absorption region. Two of the peaks corresponded to the absorbances seen at 1750 and 1710 cm<sup>-1</sup> in the spectra of uncured lacquers with a third absorption peak at a frequency between the other two absorbances. The species responsible for the absorbance at 1750 cm<sup>-1</sup> might again be ester or perester functional groups, the peak at intermediate frequency could be due to aldehyde functionality whilst that at 1710 cm<sup>-1</sup> could be due to either ketone or carboxylic acid functionality. It was also noted that the intensity of the -OH absorption at 3500 cm<sup>-1</sup> increased on irradiation. Figure 5.8 shows that the two absorbances at 1750 and 1710 cm<sup>-1</sup>, expressed as a ratio of the absorbance

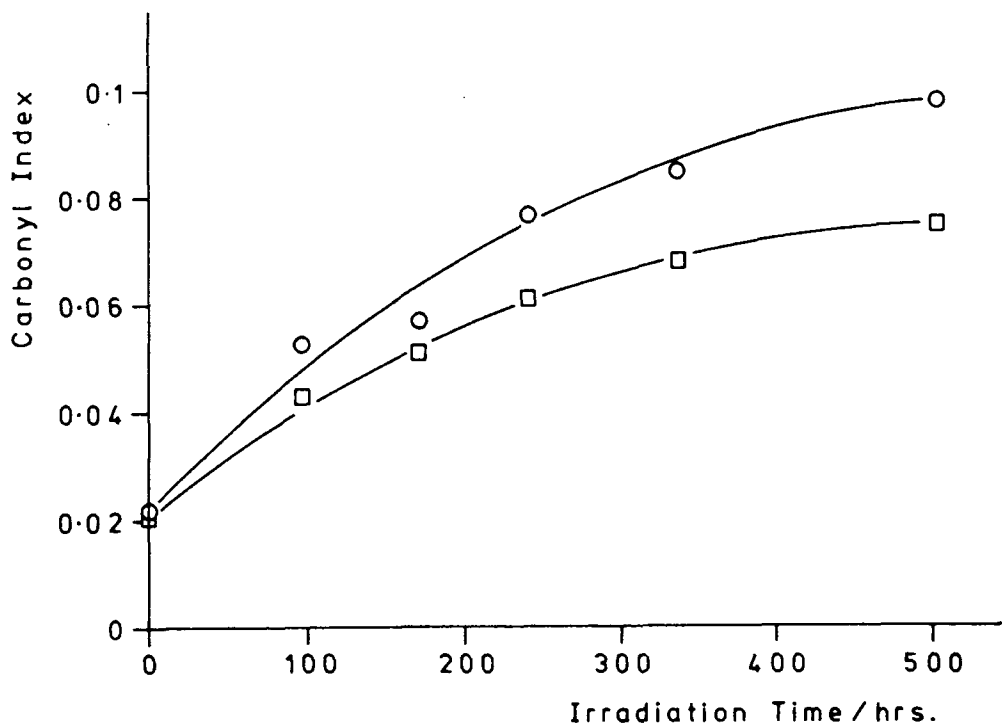


FIGURE 5.8 Growth of the Normalized Absorbances at 1750 (□) and 1710 cm<sup>-1</sup> (○) on Irradiation (λ > 300nm) of a Film Given 20 Passes

at 1605 cm<sup>-1</sup>, exhibit the trend of increasing towards a plateau value with increasing irradiation time.

It is apparent from Figure 5.8 that the growth of the carbonyl species does not exhibit autocatalytic behaviour. However, bulk photo-oxidation as detected by IR spectroscopy does occur on irradiation with longer wavelength light albeit to a relatively low level.

From the above data it was decided to irradiate films given increasing cure exposures for 192 hours with the fluorescent lamp, in the hope that differences in the surface and bulk photo-oxidation related to the initial surface photo-oxidation would become apparent. The IR spectroscopic analysis was carried out on films of 50µm thickness but otherwise in the same way as that above.

Figure 5.9 is the  $O_{1s}/C_{1s}$  ratio found in the surface of the cured films, after 192 hours' irradiation, as a function

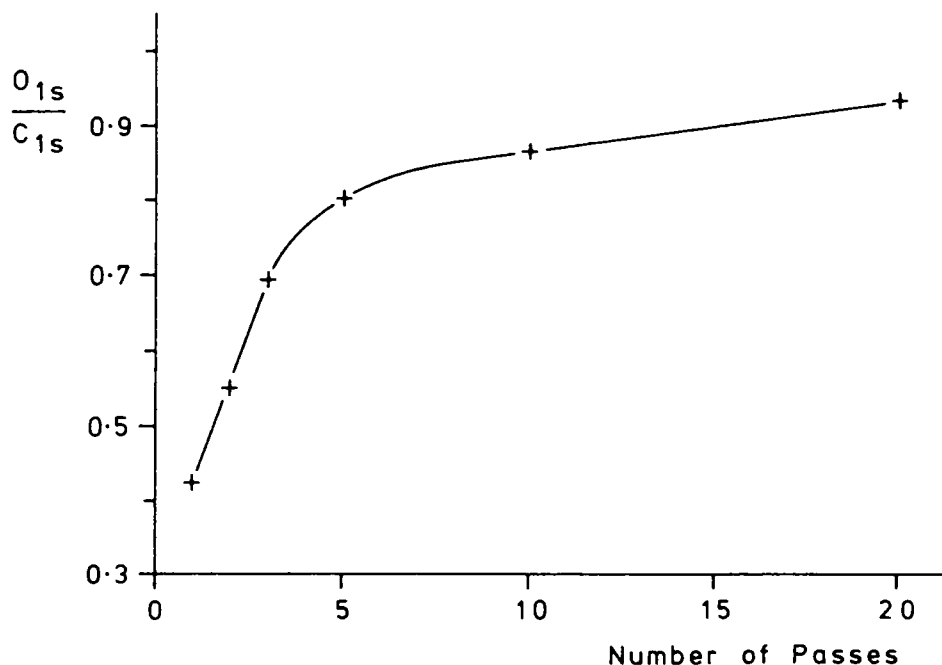


FIGURE 5.9  $\frac{O_{1s}}{C_{1s}}$  Intensity Ratio after 192 Hours Irradiation ( $\lambda > 300\text{nm}$ ) as a Function of the Initial Cure Exposure

of the initial cure exposure. This figure shows that the relative amount of oxygen present in the surface increases to a plateau value as the initial cure exposure and hence the initial surface oxidation increases.

Figure 5.10, in which the difference in  $\frac{O_{1s}}{C_{1s}}$  ratio is plotted against the initial cure exposure, indicates more clearly how the increase in the relative oxygen content due to the prolonged irradiation varies with the initial surface photo-oxidation. The increase in the  $\frac{O_{1s}}{C_{1s}}$  ratio becomes greater on going from 1 to 5 passes and then diminishes with further cure exposure. The film given 1 pass shows an increase in  $\frac{O_{1s}}{C_{1s}}$  ratio indicating that detectable amounts of carbonyl functionality after cure are not a prerequisite for subsequent photo-oxidation. In this case the chromophore responsible for initiating photo-oxidation could be due to an impurity or the aryl ether moiety of

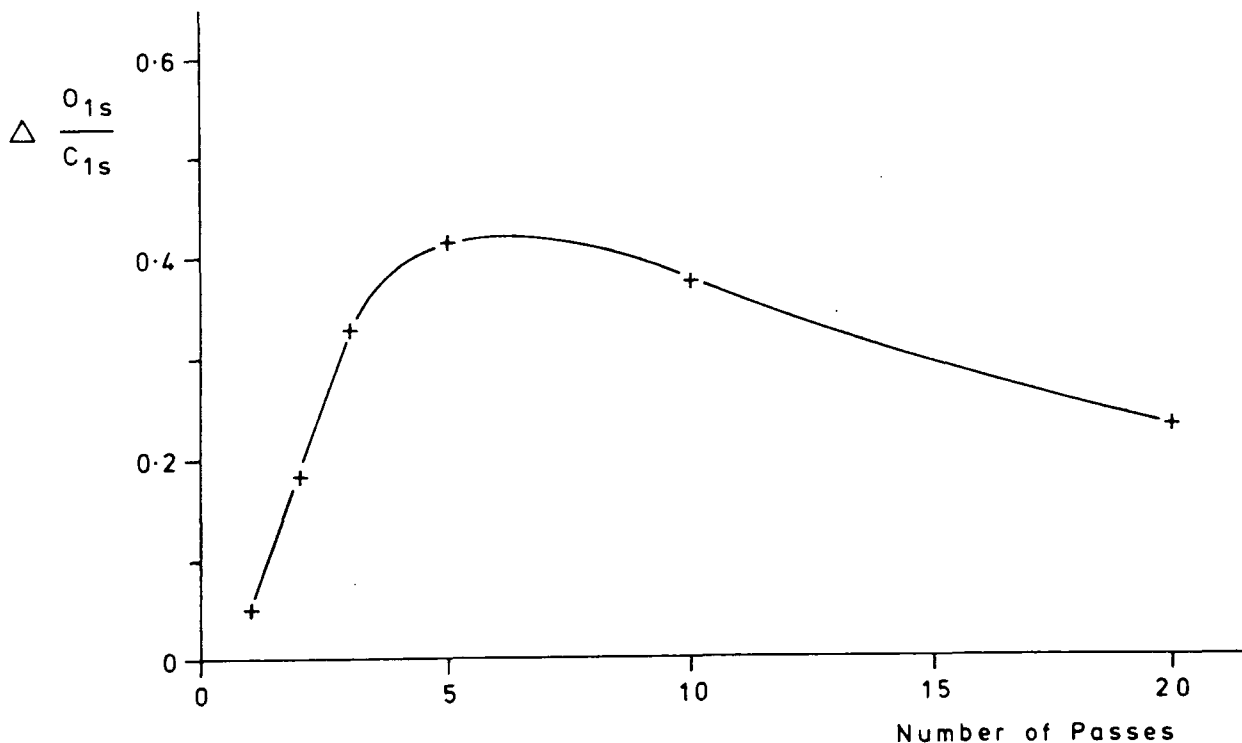


FIGURE 5.10 Change in the  $O_{1s}/C_{1s}$  Intensity Ratio resulting from 192 hours Irradiation ( $\lambda > 300\text{nm}$ ) as a Function of the Initial Cure Exposure

the resin. The oxygen uptake does, however, increase on going to 5 passes as does the relative amount of carbonyl and carboxylate functionality present initially as a result of the curing process, implying that this type of functionality photosensitizes or promotes in some other way further photo-oxidation. Since the surfaces of the films given 10 and 20 passes are quite heavily oxidized initially, it is not surprising that the magnitude of the increase in oxygen at the surface of these films is not as great as for some of the films given shorter cure exposures.

The  $C_{1s}$  component analysis of the films after 192 hours' irradiation shows that the  $\underline{C-H}$  and  $\underline{C-O}$  component intensities have decreased to plateau values whilst the  $\underline{C=O}$  and  $O-\underline{C=O}$  intensities increase to plateau values with increasing cure exposure as illustrated in Figure 5.11.

The change in the  $C_{1s}$  component intensities resulting from the prolonged irradiation are shown in Figure 5.12 as a

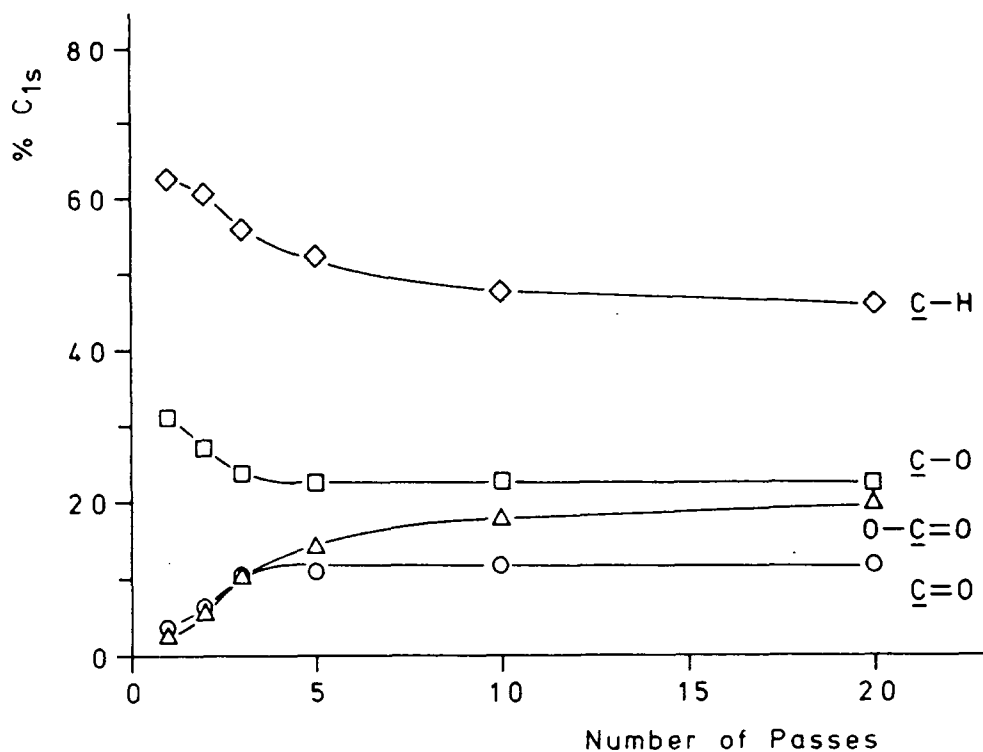


FIGURE 5.11  $C_{1s}$  Component Intensities after 192 Hours Irradiation ( $\lambda > 300\text{nm}$ ) as a Function of Initial Cure Exposure

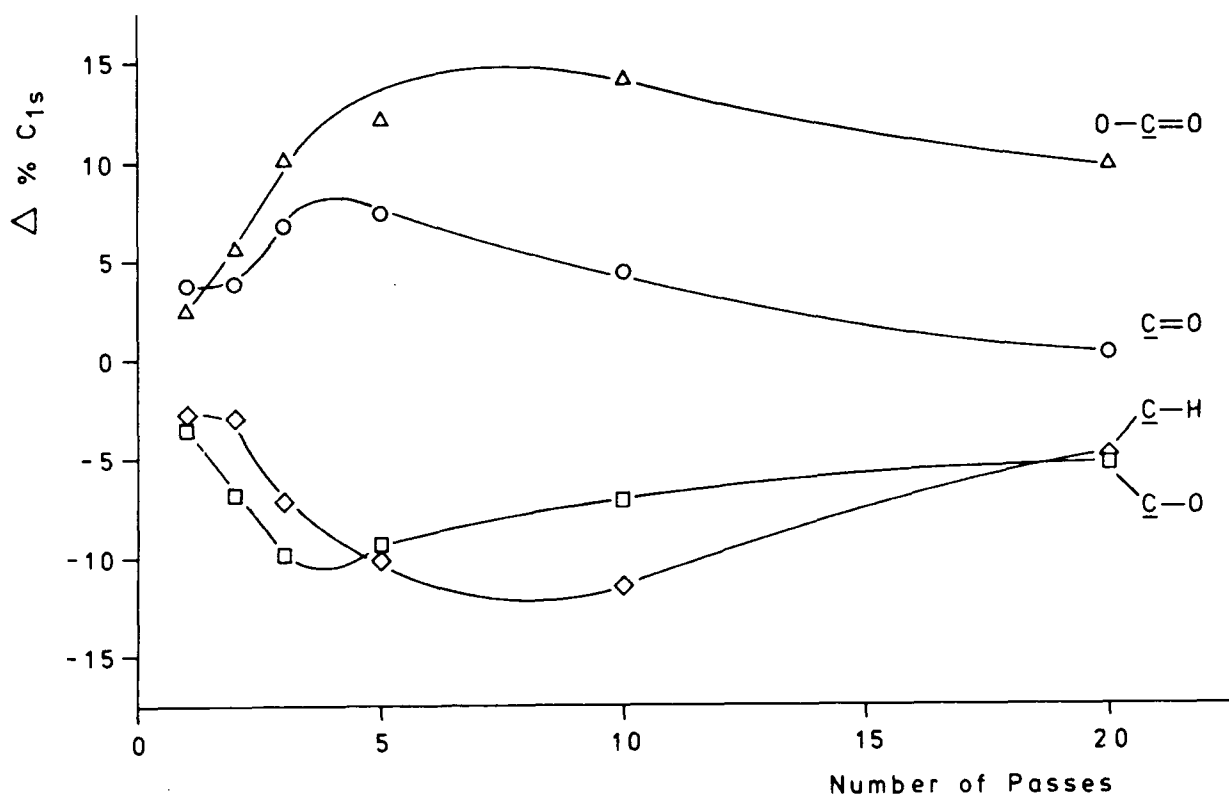


FIGURE 5.12 Changes in the  $C_{1s}$  Component Intensities Resulting from 192 Hours Irradiation ( $\lambda > 300\text{nm}$ ) as a Function of Initial Cure Exposure

function of the initial cure exposure. The overall change in surface composition increases on going from 1 to 5 passes and then diminishes although the maximum changes in the four components shown in Figure 5.12 occur at different cure exposures.

This figure also shows more clearly that as the initial surface photo-oxidation increases,  $O-\underline{C}=O$  formation predominates over  $\underline{C}=O$  formation on subsequent photo-oxidation. The intensities of the  $\pi \rightarrow \pi^*$  components are not shown in Figure 5.11 but are tabulated below as a function of the initial cure exposure.

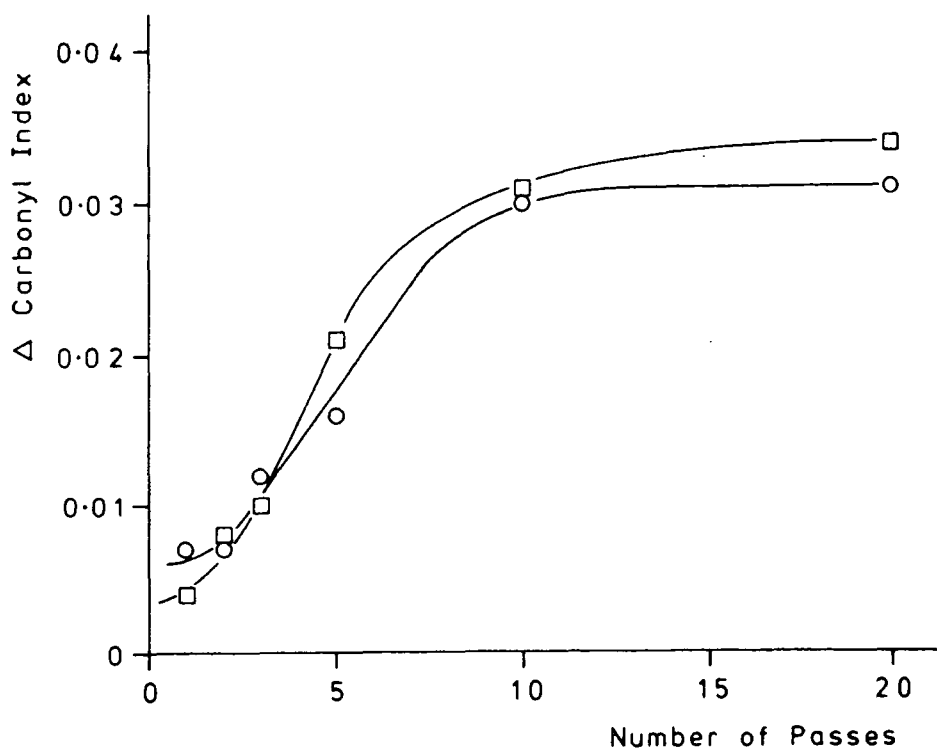
TABLE 5.3.  $\pi \rightarrow \pi^*$  Intensity after 192 Hours Irradiation ( $\lambda > 300\text{nm}$ ) as a Function of the Initial Cure Exposure

Number of passes	1	2	3	5	10	20
$\% C_{1s}$	1.4	1.4	1.6	1.2	1.1	1.0

From a comparison of the above values with those in Table 5.1 it appears that the  $\pi \rightarrow \pi^*$  intensity decreases in the films given 1 to 10 passes on prolonged irradiation implying that degradation of the aromatic moiety of the resin is occurring. No decrease in the  $\pi \rightarrow \pi^*$  intensity is observed in a film given 20 passes on prolonged irradiation. As the surface becomes heavily oxidized, carbonate,  $O-\overset{\text{O}}{\parallel}{\underline{C}}-O$ , formation may occur giving rise to a peak at a similar binding energy to the  $\pi \rightarrow \pi^*$  peak offsetting any decrease in this latter peak and hence accounting for the above observation. Whilst irradiating films for the above measurements other films were left in the dark as controls. These films showed no change in their  $C_{1s}$  component analysis or  $O_{1s}/C_{1s}$  ratio confirming that irradiation with the fluorescent lamp in the presence of air is responsible for the changes in surface oxidation.

The IR spectra of the films given increasing cure exposures recorded prior to prolonged irradiation showed the presence of the two absorptions in the  $1700\text{-}1750\text{ cm}^{-1}$  region. These two absorbances expressed as a ratio of the absorbance at  $1605\text{ cm}^{-1}$  were no greater than in the uncured lacquer nor did they increase with increasing cure exposure. After 192 hours irradiation with the longer wavelength UV light, the two normalized carbonyl absorbances had increased in all the films and Figure 5.13 shows that the magnitude of the increase becomes greater as the initial cure exposure and hence surface photo-oxidation increases, tending towards a plateau value.

FIGURE 5.13 Change in the Normalized Carbonyl Absorbances at  $1750\text{ (}\square\text{)}$  and  $1710\text{ cm}^{-1}\text{ (}\circ\text{)}$  after 192 hours Irradiation ( $\lambda > 300\text{nm}$ ) as a Function of Initial Cure Exposure



The experiment was repeated using similar films and the same trends were observed. Whilst the above films were being irradiated, other films were left in the dark. There were no significant changes in the two normalized absorbances although the one at  $1710\text{ cm}^{-1}$  did tend to decrease slightly possibly resulting from the loss of acetone. Thus the surface photo-oxidation resulting from the curing process does appear to have an effect on the subsequent photo-oxidative stability of both the surface and the bulk.

The level of photo-oxidation at the surface of the films after 192 hours' irradiation is highly unlikely to be representative of that in the bulk of the films. For example the ESCA data for the film given 1 pass indicates that ~6% of carbon atoms are associated with carbonyl functionality, equivalent to each resin molecule containing at least one carbonyl group which would be expected to give rise to an intense absorption in the infra-red spectrum. Taken in conjunction with the infra-red data this would indicate that the photo-oxidation does extend into the bulk but becomes attenuated with increasing depth. When irradiating the films of  $100\mu\text{m}$  thickness for surface analysis they were left on the polyethylene substrate. As the initial cure exposure increased it became progressively more difficult to remove the film from the substrate after the prolonged irradiation. Thus changes must have occurred at the substrate-film interface becoming more pronounced with increasing cure exposure. It is probable that the above observation arises from the photo-oxidative degradation of the films which suggests that as the initial surface photo-oxidation increases, the subsequent photo-oxidation progresses further into the bulk of the film to reach the substrate-film interface. If the photo-

oxidative degradation were to be limited to the upper regions of the film one would expect the normalized carbonyl absorptions to increase with decreasing film thickness as has been observed in a study of the photo-oxidation of conventionally cured epoxy resins reported in the literature,<sup>13</sup> although in this case the observation was attributed to unreacted amine curing agent present in greater amounts in the thicker films, acting as an antioxidant. Comparing the values of the normalized carbonyl absorption in the 50 $\mu\text{m}$  film given 20 passes in Figure 5.13 with that expected from Figure 5.8 for the 100 $\mu\text{m}$  film given 20 passes after 192 hours' irradiation shows that they are very similar. Since it appears that the photo-oxidation extends through the bulk of the films of 100 $\mu\text{m}$  given 20 passes, this will reduce the expected difference in the normalized carbonyl absorptions between the two films of different thickness. Other factors may further contribute to a reduction in the difference. For example the difference in film thickness may lead to differences in the characteristics of the cured films which, in turn, affects how the films photo-oxidize or alternatively the closeness of the samples to the source for the prolonged irradiations means that only a slight shift in the sample position (tenths of a millimetre) has a significant effect on the intensity of light incident on the sample.

If the products of photo-oxidative degradation were to absorb the wavelengths of light responsible for initiating the degradation then as the concentration of such products in the surface and sub-surface regions increases, and the results do indicate that the surface is richer in photo-oxidation products than the bulk both before and after prolonged irradiation, the depth of penetration of the damaging wavelengths of light into the film could become attenuated. This could explain

why the bulk photo-oxidation as indicated in Figure 5.8 tends towards a plateau value with increasing irradiation time and why the magnitude of the increase in bulk photo-oxidation tends towards a plateau value with increasing exposure on prolonged irradiation with longer wavelength light as in Figure 5.13. Alternatively, the above observations may be related to a lack of diffusion of oxygen into the films which could limit the occurrence of photo-oxidative degradation.

From the IR spectra of the films used in the above experiment, the effect of prolonged irradiation on the extent of reaction of epoxide functionality may be determined.

TABLE 5.4 Effect of the Prolonged Irradiation with Longer Wavelength UV Light on the Percentage Conversion of Epoxide Functionality

Conditions	Number of passes					
	1	2	3	5	10	20
0 hrs irradiation	88	88	90	89	89	91
192 hrs irradiation	92	92	92	91	89	92
0 hrs dark	90	88	89	88	91	89
192 hrs dark	90	89	90	90	91	91

The results shown in Table 5.4 indicate that a small but significant increase in the degree of conversion of epoxide functionality occurs in the films given the two lower cure exposures.

The Tg of films of 100 $\mu$ m thickness given increasing cure exposures were also measured after 192 hours' irradiation using TMA as described in Chapter Four. The values obtained are shown in Table 5.5 and indicate that there is a small increase in Tg compared with similar films left in the dark, even for the films given 10 and 20 passes which exhibited the greatest degree of bulk photo-oxidation and might be expected to show signs of chain scission if it were occurring. Any chain scission that

TABLE 5.5 Tg of Films Irradiated with Longer Wavelength UV Light

Number of passes	Tg of unirradiated film/°C	Tg of irradiated film/°C	Tg of irradiated film after heating/°C
1	55	58	68
3	66	70	93
10	72	74	112
20	76	78	114

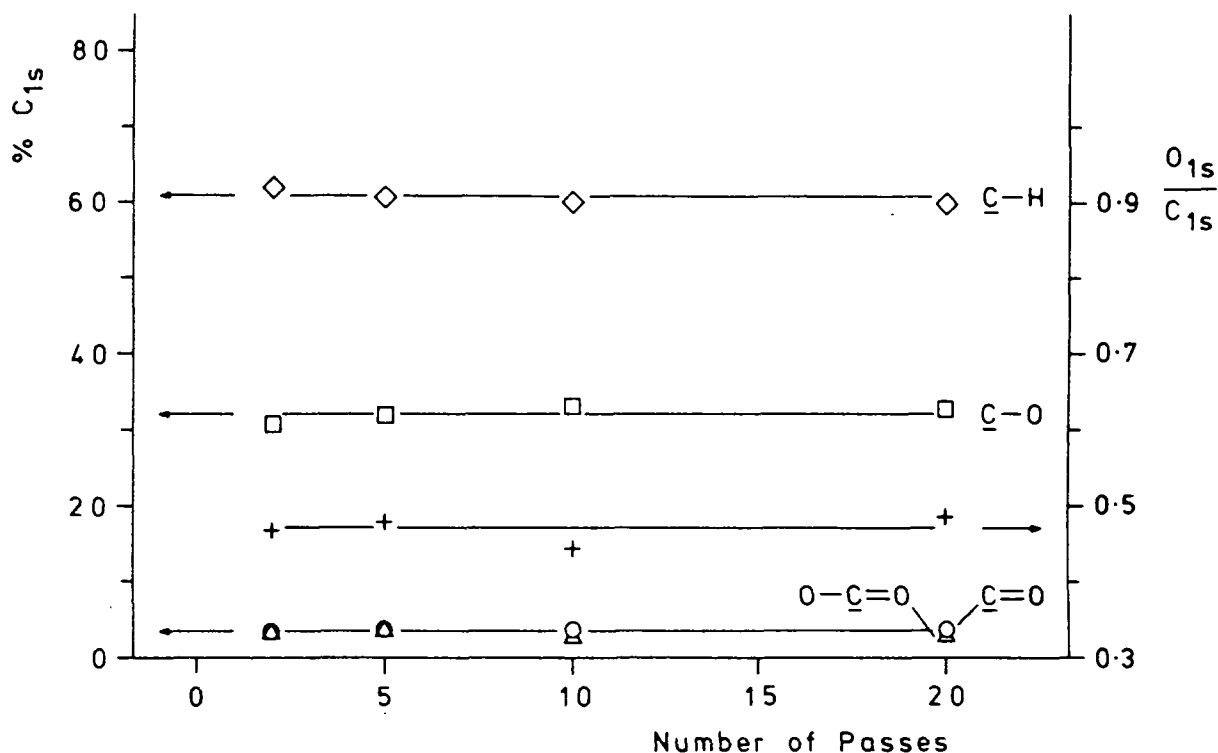
occurs must therefore be more than offset by an increase in the cross-link density possibly due to the photolysis of photo-initiator or to the temperature under the lamp accelerating the continued polymerization, which could also explain the increase in the extent of reaction of epoxide functionality. Also shown in Table 5.5 is the Tg value obtained when the measurement is repeated on the same sample. The increase in Tg shows that even after prolonged irradiation, the potential for further thermal cross-linking exists.

(ii) Effect of Increasing Cure Exposure to Filtered Light

Films given increasing cure exposures under the 1.8kW source with the "pyrex" filter in place were irradiated for 192 hours with the low intensity fluorescent lamp as in the above experiments.

Figure 5.14 shows the  $O_{1s}/C_{1s}$  ratio and the  $C_{1s}$  component intensities at the surface of the films, after irradiation, as a function of the initial cure exposure. The  $O_{1s}/C_{1s}$  ratio has increased compared with unirradiated films but remains constant with increasing cure exposure. The  $C_{1s}$  component analysis shows the presence of  $\underline{C}=\underline{O}$  and  $\underline{O}-\underline{C}=\underline{O}$  functionality with a concomitant decrease in the  $\underline{C}-\underline{H}$  and  $\underline{C}-\underline{O}$  component intensities compared with unirradiated films but the surface composition does not change

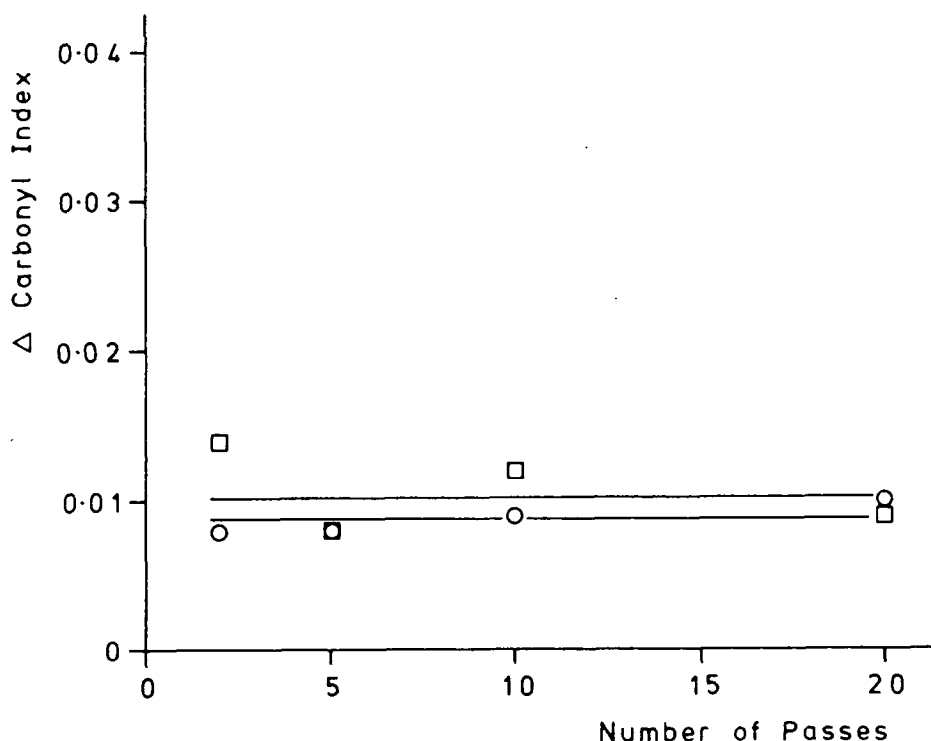
FIGURE 5.14  $O_{1s}/C_{1s}$  Intensity Ratio and  $C_{1s}$  Component Intensities after 192 Hours Irradiation ( $\lambda > 300\text{nm}$ ) as a Function of the Initial Cure Exposure to Filtered Light



significantly with increasing cure exposure. The degree of surface photo-oxidation in the above films is equivalent to that observed in a normally cured film given 2 passes. The intensity of the  $\pi \rightarrow \pi^*$  component not shown in Figure 5.14 was found to be constant at around 2%, similar to the intensity observed in un-irradiated films. The film given 1 pass cured using the full output of the lamp showed a decrease in the  $\pi \rightarrow \pi^*$  component intensity on prolonged irradiation implying that aromatic groups are degraded whereas the films cured with the filter in place show no loss of  $\pi \rightarrow \pi^*$  intensity although like the above film no photo-oxidation was apparent as a result of the curing process. It may be that the above observation results from the difference in cure conditions affecting the subsequent photo-oxidation or alternatively it may be a reflection of the

difficulty in accurately measuring the intensity of this quite small peak. These results confirm that the presence of carbonyl function as a result of the curing process is not a prerequisite for subsequent photo-oxidation to occur.

FIGURE 5.15 Change in the Normalized Carbonyl Absorbances at 1750 ( $\square$ ) and 1710  $\text{cm}^{-1}$  (O) after 192 hours Irradiation as a Function of the Initial Cure Exposure to Filtered Light



IR analysis of films after 192 hours irradiation indicated that the two normalized carbonyl absorbances had increased but the magnitude of the increase remains virtually constant with increasing cure exposure as illustrated in Figure 5.15. The increase in the absorbances is of the same level as that of a film given 3 passes under the full output of the 1.8kW lamp rather than that of a film given 1 pass which showed no surface photo-oxidation after cure. The greater than expected degree of surface and bulk photo-oxidation in the films cured with the

'pyrex' filter in place may be due to differences in the cure characteristics leading to differences in the photo-oxidative degradation or alternatively to the latter films receiving a higher intensity of light for the reasons discussed previously.

From the IR spectra recorded in the course of the above work the effect of the prolonged irradiation on the extent of reaction of the epoxide functionality of the films could be determined. The values in Table 5.6 indicate that excepting the film given 20 passes, there is a small increase in the conversion of epoxide functionality.

TABLE 5.6 Effect of the Prolonged Irradiation on the Percentage Conversion of Epoxide Functionality for Films cured with the Filter in Place

Conditions	Number of passes			
	2	5	10	20
0 hrs irradiation	92	90	89	90
192 hrs irradiation	95	94	92	90
0 hrs dark	89	91	88	87
192 hrs dark	91	91	90	86

-----

The effect of the prolonged exposure on the Tg of films of 100 $\mu$ m thickness was also investigated using TMA.

TABLE 5.7 Effect of the Prolonged Irradiation on the Tg of Films Cured with the Filter in Place

Number of passes	Tg of unirradiated film/ $^{\circ}$ C	Tg of irradiated film/ $^{\circ}$ C	Tg of irradiated film after heating/ $^{\circ}$ C
2	37,64	66	80
5	51,69	67	86
10	52,69	68	86
20	55,-	70	86

The values recorded in Table 5.7 indicate that all but one of the unirradiated films kept in the dark show two glass transitions whereas the irradiated films show only one transition; the temperature of which is quite close to that of the second glass transition observed in the unirradiated films. The above results imply that the prolonged irradiation leads to an increase in the cross-link density of the regions of low cross-link density present in the films given 2,5 and 10 passes to yield a more homogeneously cross-linked network whilst in the film given 20 passes, which appears to be quite homogeneously cross-linked initially, the prolonged irradiation results in a general increase of the cross-link density and hence  $T_g$ . Both the increased conversion of epoxide functionality and the changes in the  $T_g$  as a result of the prolonged exposure to longer wavelength UV light could be attributed to either the photolysis of residual photoinitiator or to the temperature under the lamp accelerating the continued polymerization that occurs after cure. Table 5.7 also shows that the  $T_g$  increases when the measurement is repeated indicating that the potential for thermal polymerization remains after prolonged irradiation.

### 5.7 Photo-Oxidation of the Diglycidyl Ether of Butanediol System

The previous work indicated that the DGEBA system underwent surface photo-oxidation during cure as a result of light absorption by the aryl ether moiety of the resin and that this had a deleterious effect on the subsequent photostability of the cured system. The aliphatic diglycidyl ether, (XX), does not possess an inherent chromophore capable of absorbing light above  $\sim 240\text{nm}$  emitted by the medium pressure mercury lamps and so would not be expected to undergo photo-oxidation during cure

by the direct absorption of light and might also prove to exhibit a greater degree of photostability on prolonged exposure to longer wavelength UV light.

The lacquers used in the following experiments contained 94.3% resin, 3.8% photoinitiator and 1.9% w/w acetone and 97.2% 1.9% photoinitiator and 0.9% w/w acetone or were close to these compositions. Films of 100 $\mu$ m nominal thickness were prepared for surface analysis whilst films of 50 $\mu$ m nominal thickness (actual thickness  $\sim$ 35 $\mu$ m measured using a micrometer gauge) were prepared for the IR analysis using the 'sellotape' technique, with polyethylene as the substrate. The films were cured using the 1.8kW source and prolonged irradiations were carried out as previously using the fluorescent lamp.

(A) Comments on the Cure of this System

Lacquers containing 3.8% photoinitiator were prepared so that the molar ratio of epoxide groups to photoinitiator was similar to the DGEBA lacquers. It was noted when preparing the lacquers that at least some of the photoinitiator did not dissolve in the resin but formed a fine suspension. One pass under the lamp was found to be insufficient to cure the films but 2 passes did result in the apparent through-cure of the films. The IR spectra recorded for the investigation of bulk photo-oxidation indicated that there was little unreacted epoxide functionality present in the cured films probably reflecting the higher mobility of this system. The above comments also apply to the lacquers containing 1.9% photoinitiator prepared and cured in the course of this work. In addition films containing 3.8% photoinitiator were irradiated with the 'pyrex' filter in place, requiring at least 15 passes under the lamp

before a satisfactory degree of cure was obtained. This, incidently, made it necessary to improve the wettability of the polyethylene substrate by oxidizing the surface using an oxygen plasma so that the film of uncured lacquer remained intact.

There are a number of possible explanations to account for the above observation of an induction period associated with the cure of this resin. It might be that the penetration of light into the interior of the films is seriously attenuated so that longer irradiation times are required to produce an adequate degree of photolysis of the photoinitiator and hence gelation. The results of calculations using the extinction coefficients of the resin and photoinitiator at wavelengths,  $\lambda$ , emitted by medium pressure mercury lamps and assuming that the scattering of light by undissolved photoinitiator is negligible are shown in Table 5.8.

TABLE 5.8 Depth of Penetration of Light into a Film of a Lacquer of the Aliphatic Diglycidyl Ether Resin Containing 3.8% or 1.9% w/w Photoinitiator

$\lambda$ /nm	Depth at which 50% of light is absorbed/ $\mu\text{m}$		Depth at which 90% of light is absorbed/ $\mu\text{m}$		Depth at which 99% of light is absorbed/ $\mu\text{m}$	
	1.9% photo-initiator	3.8% photo-initiator	1.9% photo-initiator	3.8% photo-initiator	1.9% photo-initiator	3.8% photo-initiator
313	1900	1200	6300	4100	12600	8100
303	1100	660	3600	2200	7200	4400
297	540	330	1800	1100	3600	2200
265	20	11	67	37	134	74
254	17	9	56	29	113	58
248	14	7	45	23	90	46

The values recorded in Table 5.8 indicate that longer wavelength UV light can pass through the films used in this work virtually without attenuation whilst, although shorter wavelength UV light

is absorbed more readily, it can still penetrate to a significant depth. Table 5.9 shows the percentage of incident light absorbed by the photoinitiator and resin at each wavelength for a given depth.

TABLE 5.9 Percentage of Total Light Absorption due to the Photoinitiator (3.8% and 1.9% w/w) and Resin

$\lambda/\text{nm}$	1.9% Photoinitiator		3.8% Photoinitiator	
	$\frac{I_{AP}}{I_A} \times 100$	$\frac{I_{AR}}{I_A} \times 100$	$\frac{I_{AP}}{I_A} \times 100$	$\frac{I_{AR}}{I_A} \times 100$
313	55	45	71	29
303	62	38	77	23
297	62	38	77	23
265	79	21	88	12
254	90	10	95	5
248	93	7	96	4

$I_A$  = Total intensity of light absorbed

$I_{AP}$  = Intensity of light absorbed by the photoinitiator

$I_{AR}$  = Intensity of light absorbed by the resin.

-----

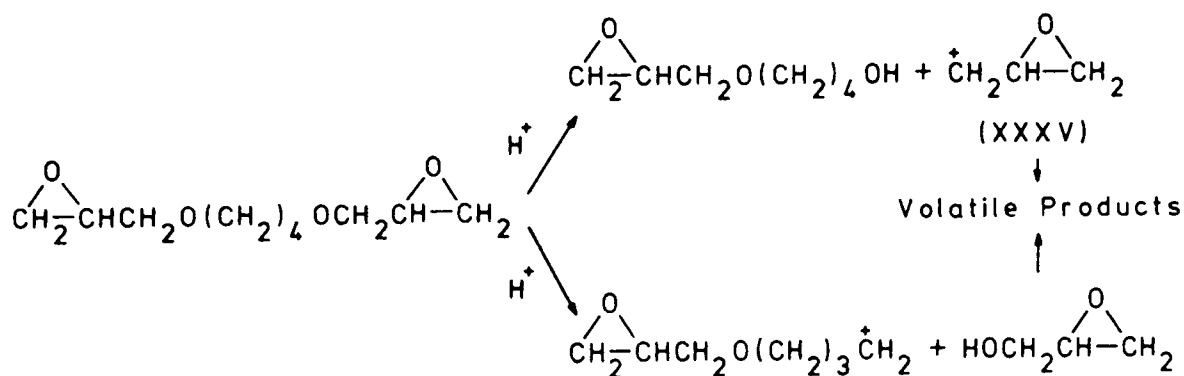
The fact that light is absorbed by the resin at wavelengths greater than 240nm is due to the presence of an impurity chromophore ( $\lambda_{\text{max}} = 276\text{nm}$ ). Comparison of the values in Tables 5.8 and 5.9 with those for the DGEBA system in Tables 4.1 and 4.2 shows that light of all wavelengths penetrates further into the films of the aliphatic resin and the percentage of light absorbed by the photoinitiator is much greater. Since the films of DGEBA lacquer cured satisfactorily, it is unlikely that the induction period associated with the cure of the above resin is related to the penetration of light into the interior of the films. In view of the effect of curing films of the above system with the 'pyrex' filter in place one might speculate that



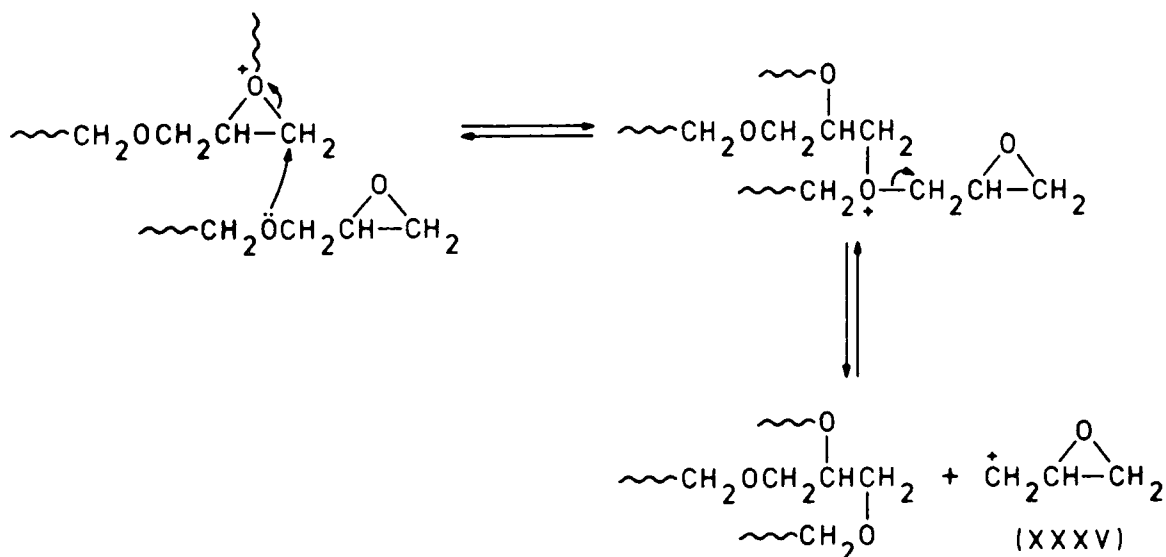
A similar reaction is likely to occur in the cure of the glycidyl ether used in this work, however one might expect that such a reaction would be more prevalent in the aliphatic diglycidyl ether resin since electron density on the aryl ether oxygen of the aryl glycidyl ethers will tend to be reduced through conjugation with the aromatic ring, represented by (XXXIV), therefore making the ether oxygen less basic:



If this type of reaction were to occur with greater ease in the aliphatic glycidyl ether then it could compete with the initiation of polymerization, having a greater chance of occurring prior to protonation of the oxirane oxygen thus giving rise to volatile species as shown below:



The photoinitiator is only present in small amounts and would not be expected to produce a significant amount of volatile product and the -OH absorption in cured films does not appear to be that much greater than in the uncured resin. However the following type of reaction could also give rise to volatile products.



Thus the above process could account for both the induction period and the evolution of a volatile species both of which are associated with the cure of this resin. An attempt was made to identify the volatile species responsible for the odour by using the 100W source to irradiate samples of the resin containing just photoinitiator in a quartz tube sealed with a rubber septum and withdrawing samples of the atmosphere above the cured resin for mass spectral analysis. The results were inconclusive although the mass spectra obtained did show species at 55, 56 and 57 mass units which could result from products formed *via* the cationic species (XXXV), there were also other peaks at higher mass units so that the peaks at lower mass units could be due to the fragmentation of higher molecular weight species.

During the course of the work it was also noted that films given 20 passes were pale yellow. UV spectra of films containing 3.8% photoinitiator given 2 and 20 passes indicated that the latter film possessed a weak absorption band at  $\sim 360\text{nm}$

tailing into the visible region of the spectrum. The UV spectrum of a film containing 1.9% photoinitiator given 20 passes however did not show this absorption band although the yellow colour was still apparent. The lack of the absorption band in the latter film might indicate that the concentration of the species responsible for the colouration is very low in this case which implies that the formation of the coloured species may be related to the concentration of photoinitiator used. The film containing 3.8% photoinitiator given 20 passes with the 'pyrex' filter in place did not show this colouration which may indicate that its occurrence is also wavelength dependent.

(B) Photo-Oxidation as a Result of the Curing Process

Films containing 3.8% photoinitiator were given an increasing number of passes and analysed using ESCA, 24 hours after cure. Figure 5.16 is the  $C_{1s}$  spectra of a film given 5 passes and

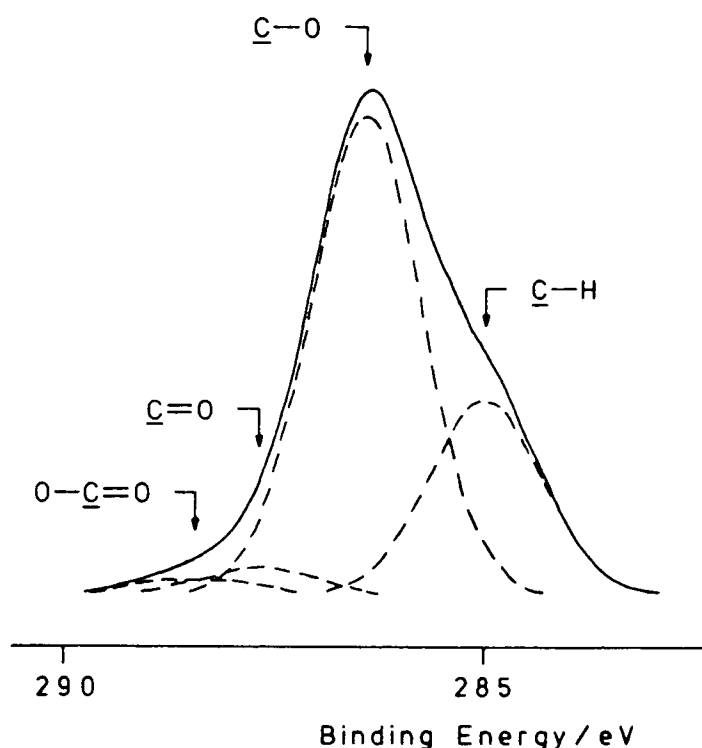


FIGURE 5.16  $C_{1s}$  Core Level Spectrum of a Film of the Aliphatic Diglycidyl Ether System containing 3.8% Photoinitiator

illustrates the form of the spectra obtained. Peak fitting showed the presence of four peaks in this and the other spectra recorded. Relative to the  $\underline{\text{C}}\text{-H}$  peak at 285 eV, the other peaks occur at binding energies of  $286.5 \pm 0.1$ ,  $287.8 \pm 0.1$  and  $288.7 \pm 0.2$  eV and are attributable to  $\underline{\text{C}}\text{-O}$ ,  $\underline{\text{C}}\text{=O}$  and  $\text{O-}\underline{\text{C}}\text{=O}$  functionality respectively, although in the latter case the binding energy of the peak is a little low.

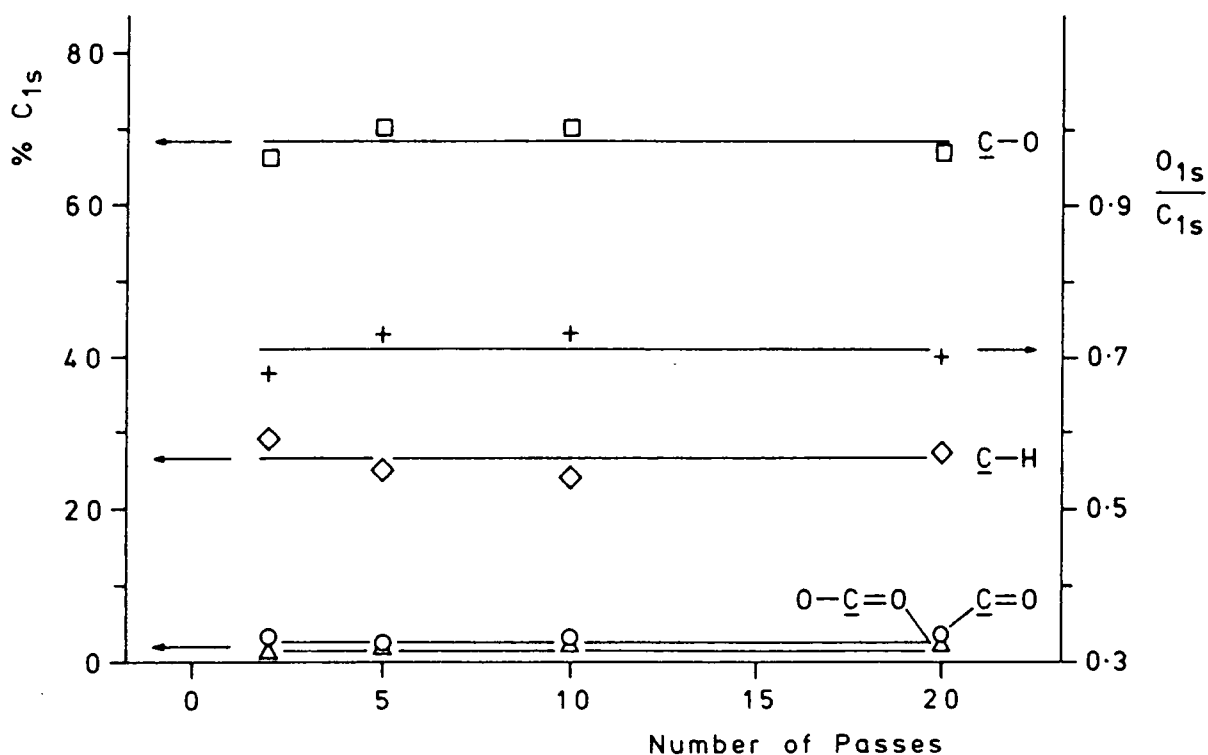


FIGURE 5.17  $\text{O}_{1s}/\text{C}_{1s}$  Intensity Ratio and  $\text{C}_{1s}$  Component Intensities as a Function of Cure Exposure for Films of the Aliphatic Diglycidyl Ether System containing 3.8% w/w Photoinitiator

The two most striking features of Figure 5.17 which is a combined plot of the  $\text{O}_{1s}/\text{C}_{1s}$  ratio and  $\text{C}_{1s}$  component intensities against cure exposure are the presence of carbonyl and carboxylate functionality and the virtual constancy of both the  $\text{O}_{1s}/\text{C}_{1s}$  ratio and the component intensities as the cure exposure increases. The underneath of a film given 5 passes was found to be of similar composition to the surface including the presence of oxidized species.

TABLE 5.10 Comparison of the Expected and the Experimentally Measured Surface Composition of Films Containing 3.8% Photoinitiator

	% C <sub>1s</sub>				$\frac{O_{1s}}{C_{1s}}$
	<u>C</u> -H	<u>C</u> -O	<u>C</u> =O	O- <u>C</u> =O	C <sub>1s</sub>
Average surface composition of the films	25.8±1.3	69.1±1.7	2.9±0.5	2.2±0.2	0.757±0.015
A. Expected surface composition	22.3	76.6	0.7	—	0.696
B. Expected surface composition	23.3	75.6	0.7	—	0.702

A. = 94.3% resin, 3.8% photoinitiator and 1.9% w/w acetone.

B. = as A, but with resin containing 12 mole % monoglycidyl impurity.

-----

Table 5.10 shows a comparison of the average surface composition from Figure 5.17 with that expected from a lacquer of pure resin and one with resin containing monoglycidyl ether impurity.

In spite of the occurrence of oxidation which might involve reaction of hydrocarbon functionality, the C-H component intensity is significantly greater than that expected whilst the C-O component intensity is significantly lower than that expected although the formation of oxidized species will account at least in part for some of the decrease. The C=O component intensity is significantly greater than the expected intensity which would, if acetone were to be present in the surface, probably be below the limits of detection whereas the O-C=O functionality is totally unexpected. Also it appears that the  $O_{1s}/C_{1s}$  ratio is slightly greater than expected.

To determine whether contamination from the 'sellotape' used in the preparation of the above films was occurring, a film was cured in the bottom of a glass petri dish, being given 5 passes under the lamp. Both the top and bottom surfaces of

this film were found to be of similar composition to those above. The effect of acetone on the surface composition was also investigated by curing a film containing 96% resin and 4% photoinitiator. Again the surface of this film given 5 passes under the lamp was found to be of similar composition to those above.

Films containing 1.9% photoinitiator were also prepared and analysed as above, to determine whether the concentration of photoinitiator had any effect on the surface oxidation.

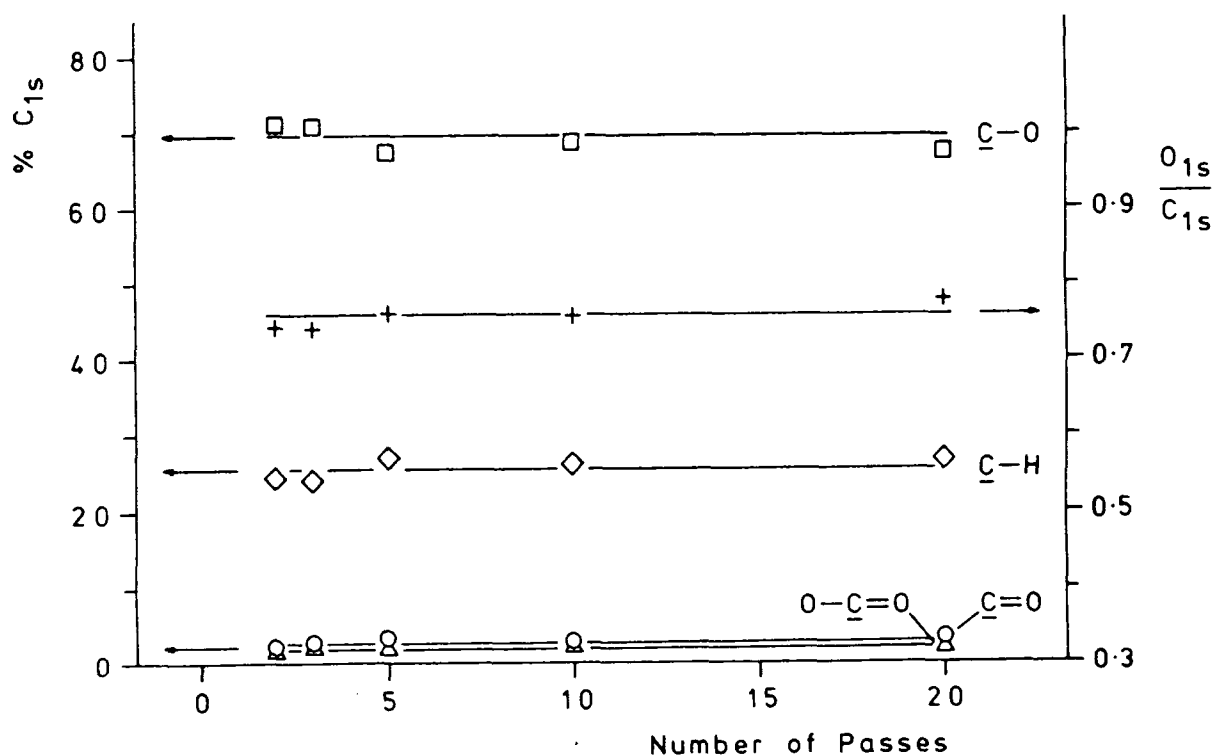


FIGURE 5.18  $O_{1s}/C_{1s}$  Intensity Ratio and  $C_{1s}$  Component Intensities as a Function of Cure Exposure for Films of the Aliphatic Diglycidyl Ether System Containing 1.9% w/w Photoinitiator

Figure 5.18 indicates that  $C_{1s}$  component intensities are quite similar to those for the films containing 3.8% photoinitiator, although the  $O_{1s}/C_{1s}$  ratio is a little lower, and like the films examined previously both the  $C_{1s}$  component intensities and  $O_{1s}/C_{1s}$  ratio remain virtually constant with increasing cure exposure. The bottom surface of the film given 5 passes under

the lamp showed a similar composition to that of the top surface. Table 5.11 shows that the disparity between the expected  $\underline{\text{C}}\text{-H}$  and  $\underline{\text{C}}\text{-O}$  component intensities and the average value from Figure 5.18 is greater than for the films containing 3.8% photoinitiator, mainly by virtue of changes in the expected intensities, whereas the  $\text{O}_{1s}/\text{C}_{1s}$  ratio is quite close to that expected. The results suggest that the concentration of photoinitiator has virtually no effect on the surface composition and oxidation.

TABLE 5.11 Comparison of the Expected and the Experimentally Measured Surface Composition of Films Containing 1.9% Photoinitiator

	% $\text{C}_{1s}$				$\frac{\text{O}_{1s}}{\text{C}_{1s}}$
	$\underline{\text{C}}\text{-H}$	$\underline{\text{C}}\text{-O}$	$\underline{\text{C}}\text{=O}$	$\text{O-}\underline{\text{C}}\text{=O}$	
Average surface composition of the films	26.5±2.0	68.4±2.1	3.2±0.4	1.9±0.4	0.710±0.026
A. Expected surface composition	21.1	78.3	0.3	-	0.705
B. Expected surface composition	21.3	77.7	0.3	-	0.714

A. = 97.2% resin, 3.9% photoinitiator and 1.9% acetone

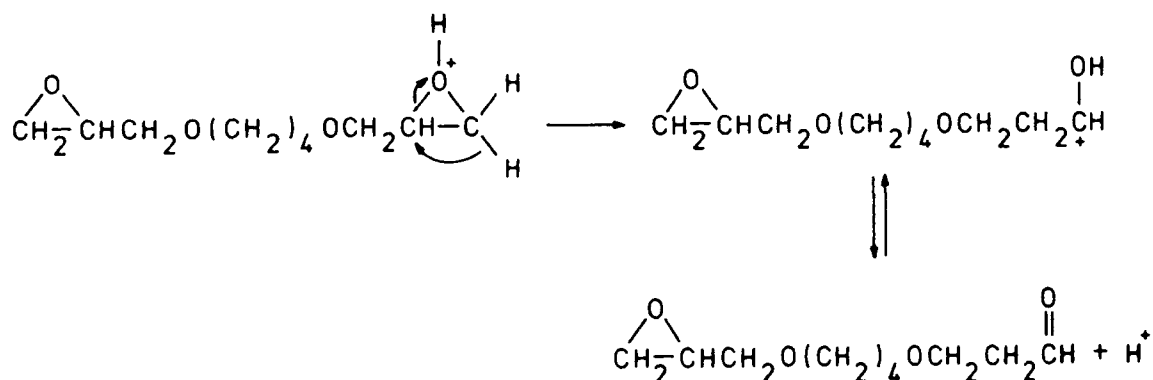
B = as A but with resin containing 12 mole% monoglycidyl impurity.

-----

The observation that the bottom surface of films appears to exhibit oxidative degradation is not surprising in view of the ease of penetration of light into the films of this system but this would imply that the bulk is also undergoing oxidation. From the ESCA data ~5% of carbon atoms at the two surfaces are associated with carbonyl or carboxylate functionality indicating that roughly one in two resin molecules contain such a functional group. On this basis one would expect a quite intense absorption in the carbonyl region of the IR spectra of cured films. Although the IR spectra of cured films do show an absorption at

1725  $\text{cm}^{-1}$ , which is attributable to aldehyde functionality, it is quite weak and also occurs in the spectrum of the uncured resin. Expressing this absorption as a ratio of one at  $1450\text{cm}^{-1}$  shows it is only slightly, if at all greater, in the cured films and it does not show any significant change with increasing cure exposure. Thus the fact that the top and bottom surfaces of a film apparently undergo photo-oxidation yet the bulk does not or at least only at a much slower rate, is somewhat paradoxical and difficult to rationalize.

Cleavage of the ether bond of the resin as described previously would account for the difference of the  $\underline{\text{C}}\text{-H}$  and  $\underline{\text{C}}\text{-O}$  component intensities in the surfaces from those expected. It is unlikely that the light absorption characteristics of the products generated by such a process would be vastly different to those of the pure resin, therefore the initiation of photo-oxidation would require an impurity chromophore. A more speculative explanation for the higher  $\underline{\text{C}}\text{-H}$  and lower  $\underline{\text{C}}\text{-O}$  component intensities that also accounts in part for carbonyl formation involves the acid catalysed rearrangement of the oxirane rings to give aldehyde groups:



The occurrence of this type of reaction catalysed by Lewis acids is quite well documented for aliphatic and cycloaliphatic epoxides with various substituents around the oxirane ring.<sup>20</sup> The formation of the aldehyde functionality may promote photo-oxidation leading to the production of carboxylate groups.

However if such a process were to be occurring, it is difficult to understand why it is limited to the film-substrate and film-air interfaces. Segregation of some impurity to the two interfaces might not only account for the increase in the  $\underline{C}$ -H and the decrease in the  $\underline{C}$ -O component intensities compared with those expected but also the limitation of photo-oxidation to the top and bottom surfaces. As to the nature of the impurity, it is suspected that the resin contains an aromatic impurity whilst IR spectroscopy has shown the presence of a carbonyl containing impurity. As indicated in Appendix Two the segregation of photoinitiator to the two interfaces is unlikely to be taking place. If the impurity were segregating and either underwent photo-oxidation giving rise to carboxylate and carbonyl functionality or photosensitized the photo-oxidation of the resin then one might expect the photo-oxidation to occur at a faster rate in the surfaces where the concentration of the impurity is greater. The above process could also occur in conjunction with the cleavage of ether links to give rise to the observed surface composition.

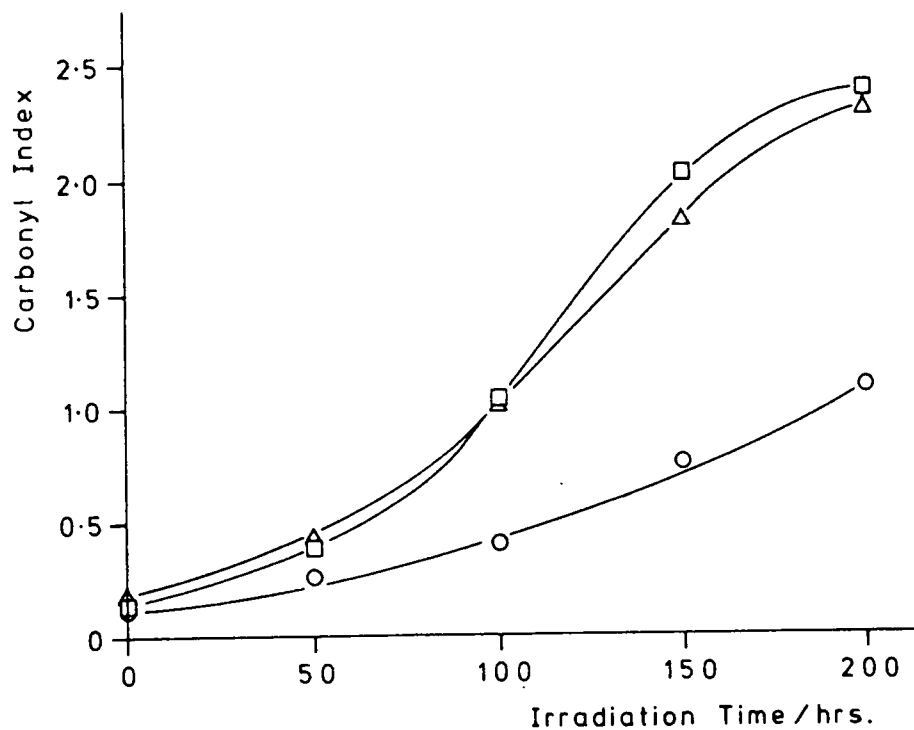
One further feature of the results is the lack of any increase in the degree of oxidation with increasing cure exposure as one might expect. The ESCA data implies that the level of oxidation at the surface is equivalent to roughly one in every two resin molecules containing a carbonyl group so it is unlikely that the maximum level has been reached. If photo-oxidation of an impurity were taking place then the degree of photo-oxidation might represent the maximum degree of degradation of the impurity. Alternatively if the resin is undergoing photo-oxidation then a stationary state may be rapidly attained in which the rate of formation of oxidized species is matched by the rate of loss of such species due to chain scission

and the evolution of volatile species. This effect may be more prevalent in the aliphatic diglycidyl ether system rather than the DGEBA system due to the greater proportion of ether links in the former system.

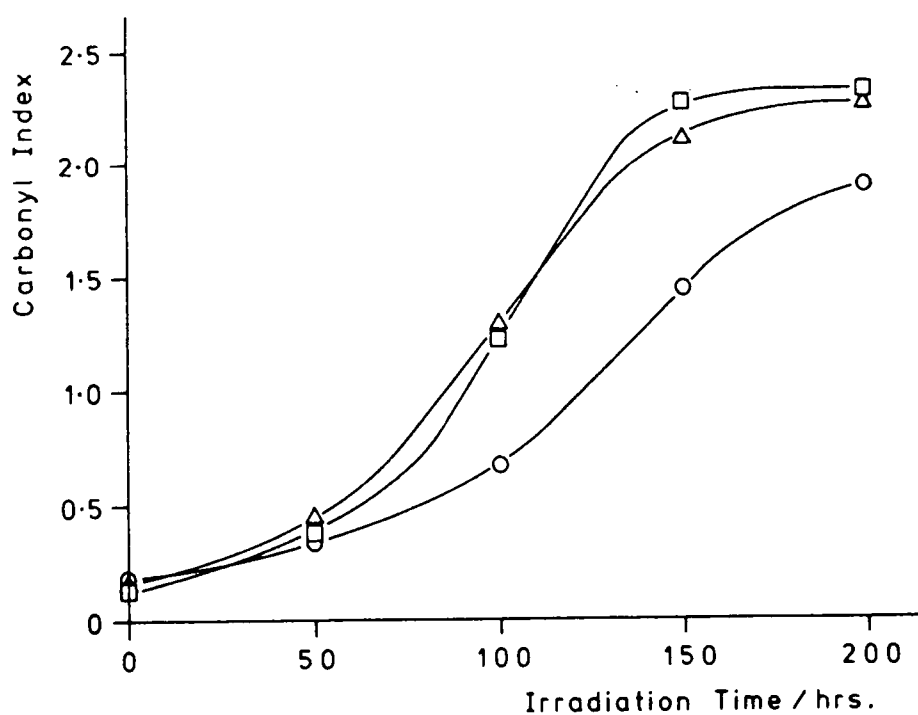
(C) Subsequent Photo-Oxidation of Cured Films on Irradiation with Longer Wavelength UV Light ( $\lambda > 300\text{nm}$ )

Films containing 3.8% photoinitiator were given 2 and 5 passes under the 1.8kW lamp, left for 24 hours and then irradiated using the fluorescent lamp. After 192 hours' irradiation, the films were found to have tacky surfaces which is indicative of chain scission and in addition the infra-red spectra of the films showed that the carbonyl absorption at  $1725\text{ cm}^{-1}$  present in the spectra recorded prior to irradiation had increased greatly. There was also some increase in the -OH absorption at  $3460\text{ cm}^{-1}$ . The irradiations were repeated using films given 2, 5 and 20 passes and IR spectra recorded as a function of the irradiation time. Figure 5.19(a) is a plot of the carbonyl absorbance at  $1725\text{ cm}^{-1}$  expressed as a ratio of that at  $1450\text{ cm}^{-1}$  against irradiation time showing that the increase of the carbonyl species exhibits a typical sigmoidal curve indicative of an autocatalytic process. The growth of carbonyl species in the film given 20 passes occurs at a slower rate and the induction period is longer than for the films given shorter cure exposures. Films containing 1.9% photoinitiator given 2, 5 and 20 passes were irradiated as in the above experiment. Like the previous films, there was no indication of yellowing as a result of the prolonged exposure in the films given 2 and 5 passes whilst that given 20 passes showed no noticeable increase in the intensity of its colouration. As indicated in Figure 5.19 (b) the growth of the

FIGURE 5.19 Growth of the Normalized Carbonyl Absorption at  $1725\text{ cm}^{-1}$  in Films of the Aliphatic Diglycidyl Ether on Prolonged Irradiation ( $\lambda > 300\text{nm}$ ) as a Function of Initial Cure Exposure ( $\Delta$ , 2;  $\square$ , 5;  $\circ$ , 20 Passes)



(a) Films Containing 3.8% Photoinitiator



(b) Films Containing 1.9% Photoinitiator

carbonyl species in these films exhibits similar trends to those observed in the films cured with a higher photoinitiator concentration although the induction period is shorter and the rate of carbonyl formation greater, especially in the film given 20 passes. Inhibition of the photo-oxidation process by reaction of the species responsible for the yellow colour and in the case of the film containing 3.8% photoinitiator, the absorption of light responsible for initiating the process by this species might account for the increased photostability of the films given 20 passes. Alternatively this may be a consequence of a difference in the characteristics of the cross-linked network resulting from the increased cure exposure. The apparent decrease in the photostability of films containing the lower concentration of photoinitiator, especially the one given 20 passes is also consistent with the above explanations since it is suspected that the concentration of the coloured species is reduced in this film and the use of a lower concentration of photoinitiator may result in a change in the characteristics of the cross-linked network. In addition it might possibly be that the two sets of films received different light intensities.

Films containing both amounts of photoinitiator given 2 and 20 passes were irradiated as above for 50 hours and then ESCA used to determine whether the surface had undergone any further photo-oxidation.

Figures 5.19(a) and (b) show that the carbonyl functionality present in the bulk has increased slightly after 50 hours irradiation so it would seem reasonable to expect that the surface photo-oxidation would show a more marked change. However comparison of the results in Table 5.12 with the average surface composition of films after cure in Tables 5.10 and 5.11 indicates that the surface composition and  $O_{1s}/C_{1s}$  ratio have changed

TABLE 5.12 ESCA Data from Films of the Aliphatic Resin System Irradiated for 50 Hours with the Fluorescent Lamp

% Photo-initiator	Number of passes	% C <sub>1s</sub>				$\frac{O_{1s}}{C_{1s}}$
		C-H	C-O	C=O	O-C=O	
1.9	2	24.6	70.1	3.2	2.1	0.75
	20	24.9	68.4	3.5	3.2	0.78
3.8	2	24.6	70.0	3.2	2.2	0.76
	20	25.8	68.9	3.2	2.1	0.76

very little if at all after 50 hours irradiation. The explanations put forward for the constancy of the surface photo-oxidation with increasing cure exposure also apply to the above observation.

Comparison of Figures 5.19 (a) and (b) with the similar plot for the film of the DGEBA system given 20 passes in Figure 5.8 shows the photostability of the cured aliphatic resin to be much less than that of the aromatic resin. In addition the photo-oxidation of the aliphatic system exhibits autocatalytic behaviour whereas the aromatic system does not. This implies that the rate of initiation is slower and the kinetic chain length of the branching steps is longer in the aliphatic system. The bulk photo-oxidation of the aliphatic system progresses to quite a high degree whilst that of the DGEBA system is limited to a relatively low level. The latter observation is attributed to the attenuation of light penetrating the film by the heavily oxidized surface regions or to a very slow rate of oxygen diffusion into the film. In the case of the aliphatic system, the surface photo-oxidation does not appear to reach a high level so that the penetration of light into the film might be less restricted and also the diffusion of oxygen into the films may

take place more readily thus facilitating the occurrence of bulk photo-oxidation.

REFERENCES - CHAPTER FIVE

1. D. Briggs and M.P. Seah, Eds., "Practical Surface Analysis by Auger and X-Ray Photoelectron Spectroscopy" , J. Wiley (1983).
2. D.T. Clark in "Polymer Surface", Eds., D.T. Clark and W.J. Feast, Wiley-Interscience (1978).
3. B. Ranby and J.F. Rabek "Photodegradation, Photo-Oxidation and Photostabilization of Polymers", Wiley-Interscience (1975)
4. D.M. Wiles and D.J. Carlsson in "New Trends in the Photo-Chemistry of Polymers", Eds. N.S. Allen and J.F. Rabek, Elsevier Applied Science Publishers (1985).
5. N.A. Weir in Reference 4.
6. N.S. Allen in Reference 4.
7. N.S. Allen, P.J. Robinson, N.J. White and G.G. Skelhorne, Eur.Polym.J., 20, 13 (1984).
8. A. Hult, Y.Y. Yuan and B. Ranby, Polymer Degradation and Stability, 8, 241 (1984).
9. J.F. McKellar and N.S. Allen, "Photochemistry of Man-Made Polymers", Applied Science Publishers, London (1974).
10. N.S. Allen, J.P. Binkley, B.J. Parsons, G.O. Phillips and N.H. Tennent, Polym.Photochem., 2, 97 (1982).
11. G.A. George, R.E. Sacher and J.F. Sprouse, J.Appl.Polym. Sci., 8, 2241 (1977).
12. V. Bellenger, C. Bouchard, P. Claveirolle and J. Verdu, Polym.Photochem., 1, 69 (1981).
13. V. Bellenger and J. Verdu, Polym.Photochem., 5, 295 (1984).
14. S.C. Lin, B.J. Bulkin and E.M. Pearce, J.Polym.Sci., Polym. Chem. Ed., 17, 3121 (1974).
15. H-J. Tempe and C. Garcia, Polym.Photochem., 6, 41 (1985).
16. D.T. Clark and H.R. Thomas, J.Polym.Sci., Polym.Chem.Ed. 14, 1671 (1974).
17. D.T. Clark and A. Dilks, J.Polym.Sci., Polym.Chem. Ed., 14, 533 (1976).
18. H.S. Munro and D.T. Clark, Polym.Deg.and Stab., 11,211 (1985).

19. J. Berger and F. Lohse, *J.Polym.Sci., Polym.Lett., Ed.*, 23, 227 (1985).
20. R.E. Parker and N.S. Isaacs, *Chem.Revs.*, 59, 737 (1959).

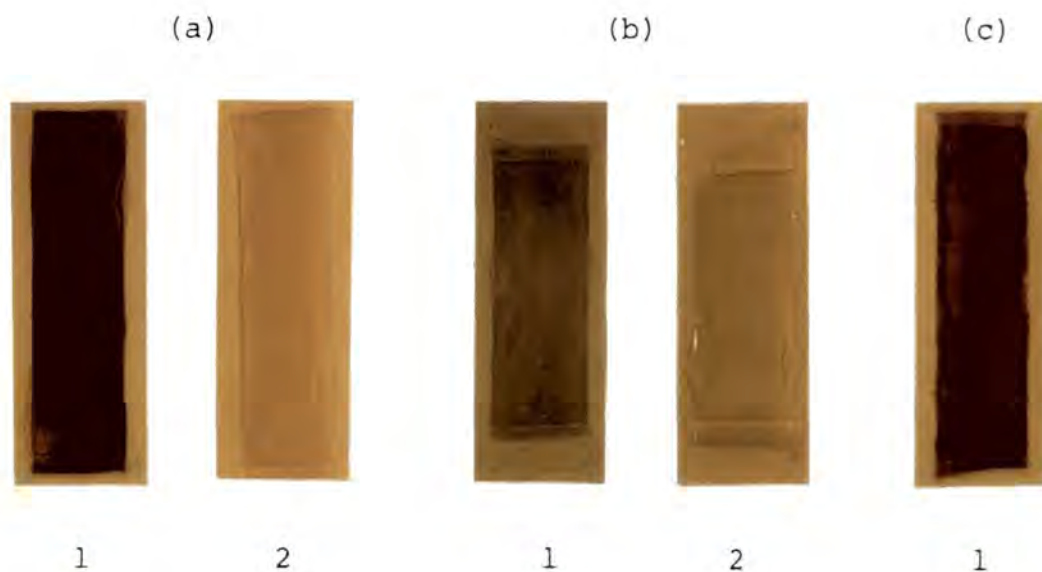
## CHAPTER SIX

AN INVESTIGATION OF THE TRANSIENT  
COLOURATION OF THE DGEBA, DGEBF  
AND EPOXY NOVOLAC SYSTEMS  
WHEN PHOTOCATIONICALLY CURED

## 6.1 Introduction

During the course of this work it was noted that films of the epoxy novolac system, given longer cure exposures using the 100W source, exhibited a red colouration. This colouration was found to be more pronounced in films irradiated using the 1.8kW source and, as indicated above, appeared to increase with increasing cure exposure. The colouration was found to fade with time or on heating the films. Similarly, films of the DGEBF system showed a transient red colouration whilst films of the DGEBA system showed a faint, transient, yellow/brown colouration. The photographs in Figure 6.1 illustrate the formation and disappearance of the coloured species.

FIGURE 6.1 Formation and Disappearance of the Coloured Species in the Epoxy Novolac, (a) DGEBA, (b) and DGEBF, (c) Systems



1. Film immediately after cure.
2. Film stored at room temperature for 1 week.

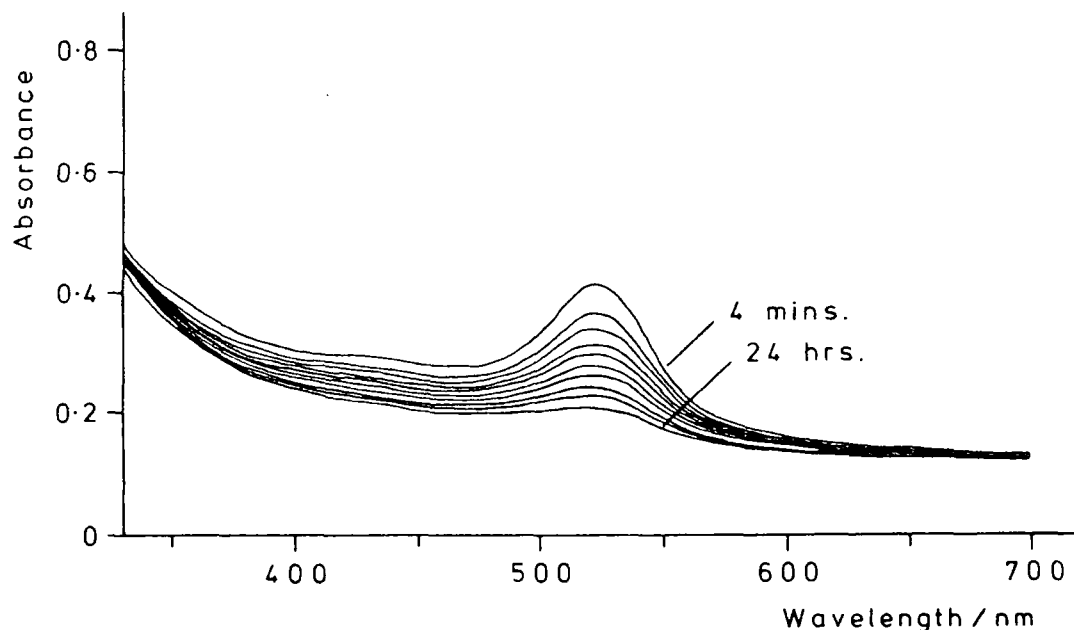
This Chapter deals with the investigation into the cause of the transient colouration which, as far as is known, has not previously been commented upon in the literature.

## 6.2 UV/Visible Spectroscopic Analysis of Cured Films

### (A) The Epoxy Novolac System

A film of a lacquer of the epoxy novolac containing 84.0% resin, 13.0% toluene, 2.0% photoinitiator and 1.0% w/w acetone was prepared on polyethylene and given 5 passes under the 1.8kW lamp. UV/visible spectra of the free-standing film (100 $\mu$ m nominal thickness,  $\sim$ 60 $\mu$ m cured thickness) were recorded at intervals after irradiation. The spectra in Figure 6.2 show an absorption band responsible for the colouration at 524nm which diminishes with time.

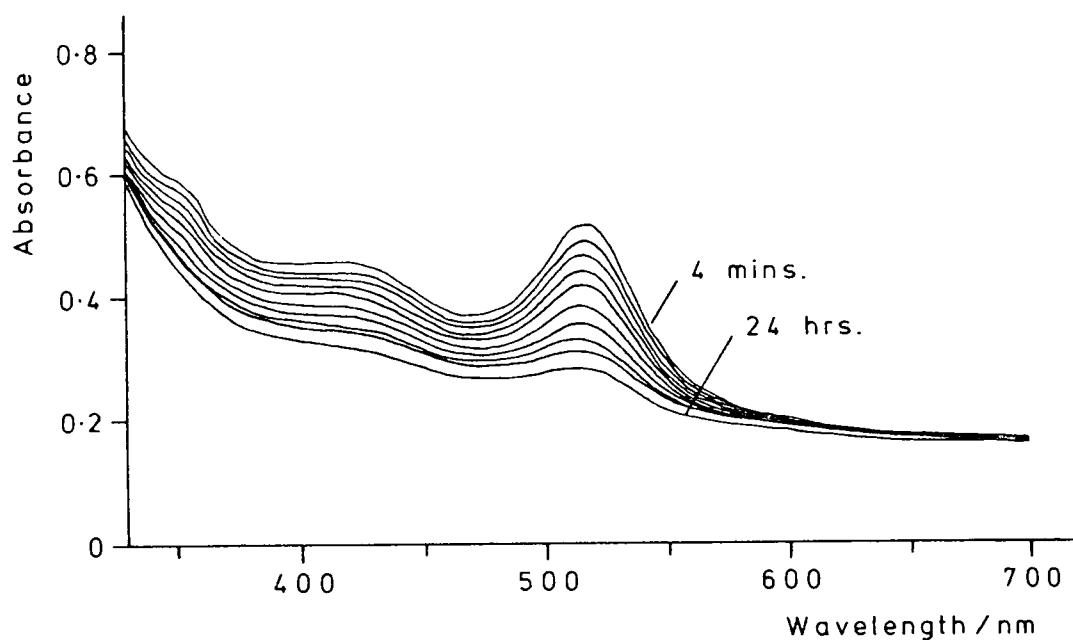
FIGURE 6.2 UV/Visible Spectra of a Film of the Epoxy Novolac System Recorded at Intervals of 4, 8, 12, 20, 30 Mins, 1, 2, 4, 8 and 24 Hrs after Irradiation



(B) The DGEBF System

A film of 100 $\mu$ m nominal thickness containing 96.4% resin, 2.5% photoinitiator and 1.0% w/w acetone was prepared on polyethylene and given 5 passes under the 1.8kW lamp. UV/visible spectra of the free-standing film were recorded at intervals after irradiation. The spectra in Figure 6.3 show an absorption maximum at 517nm responsible for the colouration that diminishes with time and additional weaker bands at  $\sim$ 428 and  $\sim$ 354nm that also diminish with time.

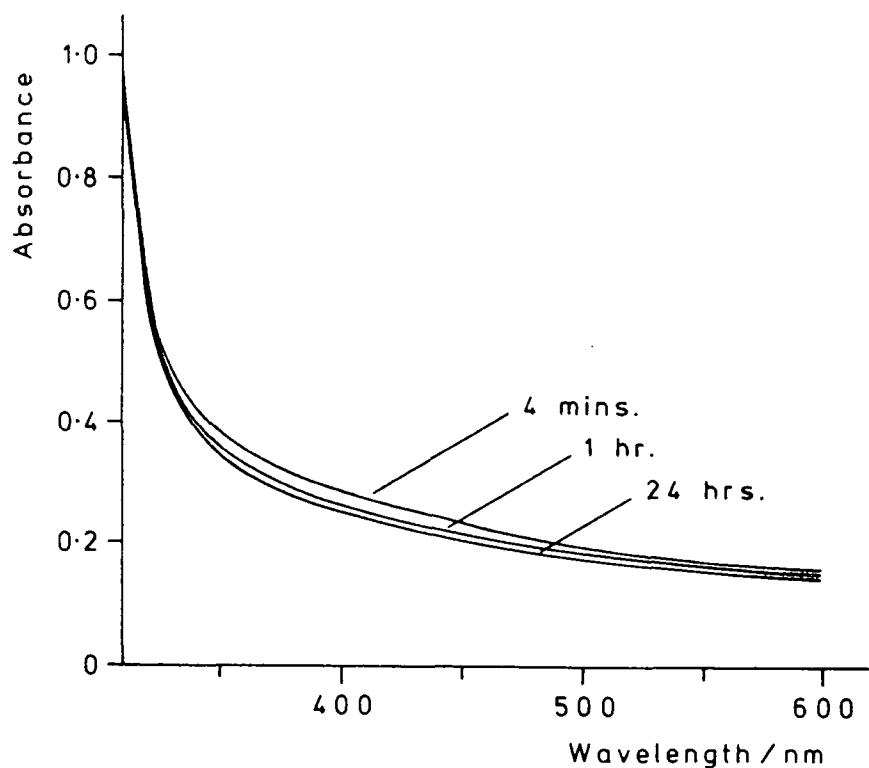
FIGURE 6.3 UV/Visible Spectra of a Film of the DGEBF System Recorded at Intervals of 4, 8, 12, 20, 30 Mins, 1, 2, 4, 8 and 24 Hrs after Irradiation

(C) The DGEBA System

A film of 100 $\mu$ m nominal thickness containing 97.0% resin, 2.0% photoinitiator and 1.0% w/w acetone was prepared and given 20 passes under the 1.8kW source. The UV/visible spectrum of the film was recorded at intervals after irradiation. Figure 6.4 shows that although the spectrum does change slightly with time,

no absorption maximum is detected in the near UV or visible regions.

FIGURE 6.4 UV/Visible Spectra of a Film of the DGEBA System Recorded at Intervals of 4 Mins, 1 and 24 Hrs. after Irradiation



Increasing the concentration of photoinitiator appeared to increase the intensity of the colouration and more pronounced changes were observed in the spectra recorded at intervals after cure but no clearly discernable absorption band in the near UV or visible regions was apparent.

### 6.3 A Possible Explanation for the Transient Colouration

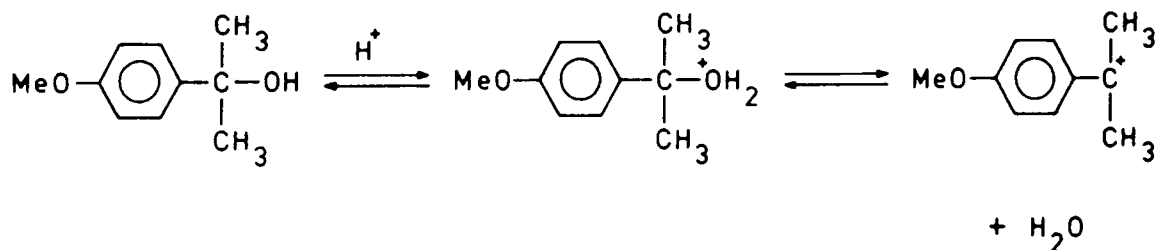
When the epoxy novolac or DGEBA resins are irradiated in the absence of photoinitiator they neither colour nor cure,

indicating that the colouration is related to the curing process. The absorption bands observed in the epoxy novolac and DGEBF systems do not correspond to any of the known or potential products of photoinitiator photolysis including the iodonium-radical cation. Furthermore the colour of cured films of the epoxy novolac system stored under high vacuum faded at a similar rate to those stored at atmospheric pressure indicating that a volatile species is not responsible for the effect.

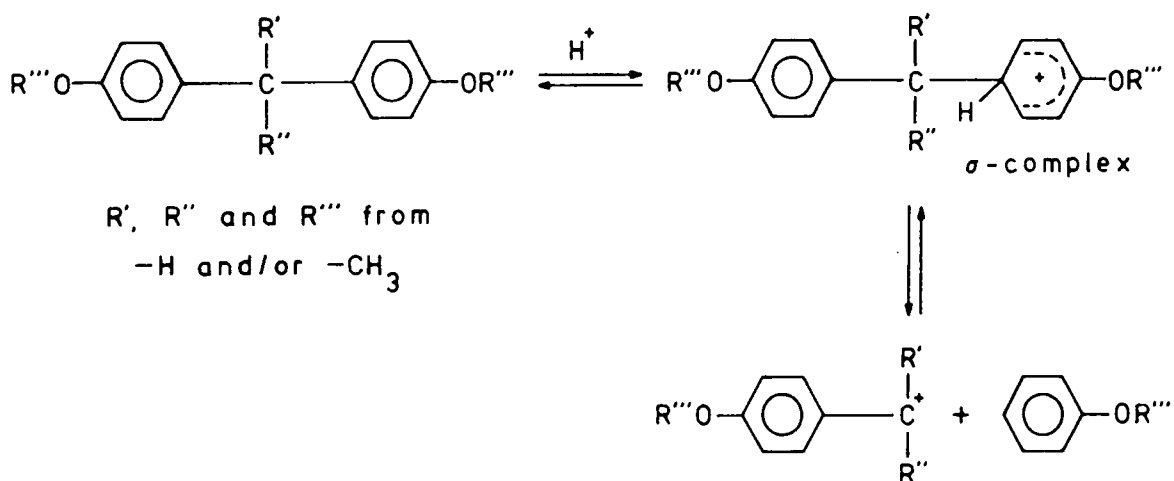
The fact that films of the aliphatic diglycidyl ether do not readily colour suggests that the species responsible for the colouration of resins (XVIII), (XIX) and (XXI) results from an interaction of a photolysis product with some moiety common to the above resins. Since the epoxy novolac and DGEBF systems exhibit a different colour to the DGEBA system it would seem likely that the bridging unit between the aromatic rings in the resin structure is involved in some way, as this is the only major structural difference between the epoxy novolac or DGEBF systems and the DGEBA system. ESR carried out on films of the epoxy novolac system in air whilst the colour was still apparent, showed that there were no radical species present in the system.

Since neither initiator products nor radical species are implicated as being responsible for the colouration it seems reasonable to consider possible ionic intermediates that could result from an interaction of a product of the photolysis of the photoinitiator with the bridged aromatic moiety of the resin structure. It has been reported in the literature that the precursor phenols of the DGEBA and DGEBF resins along with other compounds of this type give coloured solutions with absorption bands in the near UV and visible regions when dissolved in sulphuric acid.<sup>1,2,3</sup> It was also found, for example, that the

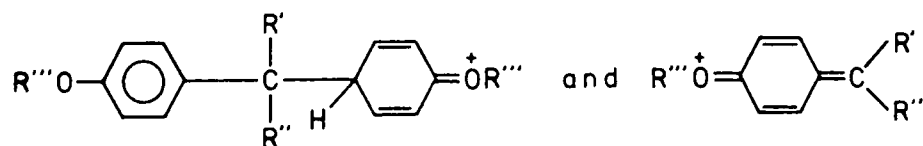
UV/visible spectra of bisphenol A and the p-methoxy derivative of  $\alpha,\alpha$ -dimethylbenzylalcohol in sulphuric acid were similar. The latter compound is expected to form a carbonium ion in acid:



This and other comparisons of a similar nature led to the proposal that the following process was occurring when, for example, bisphenol A and bisphenol F are dissolved in  $\text{c.H}_2\text{SO}_4$ :



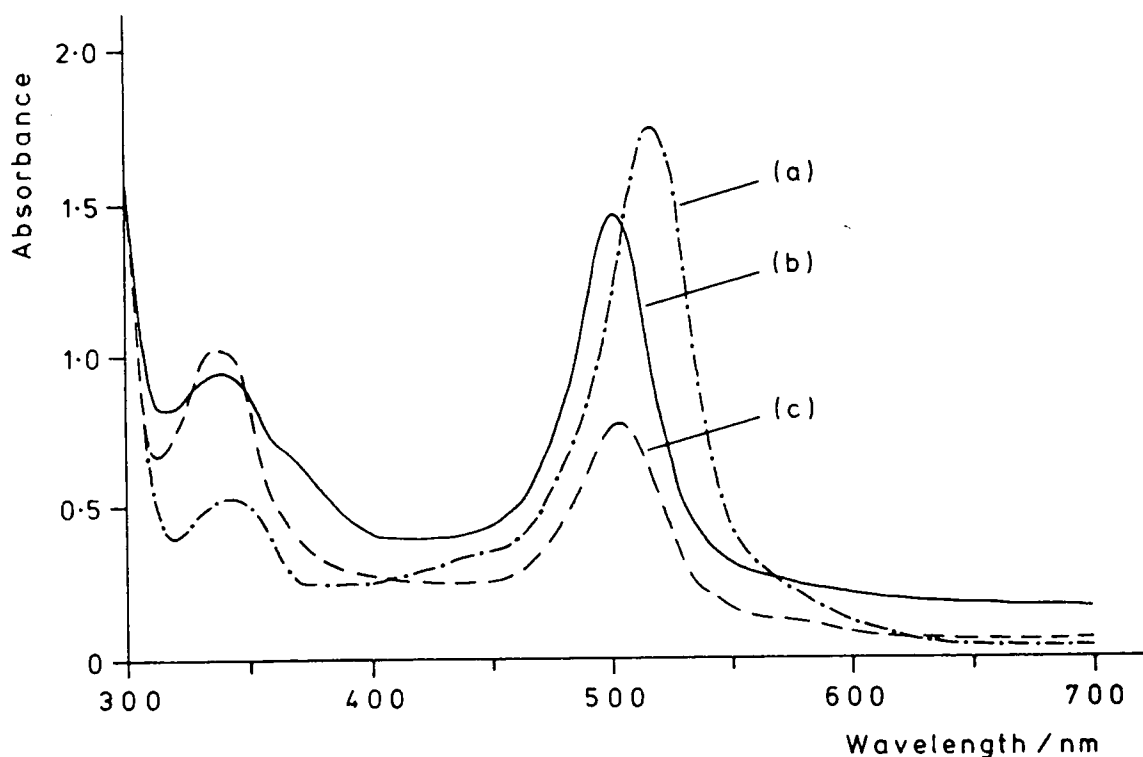
The occurrence of the above process is not unreasonable since the intermediate  $\sigma$ -complex and the cationic species produced by the cleavage of the molecule are stabilized by electron donation from the oxygen atom:



Further evidence for this process was gained by isolating phenol and hydrolysis products consistent with the formation of carbonium ions.

Solutions of the epoxy novolac and DGEBF resins in sulphuric acid exhibited a similar colour to that observed in the cured films of these resins. Before obtaining the UV/visible spectra of the solutions, they were filtered to remove any insoluble material which is presumably cross-linked polymer formed by ring-opening polymerization. The spectra are shown in Figure 6.5 along with that of 4-methoxybenzyl alcohol which if the above process is taking place, should give rise to a similar absorption spectrum. As can be seen the spectra of the three compounds are similar.

FIGURE 6.5 UV/Visible Spectra of Solutions in Concentrated Sulphuric Acid of 3-methoxybenzyl alcohol (a), the Epoxy Novolac Resin, (b) and the DGEBF Resin (c)



The absorption maxima in the visible region of the spectra of the epoxy novolac and DGEBF resins in sulphuric acid, 501 and 503nm respectively, are not in complete agreement with the absorption bands observed in the cured films but this is hardly surprising in view of the different environment of the cationic species thought to be responsible for the absorption. In the

case of the DGEBA system, solutions of this resin in sulphuric acid exhibit a yellow/brown colour, similar to that observed in cured films, with a main absorption band at 366nm, tailing into the visible region of the spectrum. The precursor phenol, bisphenol A, showed a similar colour in acid solution with an absorption maximum at 350nm.

The formation of p-alkoxybenzylic cations from the resins in sulphuric acid solution and in the curing process allows one to rationalize the shift in the absorption maximum and hence the colour on going from the epoxy novolac or DGEBF system to the DGEBA system. On the basis that the UV/visible absorption spectrum arises from a typical para-disubstituted benzene chromophore, the presence of electronically complementary groups (donor, -OR, and acceptor,  $-\overset{+}{C}R'R''$ ), will produce a red shift in the main absorption maxima.<sup>4</sup> However the effectiveness of the acceptor group is diminished when the benzyl C-H bonds are replaced by C-CH<sub>3</sub> bonds resulting in a shift to shorter wavelengths in the case of the carbonium ion derived from the DGEBA resin.

From the above it seems reasonable to propose that the colouration of the epoxy novolac, DGEBF and DGEBA systems as a result of the curing process arises from the formation of p-alkoxybenzylic cations by the interaction of the strong acid, produced by the photolysis of the photoinitiator, with the bridged aromatic moiety of the resin structure. The eventual fate of the cations thus produced is uncertain. Clearly they must have a limited life-time and there are a number of possible processes that could account for the consumption of such species. There are several nucleophilic moieties inherent to the system with which the cationic species could react such as ether groups,

unreacted epoxide groups and aromatic rings, the latter undergoing electrophilic substitution. In addition reaction with the counterion, which is presumably  $\text{PF}_6^-$ , could also take place and there is also the possibility of reaction with adventitious nucleophiles such as moisture. The process involving electrophilic aromatic substitution, if it were to be occurring, might be regarded as a mechanism for the relaxation of stress created during network formation. Further to the above processes, the benzylic carbonium ion generated in the DGEBA system has the opportunity to simply eliminate a proton to form a *para* substituted  $\alpha$ -methyl styrene moiety. This might account for the apparently low concentration of this cationic species in cured films although another possibility is that the extinction coefficient for this benzylic cation is low.

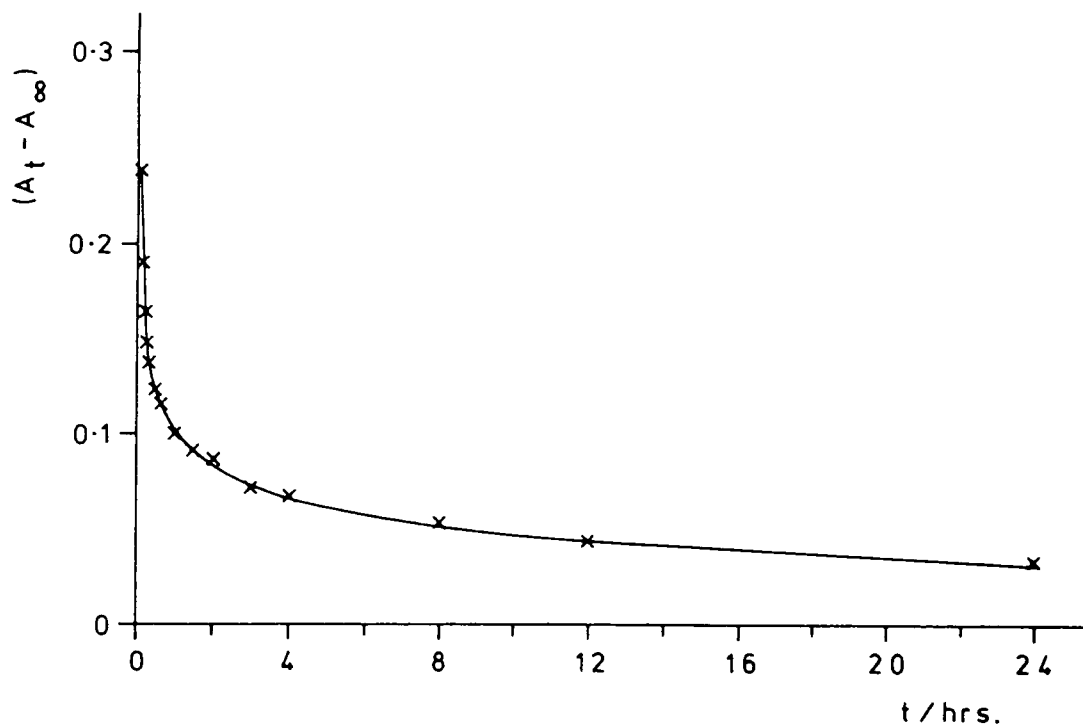
#### 6.4 The Decay Kinetics of the Coloured Species

##### (A) The Epoxy Novolac System

From the UV/visible spectra of a film of this system recorded as a function of the time after irradiation,  $t$ , the absorbance at 524nm,  $A_t$ , was measured and an infinity absorption value,  $A_\infty$ , estimated. The decay of the coloured species is shown in Figure 6.6 which is a plot of  $(A_t - A_\infty)$  versus  $t$ .

Plots of  $\ln(A_t - A_\infty)$  and  $1/(A_t - A_\infty)$  against  $t$  indicated that the decay of the species did not proceed *via* a simple first-order or second-order process. The form of the decay curve indicated that it might result from the occurrence of a number of concurrent processes. Examination of the decay curve by experienced kineticists confirmed this view, the form of the decay curve being attributable to at least two first order pro-

FIGURE 6.6 Plot of  $(A_t - A_\infty)$  versus  $t$  for the Epoxy Novolac System Showing the Decay of the Absorption Band at 524nm.

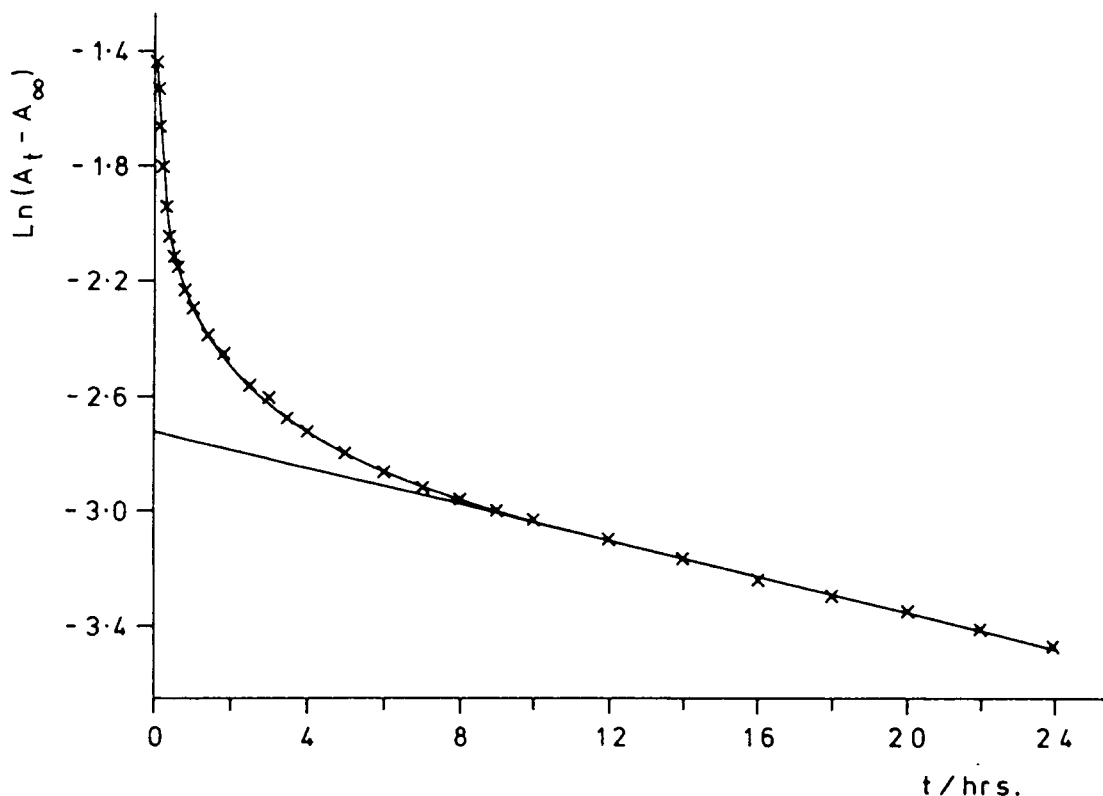


cesses. The decay of the coloured species by first-order processes is not inconsistent with the species being a *p*-alkoxybenzyl cation. Such a species would be highly unlikely to undergo a decay process that involved self-reaction, which would follow simple second-order kinetics and hence give a straight line when  $1/(A_t - A_\infty)$  is plotted against  $t$ . Of the processes indicated previously that could lead to the disappearance of such a species, reaction with the counterion would obey first-order kinetics whilst reaction with other nucleophilic species, although potentially second-order processes, would in all likelihood obey pseudo first-order kinetics since the concentration - if one can loosely use the term concentration in connection with solid state processes - of the cationic species is likely to be much lower than that of the nucleophilic species

present, even adventitious nucleophiles such as moisture.

Figure 6.7 shows that the semi-log plot is linear (correlation coefficient = -0.999) over the 8 to 24 hour period after irradiation. The gradient of the straight line corresponds to the first-order or pseudo first-order rate constant of the slowest process.

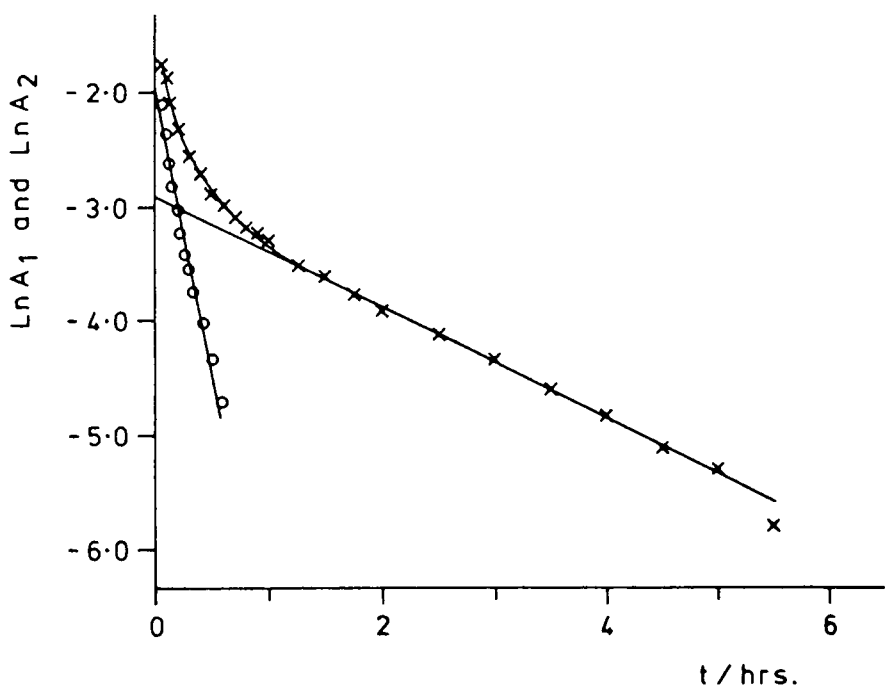
FIGURE 6.7 Plot of  $\ln(A_t - A_\infty)$  versus  $t$  for the Epoxy  
Novolac System



To determine how many processes are responsible for the decay and their rate constants the data was analysed in the following manner. The straight line was extrapolated back to zero time. Values of  $\ln(A_t - A_\infty)$  were taken from both the curve and the line for various values of  $t$ . The values of  $\ln(A_t - A_\infty)$  were converted to absorbance and for each value of  $t$ ,  $(A_t - A_\infty)$  from the line subtracted from that of the curve to give  $A_1$ .

Figure 6.8 shows a plot of  $\ln A_1$  versus  $t$  which indicates the presence of an additional process. The straight line portion

FIGURE 6.8 Plot of  $\text{Ln}A_1$  (X) and  $\text{Ln}A_2$  (O) versus  $t$  for the Epoxy Novolac System



of the plot (correlation coefficient = -0.999) gives the rate constant for the second slowest process. Treating the plot as previously gives values of  $A_2$  which, when converted to natural logarithms and plotted against  $t$ , give a straight line (correlation coefficient = -0.991) as is also shown in Figure 6.8, the gradient being equal to the rate constant of the third and most rapid process. Thus the decay curve of the coloured species in the epoxy novolac system appears to be the result of three first-order or pseudo first-order processes with rate constants of  $5 \times 10^{-4}$ ,  $80 \times 10^{-4}$  and  $820 \times 10^{-4} \text{ min}^{-1}$ . Due to the nature of the data manipulation the experimental error in the rate constants for the two faster processes will be very large.

The intercept of the three straight lines gives the amplitude of the process, which is a measure of the amount of the coloured species reacting by each process. The values of 0.066 (26%), 0.054 (21%) and 0.138 (53%) for the slow medium and fast processes respectively indicate the fast process is the most important. As indicated previously there are a number of possible reactions to account for the decay of the coloured species each having a different rate constant but it is not unreasonable, in view of the previous evidence, to suggest that there is inhomogeneous cross-linking and the slowest process corresponds to the decay of the cationic species in regions of low mobility with one of the other rate constants corresponding to the occurrence of the same process in high mobility regions.

### (B) The DGEBF System

From the UV/visible spectra of a film of this system recorded as a function of the time after irradiation,  $t$ , the absorbance at 517nm,  $A_t$ , was measured and an infinity absorption value,  $A_\infty$ , estimated. The form of the decay curve for the coloured species as shown by Figure 6.9 is similar to that for the epoxy novolac system except that the decay is slower in the initial stages.

Figure 6.10 shows  $\ln(A_t - A_\infty)$  plotted against  $t$  which is linear (correlation coefficient = -0.999) over the period between 8 and 24 hours after irradiation, the gradient corresponding to the rate constant of that slowest process.

The data was treated as for the epoxy novolac system to generate values of  $A_1$ .

FIGURE 6.9 Plot of  $(A_t - A_\infty)$  versus  $t$  for the DGEBF System  
showing the Decay of the Absorption Band at 517nm

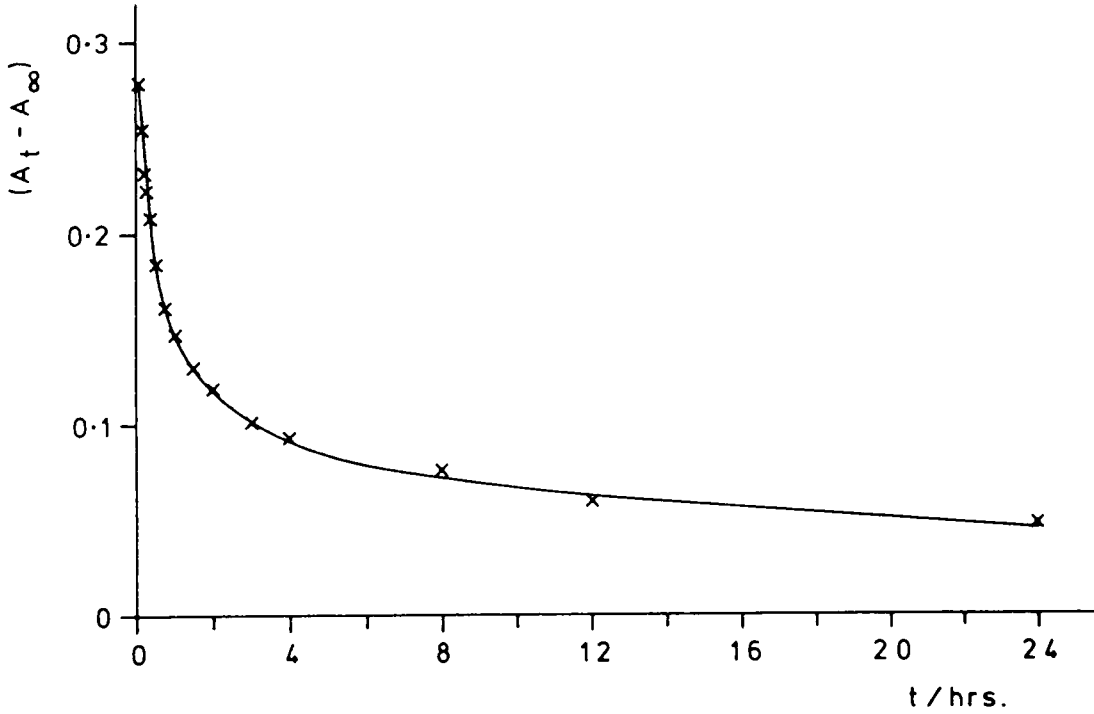
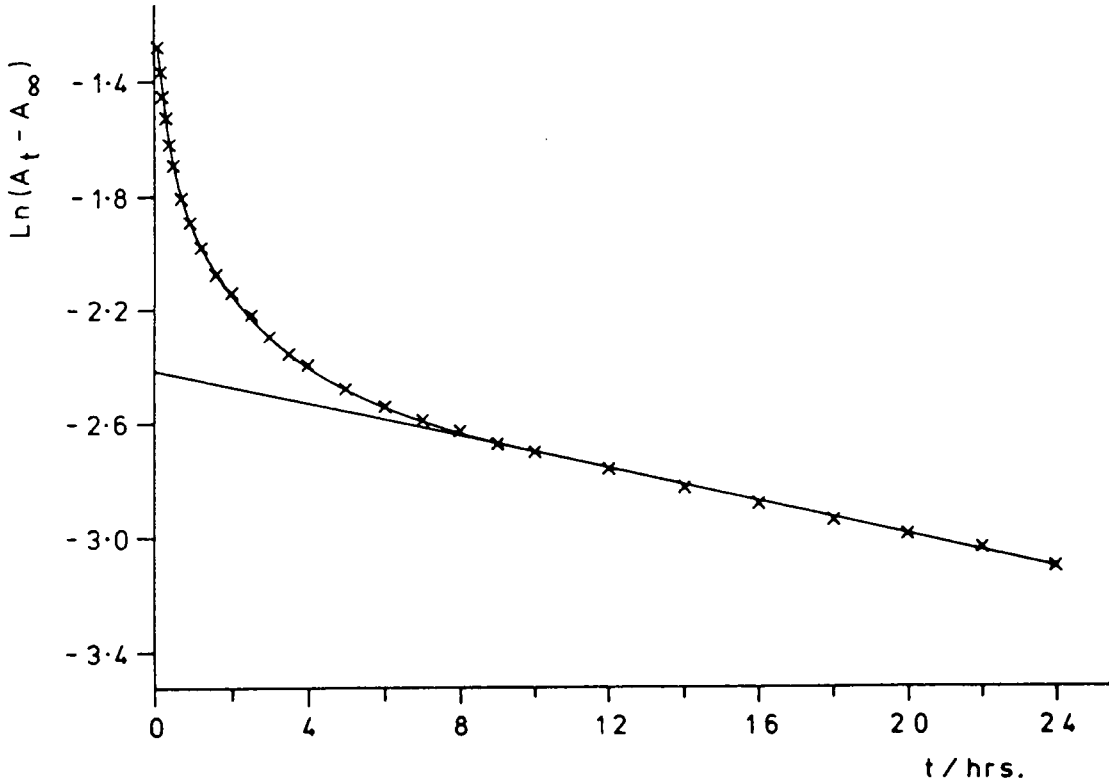
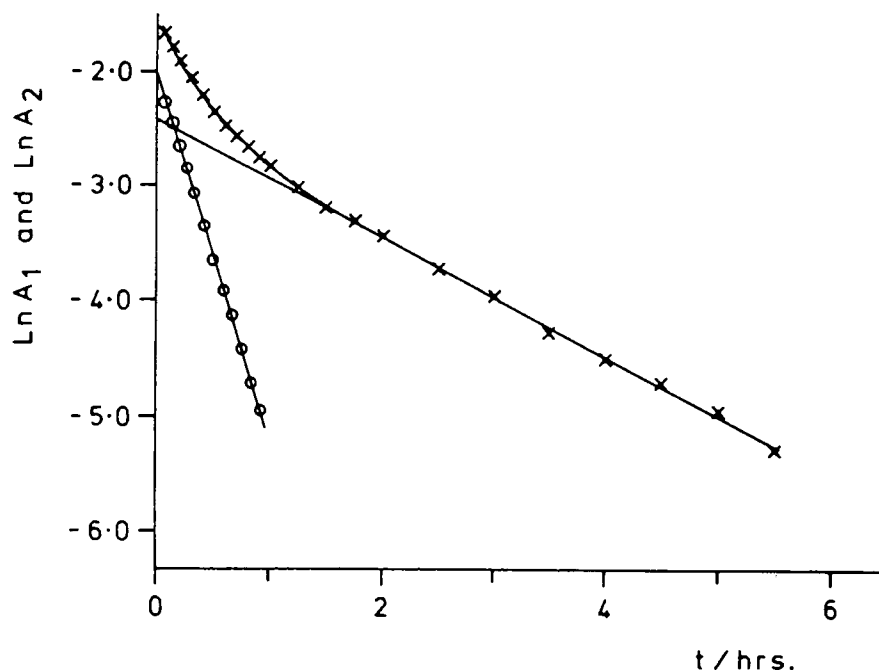


FIGURE 6.10 Plot of  $\ln(A_t - A_\infty)$  versus  $t$  for the DGEBF System



The plot of  $\ln A_1$  against  $t$ , Figure 6.11, indicates that a third process is occurring and the linear portion of the plot gives the rate constant of the second process.

FIGURE 6.11  $\ln A_1$  (X) and  $\ln A_2$  (O) versus  $t$  for the DGEBF System

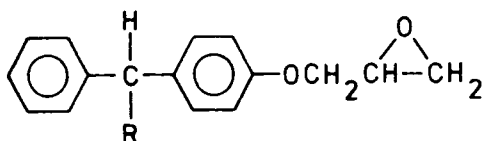


Values of  $A_2$  were calculated as for the epoxy novolac system and the natural logarithm of these values plotted against  $t$  give a straight line, Figure 6.11, the gradient corresponding to the rate constant of the fastest process. Thus, as in the epoxy novolac system, the decay of the coloured species can be attributed to three first-order or pseudo first-order processes with rate constants of  $5 \times 10^{-4}$ ,  $90 \times 10^{-4}$  and  $530 \times 10^{-4} \text{ min}^{-1}$ . Again the nature of the data manipulation will make the error

in the two larger rate constants substantial. The amplitudes of the slow, medium and fast processes are 0.089 (29%), 0.089 (29%) and 0.133 (42%) again indicating that the faster process is the most important process for the decay of the coloured species. As with the epoxy novolac system it is not unreasonable to suggest that the slower process is due to decay of the coloured species in low mobility regions with one of the other rate constants corresponding to the same reaction taking place in high mobility regions.

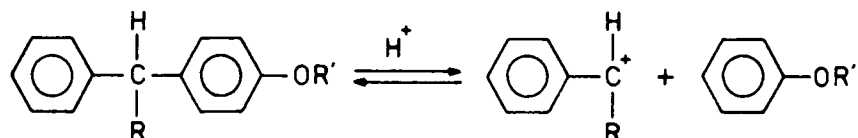
#### 6.5 The Use of Model Epoxide Compounds and Polyethers to Investigate the Potential Reaction of the Initiating Species and the Resins to Generate Benzylic Cations

From the previous work it would seem probable that the species responsible for the colouration of the three resins (XVIII), (XIX) and (XXI) during photoinitiated cationic cure is a p-alkoxybenzylic cation generated by the interaction of the acidic initiating species and the resins. In an attempt to provide further support for the occurrence of such a process, two monoglycidyl ether compounds based on the structure of the resins, but incapable of forming a network polymer, were prepared:

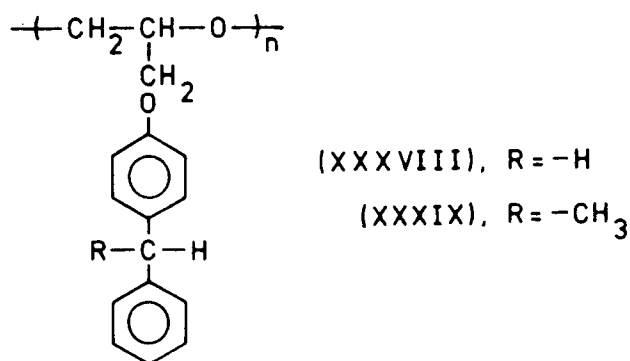


(XXXVI), R = -H; (XXXVII), R = -CH<sub>3</sub>

The aim of the the work reported in the following sections was to photocationically polymerize the above compounds and then use gas-liquid chromatography, GLC, and high resolution <sup>13</sup>C-NMR spectroscopy to determine whether products consistent with the generation of benzyl (R = -H) or phenethyl (R = -CH<sub>3</sub>) cations resulted:



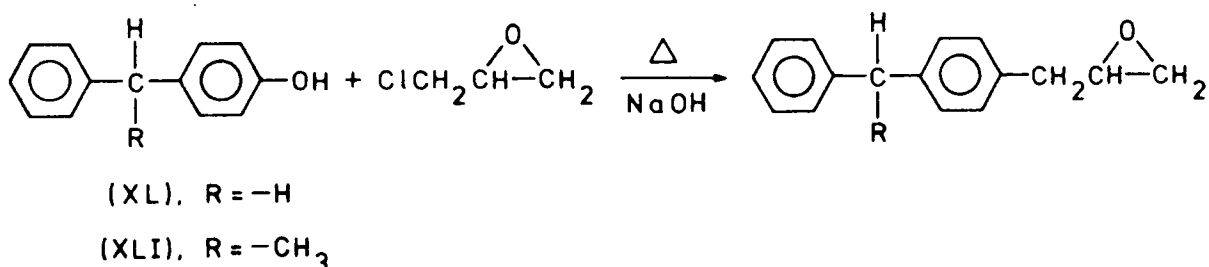
The two compounds were also polymerized using a triethylaluminium/ $\text{H}_2\text{O}$  catalyst system to yield linear polyethers of the following form:



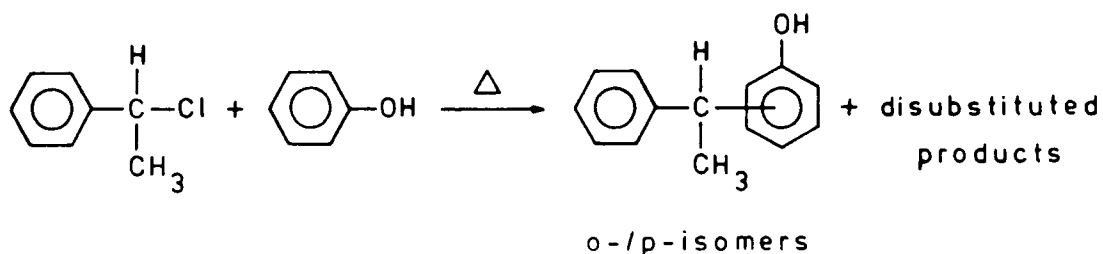
The polymers were irradiated in the presence of photoinitiator and high resolution  $^{13}\text{C}$ -NMR spectroscopy used to look for products consistent with the formation of benzyl or phenethyl cations.

### 6.6 Preparation of the Model Epoxides

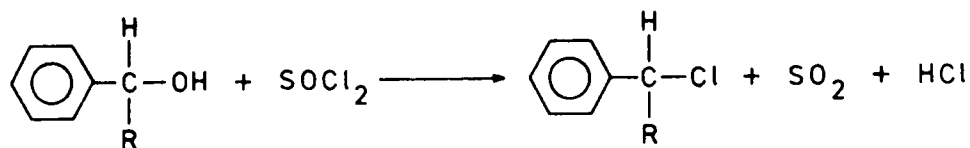
The two epoxide compounds were prepared by the reaction of the appropriate precursor phenol with ECH:



The precursor phenol (XL) was commercially available whilst (XLI) was prepared by the following route, involving the alkylation of phenol, which does not require a catalyst<sup>5</sup>:



The p-isomer was then separated from the product mixture. The phenethyl chloride used for the synthesis was prepared by the reaction of phenethyl alcohol with thionyl chloride<sup>6</sup>:



(A) Synthesis and Characterization of 4-(phenylmethyl)-phenoxymethyl oxirane (XXXVI)

The phenol (XL) was obtained from Aldrich (96% p-isomer) and reacted with ECH under nitrogen following the method used by Damont *et al.*<sup>7</sup> The phenol (XL) (47.9g, 0.26 moles), ECH (156.4g, 1.69 moles) and a few drops of water were placed in a three-neck, round bottom flask equipped with a thermometer, condenser and mechanical stirrer. The mixture was heated to 60°C and sodium hydroxide (10.4g, 0.26 moles) added in portions so that the temperature did not rise excessively. As the sodium hydroxide was added a white precipitate, presumably sodium chloride, formed. After completing the addition of sodium hydroxide, the reaction mixture was left stirring at 60-80°C for 5 hours. The white precipitate was then filtered off and the excess ECH removed using a rotary evaporator. Distillation of the impure product under high vacuum ( $5 \times 10^{-3}$  mm Hg) through a short Vigreux column gave a major fraction (44.0g) boiling at 132-136°C. This clear, colourless, viscous liquid was taken to be the product giving a yield of 71%.

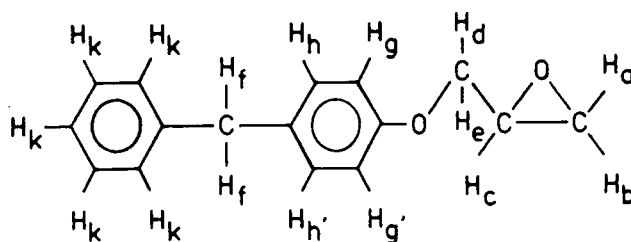
The IR spectrum of this material (Appendix 4, Spectrum No.6) is consistent with it being the desired product, Table 6.1 giving the assignment of a number of the bands present in the spectrum.

TABLE 6.1 Assignment of Absorption Bands in the IR Spectrum of (XXXVI)

Frequency/cm <sup>-1</sup>	Assignment
3070 - 2990	Oxirane C-H stretch + aromatic C-H stretch
2910 - 2830	Aliphatic C-H stretch
1605	Aromatic ring breathing
1505 - 1330	Aromatic ring breathing + C-H bend
1240	Asymmetric C-O-C stretch
1035	Symmetric C-O-C stretch
915	Oxirane ring stretch
850	Oxirane ring stretch

The <sup>1</sup>H-NMR spectrum of this material (Appendix 5, Spectrum No.9), is also consistent with it being (XXXVI). The assignments of the resonances are shown in Table 6.2.

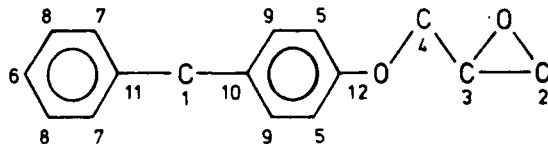
TABLE 6.2 Assignment of the  $^1\text{H}$  Resonances in the Spectrum of (XXXVI)



Proton	Shift/ppm	Splitting	Integration
$\text{H}_a$	$\delta_A = 2.67$	$\text{AB}_q$ $J_{a-b}^2 = 4.9 \text{ Hz}, J_{b-c}^3 = 4.5 \text{ Hz}$	1
$\text{H}_b$	$\delta_B = 2.82$	$J_{a-c}^3 = 2.6 \text{ Hz}$	1
$\text{H}_c$	3.27	Multiplet	1
$\text{H}_d$ or $\text{H}_e$	$\delta_A = 3.85$	$\text{AB}_q$ $J_{d-e}^2 = 11.0 \text{ Hz}, J_{d/e-c}^3 = 5.7 \text{ Hz}$	3 ( $2\text{H}_f + \text{H}_{d/e}$ )
$\text{H}_e$ or $\text{H}_d$	$\delta_B = 4.12$	$J_{e/d-c}^3 = 3.1 \text{ Hz}$	1
$\text{H}_f$	3.88	Singlet	
$\text{H}_g$ and $\text{H}_{g'}$	$\delta_A = 6.81$	Pseudo $\text{AB}_q$ $J_{g-h}^3 = J_{g'-h}^3 = 8.4 \text{ Hz}$	2
$\text{H}_h$ and $\text{H}_{h'}$	$\delta_B = 7.07$		2
$\text{H}_k$	7.20	Multiplet	5

The assignments from the  $^{13}\text{C}$ -NMR spectrum (Appendix 5, Spectrum No.10) are shown in Table 6.3.

TABLE 6.3 Assignment of the  $^{13}\text{C}$  Resonances in the Spectrum of (XXXVI)



Nucleus	Shift/ppm	Nucleus	Shift/ppm
1	41.08	7	128.48
2	44.67	8	128.86
3	50.17	9	128.96
4	68.88	10	133.91
5	114.73	11	141.49
6	126.05	12	156.98

Both the  $^1\text{H}$  and  $^{13}\text{C}$ -NMR spectra indicate there is very little, if any, of the o-isomer present.

Elemental analysis gave 80.0% carbon and 6.9% hydrogen which agrees with the expected values of 80.0% carbon and 6.7% hydrogen. The Mass Spectrum (Appendix 6) was also consistent with the material being the desired product.

(B) Synthesis and Characterization of 4-(1-phenylethyl)-phenoxyethyl oxirane (XXXVII)

(i) Synthesis and Characterization of the Precursor Phenol (XLI)

Phenethyl chloride was prepared as follows.<sup>6</sup> Thio-nyl chloride (243.0g, 2.0 moles) that had been distilled and stored under nitrogen was added to a round bottom three-neck

flask equipped with a condenser and thermometer. The contents of the flask were stirred using a magnetic follower and phenethyl alcohol (100.1g, 0.80 moles) added in portions *via* a dropping funnel. Each addition of the alcohol was accompanied by a violent evolution of gas, presumably HCl and SO<sub>2</sub>, but in spite of this, the temperature did not rise above 26°C. After completing the addition of the alcohol, the reaction mixture was left stirring for a couple of hours.

The excess thionyl chloride was removed by evaporation under reduced pressure and the remaining material was distilled under reduced pressure through a Vigreux column. The major fraction boiled at 94-98°C (23-25 mm Hg) and the IR spectrum (Appendix 4, Spectrum No.7) is consistent with this being the desired product, giving a yield of 96.5g (84%). The next step was the alkylation of phenol using the phenethyl chloride .

Phenol (131.5g, 1.40 moles) was placed in a three-neck, round bottom flask equipped with a condenser dropping funnel and mechanical stirrer. Phenethyl chloride (90.0g, 0.64 moles) was slowly added to the phenol with stirring. A light brown suspension formed initially. After an induction period of ~15 minutes the mixture cleared and turned orange, a process accompanied by a rapid evolution of gas, presumably HCl. The reaction vessel was flushed with nitrogen to help remove the HCl. When the reaction had subsided the contents of the flask were kept at 70°C for 4 hours. The excess phenol was then removed by distillation under reduced pressure (69°C, 9mm Hg). Distillation of the remaining material through a short Vigreux column under a higher vacuum (1.0mm Hg) gave two main fractions boiling at 122-124°C (31.8g) and 130-136°C (38.6g), the latter fraction solidified to give a white solid. From the <sup>1</sup>H-NMR spectrum of the mixture prior

to fractionation, two resonances of similar intensity split into quartets were readily discernible at  $\sim 4.0$  and  $\sim 4.3$  ppm. It is unlikely that significant amounts of the m-isomer are formed and it is therefore reasonable to assign the two resonances to the o- and p-isomers with the resonance at  $\sim 4.0$  ppm corresponding to the p-isomer. The  $^1\text{H-NMR}$  spectrum of the lower boiling fraction indicated that it contained mostly the o-isomer whilst the spectrum of the higher boiling fraction indicated that it contained mostly the p-isomer. The higher boiling fraction was further purified by recrystallization (twice) from 40/60 petroleum ether. The yield of the purified solid (m.pt =  $58-59^\circ\text{C}$ ) was 24.8g (20%). The product, taken to be (XLI), was then characterized using the usual techniques.

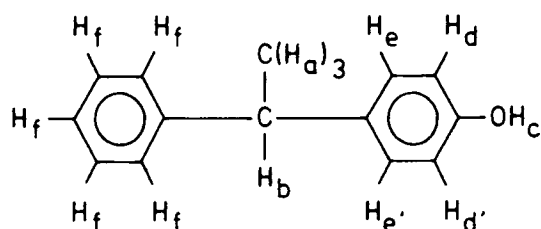
The IR spectrum (Appendix 4, Spectrum No.8) is consistent with the product being (XLI). The assignments of a number of bands are shown in Table 6.4.

TABLE 6.4 Assignment of Absorption Bands in the IR Spectrum of (XLI)

Frequency/ $\text{cm}^{-1}$	Assignment
3220	Phenolic O-H stretch
3020	Aromatic C-H stretch
2960 - 2870	Aliphatic C-H stretch
1595	Aromatic ring breathing
1510 - 1375	Aliphatic C-H bend + aromatic ring breathing
1220	Phenolic O-H bend

The assignment of the resonances in the  $^1\text{H}$ -NMR spectrum (Appendix 5, Spectrum No.11) are shown in Table 6.5.

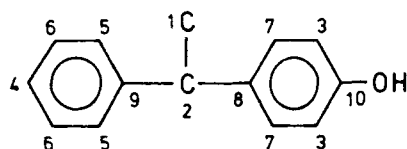
TABLEW 6.5 Assignment of the  $^1\text{H}$  Resonances in the Spectrum of (XLI)



Proton	Shift/ppm	Splitting	Integration
$\text{H}_a$	1.65	Doublet $J_{a-b}^3 = 7.2 \text{ Hz}$	3
$\text{H}_b$	4.13	Quartet $J_{b-a}^3 = 7.2 \text{ Hz}$	1
$\text{H}_c$	5.63	Broad singlet	1
$\text{H}_d$ and $\text{H}_{d'}$	$\delta_A = 6.77$	Pseudo $\text{AB}_q$ . $J_{d-e}^3 = J_{d'-e'}^3 = 8.5 \text{ Hz}$	2
$\text{H}_e$ and $\text{H}_{e'}$	$\delta_B = 7.12$		2
$\text{H}_f$	7.28	Multiplet	5

The assignments from the  $^{13}\text{C}$ -NMR Spectrum (Appendix 5, Spectrum No.12) are shown in Table 6.6.

TABLE 6.6 Assignment of the  $^{13}\text{C}$  Resonances in the Spectrum of (XLI)



Nucleus	Shift/ppm	Nucleus	Shift/ppm
1	22.12	6	128.44
2	44.01	7	128.84
3	115.33	8	138.92
4	126.05	9	146.82
5	127.63	10	153.48

Both the  $^1\text{H}$ - and  $^{13}\text{C}$ -NMR spectra indicate that any o-isomer must be present in very small amounts if at all.

Elemental analysis gave 84.1% carbon and 7.3% hydrogen which compares reasonably well with the expected values of 84.8% carbon and 7.1% hydrogen. The mass spectrum (Appendix 6) is also consistent with the product being (XLI).

(ii) Reaction of (XLI) with ECH

The reaction of the precursor phenol (XLI) with ECH was carried out as in the preparation of (XXVI). Sodium hydroxide (4.9g, 0.12 moles) was added in portions to a mixture of (XLI) (23.6g, 0.12 moles) and ECH (60.0g, 0.65 moles) with a catalytic amount of water present. After adding the sodium

hydroxide the reaction mixture was left for 4 hours at 70-80°C. The white precipitate and excess ECH were then removed and the remaining material distilled through a short Vigreux column under vacuum. The major fraction, collected between 142-147°C (0.6 mm Hg), crystallized on standing to give a white solid. The solid was further purified by recrystallization from n-hexane. The yield of the purified solid (m.pt. = 69-71°C) was 23.6g (77%). The product, taken to be (XXXVII), was then characterized using the usual techniques.

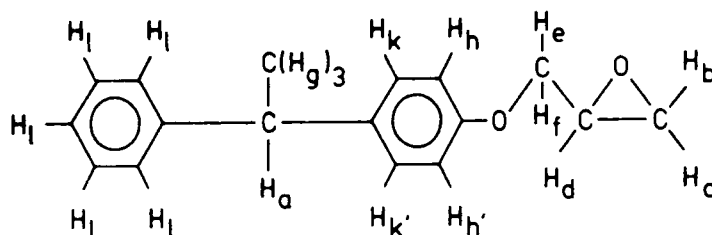
The IR spectrum (Appendix 4, Spectrum No.9) is consistent with the product being (XXXVII) the assignment of the major bands being shown in Table 6.7.

TABLE 6.7 Assignment of the Absorption Bands in the IR Spectrum of (XXXVII)

Frequency/cm <sup>-1</sup>	Assignment
3060 - 3010	Oxirane C-H stretch + aromatic C-H stretch
2970 - 2870	Aliphatic C-H stretch
1610	Aromatic ring breathing
1510 - 1350	Aliphatic C-H bend + aromatic ring breathing
1250	Asymmetric C-O-C stretch
1035	Symmetric C-O-C stretch
920	Oxirane ring stretch
840	Oxirane ring stretch

The  $^1\text{H-NMR}$  (Appendix 5, Spectrum No.13) is also consistent with the product being (XXXVII). Table 6.8 shows the assignment of the resonances.

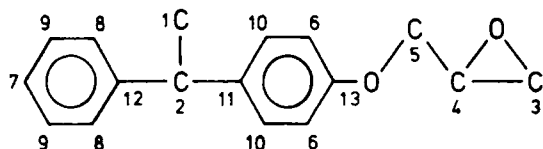
TABLE 6.8 Assignment of the  $^1\text{H}$  Resonances in the Spectrum of (XXXVII)



Proton	Shift/ppm	Splitting	Integration
$\text{H}_a$	1.70	Doublet $J_{a-g}^3 = 7.2 \text{ Hz}$	1
$\text{H}_b$	$\delta_A = 2.81$	$\text{AB}_q$ $J_{b-c}^2 = 4.9 \text{ Hz}, J_{c-d}^3 = 4.5 \text{ Hz}$	1
$\text{H}_c$	$\delta_B = 2.96$	$J_{b-d}^3 = 2.6 \text{ Hz}$	1
$\text{H}_d$	3.41	Multiplet	1
$\text{H}_e$ or $\text{H}_f$	$\delta_A = 4.00$	$\text{AB}_q$ $J_{f-e}^2 = 11.0 \text{ Hz}, J_{e/f-c}^3 = 5.6 \text{ Hz}$	1
$\text{H}_f$ or $\text{H}_e$	$\delta_B = 4.26$	$J_{f/e-c}^3 = 3.2 \text{ Hz}$	4 ( $\text{H}_{f/e} + 3\text{H}_g$ )
$\text{H}_g$	4.20	Quartet $J_{g-a}^3 = 7.2 \text{ Hz}$	
$\text{H}_h$ and $\text{H}_{h'}$	$\delta_A = 6.94$	Pseudo $\text{AB}_q$ $J_{h-k}^3 = J_{h'-k'}^3 = 8.6 \text{ Hz}$	2
$\text{H}_k$ and $\text{H}_{k'}$	$\delta_B = 7.23$		2
$\text{H}_l$	7.23	Multiplet	5

Table 6.9 gives the assignment of the resonances in the  $^{13}\text{C}$  NMR Spectrum (Appendix 5, Spectrum No.14).

TABLE 6.9 Assignment of the  $^{13}\text{C}$  Resonances in the Spectrum of (XXXVII)



Nucleus	Shift/ppm	Nucleus	Shift/ppm
1	22.12	8	127.61
2	44.03	9	128.42
3	44.77	10	128.65
4	50.24	11	139.24
5	68.90	12	146.74
6	114.61	13	156.88
7	126.04		

Elemental analysis gave 81.6% carbon and 7.6% hydrogen which is not very good when compared with the expected composition of 80.3% carbon and 7.1% hydrogen. The mass spectrum (Appendix 6) is consistent with the product being (XXXVII).

### 6.7 Conventional Polymerization of the Model Epoxides

A whole range of compounds have been shown to act as initiators or catalysts for the polymerization of epoxides by

cationic, anionic or coordinate mechanisms. An indication of the variety of initiators of cationic polymerization was given in Chapter One. The effectiveness of the catalyst systems appears to be largely dependent on the structure of the epoxide monomer. Therefore it was decided to use a catalyst system that led to the efficient polymerization of phenoxymethyl oxirane, bearing in mind the similarity of the oxirane ring environment in this compound with that in the model epoxide compounds to be polymerized.

The discovery that organometallic systems such as  $ZnR_2$ ,  $AlR_3$  and  $MgR_2$  or the products of their reaction with water act as catalysts for the polymerization of epoxides has allowed high molecular weight polymers to be prepared from a variety of monomers. In the literature it is reported that the  $AlEt_3/H_2O$  catalyst system where the molar ratio of  $AlEt_3$  to  $H_2O$  is 1:0.6 leads to the formation of high molecular weight, isotactic, poly(phenoxymethyl oxirane) in good yield (92%, 19 hours at 30°C).<sup>8</sup>

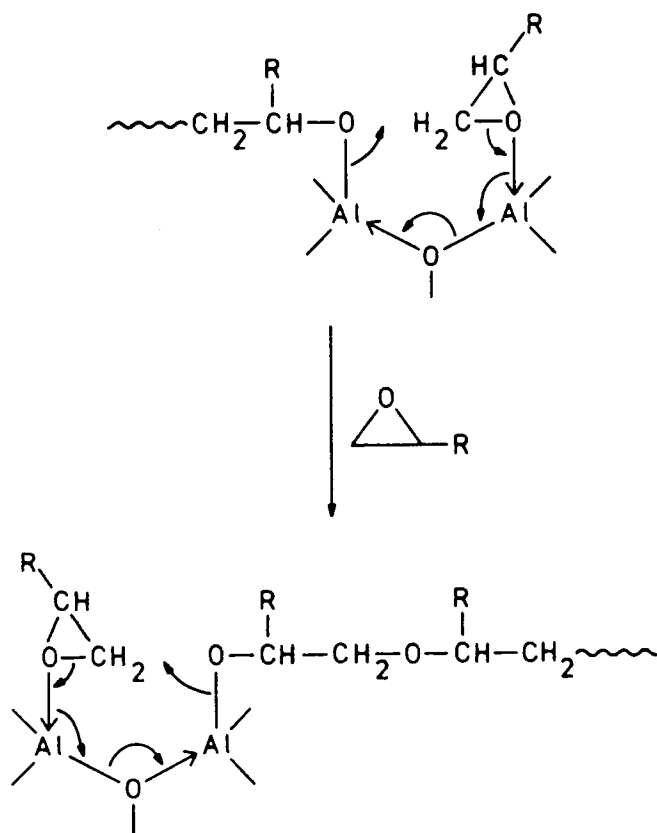
(A) Mechanistic and Stereochemical Aspects of Epoxide Polymerization using the  $AlEt_3/H_2O$  System

The exact nature of the catalytic species is unknown but it is thought to be built up by the self-association of bis-(dialkylaluminium) oxide units which are formed from the reaction of the trialkylaluminium with water:<sup>9</sup>



The presence of two or more organometal groups joined by oxygen was recognised as being a requisite for good catalytic activity.

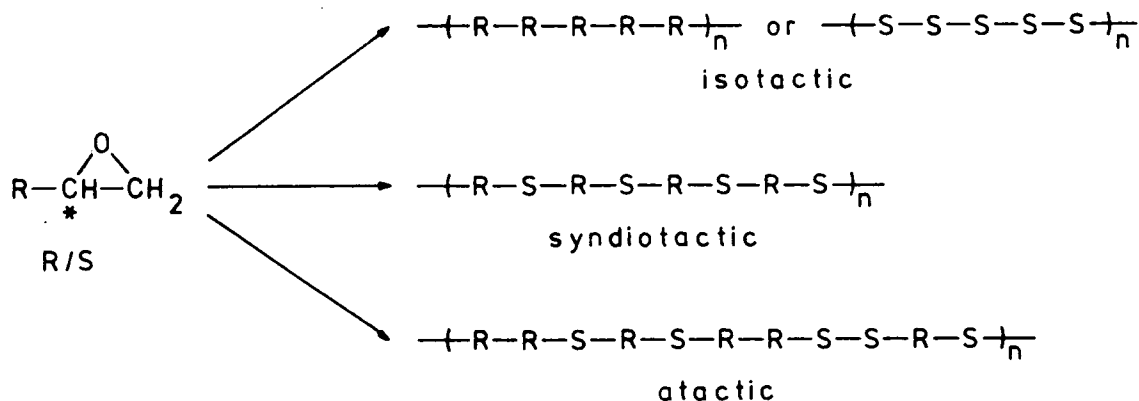
The observation that the  $\text{AlEt}_3/\text{H}_2\text{O}$  system leads to the rapid polymerization of some monomers (*e.g.* 1,2-dimethyloxirane) at low temperatures whilst other monomers (*e.g.* methyloxirane) polymerize only slowly at room temperature has led to the suggestion that the catalyst system can initiate cationic polymerization or act as a coordinate catalyst.<sup>9</sup> A mechanism for coordinate polymerization involving the coordination of a monomer unit to an aluminium atom prior to its attack by the growing chain bonded to an adjacent metal atom has been proposed:<sup>9</sup>



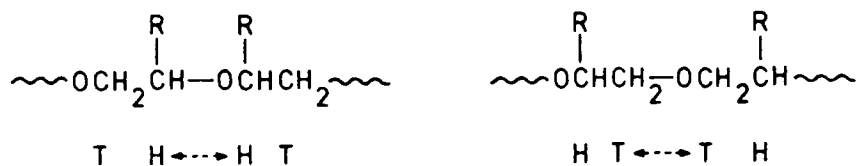
Ring-opening occurs with inversion of configuration at the carbon atom attacked, a feature common to many, if not all, epoxide polymerizations.

Monosubstituted epoxides are chiral and can be obtained in the R or S configuration. The polymer produced from such monomers generally falls into one of three classes defined by the stereochemistry of the repeat units. The absolute configuration of the monomer units comprising the polymer may be identical, alternate or random, the terms isotactic, syndio-

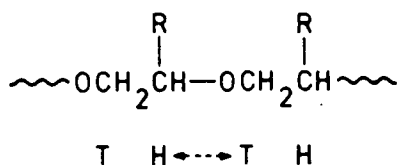
tactic and atactic being applied respectively. This can be represented as below:



Generally the polymerization of a racemic monomer using coordinate catalysts results in the formation of isotactic polymer along with low molecular weight amorphous polymer which can be separated by virtue of their different solubilities.<sup>10</sup> The crystalline, isotactic polymer tends not to be optically active suggesting that there are catalytic sites that specifically polymerize the R or S forms of the monomer.<sup>11</sup> The reason for the formation of the amorphous polymer is not clear. In the case of poly(methyloxirane) prepared using  $\text{AlEt}_3/\text{H}_2\text{O}$  and other coordination catalyst systems, the amorphous fraction is found to contain a significant proportion of head-to-head, HH, or tail-to-tail, TT, bonded units:<sup>10</sup>



The isotactic polymer contains mostly head-to-tail, HT, bonded units:



The occurrence of HT linkages in the isotactic polymer indicates that ring-opening occurs by attack of the same ring carbon atom in each propagation step. The presence of TT and HH linkages accounts for the amorphous nature of the lower molecular weight fraction and indicates that ring-opening occurs by attack at either ring carbon atom.

(B) Preparation of the Catalyst Solution

The catalyst was prepared following the method of Vandenberg.<sup>8</sup> All the solvents used had been distilled and stored under nitrogen. Immediately prior to their use they were thoroughly degassed and again placed under nitrogen. Care was taken to ensure that all manipulations were carried out under nitrogen.

Triethylaluminum ( $2.6 \text{ cm}^3$ , 0.019 moles) was carefully added to n-hexane ( $7.8 \text{ cm}^3$ ). The bulk of the above solution ( $10 \text{ cm}^3$ ) was transferred to a  $50 \text{ cm}^3$  round bottom, two-neck flask equipped with a condenser and rubber septum. Diethyl ether ( $26.6 \text{ cm}^3$ ) was then added to the solution. With the solution refluxing, water ( $0.16 \text{ cm}^3$ ), was slowly added over a 1 hour period (ratio  $[\text{AlEt}_3]/[\text{H}_2\text{O}] = 2$ ). The mixture was then refluxed for a further hour, allowed to cool, and transferred to another container for easy storage and access under nitrogen.

(C) Polymerization of (XXXVI) and the Characterization of the Resulting Polyether (XXXVIII)

The polymerization was carried out under nitrogen in a  $50 \text{ cm}^3$  round bottom, two-neck flask equipped with a mechanical stirrer. The monomer (XXXVI) (6.10g, 0.025 moles) was placed in the flask and the catalyst solution ( $3.0 \text{ cm}^3$ , ratio  $[\text{monomer}]/[\text{AlEt}_3] = 17$ ) added. On addition of the catalyst solution, the polymerization mixture turned a light green colour and was

left stirring for 30 minutes. As the polymerization mixture was then slowly heated to 85-90°C the solvent was allowed to escape. After 7 hours the viscous polymerization mixture was allowed to cool and methanol (40 cm<sup>3</sup>) added which also precipitated the polymer. After washing the polymer with methanol several times it was dried under high vacuum. Further purification was carried out by dissolving the polymer in chloroform, filtering off the small amount of insoluble material and then reprecipitating the polymer using methanol as the non-solvent. This was carried out twice. After drying under vacuum, the yield of the white, maleable material was 2.2g (36%).

The above polymerization procedure was adopted since it was found that polymerization in solution at 30°C only yielded 3% polymer after 8 hours. Cooling the polymerization mixture using an ice-bath did not increase the yield.

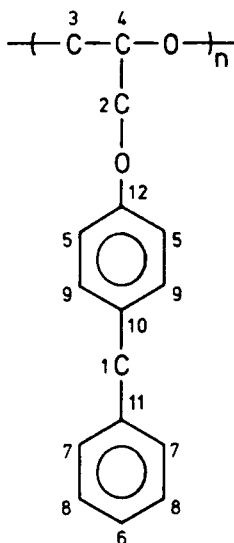
The IR spectrum of the polymer (Appendix 4, Spectrum No.10) shows many bands at similar frequencies and relative intensities to those observed in the spectrum of the monomer. However there is the appearance of a weak absorption due to hydroxyl functionality (3450 cm<sup>-1</sup>) and a band at 1110 cm<sup>-1</sup> due to an aliphatic C-O-C stretching mode along with the disappearance of absorbances due to the oxirane ring stretching modes (915 and 850 cm<sup>-1</sup>). These differences are consistent with the formation of polymer (XXXVIII) containing hydroxyl end-groups.

Elemental analysis gave 79.6% carbon and 7.0% hydrogen which is quite close to the expected composition of 80.0% carbon and 6.7% hydrogen.

The <sup>13</sup>C-NMR spectrum of the material (Appendix 5, Spectrum No.15) is consistent with it being polyether (XXXVIII). The

assignment of the resonances are given in Table 6.10.

TABLE 6.10 Assignment of  $^{13}\text{C}$  Resonances in the Spectrum of the Polyether (XXXVIII)



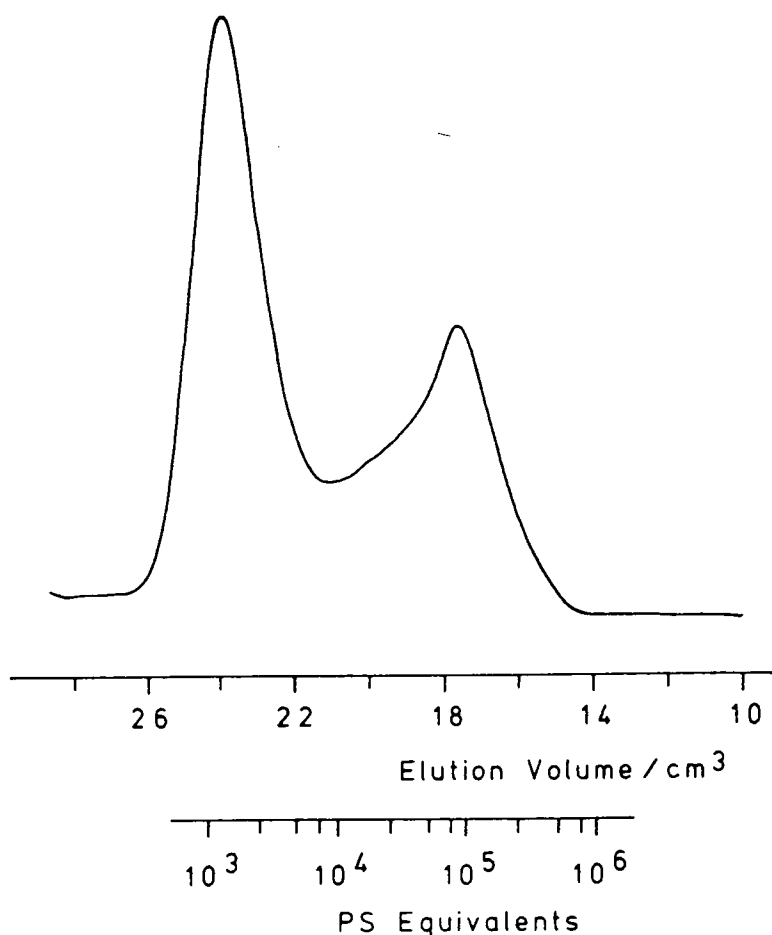
Nucleus	Shift/ppm	Nucleus	Shift/ppm
1	40.89	6	125.84
2	67.98	7	128.29
3	69.71	8	128.68
	70.02	9	129.71
4	78.09	10	133.24
	78.13	11	141.42
	78.27	12	157.04
5	114.51		

All of the signals due to the aromatic carbons, the bridging carbon and the methoxy carbon appear at similar shifts to those observed in the spectrum of the monomer. The methine and methylene carbons of what was the oxirane ring have markedly shifted downfield which is consistent with the formation of a polyether. Several small peaks of unknown origin are present in the spectrum at 30.00, 31.06, 31.44, 33.88, 45.25 and 118.75 ppm

and there are also a number of small resonances associated with the major resonances. The small resonances between 70.88 and 71.88 ppm might be connected with HH and TT linkages whilst the three resonances at 82.44, 82.75 and 83.14 appear to be due to some deuterated impurity in the solvent.

To obtain a measure of the average molecular weight of the polymer, gel permeation chromatography, GPC, was used. In this technique a liquid mobile phase is used in conjunction with polymer gels of specified pore size as the stationary phase. Smaller molecules penetrate the pores of the gel more effectively than larger molecules giving a degree of separation on the basis of molecular size which is related to molecular weight. Thus using a suitable detector to monitor the eluent gives a measure of the amount (detector response) and molecular weight (elution volume) of each species present which, after suitable calibration, allows number average molecular weights to be determined). In this work THF was used as the solvent, a differential refractometer was used as the detector and the GPC traces were calibrated using polystyrene samples of well defined  $\bar{M}_n$ .

The GPC trace of the polymer (XXXVIII) is shown in Figure 6.12. As can be seen there appears to be high and low molecular weight polymer present corresponding to  $\sim 1 \times 10^3$  and  $\sim 1 \times 10^5$  polystyrene equivalents. The occurrence of this bimodal distribution inhibits analysis of the trace to determine average molecular weights.

FIGURE 6.12 GPC Trace of Polymer (XXXVIII)(D) Polymerization of (XXXVII) and the Characterization of the Resulting Polyether (XXXIX)

Monomer (XXXVII) (5.5g, 0.022 moles) was polymerized, using the catalyst solution (2.7 cm<sup>3</sup>, [monomer]/[AlEt<sub>3</sub>] = 16), and purified by the procedure described in the previous section. The yield of the light yellow, clear, extremely viscous oil was 1.9g (34%).

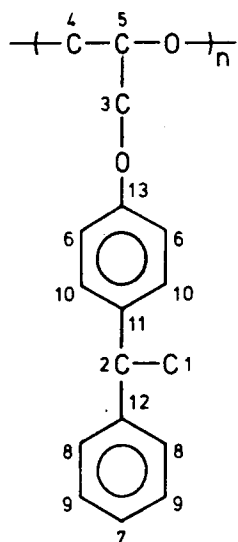
The IR spectrum (Appendix 4, Spectrum No.11) of the polymer is similar to that of the monomer but there are some differences which are consistent with the formation of a polyether with hydroxyl end-groups. A small hydroxyl absorbance (3480 cm<sup>-1</sup>) is present as is an absorbance at 1115 cm<sup>-1</sup> attributable to an aliphatic C-O-C stretching mode whilst absorbances

at 920 and 840  $\text{cm}^{-1}$  due to oxirane ring stretching modes have disappeared.

Elemental analysis of the polymer gave 80.3% carbon and 7.4% hydrogen which is in agreement with the expected values of 80.3% carbon and 7.1% hydrogen.

The  $^{13}\text{C}$ -NMR spectrum (Appendix 5, Spectrum No.16a) of the polymer is also consistent with it being the polyether (XXXIX). The assignment of the resonances is given in Table 6.11.

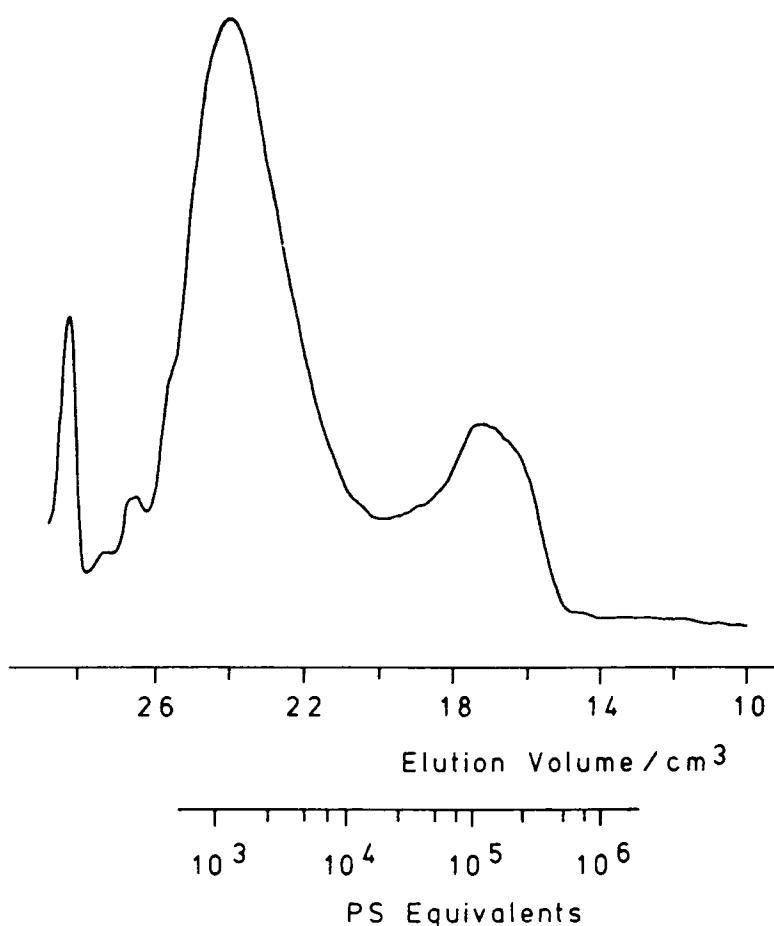
TABLE 6.11 Assignment of the  $^{13}\text{C}$  Resonances in the Spectrum of the Polyether (XXXIX)



Nucleus	Shift/ppm	Nucleus	Shift/ppm
1	21.93	6	114.36
2	43.78	7	115.78
3	67.98	8	127.39
4	69.76	9	128.18
	70.01	10	128.33
5	77.99	11	138.50
	78.11	12	146.61
	78.25	13	156.91

Many of the above resonances correspond to those observed in the spectrum of the monomer, only the signals of what were the methylene and methine carbons of the oxirane ring show a marked difference in their shift values. The resonances of the main-chain methylene and methine carbons were assigned with the help of the Distortionless Enhancement by Polarization Transfer, DEPT, spectrum (Appendix 5, Spectrum No.16b). Resonances due to unknown species are present at 15.00, 31.12, 31.37, 32.17, 33.75, 44.60, 45.19, 50.03, 68.74, 71.47, 115.75, 116.72, 137.62 and 139.09 ppm, with other small resonances associated with the main resonances. The resonances at 44.60, 50.03 and 68.74 ppm could be connected with the presence of unreacted monomer. The multiplet of small peaks at 71.47 ppm might be due to HH or TT linkages. It seems reasonable that the three resonances at 82.38, 82.75 and 83.12 ppm are due to some deuterated impurity in the solvent.

The GPC trace of the polymer, Figure 6.13, shows a bimodal molecular weight distribution similar to that observed for polymer (XXVIII). There is also a third peak present corresponding to low molecular weight material which could be due to monomer.

FIGURE 6.13 GPC Trace of Polymer (XXXIX)

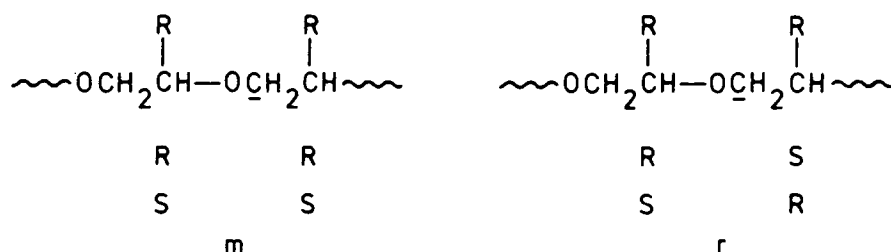
(E) Comments on the Bimodal Molecular Weight Distribution and the Tacticity of the Polyethers (XXXVIII) and (XXXIX)

As mentioned previously, when polymerizing epoxides using coordination catalysts it is not uncommon to obtain high molecular weight isotactic polymer and low molecular weight amorphous polymer. This was demonstrated in a study of the polymerization of octadecyl oxirane using a bis(dimethylglyoxine) nickel II/AlEt<sub>3</sub> catalyst system.<sup>12</sup>

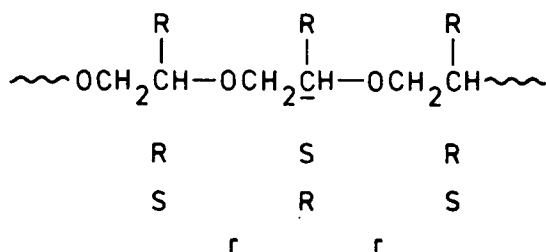
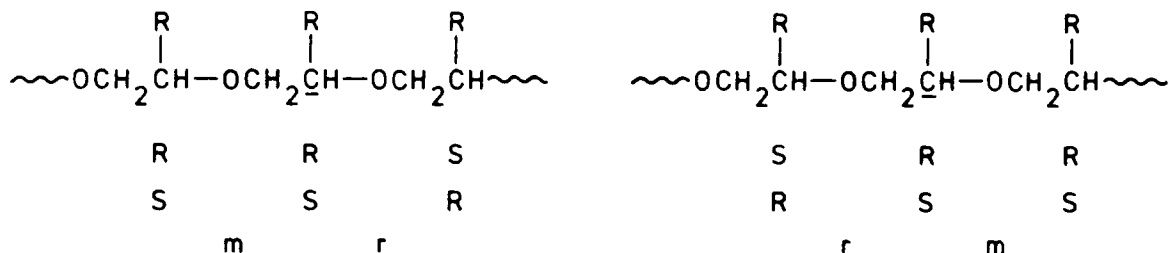
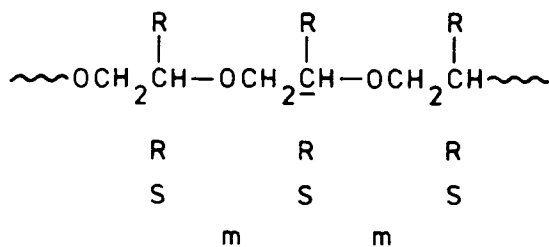
The two melting points exhibited by the resulting polymer were taken as being indicative of two crystalline phases. The higher melting temperature phase was found to have a viscosity average molecular weight,  $\bar{M}_v$ , of  $\sim 1 \times 10^6$  whilst the phase with

the lower melting point had a  $\bar{M}_v$  of  $32 \times 10^3$ . From the  $^{13}\text{C}$  NMR spectra of the two fractions the high  $\bar{M}_v$  polymer was found to be isotactic whilst the low  $\bar{M}_v$  material was found to be atactic, possibly with TT and HH linkages present. The authors offer no explanation as to why the atactic phase exhibited a melting point.

NMR spectroscopy has proved very useful for investigating the tacticity of polymers as well as other features of the microstructure.<sup>13</sup> For a polyether prepared from a monosubstituted epoxide and composed of HT linkages there are two possible environments for the main-chain methylene carbons if they are sensitive to the absolute configuration of the two nearest main-chain carbons (dyad sensitivity):



Thus for an isotactic polymer only one environment occurs, corresponding to the meso, m, dyad. Likewise, there is only one environment for such carbons in a syndiotactic polymer, corresponding to the racemic, r, dyad whereas for an atactic polymer both environments occur. Longer range interactions give rise to a greater number of possible environments and hence resonances for the main-chain methylene carbons in an atactic polymer. When the main-chain methine carbons are sensitive to the configuration of the two nearest methine carbons (triad sensitivity) four distinct environments are possible:



In isotactic and syndiotactic polyethers only one environment occurs, corresponding to the mm and rr triads respectively, whereas all four environments occur in an atactic polymer. Again, longer range sensitivity increases the number of possible environments for such carbons in an atactic polymer and hence the number of resonances.

The  $^{13}\text{C}$ -NMR spectrum of the low  $\bar{M}_v$  fraction of poly(octadecyloxirane) showed three resonances for the main-chain methine carbons which were attributed to the mm (low field), mr/rm and rr (high field) triad environments; the mr and rm environments are not usually distinguishable.<sup>12</sup> Four resonances were associated with the main-chain methylene carbons which were interpreted, perhaps incorrectly, as being due to triad sensitivity.

The monomer was also polymerized using  $t$ BuOK which gives atactic polymer with predominantly HT linkages. The  $^{13}\text{C}$  NMR spectrum of this material was found to be similar to that of the low  $\bar{M}_v$  fraction. However the different relative intensities of the main-chain methylene resonances in the spectrum of the low  $\bar{M}_v$  material from the coordinate polymerization along with the presence of additional small peaks was taken as being indicative of HH and TT linkages. The  $^{13}\text{C}$  NMR spectrum of the high  $\bar{M}_v$  fraction from the coordinate polymerization showed only one resonance for the main-chain methine and methylene carbons. The resonance for the main-chain methine carbons occurred at the same shift as that attributed to the mm triad resonance in the spectrum of the low  $\bar{M}_v$  material and similarly that of the main-chain methylene carbons corresponded to the mm triad resonance for such carbons. Therefore the high  $\bar{M}_v$  material was considered to be isotactic.

Other evidence of the formation of isotactic and atactic polymer in the coordinate polymerization of epoxides has come from the use of  $^{13}\text{C}$ -NMR spectroscopy.<sup>11</sup> The spectrum of poly(methyloxirane) prepared by anionic polymerization using  $t$ BuOK showed three resonances with an intensity ratio of 1:2:1, associated with the methine carbons which were attributed to the mm (low field), mr/rm and rr (high field) triads. Two resonances with a 1:1 intensity ratio were associated with the methylene carbons and were attributed to the m (low field) and r (high field) dyads. Thus the polymer was considered to be atactic. The spectrum of poly(methyloxirane) prepared using a  $\text{ZnEt}_2/\text{H}_2\text{O}$  coordinate catalyst system again showed three resonances associated with the main-chain methine carbons but with different relative intensities and two resonances associated with

the main-chain methylene carbons but again with different relative intensities to those observed in the atactic sample. The intensities of the resonances corresponding to the mm triad and m diad were found to be significantly increased. This was interpreted as being indicative of the presence of isotactic polymer along with atactic material.

The polyethers (XXXVIII) and (XXXIX) prepared in this work using an  $\text{AlEt}_3/\text{H}_2\text{O}$  coordinate catalyst system contain both low and high molecular weight material. The  $^{13}\text{C}$ -NMR spectra of the polymers show three resonances for the main-chain methine carbons and two resonances for the main-chain methylene carbons (Appendix 5, Spectrum Nos. 15 and 16a; Tables 6.10 and 6.11). The similarity of the relative intensities of the three methine resonances with those for the main-chain methine carbons in the spectrum of poly(methyloxirane) polymerized using a  $\text{ZnEt}_2/\text{H}_2\text{O}$  system and the presence of two fractions make it reasonable to assign the resonances to mm (low field), mr/rm and rr triads. Similarly it seems reasonable to assign the two main-chain methylene carbon resonances to the m (low field) and r (high field) dyads. Therefore it would appear that the polymers prepared in this work are composed of high molecular weight isotactic and low molecular weight atactic fractions as has been observed with other coordinate catalyst systems and/or monomers.

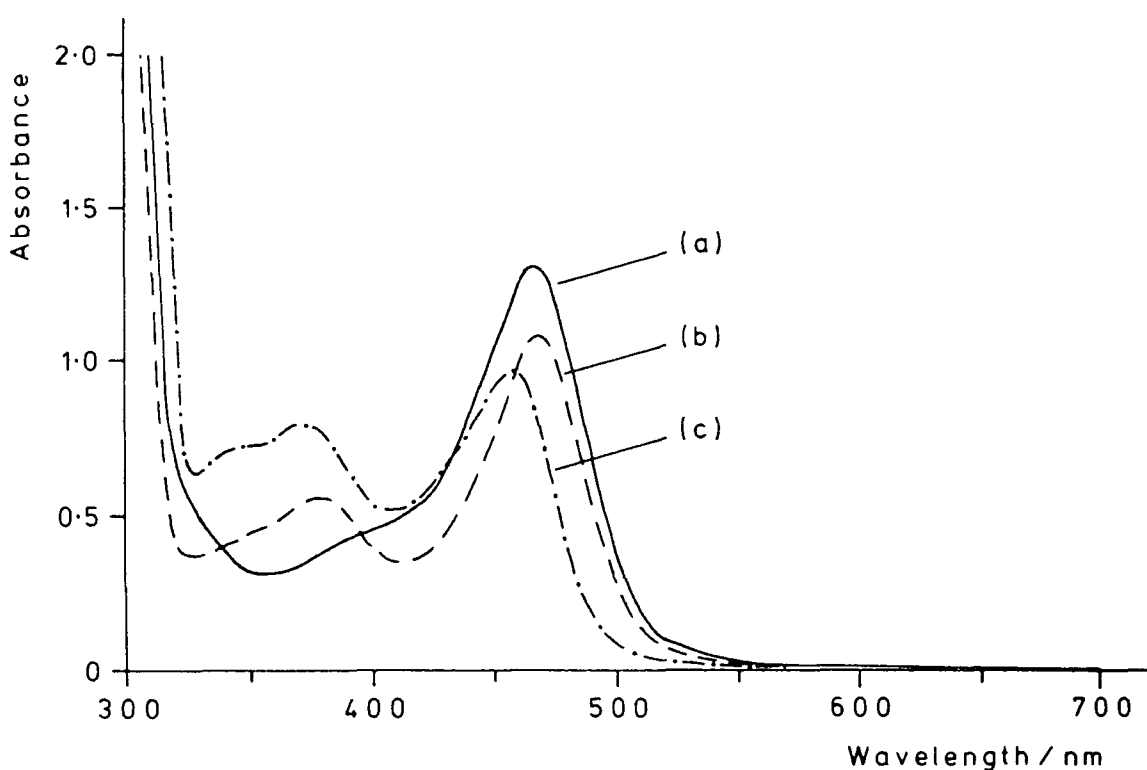
## 6.8 Addition of the Model Epoxides and Polyethers to Sulphuric Acid

### (A) Compound (XXXVI) and the Polyether (XXXVIII)

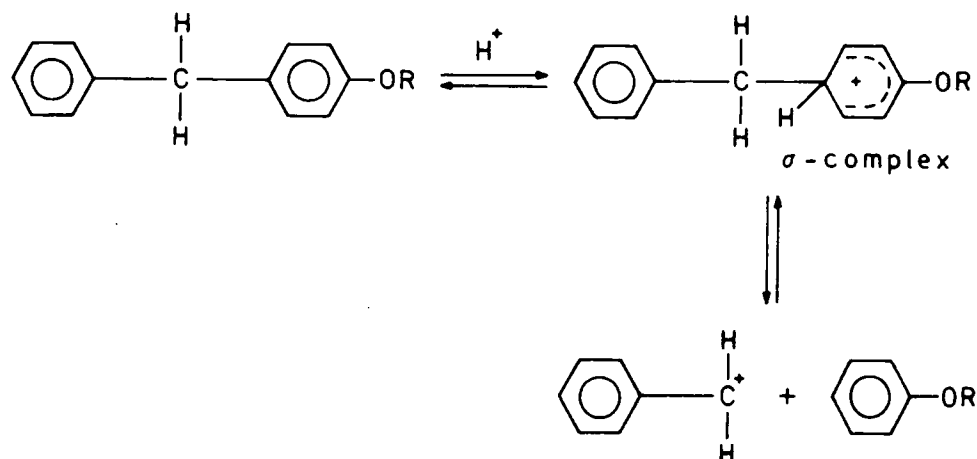
Addition of (XXXVI) and the corresponding polyether to sulphuric acid resulted in a pale yellow solution. The UV/visible spectra of the acid solutions are reproduced in Figure

6.14 and show an absorption maximum at 467nm for (XXXVI) and a main absorption maximum at 469nm with a weaker absorption at 379nm for the polyether. A pale yellow solution also resulted when the precursor phenol (XL) was added to sulphuric acid and as shown in Figure 6.14 the UV/visible spectrum shows a main absorption maximum at 457nm with a weaker one at 371nm.

FIGURE 6.14 UV/Visible Spectra of Solutions in Concentrated Sulphuric Acid of (XXXVI) (a), (XXXVIII) (b) and (XL) (c)



It is reasonable to suggest that the coloured species generated from the above compounds by the action of acid is a carbonium ion. However it is difficult to say with any certainty what the structure of the carbonium is. When commencing the synthesis of the model epoxide it was thought that in acid it would give rise to a benzyl cation as shown below:



Attempts to generate the benzyl cation by adding benzyl alcohol to sulphuric acid were fruitless due to the formation of a solid, presumably poly(benzyl), a branched polymer of methylene bridged aromatic rings. The literature pertaining to the generation and characterization of carbonium ions indicates it is unlikely that benzyl cations can be generated in solution because of their instability and hence their propensity for polymerization.<sup>14,15</sup> Only in one study was such a species thought to have been formed by the addition of benzyl alcohol to sulphuric acid.<sup>16</sup> The UV/visible spectrum of the acid solution showed an absorption maximum at 470nm. Other workers doubted that the coloured species generated in the above study was the benzyl cation since they were unable to generate such a species in an even more acidic environment ( $\text{SO}_2\text{-SbF}_5\text{-FSO}_3\text{H}$ ).<sup>17</sup>

It may be that the benzyl cation is generated from the addition of compounds such as (XXXVI) to acid but in low concentrations so that polymerization is prevented. However the fact that the species generated from the precursor phenol (XL) absorbs at a slightly different wavelength than the species generated from the epoxide (XXXVI) or the polyether (XXXVIII) suggests

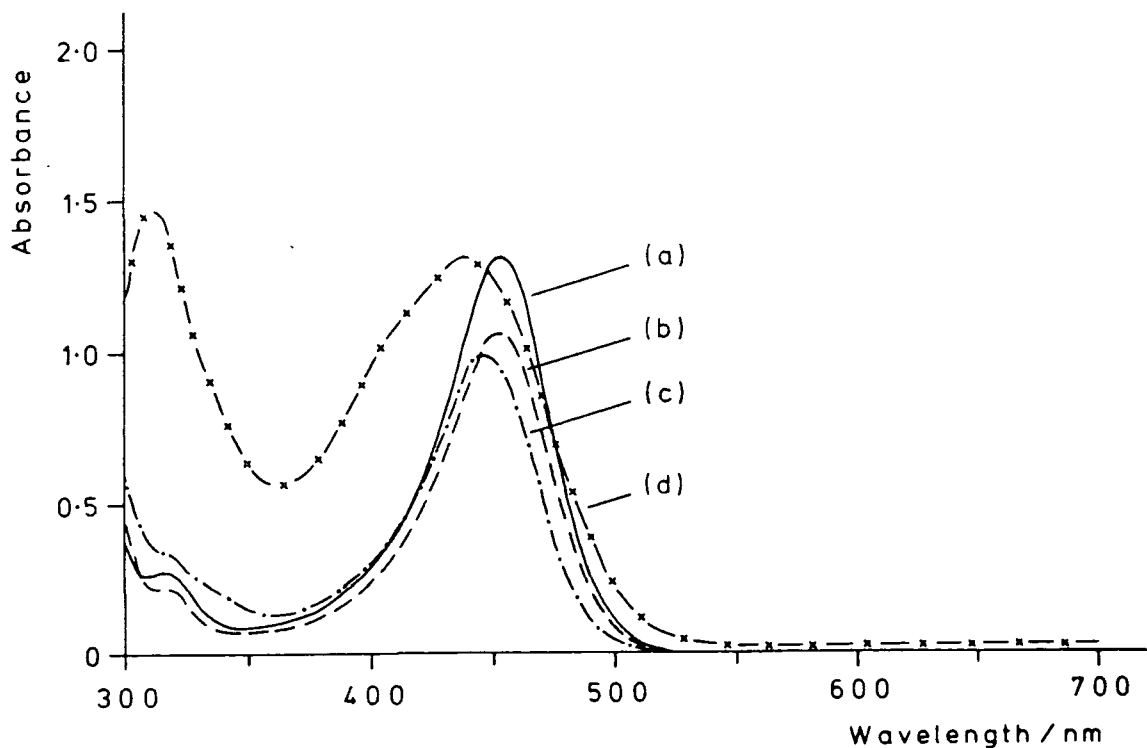
that the substituent on the oxygen atom affects the absorption characteristics of the carbonium ion formed. This would not be the case if a simple benzyl cation were being generated. A possible explanation is that the  $\sigma$ -complex is being formed which does not then undergo cleavage.

An attempt was made to obtain evidence for the formation of the benzyl cation by the action of acid on the polyether. A solution of the polymer (0.46g) in sulphuric acid (10 cm<sup>3</sup>) was cooled, ice (100g) added in portions and the solution neutralized using a dilute solution of sodium hydroxide. The neutralized solution was then washed several times with diethyl ether to remove any organic material. The ether washings were then concentrated, vacuum transferred to remove any involatile material and then further concentrated. GLC of the ether solution showed the presence of two components in minor amounts neither of which corresponded to benzylalcohol, an expected product of the hydrolysis of the benzyl cation if it were to be formed.

(B) Compound (XXXVII) and the Polyether (XXXIX)

Addition of (XXXVII) and the corresponding polyether to sulphuric acid resulted in orange/red coloured solutions with absorption maxima at 452 and 453nm respectively as shown by the UV/visible absorption spectra in Figure 6.15. Addition of the precursor phenol (XLI) to sulphuric acid yielded a similarly coloured solution with a main absorption maximum at 446nm as shown in Figure 6.15. Although phenethyl alcohol gave a red/orange coloured solution in sulphuric acid, a solid was also formed. However the solid could be filtered off and the UV/visible spectrum of the coloured solution recorded. As shown

FIGURE 6.15 UV/Visible Spectra in Concentrated Sulphuric Acid Solution of (XXXVII) (a), (XXXIX) (b), (XLI) (c) and phenethyl alcohol (d).

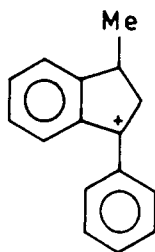


in Figure 6.15 a broad absorption maximum occurs at 438nm with a second sharper band at 312nm.

One might expect the coloured species generated from phenethyl alcohol in acid to be the phenethyl cation. Comparison of the absorption spectrum of phenethyl alcohol in sulphuric acid with those of the epoxide, polyether and precursor phenol in acid, indicates that the same species is possibly being generated from the latter compounds by the action of acid. The literature pertaining to this field, however, again suggests that the situation is more complex than one might expect.

Although several workers have assigned bands in the near UV or visible regions to the phenethyl cation, it is unlikely

that this carbonium ion is generated by the action of acid on the appropriate alcohol or alkene. It has been proposed that the species generated is an oligomeric carbonium ion<sup>17</sup> or the 1-methyl-3-phenylindane cation:<sup>18</sup>



It is asserted that this latter species results from the cyclization of unsaturated oligomers to give 1-methyl-3-phenylindane which then undergoes hydride ion abstraction to generate the cation. Various other carbonium ions can be generated from the protonation of 1-methyl-3-phenylindone depending on the conditions used, which may explain the differences in the absorption maxima quoted by other workers for what is supposedly the same species, the phenethyl cation.

Therefore it is possible that complex carbonium ions are generated from the trisubstituted bridging methane moiety of the epoxide, polyether and precursor phenol by the action of acid. However there is a slight, but significant difference between the absorption maximum of the coloured species generated from the precursor phenol and the species generated from the epoxide and polyether. This may be as a result of the formation of the  $\sigma$ -complex which does not then undergo cleavage as suggested in the previous section. It is interesting to note that the Russian worker could not detect phenol from the action of acid on (XLI).<sup>3</sup>

## 6.9 Preparation of Poly(benzyl) and Poly(phenethyl)

When benzyl alcohol on phenethyl alcohol are added to sulphuric acid, solids are formed which are assumed to be poly(benzyl) and poly(phenethyl) respectively.<sup>15</sup> It was decided to isolate the solids and obtain  $^{13}\text{C}$ -NMR spectra to compare with those of the model epoxides and polyethers irradiated in the presence of photoinitiator to determine whether such material is produced *via* benzyl and phenethyl cations formed as a result of the acidic nature of the initiating species.

### (A) Poly(benzyl)

Benzyl alcohol (2.0g) was added dropwise with cooling and rapid stirring to sulphuric acid (10 cm<sup>3</sup>). On addition of the benzyl alcohol a white solid formed. After being left stirring for 20 minutes, crushed ice (250g) was added and the excess sulphuric acid neutralized with a dilute solution of sodium hydroxide. As the solid was being filtered off it turned a light brown colour. The yield of the solid after drying under high vacuum was 1.6g. Infra-red spectroscopy, elemental analysis and  $^{13}\text{C}$  NMR spectroscopy were then used to characterize the solid.

The IR spectrum of the solid (Appendix 4, Spectrum No.12) shows a broad O-H stretching band at 3400 cm<sup>-1</sup> whilst the remainder of the spectrum is not inconsistent with the solid being poly(benzyl).

Elemental analysis gave 88.1% carbon and 6.6% hydrogen. For high molecular weight poly(benzyl) one would expect 93.3% carbon with 6.7% hydrogen. The analysis figures and IR spectrum would suggest that the material is of low molecular weight with hydroxyl end-groups.

Not surprisingly, if as seems likely, the solid is a branched polymer with methylene units linking aromatic rings the  $^{13}\text{C}$ -NMR spectrum is rather complex (Appendix 5, Spectrum No.17a). The general assignment of the resonances are given in Table 6.12.

TABLE 6.12 General Assignment of  $^{13}\text{C}$  Resonances in the Spectrum of Poly(benzyl)

Nucleus	Shift/ppm	Nucleus	Shift/ppm
Methylene carbons	38.08		128.28
	38.47		128.55
	38.87		128.66
	41.02		128.82
	41.43		129.48
Aromatic methine carbons	125.77	Quaternary aromatic carbons	130.40
	125.88		131.16
	126.39		138.76
	126.77		138.99
	126.94		140.50
	128.21		141.09

The DEPT spectrum (Appendix 5, Spectrum No.17b) was useful in assigning the resonances. The multiplicity of the resonances associated with the methylene carbons and aromatic carbons is consistent with the expected structure of polysubstituted aromatic rings linked by methylene groups. In addition the shift of the methylene carbons is consistent with them linking aromatic rings.



ment of the more intense ones being given in Table 6.13.

TABLE 6.13 General Assignment of the  $^{13}\text{C}$  Resonances in the Spectrum of Poly(phenethyl)

Nucleus	Shift/ppm	Nucleus	Shift/ppm
Methyl Carbons	15.04	Aromatic methine carbons	125.21
	15.34		125.83
	14.01		126.14
	21.87		126.45
	22.41		127.39
Methylene carbons	25.03		127.67
	28.27		128.20
Methine carbons	37.92		128.67
	43.96	Aromatic quaternary carbons	143.78
	44.34		143.91
	44.72		146.42
46.93			

The DEPT spectrum (Appendix 5, Spectrum No.18b) was useful for assigning the resonances in the spectrum.

The multiplicity of the resonances due to methyl and methine carbons associated with the bridging unit and the aromatic methine carbons is consistent with a branched polymer although the spread of shifts for the former carbons combined with the presence of resonances due to methylene carbons is indicative of some impurity or other product being present. The shift of the methine carbons is consistent with them being bridging units between aromatic rings.

## 6.10 Irradiation of the Model Epoxides and Polyethers in the Presence of Photoinitiator

### (A) Colouration of the Model Systems

#### (i) Compound (XXXVI) and the Polyether (XXXVIII)

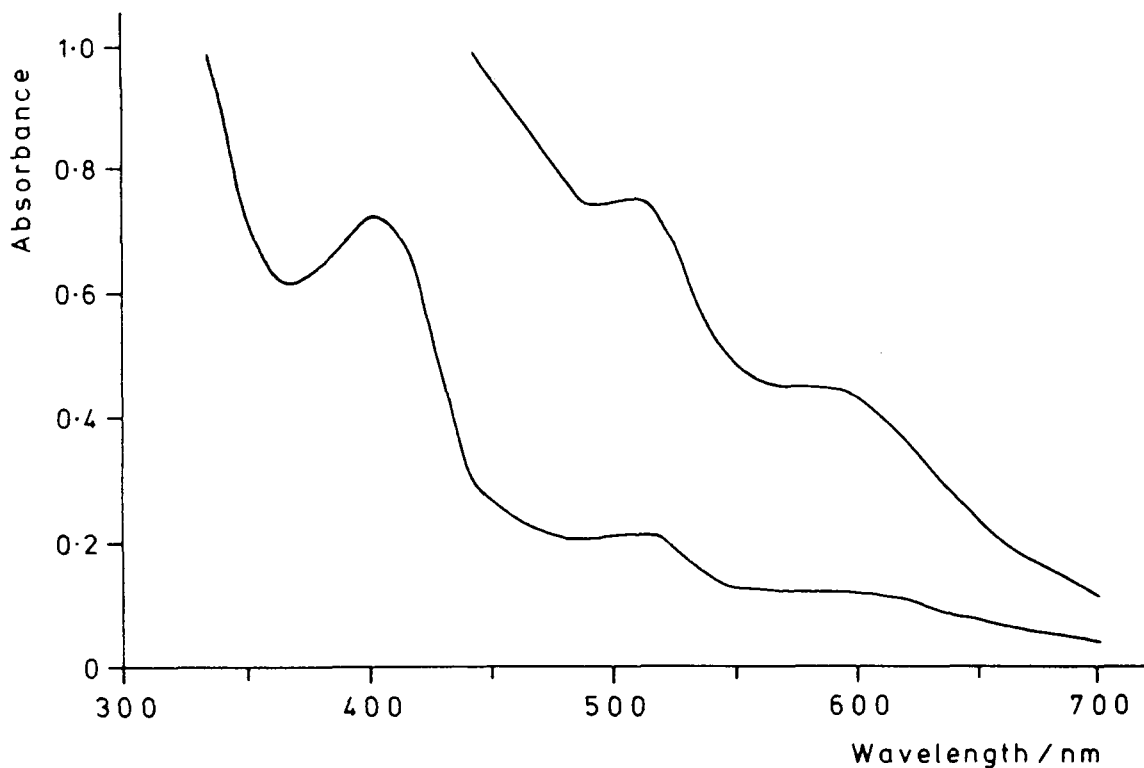
Films of (XXXVI) were prepared by dissolving the requisite amount of photoinitiator in the minimum amount of acetone, adding this solution to the epoxide and then spreading the mixture on polyethylene between pieces of "sellotape" that acted as barriers. Films of 100 $\mu$ m nominal thickness were prepared in this way. The excess acetone was allowed to evaporate and then any remaining acetone was removed under high vacuum.

Films prepared in this way containing various amounts of photoinitiator both polymerized and coloured on exposure to the 1.8kW lamp. After 1 pass the films showed a faint yellow colouration as would be expected from the colour of the acid solution of (XXXVI) but on further exposure a brown colour developed. This colouration did not fade significantly with time. Irradiation of the resin above resulted in neither polymerization nor colouration.

It was impossible to remove the films from the substrate to obtain UV/visible spectra because of their tackiness close to the substrate. However by dissolving the film in chloroform and filtering off an insoluble white solid which was identified as photoinitiator, it was possible to obtain an absorption spectrum. The ethanol used to stabilize chloroform was removed prior to its use by shaking with water and then distilling it onto molecular sieve. Figure 6.16 shows such a spectrum for a film of the epoxide containing a 3:1 molar ratio of epoxide

to initiator, given 20 passes under the 1.8kW source and dissolved in chloroform immediately after irradiation. An absorption maximum is observed at 400nm with weaker ones at 510 and 580nm.

FIGURE 6.16 UV/Visible Spectrum of a Chloroform Solution of (XXXVI) Irradiated in the Presence of Photoinitiator



Films of the polyether (XXXIX) containing photoinitiator were prepared as follows. The polymer was dissolved in chloroform whilst the photoinitiator was dissolved in acetone as no common solvent could be found. A portion of the polymer solution was spread on a glass plate and the solvent allowed to evaporate. A portion of the photoinitiator solution was then spread over the polymer film and the solvent allowed to evaporate. This was repeated several times to build up a film composed of layers of polymer and photoinitiator. Colour-

ation of films containing various amounts of photoinitiator prepared in this way occurred on exposure to the 1.8kW source. As with films of the epoxide, a faint yellow colouration was apparent after 1 pass but a brown colouration developed on subsequent exposure. No colouration was apparent when just the polymer was irradiated.

Thus a coloured species is generated on irradiation of (XXXVI) and the corresponding polyether in the presence of photoinitiator although it does not appear to be the same as that generated in acid solution. If the coloured species is a carbonium ion then it must be relatively stable.

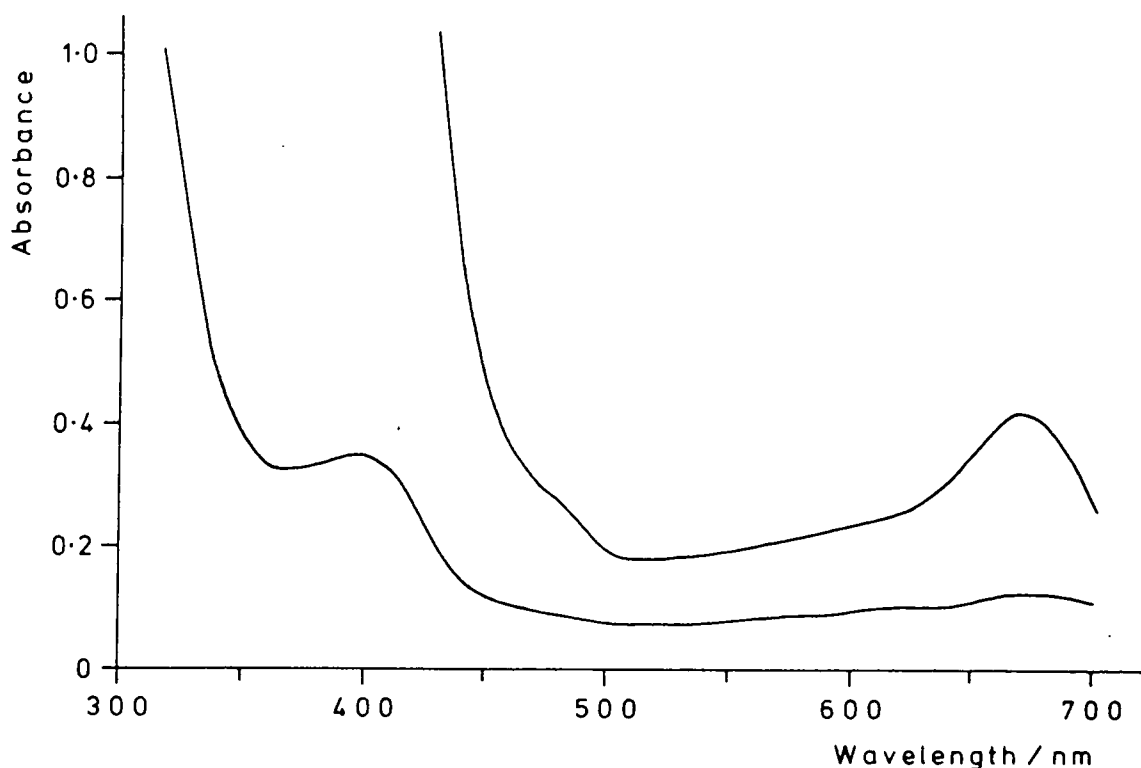
(ii) Compound (XXXVII) and the Polyether (XXXIX)

Films of (XXXVII) could not be prepared since it is a solid, however (XXVII) was mixed with photoinitiator and irradiated in the following manner. The requisite amounts of (XXXVII) and photoinitiator were dissolved in the minimum amount of acetone, the solution spread on polyethylene and the solvent allowed to evaporate slowly. Any residual solvent was then removed under high vacuum. Exposure of mixtures prepared in this way resulted in the transformation of the white powdery material to a glassy material with a faint red colouration apparent after 1 pass but then the development of a green colouration on further exposure. This colouration did not fade appreciably with time. Irradiation of the epoxide alone did not result in polymerization or the generation of coloured species.

It was again impossible to remove the film from the substrate to obtain a UV/visible spectrum so the procedure out-

lined previously was adopted. The spectrum of a chloroform solution of a mixture of (XXVII) (3 moles) and photoinitiator (1 mole) given 20 passes under the 1.8kW lamp is reproduced in Figure 6.17 and shows an absorption maximum at 397nm with a less intense one at 672nm.

FIGURE 6.17 UV/Visible Spectrum of a Chloroform Solution of (XXXVII) Irradiated in the Presence of Photoinitiator



Films of the polyether (XXXIX) containing photoinitiator were prepared in the manner described previously. Irradiation of such films containing various amounts of photoinitiator resulted in a faint red colouration after 1 pass and the development of a green colouration on subsequent exposure. Irradiation of the polymer alone did not result in colouration.

As with the previous system coloured species are generated on irradiation of (XXXVII) and the corresponding polyether in the presence of photoinitiator. Again if carbonium ions are responsible for this effect they must be relatively stable.

(B) GLC Analysis

(i) Compound (XXXVI)

A film of (XXXVI) (4.06g,  $1.69 \times 10^{-2}$  moles) containing photoinitiator (0.08g,  $2.0 \times 10^{-4}$  moles) was prepared on polyethylene by the method mentioned previously. The film was given 5 passes under the 1.8kW lamp to generate the brown colour, scraped from the substrate and placed in water. The sticky brown solid slowly turned white as it was stirred in the water. The organic material was then extracted into chloroform. The solution was then reduced in volume, vacuum transferred to remove any involatile material and then reduced further in volume. GLC analysis of this solution showed the presence of a number of components none of which corresponded to benzyl alcohol one of the expected products from benzyl cations.

The above experiment was repeated using a film containing a higher ratio of photoinitiator ( $0.26\text{g}$ ,  $6 \times 10^{-4}$  moles) to resin ( $1.48\text{g}$ ,  $6.2 \times 10^{-3}$  moles). Again there were several products detected but none of these corresponded to benzyl alcohol. One of the more abundant species present gave a mass spectrum consistent with it being iodobenzene.

A control experiment was carried out in which benzyl alcohol ( $4 \times 10^{-3}\text{g}$ ) was added to water and all the steps outlined above carried out. This amount of benzyl alcohol was

chosen on the arbitrary assumption that ~20% of the photoinitiator in the first experiment gave rise to benzyl alcohol. Under the sensitivity conditions used in the previous experiments, GLC quite clearly showed the presence of benzyl alcohol in the resulting chloroform solution.

(ii) Compound (XXXVII)

A mixture of (XXXVII) (1.04g,  $4.1 \times 10^{-3}$  moles) and photoinitiator (0.35g,  $8 \times 10^{-4}$  moles) was prepared in the manner outlined previously. The mixture was given 20 passes under the 1.8kW lamp. On placing the irradiated mixture in water, the green colour slowly disappeared. The sample was treated as those in the previous section and GLC showed the presence of two main components in ether extracts. From its retention time, one of the components corresponded to iodobenzene but the other did not correspond to phenethyl alcohol or styrene, potential products resulting from the generation of phenethyl cations.

(C)  $^{13}\text{C}$ -NMR Spectroscopic Analysis

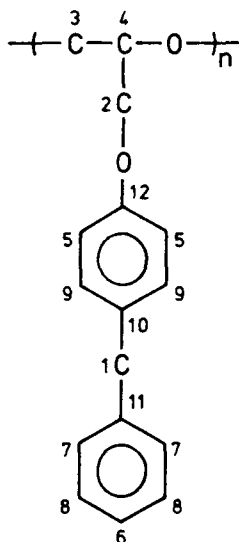
(i) Compound (XXXVI) and the Polyether (XXXVIII)

A film of (XXXVI) (0.48g,  $2.0 \times 10^{-3}$  moles) containing photoinitiator (0.29g,  $6.8 \times 10^{-4}$  moles) was prepared on polyethylene as in previous experiments. The film was given 20 passes under the 1.8kW lamp, dissolved in  $\text{CDCl}_3$  and the unphotolysed photoinitiator filtered off.

The main resonances in the  $^{13}\text{C}$ -NMR spectrum (Appendix 5, Spectrum No.19) occurred at similar shifts to those observed in the spectrum of the polyether (XXXVIII) prepared by the conventional polymerization of (XXXVI). Table 6.14 gives the

assignment of these resonances.

TABLE 6.14 Assignment of the Main Resonances in the  $^{13}\text{C}$ -NMR Spectrum of (XXXVI) Irradiated in the Presence of Photoinitiator



Nucleus	Shift/ppm	Nucleus	Shift/ppm
1	40.91	7	128.29
2	67.82	8	128.64
3	70.00	9	129.73
4	77.94	10	133.39
5	114.49	11	141.38
6	125.85	12	156.97

The relative intensities of the resonances due to the bridging and aromatic carbons do in some cases, especially the quaternary aromatic carbons, show significant differences from the relative intensities in the spectrum of the polyether prepared by conventional polymerization.

In addition to those tabulated above, other, generally small, resonances are present in the spectrum. Those at 44.61, 50.06, 68.75 and 133.88 ppm are possibly due to the presence of unreacted monomer. The resonance at 68.75 ppm might

also be connected with HH and TT linkages as might the small resonances between 70.90 and 72.50 ppm. Some deuterated impurity from the solvent is likely to be responsible for the resonances at 82.37, 82.72 and 83.08 ppm. Further resonances occur at 15.25, 30.00, 31.06<sup>\*</sup>, 31.44<sup>\*</sup>, 33.75<sup>\*</sup>, 45.19<sup>\*</sup>, 115.19, 118.75<sup>\*</sup>, 127.31, 132.43, 132.75, 135.11 and 137.38 ppm. Resonances occur at similar shifts to those marked with an asterisk in the spectrum of the polyether. There are also a number of small resonances associated with the main resonances.

There is no evidence of the presence of the known products of photoinitiator photolysis, namely, iodobenzene, biphenyl and fluorobenzene.<sup>4</sup> Also there is no conclusive evidence for the presence of benzyl alcohol or poly(benzyl) moieties, potential products of the generation of benzyl cations.

A film of the polyether (XXXVIII) (0.13g) containing photoinitiator (0.08g) was prepared on glass in the manner described previously. The film was given 20 passes under the 1.8kW lamp, removed from the substrate, dissolved in CDCl<sub>3</sub> and unphotolysed photoinitiator filtered off.

The <sup>13</sup>C-NMR (Appendix 5, Spectrum No.20) shows the expected resonances assignable to the polyether. The relative intensities of the resonances assigned to the polyether have changed significantly, the resonances at 115.41 and 129.71 for example, compared with the spectrum of untreated polyether and the resonances attributed to the quaternary aromatic carbons, particularly that at 133.25 ppm, have broadened. These changes are not generally consistent with those observed in the spectrum of the polyether prepared by the photoinitiated polymerization of (XXXVI) which may indicate that the differences are related to the conditions under which the spectra were recorded.

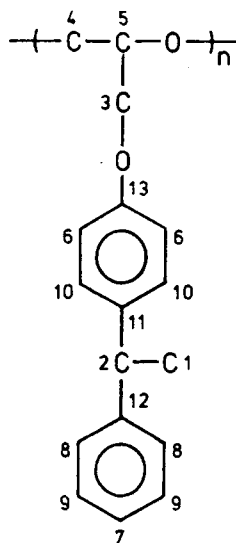
In addition to the resonances assigned to the polyether other, generally small, resonances are present. The resonances between 70.94 and 71.94 ppm occur in the spectrum of the untreated polyether as does the resonance at 127.31 ppm. Further resonances occur at 132.51, 132.68, 134.97 and 137.38 ppm with other small resonances associated with the main resonances. There is again no evidence of detectable amounts of the known products of photoinitiator photolysis nor of benzyl alcohol or poly(benzyl) moieties. Resonances with shifts close to those at 132.51, 132.68 and 134.97 ppm are observed in the spectrum of (XXXVI) irradiated in the presence of photoinitiator but not in the spectrum of the untreated polyether. Therefore these resonances might be connected with the coloured species generated by the action of the initiating species.

(ii) Compound (XXXVII) and the Polyether (XXXIX)

A mixture of (XXXVII) (0.36g,  $1.5 \times 10^{-3}$  moles) and photoinitiator were prepared on polyethylene by the method described previously. After being given 20 passes under the 1.8kW source, the material was removed from the substrate, dissolved in  $\text{CDCl}_3$  and unphotolysed photoinitiator filtered off.

The main resonances in the  $^{13}\text{C}$ -NMR spectrum (Appendix 5, Spectrum No.21) have similar shifts to those observed in the spectrum of the polyether (XXXIX) prepared by the conventional polymerization of (XXXVII). Table 6.15 gives the assignment of these main resonances.

TABLE 6.15 Assignment of the Main Resonances in the  $^{13}\text{C}$ -NMR Spectrum of (XXXVII) Irradiated in the Presence of Photoinitiator



Nucleus	Shift/ppm	Nucleus	Shift/ppm
1	21.94	6	114.38
2	43.81	7	125.79
3	68.00	8	127.41
4	69.69	9	128.20
	70.03	10	128.35
5	77.94	11	138.52
	78.14	12	146.63
	78.27	13	156.93

The relative intensities of the resonances associated with the bridging group and aromatic carbons do in one or two cases show significant differences from their relative intensities in the spectrum of the polyether prepared by conventional polymerization. Also the resonances at 138.52 ppm has broadened slightly.

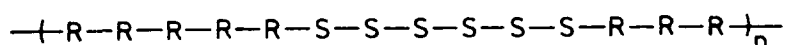
Other, generally small, resonances are present in addition to those tabulated above. The resonances at

68.69 ppm and between 70.43 and 72.50 ppm appear in the spectrum of untreated polyether and might be due to HH and TT linkages. Further resonances are observed at 15.00, 115.06, 116.19, 129.12, 129.44, 130.06 and 137.38 ppm. That at 15.00 ppm is also observed in the spectrum of the untreated polyether. Also as in the spectrum of the untreated polyether there are many small resonances associated with the main resonances. None of the above unattributed resonances appear to be connected with the known products of photoinitiator photolysis nor with three of the potential products of the generation of phenethyl cations, namely phenethyl alcohol, styrene, or poly(phenethyl) moieties.

It is interesting that there are three resonances associated with the main-chain methine carbons which have a similar relative intensity to the three resonances observed in the spectrum of the polyether (XXXIX) prepared by the conventional polymerization of (XXXVII). Similarly there are two resonances associated with the main-chain methylene carbons. In the case of the conventionally prepared polyether the multiplicity of these resonances and their relative intensities were attributed to the presence of atactic and isotactic polymer fractions.

There are two possible explanations for the apparent occurrence of atactic and isotactic material in the photoinitiated cationic polymerization of (XXXVII). Since the polymerization is carried out in the solid state, regions rich in either stereoisomer could form as the monomer is slowly deposited from solution. Thus polymer formed in these areas could be mostly isotactic. Alternatively a stereoblock polymer could be formed

as represented below:



This would require some degree of stereochemical control to be exerted over the addition of monomer, an effect observed in the polymerization of other mono- and disubstituted epoxides using catalysts not acting by a coordinate mechanism.<sup>10,19</sup> Such control has been attributed to the steric interaction between the substituents on the incoming monomer unit and the growing chain end. In this case interactions could favour the incorporation of monomer units of the same configuration as the previous monomer unit to join the polymer chain. An occasional failure of this control would give rise to a stereoblock polymer.

The presence of atactic and isotactic material is not readily apparent from the <sup>13</sup>C-NMR spectrum of the polymer of (XXXVI) prepared by photoinitiated cationic polymerization.

A film of the polyether (XXXIX) (0.26g), containing photoinitiator (0.15g) was prepared on glass by the method described previously. The film was given 20 passes under the 1.8kW lamp, removed from the substrate dissolved in CDCl<sub>3</sub> and unphotolysed photoinitiator filtered off.

The <sup>13</sup>C-NMR spectrum (Appendix 5, Spectrum No.22) shows the expected resonances due to the polyether. The relative intensities of the resonances due to the bridging group and aromatic carbons are, in some cases, markedly different from those observed in the spectrum of the untreated polyether. However the differences in the intensities are not generally consistent with those occurring in the spectrum of the polyether prepared by photoinitiated polymerization of (XXXVII).

A number of other, generally weak, resonances are apparent in the spectrum in addition to those assigned to the polyether. The resonances at 68.63 ppm and between 70.42 and 72.43 ppm appear in the spectrum of the untreated polyether and are probably due to HH and TT linkages. Other resonances are at 30.75, 31.22<sup>\*</sup>, 31.43<sup>\*</sup>, 32.23<sup>\*</sup>, 45.29<sup>\*</sup>, 129.31, 129.50, 130.16, 137.38 and 137.70<sup>\*</sup> ppm. The resonances marked with an asterisk occur at shifts similar to resonances observed in the spectrum of the untreated polyether. Other small resonances are also associated with the main resonances. There is no evidence of detectable amounts of the known products of photoinitiator photolysis nor of the presence of phenethyl alcohol, styrene or poly(phenethyl) moieties, three potential products resulting from the generation of phenethyl cations. It is noted that the resonances at 129.50 and 130.10 ppm also occur in the spectrum of (XXXVII) irradiated in the presence of photoinitiator and may therefore be connected with the species giving rise to the colouration. Also the resonance at 137.78 ppm occurs in the spectra of all four samples irradiated in the presence of photoinitiator and may be due to some product of photoinitiator photolysis.

### 6.11 Conclusions

The colouration of the DGEBA, DGEBF and epoxy novolac systems when photocationically cured can be ascribed with a reasonable degree of certainty to the formation of p-alkoxybenzylic cations. These species are produced by the protonation of the bridged aromatic moieties of the resins. In two

of the systems, the decay of the coloured species was found to result from three first-order or pseudo first-order processes which is not inconsistent with the proposed nature of the coloured species.

It was initially thought that the occurrence of such a process in the simpler model epoxide and polyether systems, chosen for their similarity to the structure of the resins, would generate products easily identifiable as resulting from the formation of benzylic cations. However it appears that the species generated by such a process in the model systems are more complex than originally envisaged and indeed no evidence for the formation of benzylic cations was obtained. The latter species lack the stabilizing influence of the p-alkoxy group of the species generated in the resin systems which greatly affects their chemistry. Coloured species were generated by the model compounds in acid solution or when irradiated in the presence of photoinitiator but since these species were unidentified the question remains as to whether they originate from the expected process or some other process. The species generated in solution appear to be different to those generated *via* photoinitiator photolysis indicating that a different process and/or final product takes precedence in the solid state. The stability of the species generated in the solid state suggests that they are not carbonium ions.

REFERENCES - CHAPTER SIX

1. V.F. Lavrushin, Doklady Akad.Nauk.SSSR, 86, 309 (1952); Chem.Abs. 47:2039c.
2. V.F. Lavrushin, Doklady Akad.Nauk.SSSR, 95, 809 (1954); Chem.Abs. 48:8650c.
3. V.F. Lavrushin and Z.N. Tarakhno, Zh.Organ.Khim. 1, 1642 (1965).
4. D.H. Williams and I. Fleming, "Spectroscopic Methods in Organic Chemistry", 2nd Edition, McGraw-Hill (1973).
5. H. Hart, W.L. Spliethoff and H.S. Eleuterio, J.Am.Chem.Soc., 76, 4547 (1954).
6. A. McKenzie and G.W. Clough, J.Chem.Soc., 103, 687 (1913).
7. F.R. Damont, L.M. Sharp and M. Schonhorn, J.Polym.Sci., Polym.Lett, B3, 1021 (1965).
8. E.J. Vandenberg, J.Polym.Sci., A1, 7, 525 (1969).
9. E.J. Vandenberg, Pure Appl.Chem., 48, 295 (1976).
10. C.C. Price, R. Spector and A.L. Tumolo, J.Polym.Sci., A1, 5, 407 (1967).
11. S. Inoue and T. Aida in "Ring-Opening Polymerization" Eds. K.J. Ivin and T. Saegusa, Vol.1, Elsevier, (1984).
12. A.L. Segre, F. Andruzzi and P.L. Magaganini, Macromol 16, 1207 (1983).
13. J.L. Koenig, "Chemical Microstructure of Polymer Chains", J.Wiley and Sons (1980).
14. H.H. Freedman in "Carbonium Ions", Ed. G.C. Olah, Wiley Interscience (1973).
15. R.L. Shriner and A. Berger, J.Org.Chem., 6, 305 (1941).
16. J.A. Grace and M.C.R. Symons, J.Chem.Soc., 958 (1958).
17. G.A. Olah, C.U, Pittman, R. Waack and D. Doran, J.Am.Chem.Soc., 88, 1488 (1966).
18. V. Bertoli and P.H. Plesch, Chem.Comm., 625 (1960).
19. C.C. Price, M.K. Akkoreddi, D.T. de Bonna and B.C. Furie, J.Am.Chem.Soc., 94, 3964 (1972).

## CHAPTER SEVEN

ATTEMPTS TO OBTAIN FLUORINATED SURFACES  
VIA THE SURFACE SEGREGATION OF  
SMALL AMOUNTS OF POLYFLUORINATED MONOMER  
ADDED TO LACQUERS OF CONVENTIONAL EPOXY RESIN

## 7.1 Introduction

Fluoropolymers offer the potential advantages of low surface energy, good chemical resistance, low coefficient of friction and good thermal stability. These properties, useful in a number of applications, stem from the high electron affinity, small atomic radius and low polarizability of fluorine. However the high cost of such materials restricts their applications to areas where such properties are essential and where a comparable performance cannot be achieved using less expensive polymers.

The desirable surface properties of fluoropolymers such as their ease of cleaning would be useful in several areas of surface coatings technology, for example, anti-fouling coatings. Since surface properties are determined by the nature and packing of the exposed species at the surface,<sup>1</sup> the bulk of such coatings need not be composed of fluoropolymer. Thus the surface properties associated with fluoropolymers might be achieved by having a hydrocarbon polymer with a surface rich in fluorinated moieties. Low surface free energy species have a tendency to migrate to the surface when incorporated into a suitable organic medium. This offers a potentially low cost route to obtaining a surface composed of fluorinated material.

Since photocurable systems only polymerize on exposure to light of a suitable wavelength it is, in principle, possible to prepare films containing small amounts of polyfluorinated monomer and leave them prior to irradiation for the fluorinated species to migrate to the surface. This approach, using photocurable systems offers two advantages over other systems.

Segregation takes place whilst the system is still mobile and should occur more rapidly, whilst the use of a monomeric species means that the fluorinated moiety is likely to be bound into the network on cure.

This chapter reports the results of attempts to obtain a fluorinated, low energy surface, by adding small amounts of polyfluorinated epoxide compounds to lacquers of conventional epoxy resin, mainly the DGEBA resin.

## 7.2 Surface Segregation of Low Surface Energy Species

The literature contains a number of studies showing that surface segregation of low surface free energy species does occur. For example, Zisman *et al* have investigated the surface segregation of small amounts of compounds containing acid or ester moieties with perfluoroalkyl chains added to polymers such as polystyrene, PS or PMMA.<sup>2,3</sup> It was found that the effectiveness of a particular additive in a polymer depended on its organophilic-organophobic nature, that is the balance between the compatibility and incompatibility of the additive with the polymer structure. The study did show that the addition of small amounts of fluorinated additives could produce a marked decrease in the surface energy and coefficients of friction of the polymers. The systems where surface segregation did occur also exhibited the property of self-healing, that is when damaged, the fluorinated surface could be regenerated by warming the film to encourage further migration of the additive.

As mentioned in Chapter Two, a surface active photoinitiator containing a perfluoroalkyl moiety has been used in free radical photocurable systems.<sup>4</sup> Using ESCA, the concentration of the photoinitiator at the film-air interface was found to increase as the viscosity of the coating decreased or the interval between application and irradiation increased. The photoinitiator was also found to migrate to the substrate-film interface.

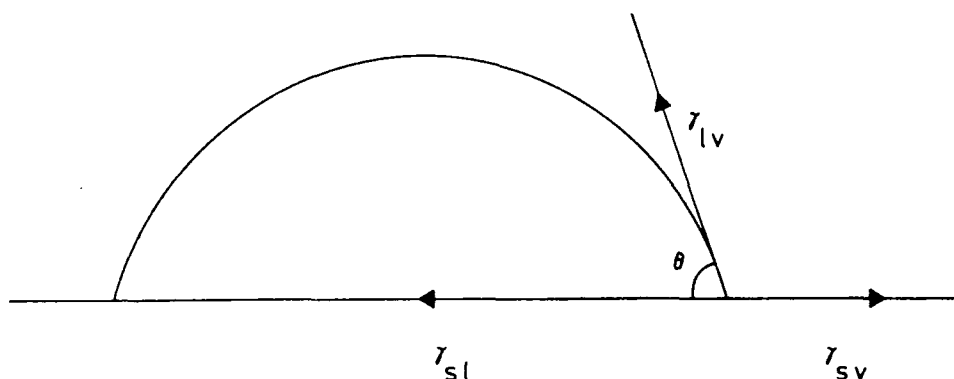
Surface segregation of the low energy components of polymer mixtures or block copolymers has also been observed<sup>5</sup> using surface energy measurements, ESCA and attenuated total reflectance infra-red spectroscopy. Using the surface sensitive infra-red spectroscopic technique, the surface of a mixture of poly-(dimethylsiloxane), PDMS, with a polyether-polyurethane type copolymer was found to be rich in the lower surface energy PDMS component.<sup>6</sup> The surface energy of a PDMS-PS block copolymer was found to be the same as that of pure PDMS and ESCA showed that the surface was mostly composed of PDMS.<sup>7</sup> Surface segregation of the PS component in a PS-poly(oxirane) block copolymer has been observed using ESCA although the difference in surface energy between the two components is quite small.<sup>8</sup> It was also found that the concentration of polystyrene in the surface was dependent on the solvent used to prepare the films.

### 7.3 Determination of the Surface Free Energy of Solid Polymers

Classically the surface energy of a solid may be defined as half the energy required to separate two unit areas of adjacent atomic planes to infinity in a vacuum.<sup>9</sup> The force of

attraction between atoms generally arises from short range dispersion forces but may also involve hydrogen bonding. The above definition is idealized and in practice it is very difficult, if not impossible, to directly determine the surface energy of a solid such as a polymer which has an important bearing, for example, the adsorption and adhesion properties of the surface. The indirect methods of measuring the surface energy of solids generally involve the determination of the wettability of the surface by various liquids of known surface tension. Wettability is quite readily defined by the contact angle,  $\theta$ , as shown in Figure 7.1.

FIGURE 7.1 Contact Angle of a Liquid Drop on a Solid



Two limiting cases are possible, either the liquid wets the surface totally and  $\theta=0^\circ$  or the liquid is totally non-wetting and  $\theta=180^\circ$ . In practice the latter case is never realized.

One of the first and possibly most successful approaches to determining the surface energy of solids was that developed by Zisman.<sup>1</sup> For a drop in equilibrium on a stress free surface the relationship, shown below, between the surface tensions at the liquid-vapour,  $\gamma_{lv}$ , solid-liquid,  $\gamma_{sl}$ , and solid-vapour,  $\gamma_{sv}$ , interfaces should hold:

$$\gamma_{sv} - \gamma_{sl} = \gamma_{lv} \cos\theta.$$

The contact angles of an homologous series of n-alkanes on various polymeric surfaces were measured and a linear relationship between  $\cos\theta$  and the surface tension of the liquid found for each surface. Extrapolation of the line to the point where  $\cos\theta = 1$ , *i.e.* the liquid just wets the surface totally, gives  $\gamma_{lv} = \gamma_{sv}$  assuming that  $\gamma_{sl}$  is zero. The value of  $\gamma_{lv}$  at which  $\cos\theta = 1$  was termed the 'critical' surface energy,  $\gamma_c$ , since it cannot be directly equated with the surface energy of the solid as  $\gamma_{sl}$  may not be zero when  $\cos\theta = 1$ .

Owens and Wendt<sup>10</sup> in an attempt to relate the contact angle of a liquid to the surface energy of a solid without the need for the unknown parameter  $\gamma_{sl}$  developed the following expression based on the work of Fowkes<sup>11</sup>:

$$1 + \cos\theta = 2 \sqrt{\gamma_s^d} \left( \frac{\sqrt{\gamma_1^d}}{\gamma_{lv}^d} \right) + 2 \sqrt{\gamma_s^h} \left( \frac{\sqrt{\gamma_1^h}}{\gamma_{lv}^h} \right)$$

The parameter  $\gamma_s^d$  is the surface energy of the solid due to dipole-dipole interactions whilst  $\gamma_s^h$  is the component of the surface energy resulting from H-bonding interactions. The parameters  $\gamma_{lv}^d$  and  $\gamma_{lv}^h$  are the corresponding components of the surface tension of the liquid, whilst  $\gamma_{lv}$  ( $= \gamma_{lv}^d + \gamma_{lv}^h$ ) is the overall surface tension of the liquid. The measurement of the contact angle of two liquids for which  $\gamma_{lv}$ ,  $\gamma_1^d$  and  $\gamma_1^h$  are known gives two simultaneous equations which can be solved for  $\gamma_s^d$  and  $\gamma_s^h$ . The overall surface energy of the solid,  $\gamma_s$ , is then given by the sum of the two components.

From contact angle measurements of water and methylene iodide, Owens and Wendt calculated the values of  $\gamma_s$  for various

polymers and compared them with values of  $\gamma_c$ . Although some objections to the method of the derivation of the above equation have been raised,<sup>12</sup> the values of  $\gamma_s$  are generally in reasonable agreement with values of  $\gamma_c$ .

In this work, the contact angles of liquids were measured by placing a 1-2 $\mu$ l drop of the liquid on the surface and measuring the height,  $h$ , and base,  $b$ , of the drop using a microscope equipped with a graticule. The contact angle,  $\theta$ , is then given by the following expression:

$$\theta = 2 \tan^{-1} \left( \frac{2h}{b} \right)$$

With some liquids the contact angle was found to decrease with time which was attributed to the effects of evaporation. Thus contact angles were measured immediately after application of the drop or followed with time and an extrapolated value of  $\theta$  corresponding to zero time obtained. Also for each surface and liquid,  $\theta$  was measured several times and an average taken.

The surface energies of commercial samples of polyethylene and polytetrafluoroethylene were estimated using the methods outlined above. The polymer samples were washed with detergent and water, rinsed thoroughly with distilled water and then left for several days under high vacuum over  $P_2O_5$ .

A plot of  $\cos\theta$  against the surface tension of a series of unpurified n-alkanes (heptane, octane, nonane, decane and hexadecane) on the polytetrafluoroethylene sample gave a good straight line from which a value of  $19 \pm 2 \text{ dyn cm}^{-1}$  for  $\gamma_c$  was obtained. This compares favourably with the literature value<sup>1</sup> of  $18 \text{ dyn cm}^{-1}$ . The n-alkanes could not be used to determine  $\gamma_c$  for the polyethylene sample since they wet the sample totally indicating that the value of  $\gamma_c$  must be above  $27.5 \text{ dyn cm}^{-1}$ .

A measure of  $\gamma_c$  for the polytetrafluoroethylene sample was made using a non-homologous series of liquids (water, glycerol, formamide, methylene iodide, benzonitrile, benzyl alcohol, n-hexadecane and n-decane) most of which were unpurified. The plot of  $\cos\theta$  against the surface tension of the series of liquids gave a good straight line with a  $\gamma_c$  value of  $14\pm 3$  dyn  $\text{cm}^{-1}$  which is lower than the literature value. Similarly  $\gamma_c$  for the polyethylene sample was measured using the above series of liquids with the exception of the two n-alkanes. The plot of  $\cos\theta$  against the surface tension of the liquids was not very good but gave a  $\gamma_c$  value of  $32\pm 4$  dyn  $\text{cm}^{-1}$  which is close to the literature value<sup>1</sup> of  $31$  dyn  $\text{cm}^{-1}$ .

Doubly distilled water and methylene iodide that had been vacuum transferred were used to estimate the surface energy,  $\gamma_s$ , of the two samples by the method of Owens and Wendt. The value of  $\gamma_s$  for the polytetrafluoroethylene sample was found to be  $16\pm 1$  dyn  $\text{cm}^{-1}$  which is lower than the literature value<sup>10</sup> of  $19$  dyn  $\text{cm}^{-1}$ . The value of  $\gamma_s$  for the sample of polyethylene was found to be  $31\pm 1$  dyn  $\text{cm}^{-1}$  which is again slightly lower than the literature value<sup>10</sup> of  $33$  dyn  $\text{cm}^{-1}$ .

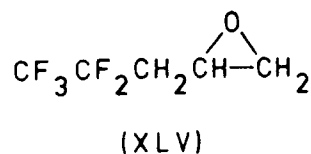
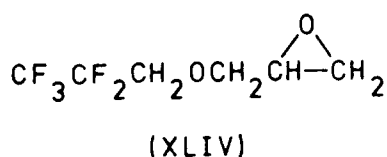
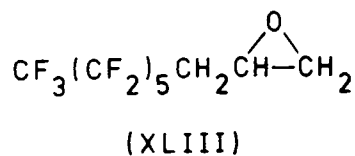
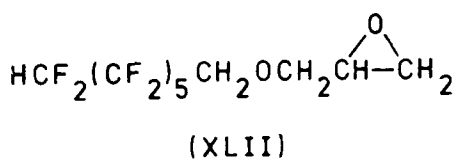
Thus, within the limits of the methods, the liquids and techniques adopted for the estimation of surface energies in this work give values in reasonable agreement to those quoted in the literature.

#### 7.4 Preparation of the Polyfluorinated Epoxides used in this Work

The work reported in the literature on poly- and perfluorinated epoxide compounds is quite extensive. Much of the

interest in fluorinated monoepoxides stems from their potential use as monomers for the preparation of linear fluorinated polyethers.<sup>13</sup> Also they may be used to obtain fluorinated surfaces by attachment *via* reaction of the oxirane ring with suitable functional groups on the surface.<sup>14</sup> Polyfluorinated diepoxide compounds have been synthesised for use in surface coatings since they give a cross-linked network on cure.<sup>15,16</sup> To obtain desirable surface properties the fluorine content of these resins must be high which makes their cost prohibitive.<sup>17</sup>

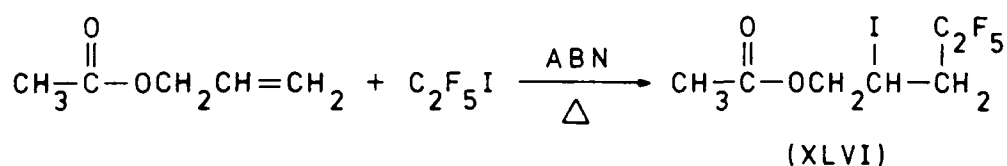
It was decided to synthesise simple monoepoxide compounds with polyfluoroalkyl chains for these surface segregation studies rather than the more complex diepoxy compounds mentioned above. The following compounds were used in this study:



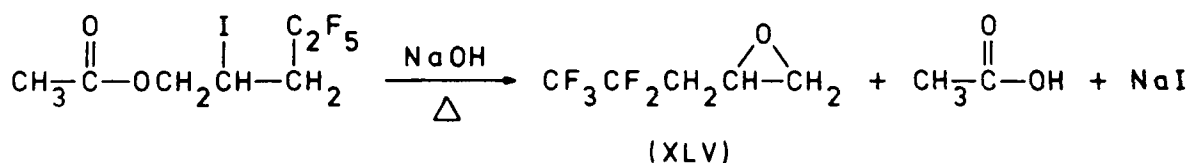
7,7,7,6,6,5,5,4,4,3,3,2,2-tridecafluoroheptyl oxirane (XLIII) (95%) was purchased from Prosynth. The IR spectrum of this material indicated that it was contaminated with a small amount of impurity containing hydroxyl and carbonyl moieties. The material was distilled through a Vigreux column under reduced pressure and the major fraction (72-75°C, 18-19mmHg) transferred under vacuum. The IR spectrum of the purified material (Appendix 4, Spectrum No.14) was consistent with the structure of (XLIII) and did not show any hydroxyl or carbonyl absorptions.

The compounds ( XLII ) and ( XLIV ) were synthesised by the simple reaction of the appropriate polyfluoroalcohol with ECH *via* the manner described previously for the synthesis of ( XXXVI ) ( Chapter 6, Section 6.6(A) ).

The compound ( XLV ) was prepared by the method of Brace<sup>18</sup> which involves the free radical reaction of allyl acetate and perfluoroethyl iodide in the presence of a small amount of azobisisobutyronitrile, ABN:



The intermediate ( XLVI ) is then treated with sodium hydroxide to generate the required product:



(A) Synthesis and Characterization of ((7,7,6,6,5,5,4,4,3,3,2,2-dodecafluoroheptyl)oxy)methyl oxirane (XLII)

The reaction of 7,7,6,6,5,5,4,4,3,3,2,2-dodecafluoroheptanol (164.8g, 0.50 moles) with ECH (231.5g, 2.50 moles) in the presence of sodium hydroxide (20.2g, 0.51 moles) and a catalytic amount of water was carried out under nitrogen in the manner described previously for the synthesis of ( XXXVI ) After the reaction mixture had been left stirring at 70°C for 5 hours, the white solid filtered off and the excess ECH removed using a rotary evaporator, the impure product was distilled through a Vigreux column under reduced pressure. The major

fraction boiled between 108-112°C (9-11 mm Hg) but GLC analysis of this material, taken to be the product, indicated that it contained some impurity. The fraction was then redistilled using a Fischer-Spaltrohr concentric ring distillation apparatus under vacuum. The major fraction (83.5g) boiled between 82-83°C (1.1 mm Hg) and GLC indicated that it contained a single component. This material was taken to be the product, giving a yield of 43%. After being transferred under vacuum using grease-free apparatus, the material was characterized using the usual techniques.

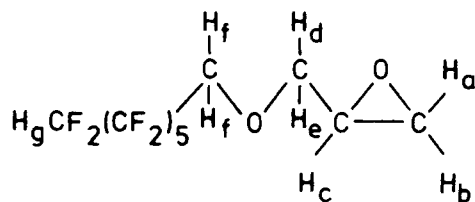
The IR spectrum of this material (Appendix 4, Spectrum No.15) was consistent with it being the desired product. Table 7.1 shows the assignment of a number of the bands in the spectrum.

TABLE 7.1 Assignment of Absorption Bands in the IR Spectrum of (XLII)

Frequency/cm <sup>-1</sup>	Assignment
3070-3010	Oxirane C-H stretch
2940-2860	Aliphatic C-H stretch
1485-1405	Aliphatic C-H bend
1210-1155	C-H stretch + aliphatic C-O-C asymmetric stretch
905	Oxirane ring stretch

The <sup>1</sup>H-NMR spectrum (Appendix 5, Spectrum No.23a) is also consistent with the material being the desired product. The assignments of the resonances are shown in Table 7.2. The spectrum with H<sub>c</sub> decoupled is also reproduced in Appendix 5, (Spectrum No. 23b).

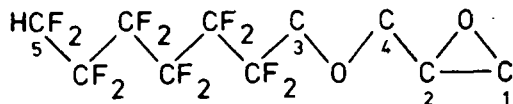
TABLE 7.2 Assignment of the  $^1\text{H}$  Resonances in the Spectrum of (XLII)



Proton	Shift/PPM	Splitting	Integration
$\text{H}_a$	$\delta_A = 2.58$	$\text{AB}_q$ $J_{a-b}^2 = 4.9\text{Hz}, J_{b-c}^3 = 4.2\text{ Hz}$	1
$\text{H}_b$	$\delta_B = 2.77$	$J_{a-c}^3 = 2.6\text{ Hz}$	1
$\text{H}_c$	3.13	Multiplet	1
$\text{H}_d$ or $\text{H}_e$	$\delta_A = 3.48$	$\text{AB}_q$ $J_{d-e}^2 = 11.9\text{Hz}, J_{d/e-c}^3 = 6.0\text{Hz}$	1
$\text{H}_e$ or $\text{H}_d$	$\delta_B = 3.93$	$J_{e/d-c}^3 = 2.5\text{ Hz}$	
$\text{H}_f$	4.00	Multiplet	3 ( $2\text{H}_f + \text{H}_{d/e}$ )
$\text{H}_g$	6.02	Triplet of triplets $J_{\text{H}_b-\text{F}}^2 = 51.9\text{ Hz}, J_{\text{H}_g-\text{F}}^3 = 5.2\text{Hz}$	1

The assignments of the resonances in the  $^{13}\text{C}$ -NMR Spectrum (Appendix 5, Spectrum No.24) of (XLII) are shown in Table 7.3.

TABLE 7.3 Assignment of the  $^{13}\text{C}$  Resonances in the Spectrum of (XLII)



Nucleus	Shift/PPM	Splitting
1	43.32	Singlet
2	50.21	Singlet
3	68.07	Triplet $J_{\text{C}_3-\text{F}}^2 = 25.6 \text{ Hz}$
4	73.12	Singlet
5	107.67	Triplet of triplets $J_{\text{C}_5-\text{F}}^1 = 254.6 \text{ Hz}, J_{\text{C}_5-\text{F}}^2 = 31.5 \text{ Hz}$
$-\text{CF}_2-$	104.51-118.68	Overlapping multiplets

Elemental analysis gave 30.4% carbon, 2.4% hydrogen and 56.1% fluorine which in the case of the fluorine analysis does not compare favourably with the expected composition of 30.9% carbon, 2.1% hydrogen and 58.8% fluorine. The mass spectrum (Appendix 6) was also consistent with the material being the desired product.

(B) Synthesis and Characterization of ((3,3,3,2,2-pentafluoropropyl)oxy)methyl oxirane (XLIV)

The reaction of 3,3,3,2,2-pentafluoropropanol (112.8g, 0.75 moles) with ECH (352.8g, 3.81 moles) in the presence of

sodium hydroxide (32.0g, 0.80 moles) and a catalytic amount of water was carried out in the manner described previously. After the reaction mixture had been left stirring for 8 hours at 70°C, the white solid was filtered off and the excess ECH removed by distillation under N<sub>2</sub> using a Vigreux column. From GLC, the distillate was thought to contain some product. The distillate and the residues were then redistilled under nitrogen using the Fischer-Spaltrôhr apparatus. The product fraction (51.0g) was collected between 144.5-144.7°C. This material was shown by GLC to be a single compound. The yield of this material was 33%. After transfer under vacuum as described in the previous section the material was characterized using the usual techniques.

The IR spectrum of the material (Appendix 4, Spectrum No.16) is consistent, it being the desired product. Table 7.4 shows the assignments of a number of bands in the spectrum.

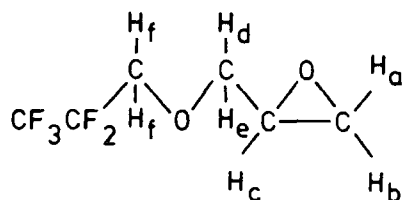
TABLE 7.4 Assignment of Absorption Bands in the IR Spectrum of (XLIV)

Frequency/cm <sup>-1</sup>	Assignment
3040-3000	Oxirane C-H stretch
2920	Aliphatic C-H stretch
1450-1350	Aliphatic C-H bend
1200-1100	C-F stretch + aliphatic C-O-C asymmetric stretch
900	Oxirane ring stretch

The <sup>1</sup>H-NMR spectrum of the material (Appendix 5, Spectrum No.25a) is also consistent with it being the desired product.

Table 7.5 shows the assignment of the resonances. The spectrum with  $H_c$  decoupled is also reproduced in Appendix 5, (Spectrum No.25b).

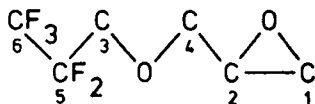
TABLE 7.5 Assignment of the  $^1H$  Resonances in the Spectrum of (XLIV)



Proton	Shift/PPM	Splitting	Integration
$H_a$	$\delta_A = 2.59$	$Ab_q$ $J_{a-b}^2 = 4.9 \text{ Hz}, J_{b-c}^3 = 4.2 \text{ Hz}$	1
$H_b$	$\delta_B = 2.78$	$J_{a-c}^3 = 2.7 \text{ Hz}$	1
$H_c$	3.4	Multiplet	1
$H_d$ or $H_e$	$\delta_A = 3.47$	$AB_q$ $J_{d-e}^2 = 11.9 \text{ Hz}, J_{d/e-c}^3 = 6.0 \text{ Hz}$	1
$H_e$ or $H_d$	$\delta_B = 3.94$	$J_{e/d-c}^3 = 2.6 \text{ Hz}$	
$H_f$	3.96	Multiplet	$\frac{3}{(2H_f + H_{f/e})}$

Table 7.6 gives the assignments of the resonances in the  $^{13}C$ -NMR spectrum (Appendix 5, Spectrum No.26a). The DEPT spectrum (Appendix 5, Spectrum No.26b) was useful in the assignment of the resonances.

TABLE 7.6 Assignment of the  $^{13}\text{C}$  Resonances in the Spectrum of (XLIV)



Nucleus	Shift/PPM	Splitting
1	42.83	Singlet
2	49.87	Singlet
3	67.38	Triplet $J_{\text{C}_3-\text{F}}^2 = 2.64 \text{ Hz}$
4	72.88	Singlet
5	112.94	Triplet of quartets $J_{\text{C}_5-\text{F}}^1 = 254.2 \text{ Hz}, J_{\text{C}_5-\text{F}}^2 = 37.1 \text{ Hz}$
6	118.61	Quartet of triplets $J_{\text{C}_6-\text{F}}^1 = 285.3 \text{ Hz}, J_{\text{C}_6-\text{F}}^2 = 35.0 \text{ Hz}$

Elemental analysis gave 35.2% carbon, 3.1% hydrogen and 45.6% fluorine which compares favourably with the expected composition of 35.0% carbon, 3.4% hydrogen and 46.1% fluorine. The mass spectrum of the material (Appendix 6) was consistent with it being the desired product.

(C) Synthesis and Characterization of 3,3,3,2,2-pentafluoropropyl oxirane (XLV)

The allyl acetate used in this preparation was distilled

under nitrogen onto molecular sieve prior to its use. ABN (4.1g, 0.025 moles) and allyl acetate (75.8g, 0.76 moles) were placed in a cylindrical, high pressure, steel reaction vessel of 1100 cm<sup>3</sup> capacity. Perfluoroethyl iodide (185.4g, 0.75 moles) was then transferred under vacuum into the cooled vessel. The vessel was then heated slowly using a furnace in an isolation cell, the temperature of the reaction mixture being monitored by means of a thermocouple placed in a well in the bottom of the vessel. As the temperature of the mixture approached 50-60°C it started to rise quite rapidly peaking at ~85°C indicating that an exothermic reaction had taken place. The reaction mixture was then left at ~77°C for 5 hours.

After allowing the vessel to cool, it was opened and the clear, pale green reaction mixture filtered to remove the small amount of insoluble material. Distillation of the reaction mixture using a Vigreux column under reduced pressure yielded a main fraction (194.2g) between 82-85°C (6-7 mm Hg). Combined GLC-mass spectral analysis indicated that this material was mostly the desired intermediate (XLVI) giving a yield of ~75%.

The intermediate (XLVI), (193.2g, 0.56 moles) was placed, along with diethyl ether (150 cm<sup>3</sup>), in a 500 cm<sup>3</sup> round bottom, three-neck flask equipped with a mechanical stirrer/nitrogen inlet, condenser and thermometer. A small portion of the sodium hydroxide (42.9g, 1.1 moles) was added and the mixture gently warmed to initiate reaction. Further portions of the sodium hydroxide were then added at intervals to keep the diethyl ether refluxing. After addition of the sodium hydroxide the mixture was refluxed for a further 7 hours.

The reaction mixture was filtered to remove the white precipitate that had formed. Distillation of the filtrate using a Vigreux column under nitrogen yielded a minor fraction boiling between 78-81°C, which combined GLC-mass spectroscopic analysis indicated was mainly the desired product. This material was then redistilled under nitrogen using the Fischer-Spaltrohr apparatus giving a fraction (20.9g) boiling between 67-69°C. GLC analysis of this fraction indicated that it was the desired product with a very small amount of diethyl ether present. After being transferred under vacuum to remove any grease, the material was characterized using the usual techniques.

The IR spectrum of the material (Appendix 4, Spectrum No.17) is consistent with it being the desired product. Table 7.7 shows the assignment of a number of the bands present in the spectrum.

TABLE 7.7 Assignment of Absorption Bands in the IR Spectrum of (XLV)

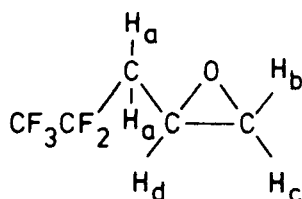
Frequency/cm <sup>-1</sup>	Assignment
3060-3010	Oxirane C-H stretch
2930	Aliphatic C-H stretch
1480-1315	Aliphatic C-H bend
1200	C-F stretch
905	Oxirane ring stretch

The <sup>1</sup>H-NMR spectrum of the material (Appendix 5, Spectrum No.27) is consistent with it being the desired product. Table 7.8 shows the assignment of the main resonances.

A small resonance present at 7.34 ppm is attributable to CHCl<sub>3</sub> whilst the small quartet and triplet resonances at 3.48

and 1.20 ppm are attributable to diethyl ether. Small resonances at 2.14 and 1.86 ppm are of unknown origin.

TABLE 7.8 Assignment of the  $^1\text{H}$  Resonances in the Spectrum of (XLV)



Proton	Shift/ppm	Splitting	Integration
H <sub>a</sub>	2.29	Multiplet	2
H <sub>b</sub>	$\delta_A = 2.56$	AB <sub>q</sub> $J_{b-c}^2 = 4.8 \text{ Hz}$ , $J_{c-d}^3 = 4.4 \text{ Hz}$	1
H <sub>c</sub>	$\delta_B = 2.85$	$J_{b-d}^3 = 2.5 \text{ Hz}$	1
H <sub>d</sub>	3.18	Multiplet	1

Table 7.9 shows the assignment of the resonances in the  $^{13}\text{C}$ -NMR spectrum of the material (Appendix 5, Spectrum No.28).

TABLE 7.9 Assignment of the  $^{13}\text{C}$  Resonances in the Spectrum of (XLV)

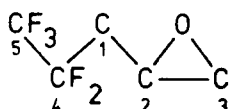


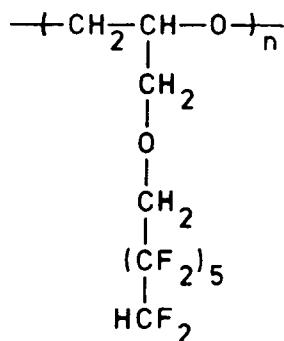
TABLE 7.9 (contd.)

Nucleus	Shift/ppm	Splitting
1	35.10	Triplet $J_{C_1-F}^2 = 21.8 \text{ Hz}$
2	44.71	Triplet $J_{C_2-F}^3 = 5.3 \text{ Hz}$
3	45.62	Singlet
4	115.05	Triplet of quartets $J_{C_4-F}^1 = 252.5 \text{ Hz}, J_{C_4-F}^2 = 38.6 \text{ Hz}$
5	119.07	Quartet of triplets $J_{C_5-F}^1 = 284.8 \text{ Hz}, J_{C_5-F}^2 = 35.6 \text{ Hz}$

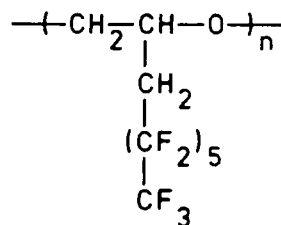
Elemental analysis gave 34.6% carbon, 3.1% hydrogen and 53.3% fluorine which compared reasonably with the expected composition of 34.1% carbon, 2.8% hydrogen and 54.0% fluorine. The mass spectrum of the material (Appendix 6) was consistent with it being the desired product.

#### 7.5 Characterization and Surface Energy Measurements of Polymers Prepared by the Conventional Cationic Polymerization of Monomers (XLII) and (XLIII)

The compounds (XLII) and (XLIII) were polymerized using the  $AlEt_3/0.5 H_2O$  catalyst system to give polymers of the following type:



(XLVII)



(XLVIII)

The polymerizations were carried out in the same way as the polymerization of compounds (XXXVI) and (XXXVII) using the same catalyst solution.

The surface energy measurements were carried out using the series of n-alkanes and the water/methylene iodide method. Glass slides that had been cleaned with nitric acid, rinsed thoroughly with distilled water and then dried were coated using solutions of the polymer. After allowing the solvent to evaporate the coated slides were stored under high vacuum for several days.

(A) Polymerization of (XLII) and the Characterization of the Resulting Polyether (XLVII)

Compound (XLII) (6.6g, 0.017 moles) was polymerized using the  $\text{AlEt}_3/0.5 \text{ H}_2\text{O}$  catalyst solution ( $1.7 \text{ cm}^3$ ,  $[\text{monomer}]/[\text{AlEt}_3] = 20$ ). The polymerization mixture was left stirring for 6 hours at  $80^\circ\text{C}$ . Methanol ( $40 \text{ cm}^3$ ) was then added which did not precipitate the polymer. The solution was filtered to remove a small amount of insoluble material and chloroform added to the filtrate to precipitate the polymer. The polymer was dissolved in methanol and reprecipitated a further two times and then dried under high vacuum. The yield of the white, very viscous oil was 4.4g (66%).

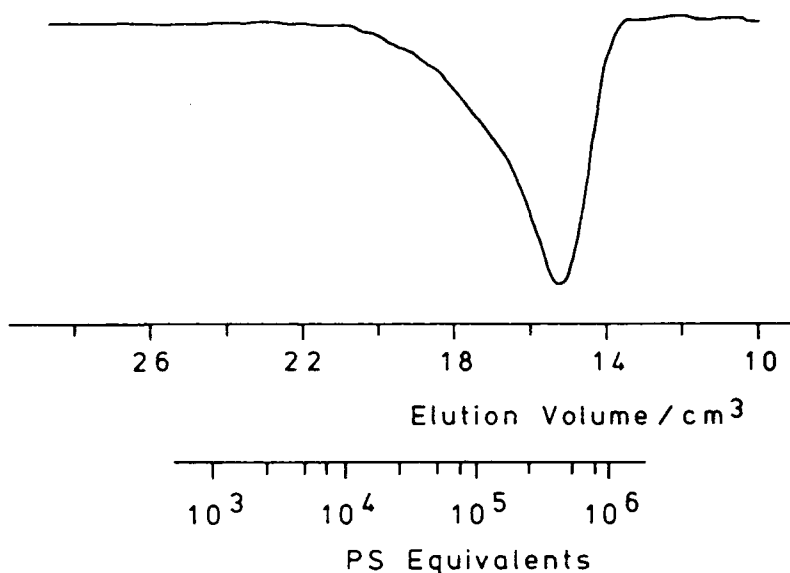
The I R spectrum of the polymeric material (Appendix 4, Spectrum No.18) shows many absorption bands at similar frequencies and with similar relative intensities to those observed in the spectrum of the monomer. However the spectrum of the polymer contains a number of differences consistent with it being a polyether with hydroxyl end groups. There is a weak, broad, hydroxyl absorption at  $\sim 3440 \text{ cm}^{-1}$ . The absorptions attributable to the oxirane C-H stretching mode ( $3070\text{-}3010 \text{ cm}^{-1}$ ) and the oxirane ring stretching mode ( $905 \text{ cm}^{-1}$ ) are not present. Absorptions attributable to aliphatic C-H stretching mode ( $2920\text{-}2880 \text{ cm}^{-1}$ ) have increased in relative intensity as has the absorption in the  $1240\text{-}1080 \text{ cm}^{-1}$  region which is assignable to aliphatic C-O-C stretching mode.

Elemental analysis gave 30.7% carbon, 2.2% hydrogen and 59.2% fluorine which is in very good agreement with the expected composition of 30.9% carbon, 2.1% hydrogen and 58.8% fluorine.

The polymer was also analysed using GPC, with THF as the solvent, as for polymers (XXXVI) and (XXXVII). The GPC trace reproduced in Figure 7.2 gives the following:

$$\begin{array}{ll} \bar{M}_n = 1.28 \times 10^5 & \bar{M}_w = 3.12 \times 10^5 \\ \bar{DP}_n = 329 & \bar{M}_w/\bar{M}_n = 2.4 \end{array}$$

Thus the polymer is of a reasonably high molecular weight.

FIGURE 7.2 GPC Trace of Polymer (XLVII)

Unlike polymers (XXXVI) and (XXXVII) prepared in a similar way, this polymer does not exhibit a bimodal molecular weight distribution although there is a tail on the low molecular weight side of the peak. The low molecular weight material observed with previous polymers may not be formed when monomer (XLII) is polymerized or alternatively it may be formed but is removed during the purification of the polymer.

Glass slides were coated using a solution of the polymer in methanol for the surface energy measurements. The plot of  $\cos\theta$  against the surface tension of the series of n-alkanes gave a reasonable straight line and a  $\gamma_c$  value of  $19 \pm 3 \text{ dyn cm}^{-1}$ . The water/methylene iodide method yielded a  $\gamma_s$  value of  $15 \pm 2 \text{ dyn cm}^{-1}$  which is lower than the value of  $\gamma_c$ . However the measurements indicate that the surface energy is quite low being of the order of that of polytetrafluoroethylene.

(B) Polymerization of (XLIII) and the Characterization of the Resulting Polyether (XLVIII)

Compound (XLIII) (8.0g, 0.021 moles) was polymerized

using the  $\text{AlEt}_3/0.5 \text{ H}_2\text{O}$  catalyst solution ( $2.7 \text{ cm}^3$ , [monomer]/ $[\text{AlEt}_3] = 16$ ). The polymerization mixture was left stirring for 5 hours at  $85^\circ\text{C}$ . Methanol ( $40 \text{ cm}^3$ ) was then added which precipitated the polymer. After washing the polymer several times with methanol it was further purified by reprecipitation from perfluoro-2-butyl THF using carbon tetrachloride as the non-solvent. The fluorinated solvent was used as no common solvent could be found. The yield of the dirty yellow coloured, very viscous oil was 4.04g (51%) after being dried under high vacuum.

The IR spectrum of the polymeric material (Appendix 4, Spectrum No.19) shows many absorption bands at similar frequencies and with similar relative intensities to those present in the spectrum of the monomer. The spectrum of polymer does however exhibit a number of differences consistent with it being a polyether with hydroxyl end-groups. There is a weak, broad, hydroxyl absorption at  $\sim 3400 \text{ cm}^{-1}$ . The absorptions attributable to the oxirane C-H stretching mode ( $3070\text{-}3010 \text{ cm}^{-1}$ ) and the oxirane ring stretching mode ( $900 \text{ cm}^{-1}$ ) are not present. Absorptions attributable to the aliphatic C-H stretching mode ( $3900 \text{ cm}^{-1}$ ) have increased in relative intensity as has the absorption in the  $1120\text{-}1020 \text{ cm}^{-1}$  region which is assignable to the aliphatic C-O-C stretching mode.

Elemental analysis gave 28.5% carbon, 1.1% hydrogen and 65.3% fluorine which is in good agreement with the expected composition of 28.7% carbon, 1.3% hydrogen and 65.7% fluorine.

Unfortunately the polymer could not be analysed using GPC as it was not soluble in THF.

Glass slides were coated using a solution of the polymer in perfluoro-2-butyl THF for the surface energy measurements. The plot of  $\cos\theta$  against the surface tension of the series of n-alkanes gave a reasonable straight line and a  $\gamma_c$  value of  $13\pm 3 \text{ dyn cm}^{-1}$  whilst the water/methylene iodide method gave a value of  $12\pm 1 \text{ dyn cm}^{-1}$ . Both values are in reasonable agreement and are somewhat lower than for polymer (XLVII). This may be attributed to the presence of a  $-\text{CF}_3$  group and the higher fluorine content.

#### 7.6 Addition of the Polyfluorinated Epoxides to Lacquers of Conventional Epoxy Resin

Unless otherwise stated films of  $100\mu\text{m}$  nominal thickness were prepared on polyethylene using a draw-down block. The films thus prepared contained approximately 2% photoinitiator and 1% w/w acetone with the remainder comprising, in most cases, the DGEBA resin alone or a mixture of the DGEBA resin and the polyfluorinated epoxides. The films were given 2 passes under the 1.8kw source and then stored for 24 hours prior to the contact angle measurements being carried out. Unless otherwise stated the measurements were carried out on the free surface (top surface) using the water/methylene iodide method to give  $\gamma_s$  values.

##### (A) Effect of Low Concentrations of (XLII) on the Surface Energy of Films

The values of  $\gamma_s$  for both the top surface and the surface adjacent to the substrate (bottom surface) were determined for films containing 0%, 2% and 5% w/w (XLII). The films containing (XLII) were either irradiated immediately after application or left for 4 hours.

TABLE 7.10 Values of  $\gamma_s$  for Films Containing  
0%, 2% and 5% w/w (XLII)

% w/w (XLII)	Time left prior to cure/hrs	$\gamma_s/\text{dyn cm}^{-1}$	
		Top	Bottom
0	0	48±1	42±1
2	0	43±2	43±1
	4	43±2	43±1
5	0	41±1	45±1
	4	39±1	38±1

From Table 7.10, the value of  $\gamma_s$  for the bottom surface of the film containing no (XLII) appears to be significantly lower than that for the top surface. The value of  $\gamma_s$  for the top surface of the film containing 2% w/w (XLII) is lower than that of the film containing none of this compound and  $\gamma_s$  shows a further slight decrease when 5% w/w (XLII) is used. There is no decrease in  $\gamma_s$  for the top surfaces of the films containing (XLII) if they are left prior to irradiation. The values of  $\gamma_s$  for the bottom surface of films containing (XLII) indicate that it is not segregating to the film-substrate interface. If segregation of (XLII) to the top surface were to be occurring then one would expect the value of  $\gamma_s$  to approach that of the polymer (XLVII). The measurement of  $\gamma_s$  for the substrate surface adjacent to the films showed that it was not significantly different from that for a pristine sample.

The series of n-alkanes were found to wet the top surfaces of the films totally indicating that  $\gamma_c$  is greater than 27.5 dyn  $\text{cm}^{-1}$ . An estimate of  $\gamma_c$  for the top surfaces of the films was made using a non-homologous series of liquids (water, glycerol, methylene iodide, benzonitrile, benzyl alcohol, glycol and

formamide). This gave a value of  $44 \pm 3$  dyn  $\text{cm}^{-1}$  for the film containing no (XLII) and values of  $39 \pm 2$  and  $38 \pm 1$  dyn  $\text{cm}^{-1}$  for the films containing 5% (XLII) left for 0 and 4 hours prior to irradiation.

An attempt was made to aid the surface segregation of (XLII) by reducing the viscosity of the DGEBA system using the reactive diluent (XX). Films were prepared from lacquers of the DGEBA resin containing 15% (XX) along with 5% w/w (XLII). The films containing (XLII) were left for 0 or 45 minutes prior to cure. The values of  $\gamma_s$  were similar to those obtained previously and there was no evidence of the surface segregation of (XLII) in the film left prior to irradiation.

Unfortunately it was found that increasing the temperature at which films were stored prior to cure reduced the effectiveness with which the lacquers wet the polyethylene. For example films prepared from lacquers of the DGEBA resin containing 2% and 5% (XLII) could only be left for 8 and 16 minutes respectively at a temperature of  $58^\circ\text{C}$ , before they started breaking up into droplets. The  $\gamma_s$  values for these films were found to be no different to the values for control films left at room temperature.

It was hoped that the use of a high surface energy substrate, steel, would encourage surface segregation of (XLII). However films prepared on mild steel panels from a lacquer of the DGEBA resin containing 5% w/w (XLII) and left for 0 or 12 hours prior to irradiation showed similar values of  $\gamma_s$  which were close to those reported previously.

The surface segregation of (XLII) in the epoxy novolac system was also investigated. Films were prepared from lacquers

containing 2% and 5% w/w (XLII) and left for 0 or 5 hours. Both lacquers also contained 13% w/w toluene. The values of  $\gamma_s$  measured for the films cured immediately after application were slightly lower than the value for a film containing none of the fluorinated epoxy. However when left for 5 hours the  $\gamma_s$  values were found to be similar to that obtained in the film containing no (XLII).

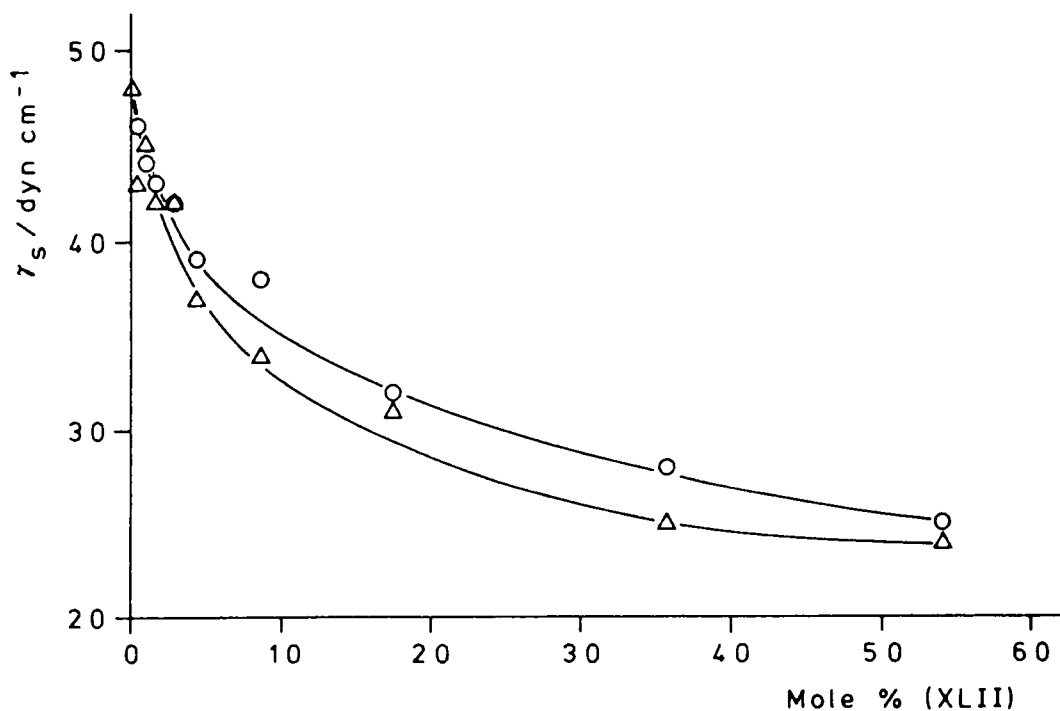
It appears that surface segregation of (XLII) is not occurring although the presence of small amounts of this compound do result in a decrease in the value of  $\gamma_s$  and it was also noted that the presence of (XLII) in such small amounts increased the lacquers' ability to wet the substrate. The non-surface segregation of (XLII) could be a result of its good compatibility with the resin or alternatively be related to the aggregation of molecules of (XLII) to form micelles with interiors composed of polyfluoroalkyl chains and the exteriors of oxirane rings. This latter possibility was investigated by using an electron microscope to examine fracture surfaces of films of DGEBA lacquers containing 0, 2 or 5% w/w (XLII). No evidence for the formation of micelles was observed, only crazing of the surfaces.

(B) Effect of Increasing the Concentration of (XLII) on the Surface Energy of Films

Films of lacquers containing up to 60% w/w (XLII) were prepared using the 'sellotape' technique and left for 0 or 4 hrs. prior to irradiation. A film containing 85% w/w (XLII) was found not to gel on irradiation and a film containing 97% w/w (XLII) was found to be still mobile and tacky even after prolonged irradiation.

Figure 7.3 shows a plot of  $\gamma_s$  as a function of the mol % of (XLII) present for films cured immediately after application. The value of  $\gamma_s$  decreases quite markedly as the concentration of (XLII) rises to 20 mole % and then shows a less pronounced decrease as the concentration is increased further, perhaps eventually becoming similar to the value of  $\gamma_s$  for the polymer (XLVII). The values of  $\gamma_s$  for films left for 4 hours prior to cure tend to be slightly higher than the values exhibited by films cured immediately after application for  $\gamma_s$  exhibits the same behaviour as the concentration of (XLII) increases as is also shown in Figure 7.3.

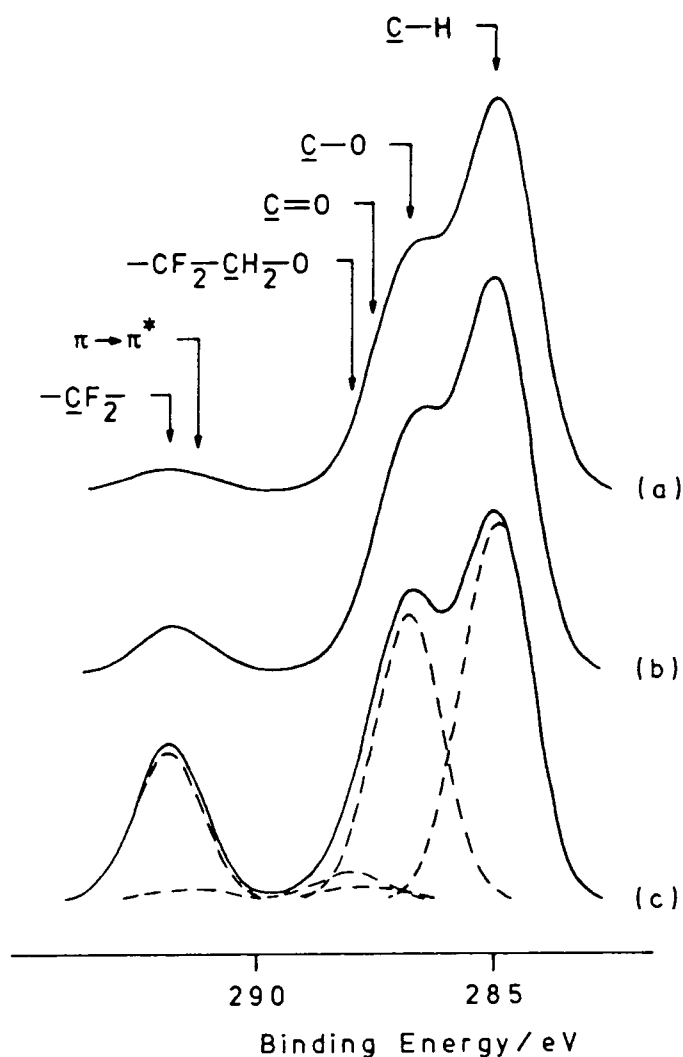
FIGURE 7.3 Decrease of  $\gamma_s$  as the Concentration of (XLII) Increases ( $\Delta$ , Films left 0 Hrs;  $\circ$ , Films left 4 Hrs.)



The results again indicate that surface segregation is not occurring although a significant reduction of  $\gamma_s$  can be achieved by increasing the concentration of (XLII).

An ESCA analysis was also carried out on a number of the films. Figure 7.4 shows the  $C_{1s}$  core level spectra of the films containing 1.7, 8.6 and 35.6 mol % (XLII) cured immediately after application. Similar spectra were obtained for the corresponding films left 4 hours prior to irradiation.

FIGURE 7.4  $C_{1s}$  Core Level Spectra as a Function of the Concentration of (XLII) (a, 1.7; b, 8.6; c, 35.6 mol %)



The two component peaks at 288.15 and 292.00 eV are attributable to  $CF_2-CH_2-O$  and  $-CF_2-$  moieties respectively and, as expected, increase in intensity as the concentration of (XLII) increases. The  $F_{1s}$  signal was also found to increase in intensity as the concentration of (XLII) increased and no signal due to  $PF_6^-$  could be detected (see Appendix 2).

The F/C atom ratio was determined from both the  $C_{1s}$  core level spectra and the  $F_{1s}/C_{1s}$  intensity ratio and compared with the expected value from the lacquer composition. Table 7.11 gives the results as a function of the concentration of (XLII) and the interval between application and irradiation.

TABLE 7.11 F/C Ratios from the  $C_{1s}$  Core Level Spectra (a) and  $F_{1s}/C_{1s}$  Intensity Ratios (b) as a Function of the Concentration of (XLII)

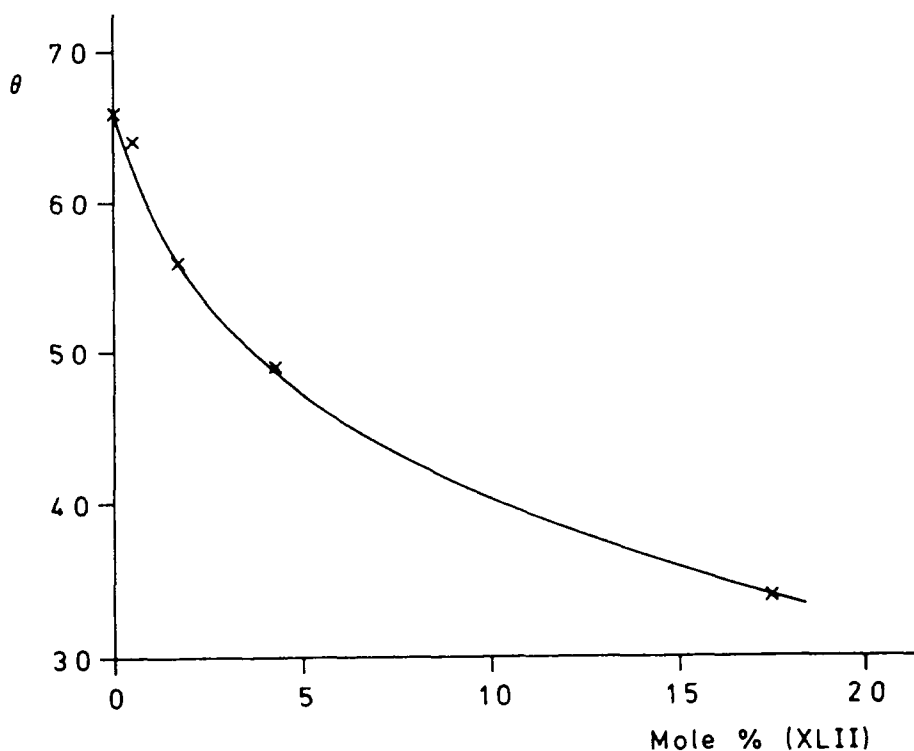
Mol % of (XLII)	Time left prior to cure /hrs.	F/C ratio		Expected F/C ratio
		(a)	(b)	
1.7	0	0.034	0.050	0.010
	4	0.038	0.043	
8.6	0	0.110	0.137	0.053
	4	0.094	0.136	
35.6	0	0.340	0.433	0.265
	4	0.340	0.435	

As expected the experimental F/C ratios increase with increasing concentration of (XLII). Both the experimental ratios however, are significantly greater than the expected value for each concentration of (XLII) and although the magnitude of the difference increases as the concentration of (XLII) increases, the proportionate increase in fluorine at the surface diminishes. This would suggest that there is a limited surface segregation of (XLII) which occurs as soon as the film is applied to the substrate since leaving films for 4 hours does not result in a significant change in the F/C ratio. Quite why the surface segregation is limited and does not progress further to give a F/C ratio of  $\sim 1.2$  corresponding to a surface composed of (XLII) is unclear.

Comparison of the experimental F/C ratios in Table 7.11 determined from the  $C_{1s}$  core level spectra and  $F_{1s}/C_{1s}$  intensity ratios shows that the latter gives a higher F/C ratio than the former. A plausible explanation for this observation, bearing in mind the shallower sampling depth for fluorine than for carbon, is that the concentration of (XLII) increases towards the surface which, if correct, provides further evidence of segregation.

It was mentioned previously that the addition of (XLII) increased the ability of lacquers to wet the substrate. Figure 7.5 in which the contact angle of lacquers on polyethylene is plotted against the mole % of (XLII) present, illustrates this point. As can be seen the contact angle,  $\theta$ , decreases and hence the ability of the lacquer to wet polyethylene increases as the concentration of (XLII) increases.

FIGURE 7.5 Decrease of the Contact Angle of Lacquers on Polyethylene as the Concentration of (XLII) Increases



(C) Effect of Low Concentrations of (XLIII) Alone or with (XLII) on the Surface Energy of Films

Lacquers containing 2 or 5% w/w (XLIII) were prepared and found to be cloudy. Attempts to prepare films from the lacquers were unsuccessful because of the incompatibility of (XLIII) with the DGEBA resin. Reducing the amount of (XLIII) to 0.6% w/w resulted in a clear lacquer from which films could be prepared. Unfortunately such films began to break up into droplets after  $\sim 20$  minutes. However the value of  $\gamma_s$  ( $40 \pm 1 \text{ dyn cm}^{-1}$ ) for such a film left 20 minutes before irradiation was slightly lower than the value ( $45 \text{ dyn cm}^{-1}$ ) for a film cured immediately after application indicating that a limited degree of surface segregation might be occurring.

In order to overcome the incompatibility of (XLIII) it was decided to prepare lacquers containing both (XLIII) and (XLII) in the hope that the latter would act as a wetting agent. Lacquers containing 5% (XLII) with 1% or 2% w/w (XLIII) were found to be clear and gave good films. Increasing the concentration of (XLIII) relative to (XLII) resulted in the problem of incompatibility reappearing.

Films of the above composition were prepared and  $\gamma_s$  measured as a function of the substrate and interval between application and irradiation. Table 7.12 shows the results.

It appears from the results in Table 7.12 that a limited degree of surface segregation of low surface energy material does occur and that the initial and final value of  $\gamma_s$  is dependant on the concentration of (XLIII) but not the substrate. The final values of  $\gamma_s$  obtained do not however reach those of either polymer (XLVII) or (XLVIII).

TABLE 7.12  $\gamma_s$  Values of Films Containing both (XLIII) and (XLII)

% w/w (XLIII)	% w/w (XLII)	Substrate	Time left prior to cure/hrs.	$\gamma_s$ /dyn cm <sup>-1</sup>
1	5	Polyethylene	0	37±2
			8	31±2
			72	32±3
2	5	Polyethylene	0	32±1
			48	25±1
2	5	Steel	0	34±1
			48	26±2

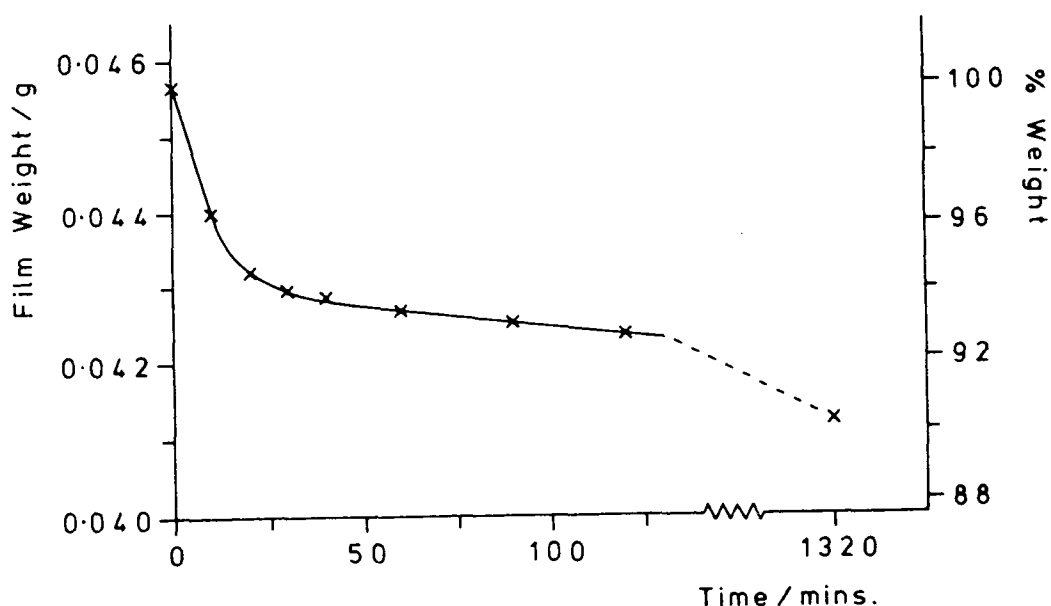
(D) Effect of Low Concentrations of (XLIV) Alone or with (XLII) on the Surface Energy of Films

In view of the relatively unsuccessful attempts to obtain a polyfluorinated surface using (XLII) and (XLIII) it was decided to prepare and use compounds (XLIV) and (XLV) in the hope that these smaller species would show a greater propensity for surface segregation.

Films containing 2% and 5% w/w (XLIV) were prepared, but unfortunately they began to break up into droplets after only 5-10 minutes. Unlike previous systems, a film cured immediately after application showed a value of  $\gamma_s$  similar to those of a film containing no fluorinated additive. Films containing 1% (XLIV) with 5% (XLII) were prepared and left for 0, 10, 20 minutes and 4 hours before being irradiated. The values of  $\gamma_s$  for the films did not vary significantly and were similar to that of a film containing 5% w/w (XLII).

The above results indicate that the presence of (XLIV) has no effect on the surface energy of films. It was then thought that the volatility of (XLIV) might result in its rapid loss from films. A film containing 10% (XLIV) with 5% w/w (XLII) was prepared and its weight followed with time. As Figure 7.6 shows, there is a rapid weight loss over the first 10-20 minutes amounting to ~6% of the initial weight of the film. After 22 hours the weight loss amounts to ~10% of the initial weight of the film.

FIGURE 7.6 Weight Loss of a Film Containing 10% (XLIV) with 5% w/w (XLII) as a Function of Time



Thus it is likely that the volatility of (XLIV) is responsible for its lack of effect. The loss of (XLIV) will be exacerbated when irradiating films due to the heat emitted by the 1.8kW source.

(E) Effect of Low Concentrations of (XLV) Alone or with (XLII) on the Surface Energy of Films

Lacquers containing 2% and 5% w/w (XLV) were prepared and found to be clear. Films were prepared from such lacquers and left for 0 or 30 minutes prior to irradiation. The values of  $\gamma_s$  for these films did not vary significantly and were similar to that of a film containing no fluorinated additive. Films were prepared containing 2% (XLV) with 5% w/w (XLII) and left for 0, 30 minutes and 4 hours prior to irradiation. The values of  $\gamma_s$  for the films did not vary significantly and were comparable to that of a film containing 5% w/w (XLII) alone.

It appears that the presence of (XLV) has no effect on the surface energy of the films. As in the case of (XLIV) this lack of effect may be attributed to the volatility of (XLV).

REFERENCES - CHAPTER SEVEN

1. W.A. Zisman, *Adv.Chem.Ser.*, 43, 1 (1964).
2. R.C. Bowers, N.L. Jarvis and W.A. Zisman, *Ind.Eng. Chem.Prod.Res.Dev.*, 4, 86 (1965).
3. N.L. Jarvis, R.B. Fox and W.A. Zisman, *Adv.Chem.Ser.*, 43, 317 (1964).
4. A. Hult and B. Ranby, *A.C.S. Polym.Preprints*, 25, 329 (1984).
5. G.L. Gaines, *Macromols.*, 14, 208 (1981).
6. J.A. Gardella, G.L. Grobe, W.L. Hopson and E.M. Eyring, *Anal.Chem.*, 56, 1169 (1984).
7. D.T. Clark, J. Peeling and J.M. O'Malley, *J.Polym.Sci., Polym.Chem. Ed.*, 14, 543 (1976).
8. H.R. Thomas and J.J. O'Malley, *Macromols.*, 12, 323 (1979).
9. E.H. Andrews and N.E. King in "Polymer Surfaces", Eds. D.T. Clark and W.J. Feast, Wiley-Interscience (1978).
10. D.K. Owens and R.C. Wendt, *J.Appl.Polym.Sci.*, 13, 1741 (1969).
11. F.M. Fowkes, *Adv.Chem.Ser.*, 43, 99 (1964).
12. Y. Lipatov and A. Feinerman, *Adv.Coll.Sci., Int.Sci.*, 11, 195 (1979).
13. P. Tarrant, G.G. Allison and K.P. Barthold, *Fluor.Chem. Revs.*, 5, 77 (1971).
14. S.A. Reines, *U.S.Pat.* 3,707,483 (1972).
15. J.G. O'Rear and J.R. Griffith, *A.C.S.Div.Org.Coat.Plast. Tech., Lett.*, 33, 657 (1973).
16. J.G. O'Rear, J.R. Griffith and S.A. Reines, *J.Paint.Tech.*, 43, 113 (1971).
17. D.E. Field, *J.Coat.Tech.*, 48, 43 (1976).
18. N.O. Brace, *J.Org.Chem.*, 27, 3033 (1962).

APPENDIX ONE

EXPOSURE OF THE UV CURABLE SYSTEMS

TO SUNLIGHT

The aim of the experiment described below was to determine whether the UV curable DGEBA and epoxy novolac systems would cure on exposure to sunlight under favourable conditions. A representative of Camrex kindly agreed to take some samples on a visit to Saudi Arabia and carry out some simple experiments.

The lacquer of the DGEBA resin contained 97.0% resin, 2.0% photoinitiator and 1.0% w/w acetone whilst that of the epoxy novolac resin contained 84.0% resin, 13.0% toluene, 2.0% photoinitiator and 1.0% w/w acetone. Films of 200µm nominal thickness were prepared on mild steel panels using the "sellotape" technique and treated as follows.

- (a) Films were exposed in the shade at an air temperature of 30°C.
- (b) One half of films were shielded and the other half exposed to direct sunlight at an air temperature of 37°C.

Films exposed as in (a) were found to be tack-free within 3 hours of being exposed. The unshielded halves of films exposed as in (b) were found to be tack-free after 20 minutes whilst the shielded halves were still soft and tacky after this period but became tack-free later. On their return to the U.K. the average hardness of the films were measured using the microhardness tester and compared with values for equivalent samples irradiated for 45 minutes, 9 cm from the 100W source.

The results in Table A1.1 show that the films exposed in the shade or to direct sunlight exhibit a hardness similar to films exposed to the 100W source. Undoubtedly the relatively high air temperatures will have aided the cure of the films but these results show that longer wavelength UV light present

TABLE A1.1 Hardness of Films Exposed to Sunlight

Conditions of exposure	Indentation / $\mu\text{m}$	
	Films of the DGEBA lacquer	Films of the epoxy novolac lacquer
(a)	13.9	15.0
(b)		
Exposed half	13.9	14.7
Shielded half	44.2	36.5
45 minutes, 9 cm from 100W source	13.9	15.7

in sunlight ( $\lambda > \sim 300\text{nm}$ ) leads to the cure of the photocurable systems. In addition to the above observations it was also noted that lacquers of the photocurable systems in glass containers gelled and became tack-free after  $\sim 3$  days when left in the laboratory at an air temperature of  $17\text{-}21^\circ\text{C}$ .

APPENDIX TWO

DETECTION OF  $\text{PF}_6^-$  AT THE SURFACE OF FILMS

---

IRRADIATED UNDER VARIOUS CONDITIONS

When carrying out the investigation into the surface photo-oxidation of the DGEBA and aliphatic diglycidyl ether systems using ESCA, the presence of fluorine at the surface from the hexafluorophosphate anion of the photoinitiator was also investigated.

(A) Films of the DGEBA System

Examination of both the top and bottom surfaces of films cured using the 1.8kW source showed an absence of fluorine. No detectable amount of fluorine was found at the surface of films cured with the 'pyrex' filter in place or after prolonged irradiation of films with the fluorescent lamp. Films cured by irradiation with the 100W source did have fluorine at the surface and the table below shows the  $F_{1s}/C_{1s}$  intensity ratios measured.

TABLE A2.1  $F_{1s}/C_{1s}$  Ratios measured in Films of the DGEBA System Cured using the 100W Lamp

Irradiation time/mins.	$F_{1s}/C_{1s}$ Ratio	
	Films irradiated with unfiltered light	Films irradiated with filtered light
3	0.008	0.008
8	0.010	0.006
13	0.011	0.005
20	0.017	0.005
30	0.015	0.008
45	0.013	0.006

From the lacquer compositions used, a  $F_{1s}/C_{1s}$  ratio in the region of 0.009 would be expected assuming the fluorine is present as  $PF_6^-$ . Therefore the values in Table A2.1 for the films irradi-

iated with the full output of the lamp tend to be similar to or greater than the expected value whilst the value for films irradiated with longer wavelength light tend to be lower than expected. It is difficult to rationalize the above observations. One could suggest, for example, that the slower cure of films irradiated with the 100W lamp allows the photoinitiator to segregate to the surface before a degree of cross-linking restricting mobility is reached and that the higher surface energy of an oxidized surface resulting from irradiation with the full output of the lamp must aid this process since films left for 4 hours prior to irradiation with the 1.8kW lamp showed no fluorine at the surface due to  $\text{PF}_6^-$ . However it is difficult to understand why  $\text{PF}_6^-$  is initially absent from the surface.

(B) Films of the Aliphatic Diglycidyl Ether System

Fluorine was detected at the surface of films of this system cured using the 1.8kW source, containing both 3.8 and 1.9% photoinitiator, although in the latter case the intensity of the signal was just about on the limits of detection. The Table below shows  $F_{1s}/C_{1s}$  intensity ratios measured in the films containing 3.8% photoinitiator.

TABLE A2.2  $F_{1s}/C_{1s}$  Ratios Measured in Films of the Aliphatic Diglycidyl Ether Containing 3.8% Photoinitiator

Number of Passes	2	3	5	10	20
$F_{1s}/C_{1s}$	0.013	0.013	0.013	0.008	0.011

The values in Table A2.2 are all significantly lower than the value of  $\sim 0.021$  expected from the lacquer composition even allowing for 12 mol% of the monoglycidyl ether. The  $F_{1s}/C_{1s}$  ratio

in the films containing 1.9% w/w photoinitiator were found to be of the order of 0.004 which is again lower than the expected value of 0.011. Similar  $F_{1s}/C_{1s}$  ratios were found in the bottom surfaces of films examined to those in the top surfaces for films cured on polyethylene. One might interpret the results as being indicative of the segregation of some impurity to the surface, decreasing the relative amount of fluorine but in view of the results from the DGEBA system, it cannot be ruled out that the actual amount of fluorine is much lower and that a loss of carbon through the formation of volatile products is occurring to give the measured  $F_{1s}/C_{1s}$  ratio. One further interesting observation is that the top surface of a film cured on glass containing 3.7% photoinitiator showed a similar  $F_{1s}/C_{1s}$  ratio in the top surface to the films in Table A2.2 whilst the bottom surface showed a significantly higher ratio of 0.022 which may indicate that the relative amount of fluorine at the bottom surface is dependent on the substrate.

APPENDIX THREE

INSTRUMENTS AND APPARATUS

### Differential Scanning Calorimetry (DSC)

This was carried out using a Perkin-Elmer DSC-2 Differential Scanning Calorimeter. The instrument was temperature calibrated using the melting point of a standard indium sample. Samples were sealed in aluminium pans and placed in the sample holder which was flushed continuously with nitrogen.

### Distillation Apparatus

The final purification of liquid compounds prepared in the course of this work was generally carried out using a Fischer-Spaltrohr HMS 500 concentric ring distillation apparatus. The column has a very low hold up and ~90 theoretical plates.

### Electron Microscopy (EM)

Samples, coated with gold, were examined using a Cambridge Instruments S 600 Scanning Electron Microscope.

### Electron Spectroscopy for Chemical Applications (ESCA)

ESCA spectra were recorded using a Kratos ES 300 Electron Spectrometer in conjunction with a Kratos DS 300 data acquisition and curve fitting system. A magnesium X-ray source and a take-off angle of  $30^\circ$  were employed.

### Electron Spin Resonance (ESR)

Spectra were recorded using a Varian V-4502-15 X-band Spectrometer.

### Elemental Analysis

For C and H analyses, a Perkin-Elmer CHN 240 Analyser was used. The fluorine content was determined by fusion with

potassium and then titration with sodium hydroxide. Phosphorous analysis was carried out spectrophotometrically after conversion to a vanadomolybdenophosphate complex. The analysis for iodine was carried out by combusting the compound in oxygen to liberate free iodine which was then quantified by titration with sodium thiosulphate.

#### Gas Liquid Chromatography (GLC)

A Pye-Unicam GCD equipped with a 152m x 4mm bore glass column packed with 10% (w/w) silicone elastomer on celite was used. A nitrogen flow rate of  $\sim 20 \text{ cm}^3 \text{ min}^{-1}$  and a flame ionization detector were used. In addition analyses were also carried out using a Hewlett Packard 5890 chromatograph equipped with a 25m x 0.2 mm bore glass column internally coated with cross-linked methylsilicone and a flame ionization detector.

#### GLC - Mass Spectroscopy

This was carried out using two systems. A Pye 104 Gas Chromatograph, equipped with a similar column to that used with the Pye-Unicam GCD, coupled to a VG Micromass 12 Chromatograph or alternatively a Hewlett-Packard Chromatograph similar to that described above coupled to a VG Analytical 7070E Spectrometer.

#### Gel Permeation Chromatography (GPC)

A Perkin-Elmer 601 Liquid Chromatography Apparatus equipped with three PL gel columns ( $10^5$ ,  $10^3$  and  $500\text{\AA}$ ) supplied by Polymer Laboratories Ltd. was used. Samples, dissolved in THF, were passed through filters of 10 and  $0.5\mu\text{m}$  pore size. A Knauer Differential Refractometer was used as the detector.

### Hardness Measurements

A Wallace Micro-Indentation Tester was used for such measurements.

### Infra-Red Spectroscopy (IR)

Infra-red spectra of compounds used in this work were recorded on Perkin-Elmer 457 or 577 Grating Infra-Red Spectrophotometers. Quantitative measurements of epoxide consumption were carried out using a Perkin-Elmer 377 Grating Infra-red Spectrophotometer whilst the measurements of bulk photo-oxidation were carried out using the PE 577 instrument.

### Mass Spectroscopy (MS)

Mass spectra were recorded using a VG Analytical 7070E instrument. For chemical ionization, isobutane was used as the carrier gas.

### Nuclear Magnetic Resonance (NMR)

Unless otherwise stated, spectra were recorded through the SERC services at Newcastle and Edinburgh Universities. At Newcastle, spectra were recorded on a Brüker WM 300 WB Spectrometer operating at 300 MHz for  $^1\text{H}$  nuclei and 75 MHz for  $^{13}\text{C}$  nuclei. At Edinburgh, spectra were recorded on a Brüker WH 360 Spectrometer operating at 360 MHz for  $^1\text{H}$  nuclei and 91 MHz for  $^{13}\text{C}$  nuclei. All spectra recorded with the samples were dissolved in  $\text{CDCl}_3$  using an internal TMS standard.

### Thermo-Gravimetric Analysis (TGA)

A Stanton Redcroft TG 750 was used for the analyses reported in this thesis. Samples were heated at a rate of  $10^\circ\text{C min}^{-1}$  under nitrogen.

### Thermo-Mechanical Analysis (TMA)

A Stanton Redcroft TMA 691 was used in the penetrometry mode with a  $1\text{mm}^2$  tip on the quartz probe. Generally a load of 50g was applied to the probe and the samples were heated at  $5^\circ\text{C min}^{-1}$  in air.

### Thermopile Detector

This detector, used to measure light intensities, was purchased from Applied Photophysics and exhibits linear sensitivity over a 200-800nm range.

### UV/Visible Spectroscopy

UV/visible spectra were recorded on a Pye-Unicam SP8-100 Ultraviolet Spectrophotometer. When following the disappearance of the coloured species present in some systems after cure, the sample compartment of the instrument was maintained at  $25\pm 1^\circ\text{C}$ .

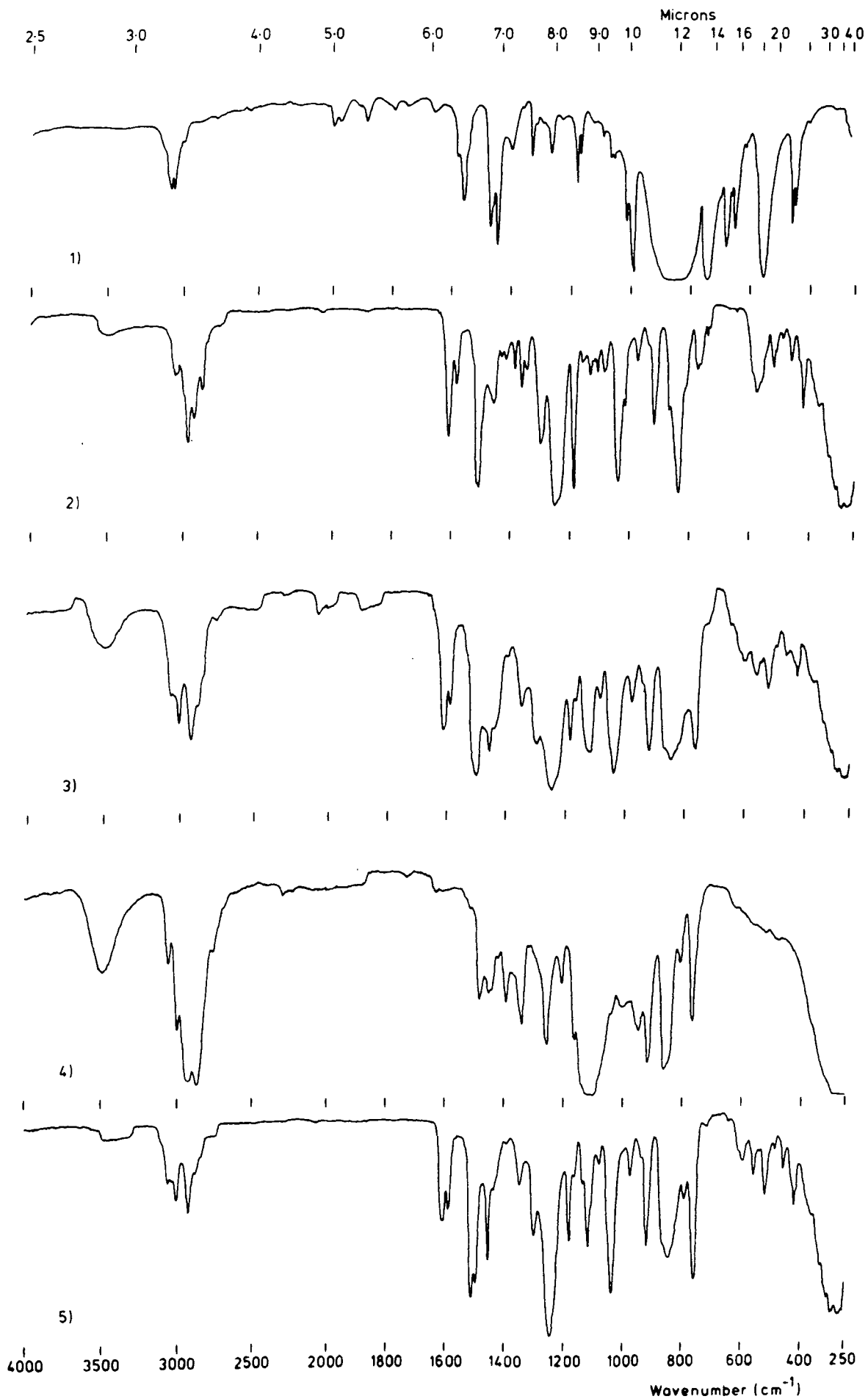
### Vacuum Systems

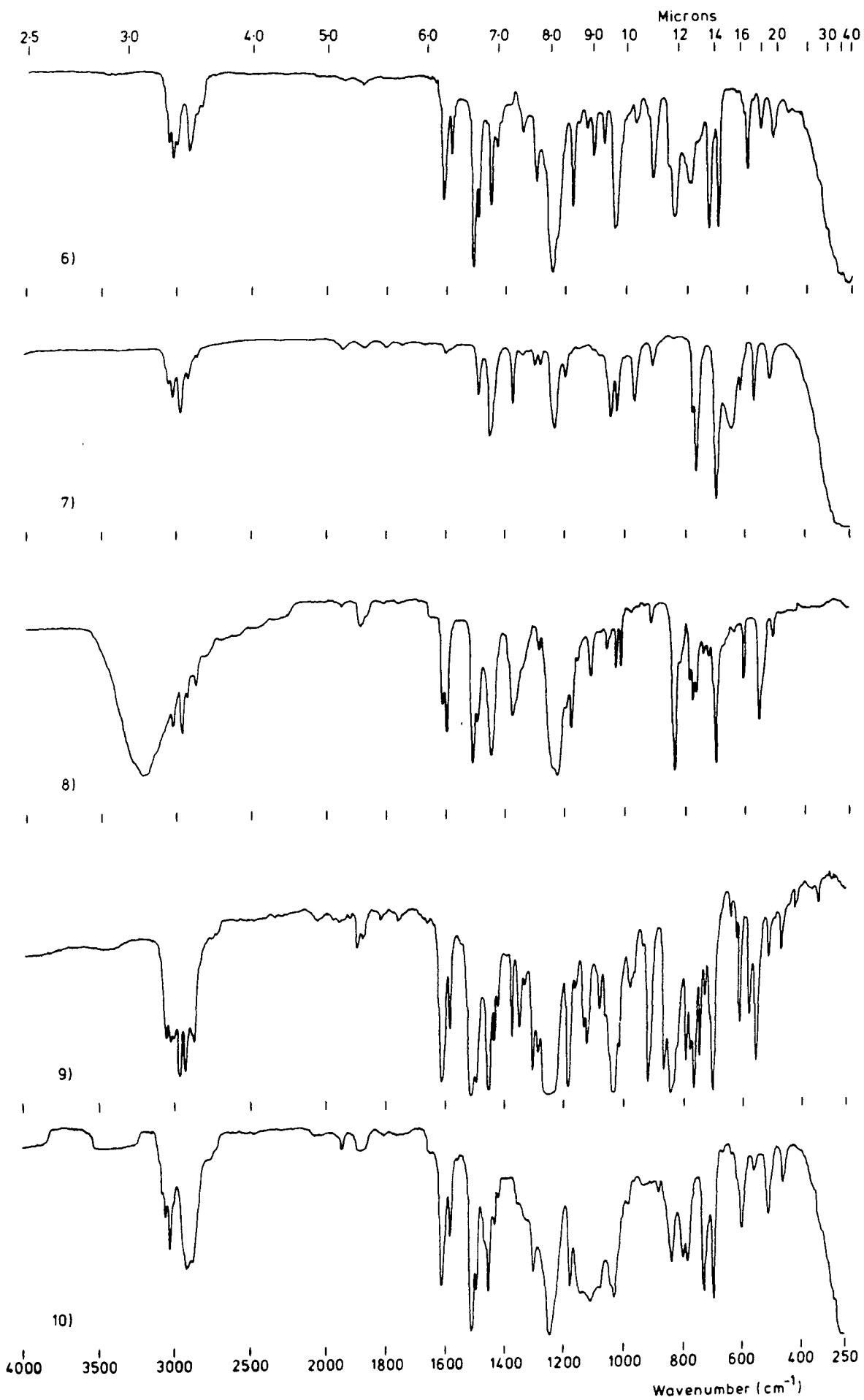
Conventional or greaseless vacuum systems incorporating a standard rotary oil pump were used for degassing materials, vacuum distillations, removing volatile residues, vacuum transfers, *etc.*

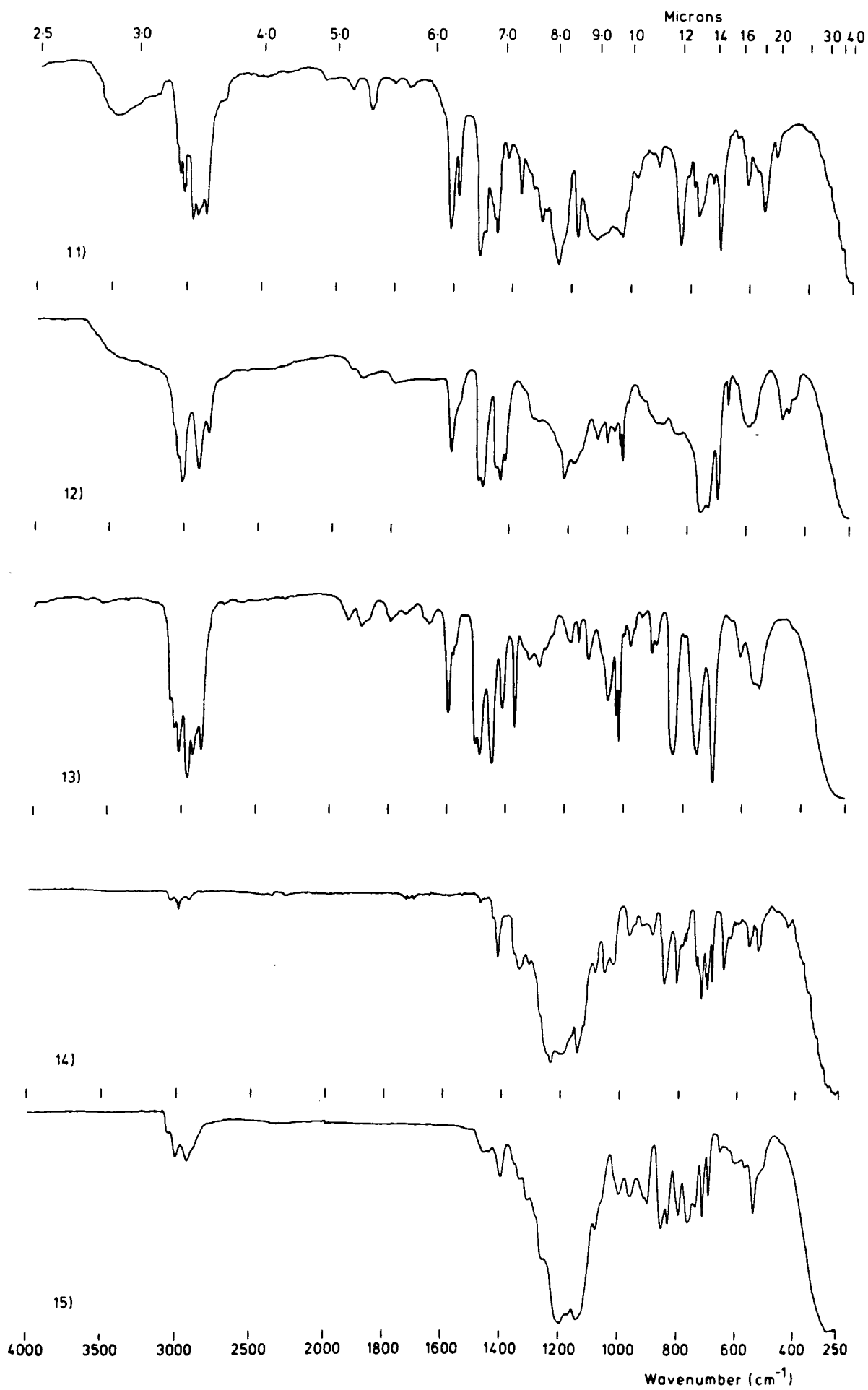
APPENDIX FOUR  
INFRA-RED SPECTRA

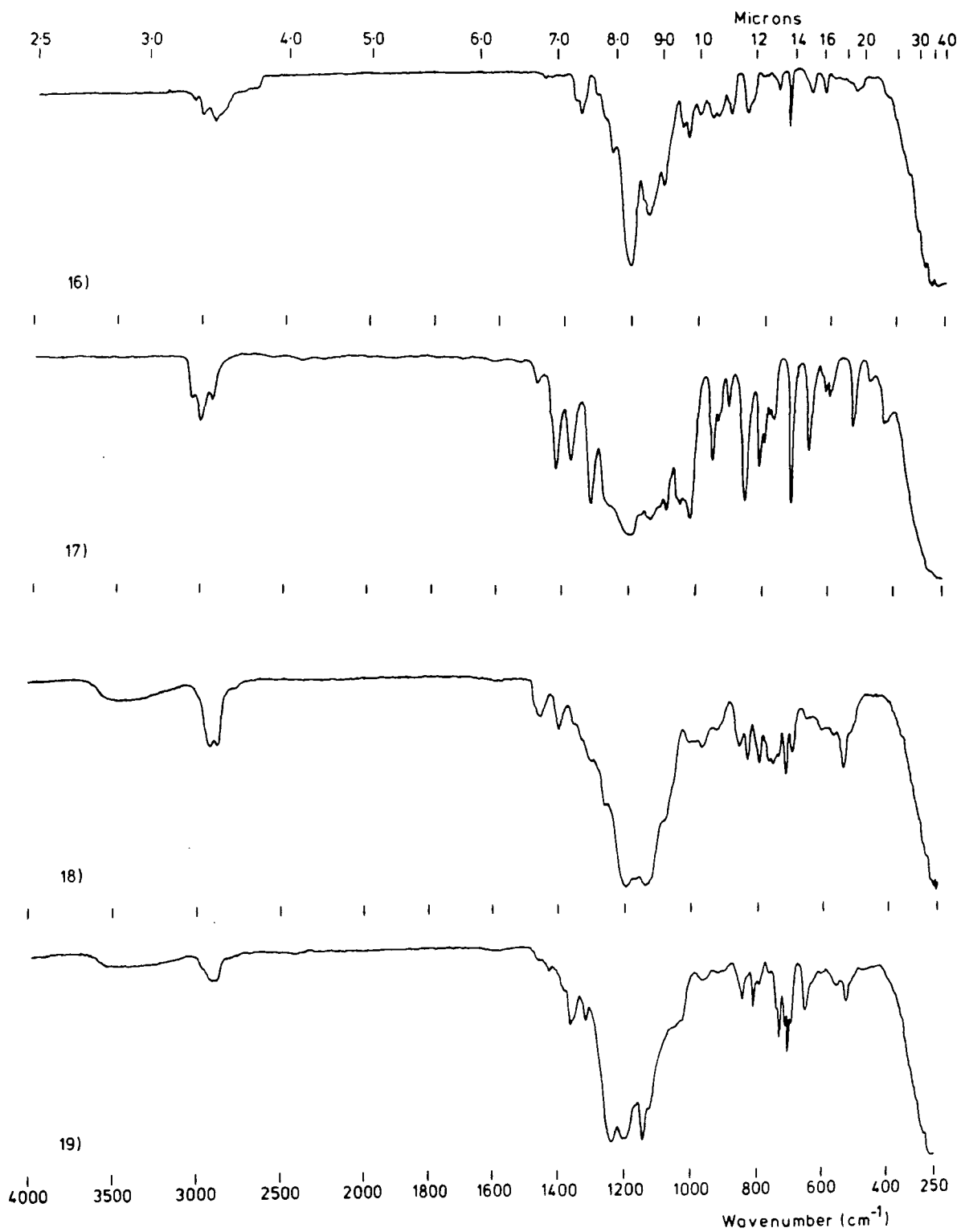
The IR spectra were recorded as a liquid film between KBr plates, LF, with the material incorporated into a KBr disc, D, in a solution cell, SC, or as a film on a KBr plate, F.

<u>Spectrum</u> <u>No.</u>	<u>Compound</u>
1	diphenyliodonium hexafluorophosphate
2	DGEBA, (XVIII), LF
3	epoxy novolac, (XIX), F
4	diglycidyl ether of butanediol, (XX), SC
5	DGEBF (XXI), LF
6	4-(phenylmethyl)-phenoxyethyl oxirane, (XXXVI), LF
7	phenethyl chloride, LF
8	4-(1-phenylethyl)-phenol (XLI), D
9	4-(1-phenylethyl)-phenoxyethyl oxirane (XXXVII), D
10	poly(4-(phenylmethyl)-phenoxyethyl oxirane) (XXXVIII), F
11	poly(4-(1-phenylethyl)-phenoxyethyl oxirane) (XXXIX), F
12	poly(benzyl), D
13	poly(phenethyl), F
14	7,7,7,6,6,5,5,4,4,3,3,2,2-tridecafluoroheptyl oxirane (XLIII), LF
15	((7,7,6,6,5,5,4,4,3,3,2,2-dodecafluoroheptyl)oxy) methyl oxirane (XLII), LF
16	((3,3,3,2,2-pentafluoropropyl)oxy)methyl oxirane (XLIV), LF
17	3,3,3,2,2-pentafluoropropyl oxirane (XLV), LF
18	poly(((7,7,6,6,5,5,3,3,2,2-dodecafluoroheptyl)oxy) methyl oxirane) (XLVII), F
19	poly(7,7,7,6,6,5,5,4,4,3,3,2,2-tridecafluoroheptyl oxirane) (XLVIII), F



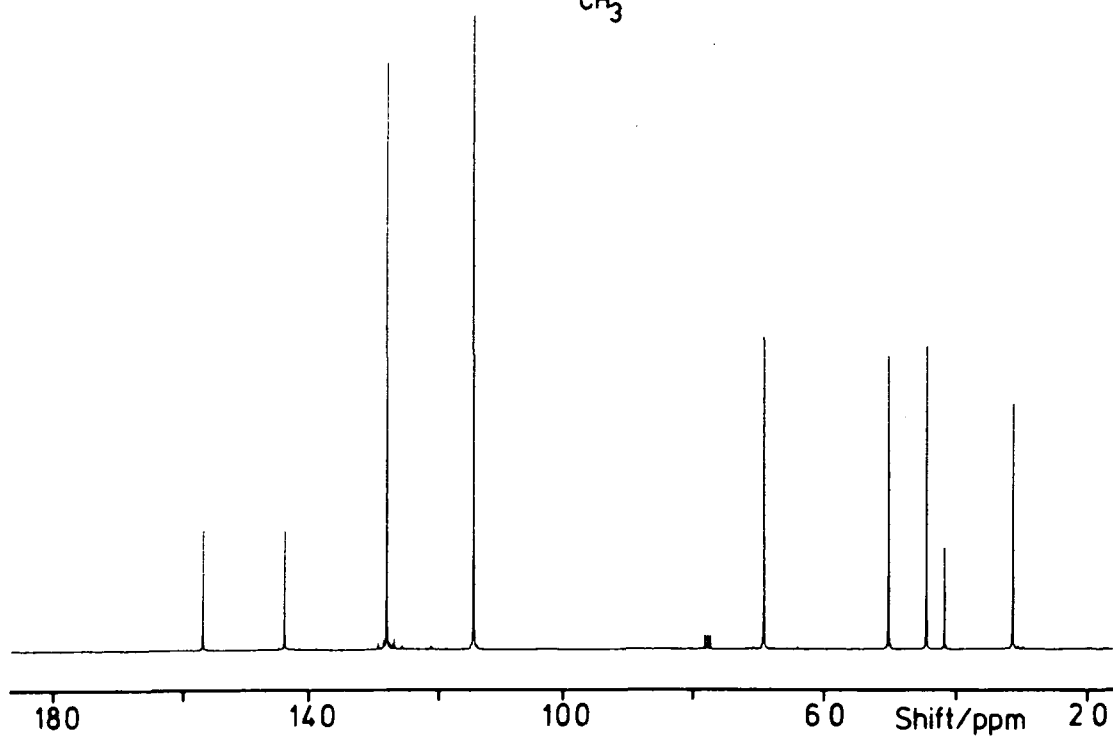
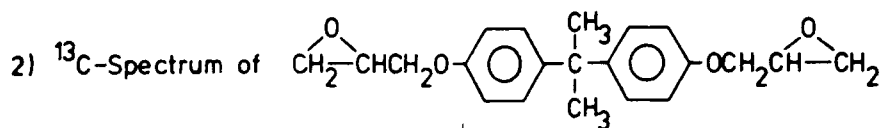
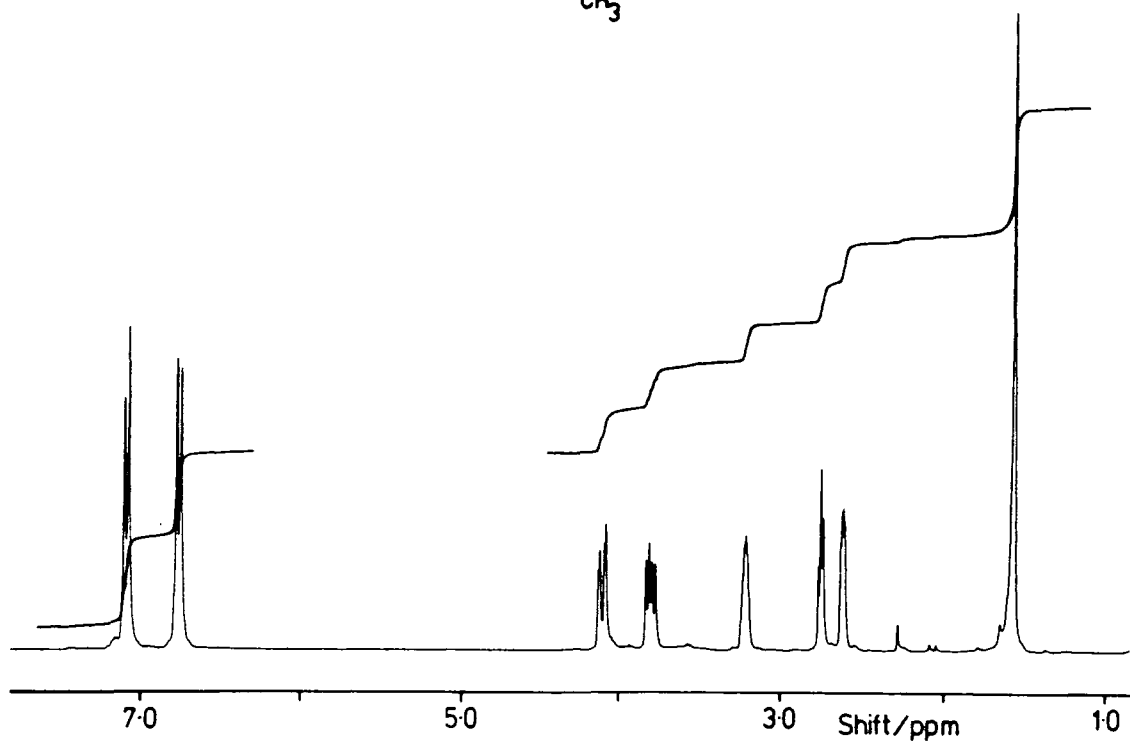
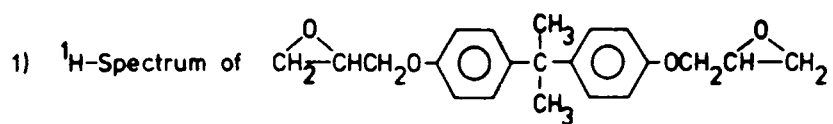


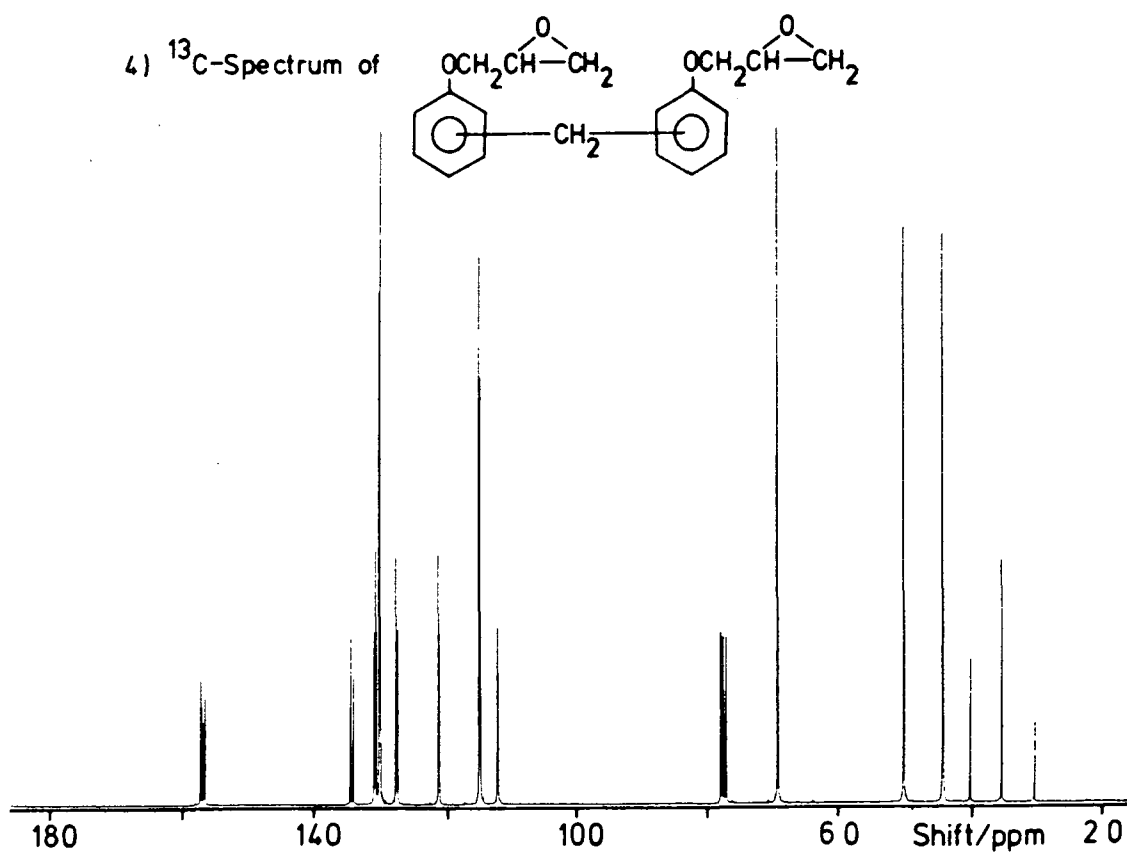
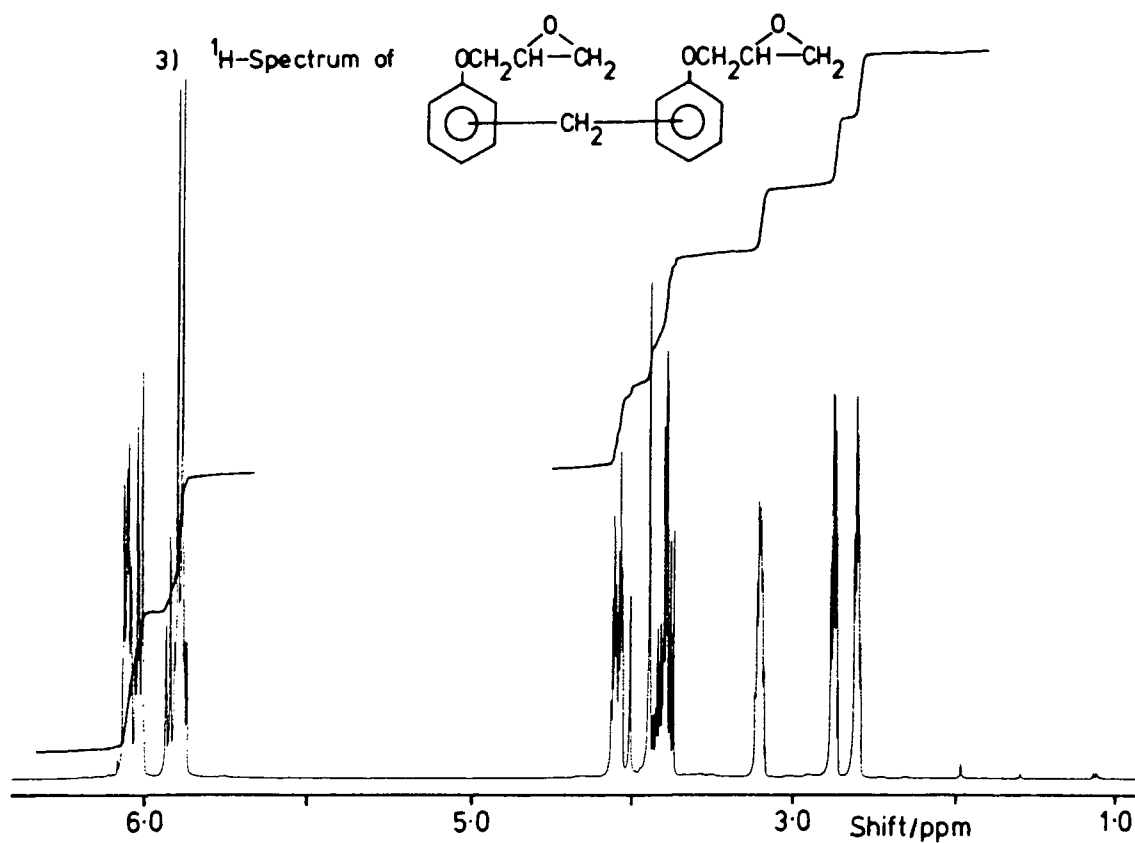




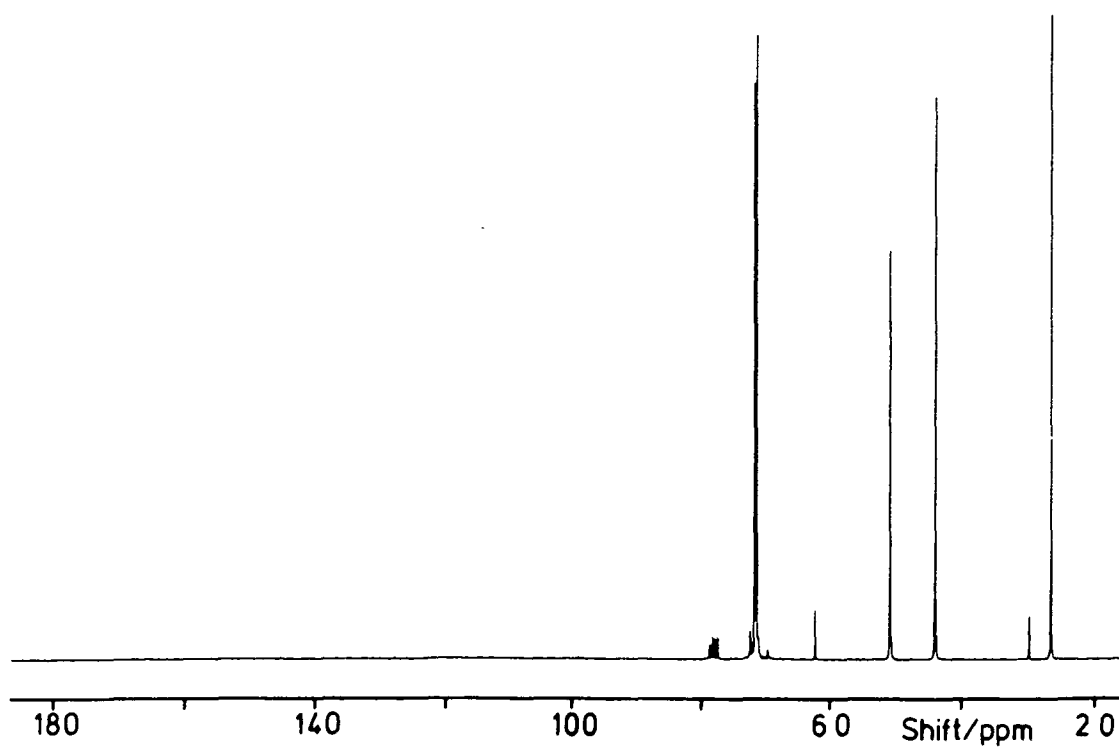
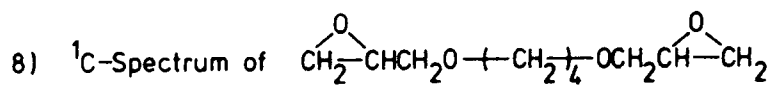
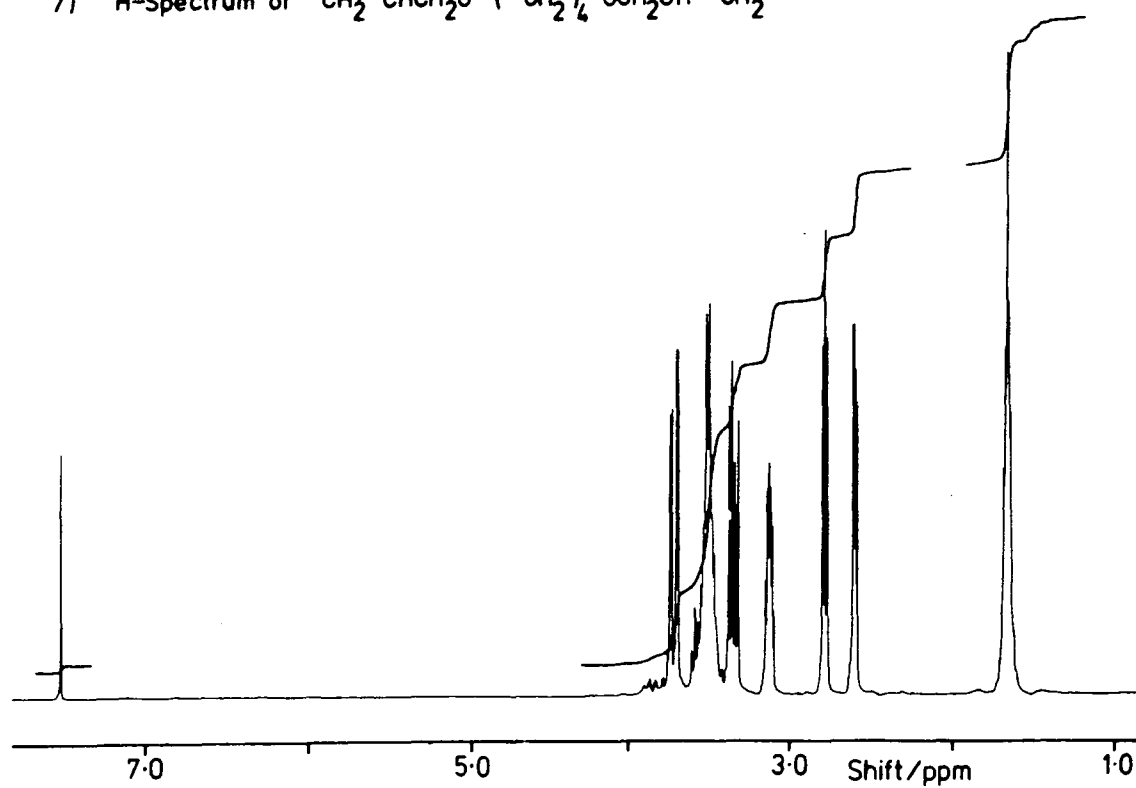
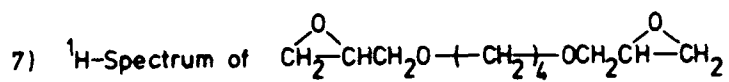
APPENDIX FIVE

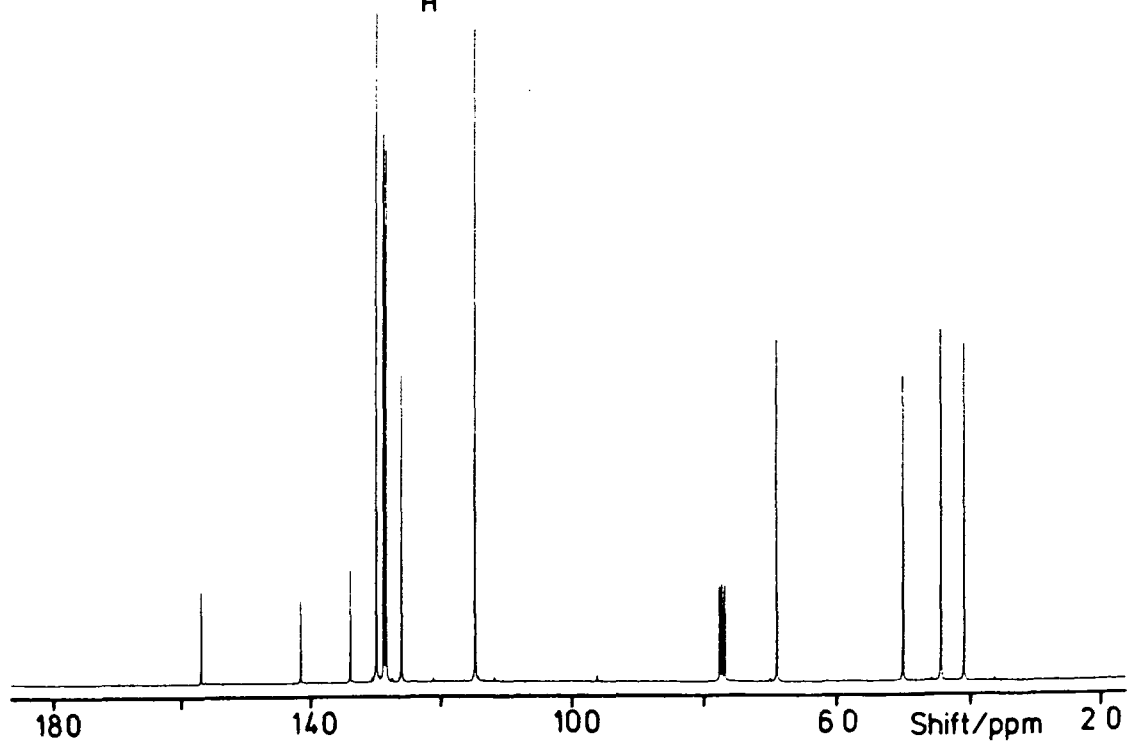
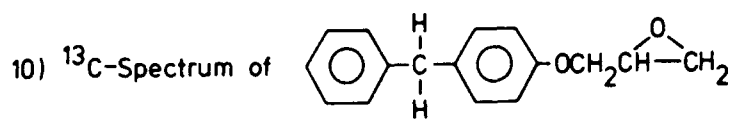
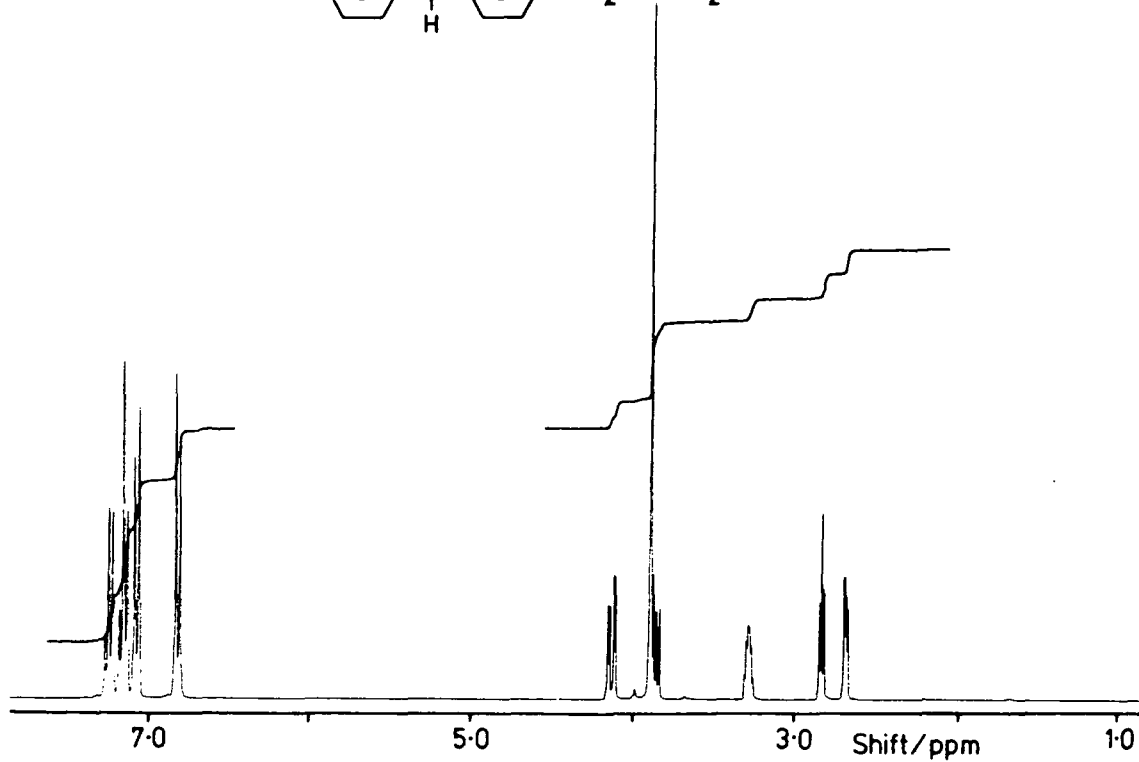
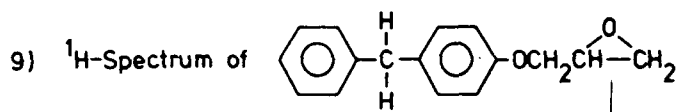
NUCLEAR MAGNETIC RESONANCE SPECTRA

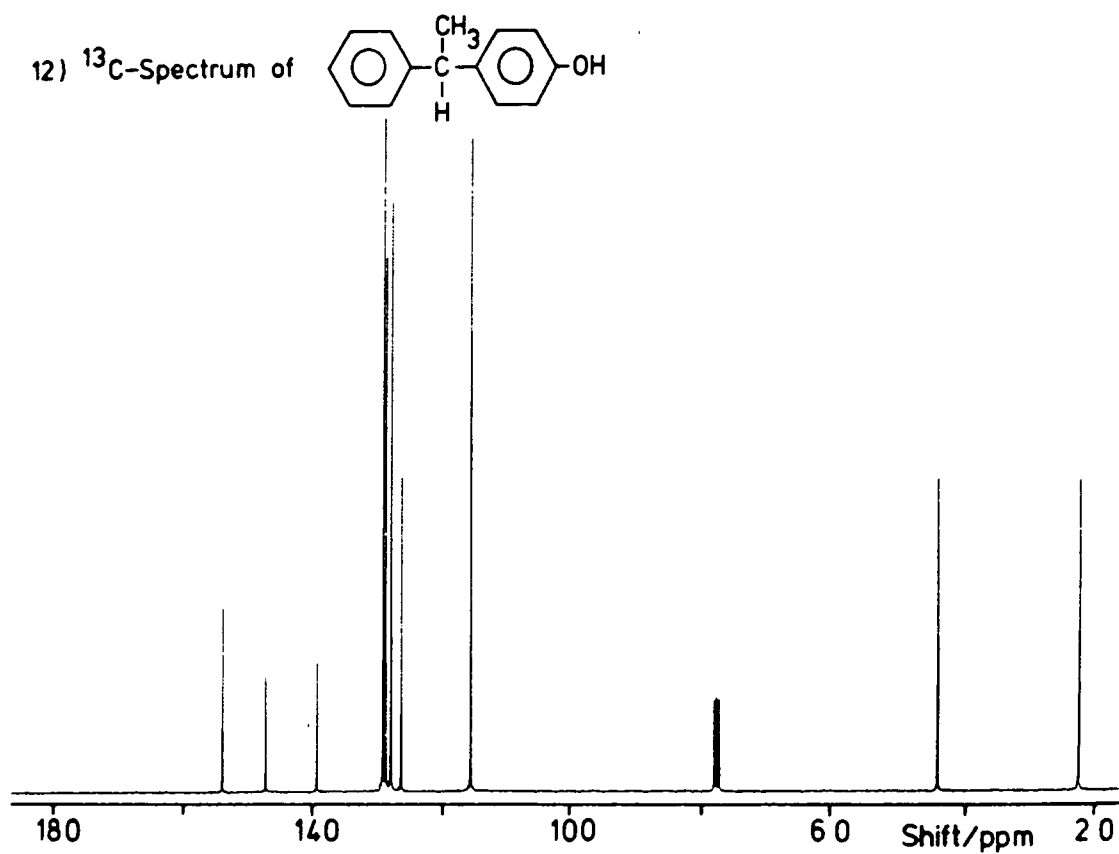
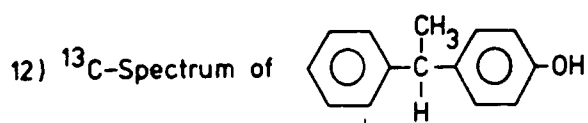
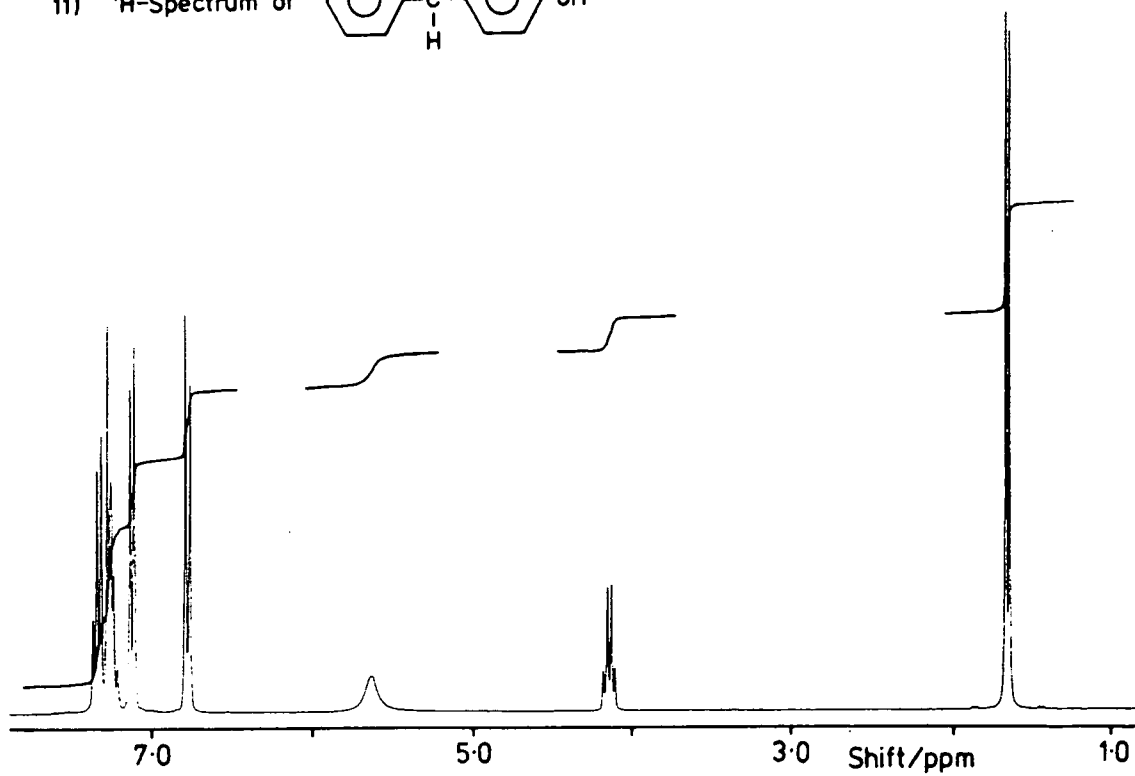
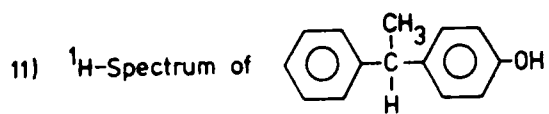


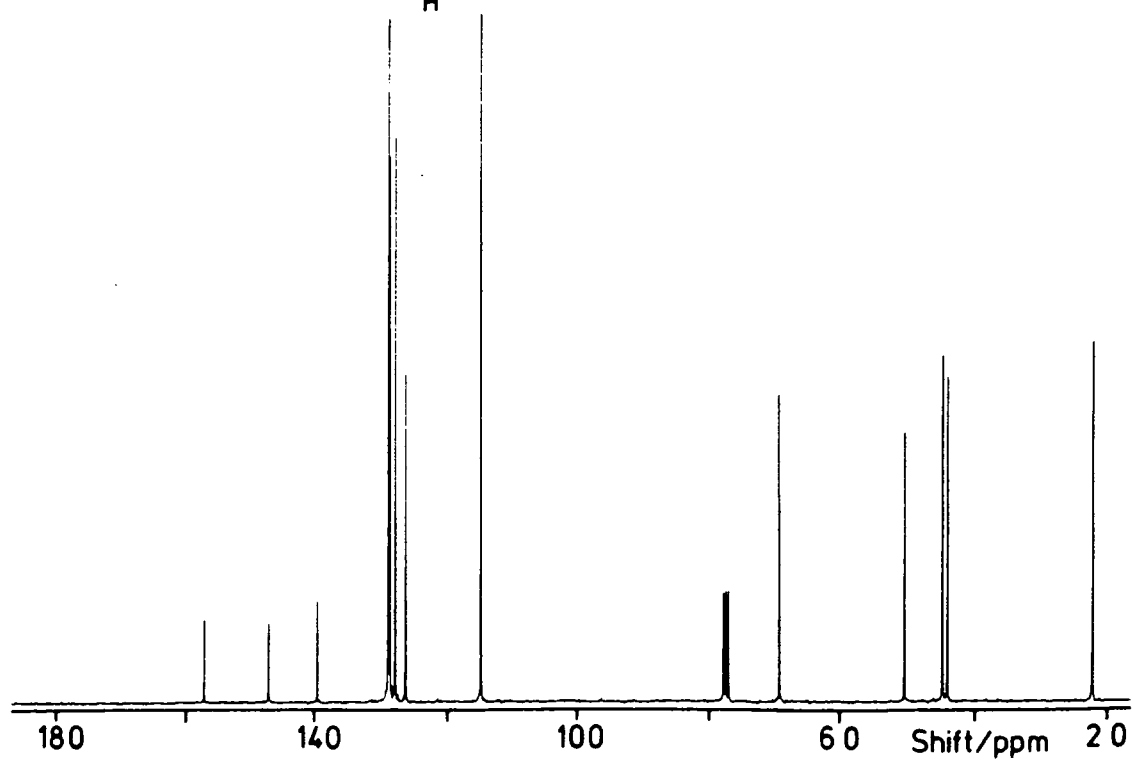
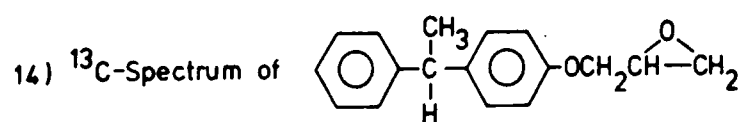
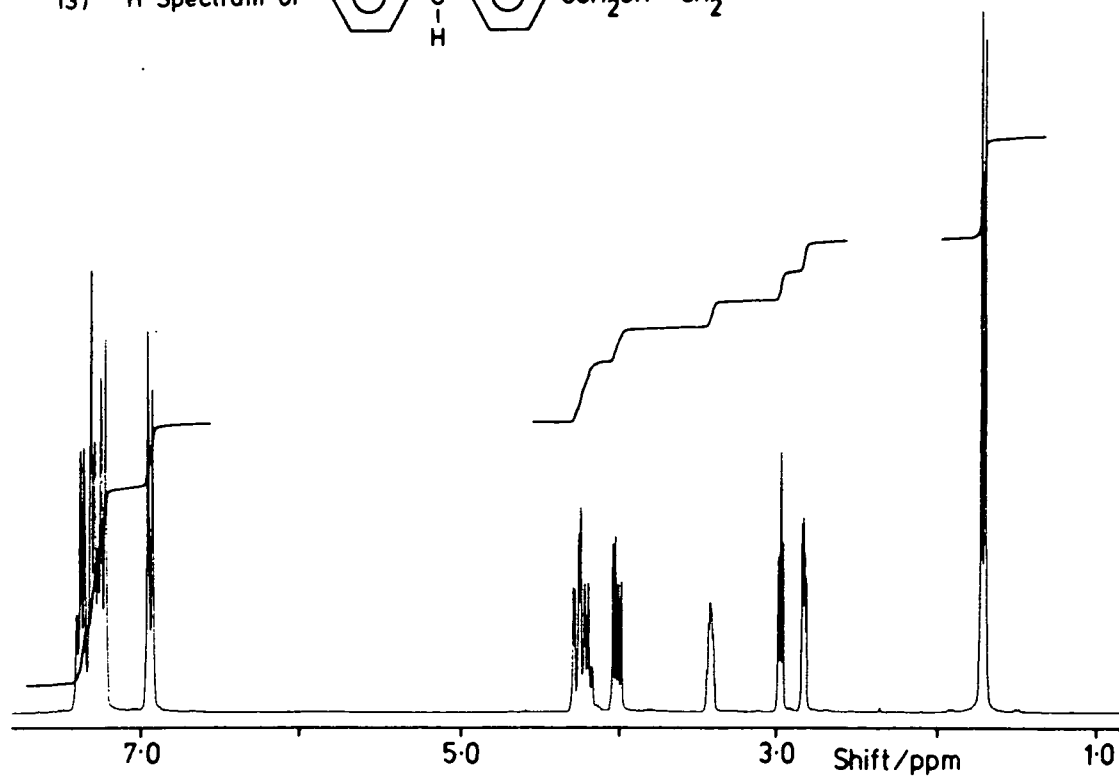
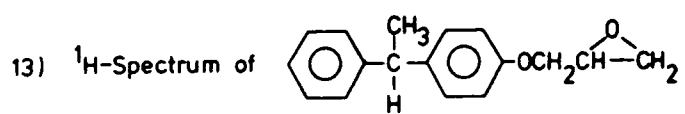


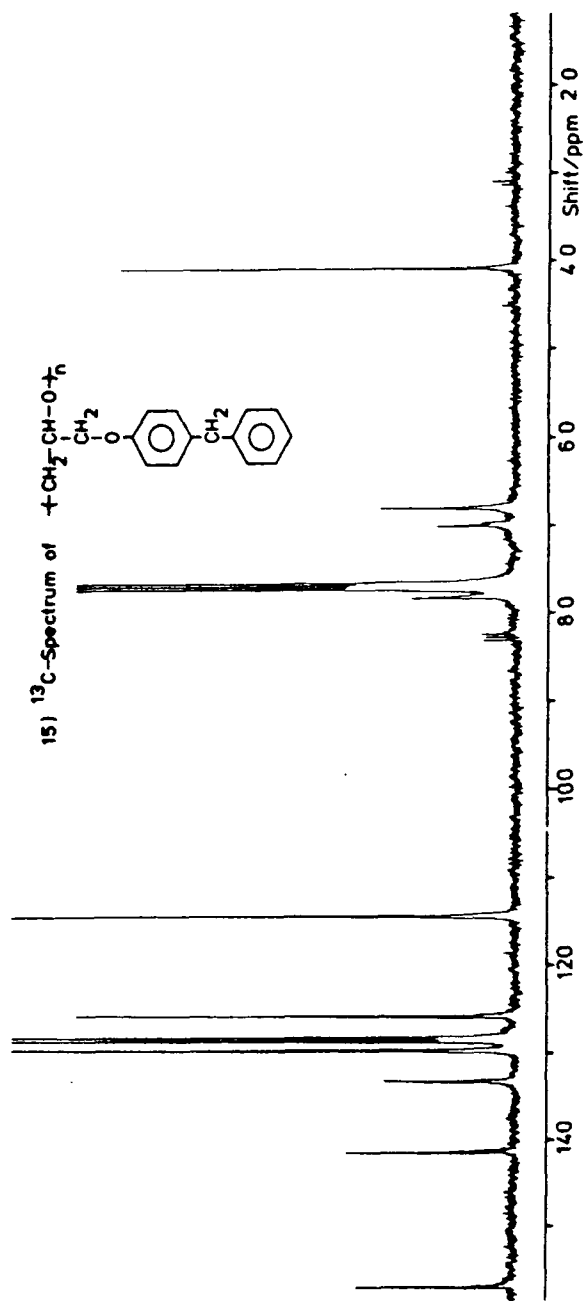


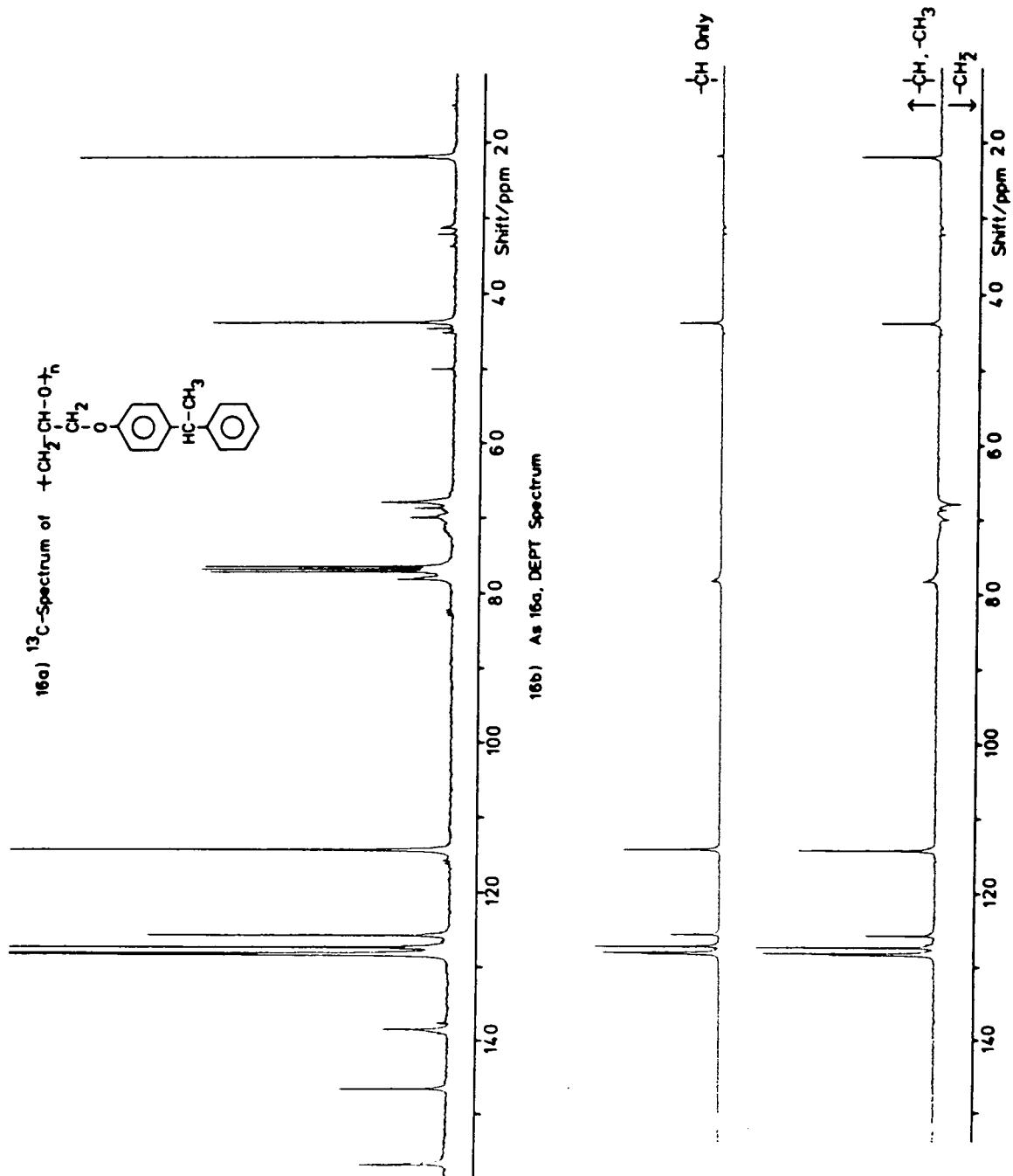


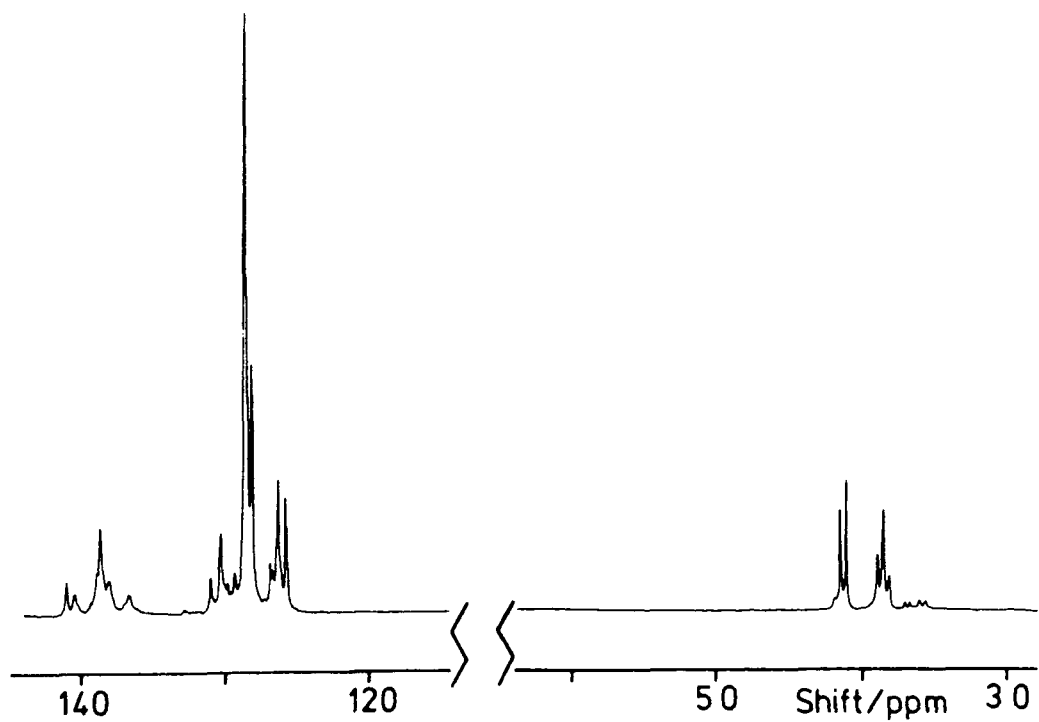




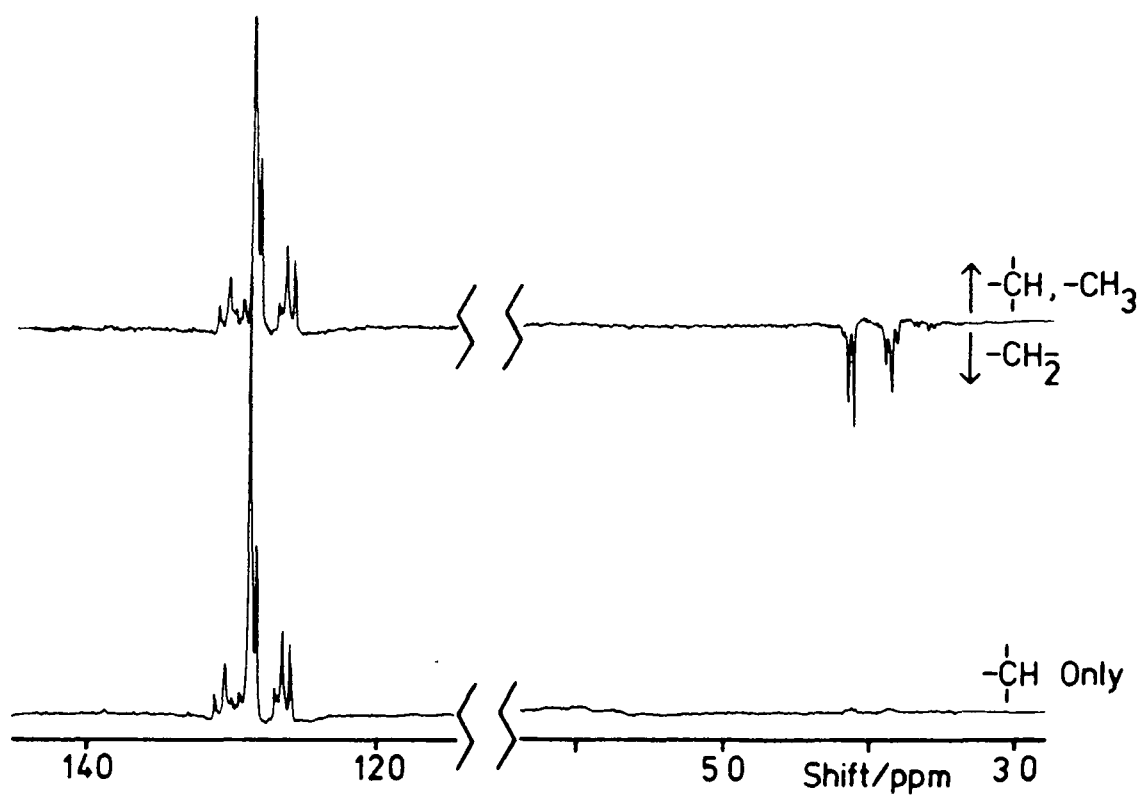


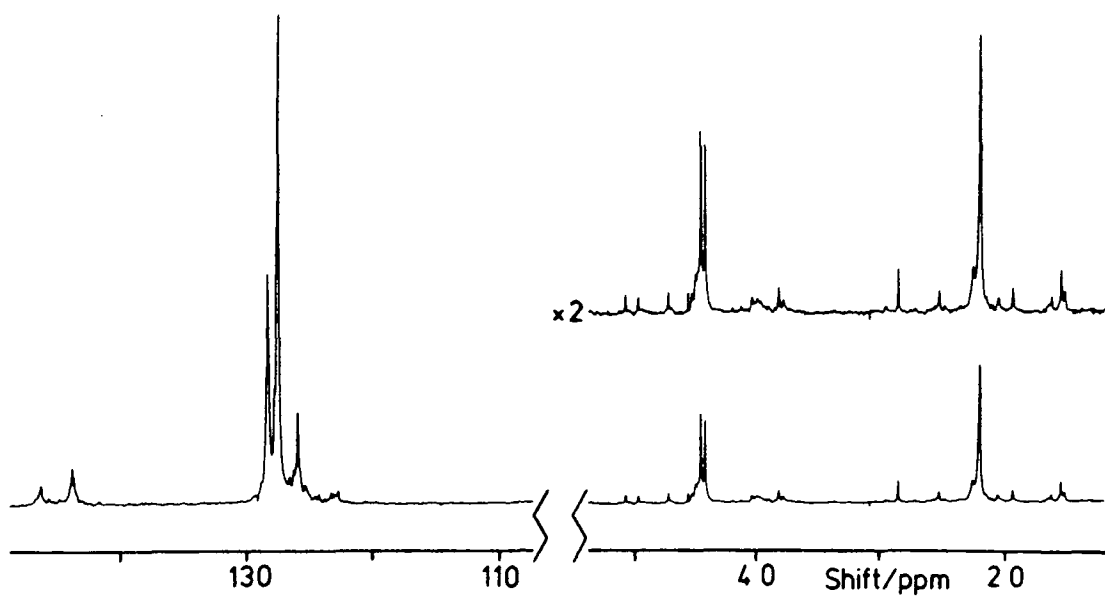




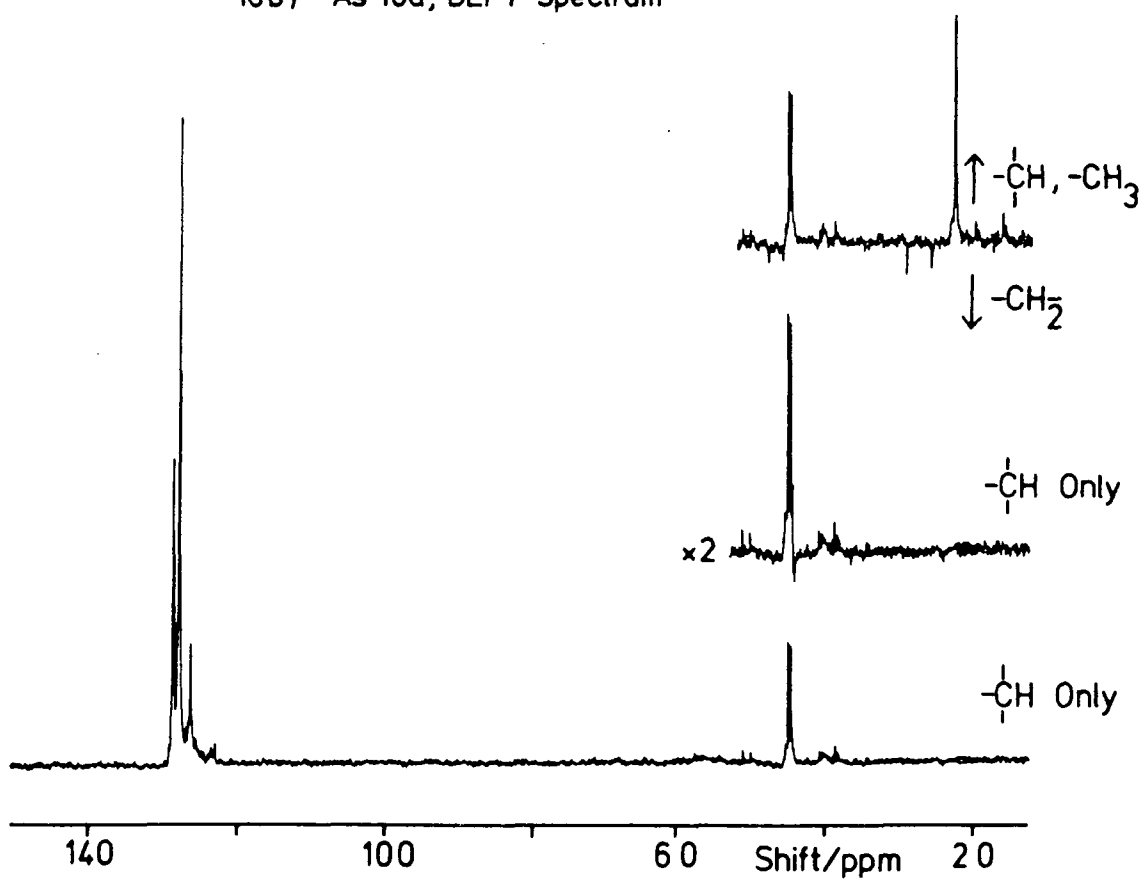
17a)  $^{13}\text{C}$ -Spectrum of Poly(benzyl)

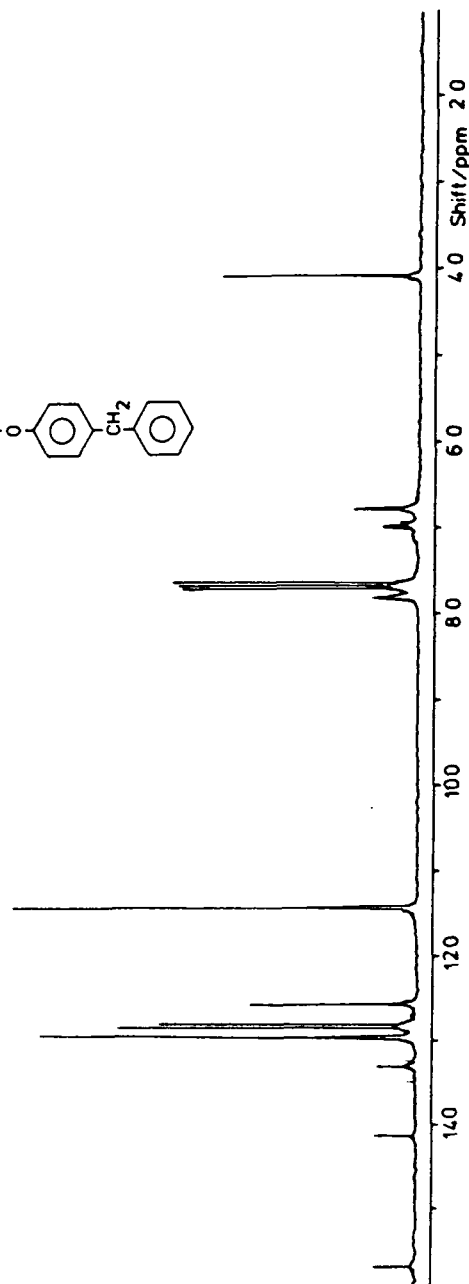
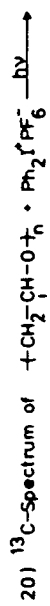
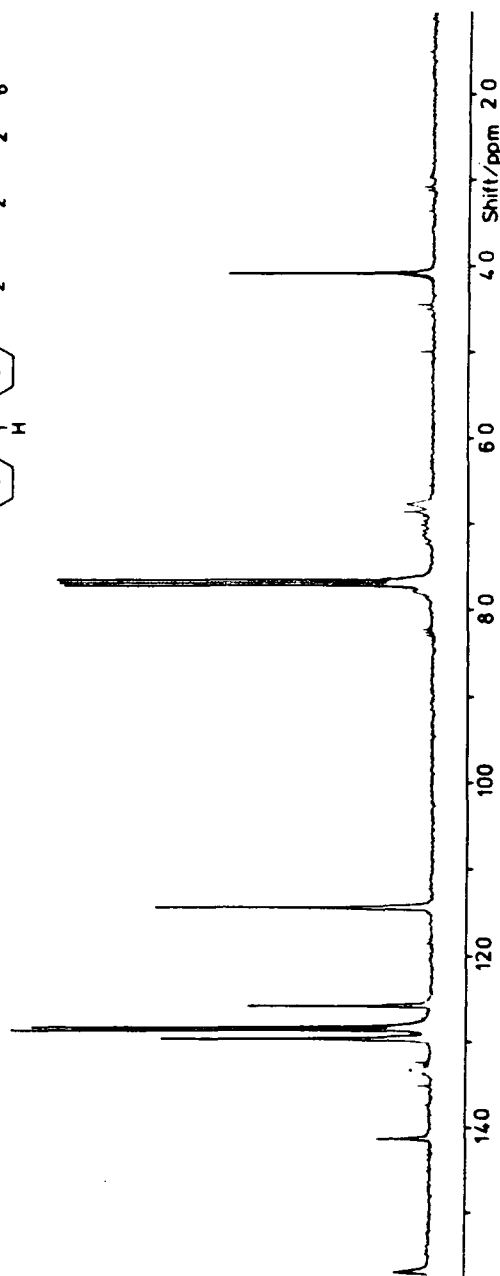
17 b) As 17a, DEPT Spectrum

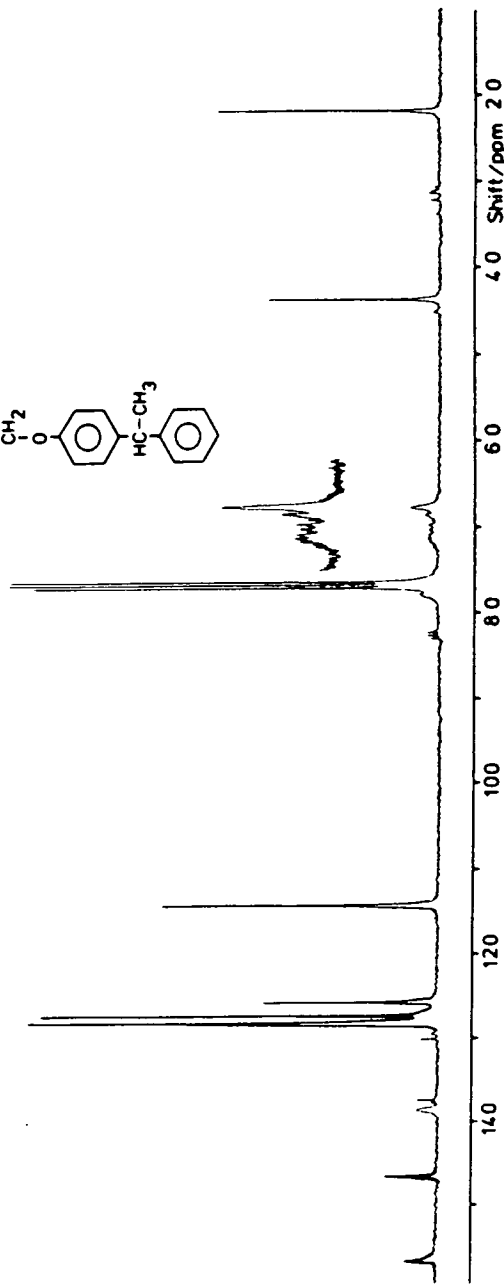
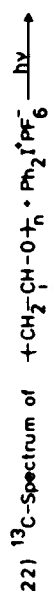
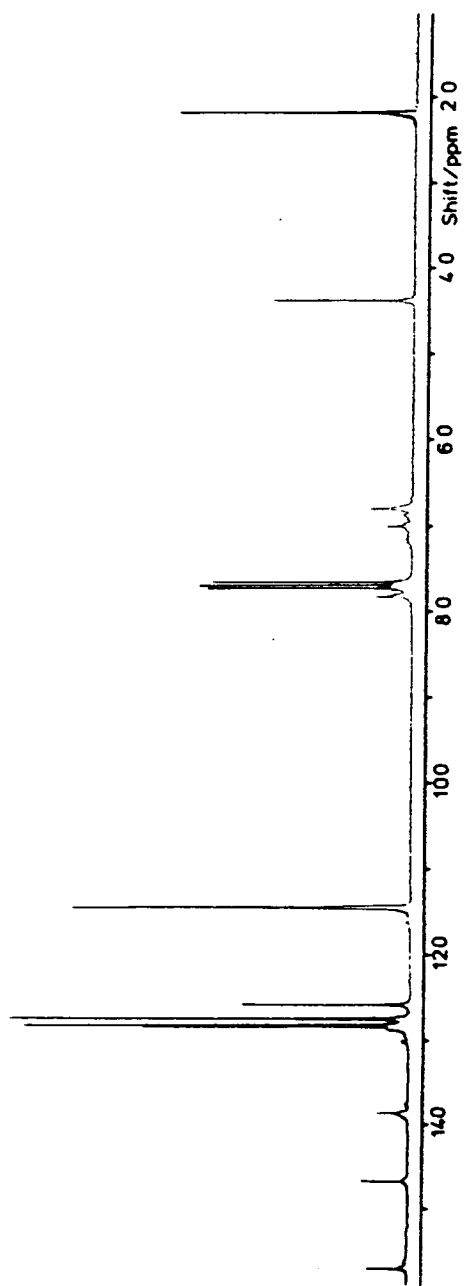
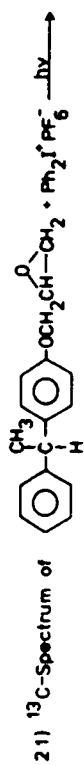


18a)  $^{13}\text{C}$ -Spectrum of Poly(phenethyl)

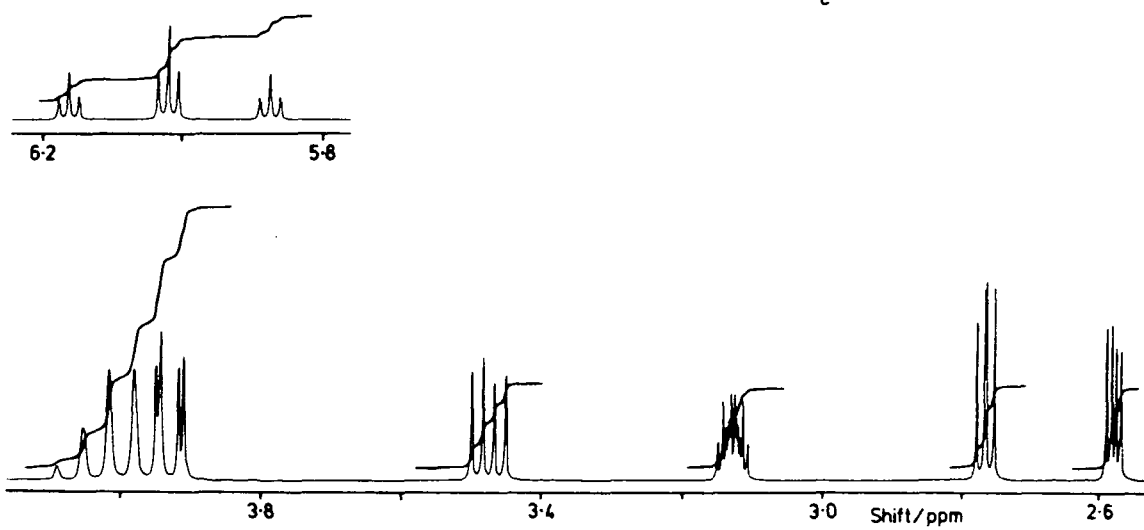
18b) As 18a, DEPT Spectrum



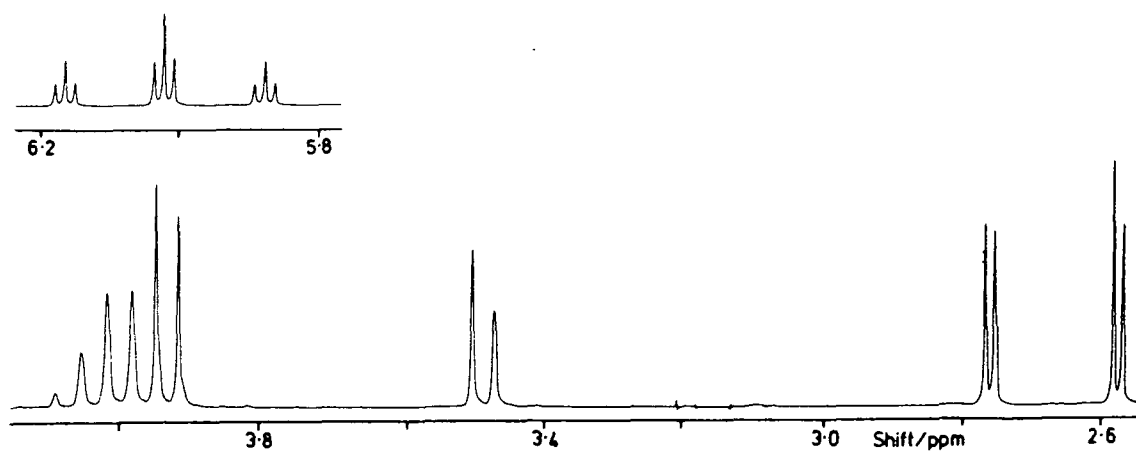




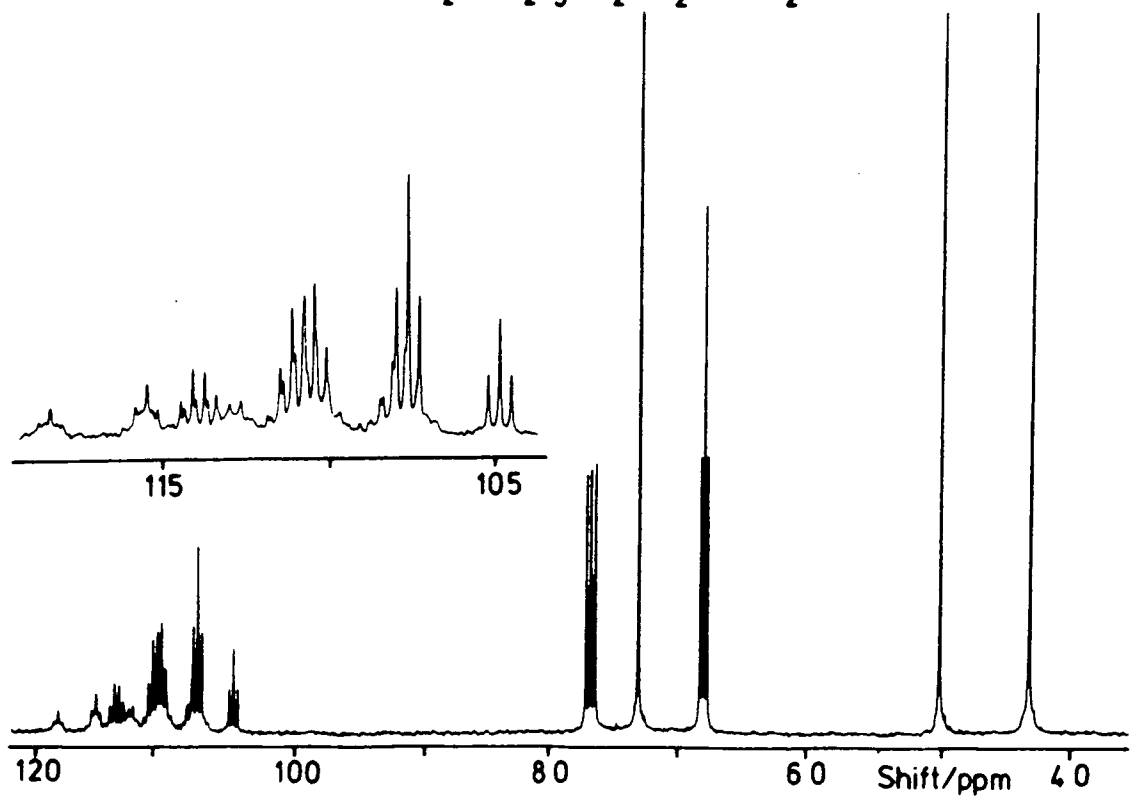
23a)  $^1\text{H}$ -Spectrum of  $\text{HCF}_2-\text{CF}_2-\text{CH}_2\text{OCH}_2\text{C}(\text{H}_c)\text{CH}_2$

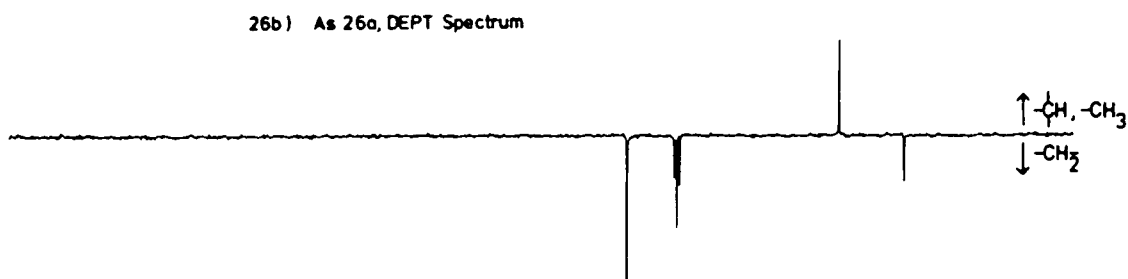
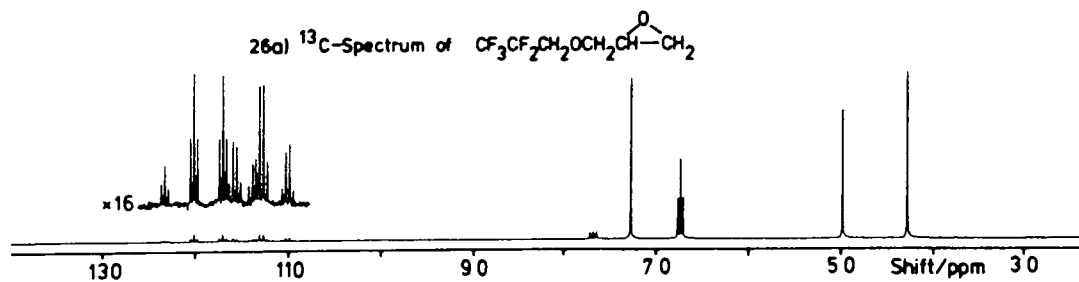
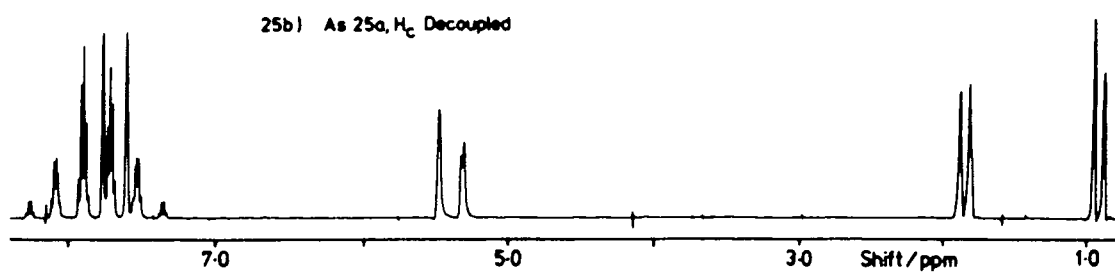
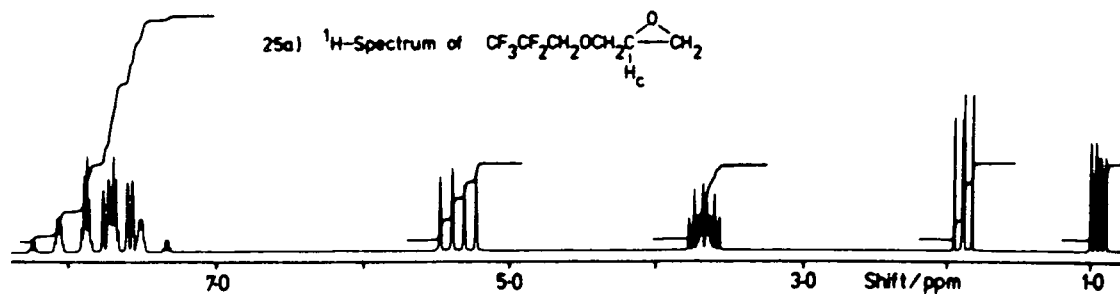


23b) As 23a,  $\text{H}_c$  Decoupled

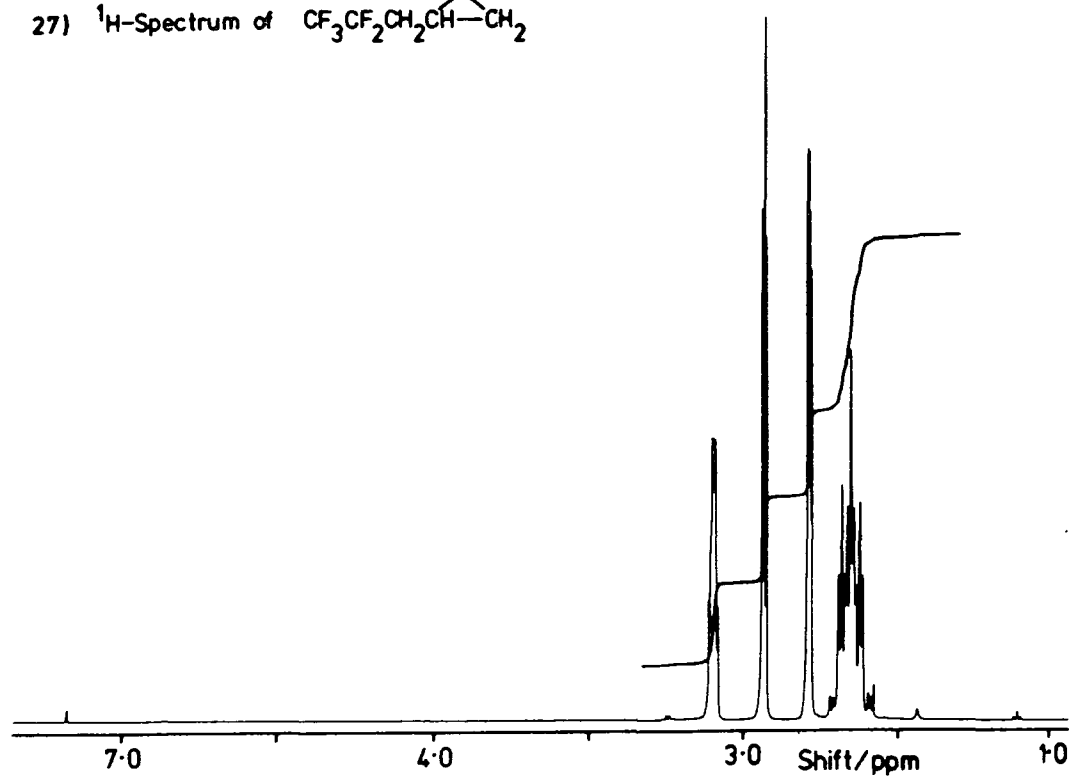


24)  $^{13}\text{C}$ -Spectrum of  $\text{HCF}_2\text{-CF}_2\text{-CH}_2\text{OCH}_2\text{CH}(\text{O})\text{CH}_2$

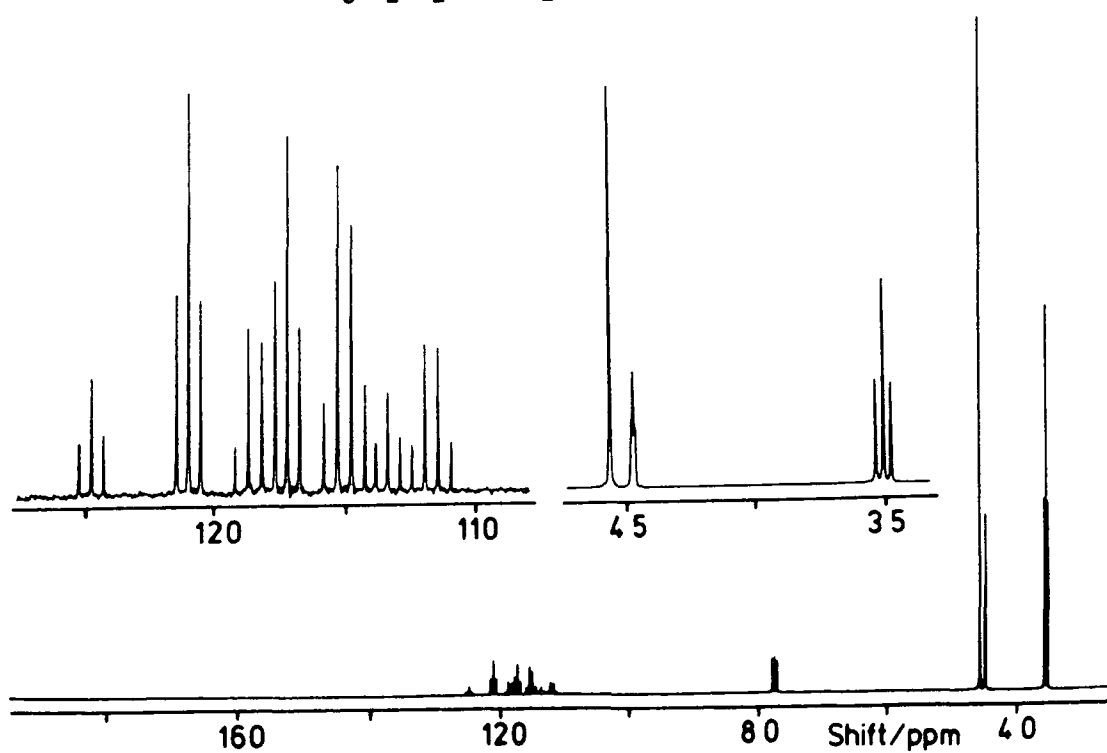




27)  $^1\text{H}$ -Spectrum of  $\text{CF}_3\text{CF}_2\text{CH}_2\text{CH}(\text{O})\text{CH}_2$



28)  $^{13}\text{C}$ -Spectrum of  $\text{CF}_3\text{CF}_2\text{CH}_2\text{CH}(\text{O})\text{CH}_2$



APPENDIX SIX

MASS SPECTRA

The more intense peaks observed in the mass spectrum of a compound are tabulated below in the following manner:

183 (3.7,  $C_{13}H_{12}O$ )

The mass-to-charge ratio,  $m/e$ , is 188, the intensity of the peak is 3.7 expressed as a percentage of the height of the base, B, peak and  $C_{13}H_{11}O$  is a species potentially present that corresponds to the  $m/e$  ratio (the +ve charge being understood). The molecular ion is designated as M.

(1) 4-(phenylmethyl)-phoxymethyl oxirane (XXXVI)

241 (1.2, M+1), 240 (7.4, M), 184 (3.4), 183 (3.7,  $C_{13}H_{11}O$ ), 167 (3.0,  $C_{13}H_{11}$ ), 165 (2.6), 119 (2.8), 105 (3.8), 94 (3.8,  $C_7H_7$ ), 91 (5.2), 83 (2.7), 82 (2.2), 77 (3.6,  $C_6H_5$ ), 71 (3.6), 70 (2.8), 69 (5.0), 65 (2.5,  $C_5H_5$ ), 57 (11.2,  $C_3H_5O$ ), 56 (3.5,  $C_3H_4O$ ), 51 (2.7), 44 (3.5), 43 (13.0,  $C_2H_3O$ ), 42 (3.1,  $C_2H_2O$ ), 41 (10.3,  $C_3H_5$ ), 40 (10.1,  $C_3H_4$ ), 39 (6.0,  $C_3H_3$ ), 29 (13.1, CHO), 28 (B, CO), 27 (8.3,  $C_2H_3$ ).

(2) 4-(1-phenylethyl)-phenol (XL1)

199 (4.6, M+1), 198 (31.6, M), 184 (14.2), 183 (B,  $C_{13}H_{11}O$ ), 182 (3.9), 181 (6.8,  $C_{14}H_{13}$ ), 166 (3.4), 165 (16.6), 155 (4.6), 154 (3.4), 153 (8.9), 152 (6.5), 150 (4.8), 149 (51.5), 121 (6.9,  $C_8H_9O$ ), 115 (5.4), 105 (3.4,  $C_8H_8$ ), 91 (8.6,  $C_7H_7$ ), 81 (3.1), 78 (3.7), 77 (5.0,  $C_6H_5$ ), 69 (6.6), 65 (7.4,  $C_5H_5$ ), 63 (5.1), 59 (6.2), 57 (20.8,  $C_3H_5O$ ), 55 (7.6,  $C_3H_3O$ ), 51 (9.3), 45 (7.6), 43 (9.9), 41 (19.6), 39 (13.8), 31 (7.6), 29 (12.5, CHO), 28 (33.0, CO), 27 (10.6,  $C_2H_3$ ).

(3) 4-(1-phenylethyl)-phoxymethyl oxirane (XXXVIII)

255 (8.4, M+1), 254 (46.1, M), 240 (19.1), 239 (B,  $C_{16}H_{15}O_2$ ),

209 (3.8), 198 (3.6), 197 (5.0,  $C_{14}H_{13}O$ ), 196 (5.1), 195 (5.5),  
 184 (8.1), 183 (50.3), 181 (9.8,  $C_{14}H_{13}$ ), 177 (2.5), 169 (2.9),  
 167 (4.6), 166 (9.4), 165 (20.0), 154 (7.6), 153 (14.3),  
 152 (8.7), 149 (9.7,  $C_9H_9O_2$ ), 141 (4.6), 128 (5.8), 115 (7.7),  
 106 (18.1), 105 (13.4,  $C_8H_9$ ), 103 (9.0), 91 (13.1,  $C_7H_7$ ),  
 85 (4.0), 83 (3.5), 81 (4.7), 77 (15.2,  $C_6H_5$ ), 69 (11.0),  
 65 (6.6), 63 (4.4), 57 (47.2,  $C_3H_5O$ ), 56 (4.2,  $C_3H_4O$ ), 55 (9.4,  
 $C_3H_3O$ ), 45 (8.9), 44 (6.1), 43 (11.0,  $C_2H_3O$ ), 41 (17.0,  $C_3H_5$ ),  
 40 (8.0,  $C_3H_4$ ), 39 (10.7,  $C_3H_3$ ), 31 (29.4), 29 (49.6, CHO),  
 28 (94.0, CO), 27 (23.2,  $C_2H_3$ ).

(4) ((7,7,6,6,5,5,4,4,3,3,2,2-dodecafluoroheptyl)oxy)methyl oxirane (XLII)

A molecular ion (m/e 388) could not be detected using electron impact.

372 (0.5,  $C_{10}H_8F_{12}O$ ), 368 (1.1,  $C_{10}H_7F_{11}O_2$ ), 358 (0.7,  
 $C_9H_6F_{12}O$ ), 345 (12.6,  $C_8H_5F_{12}O$ ), 245 (5.1,  $C_6H_5F_8O$ ), 151 (1.5,  
 $C_3F_6H$ ), 137 (2.0), 131 (2.1,  $C_3F_5$ ), 113 (2.3), 101 (3.1,  $C_2F_4H$ ),  
 95 (2.5), 83 (3.6), 81 (10.2,  $C_2F_3$ ), 63 (1.7,  $C_2F_2H$ ), 61 (6.9,  
 $C_2H_2FO$ ), 58 (11.7), 57 (B,  $C_3H_5O$ ), 56 (3.2,  $C_3H_4O$ ), 51 (18.0,  
 $CHF_2$ ), 45 (9.1,  $C_2H_2F$ ), 43 (8.8,  $C_2H_3O$ ), 42 (2.0,  $C_2H_2O$ ),  
 41 (5.6,  $C_3H_5$ ), 33 (16.9), 32 (6.3, CHF), 31 (49.2, CF), 30 (4.8,  
 $CH_2O$ ), 29 (61.3, CHO), 28 (29.1, CO), 27 (8.7,  $C_2H_3$ ).

Chemical ionization gave a species at m/e 387 which corresponds to an M-1 species commonly formed by the loss of  $H_2$  from the M+1 species but no M+1 species was detected.

(5) ((3,3,3,2,2-pentafluoropropyl)oxy)methyl oxirane (XLIV)

A molecular ion (m/e 206) could not be detected using electron impact.

205 (0.8,  $C_6H_6F_5O_2$ ), 186 (5.0,  $C_6H_6F_4O_2$ ), 177 (5.5),  
 176 (8.4,  $C_5H_5F_5O$ ), 164 (3.0), 163 (81.6,  $C_4H_4F_5O$ ), 156 (6.7),  
 133 (10.0,  $C_3H_2F_5$ ), 119 (3.4,  $C_2F_5$ ), 113 (5.4,  $C_3HF_4$ ), 111 (3.4),  
 100 (3.5,  $C_2F_4$ ), 83 (18.7), 81 (26.4,  $C_2F_3$ ), 69 (49.2,  $CF_3$ ),  
 64 (9.6,  $C_2H_2F_2$ ), 63 (4.7,  $C_2HF_2$ ), 61 (4.7,  $C_2H_2FO$ ), 58 (10.6),  
 57 (B,  $C_3H_5O$ ), 56 (3.0,  $C_3H_4O$ ), 55 (3.5,  $C_3H_3O$ ), 51 (21.8,  $CHF_2$ ),  
 45 (8.6,  $C_2H_2F$ ), 41 (5.5,  $C_3H_5$ ), 39 (3.9), 33 (9.9), 32 (4.7,  $CHF$ ),  
 31 (66.8,  $CF$ ), 30 (3.1,  $CH_2O$ ), 29 (94.5,  $CHO$ ), 28 (15.0,  $CO$ ),  
 27 (28.3,  $C_2H_3$ ).

Chemical ionization gave a species at  $m/e$  207 corresponding to the expected  $M+1$  species.

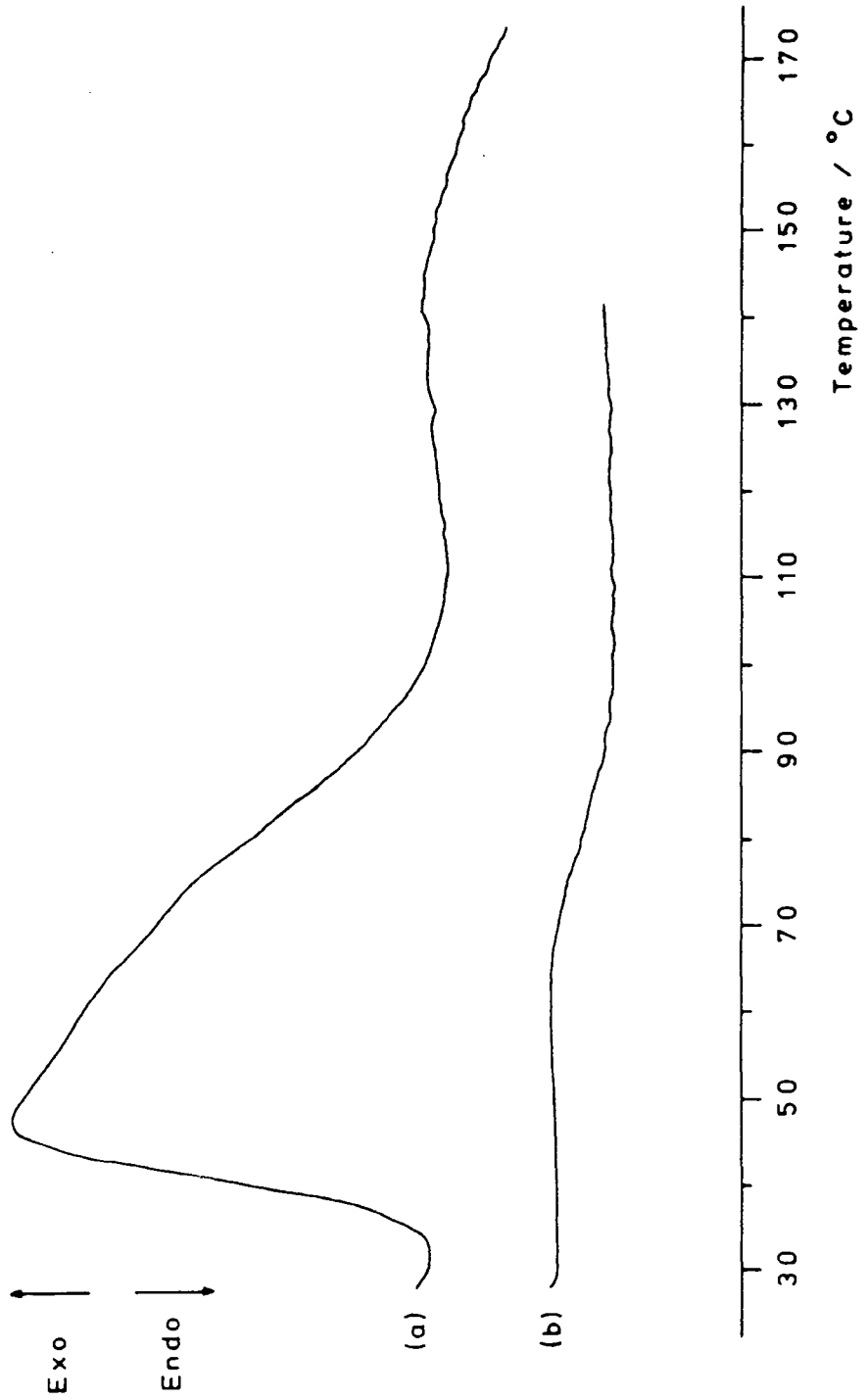
(6) 3,3,3,2,2-pentafluoropropyl oxirane (XLV)

177 (1.0,  $M+1$ ), 176 (9.7,  $M$ ), 119 (5.9,  $C_2F_5$ ), 113 (2.2,  $C_3HF_4$ ),  
 109 (6.3), 108 (4.4), 107 (B,  $C_4H_5F_2O$ ), 100 (9.7,  $C_2F_4$ ),  
 95 (8.5), 91 (2.9,  $C_4H_5F_2$ ), 89 (12.4,  $C_4H_3F_2$ ), 79 (3.6),  
 77 (44.8,  $C_3H_3F_2$ ), 76 (3.2), 75 (9.8), 69 (40.3,  $CF_3$ ), 65 (5.7),  
 64 (7.8,  $C_2H_2F_2$ ), 61 (2.5,  $C_2H_2FO$ ), 59 (19.0), 57 (63.1,  $C_3H_5O$ )  
 56 (2.3,  $C_3H_4O$ ), 51 (34.3,  $HCF_2$ ), 45 (4.7,  $C_2H_2F$ ), 43 (34.0,  
 $C_2H_3O$ ), 42 (6.2,  $C_2H_2O$ ), 41 (2.1,  $C_2HF$ ), 38 (3.4), 33 (6.4),  
 32 (4.9,  $CHF$ ), 31 (66.4,  $CF$ ), 30 (6.4,  $CH_2O$ ), 29 (83.8,  $CHO$ ),  
 28 (14.6,  $CO$ ), 27 (31.7,  $C_2H_3$ ),

APPENDIX SEVEN

DIFFERENTIAL SCANNING CALORIMETRY CURVES

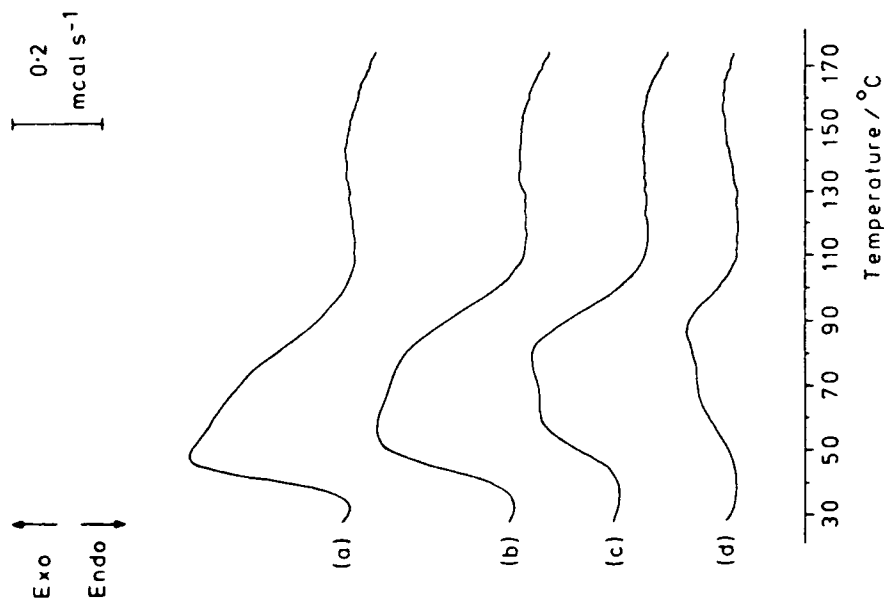
1) DSC Trace of a Film given 1 Pass under the 1.8 kW Source  
Recorded 1 Hour after Irradiation (a) and the Trace Obtained  
on Rerunning the Sample (b) Showing the Glass Transition



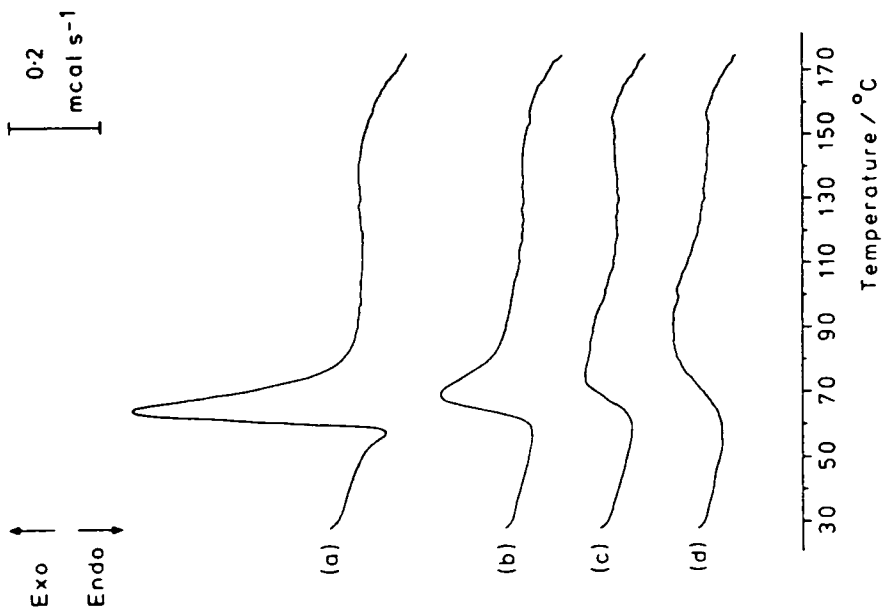
## 2) DSC Traces as a Function of Cure Exposure and

### Storage Time for Films Irradiated using the

1.8 kW Source



A) Traces Recorded 1 Hour after Irradiation



Films given :-

(a) 1 pass; 6.0 mg

(b) 3 passes; 6.0 mg

(c) 10 passes; 6.0 mg

(d) 20 passes; 6.0 mg

Films given :-

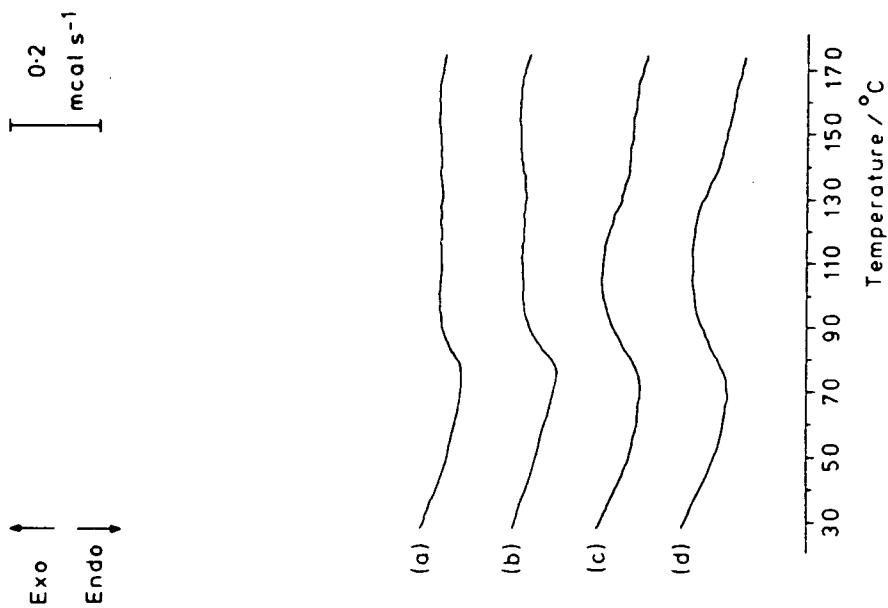
(a) 1 pass; 6.0 mg

(b) 3 passes; 6.0 mg

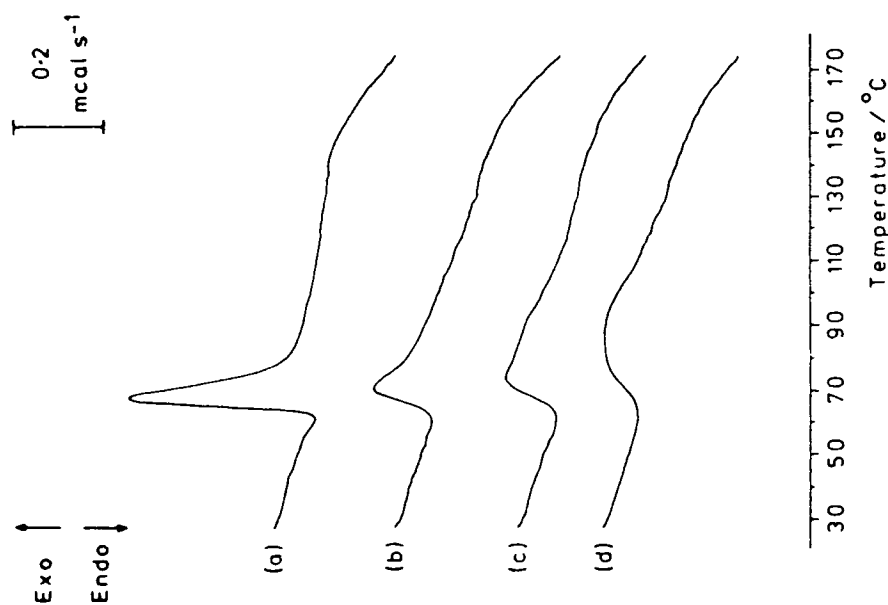
(c) 10 passes; 6.0 mg

(d) 20 passes; 6.0 mg

B) Traces Recorded 168 Hours after Irradiation

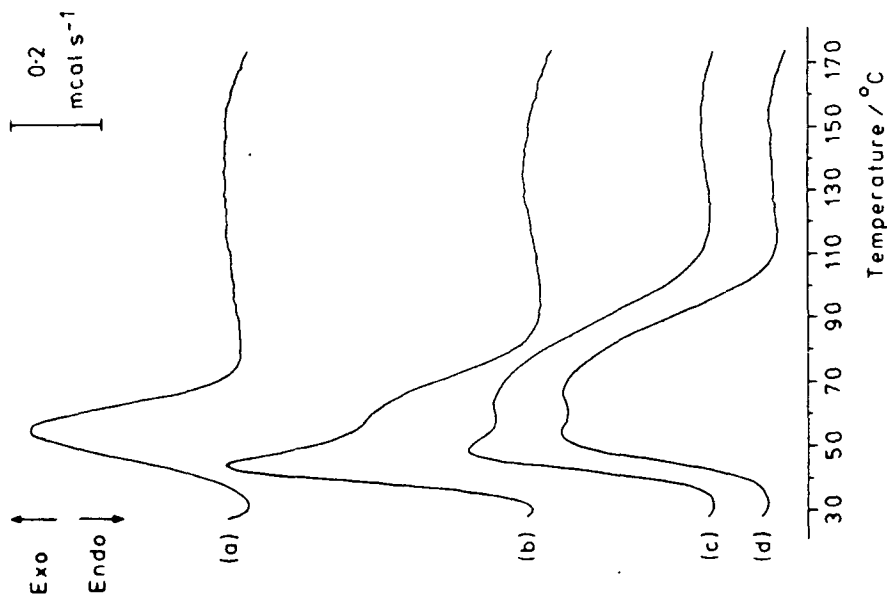


D) Traces Recorded 1 Year after Irradiation



C) Traces Recorded 504 Hours after Irradiation

3) DSC Traces as a Function of Cure Exposure and Storage Time for Films Irradiated with Filtered Light using the 1.8 kW Source

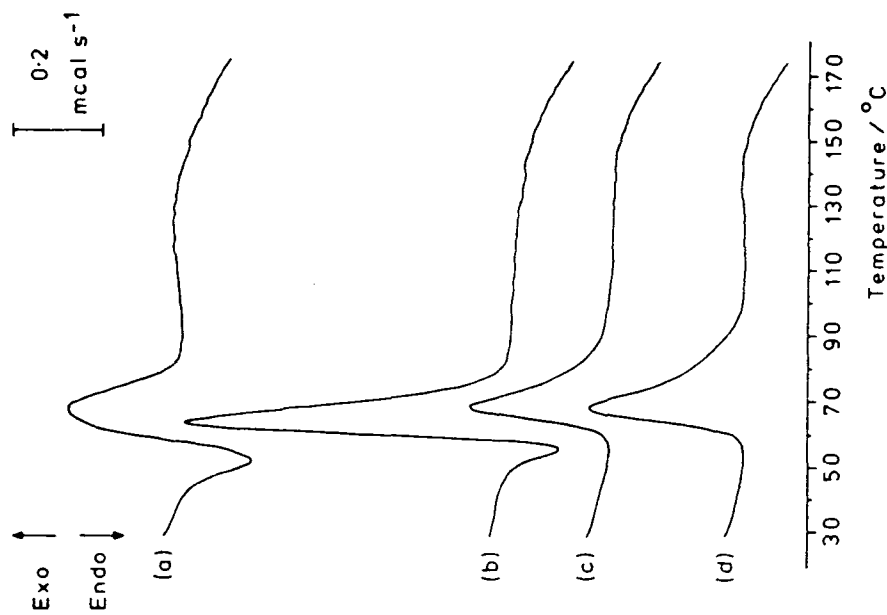


Films given:-

- (a) 1 pass; 4.8 mg\*
- (b) 3 passes; 4.9 mg
- (c) 10 passes; 5.1 mg
- (d) 20 passes; 5.0 mg

\* Trace recorded 3 hrs. after irradiation

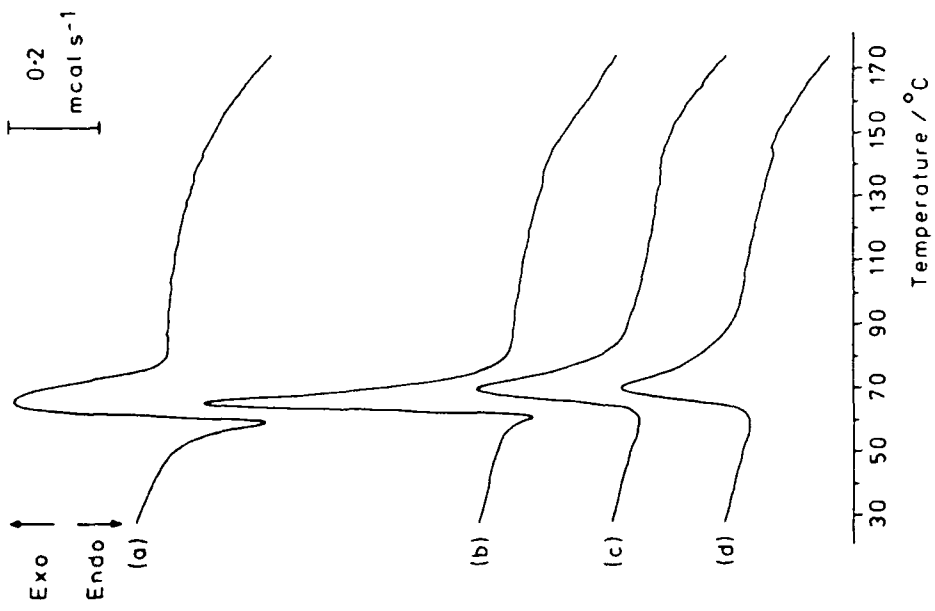
A) Traces Recorded 1 Hour after Irradiation



Films given:-

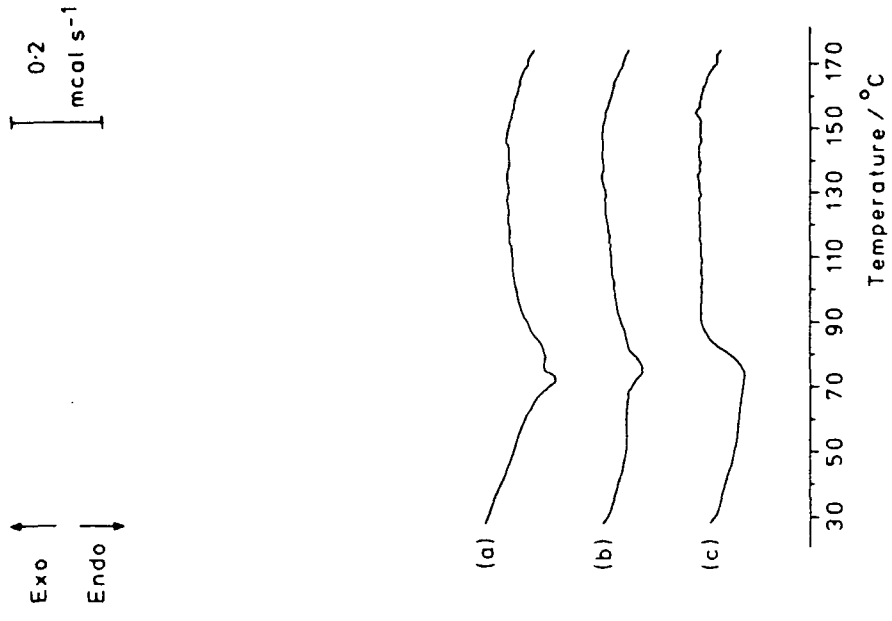
- (a) 1 pass; 4.0 mg
- (b) 3 passes; 4.0 mg
- (c) 10 passes; 4.0 mg
- (d) 20 passes; 4.1 mg

B) Traces Recorded 168 Hours after Irradiation



- Films given :-
- (a) 1 pass; 3.9 mg
  - (b) 3 passes; 4.0 mg
  - (c) 10 passes; 4.1 mg
  - (d) 20 passes; 4.1 mg

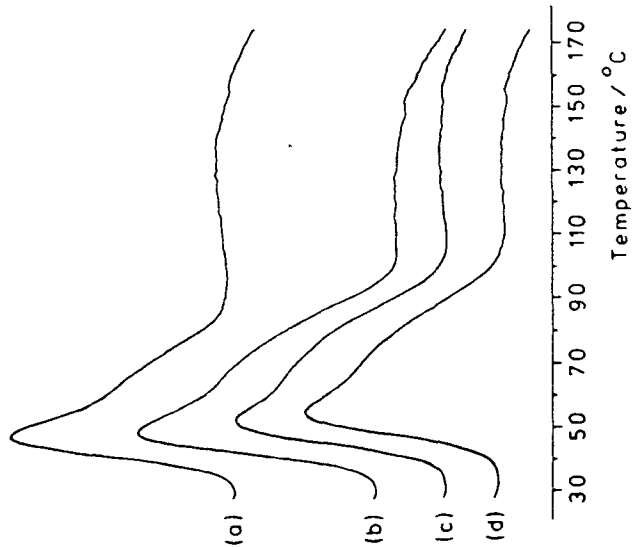
C) Traces Recorded 504 Hours after Irradiation



- Films given :-
- (a) 1 pass; 5.0 mg
  - (b) 3 passes; 5.0 mg
  - (c) 10 passes; 5.0 mg

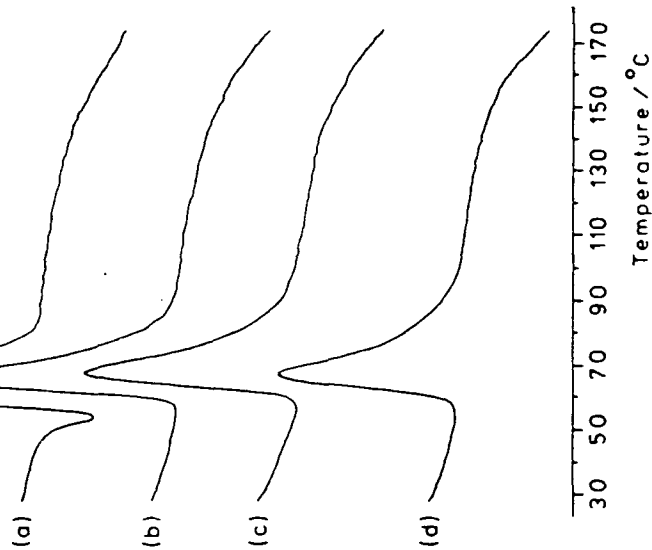
D) Traces Recorded 1 Year after Irradiation

**4) DSC Traces as a Function of Cure Exposure and Storage Time for Films Irradiated using the 100 W Source**



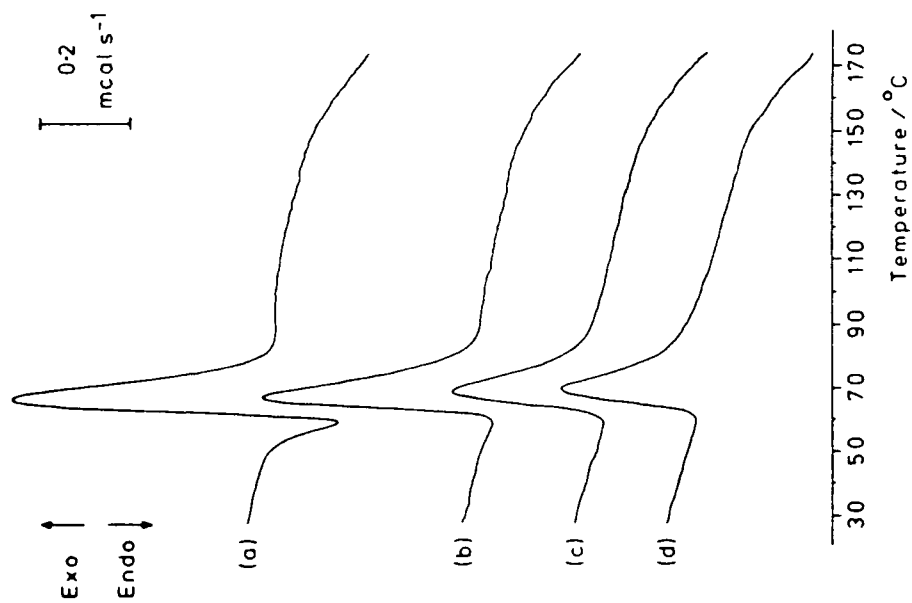
Films irradiated for :-  
 (a) 3 mins.; 3.9 mg  
 (b) 8 mins.; 4.1 mg  
 (c) 20 mins.; 4.0 mg  
 (d) 45 mins.; 4.0 mg

**A) Traces Recorded 1 Hour after Irradiation**

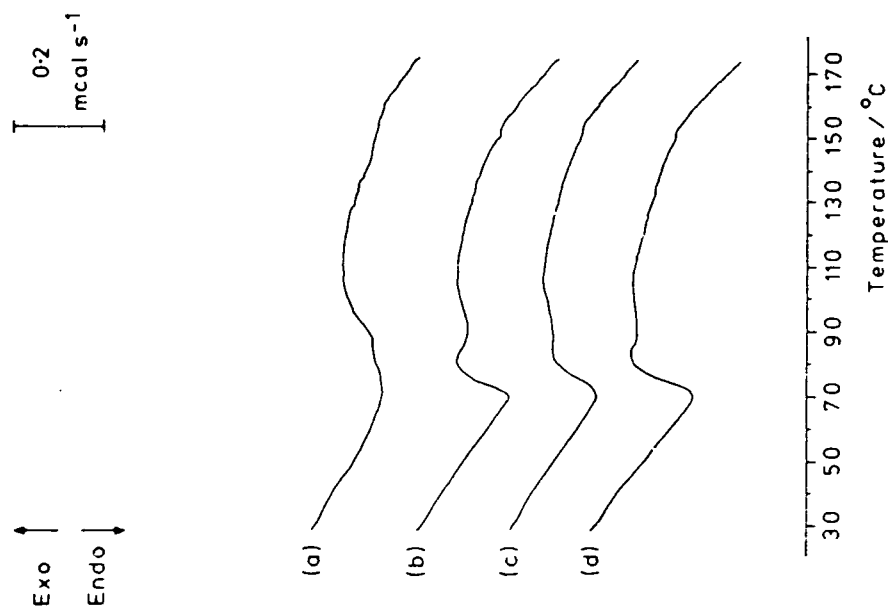


Films irradiated for :-  
 (a) 3 mins.; 3.9 mg  
 (b) 8 mins.; 4.0 mg  
 (c) 20 mins.; 4.0 mg  
 (d) 45 mins.; 4.0 mg

**B) Traces Recorded 168 Hours after Irradiation**

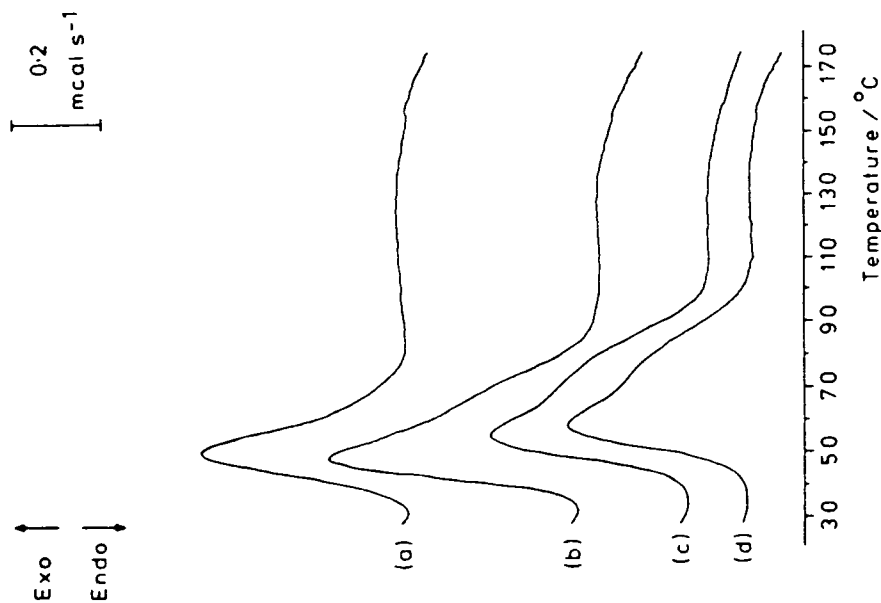


C) Traces Recorded 504 Hours after Irradiation

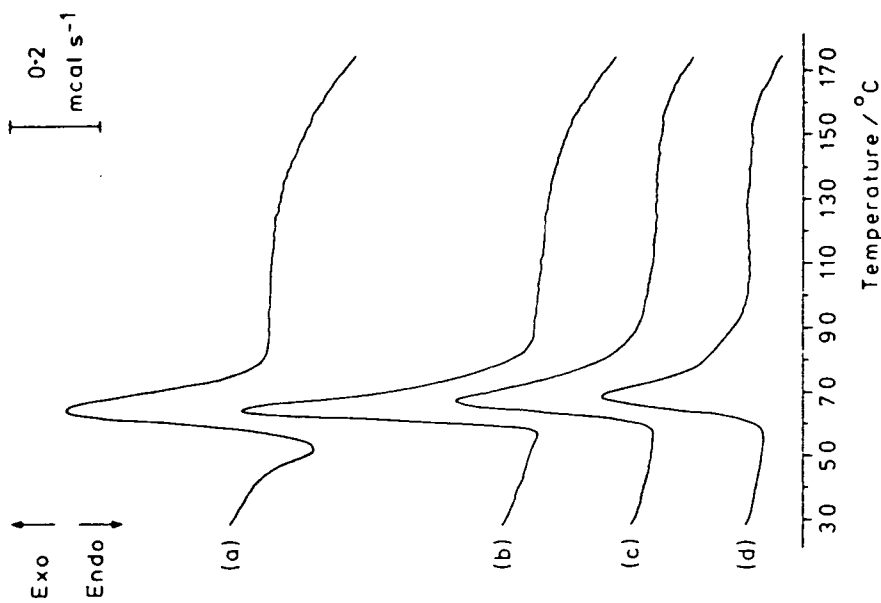


D) Traces Recorded 1 Year after Irradiation

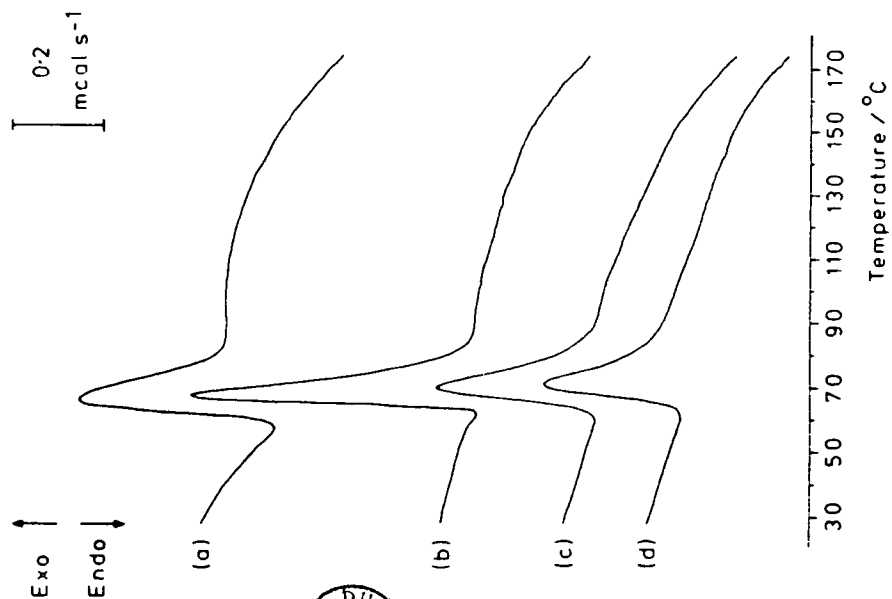
5) DSC Traces as a Function of Cure Exposure and Storage Time for Films Irradiated with Filtered Light using the 100 W Source



A) Traces Recorded 1 Hour after Irradiation

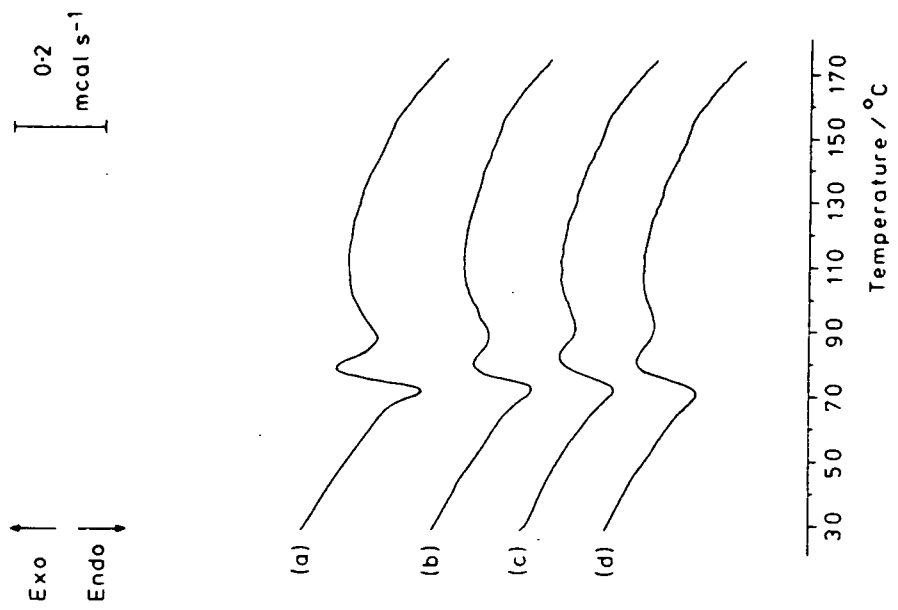


B) Traces Recorded 168 Hours after Irradiation



Films irradiated for:-  
 (a) 3 mins.; 4.0 mg  
 (b) 8 mins.; 4.1 mg  
 (c) 20 mins.; 4.1 mg  
 (d) 45 mins.; 4.0 mg

C) Traces Recorded 504 Hours after Irradiation



Films irradiated for:-  
 (a) 3 mins.; 6.0 mg  
 (b) 8 mins.; 6.1 mg  
 (c) 20 mins.; 6.1 mg  
 (d) 45 mins.; 6.0 mg

D) Traces Recorded 1 Year after Irradiation

